CA1
DTC 801
86
M571
c.2

arctec canada limited

88-00328/

ARCTEC CANADA LIMITED FR1163C

MODEL STUDIES OF ICE INTERACTION WITH SHIP RUDDERS AND STEERING SYSTEMS

VOLUME I - MAIN REPORT

TP# 8136E

November, 1986

Submitted to

Transportation Development Centre,
Complexe Guy Favreau,
200 Dorchester Blvd. West,
Suite 601, West Tower,
Montreal, Quebec.
H2Z 1X4

AUG 14 1987

Submitted by

B. Menon
L. Phillips
T. Roots

ARCTEC CANADA LIMITED
311 Legget Drive
Ottawa, Ontario
K2K 1Z8

DISCLAIMER

The contents of this report reflect the views of Arctec Canada Limited and not necessarily the official view or opinions of the Transportation Development Centre of Transport Canada.

LANGUAGE NOTE

Un sommaire en français de ce rapport est inclus avant la Table des matières.

APPROVED BY:
I.F. Glen, President

Transport Canada Transports Canada

Development Développement

REPORT DOCUMENTATION FORM

1. Transport Canada Report No. TP 8136E	2. TDC Project No. 4877	3. Recipient's Catalogue No.
4. Title and Subtitle MODEL STUDIES OF ICE INTERACTION WITH SHIP RUDDERS AND STEERING SYSTEMS		5. Report Date November 1986 6. Performing Organization Report No. 1163C
7. Author(s) B. Menon, L.D. Phillips, T. Roots		8. Transport Canada File No. D1460-179-2
9. Performing Organization Name and Address Arctec Canada Limited 311 Legget Drive Kanata, Ontario K2K 1Z8		10. DSS File No. 10SD.T8200-3-3519 11. DSS or Transport Canada Contract No. 1SD85-00077
12. Sponsoring Agency Name and Address Transportation Development Centre (TDC) Guy Favreau Complex 200 Dorchester Blvd. W., Suite 601, West Tower Montreal, Quebec H2Z 1X4		13. Type of Report and Period Covered Final (Sept./85-Oct./86) 14. Sponsoring Agency Code TDC 4877
15. Supplementary Notes Volume I - Main Report Volume II - Appendices		16. TDC Project Officer **C. Nowicki**

17. Abstract

This report presents the methodology and results of two complementary series of model scale experiments on ice loading effects on ship rudders and steering systems. In the first series, experimental data was obtained from controlled impacts of a 1:17 scale physical model of the LOUIS S. ST. LAURENT rudder into synthetic model ice. In these 'dry mode' tests, a range of parameters was investigated, including the influence of: impact velocity, ice floe size, rudder angle, ice strength, rudder stock torsional stiffness and hydraulic relief pressure. Trends in rudder stock torsional and flexural strains, rudder loads, and other response variables were identified as a function of the operating models: MV ARCTIC, PIERRE RADISSON and POLAR 8. Frequency of ice impacts on the rudder was measured in broken ice using self-propelled towed models. A range of operating conditions was investigated by means of variation in ship forms, velocity, rudder angle, draft, drift angle, direction of motion, and thrust levels. The influence of these parameters is discussed and presented by means of histograms. Rudder torque measurements in the ice basin tests provide a comparison to the dry impact test results. This work is directed towards development of rudder load design criteria for steering systems and verification of a mathematical model of rudder response.

18. Key Words Rudder, Rudder stock, Rudder loads, Physical modelling, Model tests, Ice impacts, Steering gear, Design torque		19. Distribution Statement A limited number of copies are available from the Transportation Development Centre	
20. Security Classification (of this report) unclassified	21. Security Classification (of this page) unclassified	22. No. of Pages 180	23. Price ----

TDC CDT 79-005
Rev 86

Canada

Transports Canada Transport Canada
Développement Development

FORMULE DOCUMENTAIRE DU RAPPORT

1. Nº du rapport Transports Canada **TP 8136E**	2. Nº de l'étude — CDT 4877	3. Nº de catalogue du destinataire

4. Titre et sous-titre
MODEL STUDIES OF ICE INTERACTION WITH SHIP RUDDERS AND STEERING SYSTEMS

5. Date du rapport
novembre 1986

6. Nº du rapport de l'organisme exécutant
1163C

7. Auteur(s)
B. Menon, L.D. Phillips, T. Roots

8. Nº de dossier Transports Canada
D1460-179-2

9. Nom et adresse de l'organisme exécutant
Arctec Canada Limited
311 Legget Drive
Kanata (Ontario)
K2K 1Z8

10. Nº de dossier — ASC
10SD.T8200-3-3519

11. Nº de contrat — ASC ou Transports Canada
1SD85-00077

12. Nom et adresse de l'organisme parrain
Centre de développement des transports (CDT)
Complexe Guy-Favreau
200 ouest, boul. Dorchester, suite 601, tour ouest
Montréal (Québec) H2Z 1X4

13. Genre de rapport et période visée
Final (sept.85-oct.86)

14. Code de l'organisme parrain
CDT 4877

15. Remarques additionnelles
Volume I - Rapport principal
Volume II - Appendices

16. Agent de projet — CDT
C. Nowicki

17. Résumé

Le présent rapport donne les résultats, et explique les méthodes de mise en de deux expérimentations complémentaires visant à approfondir l'action des glaces sur le gouvernail et l'appareil à gouverner d'un navire. Dans un premier temps, des données expérimentales ont été tirées des essais de choc contrôlés qui mettaient en oeuvre un modèle réduit au 1/17 du brise-glace LOUIS-SAINT-LAURENT heurtant une glace synthétique modèle. Dans ces essais dits hors bassin, des variations ont été imposées aux facteurs contrôlés suivants: vitesse à l'impact, taille des fragments de glace, angles de braquage, résistance de la glace, raideur en torsion de la mèche et pression d'ouverture du circuit hydraulique de commande. L'évolution des déformations de torsion et de flexion de la mèche, des efforts sur le gouvernail et d'autres variables a été établie à l'égard des trois modèles réduits représentant le N.M. ARCTIC, le PIERRE-RADISSON et le POLAR 8. Dans un deuxième temps, par des essais de remorquage en bassin rempli de fragments de glace, la fréquence des impacts sur le gouvernail a été chiffrée. Les facteurs contrôlés étudiés ont été les suivants: forme de la coque, vitesse, angle de braquage, tirant d'eau, angle de dérive, sens de rotation des hélices et poussée; l'influence des ces paramètres est commentée, histogrammes à l'appui. Les valeurs de couple mesurées sur le gouvernail lors des essais en bassin servent de point de comparaison aux essais hors bassin. Une fois combinés, les résultats des deux expérimentations permettront de vérifier un modèle mathématique simulant la réponse d'un gouvernail à la charge des glaces et de mettre au point les critères de calcul correspondants.

18. Mots-clés
Gouvernail, mèche, efforts, modèles réduits, modélisation physique, essais sur modèles réduits, appareil à gouverner, couple de référence, choc des glaces.

19. Diffusion
Le Centre de développement des transports dispose d'un nombre limité d'exemplaires.

20. Classification de sécurité (de ce rapport) non classifié	21. Classification de sécurité (de cette page) non classifiée	22. Nombre de pages 180	23. Prix ----

CDT TDC 79-005
Rev 86

Canada

PROJECT TEAM

The project team for Arctec Canada Limited was composed of:

- B. Menon, Program Manager
- L. Phillips, Project Engineer (Dry Impact Tests)
- L. Goossens, Project Engineer (Ice Basin Tests)
- T. Roots, Test Engineer
- R. Brown, In-House Consultant, Numerical Modelling and Data Analysis

with technical assistance from:

- D. Bourne
- A. Karton
- A. Lemieux
- A. Moonah
- R. Nelson
- V. Nisbett.

ACKNOWLEDGEMENTS

The authors would like to acknowledge the support of Mr. Chris Nowicki who, as Scientific Authority at Transportation Development Centre, has patiently directed this project to a satisfactory completion. In addition, we would like to thank Mr. Ian Bayly, also at Transportation Development Centre, who originally supported this important study on rudder/ice loading and who provided valuable guidance at the early stages of development of the experimental programs.

SUMMARY

Two complementary model scale experiments have been carried out to systematically investigate the response characteristics of ship steering systems under the influence of ice loads acting on the rudder.

- In the first phase of the project the rudder-ice interaction problem was addressed by physical modelling. A 1:17 scale model of the rudder assembly of the Canadian Coast Guard icebreaker LOUIS S. ST. LAURENT was designed and parametrically tested over a range of impact conditions. This provided a database of information on rudder loads, torques, bending strains, and other parameters.
- In the second phase of the project, three ship models were tested in the ice basin to measure frequency of ice impacts on the rudder as a function of a range of ship operating conditions.

The work is generally directed towards the development of rudder load design criteria for ship steering systems and the verification of a mathematical model of rudder response to ice impacts. The database and trends determined as a result of these two experiments represents a valuable tool in advancing the design of steering systems for ice-worthy vessels.

Physical Modelling of Dry Impact Test System

The dry mode impact tests were planned to parametrically study the loading and response of a typical rudder assembly and hydraulic steering gear from the perspective of the severe ice impact scenario. The LOUIS S. ST. LAURENT rudder was chosen as the prototype, representative of a typical icebreaker rudder assembly. Physical modelling involved the accurate scaling of pertinent geometric and dynamic properties of the test system; including rudder, stock, tiller, rams, hydraulic actuator system, and ice. A 1:17 scaling was selected on the basis of size and weight considerations. Figure 1 shows a representation of the test system. A scaled model of the rudder and matching rudder stocks were designed and machined from aluminum. The rudder was free to rotate on a pair of pintles and it was supported along the stock by a support bearing and a carrier bearing. Three rudder stocks having different diameters were fabricated to introduce variation of the rudder stock torsional stiffness.

The rudder stock attached to the tiller could be fixed rigidly or could be rotated by the rams of a hydraulic actuator system. The entire rudder assembly was bolted to a steel box which was suspended on a two meter track under the towing carriage. It was possible to add ballast weights to this box, and thereby change the mass involved in the rudder-ice interaction at the impact speed. Since the broken channel ice floes are generally much less massive than the ship, it is valid to consider that this moving box mass represents the mass of the ice pieces.

FIGURE 1

DRY IMPACT EXPERIMENTAL SET-UP

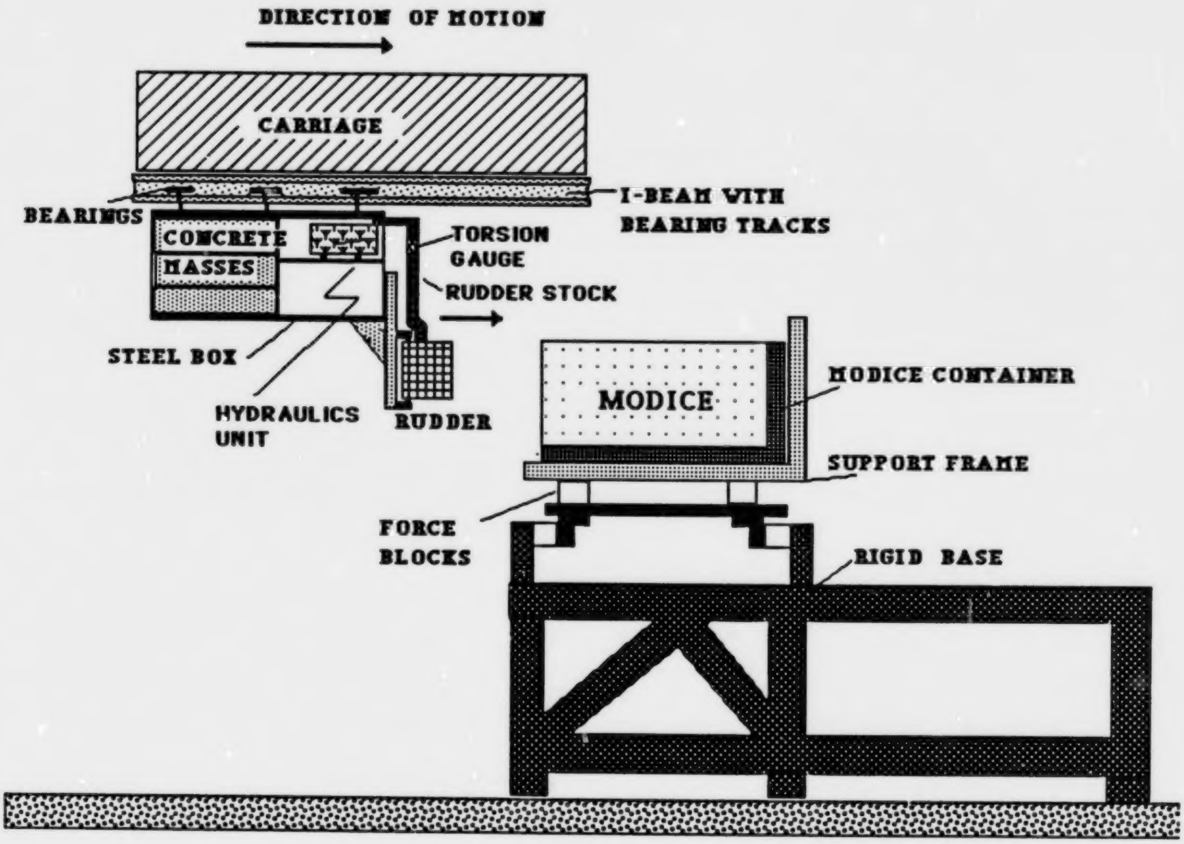
DIRECTION OF MOTION
CARRIAGE
BEARINGS
I-BEAM WITH BEARING TRACKS
CONCRETE MASSES
TORSION GAUGE
RUDDER STOCK
STEEL BOX
HYDRAULICS UNIT
RUDDER
MODICE
MODICE CONTAINER
SUPPORT FRAME
FORCE BLOCKS
RIGID BASE

The synthetic ice, MODICE, used in these tests is a wax-type material, which is formulated as a melt and allowed to set in a mold. Therefore, the testing could be carried out in a 'dry mode', with only a surface spray of water onto the MODICE to improve friction. The strength of the ice was controlled by means of an empirical scaling formula that is considered valid for crushing type application. This relationship was verified through a series of uniaxial crushing tests using Arctec's Closed Loop System. A target strength of 53 kPa was defined. This assumes that multi-year ice fragments represent the most extreme scenario. During testing the entire trailing edge of the rudder was involved in the crushing process. A series of eight ice blocks were prepared which included very strong ice, moderately strong ice, target ice, and relatively weak ice (15-22 kPa, 68 kPa, 86 kPa, 175 kPa). The blocks were mounted on a force balance which measured axial direction and lateral direction forces in the horizontal plane.

Dry Impact Test Results

The test matrix for the dry mode rudder-ice impact tests involved variation in six parameters: velocity of impact, rudder angle, rudder stock torsional stiffness, ice mass, ice strength and hydraulic pressure relief. In excess of 130 tests were carried out. Measured variables included: rudder loads (longitudinal and transverse components), stock torsional strain, bending strain (side and front components), ice indentation and ram hydraulic pressures. The influence of the operational parameters on the measured response has been assessed and represented graphically. Figure 2 provides an example showing the influence of ice strength and velocity on peak torque. The following general trends have been observed, although no definitive functional relationships have been derived in the present analysis:

- The influence of ice strength is strongest for peak rudder loading, longitudinal accelerations and torsional strain response. Indentation length appears to decrease exponentially with increasing ice strength. Torque rise time also decrease over the test range of increasing ice strength.

- Rudder loading and longitudinal acceleration appear to obey power law relationships with respect to increasing velocity, which show a coefficient less than one. Torsional strain and indentation are approximately linear with velocity. Bending strain does not show any significant trend, and torque rise time is constant.

- An increase in rudder angle is observed to cause increased rudder loads, torques and accelerations up to about 60 degrees. The trend appears approximately sinusoidal. Indentation decreases at larger angles of impact.

FIGURE 2

RUDDER STOCK TESTS
ICE STRENGTH VARIATION

A. INFLUENCE OF ICE STRENGTH ON TORSIONAL RESPONSE

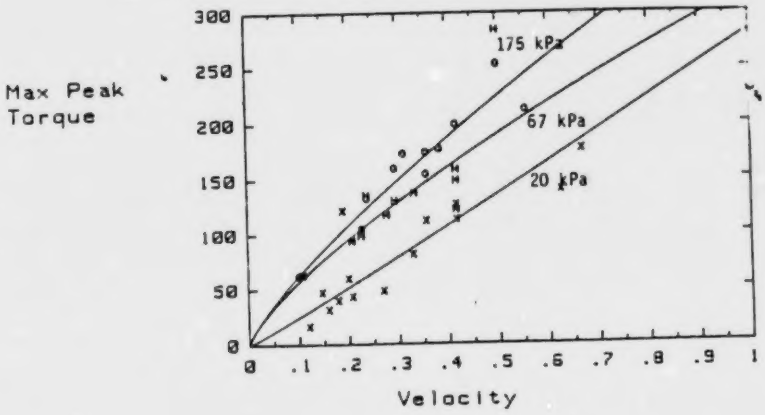

A. INFLUENCE OF VELOCITY ON NORMAL LOAD

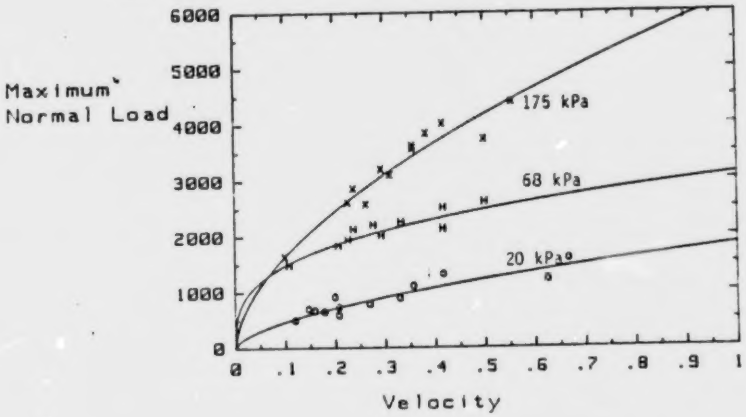

B. RELATIONSHIP OF LOAD TO CRUSHED AREA

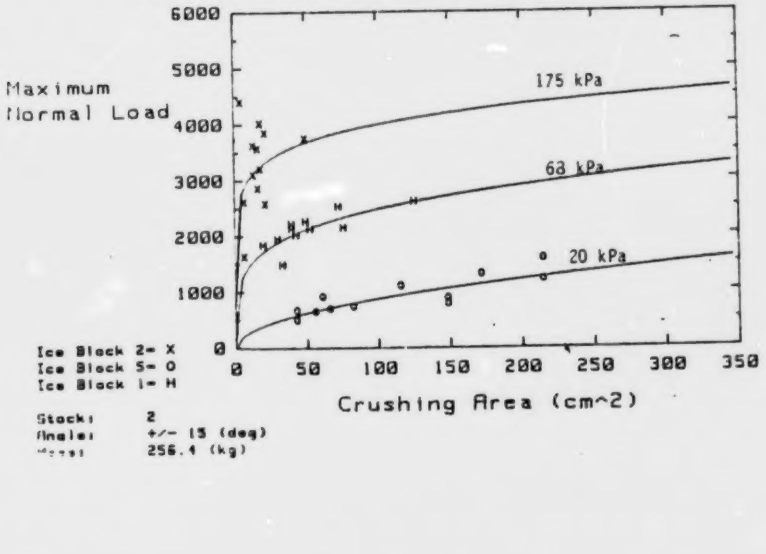

- The standard ice mass of 256 kg used in the majority of tests corresponds to about 10 percent of ship (mass) displacement. Further increases in mass up to 700 kg caused a linear increase in rudder loads, indentation and torque. Bending strains appear to depend only marginally on ice mass. Axial acceleration decreases inversely with increasing mass. It was not possible to decrease mass below 200 kg with the present set-up.

- Torsional strain and bending strain increase rapidly with reduced stock stiffness. The relationship is approximately inverse squared. The ratio of bending strain to torsional strain is less than 0.1 at target scaling, and therefore bending is only significant for very weak stock stiffnesses. This ratio does not appear sensitive to ice strength variations.

- The majority of parametric testing was carried out with the rudder stock fixed at the tiller. In one set of tests the tiller was instead connected to the hydraulic actuator system via the rams. It was observed that a release pressure of 50 psi caused a significant reduction in the peak torque and loads as compared to the fixed tiller arrangement. At increased release pressures, the maximum pressure difference was found to increase. This effect increased linearly with impact speed.

Ice Basin Towed Tests

The towed test program was developed to investigate a range of operational parameters which influence the frequency of ice impacts with the rudder. Three ship models were identified with the requisite bow forms and stern configurations. The MV ARCTIC is a large ice class bulk carrier/OBO with a single screw and single rudder. The PIERRE RADISSON is an existing Canadian Coast Guard icebreaker with twin screws and a single rudder. The POLAR 8 hull represents a proposed design for a Arctic Class 8 icebreaker. This model has triple screws and a single rudder.

Three similar series of self-propulsion tests were planned and carried out involving the three models. In the case of the MV ARCTIC tests, an additional set of tests was included at a different ice thickness. Four ice sheets were used, the thicknesses of which correspond to the maximum ice thickness for continuous icebreaking for these vessels. Each test series consisted of numerous repetitious of forward and astern trials in pre-cut floes with known dimensions. The initial test involved breaking along a herring bone pattern, which had been formed by 45° cuts outward from the ice basin centerline. The lateral width of the herring bone pattern was 1.1 times the model beam.

The separation of cuts was determined by a characteristic length calculation. The second test run involved backing in the broken channel formed by the first test. The entire ice surface was then cut into pieces corresponding to the model's characteristic cusp length. All subsequent runs in a test series were in the nominally identical piece size distribution. However, the mean size gradually became smaller as a result of interaction between the floes and the ship, as well as by ingestion of ice into the propellers. For this reason it was necessary to stagger the repetitions of a particular test condition, so that the mean ice piece size of each grouping of similar tests would be equivalent. A large range of operating parameters were investigated, including the influence of ship form, forward speed, astern speed, rudder angle, propeller thrust level and direction of rotation, ballast condition (draft), ice thickness and floe size. The principal parameters measured were frequency of impact and rudder torque.

Towed Test Results

Data sets from approximately 150 tests involving four different ice sheets were recorded. In addition, bollard test data and open water self-propulsion trials data for each of the three models was collected. This latter information was obtained at forward and backing velocities corresponding to the ice test conditions for each ship model. Torque time histories from the individual ice transiting tests were examined and the magnitude and number of significant impacts have been extracted. Figure 3 shows a typical torque time history.

The results have been presented in histograms which give the number of impact events (or peaks) at a particular magnitude of torque. For purposes of analysis, the matrix of test parameters has been consolidated into five groups. This was necessary to ensure a statistically meaningful number of impact counts within each histogram.

Table 1 shows the tests which have been included in each of the five categories; designed as: maximum forward speed, yawing forward, mid speed forward, mid speed backing and low speed backing. Histograms are normalized to show the average number of impacts per full scale kilometer of transit (forward or astern). For each ship, this corresponds to a different ice thickness and test velocities. A sample histogram is shown in Figure 4.

It has not been possible to define the influence of some parameters such as thrust level, draft condition and rudder angle because of the limited amount of significant impact data. However, the consolidated histograms have indicated the following general trends:

- There were no ice impacts observed for the MV ARCTIC during forward speed motions. This is likely a result of her length, deep draft and the protection afforded by the propeller nozzle.

FIGURE 3

INFLUENCE OF SHIP FORM IN FULL FORWARD SPEED MANOEUVRES

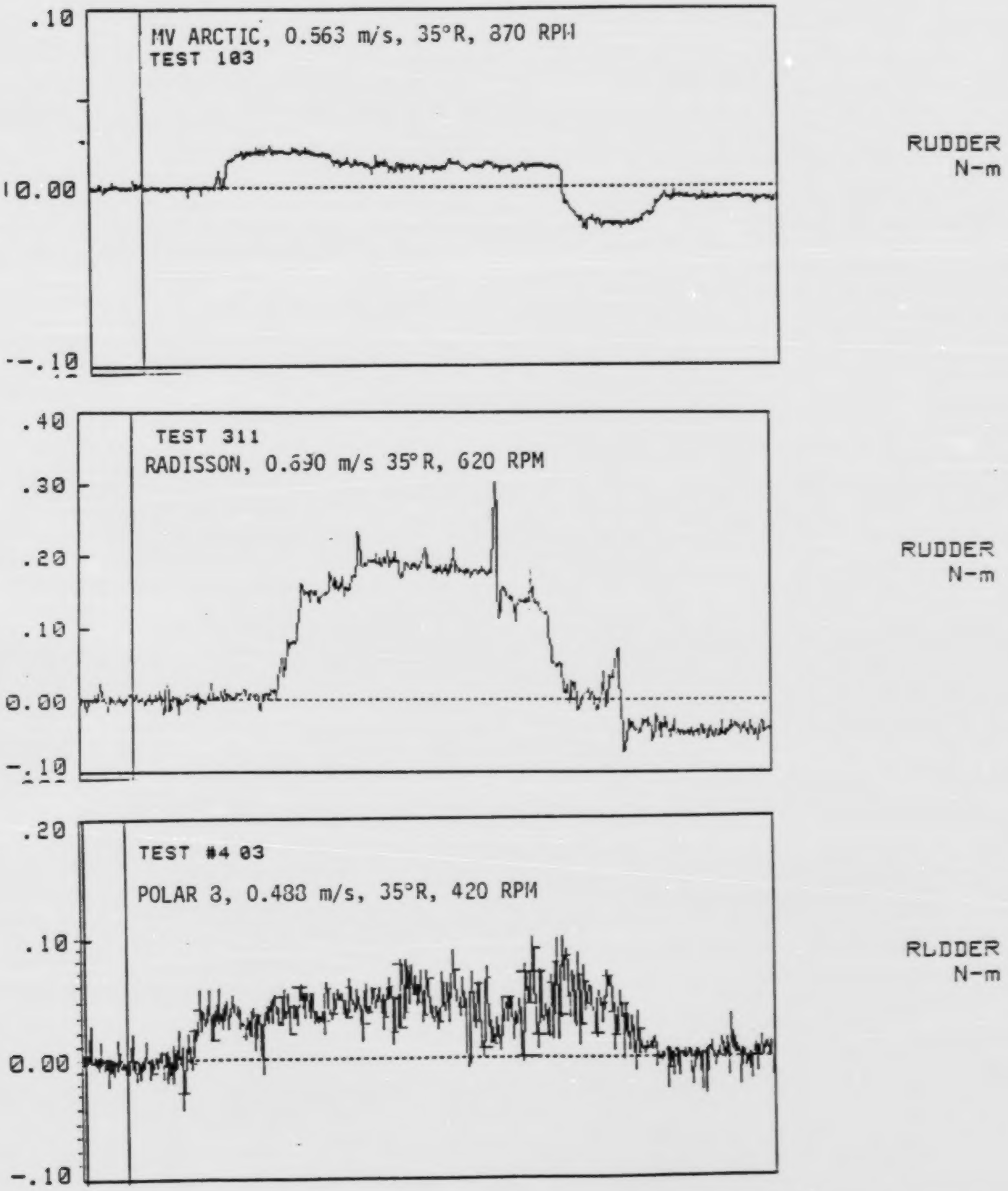

FIGURE 4

FREQUENCY and MAGNITUDE of RUDDER/ICE IMPACTS

M. V. ARCTIC - Mid-speed Backing : .282 m/s

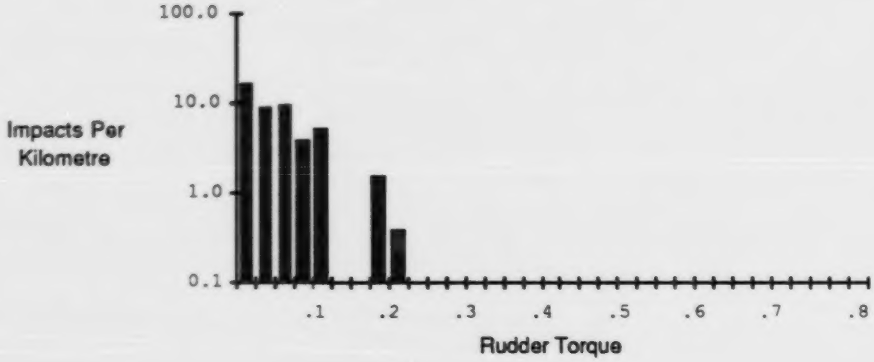

PIERRE RADISSON - Mid-speed Backing : .345 m/s

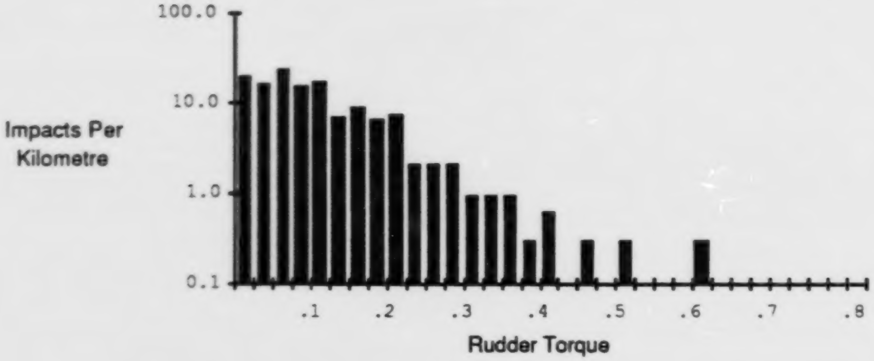

POLAR 8 - Mid-speed Backing : .244 m/s

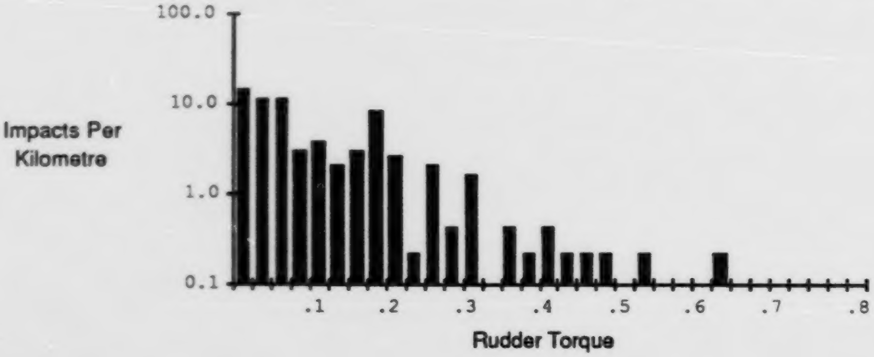

- In astern manoeuvres the MV ARCTIC exhibited a larger number of impacts with moderate torque magnitudes. Additionally, a large number of impacts with low torque values were observed. These may result from continuous ice contact or from enhanced hydrodynamic loads on the rudder. There appears to be no appreciable increase in frequency of impact with increased astern velocity, although a shift towards larger mean torque is seen.

- The PIERRE RADISSON shows the highest frequency of impacts on the rudder during both ahead motions and astern motions of all three test vessels. An increase in frequency with forward speed is observed in both the ice impact torque region and the hydrodynamic loading range. Introduction of a drift angle into the full speed manoeuvres results in an increase in the number of impacts and an upward shift in the mean torque magnitude.

- In astern manoeuvres the RADISSON exhibits a larger number of significant impacts, but about the same hydrodynamic loading as during forward motions. The impact frequency does not appear dependent on velocity; but there is an upward shift in torque magnitude with speed.

- The POLAR 8 icebreaker histograms have a similar pattern to that observed for the RADISSON. In forward motions, the POLAR 8 has a larger number of low magnitude or hydrodynamic events, but fewer ice impacts. This number is speed dependent. In backing the POLAR 8 again shows fewer impacts over a similar torque range.

Some additional comments about individual parameters may be made on the basis of a visual examination of the time histories. It appears that the relative value of steady state rudder torque for each ship in each operating mode is a major factor influencing the histograms. The steady state component in the ice impact environment is similar in magnitude to the corresponding open water value. In general, it is observed that the RADISSON has the larger value; followed by POLAR 8 and MV ARCTIC. This reflects the particular hydrodynamic characteristics of each ship's stern configuration and rudder geometry. Furthermore, it has repercussions on the interpretation of trends in various ship parameters.

The time histories suggest that decreasing draft causes a marginal increase in torque magnitudes; as does increasing RPM or ice thickness. The effect of changing the propeller rotation direction is hidden by the change in steady state torque.

Conclusions

The applicability of dry impact parametric testing by means of a large scale physical model of a ship rudder assembly has been demonstrated. A large range of operational parameters have been assessed, including the influence of: impact velocity, rudder angle, rudder stock torsional stiffness, ice mass, ice strength and hydraulic pressure release. Sets of time histories of rudder loading, stock bending strains and torsional response have been collected and a corresponding data base of peak values established. This has allowed insights into the rudder-ice interaction process and has provided a starting point from which functional relationships between parameters may be derived. Trends between rudder stock torque and other variables and a range of parameters have been presented.

A limited assessment of the influence of steering gear hydraulic pressure relief on rudder loads and motions has been made as a result of the use of the hydraulic rams and control units. The scaled hydraulics system provided a reasonable representation of the release pressure mechanism and illustrated significant trends associated with steering system hydraulic "stiffness". In particular, it showed that the fixed tiller tests represented a conservative loading condition, and that the effect of pressure relief variation was velocity dependent. However, it should be noted that there was no attempt to incorporate feedback control into this hydraulic model. Additional physical modelling using a more complete hydraulics model is needed to study the influence of the pipe orifice diameter, the response and the pumping rate of fluid during pressure release situations.

The data generally represents extreme impact conditions since the test conditions involved large ice masses, full depth ice contact with the rudder edge, large rudder angles, and strong ice. Excepting contact depth, a range of each of these parameters has been tested, which allows extrapolation to less extreme scenarios. However, it is difficult to predict torsional response for ice masses which are less than 5 percent of the RADISSON displacement because of the rapid increase of torque over the lower range of ice mass. The trends defined in this part of the study form the basis for parametric equations which will lead to a realistic validation of the mathematical model of overall rudder torsional response and to more rational design criteria.

The principal outcome of these tests has been the statistics on the frequency of impact during astern manoeuvres in the broken channel. Since it was not possible to accurately scale the crushing strength of the pre-cut urea ice, and maintain it throughout a full day of tests, distortions in the rudder torque values were expected. Nonetheless, the torque values provide an order of magnitude reference in assessing the impact severity.

The comparison between the three vessels has demonstrated the effectiveness of certain hull form characteristics in limiting the number and severity of rudder ice loads. In particular, the nozzle on the MV ARCTIC propeller, in combination with its greater length and draft, resulted in a total protection from impacts during forward manoeuvres. With the limited number of test repetitions, it has not been possible to statistically determine the meaningfulness of the data on opposing propeller rotation directions. Nor has it been possible to differentiate between minor variations of rudder angle or thrust level during astern manoeuvres. These tests have been grouped together to allow comparative statistical assessment between different ships and major operating characteristics.

Recommendations

The present analysis of the 'dry mode' impact data has identified the significant trends of influence between rudder torsional response and a range of operation parameters. A further analysis effort is necessary to reformulate the data into a dimensionless form and then to extract the individual parametric equations. The preliminary evaluation of peak data by means of power regression fits for the figures in the text has shown that this exercise will yield good numerical results. These relationships will form the basis for an validated mathematical model of rudder-ice interaction. For numerical modelling, added mass effects must also be included. In addition, model scale data should be correlated with available full scale LOUIS S. ST. LAURENT trials data.

There were several limitations in the dry impact modelling that resulted in unanswered questions after the present test program. The most serious deficiency was in the range of ice mass. The lower bound on mass in the test range corresponded to approximately seven percent of the LOUIS S. ST. LAURENT displacement. Therefore, only the case of an infinite ship and large ice masses has been treated. Two further cases should be addressed by means of additional testing:

(1) If the stern of a vessel manoeuvring in ice swings into the channel edge, the situation may be considered one of an infinite ice mass and a finite displacement ship. Physical model tests to investigate this case would use an existing ship model backing into a fixed synthetic (MODICE) ice block. Stock torsion would again be modelled. This approach is necessary since it is not possible to support the 1:17 scaled weight of the entire ship in the present experimental apparatus. Other vessels may also be examined in this manner to establish reference comparisons between the dry impact parametric equations and 'wet mode' self propulsion model tests.

(2) If the ice floe mass drops below seven percent of the LOUIS S. ST. LAURENT displacement, the present interpretation of the two body impact problem does not change. The same experimental apparatus may be used to investigate the lower range of ice mass. However, the box frame which constitutes a major part of the mass would have to be redesigned and fabricated out of a lighter material to reduce its minimum, unballasted value.

Other areas in which the dry impact database may be expanded include variation in rudder tip geometry and depth of contact with the ice. Both of these recommendations address the question of the influence of pressure-area effects on rudder loading.

Another aspect of improved physical modelling involves the development of a more complete hydraulic steering gear. This necessitates further work on the modelling of fluid flow rates in the cylinders and orifices of the control unit. In addition, scaled feedback control should be incorporated into the hydraulic control system.

The principal limitation affecting the quality of the towed ice basin test results is in the number of repetitions of each test configuration. It has not been possible to separate the ice related torque peaks from the background hydrodynamic mean values. The towed results should be further reviewed to consider the open water and bollard trials data at each operational condition which was examined in the ice tests. The limited amount of data has necessitated a coarser grouping of different test parameters in the histograms than intended, to ensure more statistically meaningful trends. Additional evaluation of at least one vessel in a significantly larger sample of tests would improve the validity of these statistics and allow a finer differentiation of parametric influences. Furthermore, as a result of the experience with the dry impact physical modelling it is recommended that MODICE should be used in a follow-up towed test program. This ice material has two principal advantages: ice crushing strength can be modelled and maintained during testing; and the density of MODICE is closer to that of full scale ice. The former implies more accurate torque values. The latter implies that ice buoyancy forces will be better simulated and therefore the flow of ice to the rudder will be more representative.

The present 'dry mode' impact tests and 'wet mode' ice basin model tests have established the basic information necessary to confirm or validate a mathematical model of steering response to rudder-ice loads. A valuable continuation involves the combination of the parametric equations of the dry impact tests, with the appropriate statistics from the ice basin tests and comparison to available full scale data. This leads towards the development of a semi-empirical model of the rudder-ice interaction with repercussions for rudder system design and regulation.

SOMMAIRE

Dans le but de caractériser la réponse de l'appareil à gouverner d'un navire à la charge des glaces sur le gouvernail, deux expérimentations complémentaires ont été faites à l'aide de modèles réduits:

- En premier lieu, l'investigation de l'interaction gouvernail-glaces s'est faite à l'aide d'un modèle réduit au 1/17 du gouvernail du brise-glace canadien LOUIS-ST-LAURENT, lequel modèle a été soumis à des essais paramétriques dans toute l'étendue du domaine considéré. Dans cette recherche, divers paramètres ont été pris en compte: efforts sur le gouvernail, couples, déformations dues aux efforts de flexion, etc.

- Ensuite, la recherche a pris la forme d'essais, dans un bassin des glaces, sur les modèles réduits de trois navires, dans le but de chiffrer le nombre d'impacts sur le gouvernail dans des conditions de marche variables.

L'objet de ces travaux était double: (1) mettre au point des critères de calcul de résistance des gouvernails et appareils à gouverner et (2) vérifier un modèle mathématique simulant la réponse d'un gouvernail à la charge des glaces. Tant l'information que les techniques résultant de ces deux expérimentations ont permis de faire progresser les méthodes de conception des appareils à gouverner pour navires appelés à naviguer dans les glaces.

Modèle réduit pour essais de choc hors bassin

Ces essais ont été étudiés en vue de mettre en évidence la charge exercée par les glaces sur un appareil à gouverner type, ainsi que les réactions de celui-ci à des chocs de forte amplitude. Le prototype choisi pour l'expérimentation a été l'appareil à gouverner du LOUIS-ST-LAURENT. Afin de réaliser la maquette, il a fallu procéder à une réduction d'échelle exacte des conditions géométriques et dynamiques des éléments constitutifs: gouvernail, mèche, barre, vérins, actionneur hydraulique et, enfin, glaces. L'échelle de réduction choisie a été de l'ordre du 1/17, pour des considérations à la fois de taille et de poids. La maquette réalisée est illustrée à la figure 1. Le gouvernail a été réalisé en aluminium, ainsi que les trois mèches dont chacune avait un diamètre différent de manière à faire varier la raideur en torsion de cet élément. Le gouvernail tournait sur deux aiguillots et était maintenu en position par l'intermédiaire de la mèche passant dans deux paliers.

FIGURE .1

Montage d'essais hors bassin

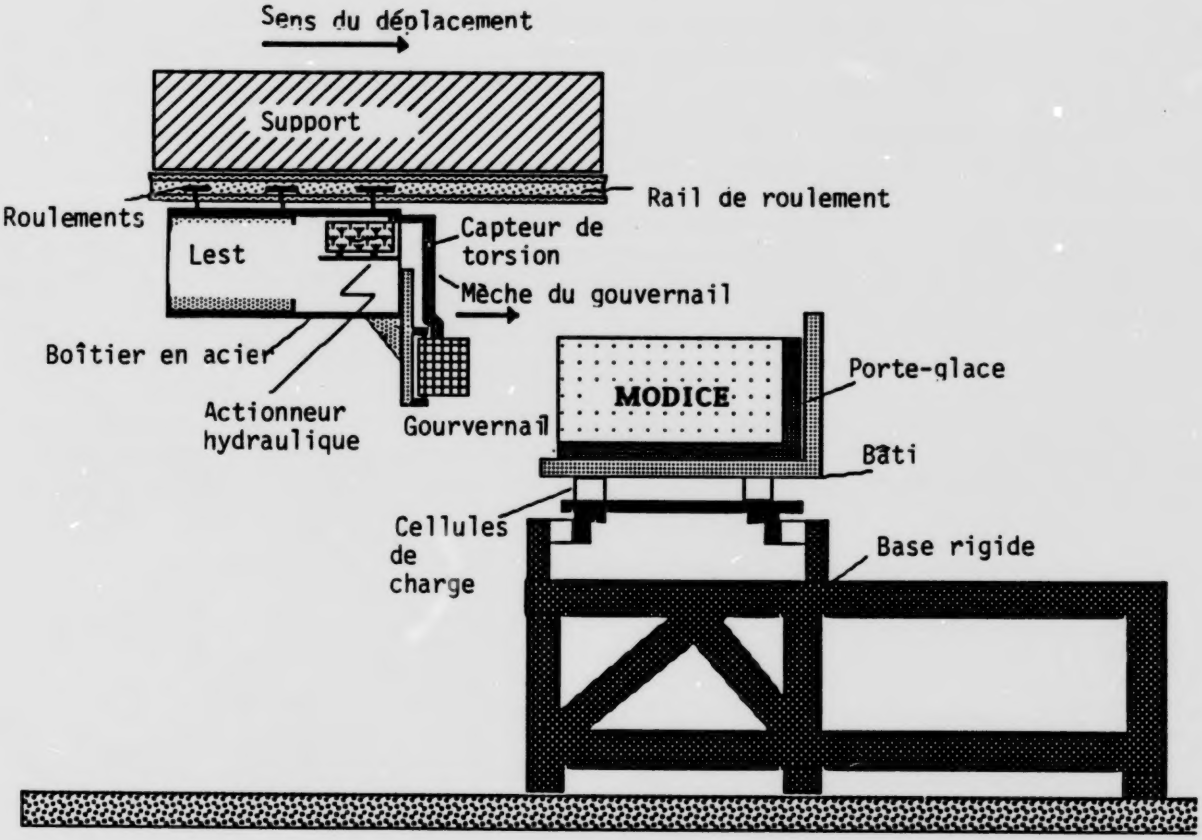
Sens du déplacement
Support
Rail de roulement
Roulements
Lest
Capteur de torsion
Mèche du gouvernail
Boîtier en acier
Actionneur hydraulique
Gourvernail
MODICE
Porte-glace
Bâti
Cellules de charge
Base rigide

La mèche était fixée à la barre, soit rigidement, soit par l'intermédiaire d'un actionneur hydraulique. La maquette était boulonnée à un boîtier en acier qui coulissait sur un rail de deux mètres de long fixé au chariot d'entraînement. Les variations dans la masse mise en oeuvre durant les essais étaient réalisées par des blocs de lest amovibles placés dans le boîtier. Étant donné que les fragments de glace dans le chenal ouvert ont une masse qui représente une petite fraction de la masse du navire, il est raisonnable de considérer la masse du boîtier en mouvement comme représentative de la masse des fragments de glaces.

La glace modèle utilisée dans les expérimentations était à base de cire, élaborée à l'état fondu et placée dans un moule pour figer. Lors des essais hors bassin, la surface des blocs de glace modèle était aspergée d'eau pour réduire le frottement. La résistance de la glace modèle a été déterminée à l'aide d'une équation de similitude obtenue empiriquement et considérée comme valide dans les cas de compression. Cette équation avait été vérifiée par des essais uniaxiaux de résistance à la compression pilotés par un programme informatique propre à Arctec. La résistance de référence de la glace modèle a été fixée à 53 kPa, partant de l'hypothèse que la plus grande probabilité d'endommagement du gouvernail est liée à la présence de fragments de glace de plusieurs années. Un total de huit blocs de glace avaient été préparés; leur résistance était de 175 kPa (très forte), 86 kPa (moyennement forte), 68 kPa (valeur de référence) et 15 à 22 kPa (relativement faible). Ces blocs étaient montés sur une balance comportant des cellules de charge qui mesuraient les forces horizontales, tant axiales que transversales.

Résultats des essais hors bassin

Le plan de l'expérimentation hors bassin prévoyait de faire varier six facteurs contrôlés, à savoir: vitesse à l'impact, angle de braquage, raideur en torsion de la mèche, masse du bloc de glace, résistance de celui-ci et pression limite du circuit hydraulique de commande. Les quelque 130 essais effectués ont permis de chiffrer les variables dépendantes, soit: contraintes dans le gouvernail (composantes axiale et transversale), déformations de la mèche en torsion, moments de flexion (composantes axiale et transversale), pénétration dans la glace et pression dans le circuit hydraulique. L'influence des facteurs contrôlés sur la réponse chiffrée a été évaluée et reproduite graphiquement. La figure 2 donne à titre d'exemple les couples maximums en fonction de la résistance de la glace et de la vitesse. Bien qu'aucune relation fonctionnelle définitive n'ait pu être tirée de la présente analyse, les constatations générales suivantes ont pu être faites:

FIGURE 2

Réponse de la mèche aux
variations de résistance de la glace

A. Influence de la résistance sur le couple de torsion

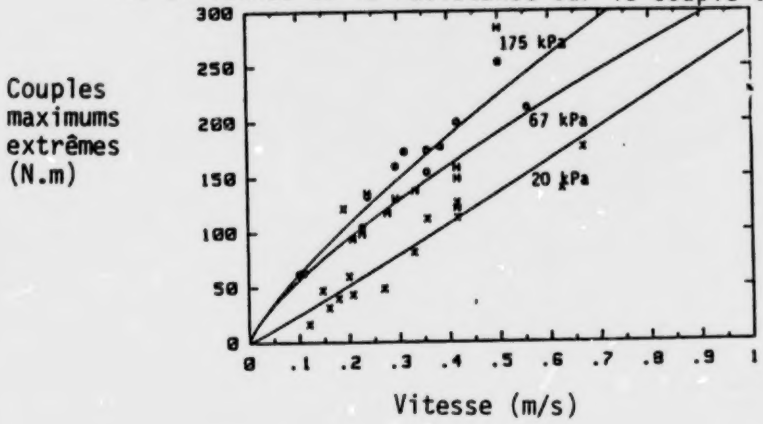

A. Influence de la vitesse sur la charge normale

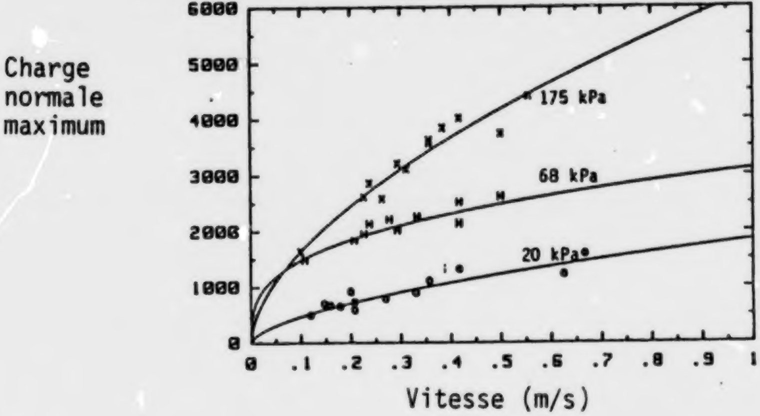

B. Évolution de la charge en fonction de la surface de compression

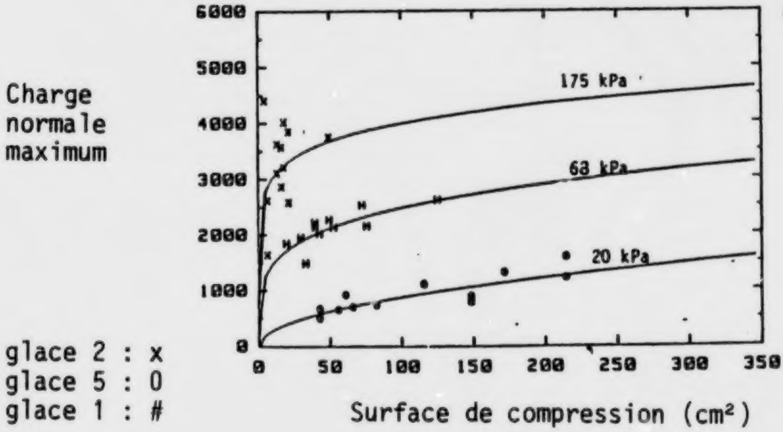

Bloc de glace 2 : x
Bloc de glace 5 : 0
Bloc de glace 1 : #

Mèche : 2
Angle : ± 15°
Masse : 256,4 kg

- Les variables dépendantes qui réagissent le plus fortement à une variation dans la résistance de la glace sont: l'effort maximum sur le gouvernail, l'accélération axiale et la déformation en torsion. La profondeur de pénétration dans la glace décroit exponentiellement à mesure qu'augmente la résistance de la glace. Le temps de réaction en torsion diminue aussi dans toute l'étendue de la plage d'essais.

- Les efforts sur le gouvernail et les accélérations axiales varient avec les vitesses croissantes selon une loi (de) puissance dont l'exposant est inférieur à l'unité. Les déformations en torsion et les profondeurs de pénétration varient à peu près linéairement avec la vitesse. Les déformations en flexion ne montrent pas de variations significatives tandis que les temps de réaction en torsion du gouvernail demeurent inchangés.

- Toute augmentation de l'angle de braquage semble s'accompagner d'un accroissement des efforts sur le gouvernail, des couples et des accélérations, et ce, jusqu'à un angle limite d'environ 60°. Une courbe quasi sïnusoidale a été obtenue dans chaque cas. Aux angles plus élevés, les pénétrations diminuent en profondeur.

- La masse de 256 kg de glace mise en oeuvre dans la plupart des essais correspond à quelque 10 p. 100 du déplacement du navire. Une masse portée graduellement à 700 kg a provoqué un accroissement linéaire des efforts sur le gouvernail, des pénétrations et des couples. Les moments de flexion ne dépendraient de la masse de glace qu'accessoirement. Les accélérations axiales décroissent en raison inverse de l'augmentation de la masse. Sur le montage utilisé, il n'a pas été possible de réduire la masse à moins de 200 kg.

- Les déformations en torsion et en flexion croissent rapidement à mesure que décroît la raideur de la mèche, et ce, dans un rapport non loin d'être inversement proportionnel au carré des valeurs considérées. Le rapport déformations en flexion/déformations en torsion est inférieur à 0,1 à la raideur en flexion de référence. Donc, la flexion ne devient significative qu'à partir de valeurs de raideur très faibles. Ce rapport ne semble pas sensible aux variations dans la résistance de la glace.

- Dans la plupart des essais paramétriques, la mèche était fixée rigidement à la barre. Dans une série d'essais, celle-ci a été reliée à un actionneur hydraulique à vérins. Il a été observé que la pression d'ouverture du circuit hydraulique, réglée à 50 lb/po^2, a provoqué une réduction notable des couples et contraintes maximums, comparativement au système rigide. À mesure qu' augmentent les pressions de réglage, la pression différentielle maximum dans les vérins croît, elle aussi, selon une relation linéaire avec la vitesse à l'impact.

Résultats des essais de remorquage en bassin

Les essais de remorquage en bassin étaient destinés à élucider les paramètres déterminant la fréquence des impacts gouvernail-glaces ainsi que leur domaine d'action. Les essais en bassin ont été conduits sur les modèles réduits de trois navires ayant les formes de proue et de poupe requises: le N.M. ARCTIC, un gros minéralier-vraquier-pétrolier de cote arctique, à une seule hélice et un seul gouvernail; le PIERRE-RADISSON, brise-glace canadien à deux hélices et un gouvernail; et la représentation de la coque du POLAR 8, brise-glace proposé doté de trois hélices et d'un gouvernail.

Trois séries d'essais en autopropulsion ont été effectuées sur chacun des trois modèles, et une série supplémentaire a été faite dans une glace d'une épaisseur différente dans le cas de l'ARCTIC. Quatre couches de glace ont été mises en oeuvre, dont l'épaisseur a été choisie pour correspondre à l'épaisseur maximum dans laquelle les navires représentés peuvent avancer en marche continue. Chaque série d'essais a comporté des marches avant et arrière répétées dans une glace préalablement entaillée pour former des fragments de dimensions précises. Le premier essai consistait à casser la glace selon un motif en chevrons formant un angle de 45° avec l'axe du bassin. La largeur de la glace ainsi découpée correspondait à 1,1 fois la largeur du modèle. Quant à la distance séparant les chevrons, elle correspondait à une longueur caractéristique obtenue par calcul. L'essai suivant consistait à lancer le modèle en marche arrière dans le chenal ouvert lors de l'essai précédent. Ensuite, la surface de la couche glacée a été coupée en fragments de longueur correspondant à la longueur caractéristique pour le modèle considéré. Pour les essais subséquents de chaque série, la taille des fragments a été maintenue afin de respecter une distribution nominalement identique. Mais comme la taille moyenne des fragments diminuait après chaque essai, en raison des chocs répétés avec les modèles et aussi du broyage par les hélices, il a fallu disperser les répétitions d' essais particuliers, de manière à assurer une distribution équivalente particuliers, de la taille moyenne des fragments, d'un groupe d'essais homologues à l'autre. Parmi les nombreux facteurs contrôlés qui ont été étudiés figurent: la forme de la coque, la vitesse avant et arrière, l'angle de braquage, la poussée, le sens de rotation de l'hélice, le tirant d'eau (ballast), l'épaisseur de la glace et la taille des fragments. Les principales variables dépendantes mesurées ont été la fréquence des impacts et l'amplitude du couple agissant sur le gouvernail.

Analyse des résultats

Les résultats de quelque 150 essais dans quatre couches de glace différentes ont été enregistrés, de même que ceux d'essais de traction au point fixe et d'autopropulsion en eau libre. Ces derniers ont été faits à des vitesses de marche avant et arrière correspondant à celles pratiquées lors des essais dans les glaces. Des courbes d'évolution des couples obtenues de chacun des essais individuels dans la glace a été extraite l'information correspondante sur l'amplitude et la fréquence des impacts. Une courbe d'évolution type des couples est illustrée à la figure 3.

Le résultat a été présenté sous la forme d'histogrammes donnant le nombre d'impacts (ou de crêtes) au regard d'une amplitude donnée. Aux fins d'analyse statistique, l'information obtenue a été organisée en cinq catégories générales, de manière à donner des histogrammes où le nombre d'impacts mis en évidence est significatif du point de vue statistique.

Le tableau 1 dénombre les essais faisant partie de ces cinq catégories: vitesse avant maximum, vitesse avant modifiée par la dérive, vitesse avant intermédiaire, vitesse arrière intermédiaire et vitesse arrière basse. Les histogrammes ont été normalisés de manière à donner le nombre moyen d'impacts par kilomètre réel de marche (avant ou arrière), paramètre qui, lors des essais, a varié en fonction de l'épaisseur de la glace et de la vitesse. Un histogramme type est illustré à la figure 4.

Il n'a pas été possible de chiffrer l'influence de certains paramètres tels que la poussée, le tirant d'eau et l'angle de braquage, vu la quantité restreinte de données utiles disponibles. Néanmoins, les constatations suivantes ont pu être faites à partir des histogrammes normalisés obtenus:

- Aucun impact avec la glace n'a été observé avec l'ARCTIC durant les essais en marche avant. Cela peut s'expliquer par la longueur du navire, son grand tirant d'eau et la protection assurée par la tuyère.
- En marche arrière, avec l'ARCTIC, un nombre élevé d'impacts ont été observés ainsi que des valeurs de couple modérées. De nombreux impacts à des valeurs de couple faibles ont également été observés. Cela peut être attribué à un contact continu avec la glace ou à une charge hydrodynamique accrue sur le gouvernail. Il ne semble pas y avoir un accroissement notable dans la fréquence des impacts lorsque la vitesse en marche arrière est augmentée, bien qu'une tendance vers des valeurs moyennes de couple plus élevées ait été observée.

FIGURE 3

Influence de la forme de coque à vitesse avant maximum

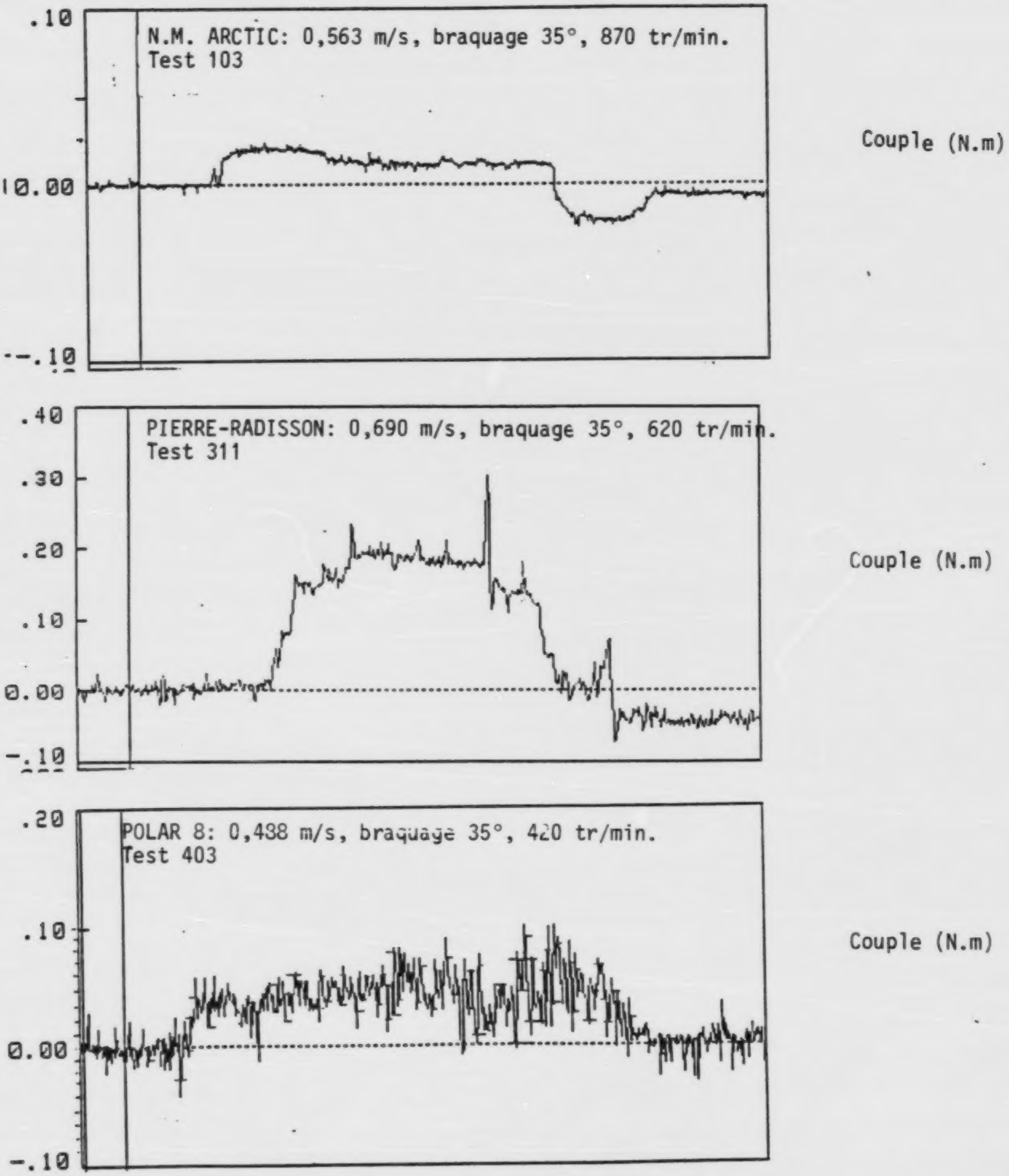

FIGURE 4

Fréquence et amplitude des impacts de glace

N.M. Arctic - Marche arrière à vitesse intermédiare : 0.282 m/s

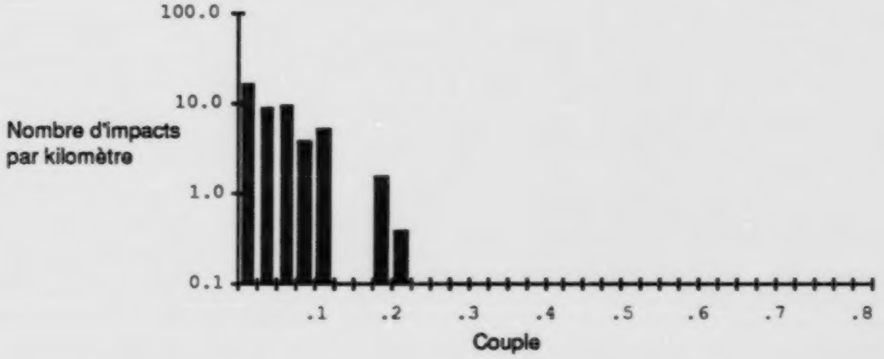

Pierre-Radisson - Marche arrière à vitesse intermédiare : 0.345 m/s

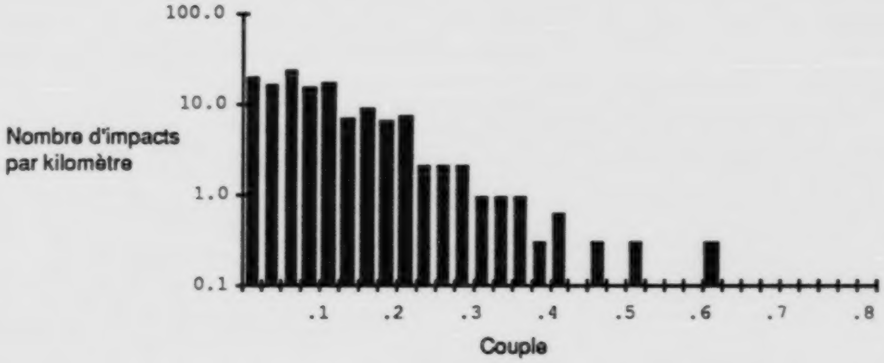

Polar 8 - Marche arrière à vitesse intermédiare : 0.244 m/s

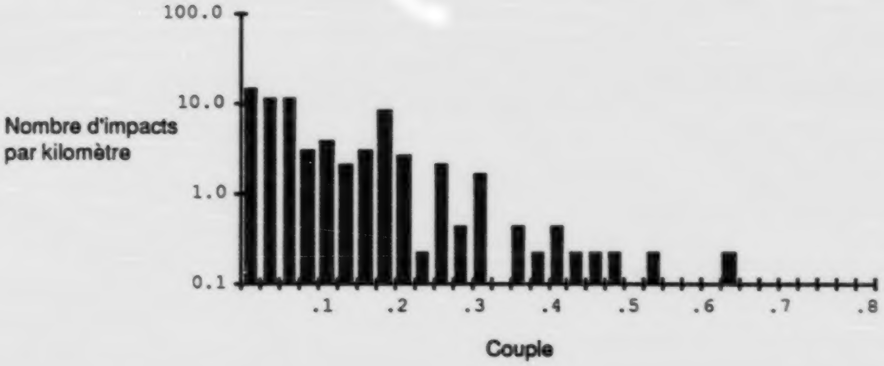

- De tous les modèles, c'est celui du PIERRE-RADISSON qui a montré la fréquence d'impact la plus élevée sur le gouvernail, tant en marche avant qu'en marche arrière. Un accroissement de cette fréquence avec la vitesse avant a également été observé, tant dans le domaine des couples correspondant au choc des glaces que dans celui des surcharges hydrodynamiques. La prise en compte d'un angle de dérive durant les essais à vitesse maximale s'est traduite par un accroissement dans le nombre d'impacts et par un relèvement des valeurs moyennes de couple.

- En marche arrière, le modèle du PIERRE-RADISSON a montré un nombre d'impacts significatifs plus élevé qu'en marche avant, le régime de surcharge hydrodynamique restant à peu près le même. Il ne semble pas que la fréquence des impacts soit fonction de la vitesse, mais un relèvement des valeurs de couple avec la vitesse a été observé.

- Les histogrammes relatifs au POLAR 8 ressemblent à ceux du PIERRE-RADISSON. En marche avant, il y a eu un nombre plus élevé d'événements à faible valeur de couple assimilables à des surcharges hydrodynamiques, mais moins d'impacts avec les glaces. Le nombre de ces événements varie avec la vitesse. En marche arrière, le POLAR 8 a eu encore une fois moins d'impacts avec les glaces, pour des valeurs de couple identiques.

D'autres constatations concernant certains paramètres peuvent être tirées d'un examen des courbes d'évolution dans le temps. Il semble que le couple en régime permanent qui agit sur le gouvernail des trois navires représentés, et à toutes les allures essayées, serait un des principaux paramètres influençant les résultats; il semble également que la composante en régime permanent durant la marche dans les glaces se compare en amplitude à la valeur correspondante en eau libre. De façon générale, il a été observé que, à ce point de vue, le PIERRE-RADISSON vient en tête, suivi du POLAR 8 et de l'ARCTIC, reflétant les caractéristiques hydrodynamiques particulières propres tant à la forme de la poupe qu'à la géométrie du gouvernail des navires représentés. L'interprétation des résultats relatifs à divers paramètres a pu également s'en ressentir.

Les courbes d'évolution dans le temps montrent que l'amplitude des couples augmente très légèrement lorsqu'on réduit le tirant d'eau ou bien lorsque le nombre de tr/min ou l'épaisseur de la glace est augmenté. Quant à l'effet apporté par un changement dans le sens de rotation de l'hélice, il a été masqué par les fluctuations dans le couple en régime permanent.

Conclusions

L'utilité des essais hors bassin, sur un gros modèle réduit du gouvernail, en vue de mettre en évidence l'influence des divers paramètres a été amplement démontrée. D'importantes variations ont été données aux facteurs contrôlés, à savoir: vitesse à l'impact, angle de braquage, raideur en torsion de la mèche, masse du bloc de glace, résistance de celui-ci et, enfin, pression d'ouverture du circuit hydraulique de commande. Des courbes d'évolution dans le temps ont été obtenues en ce qui concerne les efforts sur le gouvernail, les déformations en flexion et en torsion de la mèche et, à partir de ces courbes, une base de données sur les valeurs extrêmes a été élaborée. La recherche a débouché sur des connaissances approfondies concernant le phénomène d'interaction gouvernail-glace et a été le point de départ d'une étude sur les relations fonctionnelles pouvant exister entre les divers paramètres en jeu. Des courbes d'évolution sont présentées et montrent les variations du couple de torsion qui agit sur la mèche du gouvernail et sur d'autres variables, en fonction des paramètres pris en compte.

La mise en oeuvre d'un actionneur hydraulique en modèle réduit a permis d'évaluer dans une certaine mesure l'influence de la pression hydraulique d'ouverture sur le gouvernail: déplacements et efforts exercés. Cet actionneur, qui peut être considéré comme représentant assez fidèlement le mécanisme de déblocage hydraulique, a mis en évidence l'influence de la variation de "raaideur" de l'appareil à gouverner; il a particulièrement démontré que les essais faits à mèche rigidement fixée à la barre représentaient un mode de charge classique et que l'influence des variations de réglage de la pression hydraulique était liée à la vitesse. À noter cependant l'absence d'asservissement par rétroaction dans le modèle réduit. Des études complémentaires visant la mise au point d'un modèle réduit plus complet d'un appareil à gouverner hydraulique seront nécessaires afin d'approfondir l'influence du diamètre de la vanne de commande, la réponse du gouvernail et les débits, lorsque la pression d'ouverture du circuit hydraulique est atteinte.

Les données tirées des expérimentations se rapportent généralement à des conditions extrêmes, étant donné la mise en oeuvre de blocs de glace massifs, les contacts pleine hauteur entre le gouvernail et la glace, les angles de braquage importants et la forte résistance de la glace modèle. Excepté la hauteur du contact, chacun des facteurs contrôlés a été soumis à d'importantes variations. À partir de là, il est donc possible de procéder à des extrapolations reflétant des conditions moins rigoureuses. Mais il est difficile de calculer les déformations en torsion lorsque la masse de la glace est inférieure à 5 p. 100 du déplacement du PIERRE-RADISSON, vu l'accroissement rapide des valeurs de couple dans ces conditions. Les résultats de ces expérimentations serviront à établir les relations pouvant exister entre les facteurs contrôlés et, de la sorte, permettront de valider le modèle mathématique élaboré pour simuler la réponse d'un gouvernail à la charge des glaces et de déboucher sur des critères de calcul plus logiques.

Le principal résultat de cette recherche aura été la mise en évidence des statistiques concernant la fréquence des impacts lorsque le navire recule dans le chenal qu'il vient d'ouvrir. Étant donné qu'il est impossible d'obtenir une similitude parfaite en résistance à la compression dans le cas de la couche de glace dopée à l'urée et pré-entaillée et, au surplus, de maintenir une même résistance en compression durant toute une journée, il fallait s'attendre à une distorsion dans les valeurs de couples de torsion du gouvernail. Néanmoins, un ordre de grandeur des impacts enregistrés a pu être dégagé de ces valeurs.

La comparaison des trois modèles de navire a mis en évidence l'apport de certaines caractéristiques géométriques de leur coque à la réduction du nombre et de l'amplitude des impacts gouvernail-glaces. Dans le cas de l'ARCTIC en particulier, la conjonction d'une tuyère protégeant l'hélice, d'une grande longueur de coque et d'un grand tirant d'eau, s'est traduite par une absence totale de chocs en marche avant. À cause du nombre restreint de répétitions des essais, il n'a pas été possible de déterminer statistiquement l'utilité des données tirées des essais durant lesquels le sens de rotation des hélices a été inversé. Il n'a pas non plus été possible de distinguer l'effet des faibles variations dans l'angle de braquage ou la poussée durant les manoeuvres en marche arrière. Ces essais ont été groupés pour autoriser une analyse statistique comparée des navires en fonction de leurs principales caractéristiques.

Recommandations

L'analyse des résultats des essais hors bassin a permis d'approfondir l'influence des principaux facteurs contrôlés sur le comportement en torsion du gouvernail. Cependant, une analyse plus poussée est nécessaire pour réécrire les résultats sous forme adimensionnelle de manière à déboucher sur des équations paramétriques spécifiques. Le traitement préliminaire des valeurs extrêmes par une analyse de régression de la variable puissance promet de déboucher sur d'intéressants résultats numériques. Les relations ainsi mises en évidence seront le fondement sur lequel asseoir un modèle de simulation des forces d'interaction dûment validé qui devra également tenir compte du phénomène de la masse entraînée. En outre, une corrélation devra être faite entre, d'une part, le résultat des essais sur modèle réduit du LOUIS-ST-LAURENT et, d'autre part, les données d'essais en vraie grandeur du même brise-glace.

Diverses limitations des essais sur modèles réduits hors bassin ont fait que certaines questions sont restées sans réponse à l'issue du présent programme d'essais. La plus importante lacune a été la limitation de la masse de glace modèle pouvant être mise en oeuvre. Les valeurs minimales de masse prises en compte durant les essais correspondent à quelque 7 p. 100 du déplacement du LOUIS-ST-LAURENT. Donc, le seul scénario envisagé dans les essais a été de considérer le déplacement du brise-glace comme étant infini et la masse de glace comme quelconque, mais finie. Il faudrait faire d'autres essais pour approfondir les deux scénarios suivants:

(1) Celui de la poupe heurtant le bord du chenal ouvert par le brise-glace, où la situation est inversée: masse de glace infinie et déplacement fini. Les essais sur modèle réduit s'effectueraient au moyen du modèle existant que l'on ferait reculer dans un bloc de glace synthétique fixe. Là encore il faudrait utiliser des mèches dont la résistance en torsion aurait été calculée par voie de similitude. Cette méthode s'impose étant donné que le montage servant aux expérimentations ne peut supporter le poids du modèle réduit au 1/17. Des essais sur d'autres modèles pourraient être faits dans cette optique afin d'établir une corrélation entre les équations paramétriques résultant des essais hors bassin et les résultats des essais d'autopropulsion en bassin.

(2) Masse de glace inférieure à 7 p. 100 du déplacement du LOUIS-ST-LAURENT. Dans ce cas, l'interprétation retenue quant au choc de deux corps reste inchangée. Le montage actuel pourrait servir à la recherche dans la plage inférieure des masses de glace. Mais il faudrait alléger le boitier métallique qui représente la plus grande part de la masse mise en oeuvre.

Parmi les autres secteurs, auxquels la base de données résultant des essais hors bassin mériterait d'être étendue, citons celui des variations dans les deux paramètres suivants: géométrie du bord de gouvernail et hauteur de contact avec la glace. Cette recherche permettrait d'approfondir l'influence de la surface de contact sur les efforts s'exerçant sur le gouvernail.

Il y a aussi le perfectionnement du modèle réduit par l'adjonction d'un appareil à gouverner hydraulique plus complet; mais cela suppose des recherches sur la modélisation des débits dans les vérins et à travers la vanne de commande. En outre, il y aurait lieu de définir et de réaliser un dispositif d'asservissement par rétroaction, également en modèle réduit.

La grande faiblesse des essais de remorquage en bassin, responsable de la qualité réduite des résultats, a été le petit nombre de répétitions faites de chaque essai. À partir des résultats obtenus, il n'a pas été possible d'extraire les deux composantes que sont les impacts dus aux glaces et aux charges hydrodynamiques normales. Les résultats de ces essais devraient être examinés à la lumière des données résultant des essais en eau libre et des essais de traction au point fixe faits dans les mêmes conditions "opérationnelles" que les essais dans les glaces. Le nombre restreint de données a nécessité un groupage moins fin que prévu des paramètres d'essais, afin de pouvoir dégager des tendances statistiquement plus significatives. La solution réside dans une recherche ultérieure, sur au moins un des trois modèles, par des essais plus nombreux visant à confirmer les résultats statistiques déjà obtenus et à permettre une distinction plus fine entre le degré d'influence des différents facteurs contrôlés. De plus, suite aux expérimentations hors bassin, il est recommandé d'utiliser la glace modèle "MODICE" dans un programme ultérieur d'essais en bassin, étant donné les deux avantages offerts par ce type de glace: (1) bonne aptitude à la modélisation en résistance de compression de la glace réelle et stabilité de cette résistance dans le temps, et (2) densité plus proche de celle de la vraie glace. Le premier facteur apporte une plus grande précision dans les valeurs de couple, le deuxième une simulation plus réaliste de la flottabilité de la glace et, par conséquent, une modélisation plus fidèle de l'écoulement des fragments de glace par rapport au gouvernail.

Les essais réalisés dans le cadre de la présente recherche, tant en bassin que hors bassin, ont fourni l'information de base nécessaire pour confirmer ou vérifier un modèle mathématique permettant de simuler la réponse du gouvernail d'un navire à la charge des glaces. Il serait intéressant de poursuivre ces travaux par l'intégration des équations paramétriques découlant des essais hors bassin aux statistiques tirées des essais en bassin et d'en comparer le résultat final aux données disponibles tirées des essais en vraie grandeur. Cela autoriserait la mise au point d'un modèle semi-empirique simulant l'interaction gouvernail-glaces qui aurait certainement des répercussions sur la conception des gouvernails et appareils à gouverner ainsi que sur la réglementation en la matière.

TABLE OF CONTENTS

VOLUME I

1. INTRODUCTION..1
2. BACKGROUND AND STATE-OF-THE ART.................................3
3. DRY IMPACT TESTING OF RUDDER MODEL..............................5
   3.1 Physical Modelling of Rudder/Ice Interaction................5
      3.1.1 Physical Model System..................................5
      3.1.2 Scaling Criteria and Similitude Principle..............6
      3.1.3 Ice Model...14
   3.2 Parametric Test Program....................................19
      3.2.1 Matrix of Test Parameters.............................19
      3.2.2 Experimental Set-up...................................21
      3.2.3 Instrumentation and Data Collection...................25
      3.2.4 Test Data...27
   3.3 Discussion of Dry Impact Test Results......................41
      3.3.1 Influence of Test Parameters..........................41
   3.4 Dry Impact Tests Astern Results, Remarks and Recommendations......................65
      3.4.1 Dry Impact Astern Tests Results.......................65
      3.4.2 Remarks on Dry Impact Astern Tests....................67
      3.4.3 Recommendations Regarding Dry Impact Astern Tests...68
4. ICE BASIN TOWED MODEL TESTS....................................72
   4.1 Background...72
   4.2 Test Objectives..72
   4.3 Scope of Test Program......................................73
   4.4 Models and Modelling Criteria..............................76
      4.4.1 Ship Models...76
      4.4.2 Modelling Criteria....................................76
   4.5 Ice Basin Test set-up......................................78
      4.5.1 Rudder Torque...78
      4.5.2 Propeller Shaft RPM...................................80
      4.5.3 Model Speed and Drag..................................80
      4.5.4 Drift Angle...80
      4.5.5 Data Acquisition......................................80
   4.6 Test Procedure...82
      4.6.1 Bollard Testing.......................................82
      4.6.2 Open Water Testing....................................82
      4.6.3 Level Ice Testing.....................................82
      4.6.4 Broken Channel Testing................................84
      4.6.5 Photographic Documentation of the Towed Tests.......87
   4.7 Data Reduction and Results.................................91
      4.7.1 Histograms of Peak Torque Magnitude and Frequency of Impact...............................95
      4.7.2 Influence of Parameters..............................105

4.8 Remarks and Recommendations on Towed Tests................113
4.8.1 Remarks...113
4.8.2 Recommendations.....................................114

5. GENERAL REMARKS..115

REFERENCES..116

APPENDIX A - MATHEMATICAL MODELS OF RUDDER LOAD AND STEERING GEAR RESPONSE............................117

APPENDIX B - BIBLIOGRAPHY...................................129

APPENDIX C - DETAILED STATEMENT OF WORK.....................137

VOLUME II - TYPICAL DRY IMPACT RUDDER TORQUE AND ICE BASIN TOWED TEST DATA

APPENDIX D - TYPICAL DRY IMPACT TESTS

APPENDIX E - ICE BASIN TOWED TEST DATA

LIST OF FIGURES

1.1 ARCTIC SHIP RUDDER RESEARCH AND DEVELOPMENT PROGRAM..........2
3.1 DRY IMPACT EXPERIMENTAL SET-UP.................................7
3.2 PHYSICAL MODEL OF RUDDER ASSEMBLY.............................9
3.3 STRAIN RATE DEPENDENCE OF MODICE.............................15
3.4 TEMPERATURE DEPENDENCE OF MODICE.............................16
3.5 GRAECO-LATIN SQUARE ARRANGEMENT OF TEST VARIABLES............20
3.6 TEST ASSEMBLY..22
3.7 HYDRAULIC SYSTEM...23
3.8 TYPICAL SET OF TIME HISTORIES................................28
3.9 TYPICAL TORSIONAL RESPONSE...................................29
3.10 TORSIONAL RESPONSE ILLUSTRATING PEAK REVERSALS..............30
3.11 TYPICAL TORQUES AND BENDING MOMENTS IN TARGET STRENGTH ICE..31
3.12 RUDDER STOCK TESTS ICE STRENGTH VARIATION...................42
3.13 MAXIMUM RUDDER LOAD INFLUENCE OF VELOCITY & CRUSHING AREA...43
3.14 RUDDER STOCK TESTS ICE STRENGTH VARIATION...................45
3.15 RUDDER STOCK TESTS ICE STRENGTH VARIATION...................46
3.16 RUDDER STOCK TESTS ICE STRENGTH VARIATION...................47
3.17 RUDDER STOCK TESTS ANGLE VARIATION..........................48
3.18 RUDDER STOCK TESTS ANGLE VARIATION..........................49
3.19 RUDDER STOCK TESTS ANGLE VARIATION..........................50
3.20 RUDDER STOCK TESTS RATIO OF BENDING STRAIN TO TORQUE STRAIN.51
3.21 TORQUE RISE TIME INFLUENCE OF VELOCITY & MAX. TORQUE........53
3.22 RUDDER STOCK TESTS MASS VARIATION...........................54
3.23 RUDDER STOCK TESTS MASS VARIATION...........................56
3.24 RUDDER STOCK TESTS MASS VARIATION...........................57
3.25 RUDDER STOCK TESTS MASS VARIATION...........................58
3.26 RUDDER STOCK TESTS RELIEF VARIATION.........................59
3.27 RUDDER STOCK TESTS RELIEF VARIATION.........................60
3.28 RUDDER STOCK TESTS RELIEF VARIATION.........................61
3.29 RUDDER STOCK TESTS VELOCITY VARIATION.......................63
3.30 RUDDER STOCK TESTS VELOCITY VARIATION.......................64
4.1 TOWED TESTS EXPERIMENTAL SET-UP..............................79
4.2 SCHEMATIC OF TOWING ARRANGEMENT..............................81
4.3 PRE-SAWN PLAN..83
4.4 ICEBREAKING TEST IN PRE-CUT ICE..............................86
4.5 PRE-CUT BROKEN CHANNEL DISTRIBUTION..........................88
4.6 TYPICAL TEST RUNS..90
4.7 RADISSON MODEL ICEBREAKING TEST..............................92
4.8 INFLUENCE OF AHEAD VELOCITY ON OPEN WATER TORQUE............93
4.9 INFLUENCE OF ASTERN VELOCITY ON OPEN WATER TORQUE...........94
4.10 FREQUENCY AND MAGNITUDE OF RUDDER ICE IMPACTS...............99
4.11 FREQUENCY AND MAGNITUDE OF RUDDER ICE IMPACTS..............100
4.12 FREQUENCY AND MAGNITUDE OF RUDDER ICE IMPACTS..............101
4.13 FREQUENCY AND MAGNITUDE OF RUDDER ICE IMPACTS..............102
4.14 FREQUENCY AND MAGNITUDE OF RUDDER ICE IMPACTS..............103
4.15 INFLUENCE OF SHIP FORM IN HULL FORWARD SPEED MANOEUVRES....106
4.16 INFLUENCE OF SHIP FORM IN MID SPEED BACKING MANOEUVRES.....107

LIST OF FIGURES (CONTINUED)

4.17 INFLUENCE OF DRAFT CONDITION DURING BACKING MANOEUVRES.....109
4.18 INFLUENCE OF PROPELLER SPEED DURING BACKING MANOEUVRES.....110
4.19 INFLUENCE OF PROPELLER ROTATIONAL DIRECTION DURING FORWARD MANOEUVRES.....111
4.20 INFLUENCE OF ICE THICKNESS DURING BACKING.....112
A.1 SCHEMATIC OF A TYPICAL HYDRAULIC STEERING GEAR.....125
A.2 PRINCIPLE OF OPERATION OF A HYDRAULIC STEERING GEAR.....126
A.3 TYPES OF TILLER ARRANGEMENTS.....126

LIST OF TABLES

3.1 PERTINENT VARIABLES IN DIMENSIONAL ANALYSIS.....10
3.2 PRINCIPAL DIMENSIONLESS PARAMETERS.....11
3.3 DESIGN EQUATIONS BASED ON DYNAMIC (FROUDE) SCALING.....12
3.4 PRINCIPAL PROTOTYPE AND MODEL SCALE DIMENSIONS.....13
3.5 DENSITY, FRICTION, UNIAXIAL CRUSHING STRENGTH PROPERTIES.....18
3.6 TEST MATRIX AND PEAK DATA SUMMARY.....33
4.1 INDEPENDENT TEST VARIABLES.....74
4.2 TYPICAL TEST MATRIX.....75
4.3 TOWED TEST MODEL PARTICULARS.....77
4.4 ICE SHEET CHARACTERISTICS.....85
4.5 ICE BASIN TOWED TESTS.....96
4.6 ICE BASIN TOWED MODEL DATA.....97
A.1 DESIGN EQUATIONS BASED ON DYNAMIC (FROUDE) SCALING.....122

NOMENCLATURE

A	Area of contact
b	Width of contact area
d	Diameter
g	Acceleration due to gravity
G	Load, Force, Shear Modulus
i	Moment of Inertia
K	Torsional Stiffness
l	Characteristic length
L	Any length variable
M_I, M_R, M_S	Mass (Ice, Rudder, Ship)
p	Hydraulic pressure
Q	Torque
S	Ratio of Full Scale to Model Scale
t	Time
T	Temperature
v	Velocity
x,y,z	Displacement Coordinate
δ	Rudder Angle
μ	Friction Coefficient
σ_c	Crushing Strength
ρ	Mass Density
λ	Geometric Scale Factor
θ	Crushed depth
ε	Strain

1. INTRODUCTION

In March 1981, as part of an unsolicited proposal [1] to the Transportation Development Centre, Arctec Canada summarized the following as the state-of-the-art related to research concerning the interaction of ice with rudders and steering systems:

- Incidents of damage continue to be reported.
- Analysis of damage reports has been made and critical components and operating modes have been identified.
- There will be a significant increase in traffic in the next decade.
- No systematic analysis of the efficiencies of various rudder configurations has been carried out.
- Steering system hydraulics do not act as shock absorbers for typical ice impacts.
- Insufficient data is available to provide a high confidence level in any restructuring of present regulations.

The proposal highlighted the need for developing a large full scale data base of rudder loads and steering gear responses. Five years later, it can be said with confidence that the database required for the development of design standards for rudders and steering gears has been at least partially achieved.

This database development was a continuation of some earlier work carried out by Arctec Canada Limited in which a preliminary study of the ice/rudder problem was performed using limited full scale data and an analytical approach [2]. As a result of that study, an Arctic ship rudder research and development program was outlined (Figure 1.1) which incorporated re-analysis of existing full scale data, additional full scale trials of both a statistical long term nature and specific dedicated testing, and scale experiments of rudder/ice interaction using model ice.

This report addresses the task of conducting scale model experiments with the following objectives:

(a) To determine the magnitude and characteristics of the loads imposed on steering systems due to rudder/ice interactions, by carrying out controlled impact tests using synthetic ice on a model rudder and steering gear system.

(b) To carry out towed tests in saline ice using large scale model sterns to determine the influence of draft, rudder and ice horn designs and propeller rotation on the frequency of ice impacts in various ice environments and speeds.

FIGURE 1.1

ARCTIC SHIP RUDDER RESEARCH and DEVELOPMENT PROGRAM

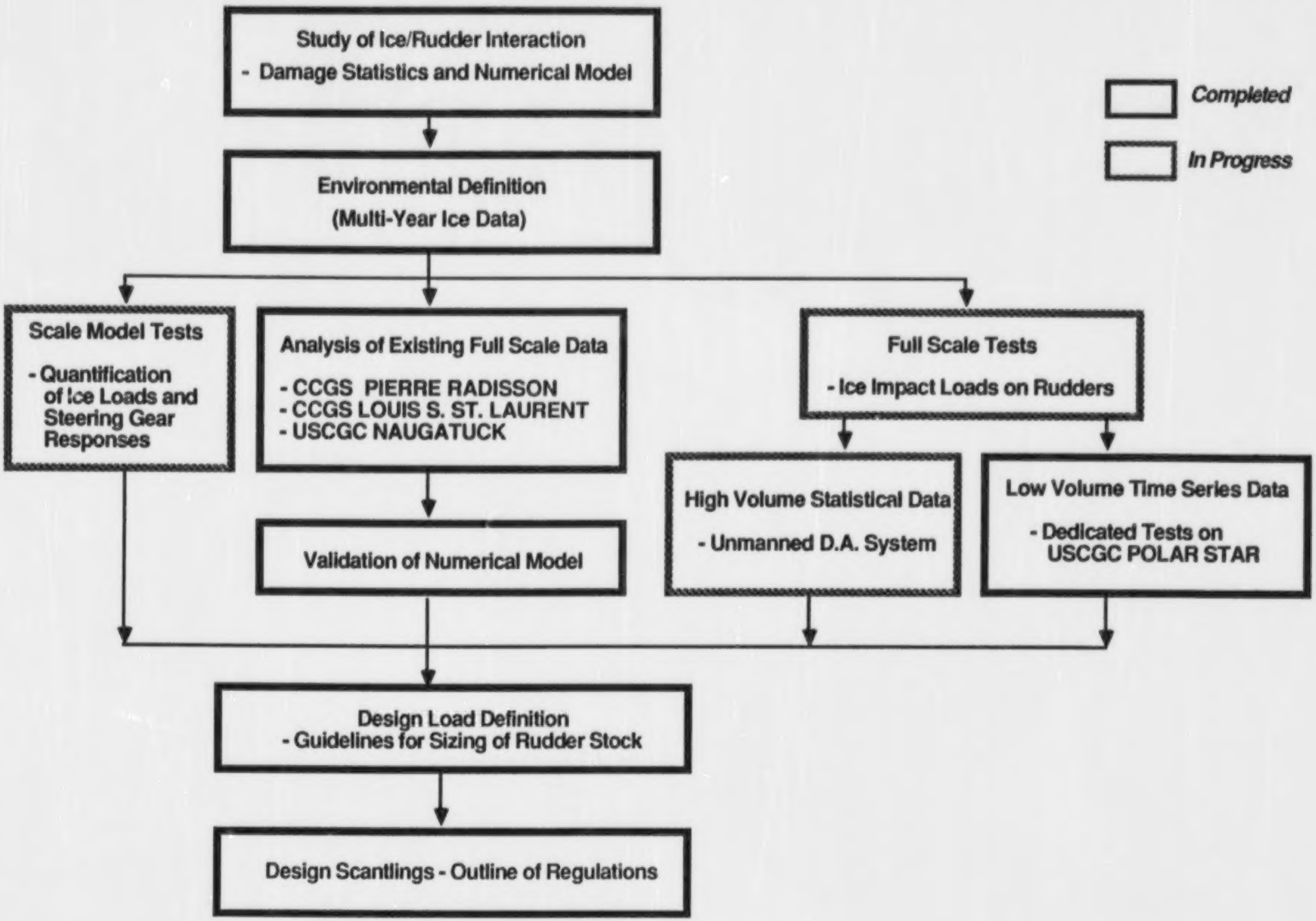
Study of Ice/Rudder Interaction
- Damage Statistics and Numerical Model
Completed
In Progress
Environmental Definition
(Multi-Year Ice Data)
Scale Model Tests
- Quantification of Ice Loads and Steering Gear Responses
Analysis of Existing Full Scale Data
- CCGS PIERRE RADISSON
- CCGS LOUIS S. ST. LAURENT
- USCGC NAUGATUCK
Full Scale Tests
- Ice Impact Loads on Rudders
High Volume Statistical Data
- Unmanned D.A. System
Low Volume Time Series Data
- Dedicated Tests on USCGC POLAR STAR
Validation of Numerical Model
Design Load Definition
- Guidelines for Sizing of Rudder Stock
Design Scantlings - Outline of Regulations

2. BACKGROUND AND STATE-OF-THE-ART

By carrying out experiments at small scale, a considerable number of data points can be acquired relatively easily and cheaply when compared to the alternative of full scale testing. In addition, conducting experiments in a laboratory allows the selection and control of variables such as ice thickness and strength, stock length, etc., which is not usually practical at full scale. Such model experiments must however, be designed with skill, as the dynamics of the steering system may not be modelled easily at small scale. Whereas model work to investigate hydrodynamic performance is acknowledged to be valid, larger scale models will be necessary to examine loading effects and reproduce system responses.

Two main types of materials are at present used to represent sea ice at model scale. Both saline ice (frozen salt water) and synthetic ice ('wax' type material) are used and both have advantages and disadvantages. For tests involving crushing or combined crushing and bending type of interactions, the synthetic ice is the best solution.

One of the most important questions to be answered in rudder design for ice going ships is "What design criteria should be applied to twin or multiple rudder ships?". It has generally been accepted that a rudder operating in the propeller slipstream provides a much more versatile manoeuvring device than one which is not. The magnitude of this improvement must be weighed against potential difficulties when operating in ice. Tests could be run both to measure the effectiveness of the rudder configuration and to determine the vulnerability to ice damage; "vulnerability to ice damage" being both a function of frequency of encounter of the rudder with ice pieces and magnitude of the forces developed when such an encounter occurs. At present, insufficient data exists concerning the movement of ice pieces along and below the hull of an icebreaker to analytically predict the size and the number of rudder/ice impacts with great certainty.

A serious case may well be when the ship is in a turn and the stern tends to sweep the outer edge of the ice sheet, breaking off pieces at the quarter. These ice pieces may go under the hull and strike the rudder. Further, the most serious case, where very high forces can occur, is in the backing condition. A single rudder stern may effectively protect the single centerline rudder with an ice horn. Placing twin rudders on such a stern may not provide such protection. In such a situation, it may be desirable to design a stern specifically for twin rudders. Such a stern might provide as much protection when backing as the single rudder stern does.

In the work reported herein, the approach adopted to provide answers to the questions raised is restricted to vessels with single rudder installations. Many model ships, some fitted with operable steering and rudder systems have been tested in Arctec Canada's towing tank at around 1:40 or 1:50 scale. At these scales it is most difficult to instrument rudder and steering system components and to reproduce the stiffness of typical steering systems. For this reason the present model test program was designed to include two distinctly separate series of tests. They are:

- Dry impact tests using synthetic ice involving controlled relative velocity, impact geometry and ice strength.

- Towed model tests, carried out ahead and astern, using scaled vessel sterns (outfitted with appendages) and broken ice of specified thickness and representative floe size in the refrigerated basin.

As part of the planning task under this project, a literature survey was carried out to identify and evaluate any similar work involving experimental determination of loads on steering system components. No new published works were discovered as contributing to the existing knowledge. However, a bibliography of the state-of-the-art was prepared and is attached as Appendix B. Also presented in Appendix B are summaries of some of the previous projects completed by Arctec in the area of rudders and steering gears.

3. DRY IMPACT TESTING OF RUDDER MODEL

3.1 Physical Modelling of Rudder/Ice Interaction

3.1.1 Physical Model System

An estimation of the ice loads on a ship rudder and the torque acting on the rudder stock may be based on a physical model of the phenomena. The first step in developing an effective physical model is to carefully state the problem at hand. In this case, impacts between a typical rudder and ice pieces during slow astern manoeuvres were identified as being of interest. The torsional response of the rudder stock was investigated since that component of the steering system assembly is most susceptible to damage during ice impacts. The modelling system, which was defined, consisted of a scaled model of the ship rudder arrangement (with its attached rudder, stock and tiller), hydraulic controls, simulated ice masses, and water.

The complexity of the interaction process was reduced by isolating the salient features of the impact process which affect the torsional response of the rudder stock. The ice fragments are generally expected to have masses which are a small fraction of that of the ship; which by comparison may be considered an infinitely massive body. This assumption reduces the two-body problem to a simpler one in which only the relative momentum of the ice mass with respect to the ship and rudder is important. Ships' steering systems are complex structural assemblies which respond dynamically to external excitation. The main ship structure is assumed rigid, and therefore is not addressed in this study. The response of the steering gear hydraulics at the tiller can be modelled by assuming the hydraulic rams to be perfectly rigid in axial loading. This is reasonable since the hydraulic fluid is effectively incompressible and therefore a fixed tiller may be considered. The torsional stiffness of the stock is the principal characteristic which has been modelled. Secondary contributions to rudder stock torsional response from rudder and tiller structural dynamics are considered of lesser importance for defining torsional models and hence were not taken into account.

The resulting physical model provides a quasi-dynamic representation of the impact phenomenon. Certain limitations on the types of data measured are introduced as a result of the decision to suppress modal effects associated with the rudder structure and the tiller. Their inclusion would have enabled the rudder model to respond in a fully dynamic manner. However, the additional complexity is not warranted since neither the distribution of torque along the stock, nor the stress distribution in the rudder are sought from this study.

Hydrodynamic forces acting on the stern appendages and on ice pieces are an important factor in properly scaling the impact process. However a major simplification is achieved by treating the hydrodynamic influences separately from the ice impact. This is a reasonable procedure since the crushing forces associated with rudder indentation into the ice and the inertial reaction of the ice mass are known to predominate. A stream of water was poured over the ice surface to improve the ship-ice friction characteristics. In this "dry mode" of testing the measured loads and responses are those associated entirely with the ice interaction.

Figure 3.1 shows a schematic representation of the physical modelling system. The ship hull is represented by a rigid I-beam framework, fixed in the test basin. This reflects the assumption that the ship mass is much larger than the ice mass. Synthetic model ice blocks are supported on this frame. The hydraulics control unit is mounted on top of the carriage.

The rudder assembly is attached to a moving frame which is shown suspended under the carriage and mounted on low friction rails. By a simple inversion of the logic in the two-body problem, the total mass of the moving frame represents the mass of the ice fragments with which the rudder interacts. The model ice blocks which are mounted on the I-beam framework do not give the ice fragment masses, but rather only provide the ice-rudder interface.

A force balance connects the ice block support frame to the rigid base below, allowing measurement of horizontal forces in the axial direction as well as the lateral directions.

3.1.2 **Scaling Criteria and Similitude Principle**

The conceptual arrangement of the physical model and experimental test loop was constrained by several practical considerations:

(1) Dimensions:
- Clearance between carriage and waterline.
- Size of synthetic model ice blocks.
- Length of sub carriage rails.

(2) Weight:
- Limitations on load which can be safely supported under carriage.

(3) Materials:
- Torsional stiffness properties for fabrication of components.

FIGURE 3.1

DRY IMPACT EXPERIMENTAL SET-UP

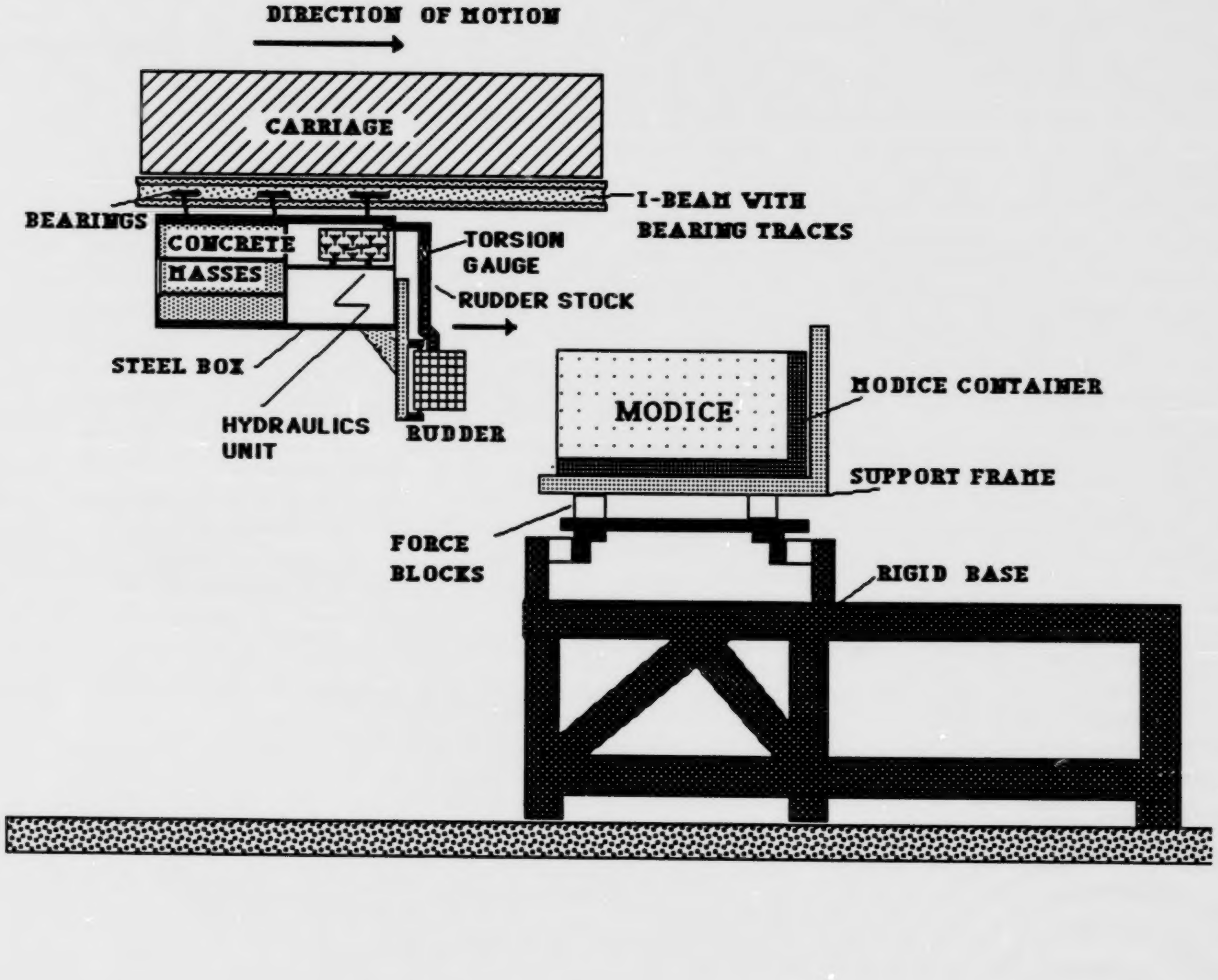
DIRECTION OF MOTION
CARRIAGE
I-BEAM WITH BEARING TRACKS
BEARINGS
CONCRETE
MASSES
TORSION GAUGE
RUDDER STOCK
STEEL BOX
HYDRAULICS UNIT
RUDDER
MODICE
MODICE CONTAINER
SUPPORT FRAME
FORCE BLOCKS
RIGID BASE

The rudder assembly of the LOUIS S. ST. LAURENT was selected as a representative configuration and it's dimensions were used as a basis for the modelling. Size restrictions resulted in a geometric scaling of the model of 1:17. At this scale, the weight supported by the carriage, was within acceptable limits. This corresponded to ice-piece masses between 5% and 15% of scaled ship (mass) displacement. Aluminum and steel materials were used judiciously to achieve reasonable dimensions and desired torsional properties. Figure 3.2 shows the physical model of the rudder assembly.

Scaling of the rudder arrangement dimensions and the derivation of a full scale prediction algorithm was based on similitude arguments. The pertinent variables of the interaction process are shown in Table 3.1. Only those variables are listed which influence torsional response. The techniques of dimensional analysis were applied and eleven dimensionless groups were defined as shown in Table 3.2. The value of each of these groups is preserved between the full scale prototype and model scale. Froude scaling of velocity was employed since these are dynamic interactions.

Given the selection of geometric scaling of length as 1:17, the resulting design equations are shown in Table 3.3. The prediction equation for full scale torque is valid only when these design conditions are satisfied.

Model scale dimensions are given in Table 3.4 as derived from the design equations. Overall physical shape was geometrically proportionate to the LOUIS S. ST. LAURENT rudder and stock; except for the stock diameter which was scaled on stiffness criteria. The prototype stock was of forged steel and the rudder was of steel plate and grillage. The model scale stock and the rudder were of machined aluminum. The mass distributions of rudder and stock are not precisely modelled. This was considered of minimum importance because the polar moment of the stock was small and the rudder mass acting torsionally was approximated. Particular details of prototype rudder and stock assembly were incorporated only as necessary to retain an accurate physical model. For example, spindle and pintles were modified and fabricated out of steel to ensure rigidity of attachments. The tiller, steady bearing, carrier bearing, and other fixtures are also simplified.

FIGURE 3.2

PHYSICAL MODEL OF RUDDER ASSEMBLY

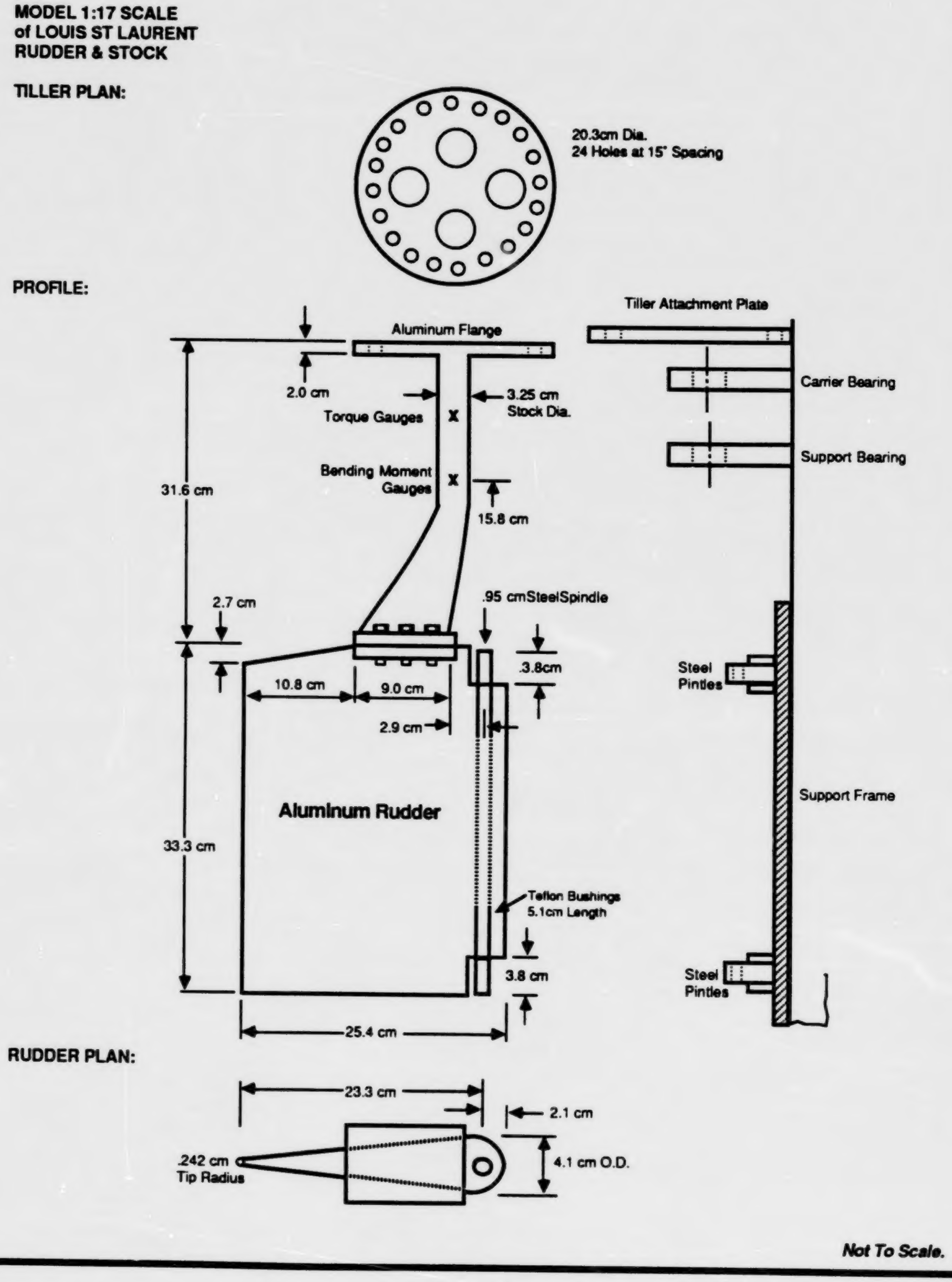
MODEL 1:17 SCALE
of LOUIS ST LAURENT
RUDDER & STOCK
TILLER PLAN:
20.3cm Dia.
24 Holes at 15° Spacing
PROFILE:
Aluminum Flange
Tiller Attachment Plate
2.0 cm
3.25 cm
Stock Dia.
Torque Gauges
Carrier Bearing
Support Bearing
Bending Moment
Gauges
31.6 cm
15.8 cm
.95 cmSteelSpindle
2.7 cm
.3.8cm
Steel
Pintles
10.8 cm
9.0 cm
2.9 cm
Aluminum Rudder
Support Frame
33.3 cm
Teflon Bushings
5.1cm Length
3.8 cm
Steel
Pintles
25.4 cm
RUDDER PLAN:
23.3 cm
2.1 cm
.242 cm
Tip Radius
4.1 cm O.D.
Not To Scale.

TABLE 3.1

PERTINENT VARIABLES IN DIMENSIONAL ANALYSIS

1.	ANY LENGTH VARIABLE	L
2.	CHARACTERISTIC LENGTH	l
3.	TIME	t
4.	MASS DENSITY	ρ
5.	MASS (ICE, RUDDER, SHIP)	M_I, M_R, M_S
6.	ACCELERATION DUE TO GRAVITY	g
7.	VELOCITY	v
8.	RUDDER ANGLE	δ
9.	UNIAXIAL CRUSHING STRENGTH	σ_c
10.	POLAR MOMENT OF INERTIA	J
11.	SHEAR MODULUS	G
12.	TORSIONAL STIFFNESS	K
13.	FRICTION COEFFICIENT	μ
14.	TORQUE, LOAD	Q, F

TABLE 3.2

PRINCIPAL DIMENSIONLESS PARAMETERS

1.	RUDDER ANGLE	δ
2.	GEOMETRIC	l/L
3.	DYNAMIC OR FROUDE	$\frac{gt^2}{l} = \frac{gl}{v^2}$
4.	TORQUE	$\frac{Q}{M_I gl}$
5.	STIFFNESS	$\frac{KL}{G_R J}$
6.	POLAR MOMENT OF INERTIA	J/l^4
7.	FRICTION COEFFICIENT	μ
8.	MASS DENSITY	$\rho l^3/M_I$
9.	VELOCITY (OR TIME)	vt/l
10.	SHEAR MODULUS	$\frac{Gt^2 l}{M_R}$
11.	CRUSHING STRENGTH	σ_c/l

TABLE 3.3

DESIGN EQUATIONS BASED ON DYNAMIC (FROUDE) SCALING

1.	$S_l = 17$	GEOMETRIC LENGTH SCALE
2.	$S_g = 1$	GRAVITY (IDENTICAL) SCALE
3.	$S_\rho = 1$ steel,3 aluminum	DENSITY SCALE
4.	$S\delta = 1$	RUDDER ANGLE SCALE
5.	$S_m = S_g S_l^3$	MASS SCALE
6.	$S_J = S_l^4$	POLAR MOMENT SCALE
7.	$S_\mu = 1$	FRICTION SCALE
8.	$S_v = (S_g S_l)^{1/2} = S_l^{1/2}$	VELOCITY SCALE
9.	$S_t = S_l S_v^{-1} = S_l^{1/2}$	TIME SCALE
10.	$S_G = S_m S_t^{-2} S_l^{-1} = S_\rho S_l$	SHEAR MODULUS SCALING
11.	$S_{\sigma_c} = S_l$	ICE STRENGTH SCALE
12.	$S_K = S_G S_I S_l^{-1} = S_\rho S_l^4$	TORSIONAL STIFFNESS SCALE

PREDICTION EQUATIONS

1. $Q_p = S_l^4 Q_M$, Torque
2. $F_p = S_l^3 F_M$, Load

NOTE: Convention $S_X = \dfrac{\text{Full Scale X}}{\text{Model Scale X}}$

TABLE 3.4

PRINCIPAL PROTOTYPE AND MODEL SCALE DIMENSIONS

DIMENSION	PROTOTYPE	MODEL TARGET
STOCK LENGTH	11.04 (36.2 ft)	64.9 cm
STOCK DIAMETER	0.675 m (26.55 inches)	3.46 cm
STOCK MATERIAL	FORGED STEEL	ALUMINUM
STOCK MASS	15,300 kg	(3.12 kg)
RUDDER DEPTH	5.66 m (18.56 ft)	33.3 cm
RUDDER LENGTH	4.33 m (14.20 ft)	25.44 cm
RUDDER WIDTH	0.700 m (27.5 inches)	4.11 cm
RUDDER MATERIAL	STEEL PLATE & FRAMES	ALUMINUM
RUDDER MASS	2187 kg	(0.65 kg)

3.1.3 **Ice Model**

An in-house synthetic model ice material, MODICE, was used to simulate field ice in the laboratory. It is a wax-like material which is formulated as a melt and allowed to set in a steel box.

A surface spray of water onto the MODICE was used to improve friction. The strength of the ice was controlled by means of an empirical scaling formula that is considered valid for crushing type application. This relationship was verified through a series of uniaxial crushing tests using Arctec's Closed Loop System. A target strength of 53 kPa was defined. This assumes that multi-year ice fragments represent the most extreme scenario. During testing the entire trailing edge of the rudder was involved in the crushing process. A series of eight ice blocks were prepared which included very strong ice, moderately strong ice, target ice, and relatively weak ice (15-22 kPa, 68 kPa, 86 kPa, 175 kPa). The blocks were mounted on a force balance which measured axial direction and lateral direction forces in the horizontal plane.

The present study utilized ice property test results from an earlier series of uniaxial crushing tests which were carried out in Arctec's Kanata Ice Laboratory. Figure 3.3 shows typical agreement in strain rate dependence of MODICE strength at 1:40 scale as compared to full scale ice. Figure 3.4 illustrates MODICE behaviour when subjected to temperature variation. On the basis of these test results, it was determined that impact tests could be conducted at room temperature.

Impact of the rudder with multi-year ice fragments is considered the upper bound damage scenario and therefore ice strength scaling in the "dry mode" tests is based on multi-year ice strength. A commonly accepted value of uniaxial crushing strength is 4.8 MPa. The design equation for ice strength in Table 3.3 shows a geometric scale relationship. Geometric scaling (1:17) would give a MODICE strength of approximately 280 kPa. However, it has been established that the actual model ice strength must be much less. Therefore ice blocks prepared for testing in the parametric study span a lower range of ice strengths.

FIGURE 3.3

STRAIN RATE DEPENDENCE OF MODICE

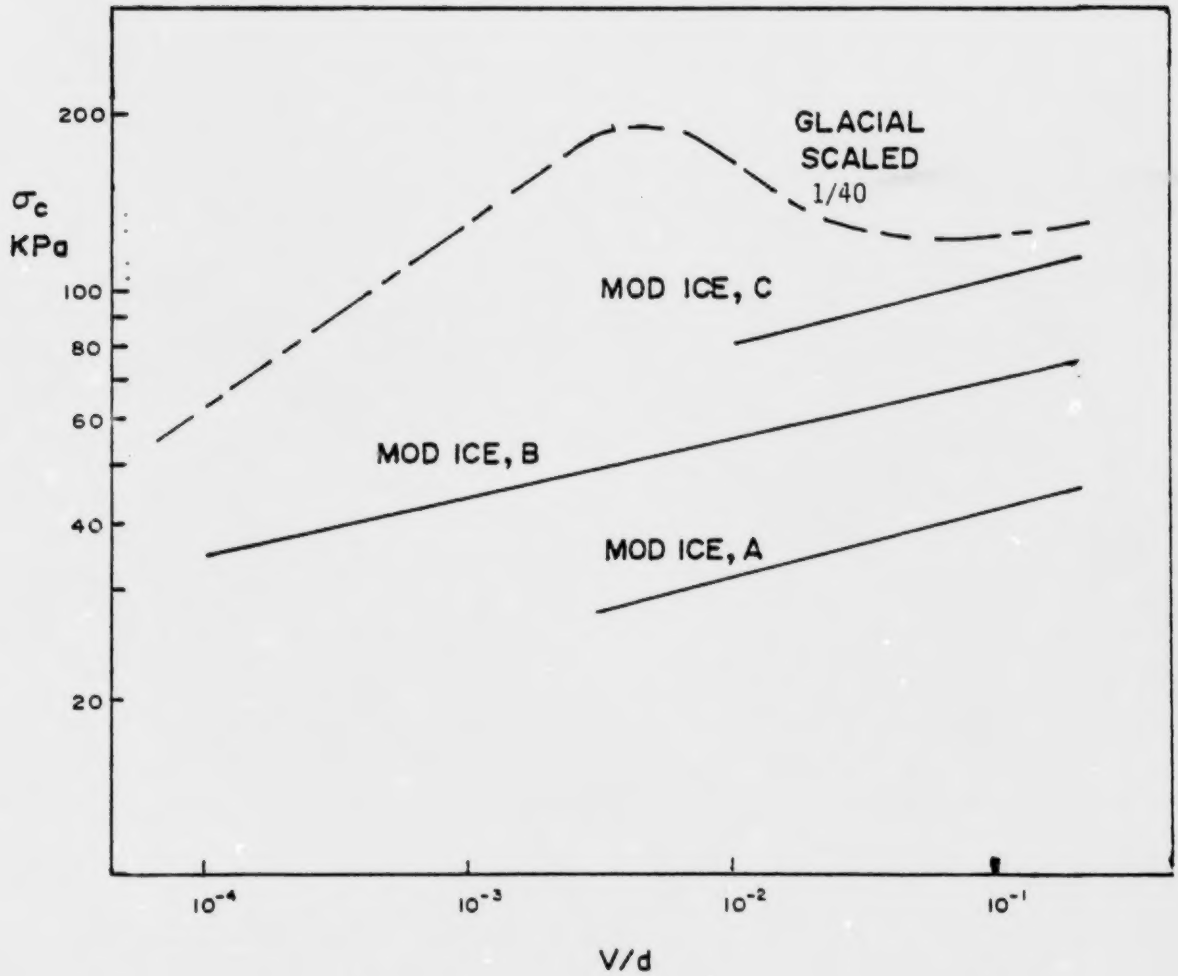

FIGURE 3.4

TEMPERATURE DEPENDENCE OF MODICE

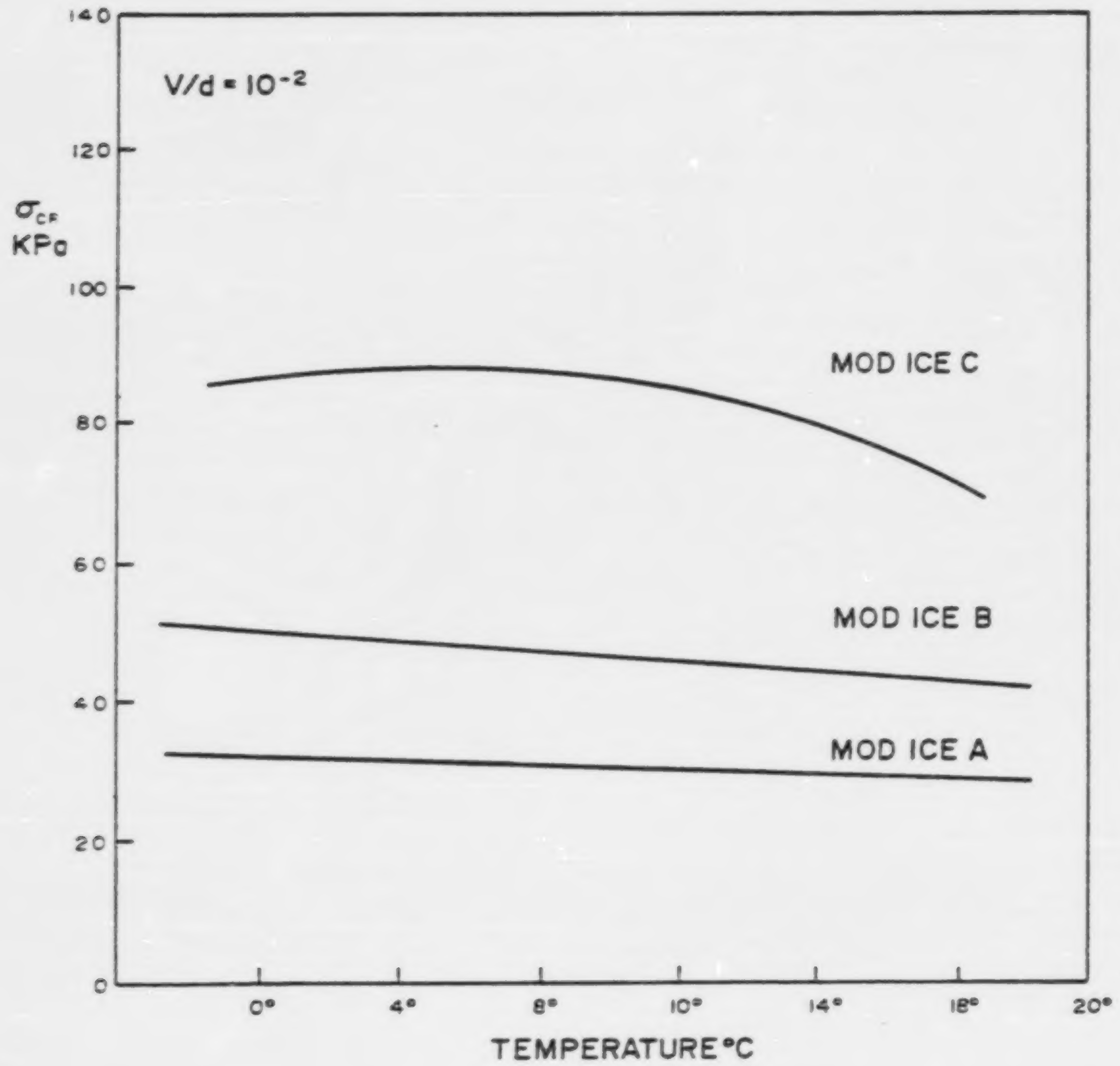

The target MODICE uniaxial crushing strength was based on an empirical scaling relationship:

$$(\sigma_{CR})_M = \frac{\sigma_c}{\lambda} (\lambda \, d/do)^{-0.88} \quad [\mathrm{MPa}] \tag{3.1}$$

where λ = geometric scale, 17

σ_c = 4.8 MPa (multi-year ice)

do = reference diameter of standard laboratory ice cores (100 mm)

d = MODICE core sample diameter (40 mm)

Therefore at $\lambda = 17$ model scale the target ice strength is:

$$(\sigma_c)_M = 52.3 \text{ kPa}$$

The pressure-area correlation term in equation 3.1 results from a comparison between full scale and model scale ramming indentations at corresponding speeds. Force was shown to depend very weakly on uniaxial crushing strength. This means that small errors in modelling of the ice strength do not result in large distortions in torque or rudder loads.

Multi-year ice is commonly characterized by temperature, salinity and structure profiles. These parameters define a brine volume factor which may be correlated with a crushing strength. It was not expected or possible that MODICE duplicate all properties of multi-year ice. The former is homogenous, whereas the latter is layered and asymmetric in structure. Table 3.5 describes density, friction and uniaxial crushing strength properties for the seven test blocks of MODICE. Specific density was 0.85. Friction factor was 0.10.

Equivalent full scale ice strengths have been calculated on the basis of equation 3.1. Test Series 3, using ice block 1, is seen to most closely approach the target ice strength. The strongest ice is observed to be 174.4 kPa, which corresponds to 16 MPa. The weakest ice was 15.4 kPa, which corresponds to 1.4 MPa in full scale. This range of strengths spans a variety of ice types; including: very strong multi-year or glacial, or multi-year, and weak multi-year or strong first year. However, it should be noted that equation 3.1 has not been strictly proven for rudder/ice interactions. It is the best available scaling relation, but caution should be employed in extrapolating to full scale ice conditions.

TABLE 3.5

TEST GROUP	MODICE BLOCK NUMBER	*MEAN UNIAXIAL CRUSHING STRENGTH (kPa)	EQUIVALENT FULL SCALE ICE STRENGTH FROM EQUATION 3.1
3	2	174.5	16 MPa, VERY STRONG MULTI-YEAR OR GLACIAL PIECES
7	7	85.8	7.7 MPa, STRONG MULTI-YEAR
4	1	67.7	6.2 MPa, TARGET MULTI-YEAR
1	5	15.4	1.4 MPa, VERY WEAK MULTI
2	6	22.3	2.0 MPa, MULTI-YEAR OR
5	8	20.5	1.9 MPa, STRONG FIRST YEAR

* Average of 6 samples

$T = 18°$

$\dot{\varepsilon} = 10^{-1}$

Specific Density = 0.85

3.2 Parametric Test Program

3.2.1 Matrix of Test Parameters

In order to give a reasonable assurance that the results of the experiments will yield well-defined relationships between the measurement parameters and at the same time achieve considerable economy in the data analysis, the experiments were planned so that all the test variables and measurement parameters are taken into account. Several techniques of experimental design have been proposed in the literature [3] which suggest the minimum number of experiments required in order to obtain the maximum amount of information. In this context a factorial arrangement known as the Graeco-Latin square was used. In a Graeco-Latin square, each variable is assumed to be 'distributed evenly' over the other variables. Thus in comparing the means obtained for one variable the effects of the other variables all average out. The influence of each test variable in the measured parameter can be assessed by analyzing the Graeco-Latin square (once all observations have been registered) using standard analysis of variance procedures. The method has proven to be useful when the number of independent variables is less than or equal to four.

The independent variables considered in the planning of the present test program were: rudder angle δ, speed v, crushing strength σ_c and equivalent ice mass m_e. Four target values for each of these variables were considered and the experiment arranged according to Graeco-Latin square shown in Figure 3.5. However, in the actual test program it was decided to consider six principal test parameters which have been studied:

- v - relative impact speed; from 0.15 m/s to 0.6 m/s
- σ_c - uniaxial ice crushing strength; from approximately 20 kPa to 175 kPa
- M_I - ice floe mass; from approximately 200 kg to 725 kg
- σ - rudder angle; from ± 15° to ± 60°
- ϕ - rudder stock diameter (stiffness); from 2.90 cm to 4.13 cm
- p_v - hydraulic pressure release; from 50 psi to 240 psi, and a fixed tiller configuration.

As the Graeco-Latin square method is capable of treating only four variables, a larger number of combinations have been included in the final test matrix. In addition, the velocity range and the ice mass range have been extended to give better coverage and to reduce the effect of scatter. Therefore the test program is more extensive than initially forecast.

FIGURE 3.5
GRAECO-LATIN SQUARE ARRANGEMENT OF TEST VARIABLES

	V_1		V_2		V_3		V_4	
δ_1	σ_{c1}	m_{e1}	σ_{c2}	m_{e2}	σ_{c3}	m_{e3}	σ_{c4}	m_{e4}
δ_2	σ_{c2}	m_{e1}	σ_{c1}	m_{e3}	σ_{c4}	m_{e2}	σ_{c3}	m_{e1}
δ_3	σ_{c3}	m_{e2}	σ_{c4}	m_{e1}	σ_{c1}	m_{e4}	σ_{c2}	m_{e3}
δ_4	σ_{c4}	m_{e3}	σ_{c3}	m_{e4}	σ_{c2}	m_{e1}	σ_{c1}	m_{e2}

UNIAXIAL ICE STRENGTH		**IMPACT VELOCITY**	
σ_{c1}	20 kPa	V_1	0.15 m/s
σ_{c2}	68 kPa (near target)	V_2	0.30 m/s
σ_{c3}	86 kPa	V_3	0.45 m/s
σ_{c4}	175 kPa	V_4	0.6 m/s

RUDDER ANGLE		**ICE FRAGMENT MASS**	
δ_1	± 15°	m_{e1}	200 kg
δ_2	± 30°	m_{e2}	375 kg
δ_3	± 45°	m_{e3}	550 kg
δ_4	± 60°	m_{e4}	725 kg

ADDITIONAL TEST VARIABLES

1. Rudder Stock Stiffness; Stock Diameter:
    - ϕ_1 2.90 cm
    - ϕ_2 3.34 cm (target)
    - ϕ_3 4.13 cm
2. Steering Gear Stiffness; Hydraulic Pressure Release:
    - P_1 50 psi
    - P_2 150 psi
    - P_3 240 psi
    - P_4 infinite (fixed end)
3. Extended Velocity Range
4. Extended Ice Mass Range

Using the combinations shown, the experiments were carried out using a constant incremental variation in each of the independent variables. The specific values used for each variable and the observed values are also shown in Figure 3.5.

No variation in the contact depth of the rudder against the ice face has been included in these tests. The maximum rudder depth has been used in all test runs, so as to represent the extreme impact condition. As a first approximation it can be assumed that smaller contact depths will result in proportionately smaller loads and torques. However, it is known from related studies that changes in contact area can produce disproportionate variations in impact pressures, and therefore further experimental work is required to define the trends associated with contact depth.

3.2.2 **Experimental Set-Up**

Figure 3.6 illustrates the dry impact rudder assembly and shows the general arrangement of ice and the force balance. The rudder was accurately machined from a single aluminum piece. Upper and lower portions were hollowed out with a central web in between. The tip region is solid and its curvature was carefully scaled. The pintles and bearing supports were of steel for greater rigidity. Teflon bushings were used to minimize frictional effects. The upper and lower rudder surfaces were sealed with thin aluminum sheets. A flange along the top surface of the rudder provided a means to fasten it to the stock. Figure 3.7 shows the hydraulic system which drives the tiller. The hydraulic rams were mounted in the moving mass frame; whilst the the larger control unit was placed on top of the basin carriage.

Three rudder stocks having different stiffnesses were fabricated. Each was machined from a single aluminum plate. The upper length of the stock was circular in diameter. The foot was flattened on the sides and maintained the diameter's curvature along the front and back edges. A base plate was welded to the foot, which in turn mated with the rudder flange. At the top of the stock there was a circular aluminum flange. Holes were drilled every 15 degrees around its circumference. This could be connected to a matching circular flange to form a rigid tiller. Rudder angle was chosen by rotating the stock through a fixed number of drill holes and bolting. Alternately the stock could be manually positioned by means of the hydraulic rams and control unit.

Two sets of steel bearings supported the stock but did not impede freedom of rotation. Each bearing was provided with three sets of bronze bushings to accommodate the three different stock diameters. Torsional gauges were mounted on the circular stock shaft between the two bearings. Bending gauges for front and side bending were positioned immediately below the lower support bearing.

FIGURE 3.6

TEST ASSEMBLY

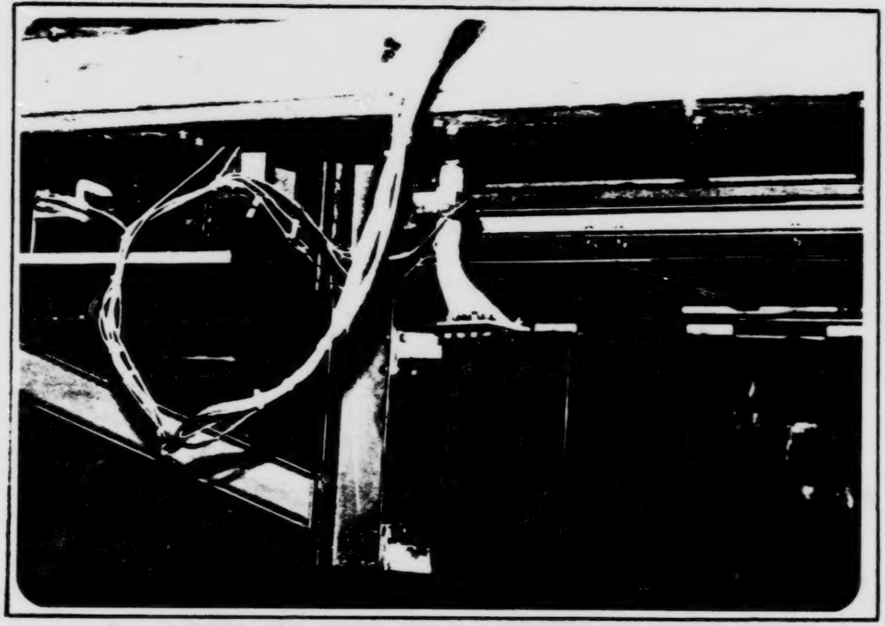

A. RUDDER AND STOCK ON MOVING MASS ASSEMBLY

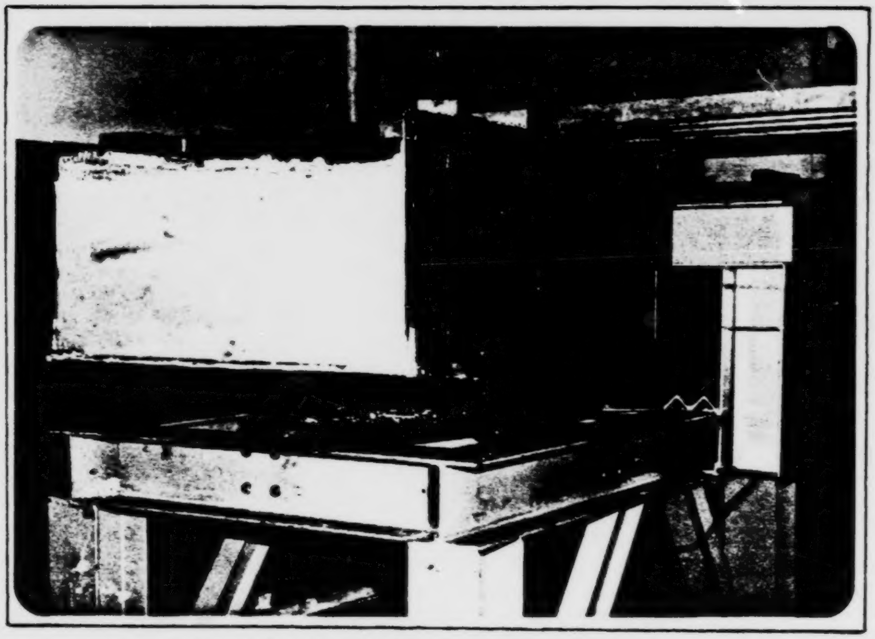

B. MODICE BLOCK ON FORCE BALANCE

FIGURE 3.7

HYDRAULIC SYSTEM

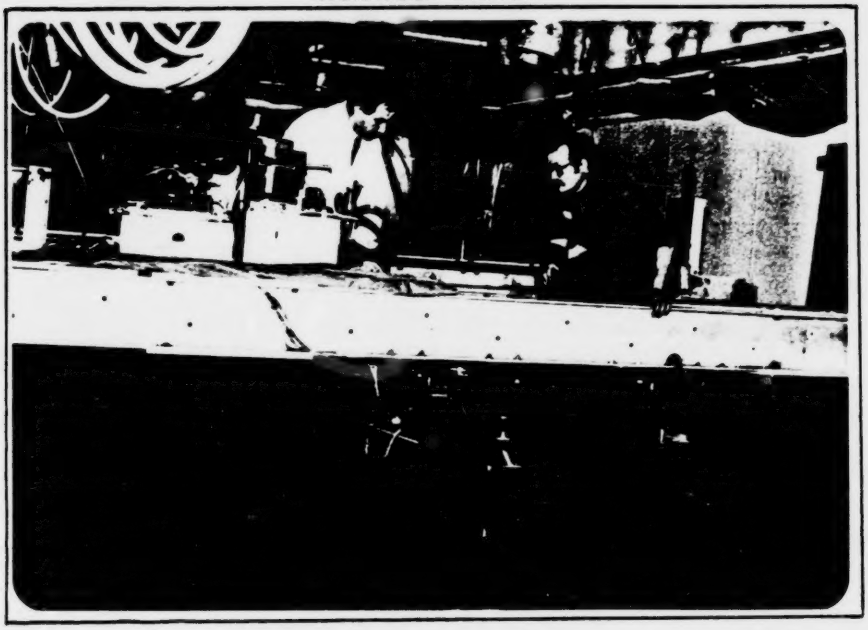

A. HYDRAULIC STEERING GEAR CONTROLLING RUDDER ANGLE

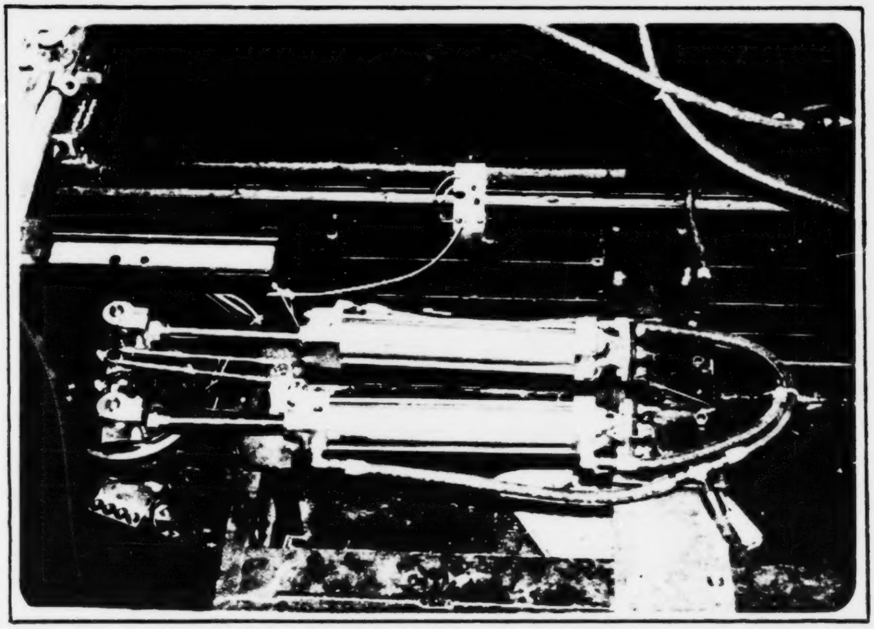

B. HYDRAULIC RAMS DRIVING TILLER

The pintles, bearings and tiller flange connected the rudder stock unit to a steel, box-like frame. This box frame comprised the moving mass. It included the hydraulic rams and any additional lead weights which were added. Along either top edge of the frame, a series of bearings were located. This allowed the box to freely move forward and back along two parallel circular steel shafts which pointed toward the ice block face. A back-weight arrangement was added to overcome friction. The entire track system was connected to the towing carriage through four bearing assemblies which permitted lateral movement. Lateral positioning of the rudder was possible through a range of 30 centimeters. This permitted several tests on each fresh face of the ice block, which significantly increased the total number of data points obtained.

The total axial moving mass was generally set at 256 kg during the testing, except during specific runs to study the influence of mass. The lateral mass was approximately 200 kg greater, as a consequence of the additional weight associated with the support rails and additional bearing components in this part of the moving mass assembly. The difference in mass acting in the lateral and axial directions will affect the measured loads and torques. However the distortion is not expected to be significant since the majority of testing is at a rudder angle of ± 15 degrees, for which the lateral component of rudder load is very small. It is also felt that this arrangement was preferable to rigidly constraining lateral motions, which would in theory give an infinite lateral mass, and thereby introduce greatly distorted confinement effects into the rudder/ice interaction.

When it was utilized, the hydraulic actuator system on the carriage was connected by flexible hosing to the tiller rams. Two calibrated pressure transducers were incorporated into the line to measure pressure differences.

The ice blocks were mounted on an I-beam support structure which was weighted to the basin floor. A two-layer force balance provided a connecting link between the ice block and the framework. Axial forces and lateral forces were measured in the horizontal plane. The entire structure had a first natural frequency of about 15 Hertz. It was important to avoid coupling with lower torsional modes of the rudder stock.

3.2.3 Instrumentation and Data Collection

A Hewlett Packard 9816 computer-based data acquisition system was utilized to expedite data collection and file management. All raw data during testing was recorded in analogue form onto a 28 channel FM back-up tape. Vishay units provided excitation and balancing of the strain gauge channels. All data was filtered at 30 Hz and passed through a system of amplifiers and analogue-to-digital converters. In this process the data was digitized at a rate of 248 Hz and the resulting time histories stored in Arctec's ACLDAT program file format. There were 14 instrumentation channels which were used:

- Three horizontal sensing force blocks in the force balance were aligned to measure the component of force in the axial direction. Calibration coefficients were determined by means of static loading with known weights.

- Three horizontal sensing force blocks measured the force component in the lateral direction. Calibration coefficients were determined by means of static loading with known weights.

- Rudder stock torque was measured by a pair of full bridge aluminum torque gauges which were applied to the stock at a point midway between the steady bearing and the carrier bearing. For each of the three stocks tested a calibration coefficient was determined by applying a range of known torsional moments.

- Side bending moment was measured by means of a pair of full bridge aluminum bending strain gauges which were affixed to opposite side surfaces of the rudder stock. They were positioned immediately below the steady bearing where the bending moment was expected to reach its maximum value. Calibration for each of the three stocks tested was by means of known static bending moments.

- Front bending moment was measured by means of a pair of full bridge aluminum bending strain gauges which were affixed to the front and back surfaces of the stock. They were positioned immediately below the steady bearing near the point of maximum bending strain. Calibration for each of the three stocks tested was by means of known static bending moments.

- A Schavitz type accelerometer was mounted on the moving frame and aligned to sense in the axial direction. It was gravity calibrated by rotations through a range of known angles. Vertical alignment corresponds to 9.807 m/s^2 and a horizontal alignment corresponds to zero.

- A multiple turn rotary potentiometer was used to measure velocity at impact. The potentiometer was fixed to the moving box frame; but the teeth of the rotor were connected to links in a track along the rail surface. This arrangement allowed measurement of rudder position and motion in the axial direction. It was calibrated from known distances along the track. Video camera records provided a check on this data.

- Carriage position was recorded via a magnetic pick-up which was pre-calibrated by known distance. However, this measurement was not utilized in the analysis since rudder impact speed, not carriage speed, was important.

- Two pressure transducers were attached to the steering hydraulic system to measure pressure differences in the cylinder rams. Calibration was by means of known pressures, as observed on a manual pressure gauge.

Information describing all of the test runs is listed in Table 3.6 of subsection 3.2.4. During each test run the following operations were repeated:

- The basin carriage was positioned at a distance from the exposed ice block face. The moving mass was shifted to its furthest back extent on the rails and the back-weight pulley adjusted to ensure a low friction motion during the impact.

- The computer console operator collected preliminary 'zero' readings from all channels once all of the sensors were undisturbed. This data was recorded into Arctec's ACLDAT data acquisition program and also onto an analogue back-up tape. It was subsequently used during data reduction to correct time histories to a zero value prior to contact.

- The carriage was accelerated to the required test speed and then abruptly stopped at a fixed distance from the ice face. With this procedure, the moving mass continued forward along the low friction rails; arriving at impact with the required speed.

- Immediately prior to impact, the computer console operator initiated the data sampling into the ACLDAT program and onto analogue back-up tape. A video recording was also started.

- After the impact was completed, the rudder indentation into the ice was measured with a ruler. The next configuration of the steering system was set up and the moving mass shifted laterally to allow the next contact to take place on an undamaged portion of the ice face. Three or four impacts could be tested on one face and then it was generally necessary to cut away the edge of the ice block to expose a new face.

3.2.4 **Test Data**

Figure 3.8 illustrates a typical set of time histories recorded during a rudder/ice impact test. The three axial sensing force blocks (one, two and three) are summed to give the total axial force time history. Similarly, force blocks four, five and six give the side (or lateral) force component. A low frequency oscillation in the lateral force data can be observed, which results from inadequate lateral stiffness in the force balance. This causes a reduction in the peak lateral force of approximately 20 percent in the test shown, during which the rudder was at its maximum angle of 60 degrees. The majority of the testing was done at 15 degrees, where the effect of force balance response was not significant. The three axial force channels have peaks and values that are much greater than the lateral forces. The signal quality is also much better. Therefore, the normal force on the rudder, which is calculated from the vector sum of the axial and lateral forces, is not significantly affected by the distortion in the lateral component.

The torque measured in the rudder stock was generally a single, smooth peak as shown in Figure 3.9. The curve did not exhibit any noticeable dynamic response during testing in the fixed tiller configuration, except at large rudder angles or higher speeds of impact. Under those conditions reversals in the torque peak were observed; the initial positive peak torque caused by the axial force, succumbing to the gradually larger moment associated with the lateral force component. The influence of the small lateral force is amplified by the large moment arm between the rudder tip and the stock centerline. Figure 3.10 shows the torsional response in three relatively high speed impacts which illustrate this phenomenon. In the present analysis of the data, only the absolute maximum peak has been used.

The typical front and side bending moments shown in Figure 3.11 are also found to exhibit single peaks. Their strain magnitudes are generally much less than the corresponding torsional strains. Reverse peaking and dynamics occur under similar conditions as observed for torque.

Table 3.5 of Section 3.1.3 has identified the uniaxial crushing strength of the MODICE blocks which were used in the different parts of the test program. For qualitative purposes the four strength categories are referred to as very strong, moderately strong, target, and relatively weak ice. Table 3.6 lists the expanded matrix of test runs and summarizes the peak values of the principal variables for each test condition. A total of 132 tests were carried out on eight blocks of MODICE. The testing was divided into seven parts, which each investigating different parameters. The three rudder stocks had different diameters which translated to three torsional stiffnesses.

FIGURE 3.8

TYPICAL SET OF TIME HISTORIES

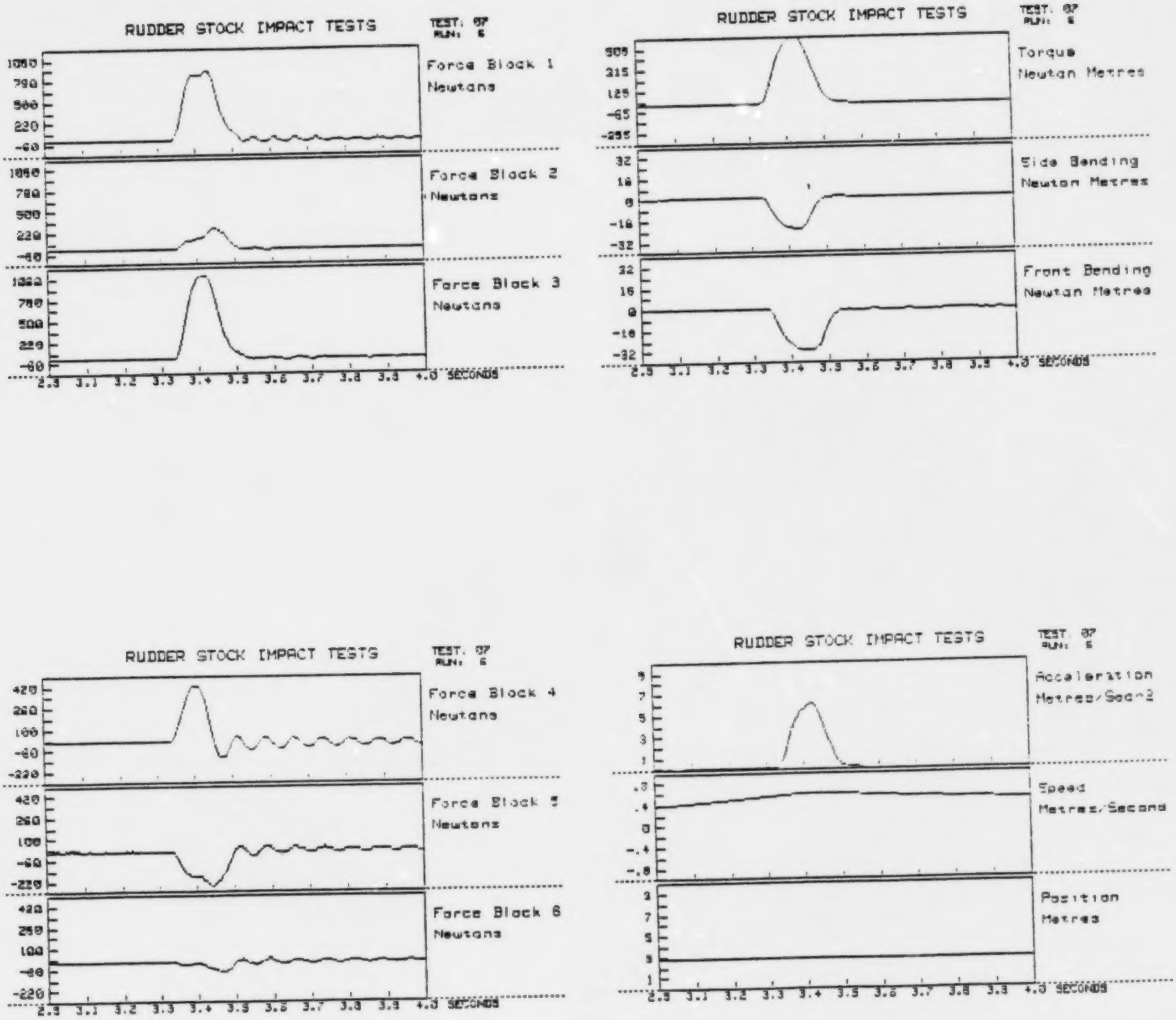

FIGURE 3.9
TYPICAL TORSIONAL RESPONSE

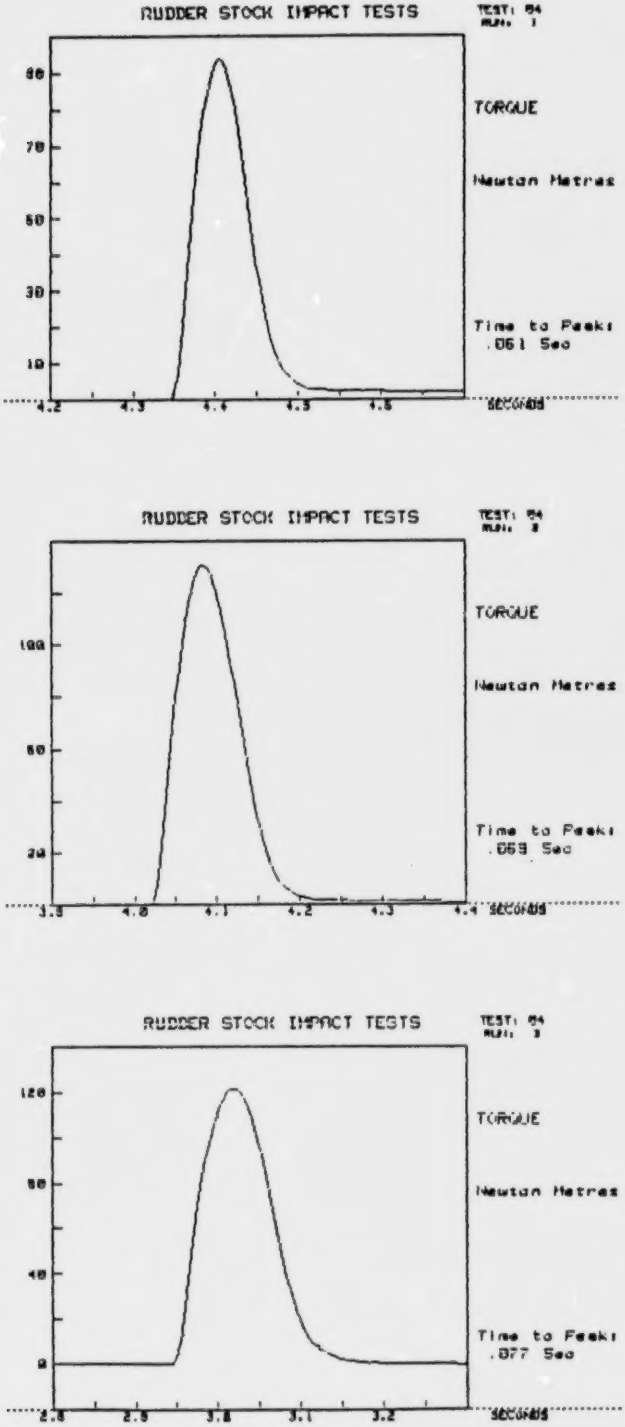

FIGURE 3.10

TORSIONAL RESPONSE ILLUSTRATING PEAK REVERSALS

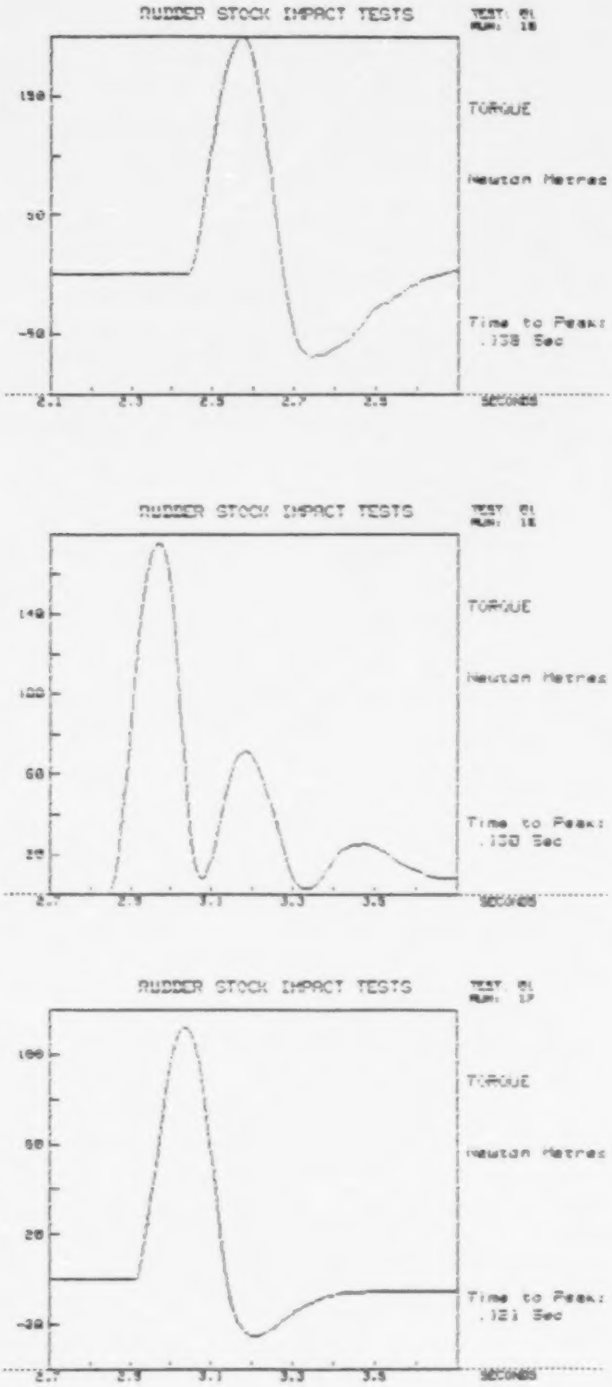

FIGURE 3.11
TYPICAL TORQUES AND BENDING MOMENTS IN TARGET STRENGTH ICE

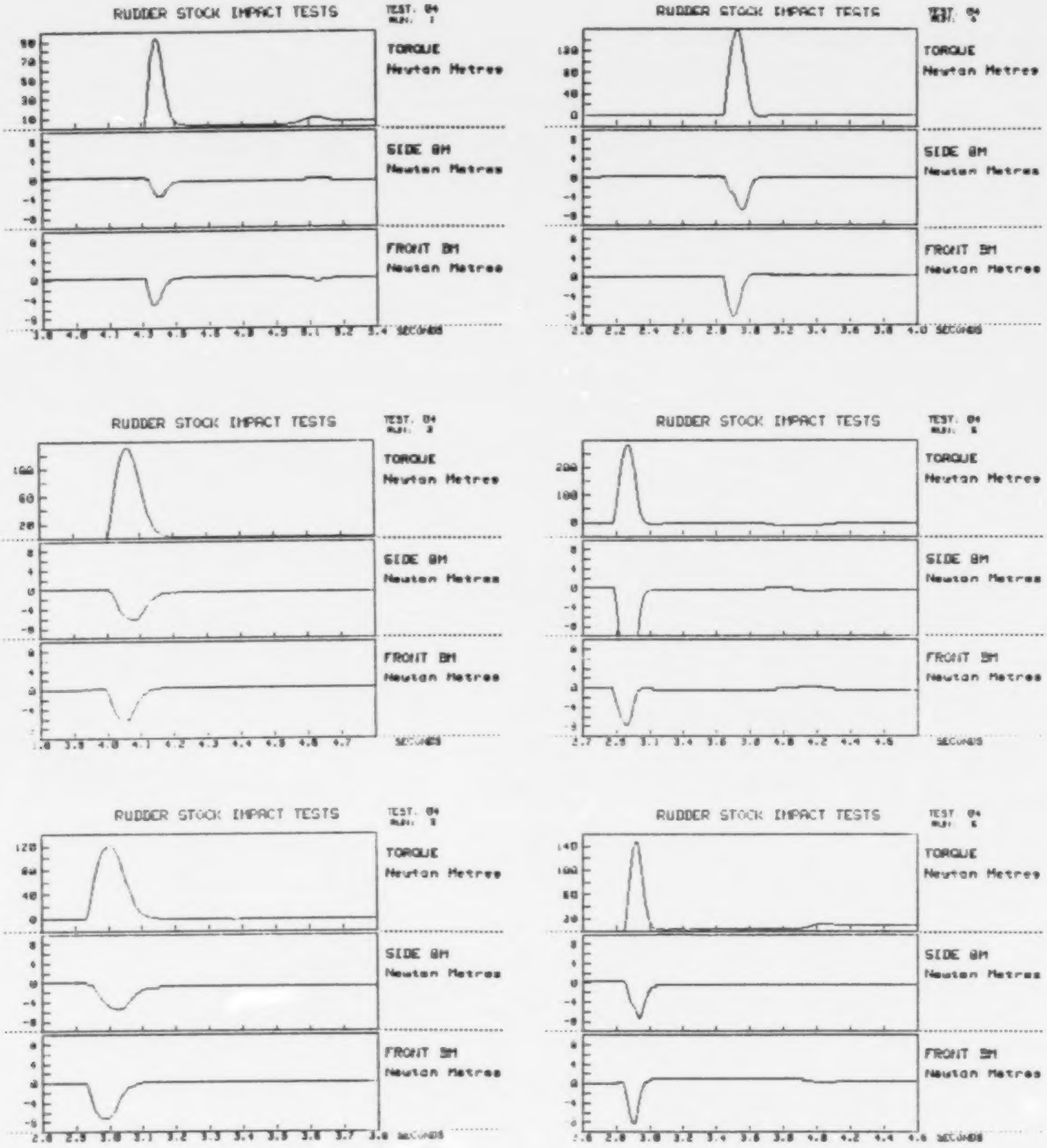

FIGURE 3.11 (CONTINUED)

TYPICAL TORQUES AND BENDING MOMENTS IN TARGET STRENGTH ICE

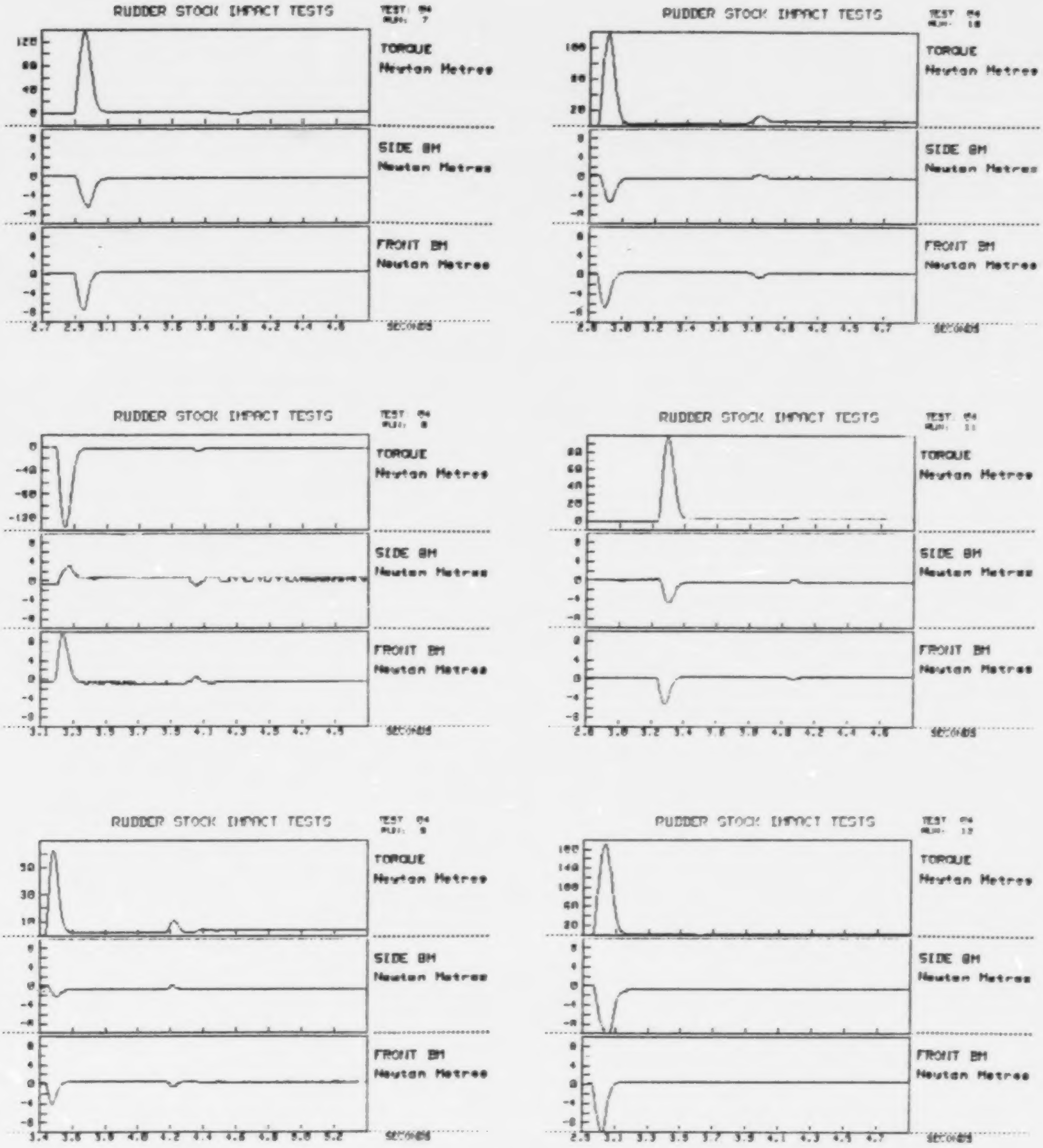

TABLE 3.6

TEST MATRIX AND PEAK DATA SUMMARY

TEST MATRIX

TEST	RUN	ICE BLOCK #	VELOCITY (m/s)	RUDDER STOCK #	ICE MASS (kg)	RUDDER ANGLE (deg)	RELEASE PRESSURE (psi)
1	1	5	.19	2	256	15	
1	2	5	.18	2	256	15	
1	3	5	.21	2	256	15	
1	4	5	.20	2	256	-15	
1	5	5	0.00	2	256	-15	
1	6	5	.16	2	256	15	
1	7	5	.35	2	256	15	
1	8	5	.27	2	256	15	
1	9	5	.42	2	256	-15	
1	10	5	.12	2	256	-15	
1	11	5	.63	2	256	15	
1	12	5	0.00	2	256	15	
1	13	5	0.00	2	256	15	
1	14	5	0.00	2	256	15	
1	15	5	.83	2	256	-15	
1	16	5	.67	2	256	-15	
1	17	5	.36	2	256	-15	
1	18	5	0.00	2	256	-15	
1	19	5	.33	2	256	-15	
1	20	5	.15	2	256	15	
1	21	5	.21	2	256	15	
1	22	5	.56	2	256	15	
1	23	5	.42	2	256	15	
1	24	5	0.00	2	256	15	
1	25	5	0.00	2	256	-15	
2	1	6	.33	2	256	0	
2	2	6	.33	2	256	0	
2	3	6	.42	2	256	-15	
2	4	6	.36	2	256	15	
2	5	6	.36	2	256	30	
2	6	6	.38	2	256	30	
2	7	6	.39	2	256	45	
2	8	6	.40	2	256	45	
2	9	6	.36	2	256	-45	
2	10	6	.42	2	256	-45	
2	11	6	.31	2	256	0	
2	12	6	.39	2	256	0	
2	13	6	.42	2	256	0	
2	14	6	.42	2	256	60	
2	15	6	.36	2	256	60	
2	16	6	.31	2	256	-60	
2	17	6	.36	2	256	-60	
2	18	6	.36	2	256	-15	
2	19	6	.36	2	256	15	
2	20	6	.42	2	256	-30	
2	21	6	.42	2	256	-30	
2	22	6	.42	2	192	15	
2	23	6	.36	2	329	15	
2	24	6	.39	2	397	15	
2	25	6	.36	2	465	15	

TABLE 3.6 (CONTINUED)

REDUCED TEST DATA

TEST	RUN	INDENT (cm)	MAXIMUM TORQUE (NM)	SIDE BEND (NM)	FRONT BEND (NM)	FORCE AXIAL (N)	FORCE LATERAL (N)	PRESSURES 1 (kPa)	PRESSURES 2 (kPa)
1	1	0.0	-121.1	6.5	-4.6	1434	-343		0.0
1	2	1.7	-39.3	1.5	-3.0	628	-130		0.0
1	3	0.0	-93.5	6.5	-2.4	453	-359		0.0
1	4	1.9	59.3	-2.7	1.7	891	162		0.0
1	5	3.3	89.2	-4.2	-3.4	967	242		0.0
1	6	1.3	-31.0	-2.7	-6.4	650	97		0.0
1	7	10.5	0.0	0.0	0.0	0	0		0.0
1	8	4.5	-48.1	2.3	-6.6	766	-119		0.0
1	9	5.2	126.2	-18.6	-17.6	1234	421		0.0
1	10	1.3	16.1	-2.7	-8.1	488	28		0.0
1	11	6.5	-138.7	4.9	-2.7	1133	-423		0.0
1	12	0.0	-9.0	6.5	-13.2	206	-41		0.0
1	13	5.5	-154.5	11.4	-6.1	1283	-491		0.0
1	14	7.0	170.6	-19.8	-12.9	1307	610		0.0
1	15	12.0	199.3	-25.1	-10.8	3190	938		0.0
1	16	6.5	175.7	-20.1	-16.6	1475	567		0.0
1	17	3.5	111.6	-13.4	-15.2	1040	339		0.0
1	18	0.0	1.6	-11.0	-31.4		-12		0.0
1	19	4.5	81.0	-12.9	-14.9	849	221		0.0
1	20	2.0	-46.8	-1.1	-5.8	683	-95		0.0
1	21	2.5	-42.8	1.1	-6.4	721	-90		0.0
1	22	0.0	2.5	7.6	-16.3		-22		0.0
1	23	0.0	-112.6	-6.5	-5.1	1071	-319		0.0
1	24	0.0	-177.2	12.9	-9.2	1047	-632		0.0
1	25	0.0	108.7	-12.2	-15.9	1190	318		0.0
2	1	3.5	2.4	-.8	-5.1	1373	80		0.0
2	2	3.6	-10.5	1.5	-4.7	1321	-67		0.0
2	3	5.5	51.5	-2.7	-3.4	1276	-273		0.0
2	4	5.6	-62.9	-6.5	-5.8	1056	349		0.0
2	5	5.8	-273.1	14.5	-7.1	1733	-665		0.0
2	6	3.2	-222.4	4.2	-2.6	1578	-474		0.0
2	7	2.0	-409.1	11.0	-3.0	2173	-421		0.0
2	8	2.0	-441.4	11.4	3.4	2334	-485		0.0
2	9	2.3	317.2	-26.2	-10.8	1925	569		0.0
2	10	2.4	321.9	-25.5	-7.1	1842	688		0.0
2	11	3.4	13.7	-2.7	-7.8	1330	124		0.0
2	12	0.0	59.3	-5.7	-8.5	1390	344		0.0
2	13	4.0	-14.1	1.1	-6.1	1189	87		0.0
2	14	2.2	-433.5	3.8	2.7	2346	-476		0.0
2	15	2.0	-437.8	5.7	-2.4	2398	-437		0.0
2	16	2.5	369.0	-32.3	-7.8	2115	488		0.0
2	17	2.0	415.0	-32.7	-8.1	2290	551		0.0
2	18	3.5	117.9	-6.1	-6.3	1497	302		0.0
2	19	4.5	-82.5	-6.1	-5.1	1398	-401		0.0
2	20	3.0	222.6	-14.7	-6.4	1602	447		0.0
2	21	2.9	220.3	-14.1	-6.8	1573	476		0.0
2	22	3.5	-147.0	3.4	3.7	1431	-396		0.0
2	23	6.2	-47.6	-4.5	-3.4	1161	219		0.0
2	24	5.0	-165.5	-3.4	4.7		-366		0.0
2	25	5.2	-223.2	4.6	4.4	1395	-795		0.0

TABLE 3.6 (CONTINUED)

TEST MATRIX

TEST	RUN	ICE BLOCK #	VELOCITY (m/s)	RUDDER STOCK #	ICE MASS (kg)	RUDDER ANGLE (deg)	RELEASE PRESSURE (psi)
2	26	6	0.00	2	**533**	15	
2	27	6	.33	2	**533**	15	
2	28	6	.38	2	**600**	15	
2	29	6	.36	2	**669**	-15	
2	30	6	.36	2	**737**	-15	
2	31	6	.36	2	**600**	-15	
3	1	2	.23	2	256	-15	
3	2	2	.31	2	256	-15	
3	3	2	.36	2	256	-15	
3	4	2	.38	2	256	-15	
3	5	2	.50	2	256	-15	
3	6	2	.42	2	256	-15	
3	7	2	.36	2	256	-15	
3	8	2	.26	2	256	-15	
3	9	2	.10	2	256	-15	
3	10	2	.29	2	256	-15	
3	11	2	.24	2	256	-15	
3	12	2	.56	2	256	-15	
4	1	1	.21	2	256	-15	
4	2	1	.29	2	256	-15	
4	3	1	.42	2	256	-15	
4	4	1	.42	2	256	-15	
4	5	1	.50	2	256	-15	
4	6	1	.42	2	256	-15	
4	7	1	.33	2	256	-15	
4	8	1	.24	2	256	-15	
4	9	1	.11	2	256	-15	
4	10	1	.28	2	256	-15	
4	11	1	.23	2	256	-15	
4	12	1	0.00	2	256	-15	
5	1	8	.31	1	256	-15	
5	2	8	.23	1	256	-15	
5	3	8	.22	1	256	-15	
5	4	8	.31	1	256	15	
5	5	8	.12	1	256	15	
5	6	8	.63	1	256	15	
5	7	8	.28	1	256	15	
5	8	8	0.00	1	256	15	
5	9	8	.28	1	256	15	
5	10	8	.32	1	256	-15	
5	11	8	.50	1	256	-15	
5	12	8	.50	1	256	-15	
5	13	8	.42	1	256	-15	
6	1	8	.18	**3**	256	15	
6	2	8	.13	**3**	256	15	
6	3	8	.23	**3**	256	15	
6	4	8	.50	**3**	256	15	
6	5	8	.63	**3**	256	15	
6	6	8	0.00	**3**	256	15	
6	7	8	.28	**3**	256	15	

TABLE 3.6 (CONTINUED)

REDUCED TEST DATA

TEST	RUN	INDENT (cm)	MAXIMUM TORQUE (NM)	SIDE BEND (NM)	FRONT BEND (NM)	FORCE AXIAL (N)	FORCE LATERAL (N)	PRESSURES 1 (kPa)	2 (kPa)
2	26	4.5	-190.6	-7.2	-6.1	1522	-583		0.0
2	27	5.8	-165.1	3.4	5.1	1708	405		0.0
2	28	5.5	-132.5	2.7	2.7	1496	-340		0.0
2	29	5.9	169.6	-14.2	-4.7	1714	473		0.0
2	30	6.0	203.2	-19.8	-5.4	1511	700		0.0
2	31	7.0	189.8	-14.8	-5.8	1698	592		0.0
3	1	.2	104.2	-4.9	-9.0	2585	325		0.0
3	2	.4	172.5	-10.6	-9.5	3039	601		0.0
3	3	.5	154.1	-8.4	-13.6	3505	625		0.0
3	4	.7	176.9	-11.4	-14.9	3769	713		0.0
3	5	1.5	252.3	-18.2	-13.9	3564	1093		0.0
3	6	.6	198.5	-12.2	-14.9	3946	711		0.0
3	7	.4	173.7	-11.0	-13.2	3543	719		0.0
3	8	.7	113.2	-4.2	-9.8	2556	291		0.0
3	9	.2	61.3	-3.0	-6.4	1618	192		0.0
3	10	.6	159.6	-6.8	-10.5	3158	506		0.0
3	11	.5	132.1	-5.3	-10.2	2820	421		0.0
3	12	.1	211.4	-9.5	-15.9	4362	531		0.0
4	1	.6	93.5	-3.4	-5.1	1816	253		0.0
4	2	1.3	130.5	-6.1	-6.4	1983	329		0.0
4	3	1.6	121.4	-5.7	-7.1	2107	260		0.0
4	4	2.3	158.0	-6.8	-8.1	2104	399		0.0
4	5	3.8	283.4	-22.4	-7.8	2396	1031		0.0
4	6	2.2	148.2	-7.3	-8.1	2477	405		0.0
4	7	1.5	137.1	-6.5	-7.5	2234	304		0.0
4	8	1.2	-134.7	3.1	9.5	2115	197		0.0
4	9	1.0	62.5	-2.3	-4.1	1473	144		0.0
4	10	1.2	117.1	-5.3	-6.8	2194	242		0.0
4	11	.9	98.2	-4.6	-5.1	1930	229		0.0
4	12	2.2	192.2	-10.6	-10.2	2982	411		0.0
5	1	3.6	-476.2	-76.9	18.5	1224	315		0.0
5	2	3.3	-313.0	-56.1	15.3	933	209		0.0
5	3	2.2	-276.3	-49.3	13.9	838	168		0.0
5	4	3.1	366.9	38.4	-24.2	1037	-286		0.0
5	5	1.8	-35.0	-4.2	-10.9	391	180		0.0
5	6	5.8	716.0	81.0	-24.6	1629	-463		0.0
5	7	2.2	319.5	34.3	-22.3	893	-203		0.0
5	8	0.0	0.0	0.0	0.0	0	0		0.0
5	9	3.8	530.7	63.4	-14.2	917	-367		0.0
5	10	3.5	-455.3	-35.3	-30.3	1355	277		0.0
5	11	4.7	-313.0	-30.6	-26.5	1039	158		0.0
5	12	5.2	-604.5	-41.0	-34.1	1634	396		0.0
5	13	5.3	-478.0	-33.0	-21.7	1273	559		0.0
6	1	1.9	0.0	0.0	0.0	0	0		0.0
6	2	.9	9.2	1.1	-.7	684	61		0.0
6	3	3.4	6.7	.7	-.7	837	110		0.0
6	4	4.5	38.3	7.6	-2.4	1522	-426		0.0
6	5	5.9	47.5	9.4	-2.7	1641	-604		0.0
6	6	0.0	0.0	0.0	0.0	0	0		0.0
6	7	2.2	20.9	3.6	-1.2	955	-201		0.0

TABLE 3.6 (CONTINUED)

TEST MATRIX

TEST	RUN	ICE BLOCK #	VELOCITY (m/s)	RUDDER STOCK #	ICE MASS (kg)	RUDDER ANGLE (deg)	RELEASE PRESSURE (psi)
6	8	8	.29	3	256	15	
6	9	8	.33	3	256	15	
6	10	8	.39	3	256	15	
6	11	8	0.00	3	256	15	
6	12	8	.39	3	256	15	
6	13	8	.46	3	256	15	
6	14	8	.31	3	256	15	
7	1	7	.42	2	256	0	50
7	2	7	0.00	2	256	45	50
7	3	7	.42	2	256	45	50
7	4	7	.36	2	256	45	50
7	5	7	.36	2	256	30	50
7	6	7	.42	2	256	60	50
7	7	7	.31	2	256	15	50
7	8	7	0.00	2	256	15	50
7	9	7	.25	2	256	15	50
7	10	7	.33	2	256	15	50
7	11	7	.50	2	256	15	50
7	12	7	.63	2	256	15	50
7	13	7	.12	2	256	15	150
7	14	7	.19	2	256	15	150
7	15	7	.28	2	256	15	150
7	16	7	.36	2	256	15	150
7	17	7	.42	2	256	15	150
7	18	7	.50	2	256	15	150
7	19	7	.13	2	256	15	240
7	20	7	.31	2	256	15	240
7	21	7	.36	2	256	15	240
7	22	7	.42	2	256	15	240
7	23	7	.50	2	256	15	240
7	24	7	.63	2	256	15	240

TABLE 3.6 (CONTINUED)

REDUCED TEST DATA

TEST	RUN	INDENT (cm)	MAXIMUM TORQUE (NM)	SIDE BEND (NM)	FRONT BEND (NM)	FORCE AXIAL (N)	FORCE LATERAL (N)	PRESSURES 1 (kPa)	PRESSURES 2 (kPa)
6	8	4.5	11.8	1.5	-1.0	1007	62		0.0
6	9	4.8	29.6	5.4	-2.0	1265	-296		0.0
6	10	3.5	30.0	6.2	-1.8	1322	-294		0.0
6	11	0.0	15.6	2.2	-1.4	1190	126		0.0
6	12	4.5	38.4	8.0	-2.1	1531	-383		0.0
6	13	4.9	45.2	9.4	-2.4	1531	-558		0.0
6	14	3.2	8.0	1.5	-.7	891	189		0.0
7	1	2.3	11.8	7.3	8.5			-131.0	-134.3
7	2	1.2	346.3	22.8	-18.6	1448	-382	17.9	-48.8
7	3	1.2	405.2	23.2	-20.0	1771	424	17.9	-54.9
7	4	1.4	397.2	26.1	-24.7	1711	388	11.9	-54.9
7	5	1.5	289.3	22.5	-33.2	1752	-418	11.9	-41.9
7	6	1.6	623.0	-22.6	-30.8	2170	-370	11.9	6.1
7	7	2.0	168.1	-3.6	13.6	1731	-291	11.9	-18.3
7	8	2.0	60.1	-1.8	6.1	830	81	0.0	-6.1
7	9	1.4	118.2	6.5	-15.2	1535	217	12.0	-12.2
7	10	1.6	165.7	9.4	-25.8	1957	317	11.9	-18.3
7	11	2.8	152.4	6.8	-23.4	2183	421	17.9	-18.4
7	12	3.4	253.9	11.2	-28.1	2546	-445	23.0	-36.6
7	13	.3	57.0	.6	2.0	866	-95	0.0	-6.1
7	14	.7	69.9	6.9	-22.0	1440	224	6.0	-12.2
7	15	1.3	139.1	2.2	-2.4	1822	-244	11.7	-24.4
7	16	1.4	80.6	-2.5	-4.4	1923	644	6.0	6.1
7	17	3.2	149.8	1.8	-10.2	2215	359	11.9	-37.1
7	18	3.8	199.2	4.4	-12.2	2470	259	11.9	-54.9
7	19	.5	71.1	-6.9	22.0	1170	182	11.9	-12.6
7	20	1.0	166.5	2.9	-5.1	1637	221	11.9	-42.7
7	21	1.5	233.3	8.7	-15.6	1956	-350	11.9	-60.9
7	22	2.8	87.0	-3.6	7.1	2149	736	11.9	-18.2
7	23	4.6	97.3	-3.2	-6.1	2666	711	11.9	12.2
7	24	4.9	56.6	5.8	-25.8	2198	686	6.0	-6.1

Rudder #2 was a scaled replica of the LOUIS S. ST. LAURENT rudder stock. Rudder #1 was a smaller diameter stock corresponding to one half the target stiffness. Rudder #3 was twice the target stiffness of Rudder #2.

- Test group 1 studied the influence of impact velocity. The tiller was rigidly fixed during these impacts and during all subsequent testing except group 7. Relatively weak MODICE was used and Rudder #2. The axially moving ice mass was fixed at 256 kg, which corresponds to approximately 10 percent of the LOUIS S. ST. LAURENT mass displacement. The rudder was fixed at ± 15 degrees, which represents an extreme for impacts during normal backing manoeuvres in ice. A range of impact velocities up to 0.83 m/s was investigated.

- Test group 2 involved the variation of rudder angle to assess its influence on rudder loads, bending moments and torsional response. The rudder angle was varied in steps of 15 degrees from zero to 60 degrees. Although 15 degrees is considered a maximum in normal backing, larger impact angles may be caused by yaw or sway of the ship's stern into ice masses in the broken channel. These tests used weak ice, Rudder #2 and a 256 kg ice mass. The mean velocity in these tests was 0.369 m/s. The maximum and minimum masses were 600 kg and 192 kg respectively.

- Test group 3 and 4 extended the velocity variation testing of group 1 to include the influence of ice strength. Test group 3 used the very strong ice at 174 kPa and test group 4 used the target strength ice. Rudder stock #2 was again used. The rudder angle was set at ± 15 degrees and the ice mass was 256 kg; and the ice was relatively weak, as during the testing of Rudder #2.

- Test group 7 investigated the response of the steering system for a range of pressure release settings of the hydraulics control unit. The rudder assembly was not fixed at the tiller in these tests. Instead the tiller was connected to the hydraulic rams. Three release pressures were assessed: 50 psi, 150 psi and 240 psi. The lowest value was the target scaled hydraulics setting. The largest value was the maximum attainable from the hydraulics unit. A small set of velocities was tested at each setting and a range of angles was also tested at 50 psi.

Table 3.6 also summarizes the peak values of torque, side bending moment, front bending moment, axial rudder force, and lateral force. Peak hydraulic pressures in the ram cylinders are also listed in the test series 7 runs. Where double or reverse peaking occurs, only the absolute maximum has been reported. Indentations have been manually recorded and represent the axial directed length of the notch caused by the impact. The accumulated data in this table has been analyzed and discussed in Section 3.3.

3.3 Discussion of Dry Impact Test Results

3.3.1 **Influence of Test Parameters**

The influence of the principal test parameters has been assessed on the basis of the peak values of the dependent variables which were extracted from the time histories. In the context of the present analysis it has not been possible to define a mathematical surface which describes the parametric variations. However the trends associated with each dependent variable have been identified as a function of the individual test parameters. Power regression curves are fitted to the data sets; but numerical equations have not been given, since the model test data has not been corrected to a common, reference condition.

Ice Strength Variation

The influence of ice strength is indicated in Figure 3.12. Rudder angle and moving mass were constant in these tests. Longitudinal impact loading is observed to follow a power relation in which the exponent on speed is less than one. The multiplicative constant in this relation increases sharply with increased ice strength. The sensitivity of the longitudinal impact loading to variation in ice strength was clearly evident. The transverse load shows a more linear trend with increasing speed.

The upper most plot of the longitudinal component load corresponds to tests in the very strong, 174 kPa MODICE. Over the mid range of impact velocities, these loads are nearly twice as severe as found in tests on ice block 1 which is close to the target strength. The relatively weak ice from block 5 resulted in axial forces which are half of those observed at target strength. The lateral loads show a similar increase with ice strength.

Figure 3.13(a) shows the peak normal loads on the rudder as a function of impact velocity. Normal load has been calculated as the vector summation of the axial component and the lateral component of the measured load. This depends on the rudder angle, which was fixed at 15 degrees during these tests. This condition represents the extreme expected impact angle during backing manoeuvres. The power regression curves through this data are only slightly modified from the longitudinal load plots by the inclusion of the transverse loads. The trend is very well defined and there is little scatter in the results.

Figure 3.13(b) illustrates the relationship between the peak normal load on the rudder and the crushed area of the notch formed by the impact. This area is defined by the measured indentation length and the rudder angle. It assumes that only the hypotenuse surface of the notch is active in crushing. The three curves show that crushing area rapidly decreases with ice strength and that peak normal rudder loads increase rapidly with crushing area. Only the 15 degree rudder angle data has been assessed in the present analysis. The influence of ice mass has not been investigated.

FIGURE 3.12

DRY IMPACT TESTS
ICE STRENGTH VARIATION

A. LONGITUDINAL DIRECTION COMPONENT OF RUDDER LOAD

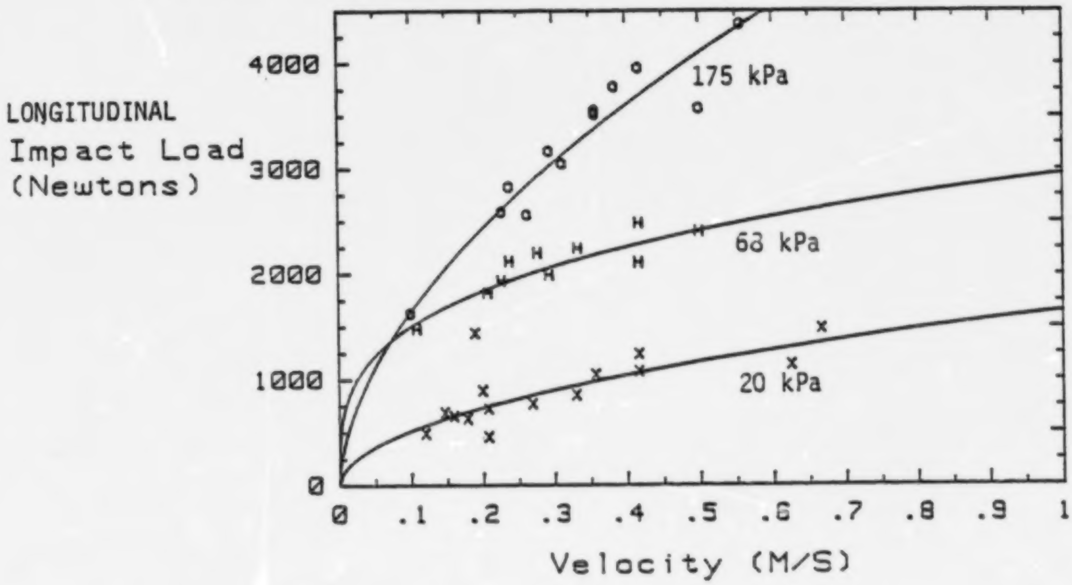

B. TRANSVERSE COMPONENT OF RUDDER LOAD

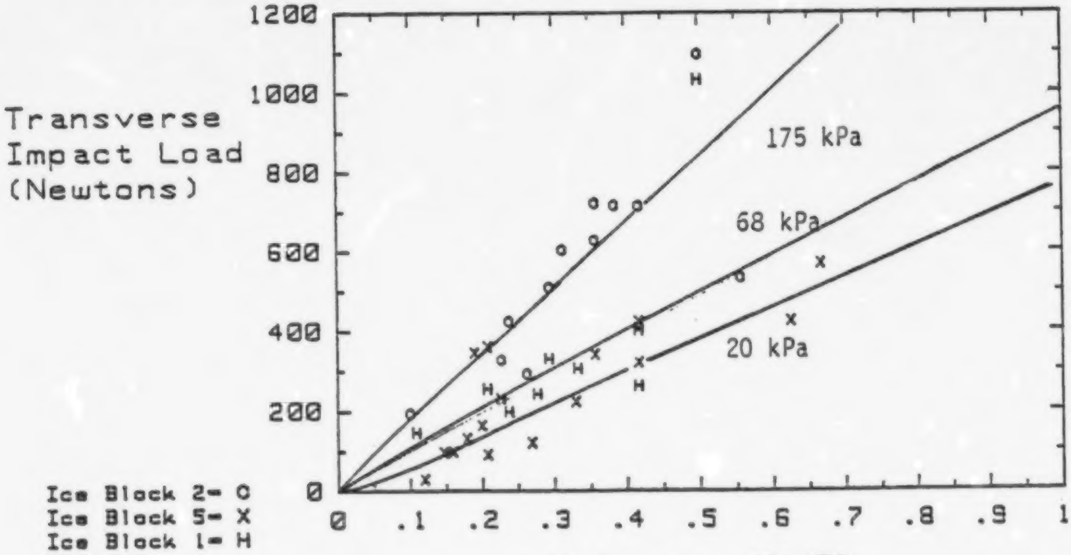

Stock: 2
Angle: +/- 15 (deg)
Mass: 256.4 (kg)

FIGURE 3.13

MAXIMUM RUDDER LOAD
INFLUENCE OF VELOCITY & CRUSHING AREA

A. INFLUENCE OF VELOCITY ON NORMAL LOAD

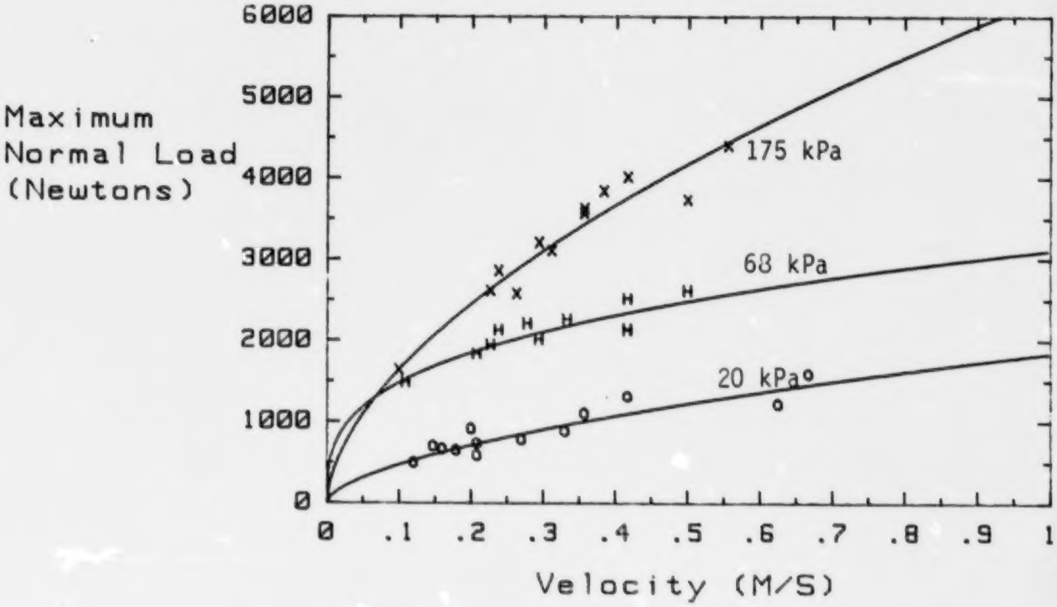

B. RELATIONSHIP OF LOAD TO CRUSHED AREA

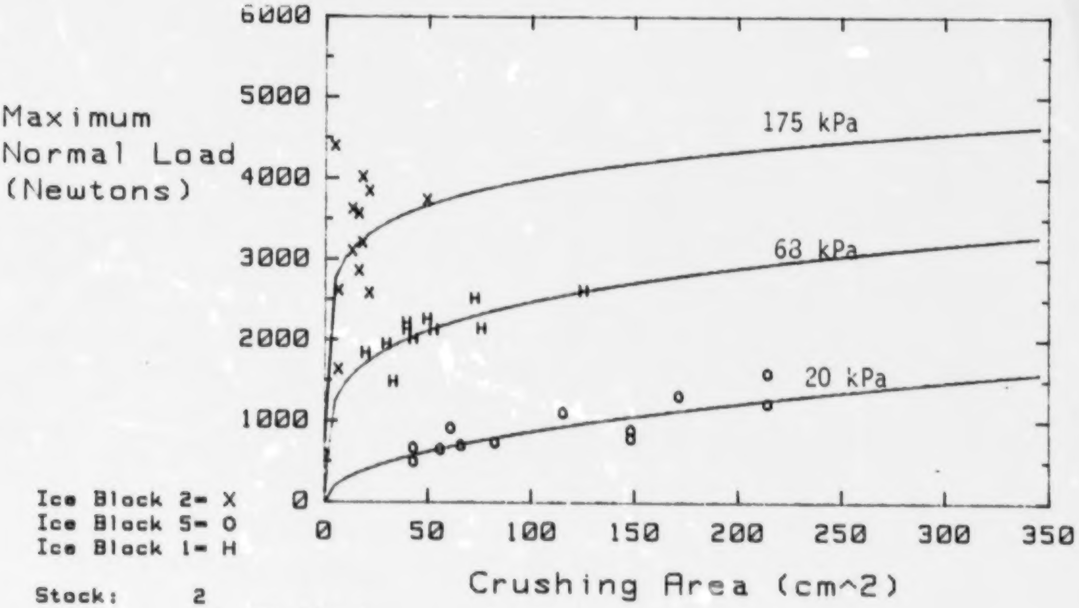

Stock: 2
Angle: +/- 15 (deg)
Mass: 256.4 (kg)

Figure 3.14 shows the corresponding effect on maximum peak acceleration and peak torque experienced by the stock. Acceleration followed a trend analogous to the longitudinal loading. The torque is closely associated with the transverse loading and therefore shows a similar curve.

The trends in Figure 3.15 for variation of side bending moment and front bending moment are less clearly defined. This was due in small part to scatter of the data, but primarily to insulation of those strain gauges by the pintles and bearings. However, values increased with velocity and generally increased with ice strength. It was observed that indentation of the rudder into the ice face increased linearly with speed in Figure 3.16 for a rudder angle of 15 degrees. As ice strength increased the indentations decreased in an approximately exponential decay. At an impact velocity of 0.5 m/s the indentation for 175 kPa ice is less than 1.0 cm. The corresponding 20 kPa ice indentation is 5.5 cm.

Rudder Angle Variation

The influence of rudder angle was investigated by conducting a series of impact tests in which the velocity, mass and ice strength were held constant. Weak ice from block 6 was used in these tests. The mean velocity was 0.375 m/s. The rudder angle was varied in steps of 15 degrees through 60 degrees.

Longitudinal impact loading is shown in Figure 3.17. It increases in a sinusoidal manner from a minimum at zero degrees to a maximum above 60 degrees. Transverse loading increases more rapidly and goes through a maximum at about 45°, then decreases.

The peak acceleration of the moving mass and rudder assembly (in Figure 3.18) increases towards a maximum above 60 degrees. As expected, this is a similar trend to that observed for the longitudinal component of the rudder load. The torque is influenced by both axial and transverse components as the rudder angle increases. Therefore it increases from a minimum at zero degrees in a nearly linear manner. However, it has a lower slope initially and also tends toward a maximum above 60 degrees. Indentation is observed in Figure 3.19 to decrease with rudder angle and to reach a minimum above 45 degrees.

The relative influences of bending strain and torsional strain on the target rudder stock #2 have been calculated and are shown in Figure 3.20.

FIGURE 3.14

DRY IMPACT TESTS
ICE STRENGTH VARIATION

A. INFLUENCE OF VELOCITY ON TORSIONAL RESPONSE

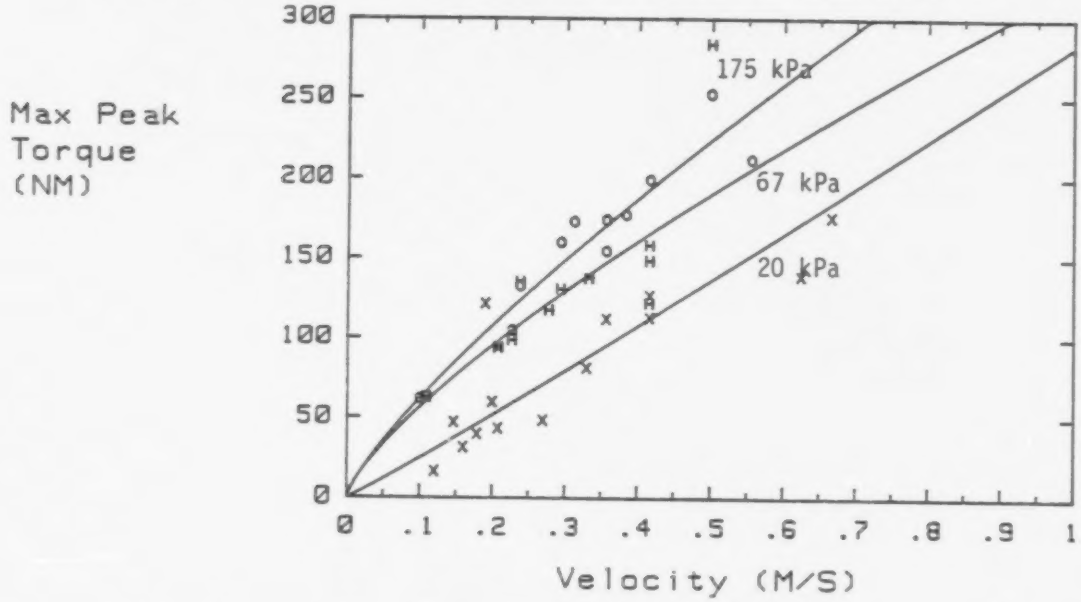

B. INFLUENCE OF VELOCITY ON ACCELERATION

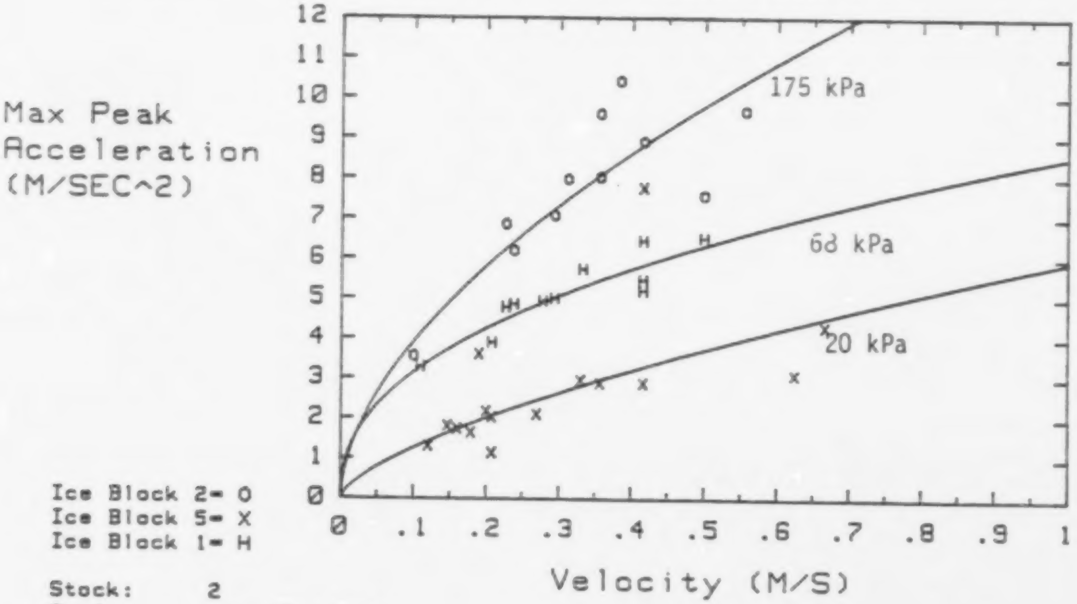

Stock:	2
Angle:	+/- 15 (deg)
Mass:	256.4 (kg)

FIGURE 3.15

DRY IMPACT TESTS
ICE STRENGTH VARIATION

A. INFLUENCE OF VELOCITY ON SIDE BENDING MOMENT

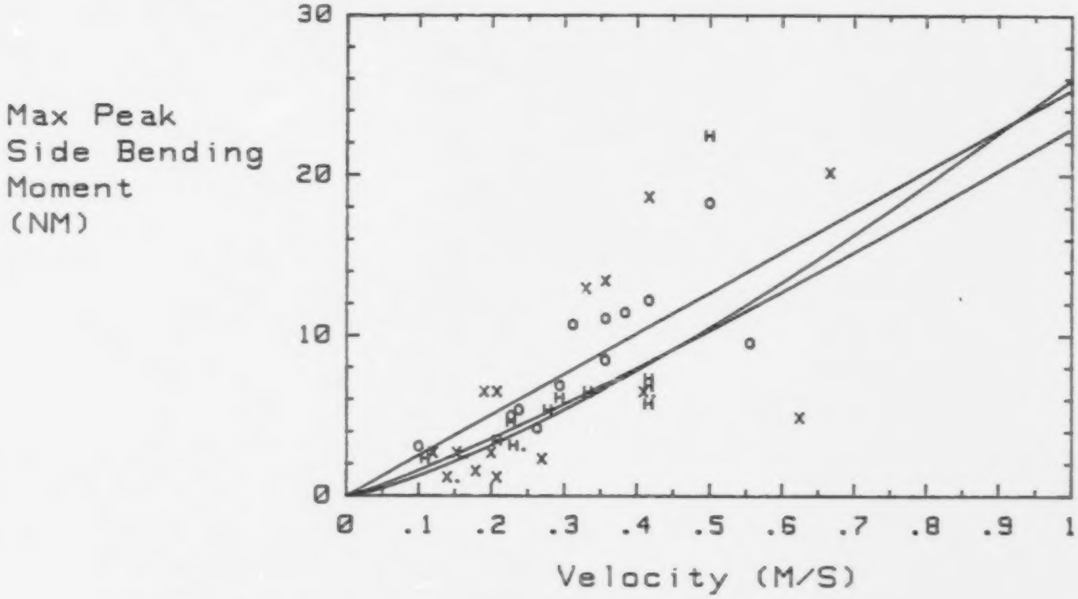

B. INFLUENCE OF VELOCITY ON FRONT BENDING MOMENT

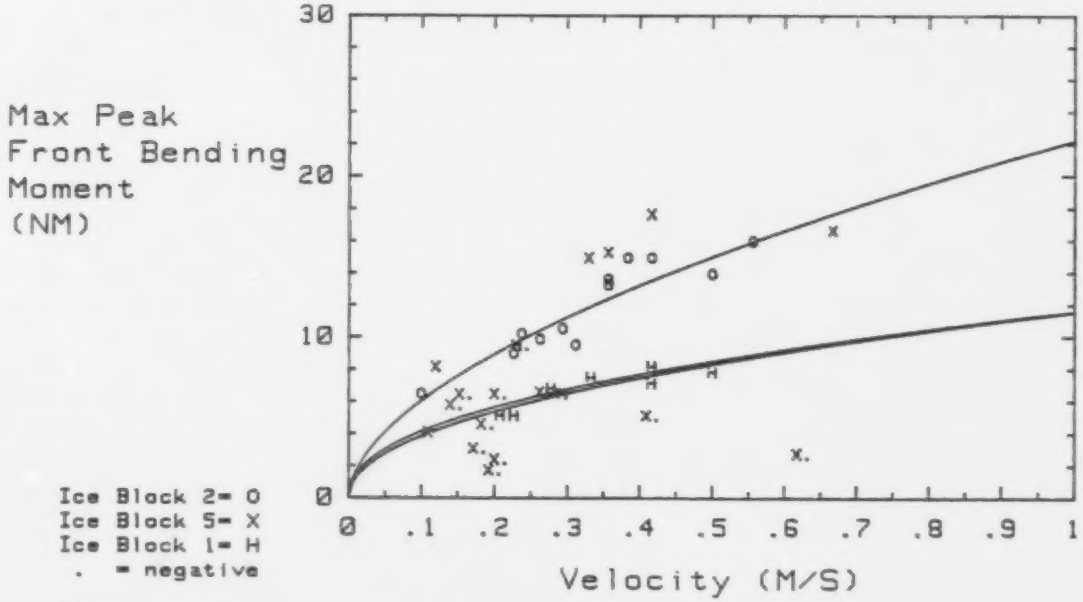

Stock	2
Angle:	+/- 15 (deg)
Mass:	256.4 (kg)

FIGURE 3.16

DRY IMPACT TESTS
ICE STRENGTH VARIATION

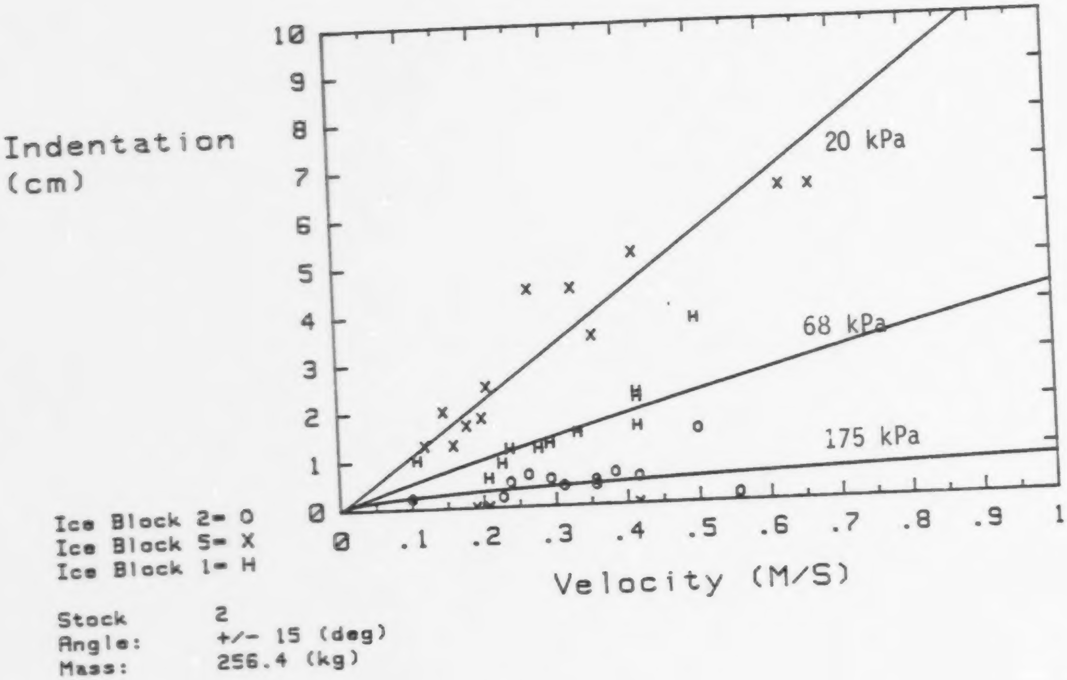

FIGURE 3.17

DRY IMPACT TESTS
RUDDER ANGLE VARIATION

A. LONGITUDINAL LOADS

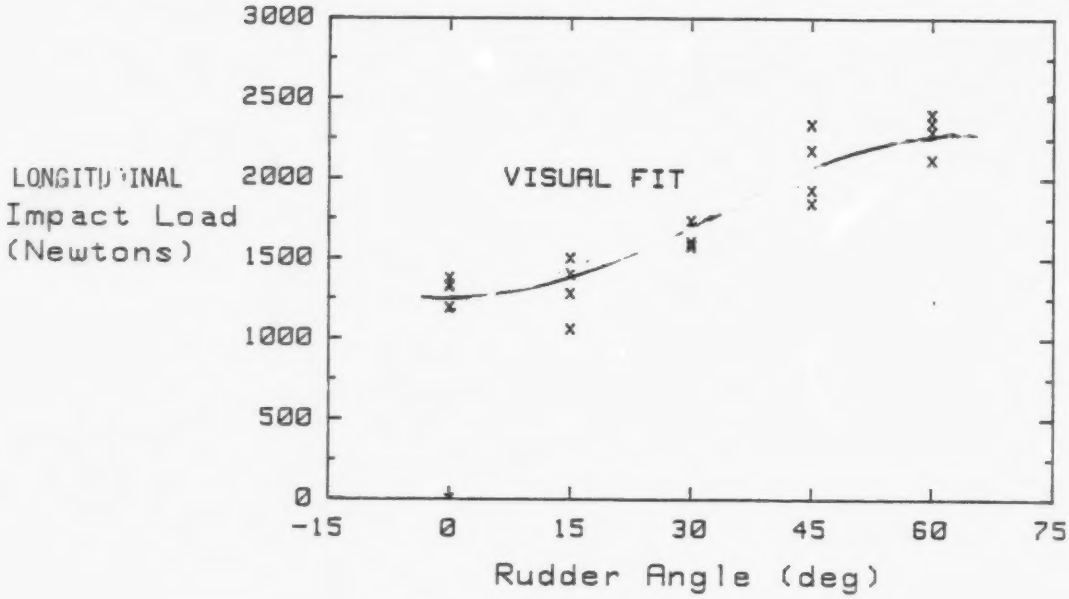

B. TRANVERSE LOADS

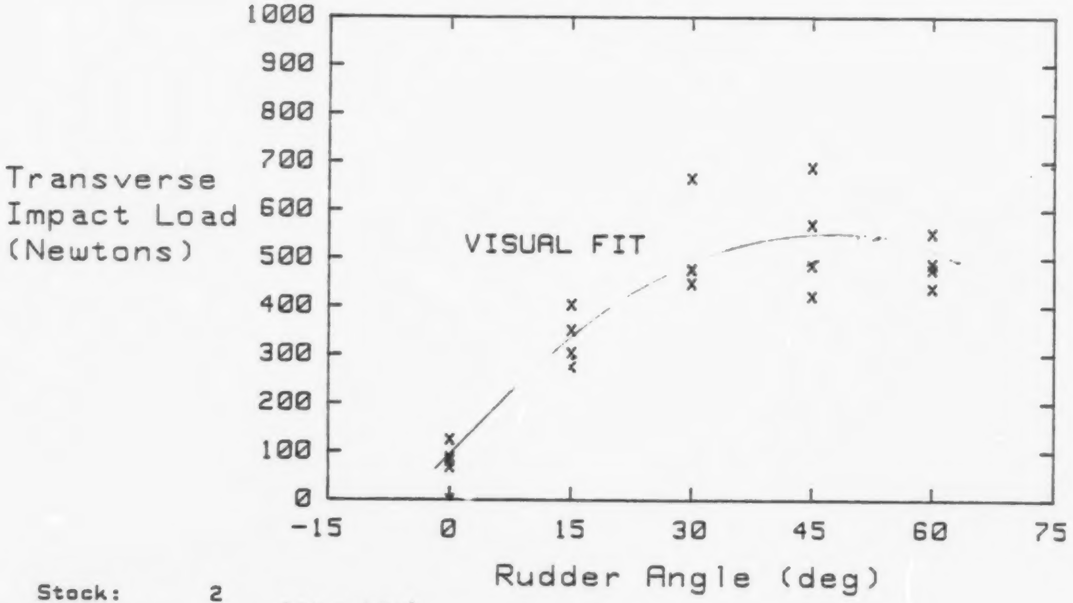

Stock: 2
Ice Block: 6 (22.3 kPa)
Velocity: .375 (M/S)
Mass: 256.4 (kg)

FIGURE 3.18

DRY IMPACT TESTS
RUDDER ANGLE VARIATION

A. TORQUE VARIATION WITH RUDDER ANGLE

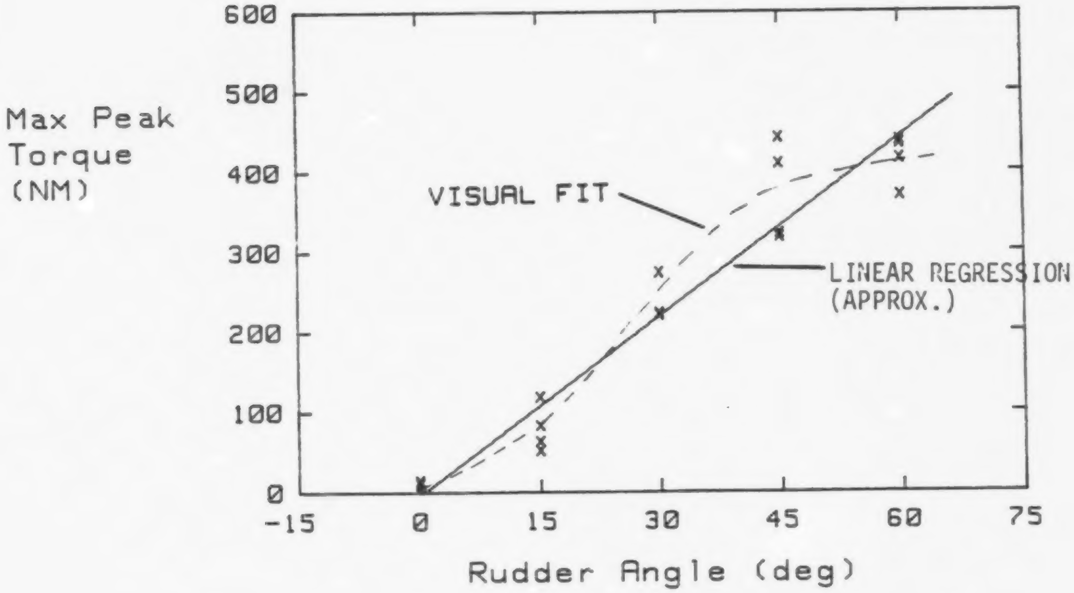

B. ACCELERATION DEPENDENCE ON RUDDER ANGLE

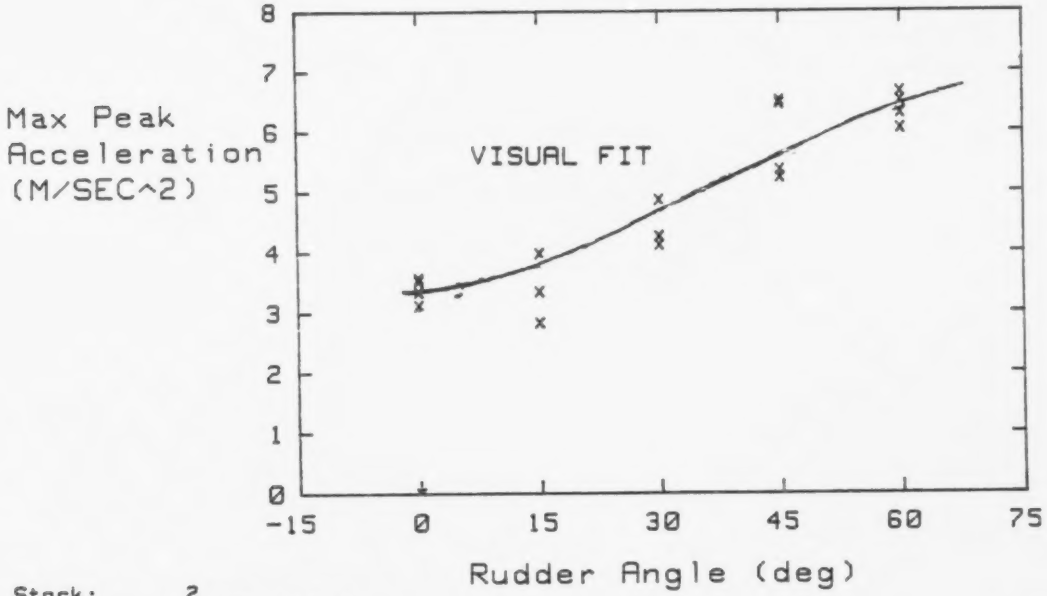

Stock:	2
Ice Block:	6 (22.3 kPa)
Velocity:	.375 (M/S)
Mass:	256.4 (kg)

FIGURE 3.19

DRY IMPACT TESTS
RUDDER ANGLE VARIATION

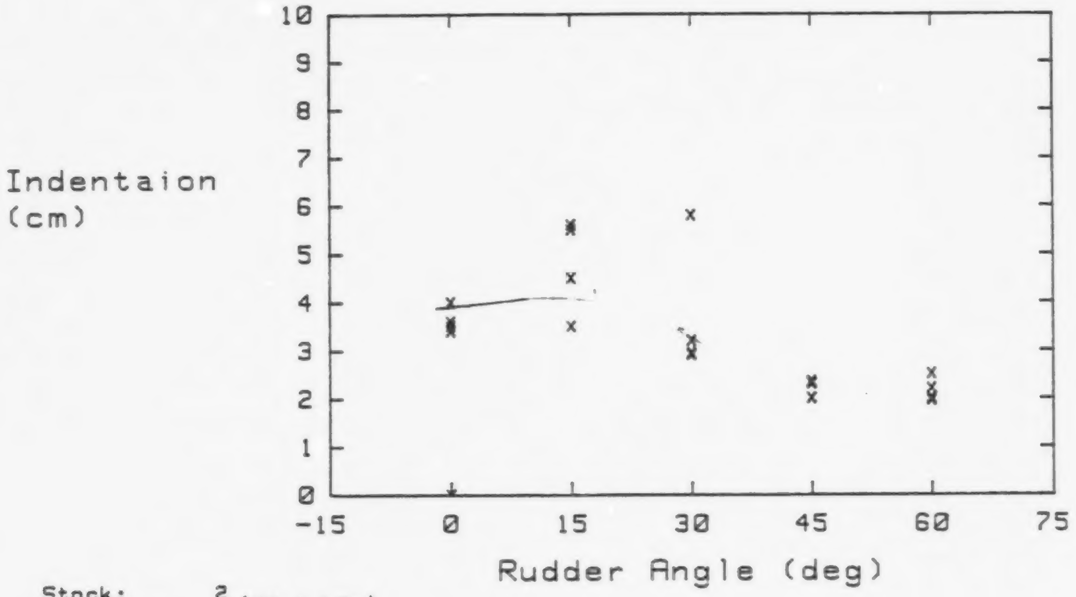

Stock: 2 (22.3 kPa)
Ice Block: 6
Velocity: .375 (M/S)
Mass: 256.4 (kg)

FIGURE 3.20

DRY IMPACT TESTS
INFLUENCE OF IMPACT VELOCITY

A. RATIO OF BENDING STRAIN TO TORSION STRAIN

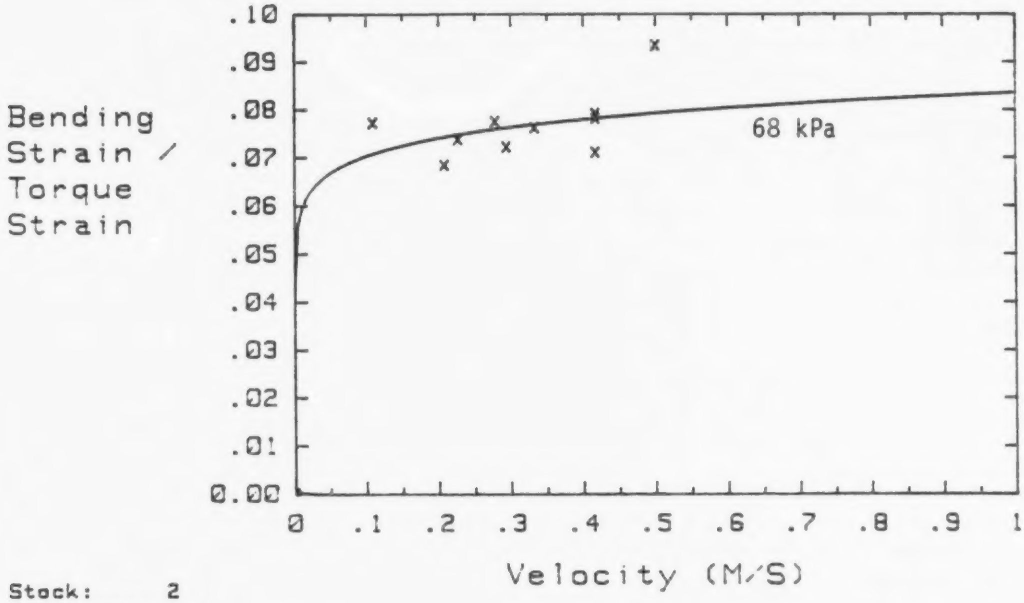

Stock: 2
Ice Block: 1
Angle: +/- 15 (deg)
Mass: 256.4 (kg)

MOMI

B. RATIO OF TORQUE TO BENDING MOMENT

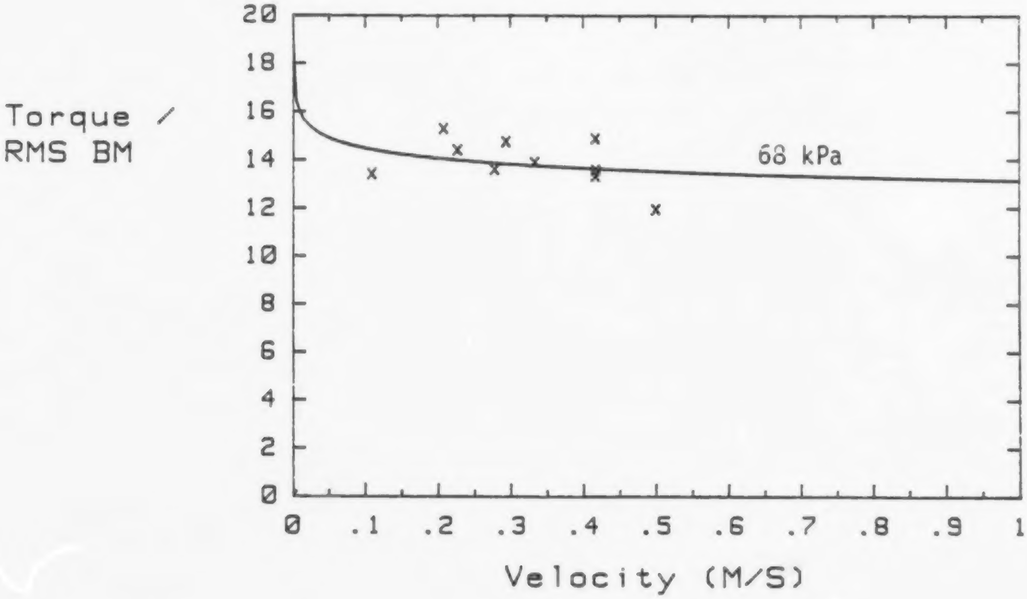

The bending strain is the composite strain calculated by the vector summation of the side bending strain and the front bending strain. At a rudder angle of 15 degrees, the bending strain is observed to be less than 10 percent of the torsional strain. The ratio of 0.08 remains approximately constant over the tested velocity range. It is expected that at larger angles the ratio will be much smaller, since the torque area will increase rapidly with angle. This result is in general agreement with typical observations from full scale trials. The present calculations have been based on the 68 kPa MODICE (Block 1). It is assumed that variation in ice strength will not significantly alter this ratio, on the grounds that individual bending moment and torque trends have been seen to be similar at different ice strengths. Figure 3.20 (b) shows an equivalent ratio based on measured torque and bending moment, rather than on the more fundamental strains.

Rise Time

Torque rise time has been defined as the time interval between contact of the rudder tip with the ice face and the point of maximum torsional response. Trends are shown in Figure 3.21 (a) giving the influence of impact velocity on the rise time at three ice strengths. In each case the rise time appears to be approximately constant with velocity. It is observed to increase as ice strength is decreased. For 20 kPa ice strength, the rise time is about 0.13 sec. At 68 kPa, it is 0.07 sec. and at 175 kPa, it is 0.05.

A similar trend is noticeable in Figure 3.21 (b), which shows the relationship between torque rise time and peak torsional response for three variations in ice strength. It appears that rise time is approximately constant with increases in peak torque and decreases with increasing ice strength.

Mass Variation

The influence of ice floe displacement was investigated by loading of the moving frame with lead weights. Rudder angle was fixed at 15 degrees. The impact speed was nominally constant with a mean value of 0.37 m/s. In this preliminary analysis the nominal speeds were used, and speed corrections have not been incorporated. Weak ice (at 22.3 kPa) was used in these tests.

Figure 3.22 shows that longitudinal impact loading obeys a power relationship with a coefficient on mass which is less than one. It is approximately linear above 300 kg. The transverse loading follows a similar relationship. Its coefficient was less than one, but larger than for the longitudinal load case. However, transverse loads are expected to be smaller at 15 degrees of rudder angle. The relationship of transverse loading to mass is also nearly linear above 300 kg. Its larger slope means that it contributes to a normal loading on the rudder which increases with mass at a faster rate than the longitudinal load.

FIGURE 3.21

TORQUE RISE TIME
INFLUENCE OF VELOCITY & MAX TORQUE

A. VARIATION WITH VELOCITY

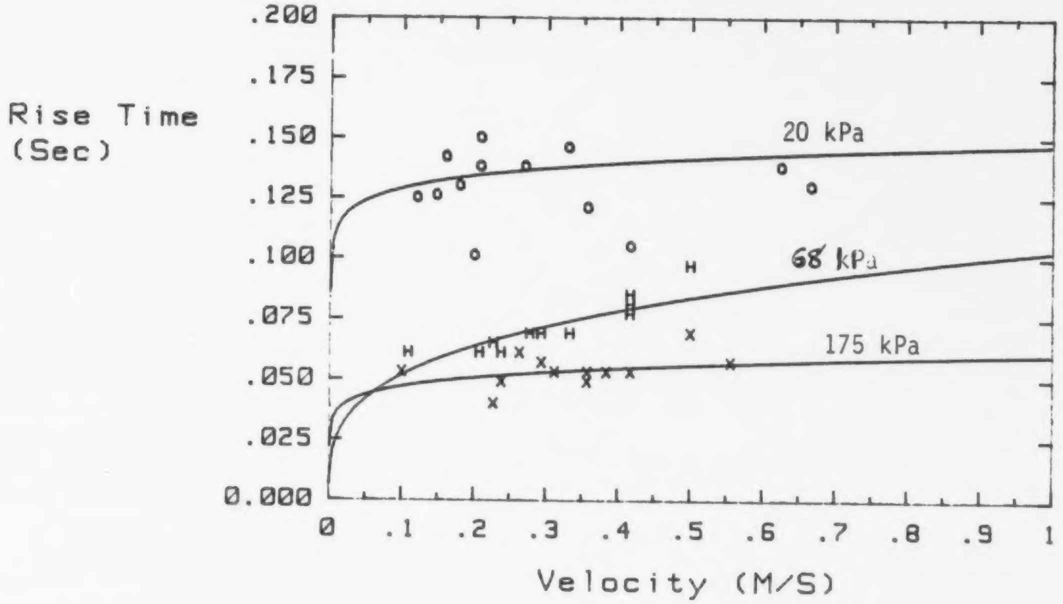

B. VARIATION WITH TORQUE

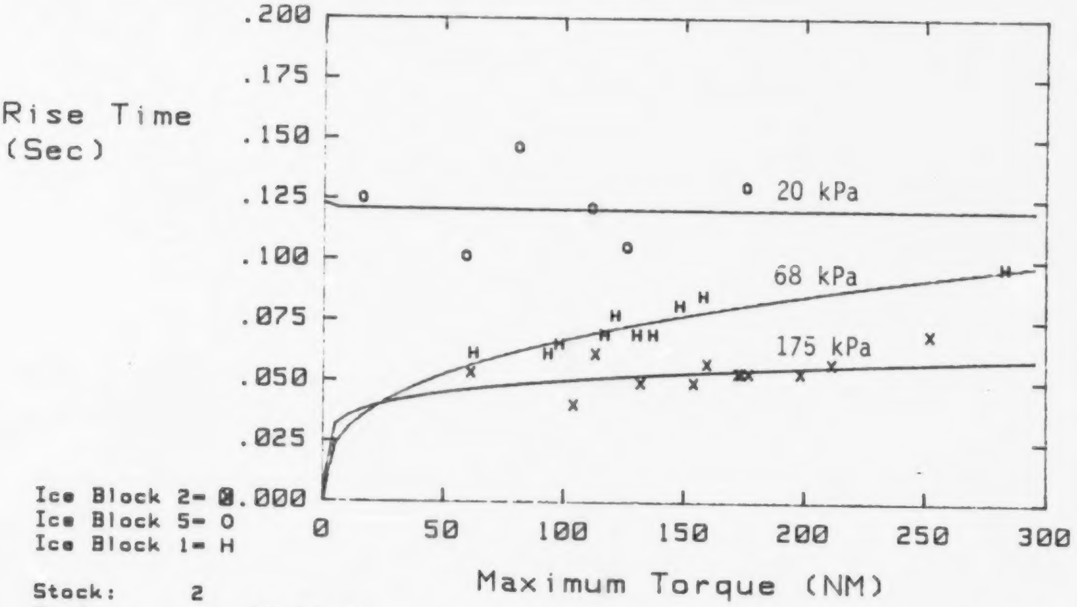

Stock: 2
Angle: +/- 15 (deg)
Mass: 256.4 (kg)

FIGURE 3.22

RUDDER STOCK TESTS
MASS VARIATION

A. LONGITUDINAL LOAD VARIATION

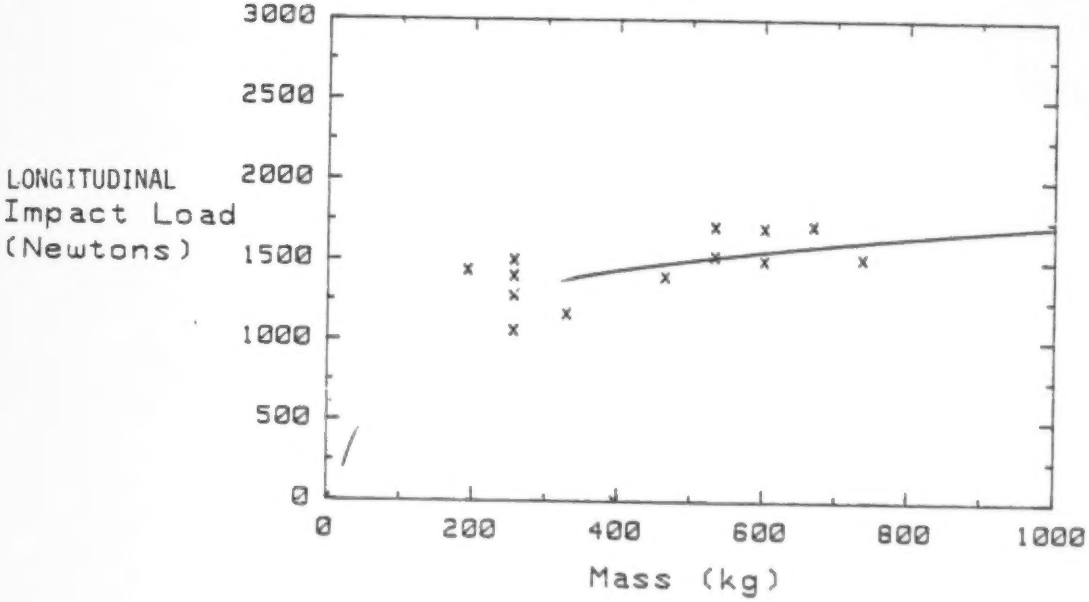

B. TRANSVERSE LOAD VARIATION

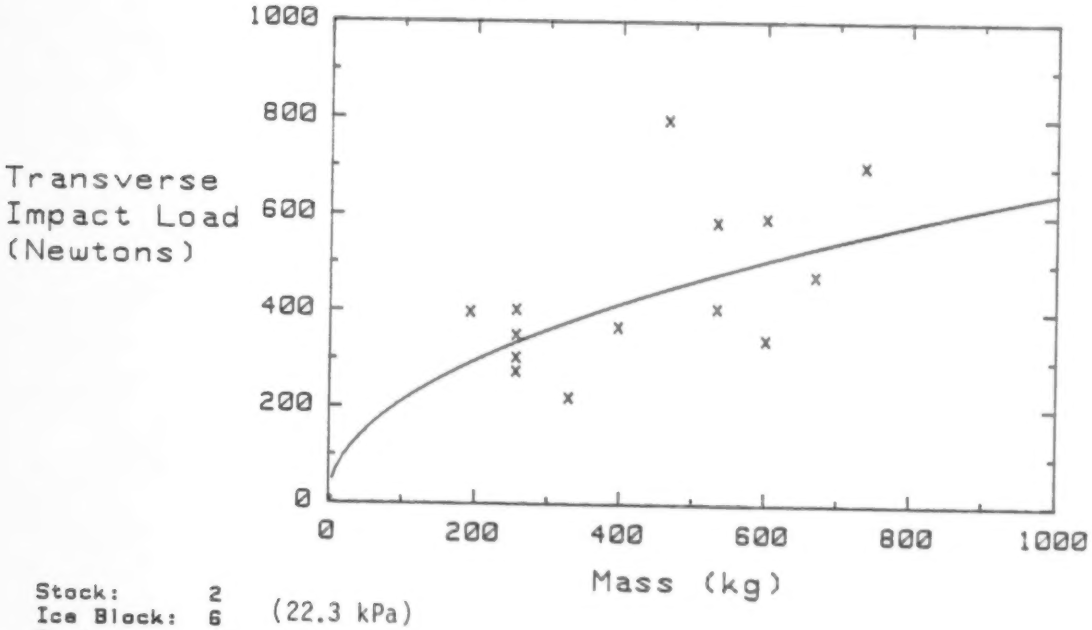

Stock: 2
Ice Block: 6 (22.3 kPa)
Angle: 15 (deg)
Velocity: .37 (M/S)

The increase in peak torque with mass is observed in Figure 3.23 to be approximately linear with mass. However, there is sufficient scatter in the uncorrected data to suggest a power relationship. Peak acceleration decreases inversely with increased mass at a nominally constant impact speed. This is consistent with Newton's Law: $F = m \cdot a$ or $a \propto m^{-1}$.

Side bending increases slowly with mass in Figure 3.24 but neither the manner nor the amount of increase is clear. Front bending moments remain constant at approximately 4.5 Nm. Indentation in Figure 3.25 follows a trend similar to longitudinal impact, with a power relationship with mass that has a coefficient less than one. The linearity of force and inverse linearity of acceleration with increasing mass indicates that the ice failure behaviour remains similar over a range of displacement.

Hydraulics Relief Pressure

The influence of the pressure relief setting on the hydraulic steering gear was studied. Only a limited number of trials were possible within the test schedule and therefore results are tentative at this point.

Figure 3.26 shows that pressure difference increases in a roughly linear manner with impact speed for the three relief settings tested. The 240 psi setting was the maximum attainable and it showed the largest pressures. The 50 psi setting was the target scaled relief. The pressures obtained at this setting are significantly lower. This means that the 50 psi system will exhibit larger motion responses and therefore reduced torques as compared to the fixed tiller configuration.

The longitudinal and transverse loading in Figure 3.27 show equivalent curves for each pressure relief case. The transverse loading was slightly higher for the 240 psi setting. Trends in the torque curves of Figure 3.28 are insufficiently clear to draw conclusions. Acceleration does not appear to be affected by the pressure release, although there is a slightly increasing trend.

FIGURE 3.23

RUDDER STOCK TESTS
MASS VARIATION

A. TORQUE VARIATION

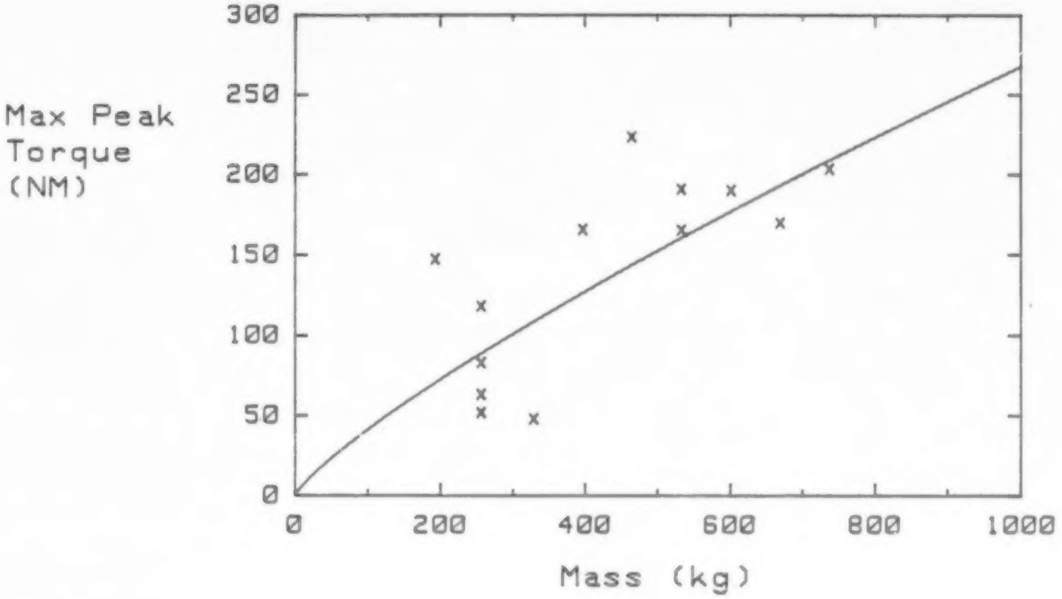

B. LONGITUDINAL ACCELERATION VARIATION

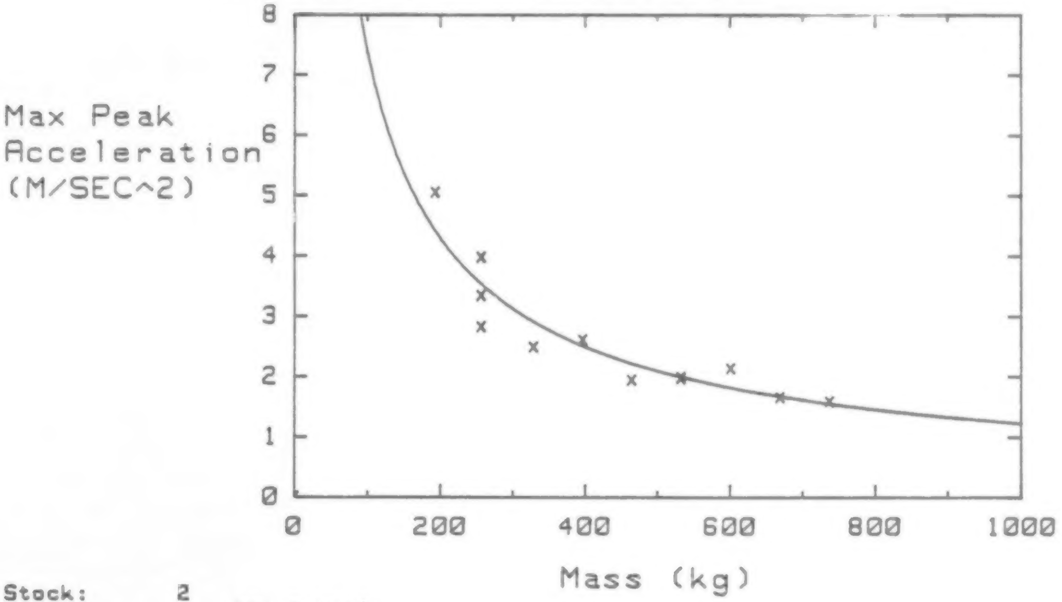

Stock: 2
Ice Block: 6 (22.3 kPa)
Angle: 15 (deg)
Velocity: .37 (M/S)

FIGURE 3.24

RUDDER STOCK TESTS
MASS VARIATION

A. SIDE BENDING MOMENT VARIATION

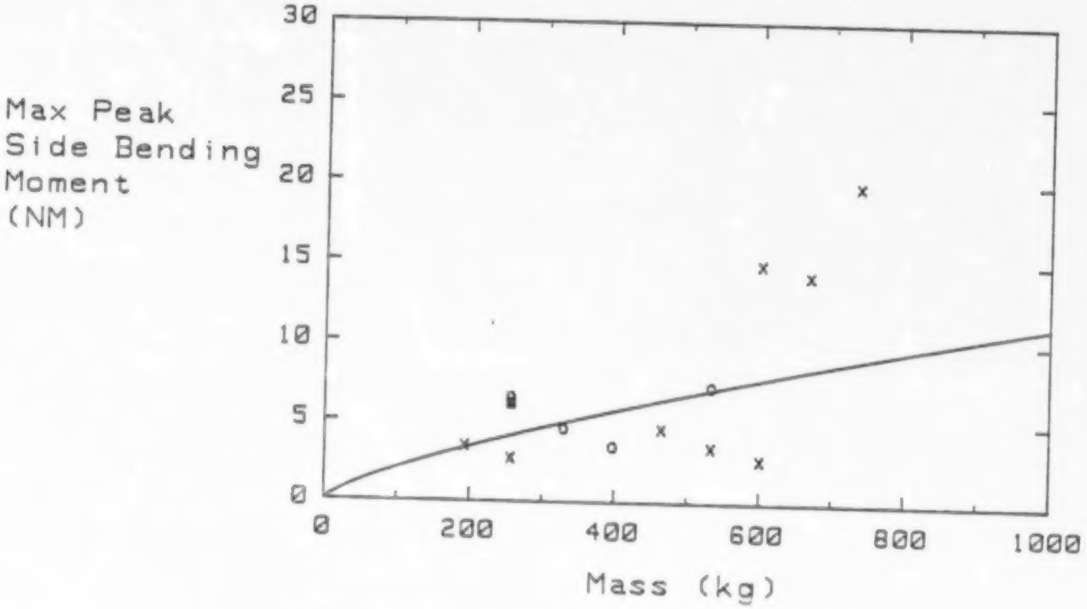

B. FRONT BENDING MOMENT VARIATION

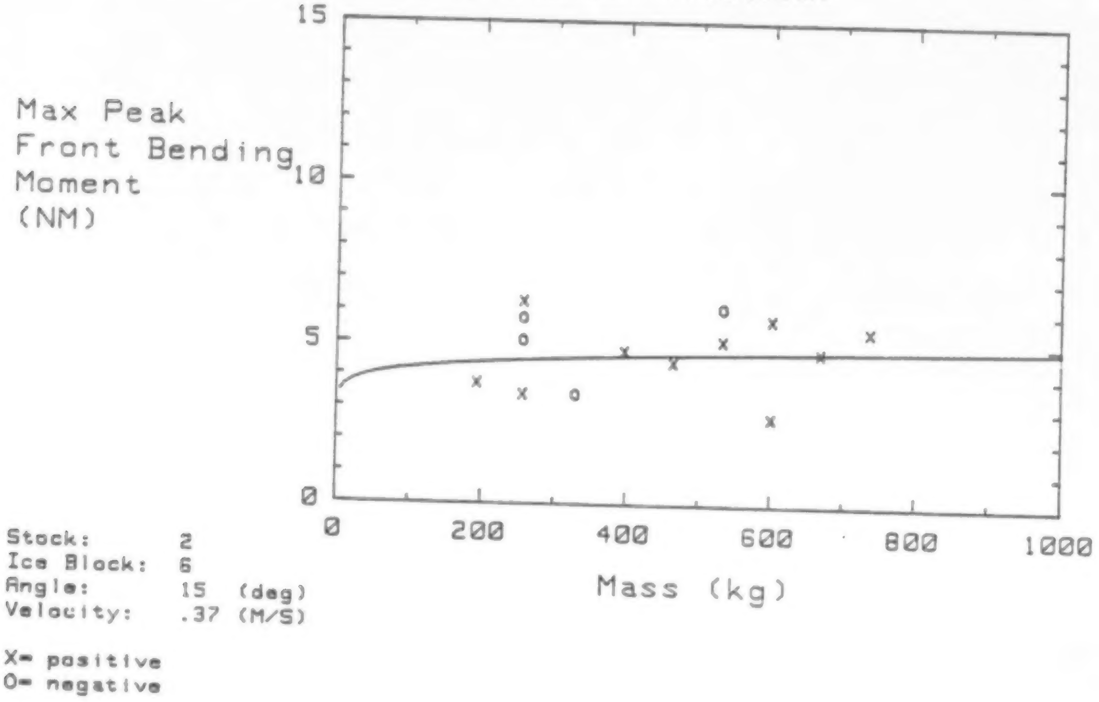

FIGURE 3.25

RUDDER STOCK TESTS
MASS VARIATION

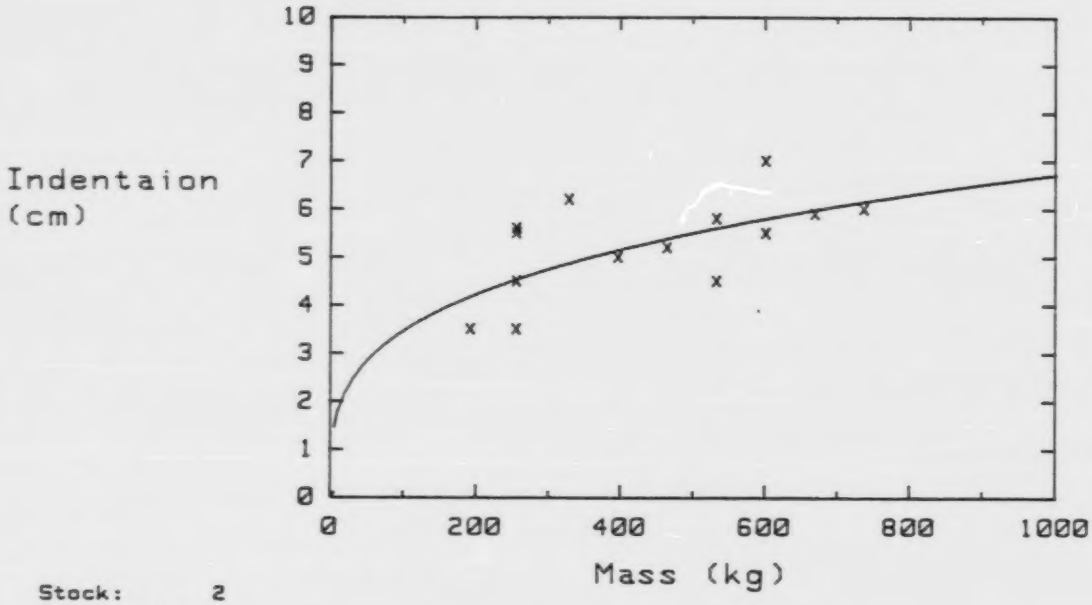

Stock: 2
Ice Block: 6
Angle: 15 (deg)
Velocity: .37 (M/S)

FIGURE 3.26

TESTS
PRESSURE RELIEF VARIATION

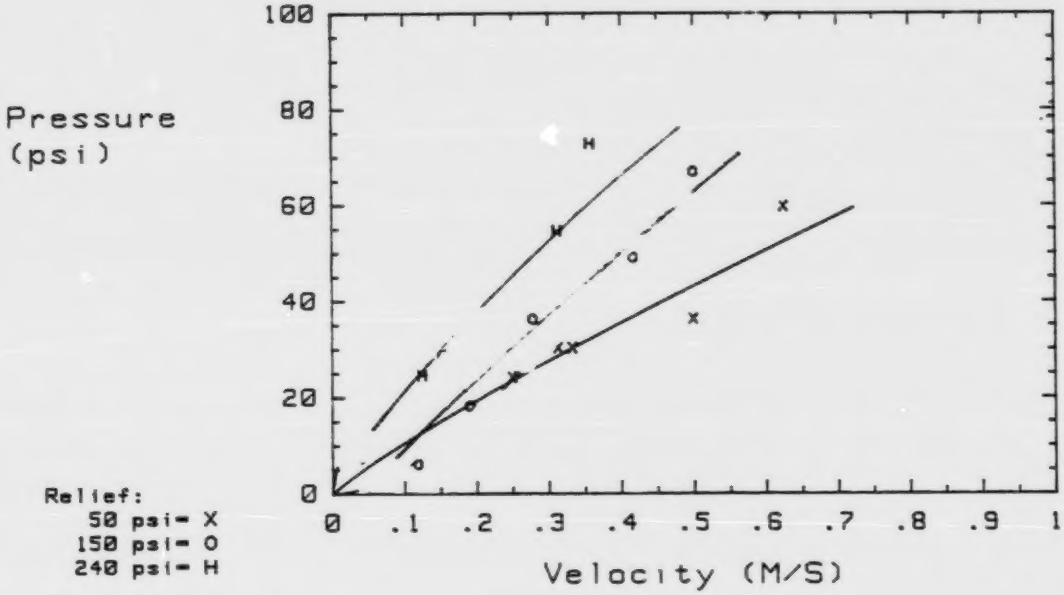

Stock 2
Angle: +/- 15 (deg)
Mass: 256.4 (kg)

FIGURE 3.27

TESTS
PRESSURE RELIEF VARIATION

A. LONGITUDINAL IMPACT VARIATION

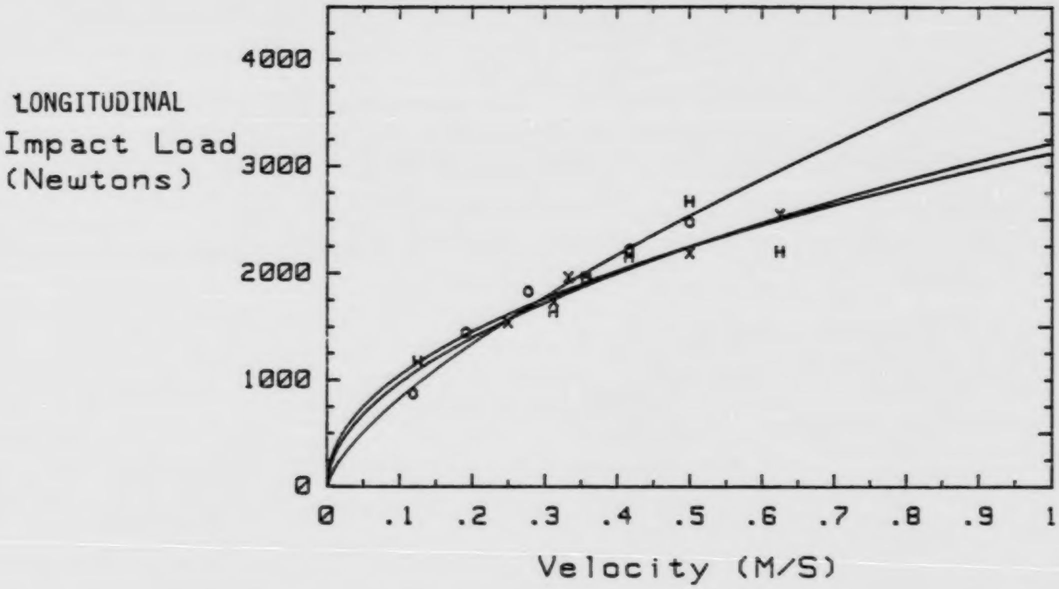

B. TRANSVERSE IMPACT VARIATION

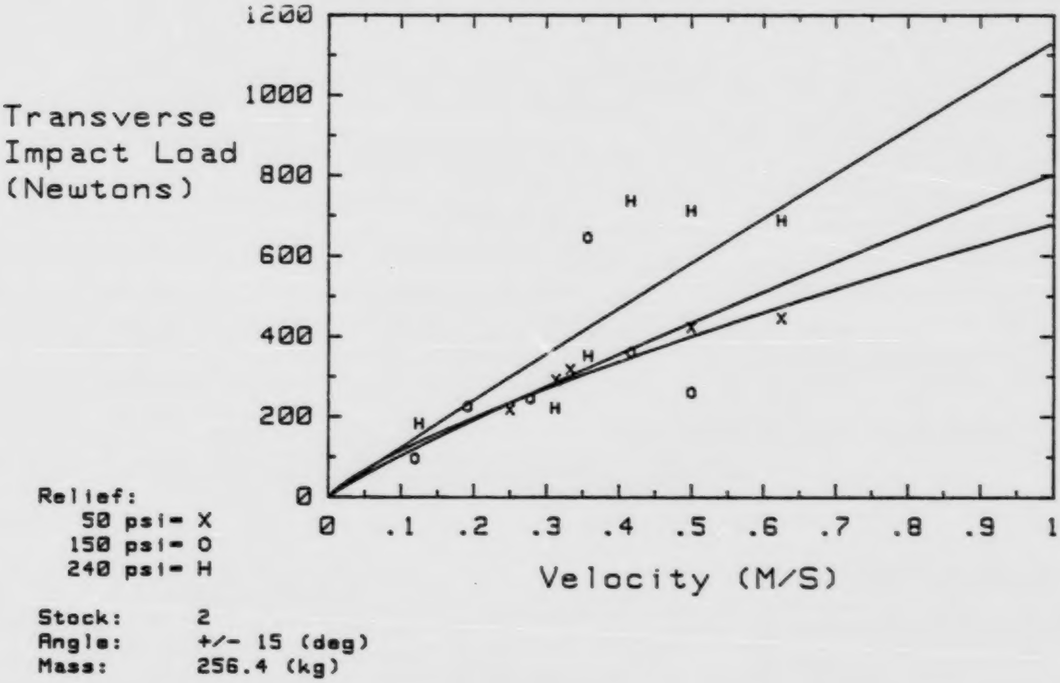

FIGURE 3.28

TESTS
PRESSURE RELIEF VARIATION

A. TORQUE VARIATION

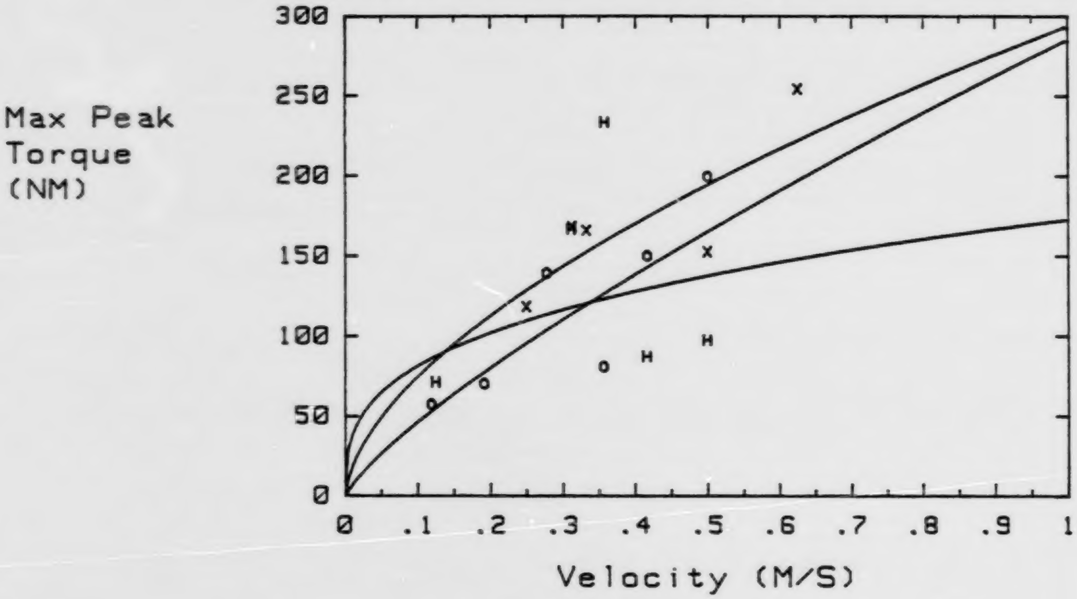

B. LONGITUDINAL ACCELERATION VARIATION

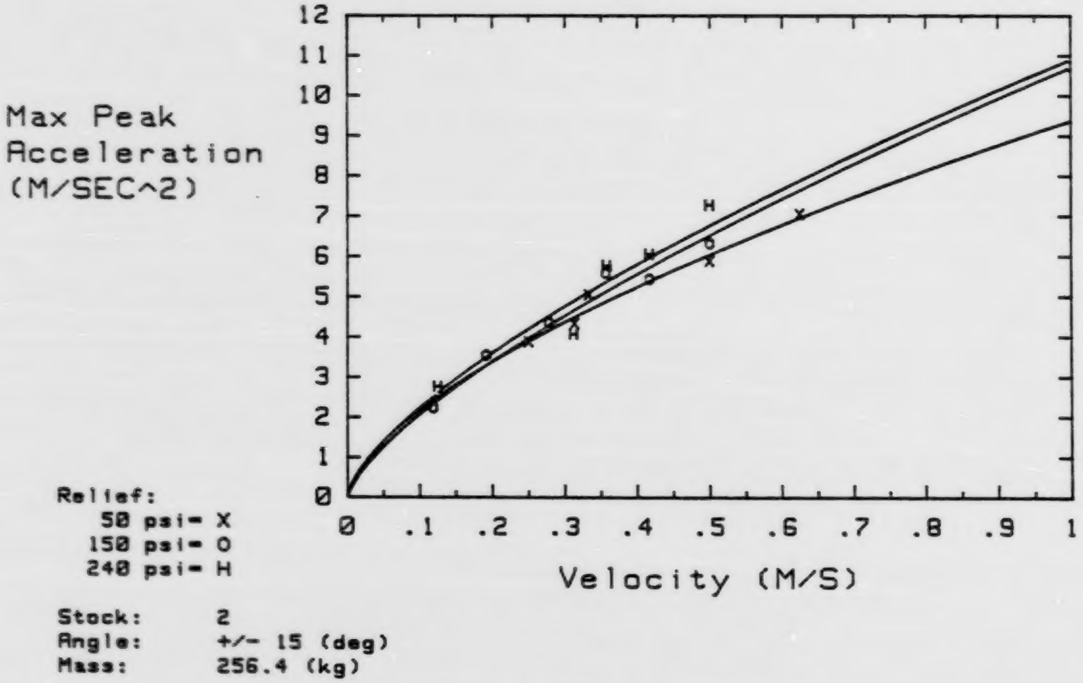

Rudder Stock Stiffness Variation

Three diameters of rudder stock have been tested in order to investigate the influence of stock stiffness on measured torque and bending moments. The stocks were rigidly fixed at the tiller to the moving mass frame. Rudder angle was 15 degrees; mass was held constant at 256 kg and speed was varied up to 0.7 m/s. Weak MODICE from blocks 5 and 8 were used in these tests. Rudder #2 is the stock with dimensions giving the target scaled torsional stiffness. Rudder #1 has a stock diameter which results in a stiffness which is one half of the target value. Rudder 3 had a stiffness which was twice the target value.

The peak acceleration and torsion curves for the three variations of stiffness are shown in Figure 3.28. The maximum stiffness is calculated as twice the target torsional stiffness. The minimum stiffness value is one half of the target. No significant variation with speed was observed. On the other hand, the measured peak torques vary greatly. All three curves are approximately linear with speed. The maximum side bending moments and front bending moments followed similar trends.

The peak torsional response is plotted in Figure 3.29 for the three series of rudder stock tests. For each rudder stock the torque is found to increase approximately linearly with increasing velocity. It appears that the torque decreases quite rapidly with increasing torsional stiffness. At an impact velocity of 0.37 m/s the target stock (Rudder #2) shows maximum torques of about 100 Nm. The doubly stiff Rudder #3 shows torques are reduced to 25 Nm. For the halved stiffness, Rudder #1 is about 475 Nm.

Acceleration is not expected to be affected by changes in the stock diameter. This is shown in Figure 3.29 (b) where all three curves are observed to overlap.

Figure 3.30 shows side bending moment and front bending moment as a function of velocity and rudder torsional stiffness. The results for each stock are plotted using a power regression curve. However, there is sufficient scatter in this data that a linear increase is more justifiable. Both side bending moment and front bending are observed to increase with smaller stock diameters. At 0.37 m/s the smaller diameter stock (Rudder #1) has a side bending moment of 45 Nm and a front bending moment of about 24 Nm. A comparison to the corresponding torque shows that the bending strain to torque ratio is about 0.1 which is similar to that observed for the target stiffness stock. The largest diameter stock (Rudder #3) has a side bending moment of 5 Nm and a front bending moment of about 5 Nm at 0.37 m/s and a rudder angle of 15 degrees. Since the torsional response is significantly reduced at this stiffness, the ratio of bending strain to torsional strain is somewhat larger than for Rudder #2.

FIGURE 3.29

TESTS
VELOCITY VARIATION

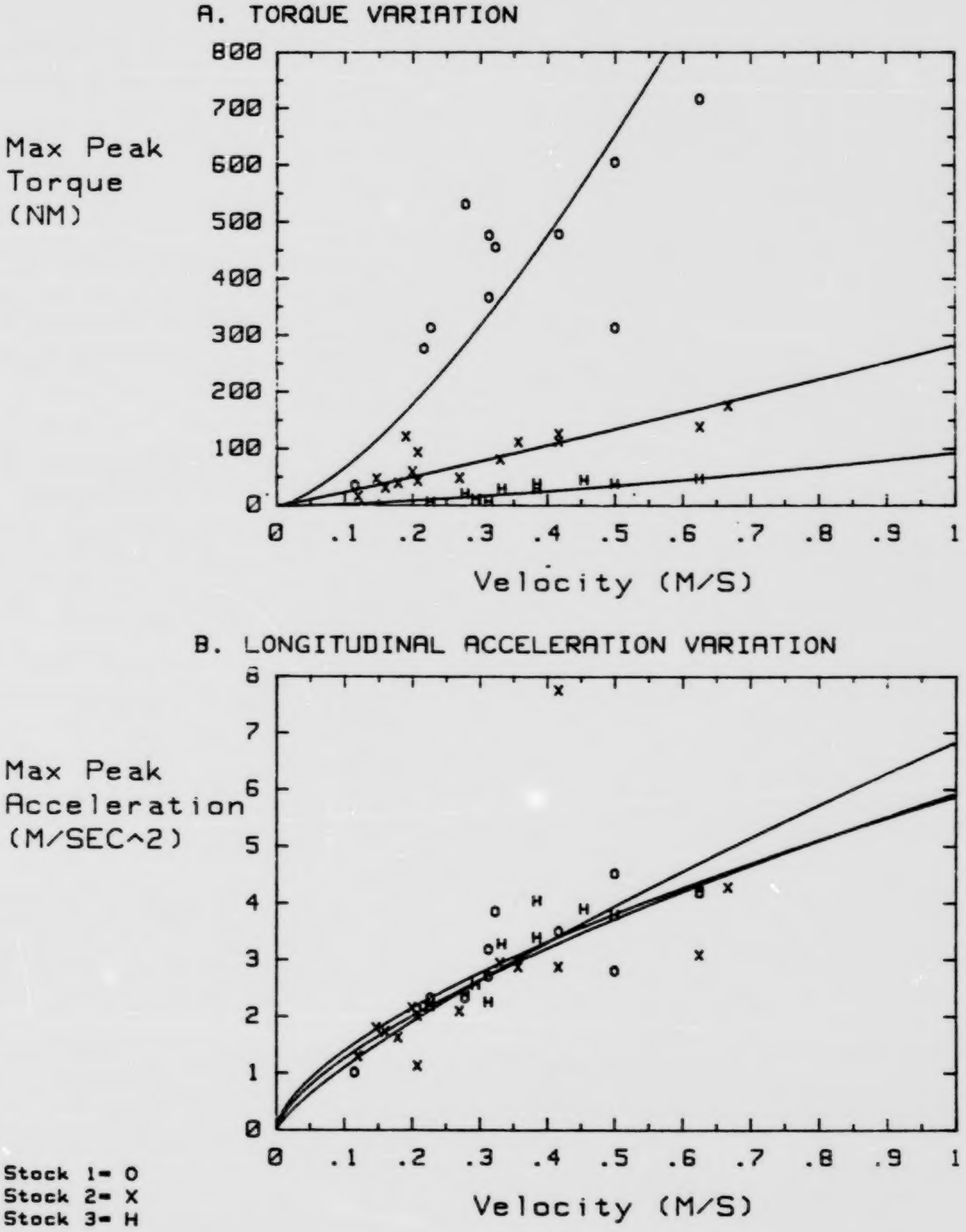

Ice Block: 5,8 (20, 22.3 kPa)
Angle: +/- 15 (deg)
Mass: 256.4 (kg)

FIGURE 3.30

DRY IMPACT TESTS
VELOCITY VARIATION

A. SIDE BENDING VARIATION WITH STOCK TORSIONAL STIFFNESS

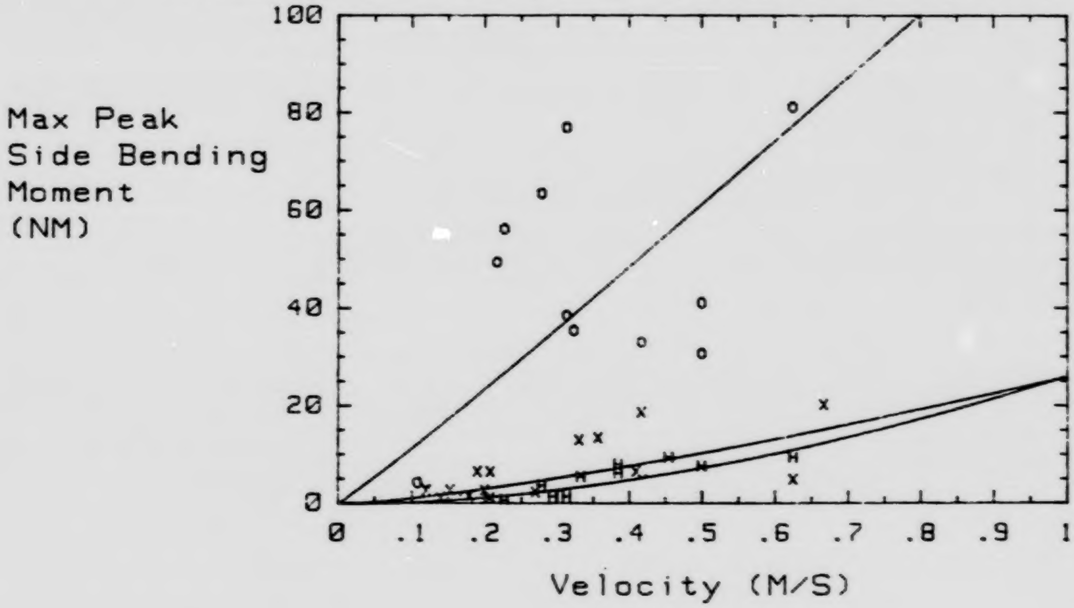

B. FRONT BENDING VARIATION WITH STOCK TORSIONAL STIFFNESS

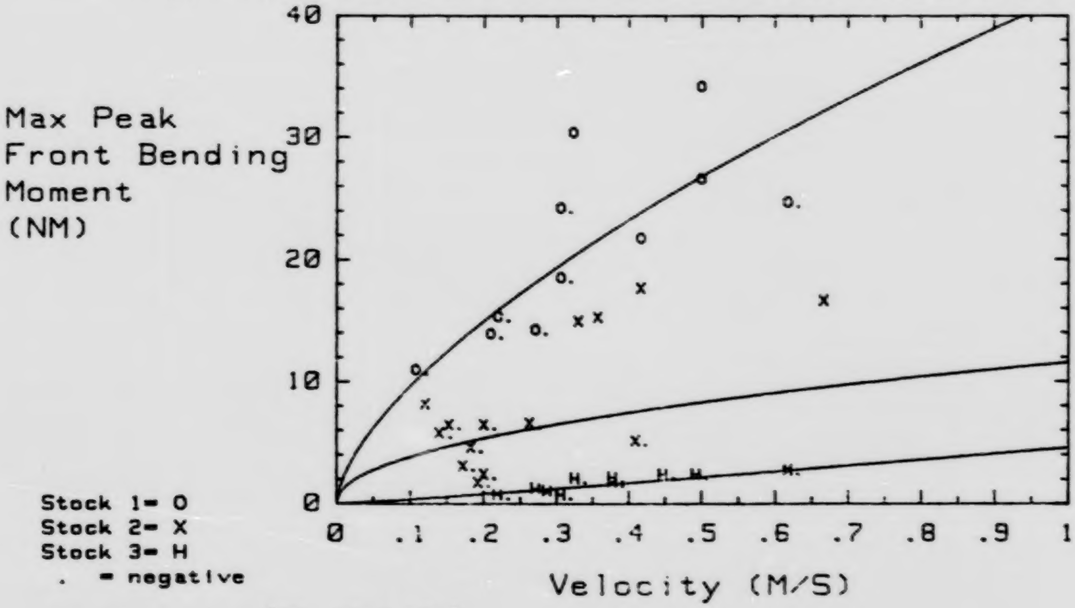

Ice Block: 5,6 (20, 22.3 kPa)
Angle: +/- 15 (deg)
Mass: 256.4 (kg)

3.4 Dry Impact Tests Astern
Results, Remarks and Recommendations

3.4.1 **Dry Impact Astern Tests Results**

An extensive parametric investigation has been carried out using a 1:17 scale model of the rudder assembly of the Canadian Coast Guard icebreaker LOUIS S. ST. LAURENT. The components of the steering system have been physically modelled to permit variation in a range of controlled parameters and to measure ice loads on the rudder, torsional response and bending moments acting on the stock and pressures in the hydraulics control system. The independent parameters tested included: impact, velocity, rudder angle, ice mass, stock torsional stiffness, ice strength and hydraulics release pressure.

Trends in each of the dependent variables have been defined in terms of the independent parameters. The principal results are as follows:

- The influence of ice strength was investigated by means of testing over a range of model scale uniaxial crushing strengths between 20 kPa and 175 kPa. The target ice strength of 53 kPa was defined using an empirical scaling relationship developed at Arctec Canada Limited and assuming that multi-year ice pieces represent the extreme damage scenario for a vessel backing in a broken channel. It was observed that peak rudder loading, longitudinal accelerations, and torsional response increased with ice strength. A one seventh power relationship may be postulated on the basis of results from similar test programs. Indentation appears to decrease exponentially with increasing ice strength. Torque rise times also decrease in a similar manner, although no definitive rise time equation can be established on the basis of these tests.

- The influence of impact velocity has been assessed in many of the tests. Rudder loading and acceleration obey power relationships with respect to velocity, where the exponents are less than one. Variation in torsional response and indentation appear to be nearly linear with velocity. Bending strain does not show any significant change with velocity. Torque rise time is also constant.

- An increase in rudder angle is observed to result in increased rudder loading, up to a maximum near 60 degrees. Torque and longitudinal acceleration are also found to approach maximum values near 60 degrees. The trend appears sinusoidal in form. Indentation decreases at larger angles of impact.

- The influence of ice mass has been studied by means of varying the ballast weight added to the moving box frame which supports the rudder assembly. Rudder loading and indentation increases rapidly up to 200 kg and then are observed to increase slowly and in a linear manner with further mass increases. Torque follows a more linear trend over the range of mass test. However, there is considerable scatter in this data from the lighter mass tests which obscures the overall trend. Longitudinal acceleration decreases inversely with increasing mass. Bending moment does not appear to depend on ice mass; although side bending shows a slight tendency to increase.

- The effect of the hydraulics control system on the loads and torque has been investigated by testing at three settings of hydraulic pressure release. An increase in release pressure was found to result in an increase in maximum pressure difference in the rams during an impact. This affect increased linearly with speed. This suggests that the loading and torque results obtained during the majority of testing, with the tiller rigidly fixed, will be conservative. In normal operation, the pressure build-up in the cylinders would release the tiller, thereby reducing the torque loads and bending moments. However, from the limited set of pressure release data in these tests it has not been possible to further clarify these effects. Trends in axial load and torque are unclear; and transverse load and acceleration show only marginal increases with increase in release pressure.

- The influence of torsional stiffness has been studied by means of comparable testing of three different diameter rudder stocks. Reducing torsional stiffness causes a rapid increase in measured torque, approximately in an inverse squared manner. A similar increasing trend with decreasing torsional stiffness is observed in bending moment. The ratio of bending strain to torque strain was generally less than 0.1 for all of the rudder test configurations, and not significantly affected by ice strength variations.

3.4.2 Remarks on Dry Impact Astern Tests

The applicability of dry impact parametric testing by means of a large scale physical model of a ship rudder assembly has been demonstrated. A large range of operational parameters have been assessed, including the influence of: impact velocity, rudder angle, rudder stock torsional stiffness, ice mass, ice strength and hydraulic pressure release. Sets of time histories of rudder loading, stock bending strains and torsional response have been collected and a corresponding data base of peak values established. This has allowed insights into the rudder/ice interaction process and has provided a starting point from which functional relationships between parameters may be derived. Trends between rudder stock torque and other variables and a range of parameters have been presented.

A limited assessment of the influence of steering gear hydraulic pressure relief on rudder loads and motions has been made as a result of the use of the hydraulic rams and control units. The scaled hydraulics system provided a reasonable representation of the release pressure mechanism and illustrated significant trends associated with steering system hydraulic "stiffness". In particular, it showed that the fixed tiller tests represented a conservative loading condition, and that the effect of pressure relief variation was velocity dependent. However, it should be noted that there was no attempt to incorporate feedback control into this hydraulic model. Additional physical modelling using a more complete hydraulics model is needed to study the influence of the pipe orifice diameter, the response and the pumping rate of fluid during pressure release situations.

The data generally represent extreme impact conditions since the test conditions involved large ice masses, full depth ice contact with the rudder edge, large rudder angles, and strong ice. Excepting contact depth, a range of each of these parameters has been tested, which allows extrapolation to less extreme scenarios. However, it is difficult to predict torsional response for ice masses which are less than 5 percent of the LOUIS S. ST. LAURENT displacement because of the rapid increase of torque over the lower range of ice mass. The trends defined in this part of the study form the basis for parametric equations which will lead to a realistic validation of the mathematical model of overall rudder torsional response and to more rational design criteria.

3.4.3 Recommendations Regarding Dry Impact Astern Tests

Detailed Analysis

The present analysis of the 'dry mode' impact data has identified the significant trends of influence between rudder torsional response and a range of operation parameters. A further analysis effort is necessary to reformulate the data into a dimensionless form and then to extract the individual parametric equations. The preliminary evaluation of peak data by means of polynomial regression (for the figures in the text) has shown that this exercise will yield good numerical results. These relationships will form the basis for a validation of the mathematical model of rudder/ice interaction. For numerical modelling, added mass effects must also be included. In addition, model scale data should be correlated with available full scale LOUIS S. ST. LAURENT trials data.

An important aspect of this process is ensuring that model ice strengths adequately reflect the prototype situation. This necessitates a statistical interpretation of the ice strengths and piece-size distribution that the rudder will see. The refinement of results involves:

1. Development of a non-dimensional presentation of the parametric results on the basis of measured ice strength. A 1/7th power relationship for collapsing ice strength has proven a good approximation in related applications using MODICE.

2. Correction of all data to account for deviation from nominal conditions (e.g. speeds, ice strengths).

3. Regression analysis of the accumulated database of non-dimensional results to establish parametric equations. Coefficients will then be corrected to target model ice strength. A rational assessment of the data will then be possible.

4. Correlation to full scale LOUIS S. ST. LAURENT torque trials data. This can be achieved by means of the physical modelling prediction equations.

5. Validation of numerical model (correcting for surge, added mass and other hydrodynamic effects) based on the rationalized parametric equations.

Physical Modelling Task

There were several limitations in the dry impact modelling that resulted in unanswered questions after the present test program. The most serious deficiency was in the range of ice mass. The lower bound on mass in the test range corresponded to approximately seven percent of the LOUIS S. ST. LAURENT displacement. Therefore, only the case of an infinite ship and large ice masses has been treated. Two further cases should be addressed by means of additional testing:

(1) If the stern of a vessel manoeuvring in ice swings into the channel edge, the situation may be considered one of an infinite ice mass and a finite displacement ship. Physical model tests to investigate this case would use an existing ship model backing into a fixed synthetic (MODICE) ice block. Stock torsion would again be modelled. This approach is necessary since it is not possible to support the 1:17 scaled weight of the entire ship in the present experimental apparatus. Other vessels may also be examined in this manner to establish reference comparisons between the dry impact parametric equations and 'wet mode' self propulsion model tests.

(2) If the ice floe mass drops below seven percent of the LOUIS S. ST. LAURENT displacement, the present interpretation of the two body impact problem does not change. The same experimental apparatus may be used to investigate the lower range of ice mass. However, the box frame which constitutes a major part of the mass would have to be redesigned and fabricated out of a lighter material to reduce its minimum, unballasted value.

Other areas in which the dry impact database may be expanded include variation in rudder tip geometry and depth of contact with the ice. Both of these recommendations address the question of the influence of pressure-area effects on rudder loading.

In the process of conducting the 'dry mode' tests and analyzing the results, several additional physical modelling tasks have been identified as leading to an improved understanding of the rudder/ice impact problem.

1. The dry mode impact tests have addressed the case where ice masses are finite and the ship is infinite. The case where the ship mass is smaller than or equivalent to the ice mass must also be included, since it represents an extreme damage condition. Further experimental work should study ship models backing into infinite ice:

i) To define the influence of displacement; which provides an anchor point in correlating dry mode tests to wet tests and in correlating model data and full scale results.

ii) To address the problem of added mass and fluid stress effects. This influence may be calculated approximately and inserted into the model validification process - however, it is better to use measurements where possible.

Existing models, such as the POLAR 8, LOUIS S. ST. LAURENT and MV ARCTIC may be tested with scaled stocks.

2. Another scenario that has not been addressed is the case where ice masses are much smaller than 10 percent of ship displacement. This is the normal operating regime for ships in the broken channel. However, the relationship between torque and mass is not well defined in this region. Testing with the present apparatus could be used provided that the moving mass frame is redesigned to reduce its unballasted weight.

3. The influence on torque of the depth of contact between the rudder and ice face has not been identified. The specific pressure-area relationships and scale effects governing the importance of contact depth should be investigated experimentally. This involves a systematic variation of rudder contact length and tip geometry.

Hydraulics Modelling Task

Hydraulic control of the steering gear and its influence on the rudder loads and stock torque has been introduced in this work. However a concerted modelling effort must be carried out to incorporate this element within the numerical model and to provide guidelines on its use in protecting the steering system.

Another aspect of improved physical modelling involves the development of a more complete hydraulic steering gear. This necessitates further work on the modelling of fluid flow rates in the cylinders and orifices of the control unit. In addition, scaled feedback control should be incorporated into the hydraulic control system.

1. Detailed physical modelling of a scaled hydraulics system should include:
    - (i) Scaling of Ram/cylinder dimensions
    - (ii) Refinement of valve orifice scaling to provide a correct flow rate
    - (iii) Auto feedback control of hydraulic pumping
    - (iv) Redesign of tiller arrangement to improve rotational inertia characteristics during impact response.
2. Other instrumentation changes are required to extend the model's capability for investigating the influence of released rudder motions and consequent forces on various structures. This includes studies of:
    - (i) Foundation stresses, and
    - (ii) Loads on rudder stops

4. ICE BASIN TOWED MODEL TESTS

4.1 Background

The purpose of the towed tests (rudder vulnerability test) was to determine if the rudder installed on the model with the model operating at the DWL, would be vulnerable to ice impact damage during normal manoeuvring operations. The method was to tow the model at various drift angles (drag the model at various headings not parallel to the length of the basin) with the rudders hard over. In order to account for the influence of propeller thrust on the frequency and magnitude of ice impacts on the rudders, the ahead towing tests were conducted with all screws full power ahead, and the astern tests were carried out at half power. As the direction of propeller rotation plays an important role in ice loads embodied on propellers and rudders, due consideration was given to this factor. Past experience with model tests of multiple-screw hulls [3] have shown that outboard turning screws produce less ice ingestion in the propellers and rudders in the astern model of operation. This has also been reported by similar outside investigations (see, for example, reference [4]). All rudder vulnerability tests have been carried out with outboard turning screws in astern towed tests. During these tests the rudders were instrumented to measure rudder torque.

4.2 Test Objectives

The towed test program was developed to investigate a range of operational parameters which influence the frequency of ice impacts with the rudder. Three ship models were identified with the requisite bow forms and stern configurations. The MV ARCTIC is a large ice class bulk carrier/OBO with a single screw and single rudder. The PIERRE RADISSON is an existing Canadian Coast Guard icebreaker with twin screws and a single rudder. The POLAR 8 hull represents a proposed design for a Arctic Class 8 icebreaker. This model has triple screws and a single rudder.

The objective of the towed tests in broken floes was to determine the degree of rudder vulnerability to ice impacts during normal manoeuvring operations. Generally in ahead tests the rudder was 'hardover' at 35°. In order to account for the influence of propeller thrust on the frequency and magnitude of ice impacts on the rudder, the ahead tests were conducted with the screws full power ahead. The astern tests were carried out at half power. As the direction of propeller rotation plays an important role in ice loads on rudders and propellers, due consideration was given to this factor. The usual mode of testing was with wing screws turning outboard in the ahead mode.

4.3 Scope of Test Program

Three similar groups of self-propulsion tests were planned and carried out involving the three models. In the case of the MV ARCTIC tests, an additional set of tests was included at a different ice thickness. Four ice sheets were used, the thicknesses of which corresponded to the maximum ice thickness for continuous icebreaking for these vessels. Each test group consisted of numerous repetitions of forward and astern trials in pre-cut floes with known dimensions. The initial tests involved breaking along a herringbone pattern, which had been formed by 45° cuts outward from the ice basin centerline.

A large range of operating parameters was investigated, including the influence of ship form, forward speed, astern speed, rudder angle, propeller thrust level and direction of rotation, ballast condition (draft), ice thickness and floe size. The principal parameters measured were frequency of impact and rudder torque.

Towing tests were performed on three ship models to determine the frequency and relative severity of rudder/ice impacts. These tests were carried out in level, unbroken ice and in broken floes. Baseline tests were also carried out in open water. The latter tests were carried out to determine the reference hydrodynamic loads on the rudders. Ahead and astern tests were performed at two model speeds, two propeller rpms, two rudder angle settings, two drift angles and two drafts. A description of these variables is given in Table 4.1. A total of 36 tests were performed for each rudder configuration and ice thickness. A typical test matrix is shown in Table 4.2.

TABLE 4.1

INDEPENDENT TEST VARIABLES

ICE SHEET:	- continuous mode thickness
	- upper limit thickness
DRAUGHT:	- fully loaded
	- light loaded
DRIFT ANGLE:	- zero drift, straight course
	- 5° drift angle, simulating turning of ship
SPEED:	- ahead, full speed
	- ahead, half of full speed
	- astern, nominal speed
	- astern, half nominal speed
SHAFT SPEED:	- RPM, required to maintain speed
	- RPM, propellers trailing (vindmilling)
RUDDER ANGLE:	- midship
	- 35° to starboard (ahead testing)
	- 10° to port (astern testing)
ICE CONDITIONS:	- level ice
	- broken floes, large floe size
	- broken floes, small floe size
	- rubble pile

TABLE 4.2

TYPICAL TEST MATRIX

A = AHEAD
B = BACKING
BF = BROKEN FLOES
CH = CHANNEL
LU = LEVEL UNBROKEN
RI = RAFTED AND IRREGULAR ICE

SHEET NO.	TEST NO.	ICE COND.	DRAUGHT COND.	DRIFT ANGLE	RUDDER ANGLE	SPEED KNOTS	THRUST LEVEL	STANDARD CASE
1	1A	LU	D	0	35S	2	FF	
	2A	BF	D	0	35S	6	FF	X
	3A	BF	D	0	35S	6	TF	
	4A	BF	D	5S	35S	6	FF	
	5A	BF	D	0	35S	3	FF	
	6A	BF	D	0	35S	6	FF	X
	7A	BF	D	0	35S	6	TF	
	8A	BF	D	5S	35S	6	FF	
	9A	BF	D	0	35S	3	FF	
	10A	BF	D	0	35S	6	FF	
	11A	BF	D	0	35S	6	TF	
	12A	BF	D	5S	35S	6	FF	
	13A	BF	D	0	35S	3	FF	
	14A	BF	L	0	35S	6	FF	
	15A	BF	L	0	35S	6	TF	
	16A	BF	L	5S	35S	6	FF	
	17A	BF	L	0	35S	3	FF	
	18A	RI						
	1B	CH	D	0	0	3	FB	
	2B	BF	D	0	0	3	FB	X
	3B	BF	D	0	0	3	TB	
	4B	BF	D	0	10P	3	FB	
	5B	BF	D	0	0	1.5	FB	
	6B	BF	D	0	0	3	FB	X
	7B	BF	D	0	0	3	TB	
	8B	BF	D	0	10P	3	FB	
	9B	BF	D	0	0	1.5	FB	
	10B	BF	D	0	0	3	FB	
	11B	BF	D	0	0	3	TB	
	12B	BF	D	0	10P	3	FB	
	13B	BF	D	0	0	1.5	FB	
	14B	BF	L	0	0	3	FB	
	15B	BF	L	0	0	3	TB	
	16B	BF	L	0	10P	3	FB	
	17B	BF	L	0	0	1.5	FB	
	18B	RI						

4.4 Models and Modelling Criteria

4.4.1 **Ship Models**

The model configurations which were tested are given below:

- Single screw, single rudder - MV ARCTIC
- Twin screw, single rudder - CCGS PIERRE RADISSON
- Triple screw, single rudder - POLAR 8

For comparison purposes, the principal particulars of these models are shown in Table 4.3. The first two models used were built of wood and were provided on loan by NRC/IMD of St. John's, Newfoundland. The third (POLAR 8 hull form) also made of wood was available in-house. The two NRC models came in two halves with water-tight bulkheads and complete appendage assembly. The fibreglass nozzle on the MV ARCTIC model required adjustments prior to fitting propulsion gear. Although the propeller on the ship is controllable pitch, the model's propeller had a fixed pitch of 20.44 degrees.

4.4.2 **Modelling Criteria**

If the model propellers produce the correct model thrust, the propeller flow field in the model will closely scale that of the full sized vessel, since propeller diameter, vessel speed and developed thrust are correctly modelled. The model ice density, friction and size are analogous to full size. An irregular object in a flow field is primarily actioned on by dynamic forces (ρAV^2 type) and, if the mass flow through the propeller is correctly scaled, so too will be the flow field velocities. Thus all the requirements necessary for correctly scaling the ice ingestion and ice impact problems are met, with the exception of viscous forces, which are assumed to be of minor importance.

TABLE 4.3

TOWED TEST MODEL PARTICULARS

MODEL	NAME	PROPELLER CONFIGURATION	RUDDER CONFIGURATION	MODEL SCALE	MODEL LENGTH (m)	BREADTH (m)	DRAFT DEEP (m)	DRAFT LIGHT (m)
1	MV ARCTIC	SINGLE SCREW IN NOZZLE	SINGLE RUDDER	1/30	6.55	0.763	0.367	0.305
2	RADISSON	TWIN SCREW	SINGLE RUDDER	1/20	4.397	0.968	0.347	0.254
3	POLAR 8	TRIPLE SCREW WITH CENTRE NOZZLE	SINGLE RUDDER	1/40	4.49	0.764	0.305	

4.5 Ice Basin Test Set-Up

An identical outfitting procedures has been followed in preparing each of the three models for testing. In this section, the means by which the test parameters were set up and varied is described. Each model was instrumented to measure:

- Propeller shaft RPM
- Carriage position and speed
- Rudder torque
- Thrust difference (under/over-propelled).

These parameters were digitally sampled during a test. Rudder angle, drift angle, ice floe thickness and floe size were manually recorded. A video recording of ice impacts on the rudder was obtained by means of an underwater camera system. In addition, a limited set of 35 mm slides were taken from an overhead gantry. Above water colour video was used to document the test series.

4.5.1 Rudder Torque

The torque resulting from ice loading impacts on the rudder was the main observable variable. It was determined using the arrangement shown in Figure 4.1.B. A force block measured the force acting perpendicular to a 50 mm tiller arm. The tiller was positioned on the model's stern post using set screws. Since it was necessary to maintain the perpendicular orientation between the tiller arm and the force block over a range of rudder angles; a series of pre-drilled holes were bored into the stock stern post. This allowed easy re-attachment of the tiller arm. The torque was defined as the product of the measured force and the tiller arm length.

FIGURE 4.1
TOWED TESTS EXPERIMENTAL SET-UP

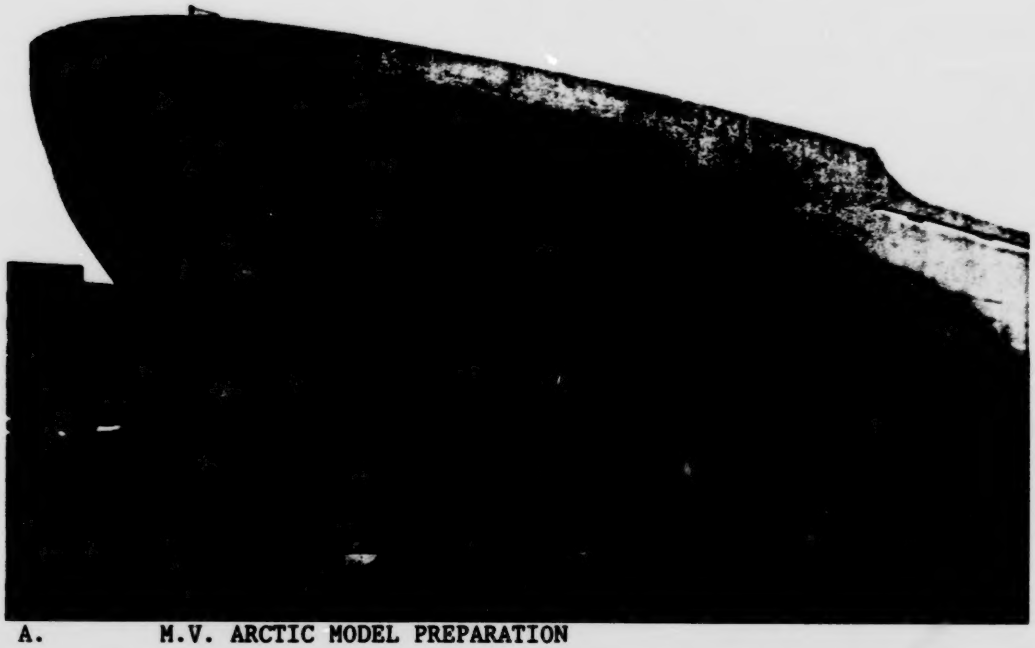

A. M.V. ARCTIC MODEL PREPARATION

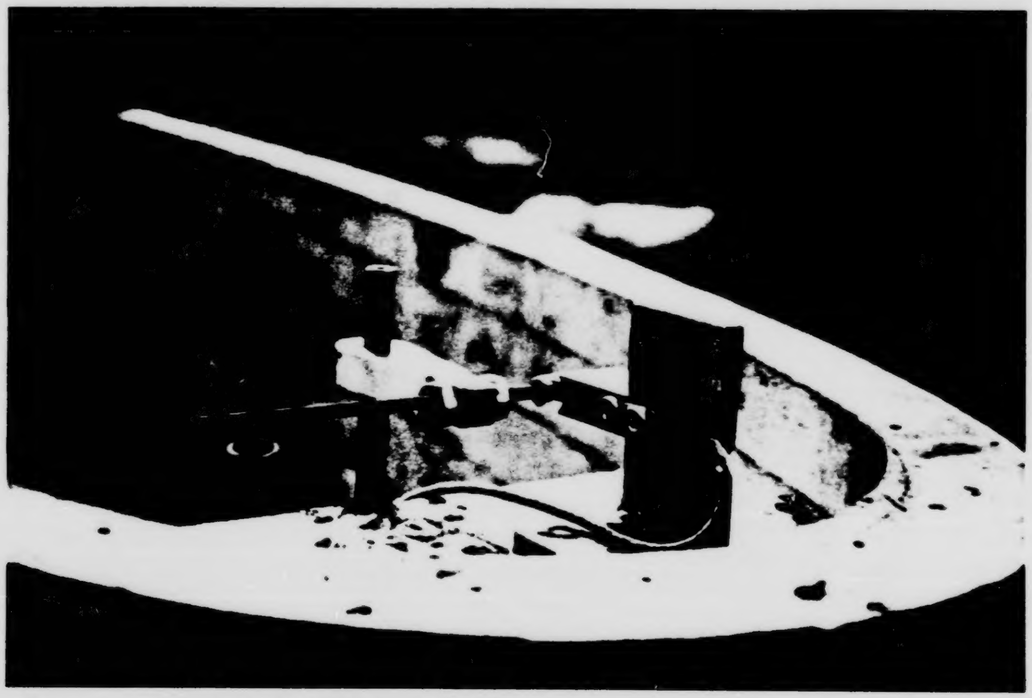

B. TORQUE MEASUREMENT SYSTEM

4.5.2 Propeller Shaft RPM

The propellers were driven by a variable speed DC electric motor. Shaft speed was set prior to each run to provide the required thrust levels. In the case of the two and three shaft models the shafts were connected together by chains and sprockets so that all shafts ran at the same RPM. Reversing of one wing shaft was accomplished through a lay shaft and an alternate chain drive. The propeller shaft rotational speed was measured using a tachometer which gave a voltage signal proportional to the RPM.

4.5.3 Model Speed and Drag

The models were attached to the towing carriage by means of a heavestaff which was located approximately one third of the overall length aft of the bow. The heavestaff allowed freedom to heave, pitch and roll without restraint. It is illustrated in Figure 4.2. Force in the direction of carriage movement was measured by a force block mounted on the heavestaff. The model speed and position were measured by a transducer mounted in the carriage drive machinery.

4.5.4 Drift Angle

In usual towed tests the heavestaff permits the model to yaw without restraint. However, in the present tests, the model was held at a steady yaw angle by a yaw restraint at the stern of the model. This yaw restraint consisted of a wire connecting the centerline of each model with the carriage at the basin wall. The yaw angle could be varied by altering the length of each side of the yaw restraint, while the yaw angle itself was measured by measuring the difference between distance the stern of the model was from the side of the basin and the heavestaff position.

4.5.5 Data Acquisition

The signals from the rudder torque, shaft speed, towing force and carriage position/speed transducers were amplified and recorded both by a 28 channel FM tape recorder and by a digital data acquisition system. The digital system stored the data on 8 inch flexible disks for analysis while the tape recorder provided backup.

FIGURE 4.2 SCHEMATIC of TOWING ARRANGEMENT

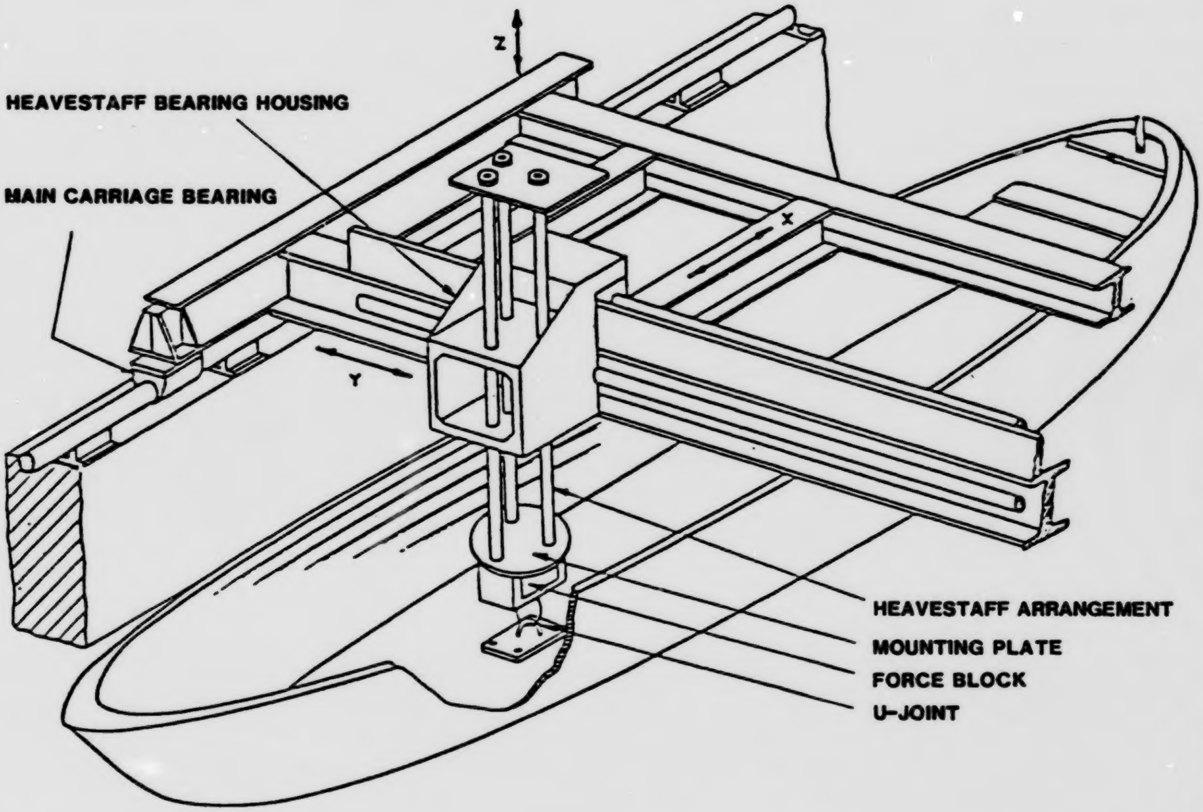
Z
HEAVESTAFF BEARING HOUSING
MAIN CARRIAGE BEARING
X
Y
HEAVESTAFF ARRANGEMENT
MOUNTING PLATE
FORCE BLOCK
U-JOINT

4.6 Test Procedure

In general the same test procedure was followed for all three stern configurations. The single rudder, single propeller MV ARCTIC model was tested in two ice sheets of different thicknesses while the two propeller single rudder "RADISSON" model and the three propeller single rudder "POLAR 8" model were tested in only one ice sheet each.

4.6.1 Bollard Testing

In order to obtain the correct thrust levels required for each type of test, ahead and astern, zero thrust and full thrust, a curve of propeller RPM versus thrust was obtained for all three models. This test was performed with the model secured to the towing carriage at the heave staff and with the yaw restraint holding the model straight. The rudder was set to a dead ahead position and the shaft speed was stepped through a series of increasing RPM. The thrust developed by the propellers was measured at the heavestaff force block enabling a curve of thrust versus shaft RPM to be plotted. This curve was necessary because the thrust from the model propellers could not be calculated with sufficient accuracy. The thrust curve obtained from the bollard test enabled the correct shaft RPM to be chosen for each testing mode.

4.6.2 Open Water Testing

Following the bollard trials each model was run through a full set of trials in open water similar to the actual ice testing. The purpose of these tests was to obtain the hydrodynamic loads resulting from the testing but without the ice impacts. These loads provide a reference to which model drag and rudder torque, obtained during ice testing, can be compared to determine the additional loads resulting from the presence of ice.

4.6.3 Level Ice Testing

Prior to the first test in each level ice sheet, a channel was precut along the ice basin centerline to provide a regular formation of ice pieces. This was done in a herringbone fashion as shown in Figure 4.3 so that the ice pieces broke at their characteristic length. The characteristic length is determined by the thickness and density for any material supported on a floating foundation, according to the formula in Table 4.4, together with the characteristic length and channel width cut for each ice sheet. Channel widths were set at 1.1 times the model breadth.

FIGURE 4.3

PRE-SAWN PLAN

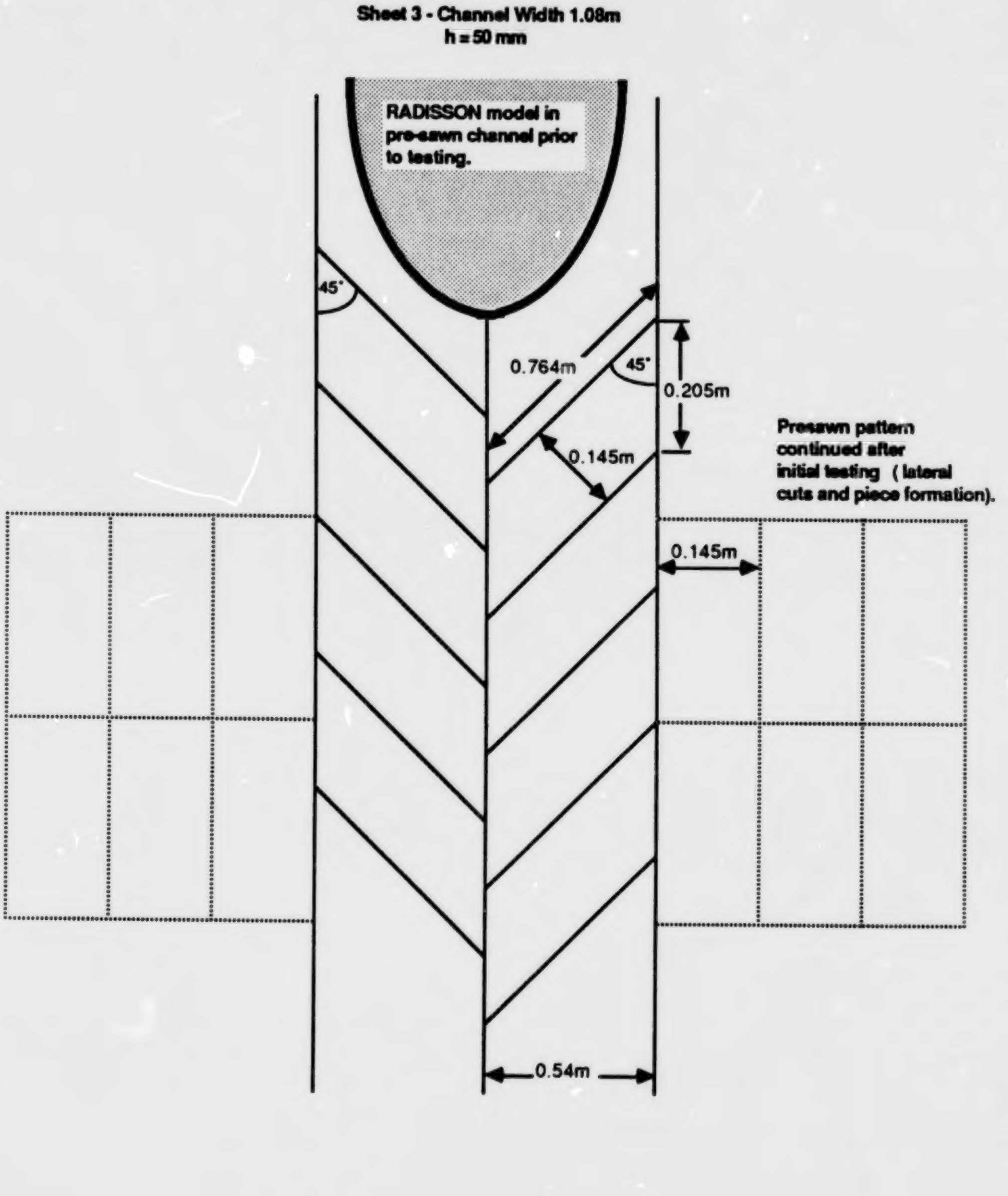
Sheet 3 - Channel Width 1.08m
h = 50 mm
RADISSON model in pre-sawn channel prior to testing.
45°
45°
0.764m
0.205m
0.145m
Presawn pattern continued after initial testing (lateral cuts and piece formation).
0.145m
0.54m

The separation of cuts was determined by the characteristic length. The second test run involved backing in the broken channel formed by the first test. The entire ice surface was then cut into pieces corresponding to the model's characteristic cusp length. All subsequent runs in a test series were in the nominally identical piece size distribution. However, the mean size gradually became smaller as a result of interaction between the floes and the ship, as well as by ingestion of ice into the propellers. For this reason it was necessary to stagger the repetitions of a particular test condition, so that the mean ice piece size of each grouping of similar tests would be equivalent.

During the level icebreaking test, the model was started approximately 0.1 ship lengths from the ice edge to permit acceleration to test speed before entering the ice sheet. The run then continued over the length of the basin while data was recorded through the force blocks and by the video camera. A single run at full thrust was made in the ahead direction. Figure 4.4 shows the POLAR 8 positioned for testing in the precut pattern and during icebreaking.

4.6.4 Broken Channel Testing

Following the level ice test the remainder of the ice sheet was cut into regular sized and shaped pieces, with a width equal to the characteristic length. These pieces were arranged over the basin to provide about 8 - 9 tenths ice cover in the broken channel directly in the model path. The model tended to push the ice ahead of it thus creating a higher concentration than intended unless steps were taken to prevent this. After each run the ice was re-arranged before the next run.

Thirty-four tests were performed on the single propeller MV ARCTIC model. A similar series of tests were carried out for the RADISSON and POLAR 8 models. Six additional tests were performed on the two and three screw sterns, with opposing thrust on the wing screws. These tests were intended to simulate typical operating conditions of such a ship when turning in ice.

Each test was run in the same manner as the open water and level ice testing. The rudder angle, yaw angle, and shaft speed were set before each run, then the model and carriage accelerated to the desired test speed. Zero readings of all measured parameters were taken before and after each run. Video and still photographs were taken during the astern runs, but only video was shot during the ahead runs. This was done in order to obtain a record of the number and size of floes entering the stern area of the model when going astern.

TABLE 4.4

ICE SHEET CHARACTERISTICS

CHARACTERISTIC LENGTH FORMULA

$$l_c = \left(\frac{Eh^3}{12(1-\nu)\gamma}\right)^{1/4}$$

$E = 2$ GPa

$\gamma = 10$ kN/m^3

$\nu = 0.3$

SHIP	ICE THICKNESS FULL SCALE m	ICE THICKNESS MODEL SCALE mm	CHARACTERISTIC LENGTH m	SHIP BREADTH MODEL m	CHANNEL WIDTH m
MV ARCTIC	2.1	70	0.676	0.763	0.84
MV ARCTIC	1.2	40	0.44	0.763	0.84
RADISSON	1.0	50	0.5815	0.968	1.065
RADISSON	1.6	80	0.827	0.968	1.065
POLAR 8	3.6	90	0.19	0.764	0.840

FIGURE 4.4
ICEBREAKING TEST IN PRE-CUT ICE

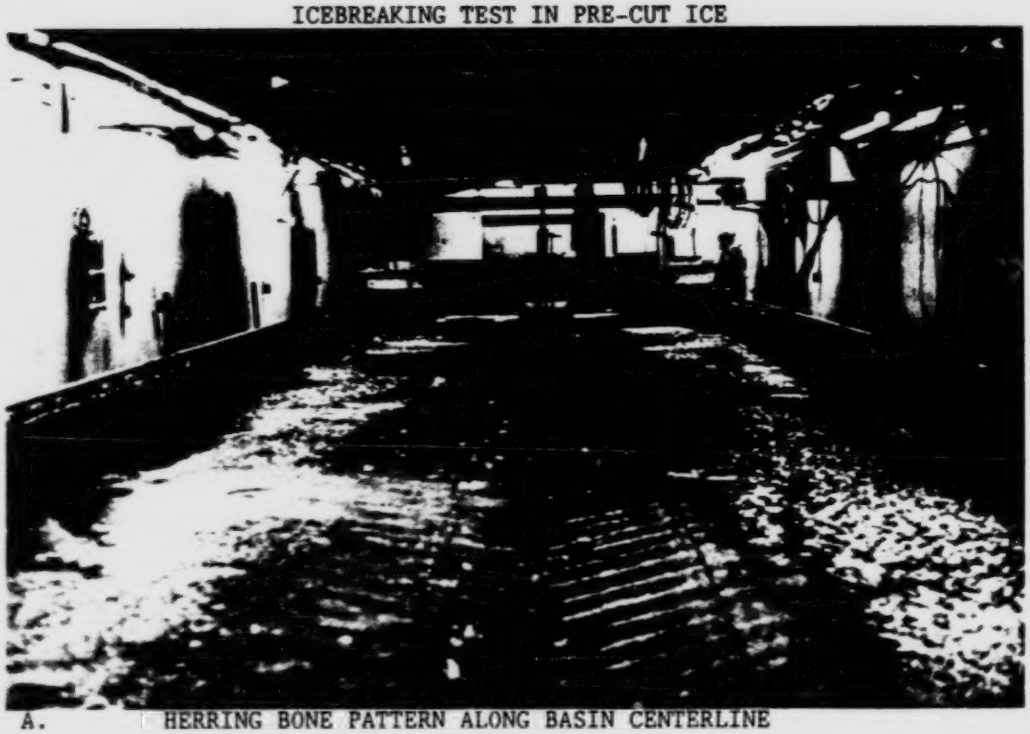

A. HERRING BONE PATTERN ALONG BASIN CENTERLINE

B. POLAR 8 FIRST TEST: BREAKING PRE-CUT ICE

4.6.5 Photographic Documentation of the Towed Tests

The relative effectiveness of the three stern configurations can be assessed if a visual observation can be made of the stern region of the models during ice operations. This was achieved by means of a time-scaled colour video of the underwater portion of the stern of the model as it was towed through the broken field. A colour video camera installed inside a water-tight housing was used to view the ice-rudder interactions. The underwater camera housing was mounted (approximately one metre on the port side of the model) on an auxiliary carriage moving along the rails on the basin floor. This carriage is fixed relative to the main towing carriage so that the camera always had the stern of the model in view with the rudder clearly in the middle. A grid placed on the rudder divided it into approximately 40 cm^2 squares was used to observe the impact location of the ice floe on the rudder.

A general view of the stern of the model and the ice floes either emerging behind the model when moving ahead or being drawn into the rudder and propeller while going astern was recorded using an overhead camera. This camera was mounted approximately two metres above the ice cover and 0.1 m behind the stern looking directly downward. It was controlled by an automatic timer so that an overlapping series of photographs could be taken during each test. Figure 4.4 and Figure 4.5 show typical distributions of ice pieces around the stern during backing manoeuvres.

Figure 4.6.A shows the broken channel astern of the RADISSON during ahead testing. Figure 4.6.B provides an underwater view of ice pieces interacting with the rudder during astern manoeuvres. Two ice pieces in the photograph have been up-ended and forced downward along the stern and into the rudder.

FIGURE 4.5
ICE FLOE DISTRIBUTION IN PRE-CUT BROKEN CHANNEL

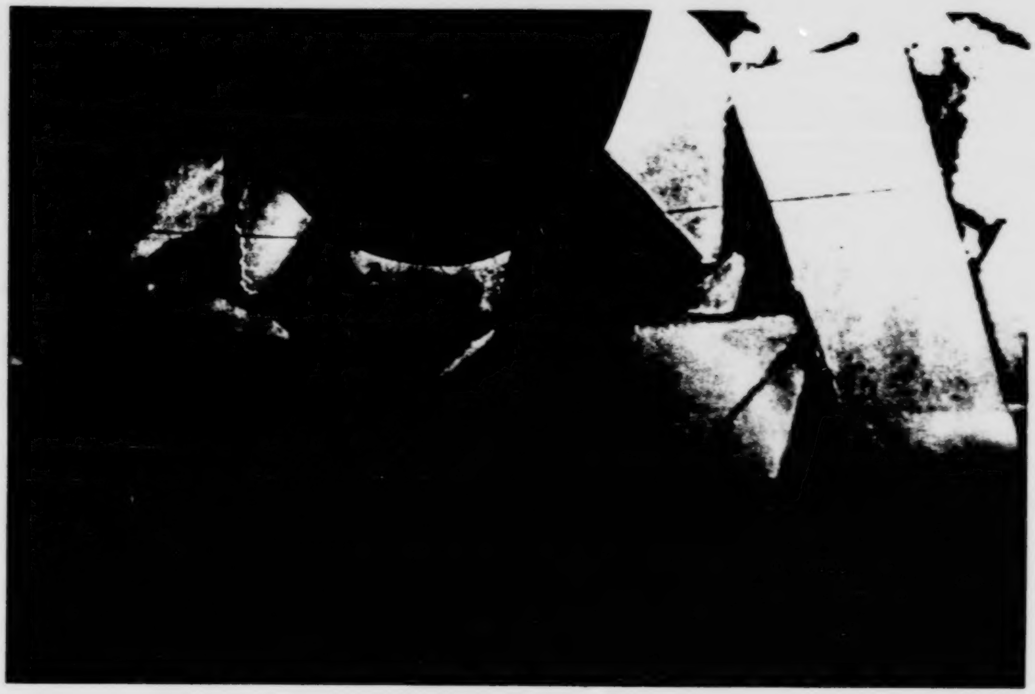

A. BACKING: PHOTOGRAPH ONE

B. BACKING: PHOTOGRAPH TWO

FIGURE 4.5
ICE FLOE DISTRIBUTION IN PRE-CUT BROKEN CHANNEL

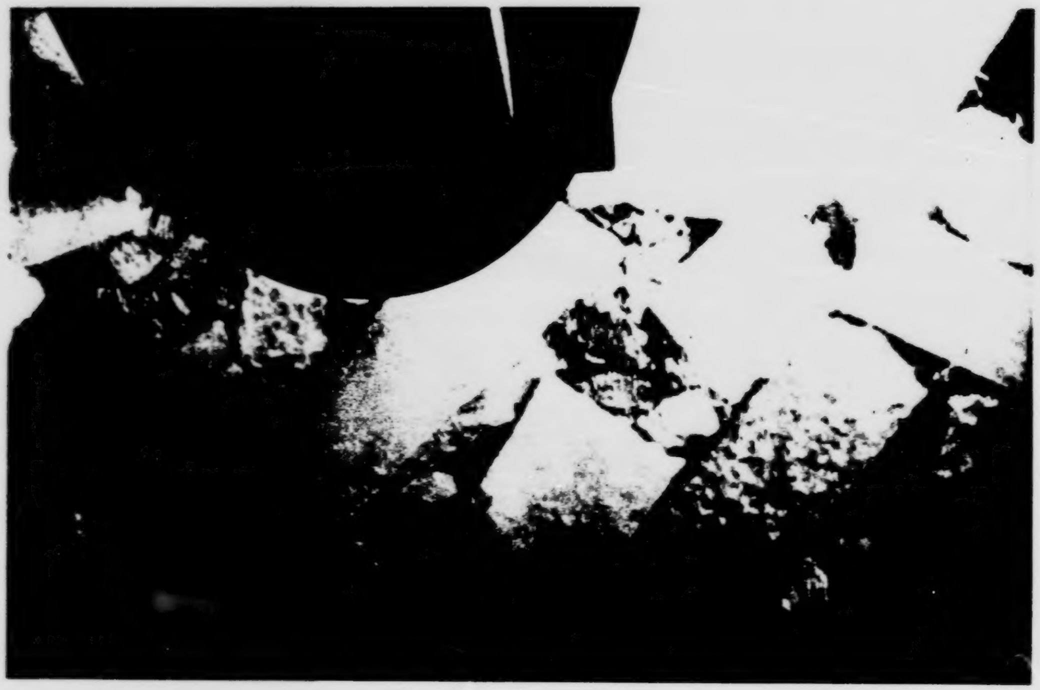

C. PHOTOGRAPH ONE

D. PHOTOGRAPH TWO

FIGURE 4.6
TYPICAL TEST RUNS

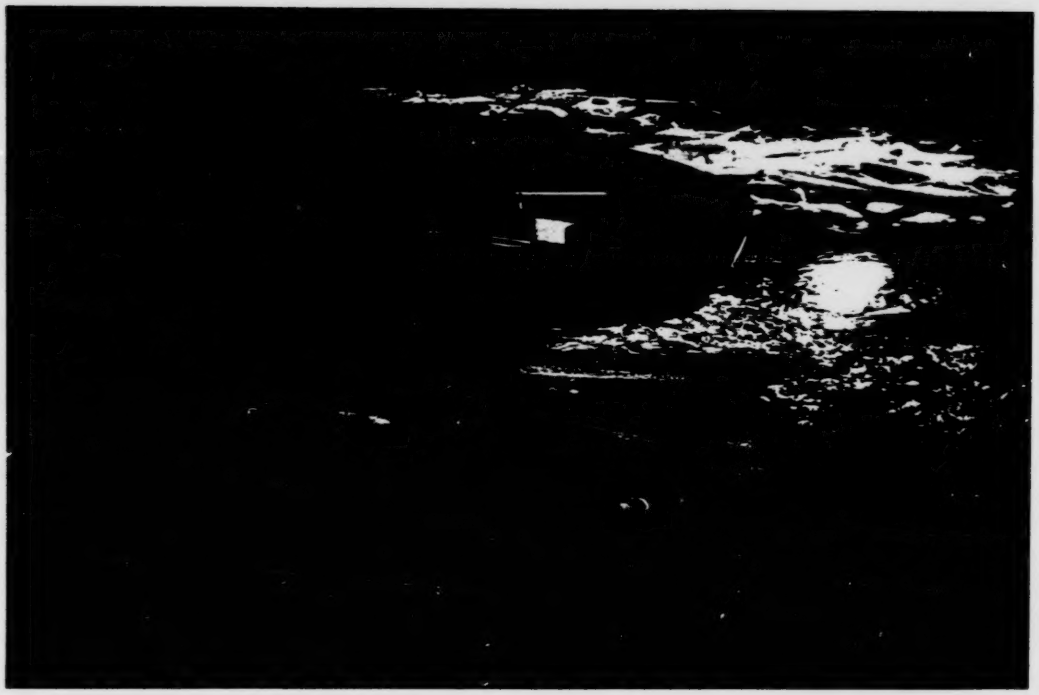

A. RADISSON MODEL MOVING FORWARD IN BROKEN CHANNEL

B. VIEW OF RUDDER-ICE IMPACT IN ASTERN TESTS

4.7 Data Reduction and Results

The digitally sampled data which was recorded during each of the test runs forms the basis for a comparative analysis of the influence of various parameters on rudder torque. Figure 4.7 shows the five time histories for the first run in the series of testing on the RADISSON model. During this test the model is breaking the herring bone pattern which has been cut into the ice sheet. At the start of the time interval the propeller speed is adjusted to approximately 800 RPM. The thrust (force) recorded at the heave staff is a large negative value since the model is constrained. Subsequently, the basin carriage is accelerated to a speed of 0.23 m/s and the model moves forward through the ice. The thrust remains negative during the time until the propeller RPM is decreased to zero since the model is over propelled at this RPM. Approximately 15 metres of forward motion is covered in this run. The rudder torque shows significant peaking during this period as a result of both hydrodynamic loading and ice interactions. During the final two metres of motion, the propellers are stopped and the magnitude and number of the peaks decreases appreciably. In this particular example a small torque offset is observed at the completion of the test. In the data reduction process, a window is defined in the time history which correspond to the period of interest. Generally it begins once the model has fully entered the ice field and it concludes immediately prior to the decrease in the RPM and velocity.

Data sets from approximately 150 test runs involving four different ice sheets were recorded. In addition, bollard test data and open water self propulsion trials data for each of the three models was collected. This latter information was obtained at forward and backing velocities corresponding to the ice test operating conditions for each of the models. Figure 4.8 shows samples of open water torque time histories for the MV ARCTIC at a range of forward velocities. The rudder angle was 35° and RPM approximately constant at each of these runs. The influence of astern velocity is shown in Figure 4.9. Similar trials were recorded for the RADISSON and POLAR 8 models.

The availability of this baseline hydrodynamic database allows the option of a detailed breakdown of the total rudder torque measured in an ice field into its pure ice impact and hydrodynamic loading components. However, the present analysis is intended to investigate only the relative magnitudes of torque and frequency of impact for the selected test conditions.

The magnitude and frequency of torque peaks due to ice impacts on the rudder have been manually extracted from each of the time histories. Several repetitions of each combination of parameters was included in the test matrix to improve the value of these statistics. For purposes of comparison, the database of torque magnitudes and impact frequencies has been further arranged into five general categories.

FIGURE 4.7

RADISSON MODEL ICEBREAKING TEST

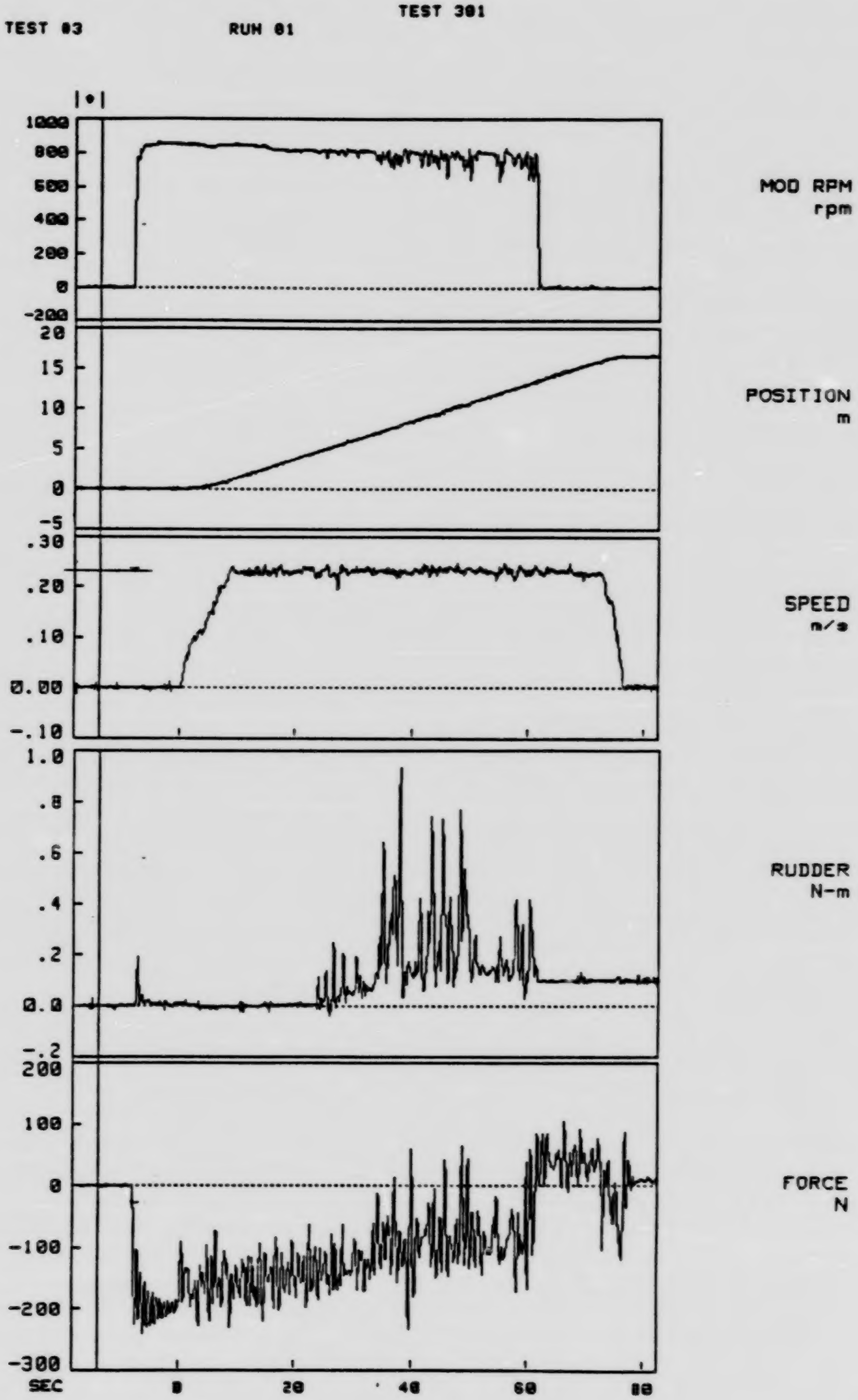

FIGURE 4.8

INFLUENCE OF AHEAD VELOCITY ON OPEN WATER TORQUE

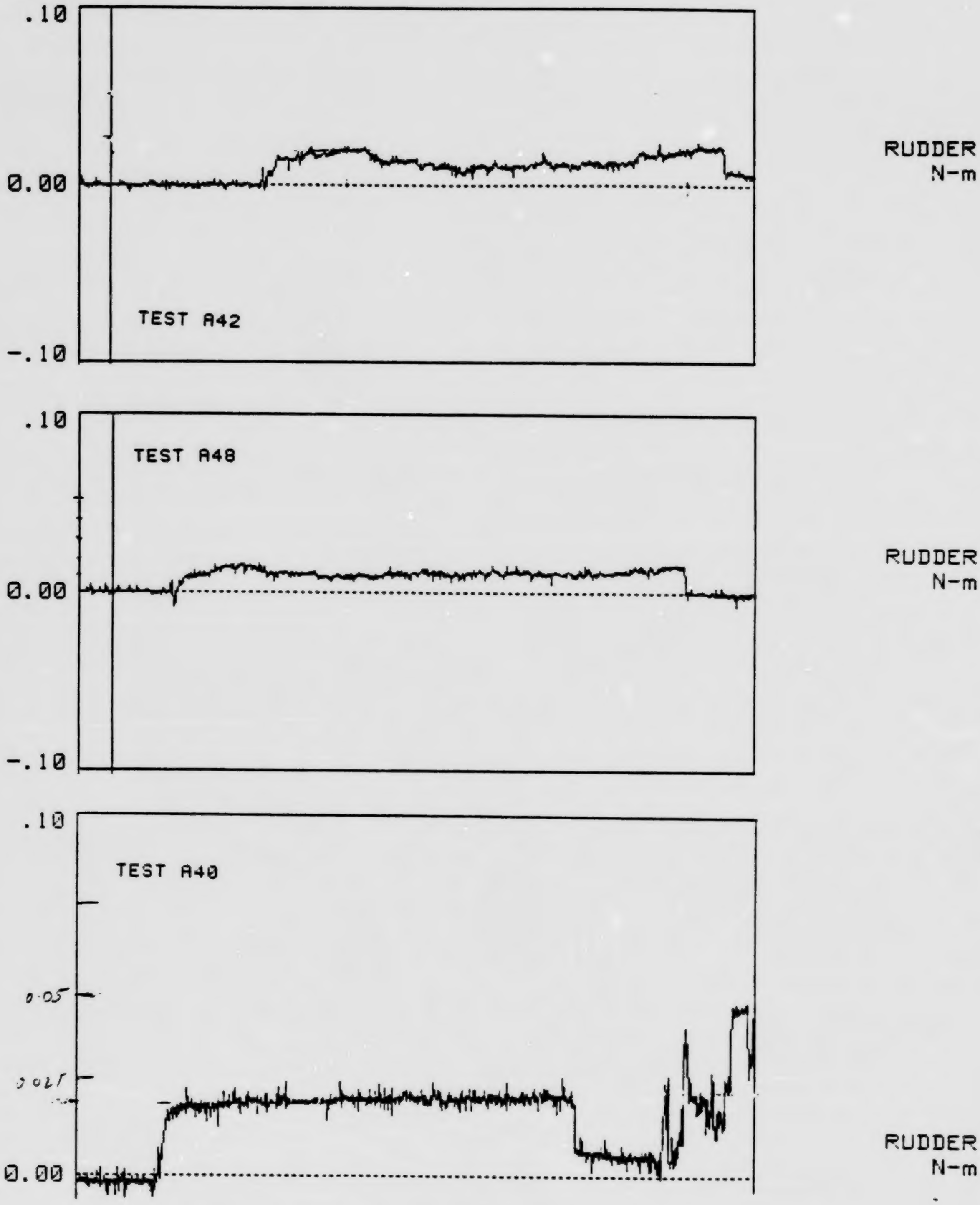

FIGURE 4.9

INFLUENCE OF ASTERN VELOCITY ON OPEN WATER TORQUE

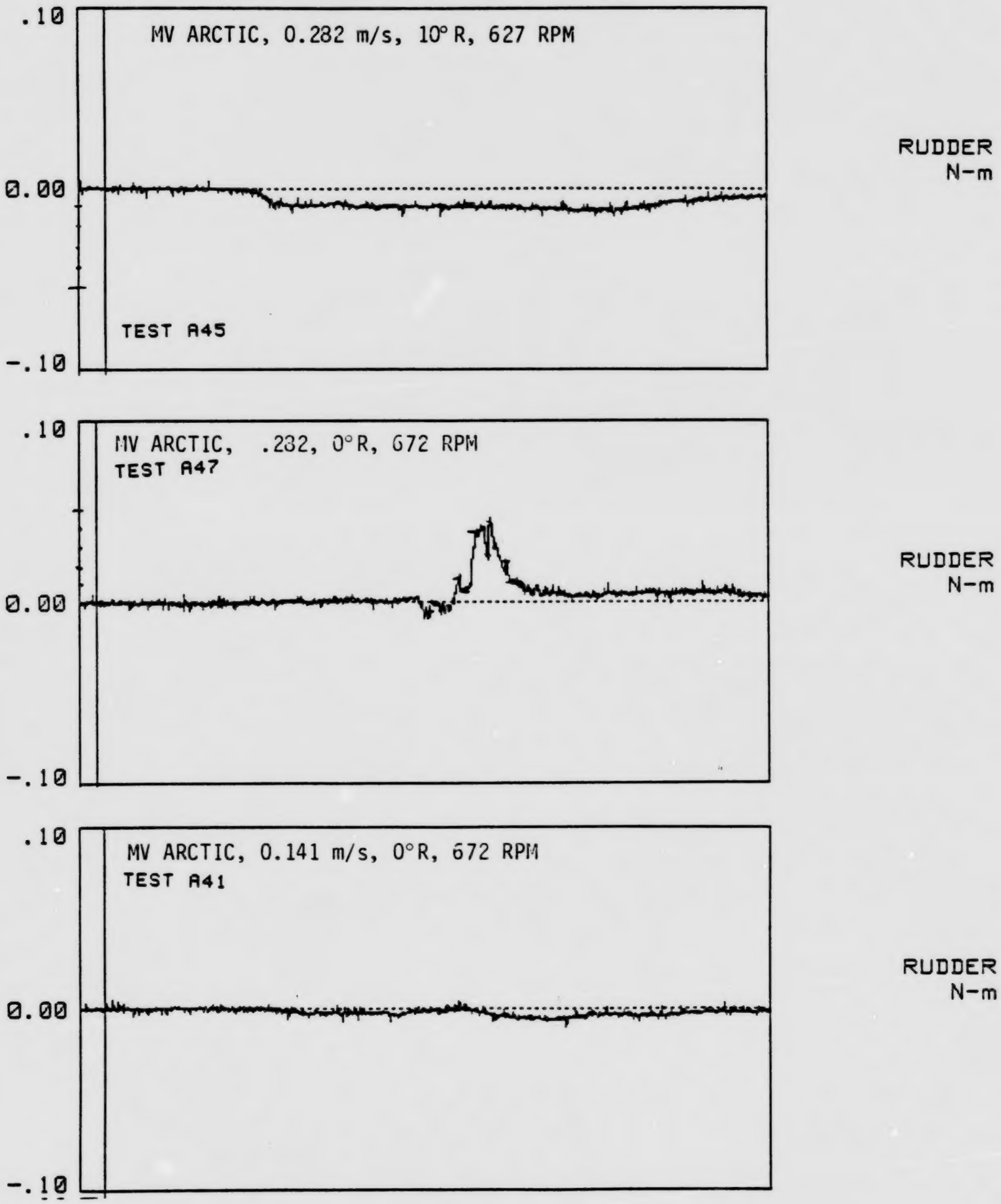

Table 4.5 lists the runs from each test series which are included within each grouping. Three forward speed categories and two astern speed categories have been defined. These have been designated as:

(1) Full Speed Forward
(2) Yawing Forward (5° drift angle)
(3) Mid Speed Forward
(4) Mid Speed Backing
(5) Low Speed Backing

The speeds differ for the three ships. Neither the level of propeller thrust, nor the draft condition have been separately distinguished. Ship velocity, rudder angle and drift angle are common to all runs within a group. One exception is the mid speed backing category which includes both 0° and 10° rudder angles.

Table 4.6 lists the cumulative statistics resulting from the extraction of peaks according to the above grouping. The number of test runs which have contributed to each of the 15 histograms is noted. The frequency of impact at each torque magnitude has been presented as impacts per kilometre of broken channel transit.

4.7.1 Histograms of Peak Torque Magnitude and Frequency of Impact

Figure 4.10 provides a comparison of the relative frequencies and torque magnitudes for the MV ARCTIC, PIERRE RADISSON and POLAR 8 models at full forward speeds. The frequency results are presented using a logarithmic scale, rather than a linear scale. This has the advantage of highlighting the more significant ice impacts, which are small in number. In viewing these histograms it should be remembered that torques with magnitudes less than 0.1 Nm generally represent hydrodynamic effects, rather than ice loading impacts. Therefore the large frequency values occuring in this range should be interpreted accordingly.

Figure 4.11 shows the relative histograms in 'mid speed forward' manoeuvres in the broken channel. Figure 4.12 shows the effect of constraining the models at a drift angle of 5°. Figure 4.13 presents the statistics on mid speed backing. It is this condition which exhibits the largest magnitudes of impacts. Figure 4.14 shows the relative statistics in the low speed astern mode of operation.

TABLE 4.5
ICE BASIN TOWED TESTS

HISTOGRAMS: CATEGORIES SELECTED AND TEST RUNS INCLUDED

CONDITIONS THRUST (FWD/BACK) VELOCITY RUDDER ANGLE DRIFT ANGLE		SHIPS MVA / R / P8 TEST 01, 03, 04 RUNS AT DESIGN DRAFT	SHIPS MV / R TEST 01, 03 RUNS AT LIGHT DRAFT	SHIPS P8 TEST 04 OTHER RUNS, DESIGN DRAFT
1 FULL SPEED	FF,V_1,35°R, 0°D	3, 11, 19	27	3a
FRWD	TF	5, 13, 21	23	5a
2 YAWED FRWD	FF,V_1,35°R,5°D	7, 15, 23	31	7a
3 MID SPEED FRWD	FF,V_2,35°R,0°D	9, 17, 25	33	
4 MID SPEED	FB,V_2, 0°R,0°D	4, 12, 20	28	49
BACK	TB,V_2, 0°R,0°D	6, 14, 22	30	69
	FB,V_2,10°R,0°D	8, 16, 24	32	89
5 SPEED BACK	FB V_3 0°R 0°D	10 18 26	34	

NOMINAL SPEEDS	MVA(01)	MVA(02)	R(03)	P8(04)
V_1 m/s	.563		.690	.488
V_2 m/s	.282		.345	.244
V_3 m/s	.141		.173	.122
SCALE	30	30	20	40
NOMINAL ICE (mm) THICKNESS	70	40	50	50

NOTE: Open water test runs are not shown.

TABLE 4.6

ICE BASIN TOWED MODEL DATA

TORQUE Nm	FORWARD MANOEUVRES: IMPACTS PER KILOMETER								
	MV ARCTIC			RADISSON			POLAR 8		
	FULL	YAW 5°	MID	FULL	YAW 5°	MID	FULL	YAW 5°	MID
0-0.025	0.56	24.44	2.2	28.89	-	19.2	27.4	6.67	51.7
0.05	1.11	15.56	-	20.0	2.0	8.3	20.0	18.89	48.9
0.075				6.66	6.0	7.5	24.5	39.45	37.2
0.100				5.19	10.0	-	5.24	7.22	1.1
0.125				4.08	38.0	0.83	1.90	1.67	
0.150				3.33	20.0	0.83	-	-	
0.175				2.97	36.0	0.83	0.24	-	
0.200				2.60	38.0	-	-	-	
0.225				0.375	36.0	-	-	1.67	
0.250				-	28.0	-	-	0.56	
0.275				0.375	10.0	-	-	1.11	
0.300					4.0		-	-	
0.325					-		0.24	1.67	
0.350					-		-	-	
0.375					-		-	0.56	
0.400					2.0		-	-	
0.425					4.0		-	0.56	
0.450					-		-	1.67	
0.475							-	1.11	
0.500							-	-	
0.525							-	2.22	
0.550							-	0.56	
0.575							-	0.56	
0.600							-	0.56	
0.6-0.800							-	0.56	
0.8-1.00							-	0.56	
VELOCITY m/s	0.563	0.282	0.282	0.690	0.345	0.345	0.488	0.244	0.244
NO. OF RUNS	4	1	2	9	5	4	7	3	3

TABLE 4.6
(CONTINUED)

ICE BASIN TOWED MODEL DATA

TORQUE	FORWARD MANOEUVRES: IMPACTS PER KILOMETER					
Nm	MV ARCTIC		RADISSON		POLAR 8	
	YAW 5°	MID	YAW 5°	MID	YAW 5°	MID
0-0.025	16.3	16.7	19.7	18.3	14.35	20.6
0.05	8.89	4.4	16.7	28.3	11.35	16.7
0.075	9.26	14.4	23.9	41.7	11.02	6.1
0.100	3.70	2.2	15.8	16.7	2.92	3.3
0.125	5.19	4.4	17.6	17.5	3.75	5.0
0.150	-	-	6.79	9.2	2.08	0.56
0.175	-	-	8.79	8.3	2.92	2.8
0.200	1.48		6.36	10.0	0.83	0.56
0.225	0.37		7.27	5.0	2.7	0.56
0.250			2.12	2.5	0.21	1.67
0.275			2.12	-	2.1	-
0.300			2.12	0.83	0.42	-
0.325			0.91	2.5	1.66	0.56
0.350			0.91	-	-	-
0.375			0.91	1.67	0.42	-
0.400			0.30		0.21	-
0.425			0.61		0.42	0.56
0.450			-		0.21	
0.475			0.30		0.21	
0.500			-		0.21	
0.525			0.30		-	
0.550			-		0.21	
0.575			-		-	
0.600			-		-	
0.6-0.800			0.30		0.21	
0.8-1.00					-	
VELOCITY m/s	0.282	0.141	0.345	0.173	0.244	0.122
NO. OF RUNS	6	2	11	4	15	3

FIGURE 4.10

FREQUENCY and MAGNITUDE of RUDDER/ICE IMPACTS

M. V. ARCTIC - Full Speed Forward : .563m/s

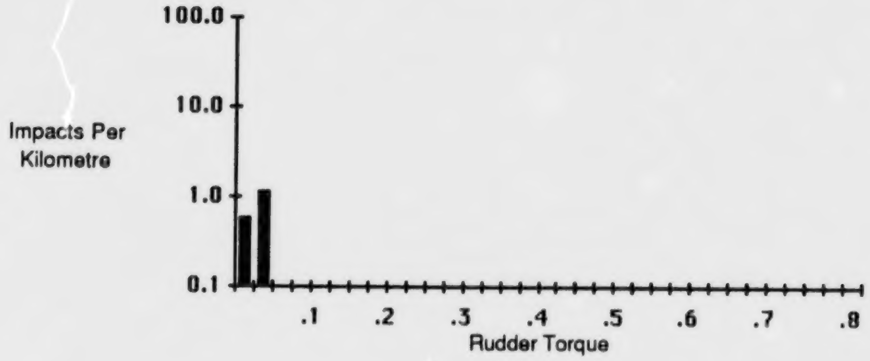

PIERRE RADISSON - Full Speed Forward : .690 m/s

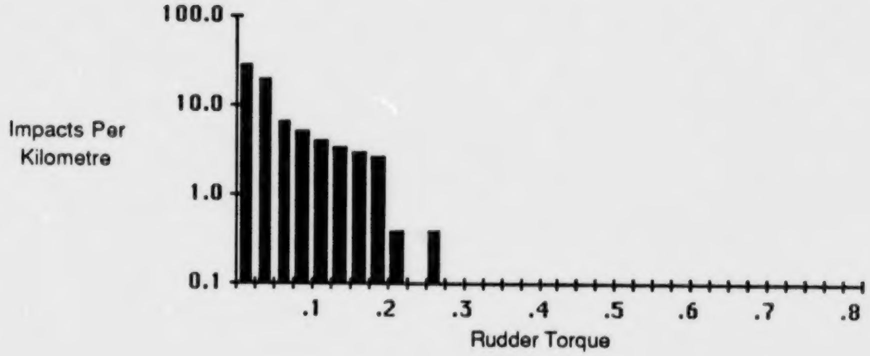

POLAR 8 - Full Speed Forward : .488 m/s

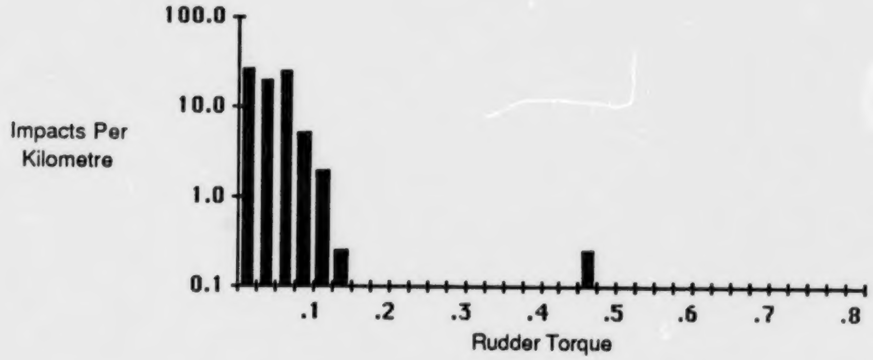

FIGURE 4.11

FREQUENCY and MAGNITUDE of RUDDER/ICE IMPACTS

M.V.ARCTIC - Mid-speed Forward : .282m/s

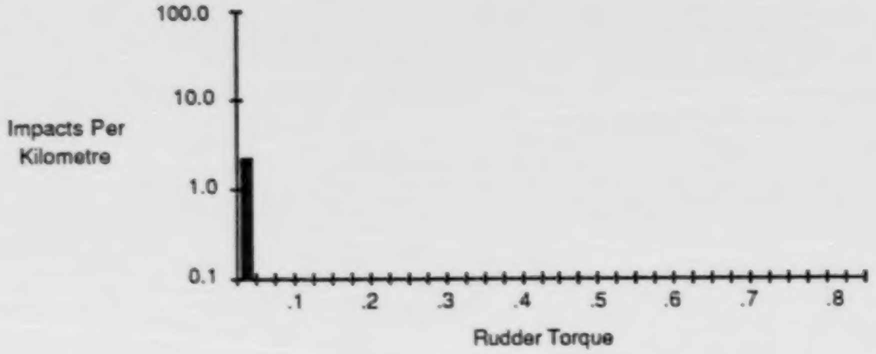

PIERRE RADISSON - Mid-speed Forward : .345 m/s

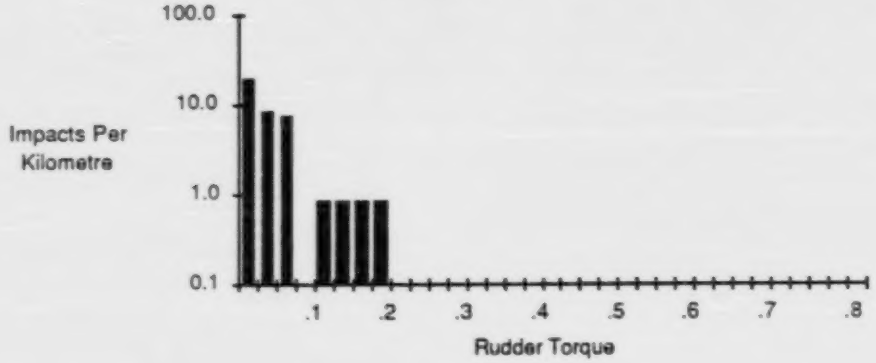

POLAR 8 - Mid-speed Forward : .244 m/s

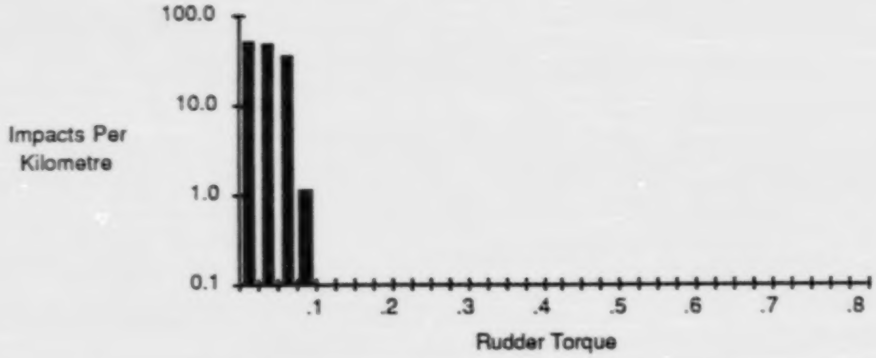

FIGURE 4.12

FREQUENCY and MAGNITUDE of RUDDER/ICE IMPACTS

M. V. ARCTIC - Yaw Angle 5° : .282 m/s

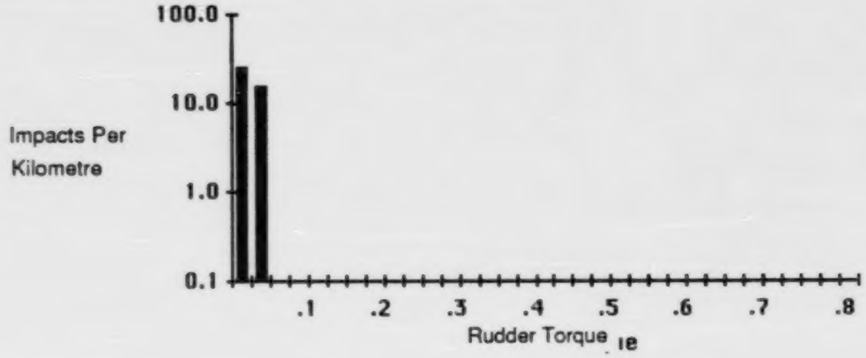

PIERRE RADISSON - Yaw Angle 5° : .345 m/s

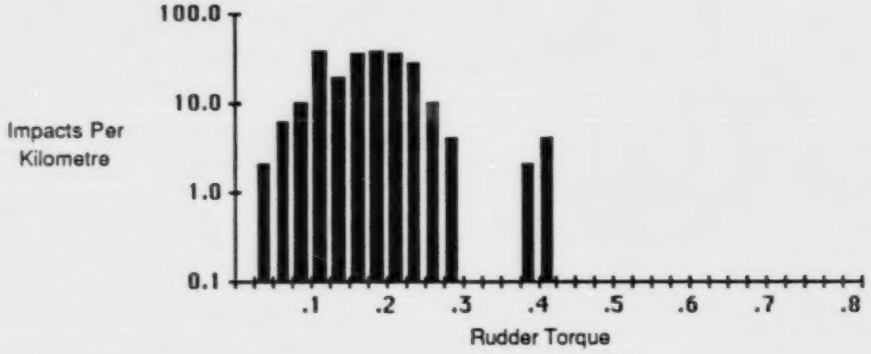

POLAR 8 - Yaw Angle 5° : .244 m/s

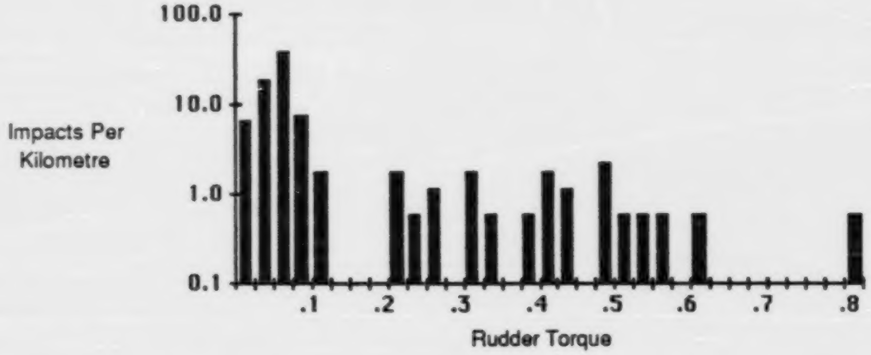

FIGURE 4.13

FREQUENCY and MAGNITUDE of RUDDER/ICE IMPACTS

M. V. ARCTIC - Mid-speed Backing : .282 m/s

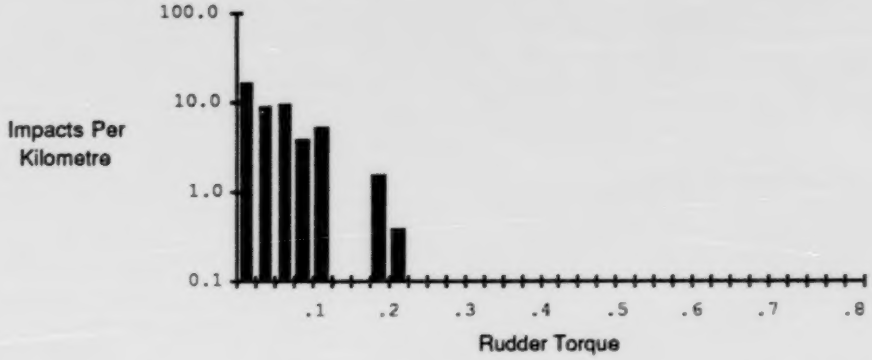

PIERRE RADISSON - Mid-speed Backing : .345 m/s

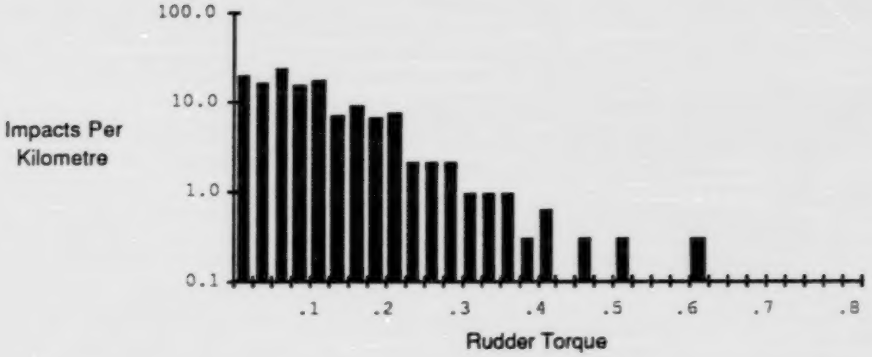

POLAR 8 - Mid-speed Backing : .244 m/s

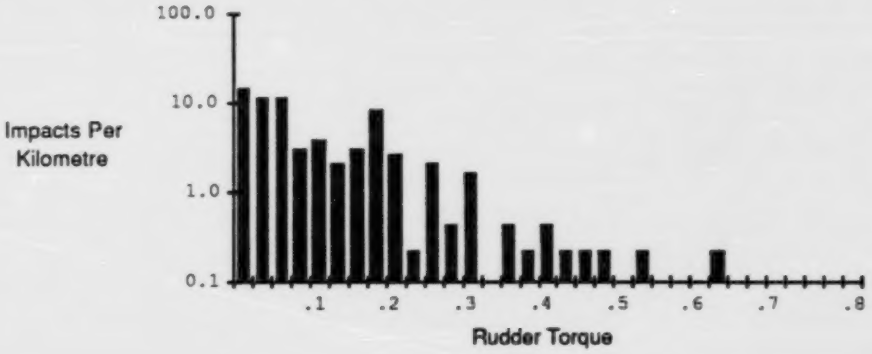

FIGURE 4.14

FREQUENCY and MAGNITUDE of RUDDER/ICE IMPACTS

M. V. ARCTIC - Low Speed Backing : .141 m/s

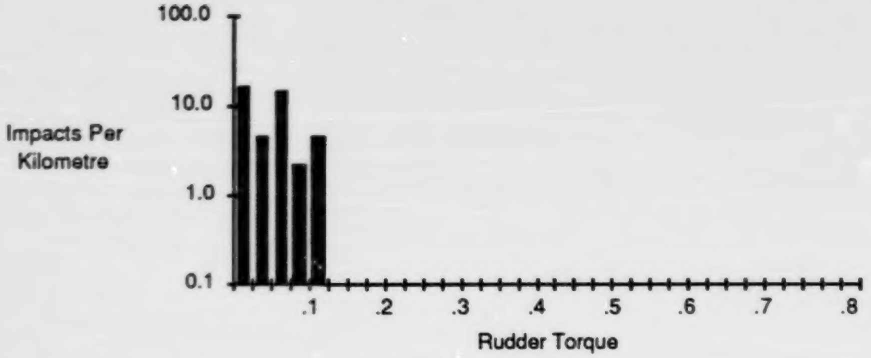

PIERRE RADISSON - Low speed Backing : .173 m/s

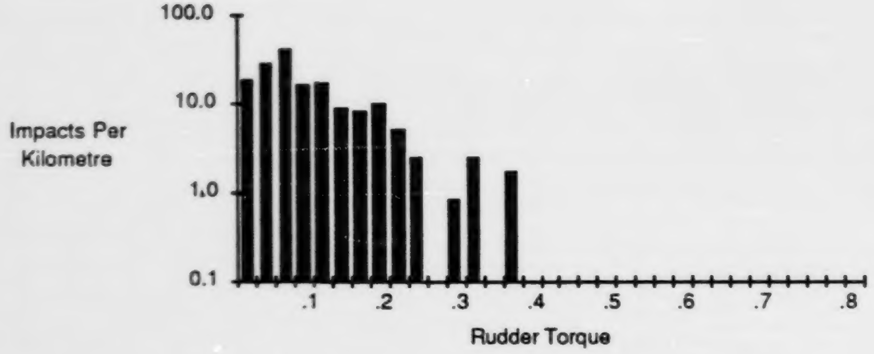

POLAR 8 - Low Speed Backing : .122 m/s

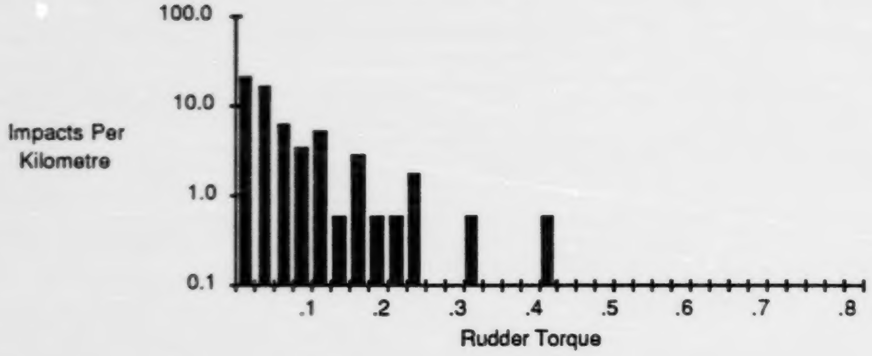

It has not been possible in assessing the histograms to distinguish the effect of certain individual parameters such as thrust level, draft condition and rudder angle because of the limited amount of impact data. However, the consolidated histograms have indicated the following general trends:

- There were no ice impacts observed for the MV ARCTIC during forward speed motions. Only hydrodynamic torques with magnitudes less than 0.05 Nm were measured. This is likely a result of her length, deep draft and the protection afforded by the propeller nozzle.

- In astern manoeuvres the MV ARCTIC exhibited a larger number of impacts with moderate torque magnitudes. Additionally, a large number of impacts with low torque values were observed. These may result from continuous ice contact or from enhanced hydrodynamic loads on the rudder. There appears to be no appreciable increase in frequency of impact with increased astern velocity, although a shift towards larger mean torque is seen.

- The PIERRE RADISSON shows the highest frequency of impacts on the rudder during both forward motions and astern motions of all three test vessels. An increase in frequency with forward speed is observed in both the ice impact torque region and the hydrodynamic loading range. Introduction of a drift angle into the full speed manoeuvres results in a significant increase in the number of impacts and an upward shift in the mean torque magnitude to about 0.2 Nm.

- In astern manoeuvres the RADISSON exhibits a larger number of significant impacts, but about the same hydrodynamic loading as during forward motions. The impact frequency does not appear dependent on velocity; but there is an upward shift in torque magnitude with speed.

- The POLAR 8 icebreaker histograms have a similar pattern to that observed for the RADISSON. In forward motions, the POLAR 8 has a larger number of low magnitude or hydrodynamic events, but fewer ice impacts. The exception is the 5° drift condition for which the POLAR 8 shows a spread of very large torques, up to 1 Nm. This number is speed dependent. In backing the POLAR 8 again shows fewer impacts over a similar torque range.

4.7.2 Influence of Parameters

Although it has not been possible to define the influence of many parameters within the context of the statistical representation, some insights may be gained from the individual time histories.

Some additional comments about individual parameters may be made on the basis of a visual examination of the time histories. It appears that the relative value of steady state rudder torque for each ship in each operating mode is a major factor influencing the histograms. The steady state component in the ice impact environment is similar in magnitude to the corresponding open water value. In general, it is observed that the RADISSON has the larger value; followed by POLAR 8 and MV ARCTIC. This reflects the particular hydrodynamic characteristics of each ship's stern configuration and rudder geometry. Furthermore, it has repercussions on the interpretation of trends in various ship parameters.

Figure 4.15 compares three time histories representing equivalent operating conditions for the three ships. The speed is the full forward value for each ship. Propeller RPM varies somewhat, but each corresponds to a similar over propelled condition in each case. The different in RPM reflects the differing numbers of screws and propeller diameters. Rudder angle is 35°. The MV ARCTIC has a constant and small magnitude torque, which is below 0.05 Nm and shows little peaking response. The RADISSON has a steady state torque of 0.2 NM and shows significant peaks up to 0.3 Nm. The POLAR 8 model results have a steady state of about 0.04 Nm and peaks up to 0.1 Nm. This comparison agrees with the histogram in Figure 4.10 and further suggests that the steady state torque may be a major factor affecting the statistics.

By referring to the open water torque time histories for the RADISSON it appears that the steady state torque is largely determined by the open water torque.

Figure 4.16 shows comparative time histories for the three models during mid speed backing manoeuvres. Rudder angle is 10°. The MV ARCTIC experiences an appreciable number of impact peaks which are several times larger than the open water torque loading. However, the magnitudes are relatively small as compared to the RADISSON and POLAR 8. The RADISSON exhibits a similar number of peaks but the magnitudes are larger. This again appears partly due to a larger steady state hydrodynamic loading. The POLAR 8 has fewer peaks over most of its test period. However, near the end it has several very large impacts of longer duration.

FIGURE 4.15

INFLUENCE OF SHIP FORM IN FULL FORWARD SPEED MANOEUVRES

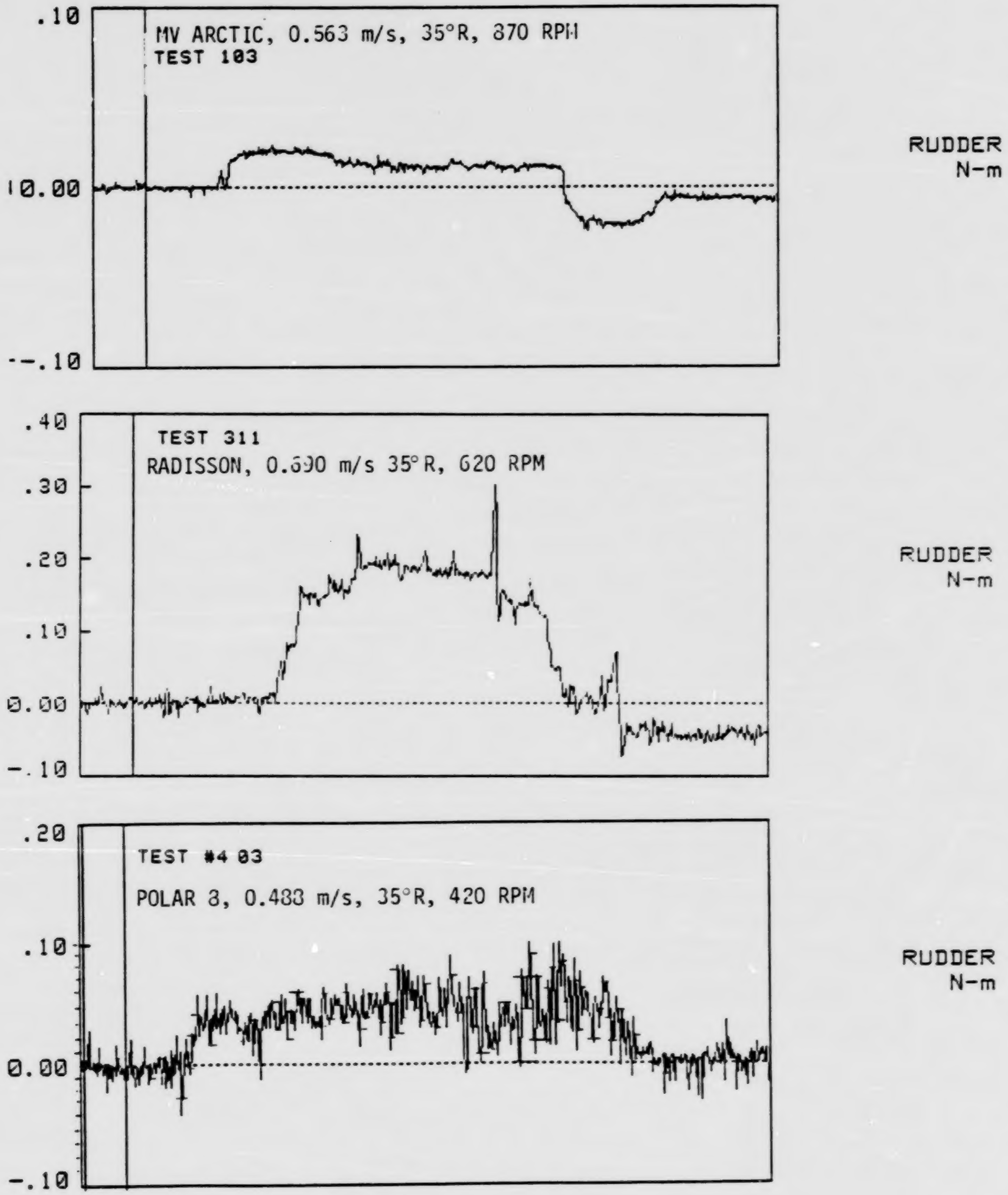

FIGURE 4.16

INFLUENCE OF SHIP FORM IN MID SPEED BACKING MANOEUVRES

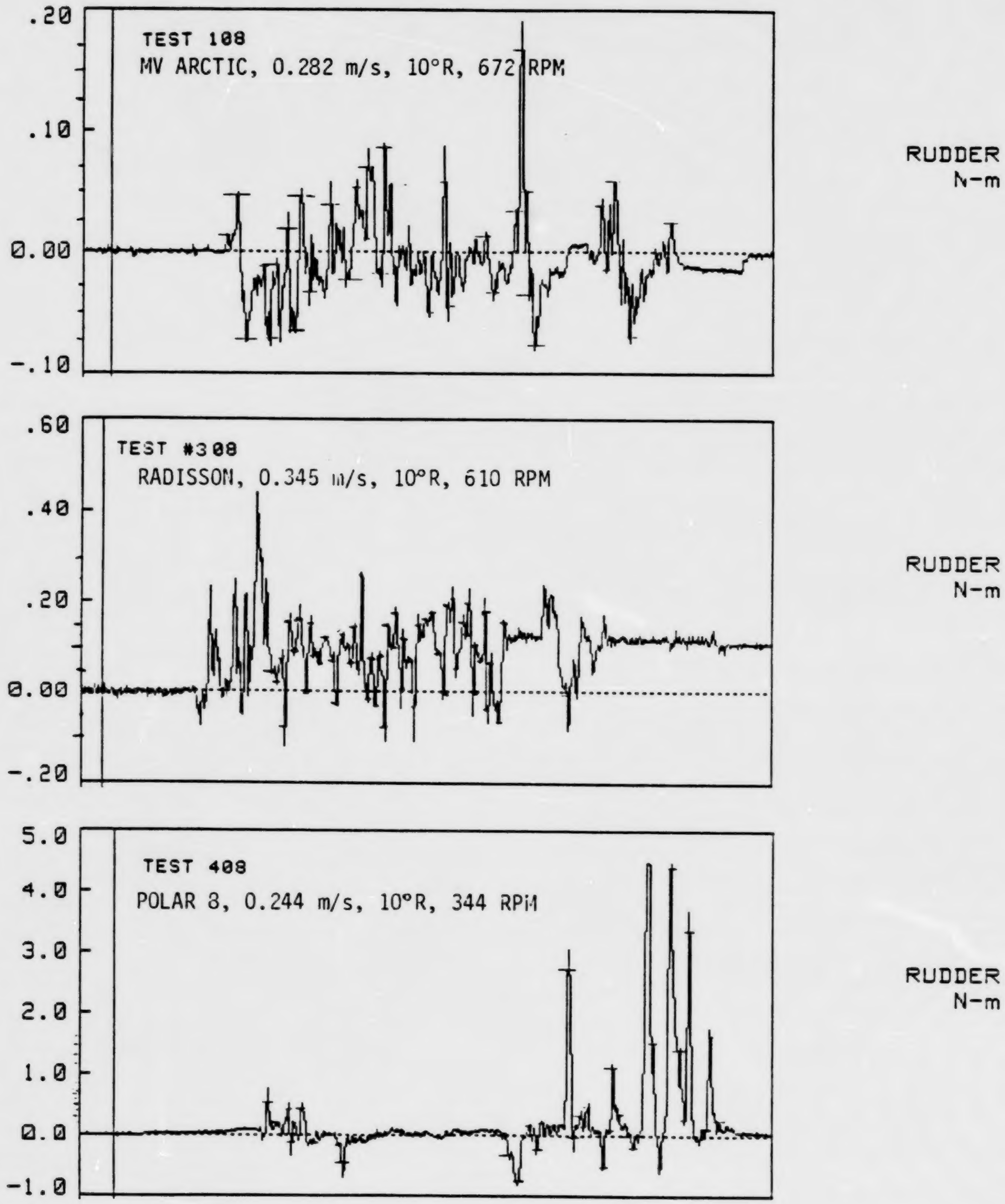

The influence of draft or ballast condition is shown in Figure 4.17 RADISSON time histories are shown for both deep and light draft test conditions during mid speed backing. The rudder angle was 0° and the propeller speed about 620 RPM. The light draft condition appears to show marginally larger torque magnitudes. A maximum in excess of 0.6 Nm is recorded, as compared to 0.4 Nm for the deep draft. However, it is difficult to assess the difference since there is a gradual offset in the light draft time history.

The time histories suggest that decreasing draft causes a marginal increase in torque magnitudes, as does increasing RPM or ice thickness. The effect of changing the propeller rotation direction is hidden by the change in steady state torque.

Figure 4.18 illustrates the affect of propeller speed during backing manoeuvres. The RADISSON model has twin screws. In Test 304 the propellers were operating at 490 RPM. Test 306 the propellers were either stopped or at 102 RPM. The model is towed at the same speed in both cases. The larger magnitudes of torque and greater numbers of peaks in the former case suggests that the propeller race may cause additional ingestion of ice onto the rudder. However, there is conflicting evidence as to its importance in view of the large peaks in Test 306 which occur when the propeller is stopped.

The influence of propeller rotational direction is investigated for full speed forward motions of the RADISSON in Figure 4.19. Test 331 features inward turning propeller rotations. This is contrary to normal operating conditions and has been physically arranged by means of pulleys and belts. Test 307 is the more usual outward turning configuration. The principal differences between the two cases appears to be that the outward condition has a larger steady state torque. Although the outward case exhibits one large peak. There is insufficient ice impact data on which to base any conclusions. A much larger set of measurements is necessary to see if additional ice is drawn into the rudder as a consequence of propeller rotation direction during forward motions.

Two ice thicknesses have been employed in the testing of the MV ARCTIC. Figure 4.20 shows two time histories from backing trials in equivalent operating conditions, other than ice thickness. Test 226 was in 40 mm thick ice. Test 110 was in 70 mm thick ice. Rudder angle was 0° and velocity, 0.141 m/s. Several larger peaks are observed in the 70 mm thickness data, but no definitive trend can be determined from the limited set of data compared. A more extensive assessment of the effect of thickness is possible from a further analysis of the Test 2 series statistics.

FIGURE 4.17

INFLUENCE OF DRAFT CONDITION DURING BACKING MANOEUVRES

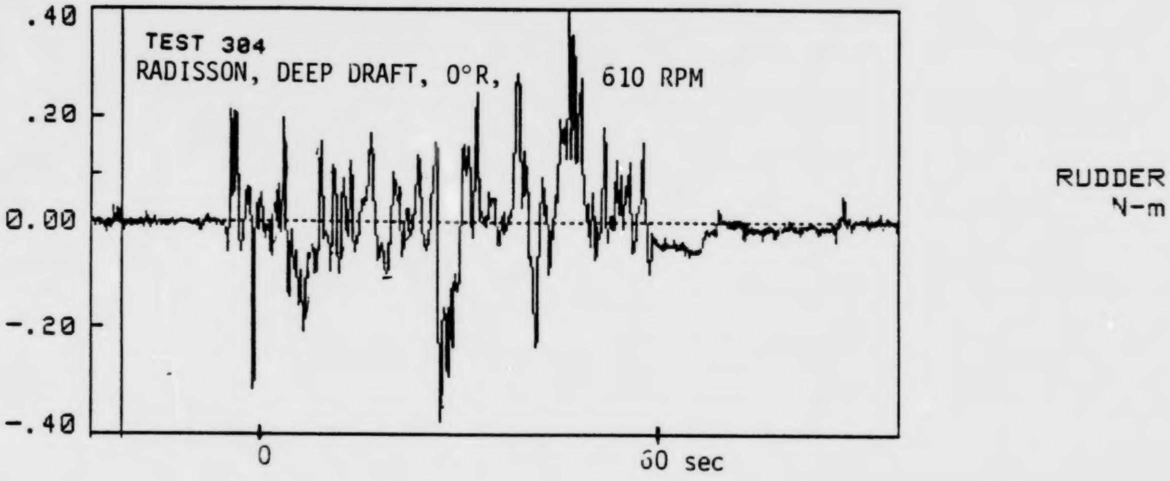

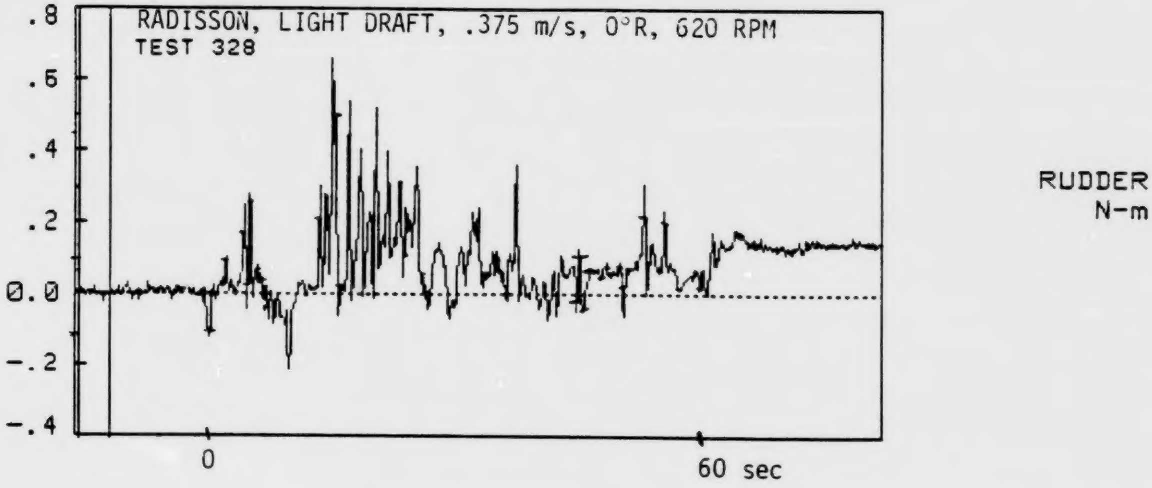

FIGURE 4.18

INFLUENCE OF PROPELLER SPEED DURING BACKING MANOEUVRES

RADISSON, 0.345 m/s, 0°R, 490 RPM

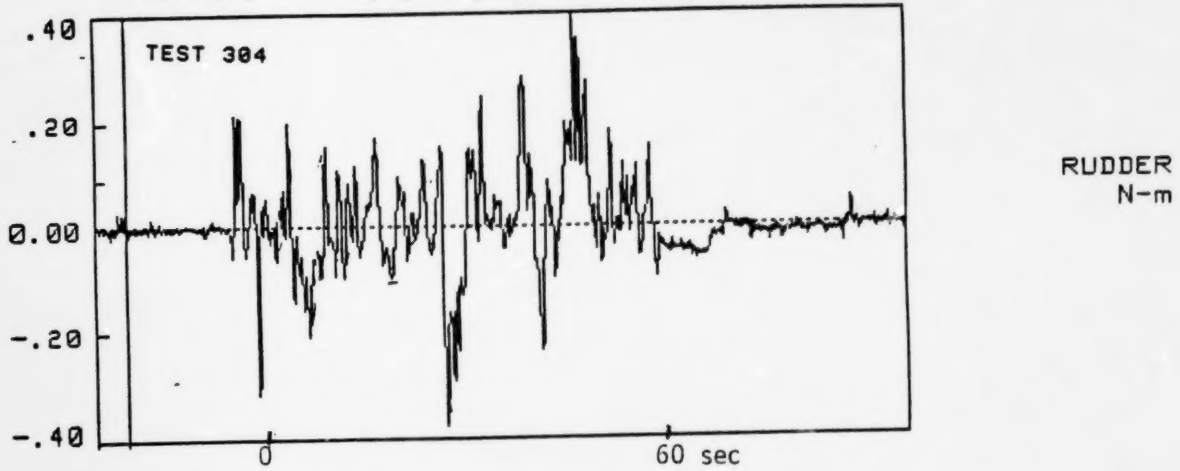

RADISSON, 0.345 m/s, 0°R, 0 - 102 RPM

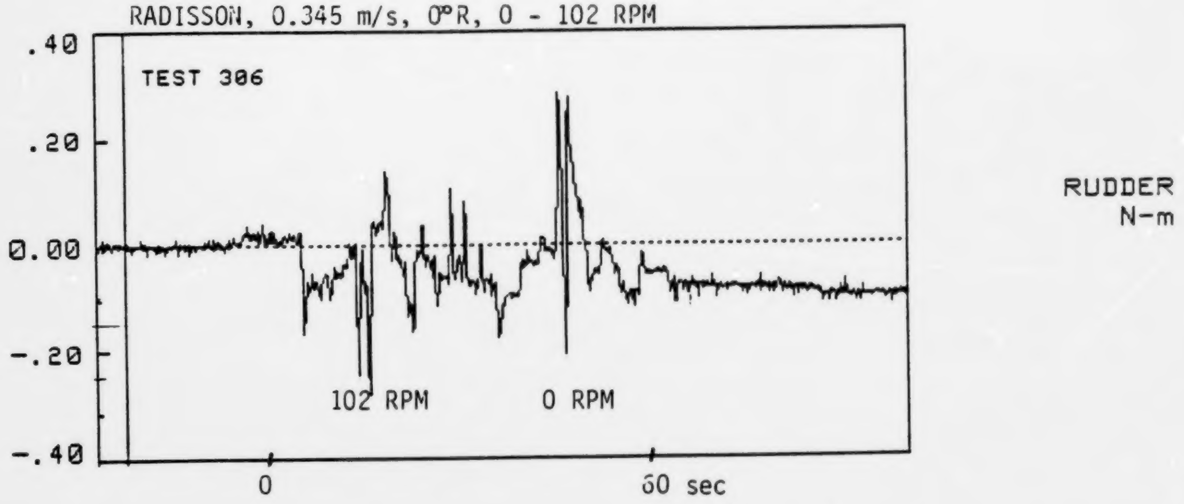

FIGURE 4.19

INFLUENCE OF PROPELLER ROTATIONAL DIRECTION DURING FORWARD MANOEUVRES

RADISSON: (INWARD PROPELLERS), 0.690 m/s, 35°R, 610 RPM

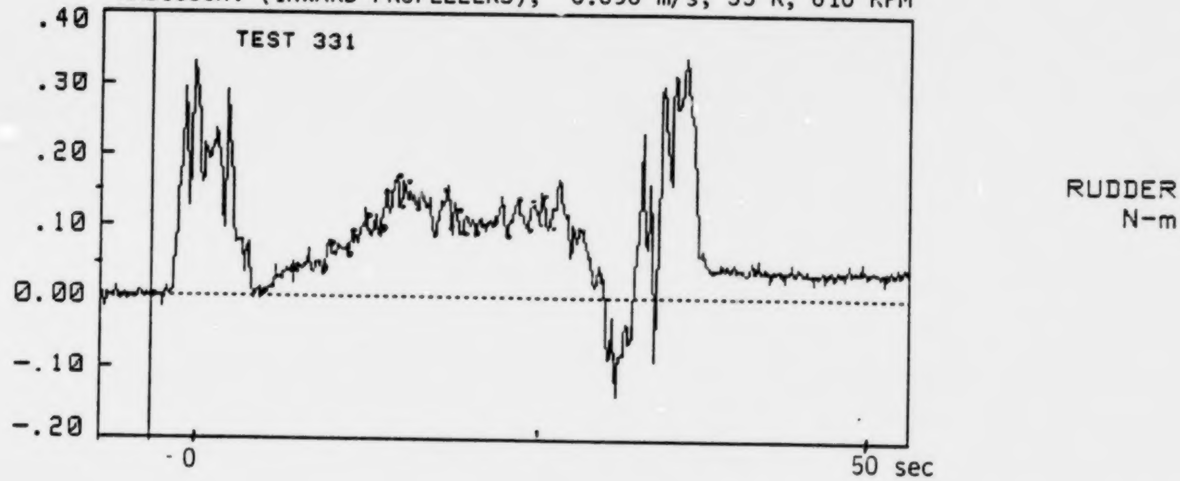

RADISSON: (OUTWARD PROPELLERS), 0.690 m/s, 35°R, 610 RPM

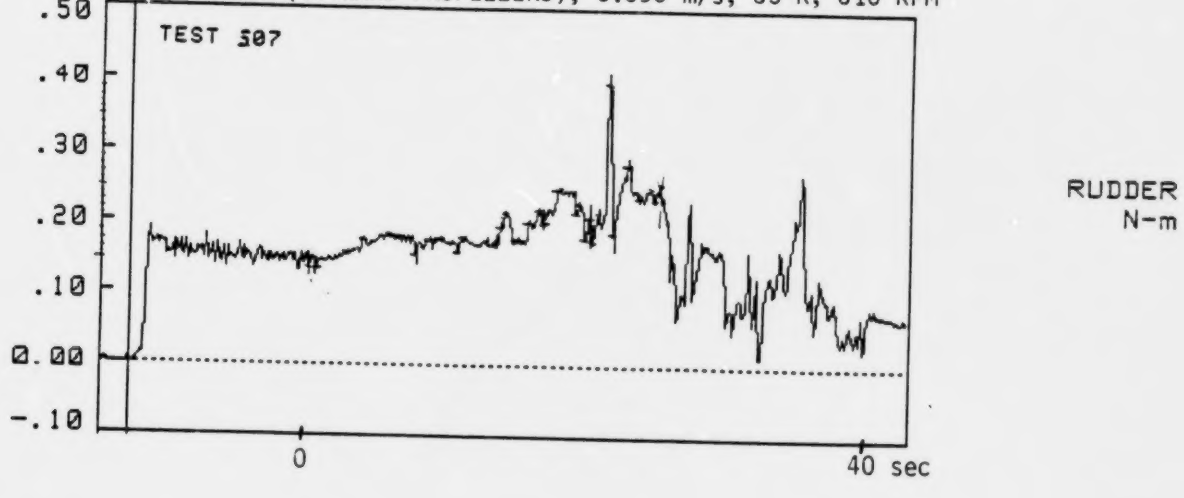

FIGURE 4.20

INFLUENCE OF ICE THICKNESS DURING BACKING

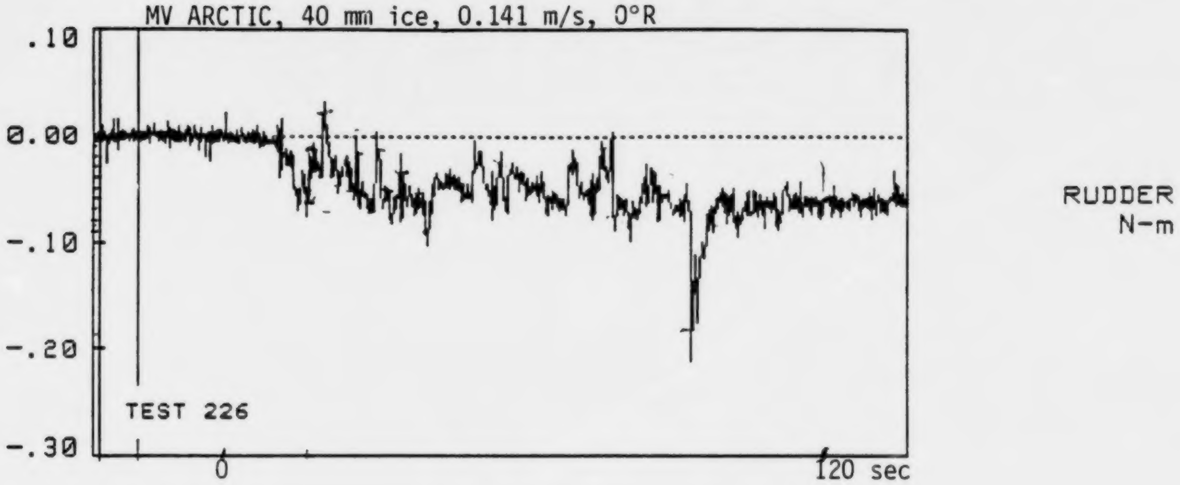

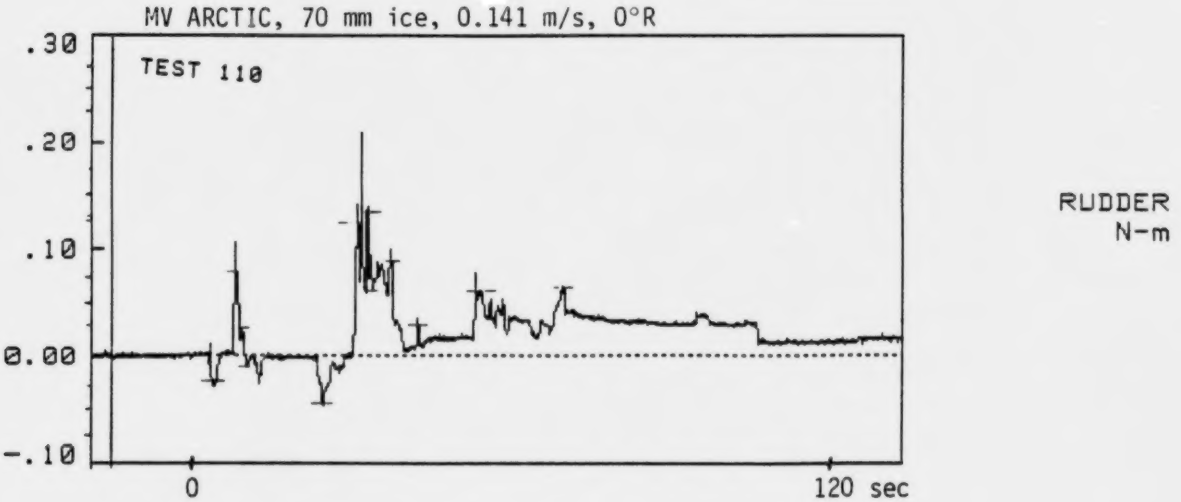

4.8 Remarks and Recommendations on Towed Tests

4.8.1 Remarks

An extensive program of model testing in pre-cut ice floes has been carried out involving three ship models: MV ARCTIC, PIERRE RADISSON and POLAR 8. The hull form and stern configuration of each model are scaled from the corresponding prototype. The POLAR 8 has been represented by a triple screw, single rudder design. Ice impact torques on the rudder were measured during a range of ship manoeuvres to determine the frequency and severity of rudder/ice impacts. Variation in test parameters included: ahead and astern tests, two velocities, two propeller speeds, two rudder angles, two drift angles, two drafts and difference ice thickness. Approximately 150 data sets were obtained. The testing involved several repetitions of test conditions to extend the statistical database.

Each ship has been investigated up to specific velocities and at an ice thickness corresponding to their design maximum operating environments. The measured torques are therefore representative of normal operating conditions, rather than extreme cases as measured in the dry impact tests. A limited number of tests in rafted and irregular ice features have also been carried out.

Open water torque data for each ship model was also accumulated, corresponding to each ice test condition. This data is important in view of the magnitude of the steady state torque which is observed during the tests in the broken ice fields. The relative statistics on frequency and peak magnitude of torque are affected since each ship has a significantly different hydrodynamic component of rudder loading. It was observed that RADISSON has the largest open water torque, followed in decreasing order by POLAR 8 and MV ARCTIC. This factor has contributed to the difficulty in assessing the influence of certain parameters, such as propeller speed, direction of rotation and draft condition. The accumulated database of statistics on the frequency and magnitude of torque peaks in different test conditions has been organized into five general categories. Three are ahead manoeuvres, one of which features at 5° drift angle. Two are astern manoeuvres at different velocities. The imposition of these five categories has allowed more statistically meaningful histograms to be plotted for each of the three vessels.

A series of general trends have been observed as a result of the consolidated histograms. The astern manoeuvres are the most significant, involving appreciably larger number of impacts with larger magnitudes. A shift in the histogram towards larger torque magnitudes is seen as velocity increases. It appears that the PIERRE RADISSON exhibits the highest frequency of impacts during both ahead and astern motions. The POLAR 8 shows similar frequency trends to the RADISSON, but smaller magnitudes. This appears partly as a result of POLAR 8's smaller open water torque.

The principal outcome of these tests has been the statistics on the frequency of impact during astern manoeuvres in the broken channel. Since it was not possible to accurately scale the crushing strength of the pre-cut urea ice, and maintain it throughout a full day of tests, distortions in the rudder torque values were expected. Nonetheless, the torque values provide an order of magnitude reference in assessing the impact severity.

The comparison between the three vessels has demonstrated the effectiveness of certain hull form characteristics in limiting the number and severity of rudder ice loads. In particular, the nozzle on the MV ARCTIC propeller, in combination with its greater length and draft, resulted in a total protection from impacts during forward manoeuvres. With the limited number of test repetitions, it has not been possible to statistically determine the meaningfulness of the data on opposing propeller rotation directions. Nor has it been possible to differentiate between minor variations of rudder angle or thrust level during astern manoeuvres. These tests have been grouped together to allow comparative statistical assessment between different ships and major operating characteristics.

4.8.2 Recommendations

Extension of Analysis

The current test program has collected time history data which spans a broad range of parametric variations. Within the scope of the present project, only a limited analysis of the data has been possible. This has focussed on the major parameters. However, it would be possible to extract a significantly larger and more accurate set of conclusions if an expanded analysis effort was undertaken. This involves:

- Derivation of steady state rudder torque for each ship at each open water test condition. This information will be used to correct the time histories obtained din equivalent tests in the broken channel.

- Recomposition of the existing histograms of ice impact frequency and severity to represent pure ice torque magnitudes. Extraction of histograms for the MV ARCTIC ice thickness variation, test series 2.

- Further assessment of individual time histories within each histogram category to investigate the influence of ship draft, propeller RPM, propeller direction, and rudder angle.

5. GENERAL REMARKS

The principal limitation affecting the quality of the towed ice basin test results is in the number of repetitions of each test configuration. It has not been possible to separate the ice related torque peaks from the background hydrodynamic mean values. The towed results should be further reviewed to consider the open water and bollard trials data at each operational condition which was examined in the ice tests. The limited amount of data has necessitated a coarser grouping of different test parameters in the histograms than intended, to ensure more statistically meaningful trends. Additional evaluation of at least one vessel in a significantly larger sample of tests would improve the validity of these statistics and allow a finer differentiation of parametric influences. Furthermore, as a result of the experience with the dry impact physical modelling it is recommended that MODICE should be used in a follow-up towed test program. This ice material has two principal advantages: ice crushing strength can be modelled and maintained during testing; and the density of MODICE is closer to that of full scale ice. The former implies more accurate torque values. The latter implies that ice buoyancy forces will be better simulated and therefore the flow of ice to the rudder will be more representative.

A minimum number of peaks are required to produce a statistically meaningful histogram. This problem could be addressed by means of a further series of towed model tests on at least one of the current models. This test series should significantly increase the number of test runs at each specified ship operating condition.

Furthermore, as a result of the success of the 'dry impact' physical modelling tests, it is recommended that any follow-up towed test program should use synthetic (MODICE) model ice sheets. This has several advantages; the foremost being that the ice crushing strength can be modelled. This was not the case for the urea-type refrigerated ice in the present tests, which was not scaled, other than for thickness. The MODICE does not deteriorate with time and additional pieces may be added during testing to maintain the same coverage and piece size distribution in the broken channel. The density of MODICE is also closer to that of full scale ice, and therefore buoyancy forces will be better modelled. d This means that the flow of MODICE pieces along the hull in ahead manoeuvres, or under the stern in backing manoeuvres will be more representative.

A combination of the parametric torque results from the dry impact tests and the statistics from the towed trials allows the possibility of formulating a semi-empirical model of the rudder/ice interaction torques. This would greatly extend the prediction capabilities of the existing mathematical model and provide insights with repercussions for rudder system design and regulation.

REFERENCES

[1] Proposal to Investigate Ice Loads on Rudders and Steering Gear, ACL,937P, June 1981.

[2] Study of Steering System Components of Arctic Class Ships Amended Final Report, ACL 329C, Feb. 1979.

[3] Ice Worthiness Tests of Two Candidate Hulls for a Cabot Strait Ferry, Final Report 91C, Contents Proprietary, August 1975.

[4] Model Testing of Quadruple Screws, Double-Ended Ferry, NRC report to German & Milne, 1976.

APPENDIX A

MATHEMATICAL MODELS OF RUDDER LOAD AND STEERING GEAR RESPONSE

Mathematical Models of Rudder Load and Steering Gear Response

A.1 Rudder Loads

Assuming that the rudder dimensions and shape are properly scaled, the next problem was that of structural sufficiency. Overly bulky steering gear components would produce strains too small for accurate measurement, while under-designed metalwork would quickly loose its effectiveness and permanently set under heavy loads.

Newton's Law describes the impact between a moving mass and a rigid rudder on an elastic shaft is:

$$\Sigma F = \frac{d}{dt}(mV) \tag{A.1}$$

For a frangible material like ice, the force transmitted to the rudder at any time will be equal to the penetration strength multiplied by the crushed area:

$$F(t) = \sigma_c \; A = k_s \theta(t) \tag{A.2}$$

The rudder stock has a certain stiffness k and deflects a distance θ under the influence of force F.

For simplicity the impact may be assumed a central impact and friction ignored. The peak impact load on an appendage may then be determined from energy considerations as follows:

KINETIC ENERGY OF FLOE		STRAIN ENERGY OF APPENDAGE		ENERGY DISSIPATED IN CRUSHING	
$1/2 \; MV_I^2$	$=$	$1/2 \; k_s \theta^2_{max}$	$+$	$\sigma_c A_{max} \; d_{crush}$	(A.3)

and

$$F_{max} = k_s \; \theta_{max} = \sigma_c A_{max} \tag{A.4}$$

If the ice fragment is assumed to be a wedge shape of width (b), then the crushed area will be proportional to the depth crushed.

$$A_{crush} = bd_{crush} \tag{A.5}$$

Substituting (A.5) into equation (A.3) produces:

$$\frac{MV^2_i}{2} = \frac{k_s\theta^2_{max}}{2} + \sigma_c bd^2 \text{ cm} \tag{A.6}$$

where 'cm' denotes 'crushed maximum'.

In addition:

$$F_{max} = k_s\theta_{max} = \sigma_c bd \text{ cm} \tag{A.7}$$

Solving for θ_{max} in equation (A.7) gives:

$$\theta_{max} = \frac{\sigma_c bd \text{ cm}}{k_s} \tag{A.8}$$

Substituting for θ_{max} in equation (A.6) results in:

$$\frac{MV^2_i}{2} = \frac{\sigma_c{}^2 b^2 d^2 \text{ cm}}{2k_s} + \sigma_c bd^2 \text{ cm} \tag{A.9}$$

Simplifying (A.9) produces:

$$\frac{MV^2_i}{2} = \left[\frac{\sigma_c{}^2 b^2}{2k_s} + \sigma_c b\right] d^2 \text{ cm} \tag{A.10}$$

$$d^2 \text{ cm} = \frac{MV^2_i}{2\left[\dfrac{\sigma_c{}^2 b^2}{2k_s} + \sigma_c b\right]} \tag{A.11}$$

Finally we have:

$$F_{max} = \sigma_c bd \text{ cm} = V_i \sqrt{\frac{M}{\dfrac{1}{2k_s} + \dfrac{1}{\sigma_c b}}} \tag{A.12}$$

This shows that the impact load on an appendage is dependent upon the following parameters:

- mass of the ice fragment,
- relative velocity between the ice fragment and the appendage
- stiffness of the appendage
- crushing strength of the ice.

Using the scaling laws in Table A.1, the ice piece sizes are properly scaled since the thickness and elastic modulus of the model ice are correctly scaled. Since the model ice density is correct, the ice fragment mass in the model will correspond properly to the full scale mass. The stiffness of the model appendage is properly scaled in the model as shown later. The crushing strength of the model ice can also be scaled approximately. Hence:

$$(F_{max,p}/F_{max,m})=(V_i/V_{im})\sqrt{(M_p/M_m)(1/K_{sm}+2/\sigma_m b_m)(1/K_{sp}+2/\sigma_p B_p)} \qquad \text{(A.13)}$$

Where p = prototype
m = model

Now:

$$\frac{V_i}{V_{im}} = \lambda^{1/2}, \quad \frac{M_p}{M_m} = \lambda^3, \quad \frac{b_p}{b_m} = \lambda, \quad \frac{\sigma_p}{\sigma_m} = \lambda, \quad \frac{k_{sp}}{k_{sm}} = \lambda^2 \qquad \text{(A.14)}$$

Substituting in the above scale ratios produces the following results:

$$\frac{F_{max,p}}{F_{max,m}} = \lambda^{1/2} \sqrt{\frac{\lambda^3}{\frac{1}{2\lambda^2} + \frac{1}{2\lambda^2}}} \qquad \text{(A.15)}$$

Hence:

$$\frac{F_{max,p}}{F_{max,m}} = \lambda^3 \qquad \text{(A.16)}$$

Therefore the impact loads will be properly scaled.

TABLE A.1

DESIGN EQUATIONS BASED ON DYNAMIC (FROUDE) SCALING

1.	$S_l = 17$	GEOMETRIC LENGTH SCALE
2.	$S_g = 1$	GRAVITY (IDENTICAL) SCALE
3.	$S_\rho = 1$ steel,3 aluminum	DENSITY SCALE
4.	$S\delta = 1$	RUDDER ANGLE SCALE
5.	$S_m = S_g S_l^3$	MASS SCALE
6.	$S_J = S_l^4$	POLAR MOMENT SCALE
7.	$S_\mu = 1$	FRICTION SCALE
8.	$S_v = (S_g S_l)^{1/2} = S_l^{1/2}$	VELOCITY SCALE
9.	$S_t = S_l S_v^{-1} = S_l^{1/2}$	TIME SCALE
10.	$S_G = S_m S_t^{-2} S_l^{-1} = S_\rho S_l$	SHEAR MODULUS SCALING
11.	$S_{\sigma_c} = S_l$	ICE STRENGTH SCALE
12.	$S_K = S_G S_I S_l^{-1} = S_\rho S_l^4$	TORSIONAL STIFFNESS SCALE

PREDICTION EQUATIONS

1. $Q_p = S_l^4 Q_M$, Torque
2. $F_p = S_l^3 F_M$, Load

NOTE: Convention $S_X = \dfrac{\text{Full Scale X}}{\text{Model Scale X}}$

If the model and prototype rudders are geometrically similar and if a model material with a shear modulus of

$$(G_{steel}/\lambda)$$

is used for the appendages, then the deflections of the model rudder stock will be proportional to the deflections full scale. The deflections will be in the ratio:

$$\frac{D_m}{D_{fs}} = 1/\lambda \qquad (A.17)$$

The general relationship for deflection is:

$$\text{deflection} \propto k \frac{Wl^3}{EI}, \ k = \text{end constraint constant} \qquad (A.18)$$

and therefore the scaling ratio of deflections reduces to:

$$\frac{\text{deflection}_{fs}}{\text{deflection}_{model}} \quad \frac{\frac{W_{fs}}{W_m} \frac{l^3{}_{fs}}{l^3{}_m}}{\frac{E_{fs}}{E_m} \frac{I_{fs}}{I_m}} = \frac{\lambda^3 \cdot \lambda^3}{\lambda \cdot \lambda^4} = \lambda. \qquad (A.19)$$

Furthermore, the stiffness of the rudder stock was accurately scaled although the rudder itself was not. Hence strain in the model appendage will be equal to strain in the full scale unit. Consequently, one of the criteria for properly modelling impact loads will be met (total stiffness scaling).

In summary, by judicious choice of materials and arrangement of the model appendages and steering gear, by maintaining geometric similarity of the model appendages, and by strain gauging the model appendages; it was possible to obtain good estimates of the forces on the appendages and insure proper modelling of the impact phenomena.

A.2 Steering Gear Response

Prior to designing an electro-hydraulic steering gear, an analysis of the performance of a typical system in terms of the response and loading of the components was carried out. Figure A.1 shows the schematic of a typical hydraulic steering gear in a situation where the solenoid valve is activated to provide oil pressure in pipe B with return through pipe A. This results in the steering gear turning the rudder to port. The pressure relief valves (or the shock valves) are set at a pressure which will allow the rudder to give way when it is subjected to severe shock from ice impacts. In giving way, the rudder moves the pump control mechanism thereby putting the pump on stroke. When the external pressure is relieved, the rudder returns automatically to its former position.

We limit the following analytical development to steering gears of the electro-hydraulic type since they are the most widely used in practice. Figure A.2 shows the schematic operation of hydraulic servo-controlled steering gear. The sketch depicts only one cylinder for convenience of illustrating the principle. The displacement 'x' may be accomplished either by telemotor or by manual control. Since the bottom of the linkage is initially held fixed by the tiller arm, the top end of the link must move through a distance 'y' thereby activating the pump control mechanism. The pump then draws oil from the other pair of cylinders and discharges into the cylinder shown in the sketch and its companion (not shown in the figure). The ram is therefore forced to move to the left, thereby rotating the tiller arm through an angle δ. It must be pointed out that the motions of the pump control mechanism and that of the ram together, constitute a nearly perfect integration (if the oil can be considered incompressible and provided there is no leakage in the system). That is, the ram will move at a rate of $\dot{z}$ which is proportional to the opening of the valve y, i.e. $\dot{z} = cy$.

As the tiller arm rotates, the point P is moved to the right, thereby bringing the link back to its vertical position. At this point, the pump stops and the delivery of oil ceases. The position of the rudder is held fixed until the control linkage is again moved.

If the initial displacement at the controls is x and the instantaneous displacement of the pump control mechanism and the rudder angle are y and δ respectively, then from geometry, we have:

$$y = \frac{(l_1+l_2)}{l_2} x - \frac{(l_1 l_4)}{l_2} \delta \qquad \text{(A.20)}$$

Also $z = l_3\delta$, so that $\dot{z} = l_3\dot{\delta}$

FIGURE A.1

SCHEMATIC OF A TYPICAL HYDRAULIC STEERING GEAR

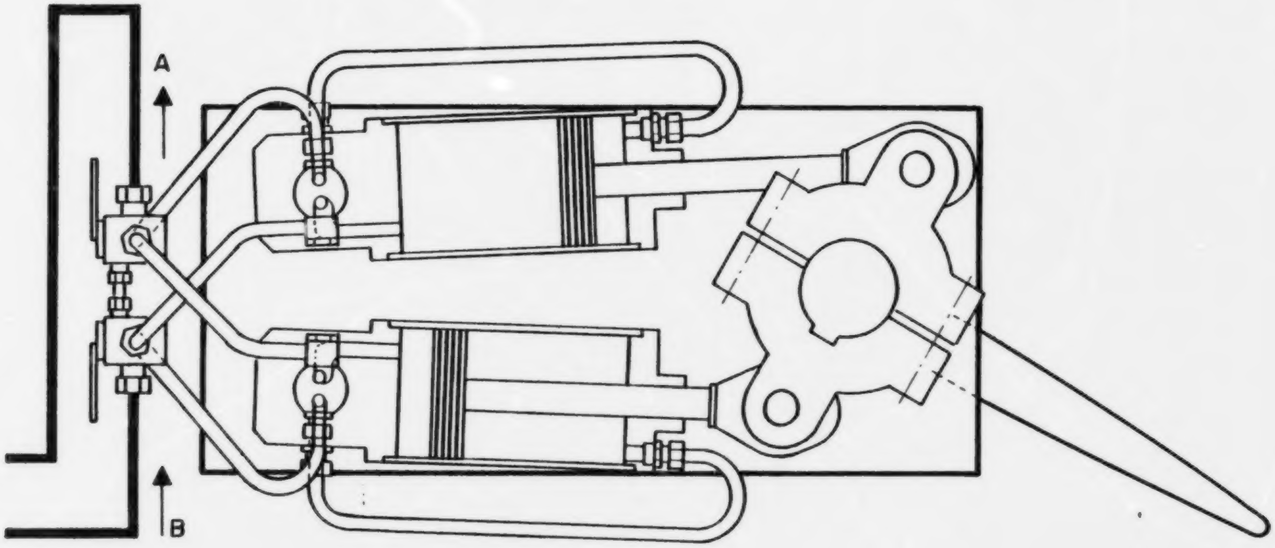

FIGURE A.2

PRINCIPLE OF OPERATION OF A HYDRAULIC STEERING GEAR

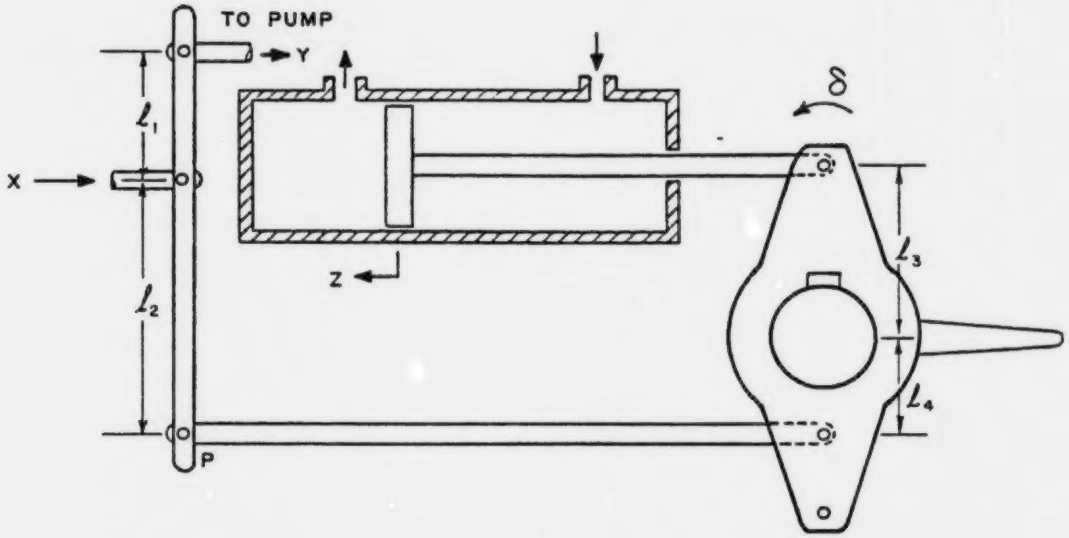
TO PUMP
Y
X
Z
P
δ
l_1
l_2
l_3
l_4

FIGURE A.3

TYPES OF TILLER ARRANGEMENTS

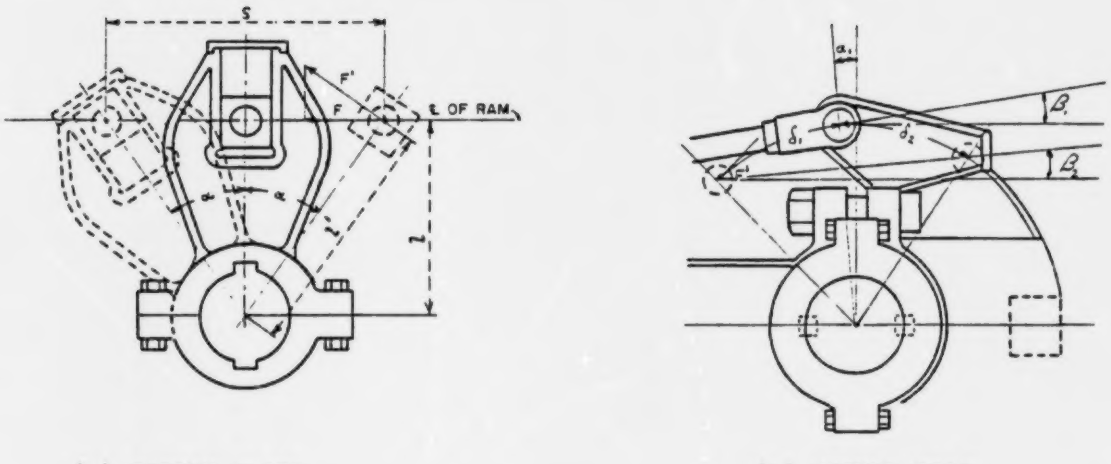
S
F'
F
℄ OF RAM
α
α
l
l
α_1
β_1
β_2
δ_1
δ_2
F'

(a) RAPSON SLIDE

(b) WAGNER GEAR

The equation governing the instantaneous rudder angle is then: (from equation A.20)

$$\dot{\delta} = \frac{C}{l_2 l_3} [(l_1+l_2)x - l_1 l_4 \delta] \qquad (A.21)$$

or

$$\dot{\delta} + \frac{Cl_1 l_4}{l_2 l_3} \delta = \frac{C(l_1+l_2)}{l_2 l_3} x \qquad (A.22)$$

The differential equation (A.22) can easily be solved by separating the variables. The solution is:

$$\delta(t) = \frac{a_2}{a_1} - \left(\frac{a_2}{a_1} - \delta_0\right) \exp(-a_1 t) \qquad (A.23)$$

where

$$a_1 = \frac{Cl_1 l_4}{l_2 l_3} \qquad (A.24)$$

$$a_2 = \frac{C(l_1+l_2)x}{l_2 l_3} \qquad (A.25)$$

In equation (A.23) $1/a_1$, which has units of time, is called the "time constant" of the steering gear. The definition of the term "time constant" can be obtained by noting the amount by which δ has "decayed" at the end of time $t = 1/a_1$. This is given as:

$$\delta(1/a_1) \equiv 0.6321 \frac{a_2}{a_1} + 0.3679\ \delta_o \qquad (A.26)$$

A.3 Forces in Hydraulic Rams

The ram groups of hydraulic steering gears are of two general types: the link-connected mechanism and the Rapson slide. The principle of Rapson slide is made use of in Hastie steering gears, while a modified link-connected version is incorporated in the Wagner gears.

The Rapson-slide (Hastie gear) force diagram is shown in Figure A.3(a) which indicates that the torque for each ram is (assuming double-ram construction):

$$\frac{Q}{2} = F'l' = \frac{F}{\cos\delta} \cdot \frac{l}{\cos\delta} \qquad (A.27)$$

where δ = the rudder angle

l = the crosshead radius

F = axial force on the ram

Therefore, the axial force on the ram

$$F = \frac{Q\cos^2\delta}{2l} \qquad (A.28)$$

In the Wagner-type gears, the ram cylinders pivot about a fixed point, thereby eliminating the need for slides. In this case then, (from Figure A.3(b)):

$$F = \frac{Q}{2l\cos(\delta_1 + \alpha_1 - \beta_2)} \qquad (A.29)$$

Equations A.28 and A.29 can be used to determine the ram forces if the maximum hydraulic pressure is known. In non-dimensional form the ram forces can be written as:

$$F' = F/p_v \frac{\pi}{4} d_r^{\,2} \qquad (A.30)$$

where p_v = relief valve pressure setting

d_r = diameter of hydraulic ram.

APPENDIX B

BIBLIOGRAPHY

"Arctic Deployment of USCGC POLAR STAR, Winter 1982, Volume IV, IVA - Ice Loads on Steering Gear Systems", TP 4125E, Arctec Canada Report FR937C-2.

"Design of Ship Rudders", by H. Thieme, Translation 321 DTNSRDC, November 1965.

"Design of Steering Gears, Rudders, Rudder Stocks and Propeller Protection for Arctic Class Ships", N.V. Laskey, SNAME, 1979.

"Feasibility Study, Employing the Rudder as Anti-Rolling Device", K. Huang, Report No. 518, Delft University of Technology, April 1981.

"Study of Steering System Components for Arctic Class Ships", Arctec Canada Limited FR329C, November 1978.

"Hydrodynamic Added Mass and Moments of Inertia of Ship Rudders", J. Brix, HANSA Vol. 114, 1977, p. 1151 (in German).

"Identify and Control of Ship Steering Process", A. Tiano, Ship Operation Automation, North Holland Publishing Company, 1977.

"Lifting Surface Theory Applied to Ship Rudder Systems", F. Hess, International Journal of Shipbuilding Progress, November 1978.

"Notes on Rudder Design Practice", A. Taplin, First Symposium on Ship Manoeuvrability, Department of U.S. Navy, 1960.

"Propellers, Rudders and Manoeuvring Devices", J.W. English, Translation, North-East Coast Institution of Engineers and Shipbuilders, 1976.

"Reliability Improvements for Vessel Steering Systems", Final Report by J.J. Henry Co., Inc., Report to MARAD No. RD-920-79011, December 1978.

"Rudder and Steering Gear Load Measurements on RADISSON", Arctec Canada Report, TP 6250E, March 1985.

"Iceworthiness Tests of Two Candidate Sterns for a Cabot Strait Ferry", Arctec Canada Limited Report FR91C, August 1975.

Brief summaries of past projects related to rudder loads carried out by Arctec Canada Limited are given below.

1974 ACL 15C Manoeuvring Model Tests - CCGS LABRADOR

Rudder effectiveness in steady turning in level ice and the influence of hull form on turning and directional stability. First ever rotating arm tests in ice to measure manoeuvring performance.

1978 ACL 245C Measurement of Rudder & Steering Gear Loads CCGS PIERRE RADISSON

Full-scale trials in ice and in open water were conducted near Cambridge Bay, N.W.T., Rudder stock torque, axial loads in hydraulic rams and rudder angles were measured. Analysis of torque data for a sample 4-hour period produced typical statistical parameters such as average and peak torque as well as log-normal distributions for ahead and astern operations. The maximum torque recorded corresponds to 1.8 times the hydrodynamic design torque.

1979 ACL 329C Study of Ice/Rudder Interaction

This project reviewed all available damage data, design criteria and regulations related to rudders, stocks, steering gears and protection devices for ships operating in ice-covered waters.

The damage statistics indicated that the most common case of steering system damage consisted of torsional failure of the rudder stock. Various modes of ice/rudder interaction were studied from which it was concluded that backing and ramming operation generated the most severe loads on the rudder. A mathematical model of the rudder/ice impact process was developed which predicts the torque in the rudder stock, the responses of the steering gear and the pintle loads. Predicted torque time-histories were compared with full-scale torques measured during the 1978 RADISSON trials listed above. It was concluded from the model predictions that the time constants (reaction times) of conventional hydraulic steering gears are longer than the typical duration of ice impact so that the steering gears do not act as shock-absorbing devices, and hence do not offer overload protection to rudder stocks.

1979 ACL 357C LOUIS S. ST. LAURENT - Full Scale Trials

During the trials conducted en route to Nanisivik, steering gear loads due to backing and ramming operations were measured. The instrumentation consisted of hydraulic ram gauges and rudder angle indication. About 36 hours of recorded data were obtained in ice up to 1.7 m thick.

1982 ACL 881C Manoeuvring Tests and Rudder Vulnerability Tests with POLAR 8 Icebreaker Model

Measurements and observations relating to manoeuvring in ice of the proposed triple-screw polar-class icebreaker design were carried out using a 40:1 scale model. A series of towed tests at various drift angles were conducted with instrumented rudders to assess rudder vulnerability in a turn. These gave the order of magnitudes of the ice torques that are likely to be experienced by the rudder stocks. Recommendations for possible improvements to the manoeuvring performance were made and design torques for full-scale rudder stock design were given.

1982 ACL 937C Measurement of Ice Loads on Rudders and Steering Gear of USCGC POLAR STAR

This was a major Canadian participation in the on-going U.S. Polar Class test series and involved measurement of torsional and flexural strains in the rudder stock, pressures in the hydraulic cylinders, strains in hydraulic rams, strains in the steering gear foundation and the rudder angle. In addition, accelerometers, yaw-rate sensor, and astern-looking video cameras were fitted to monitor vibration levels in the steering gear, ship's rotational velocities and ice conditions around the stern. A micro-computer based digital data acquisition system was used to collect, reduce, and analyse the data. Parallel to the data analysis task subsequent to the trials, this project also involved procurement, review and analysis of all available full-scale data on rudder and steering gear loads and responses. The data included those obtained onboard the CCGS RADISSON, CCGS LOUIS, and USCGC NAUGATUCK and the 14500 Soviet tanker. A statistical analysis of all the data was carried out to examine the effect of varying ship operational modes, ice conditions and rudder configurations. The results of the analysis were used to develop a preliminary ice-strengthening procedure for other ships and ice conditions. Gaps in the current data base have been identified for future research.

1984 ACL 1554C Study of Rudders, Rudder Stocks, Steering Gears and Manoeuvrability of Arctic Class Ships

This study started off with a review of the current status of design, construction and operations of rudders and steering gears onboard vessels in an Arctic environment. In this task experience of ship owners, operators, steering gear manufacturers and repair-maintenance groups were surveyed by means of formal enquiries in the form of a questionnaire. This was followed by a review of the rules for design and classification of the ice class rudders as set forth by about ten (10) authorities and a comparison of the rules for rudder stock sizing. Current practices for the protection of steering gears, steering gear control, single failure criteria and the effects of material and vibration were surveyed. A comprehensive review of all available full-scale and model-scale rudder load data was conducted to update the current status of the data base. In order to document the present level of understanding of the manoeuvring characteristics of ships in ice, all available full-scale and model-scale data on steady turning circles in ice were procured, analyzed and interpreted. It was concluded that although the data base represented a variety of hull forms and vessel types, consistent parametric sets of data were lacking. A brief survey of work related to the mathematical modelling of rudder ice interaction and rudder hydrodynamics was carried out identifying the areas of application and the limitations of the models. A number of possible scenarios associated with various types of vessels (from tankers to fishing vessels) were developed and the applicability of the available data base to the scenarios were assessed. Methods of assessing steady turning performance in level ice and preliminary guidelines for estimating design torques in rudder stock were discussed and the need for improvements to these methods were identified.

1985 ACL 1776C Rudder and Steering Gear Load Measurements on CCGS PIERRE RADISSON

This project is particularly relevant to the proposed work. The development of a 4-channel statistical data collection package and its installation on the steering system of CCGS PIERRE RADISSON is the basis of this project. The instrumentation system was aimed at measuring rudder stock torque, hydraulic ram force and the rudder angle for an unattended period of two months. The data retrieved was reduced and analyzed, which indicated that the vessel's steering system experienced moderately severe loads under normal escort operations in the St. Lawrence Seaway. Refinements to the data acquisition unit have been identified which will improve the reliability of the instrumentation system and provide ease of operation.

1985 ACL 1723C Antarctic Manoeuvring Trials of USCGC POLAR STAR

This project consisted of a comprehensive program of assessment of the manoeuvring performance of POLAR CLASS vessels involving full-scale, level ice turning trials as well as development of mathematical models to predict steady turning radius. The trials were carried out in McMurdo Sound, Antarctica which generated 19 data points. Two mathematical models were developed, one making use of a time history method utilizing approximate model test data for hull coefficients. The second model makes use of a force balance method involving an assumed hull-side force distribution. Preliminary comparisons of the predicted and measured turning radii have been made. Analysis of the full-scale data showed that further controlled tests at larger rudder angles will be required for complete validation of the mathematical models.

1985 ACL 1163C Modelling of Steering System Interaction with Ice

This is a scale-model test program (in progress) to determine the magnitude and time history of the loads imposed on steering systems due to rudder/ice interactions. By carrying out controlled impact tests using synthetic ice on a model rudder and steering gear system, these loads will be measured as a function of ice strength, speed and rudder angle. The project also includes a series of towed tests in refrigerated ice using large scale model sterns to determine the influence of draft, rudder and ice horn designs and propeller rotation on the frequency of ice impacts in various ice thicknesses and speeds.

APPENDIX C

DETAILED STATEMENT OF WORK

NOTES ON COMPLETION OF TASKS IN WORK STATEMENT

The report documenting this project has been prepared to describe the work carried out under specific tasks, which are defined in the 'Detailed Statement of Work'. The work statement has been included herein to provide a reference in assessing the means by which each task has been completed and the technical advances which this completion represents. In certain instances, deviations from the initial task wording occurred as the work evolved. These differences are explained below and generally represent extensions to the scope of work, rather than reductions. Table A.1 gives a cross-reference listing showing task sections from the work statement and corresponding sections in the text.

As a first step in defining the experimental program, a brief state-of-the-art review of rudder-ice loading and steering system dynamics was carried out. This involved a search of in-house material and a review of public domain sources. On this basis, a bibliography has been developed, which is included in the text. This review provided additional impetus for the two experimental tasks, since it was found that there is very limited model test data and no detailed physical modelling results available to the scientific community. The dearth of information has had a significant impact on the level of effort applied to designing the 'dry mode' tests and the 'towed' model tests.

In preparing the test plan (Section 4.4) it was considered of most importance to arrange the test matrices to obtain data on a large range of operating conditions, so as to establish reference trends for verification of a mathematical model. The 'dry mode' impact tests were therefore designed to parametrically assess the response of a typical rudder mechanical assembly and control system in the context of the extreme ice load scenario. By accurately scaling the geometric and dynamic properties of the test system, it has been possible to assemble a substantial data base of information on rudder ice loads, stock torsional strain and other response variables.

As per 4.4.1, the detailed physical modelling of the 'dry mode' rudder model was developed; involving a careful assessment of weights and sizes of components associated with different possible sections of scale. This resulted in a 1:17 scaling of the LOUIS S. ST. LAURENT rudder. In particular, the materials selection for the stock considered the minimum diameter of aluminum or steel could reliably be strain gauged and would have the correct torsional stiffness. The properties of the synthetic MODICE used in Task 7 were derived in 4.4.2 as a result of a series of uniaxial crushing tests, which validified an empirical ice strengths scaling relationship for this material. The thickness of the urea-type model ice used in the towed tests was based on calculation of the maximum thickness at which continuous icebreaking is possible for each of the three test ships. The equations of motion and a description of an amplified mathematical model of a conventional hydraulic system have been included (4.4.3) and a description of instrumentation and test procedures for both test phases (4.4.4).

In defining the test matrix (4.5) for the 'dry mode' rudder impact tests a Graeco-Latin square factorial arrangement was utilized to prepare an optimal number of tests. However, it was necessary to increase the number of test variables to adequately assess the physical model response, and therefore a larger range of parametric variation and a significantly larger number of test runs were carried out. This addressed variation in impact velocity, rudder angle, ice mass, ice strength, stock torsional stiffness and hydraulic pressure release. The measured response included: torsional strain, bending strains, rudder loads and hydraulic ram pressures.

The towed test program (4.6) was developed to investigate a range of parameters. Three test vessels were identified with the requisite hull and screw variations. A large matrix of tests was prepared to consider forward and ahead manoeuvres, rudder-ice impact angle, propeller rotation direction, RPM, ice floe size and irregular features. The principal output variable was frequency of impacts on the rudder. Rudder loading (torques) were also recorded.

Data analysis of the dry impact tests (4.7.1) involved an assessment of the time history data from a large set of parametric results. Peak values of torque, bending moments, rudder load components, indentation, and other variables have been tabulated. The influence of each of the parameters on the rudder system response variables has been parametrically investigated by means of graphical comparisons using the peak data.

Data analysis of the ice basin towed tests (4.7.2) has emphasized the histograms which show frequency of impact for different categories of ship operating and environmental conditions. The rudder-ice impact geometry was observed by means of underwater video. This was an improvement on the original plan to utilize an above water high speed camera. Slides and an above water colour video camera were used to measure ice floe sizes and to document the tests. A limited comparison of results from the dry impact tests and the ice basin tests has been carried out. This has involved an assessment of the torque time histories which were observed under the two test conditions. It has not been possible to provide a numerical correlation, since the dry mode testing involves an extreme test scenario with the rudder-ice contact depth at a maximum and the ice masses very large. Individual parametric test phase results and their comparison forms the basis for a formulation of a design criteria for rudder-ice interactions. Statistics of flow of ice into the rudder is given by the ice basin tests, and magnitudes of response are defined by the dry impact tests.

As specified in 4.8 the findings of the entire test program have been reported in the text of the final report. The special instructions (7) have been followed as a guideline in preparing the report. Where additional technical information is considered of supplementary value to the text, it has been placed in the appendices.

4. DETAILED STATEMENT OF WORK

DEGREE OF
COMPLETION

The work constituting this project shall include the following elements and shall be consistent with the relevant segments of Arctec Canada Limited proposal 937P (The Proposal). Items specified below in relation to the several tasks, are to be read in conjunction with the task definitions in the Proposal.

4.1 Work Plan

Develop a detailed work plan, including activity schedule, cash flow projection, project management control and documentation procedures, within four weeks of the effective commencement date. Sequential activities are to be shown on a network diagram and milestone points at which the draft summaries of working papers described in paragraph 7.2 will be made available. The plan is to be updated as work progresses and plans are further developed or modified.

100%

4.2 State-of-the-Art Bibliography

Being well informed as to the subject matter of this project, the Contractor is to provide a bibliography listing of works, published or not, known to him and relevant to the project. Those which are particularly useful are to be so indicated, and an abstract supplied. Where the proprietary nature of an item is felt to preclude its listing as above, a reduced method of indicating its existence may be employed in order to avoid any unethical disclosure.

100%

In addition to the above, a brief literature survey is to be carried out to discover and evaluate any work of which the contractor is not aware; any information which could influence the conduct of this project is to be promptly notified to the Scientific Authority.

4.3 Tasks

Tasks outlined in the proposal are modified and further defined as outlined below; if there is any inconsistency, this work statement is to take precedence.

4.4 Preparation of Test Plan (Task 6 of Proposal)

This task will address the following aspects:

4.4.1 Models of rudder, rudder stock - their sizes, materials and construction. 100%

4.4.2 Required synthetic ice properties, sizes and shapes of floes and irregular ice features. Choice of the parameters will depend on the scale factor required to model the torsional stiffness of rudder stock. Selection of a convenient scale factor will be addressed in sufficient detail. Properties of synthetic ice to be used in the dry impact tests (Task 7) to be established by independent measurements prior to actual tests; data presented need not be fresh, but must be relevant to mixtures and procedures to be used. 100%

4.4.3. A simplified mathematical model of conventional hydraulic steering gears and their responses to externally imposed loads on the rudder will be developed to obtain a qualitative understanding of the influence of the various system parameters on the steering gear response. The analysis is aimed at identifying non-dimensional quantities governing the response of and load in the steering gear, involving parameters such as rudder turning rate, relief valve pressure, and the elasticity, inertia and damping in the system. The analysis will produce the sensitivities of the loads and responses to variations in system parameters. At this stage, consultations will be made with a manufacturer to work out the details of a simple physical model of a hydraulic steering gear to the required scale. 100%

4.4.4 Planning of the towed model test program in saline ice. Details of instrumentation and photographic coverage will be worked out. Methods of reducing and analyzing the data will be drawn up. A preliminary test schedule will be prepared and submitted for discussion and approval. 100%

4.5 Rudder Load Dry Model Tests (Task 7)

These will consist of controlled impacts on a model rudder with a synthetic ice sample of uniform crushing strength, at prescribed velocities. The parameters measured will include torsional and flexural strains, rudder movement, impact location on the rudder. Rudder angle and impact velocity will be varied. Reaction forces on the synthetic ice block will also be measured, and the areas and characteristics of rudder imprints. The experiments will be repeated at three different crushing strengths and also with various representative response characteristics representing the steering gear, as well as "infinite stiffness" as originally proposed. A matrix of the test parameters will be developed along with their target values and a Graeco-Latin square factorial arrangement will be used to optimize the number of tests to be performed and to organize the data reduction techniques. 100%

4.6 Towed Tests in Level Ice and Broken Floes, etc. (Task 8)

The tests will consist of investigation of the following parameters:

- Frequency of rudder/ice impacts in the astern and ahead maneuvering modes. 100%

- Influence of operating draft, rudder angle, propeller rotation and size of floes and irregular features.

- Geometry of ice impact on the rudder for the various rudder configurations:

  - single screw, single rudder
  - twin screw, single rudder,
  - triple screw, single rudder

These configurations ar covered by the models to be selected.

Some irregular ice configurations will also be modelled and tested.

4.7 Data Analysis (Task 8a)

This is essentially the parts of tasks 9 and 10 as originally defined, which consists of reduction and analysis of data acquired from the model experimental program. 100%

4.7.1 Dry Impact Tests

The data analysis will emphasize the following:

- Torque time history - peark value and rise time.
- Ratio flexural strain to torsional strain in rudder stock.
- Influence of ice crushing strength and impact velocity on rudder loads. 100%
- Rudder load - crushed area relationships.
- Influence of rudder stock diameter, length and dynamic characteristics on rudder loads.
- Response of hydraulic steering gear system to the imposed loads and the effect of the response characteristic on the loads.

4.7.2 Ice Basin Tests

- Frequency of ice impacts.
- Rudder/ice floe impact geometry from high speed movies.
- Limited comparison of results with those from Phase I. 100%
- Formulation of design criteria.

4.7.3 General

a) Raw data is to be preserved and catalogued with a clear and complete explanation as to how all or any part of it may be accessed for review or re-examination. Cross reference keys are to be provided or identified, and explained so that separate records of the same event may be correlated readily with each other. 100%

b) Data reduction procedures are to be fully explained, with sample calculations and full particulars (by reference if appropriate) of any computer programs or processes used. Where appropriate, records of reduced data are to be preserved and catalogued as in 4.4.1 above. 100%

c) A representative number of typical segments of data involving incidents of interest, including but not only those which are selected for analysis, are to be presented in the report with pictures and diagrams, etc. as appropriate and an explanation to give a clear understanding of what is recorded, how, and the behaviour of each parameter during the event. 100%

d) Information as to the instrumentation used to measure and record the data is to be reported, including its nominal accuracy, calibration procedures and results, with a sample calculation of results. Where specific information as to the accuracy of measurements is not available, estimates are to be made and explained. 100%

e) Full particulars of analyses are to be reported: analysis methods are to be fully explained, with supporting rationale and sample calculations. Existing methods are to be critically reviewed and updated if appropriate. 100%

4.8 Reports

Interim reports will be submitted at completion of each task. Details and findings of the entire test program will be part of the final report. The requirements of paragraph 7 "Special Instructions" will be followed for both interim and final reports, as also will the requirement of paragraph 9 "Reporting Requirements".

Progress reports will be as specific in paragraph 9.1.

Library and Information Centre /
Centre [illegible]
REC[illegible]
AUG 14 1987
Transport Canada / Transports Canada

Volume

2

CA1
DTC 801
86
M572
c.2

arctec canada limited

MODEL STUDIES OF ICE INTERACTION WITH SHIP RUDDERS AND STEERING SYSTEMS

VOLUME II

TYPICAL DRY IMPACT RUDDER TORQUES AND ICE BASIN TOWED TEST DATA

TP# 8136E

November, 1986

Submitted to

Transportation Development Centre,
Complexe Guy-Favreau,
200 Dorchester Blvd. West,
Suite 601, West Tower
Montreal, Quebec.
H2Z 1X4

AUG 31 1987

Submitted by

B. Menon
L. Phillips
T. Roots

ARCTEC CANADA LIMITED
311 Legget Drive
Ottawa, Ontario
K2K 1Z8

DISCLAIMER

The contents of this report reflect the views of Arctec Canada Limited and not necessarily the official view or opinions of the Transportation Development Centre of Transport Canada.

LANGUAGE NOTE

Un sommaire en français de ce rapport est inclus avant la Table des matières.

APPROVED BY: ______________________
I.F. Glen, President

Transport Canada Transports Canada
Development Développement

REPORT DOCUMENTATION FORM

1. Transport Canada Report No. TP 8136E	2. TDC Project No. 4877	3. Recipient's Catalogue No.
4. Title and Subtitle MODEL STUDIES OF ICE INTERACTION WITH SHIP RUDDERS AND STEERING SYSTEMS		5. Report Date November 1986 6. Performing Organization Report No. 1163C
7. Author(s) B. Menon, L.D. Phillips, T. Roots		8. Transport Canada File No. D1460-179-2
9. Performing Organization Name and Address Arctec Canada Limited 311 Legget Drive Kanata, Ontario K2K 1Z8		10. DSS File No. 10SD.T8200-3-3519 11. DSS or Transport Canada Contract No. 1SD85-00077
12. Sponsoring Agency Name and Address Transportation Development Centre (TDC) Guy Favreau Complex 200 Dorchester Blvd. W., Suite 601, West Tower Montreal, Quebec H2Z 1X4		13. Type of Report and Period Covered Final (Sept./85-Oct./86) 14. Sponsoring Agency Code TDC 4877
15. Supplementary Notes Volume I - Main Report Volume II - Appendices		16. TDC Project Officer C. Nowicki

Abstract

This report presents the methodology and results of two complementary series of model scale experiments on ice loading effects on ship rudders and steering systems. In the first series, experimental data was obtained from controlled impacts of a 1:17 scale physical model of the LOUIS S. ST. LAURENT rudder into synthetic model ice. In these 'dry mode' tests, a range of parameters was investigated, including the influence of: impact velocity, ice floe size, rudder angle, ice strength, rudder stock torsional stiffness and hydraulic relief pressure. Trends in rudder stock torsional and flexural strains, rudder loads, and other response variables were identified as a function of the operating models: MV ARCTIC, PIERRE RADISSON and POLAR 8. Frequency of ice impacts on the rudder was measured in broken ice using self-propelled towed models. A range of operating conditions was investigated by means of variation in ship forms, velocity, rudder angle, draft, drift angle, direction of motion, and thrust levels. The influence of these parameters is discussed and presented by means of histograms. Rudder torque measurements in the ice basin tests provide a comparison to the dry impact test results. This work is directed towards development of rudder load design criteria for steering systems and verification of a mathematical model of rudder response.

18. Key Words Rudder, Rudder stock, Rudder loads, Physical modelling, Model tests, Ice impacts, Steering gear, Design torque		19. Distribution Statement A limited number of copies are available from the Transportation Development Centre	
20. Security Classification (of this report) unclassified	21. Security Classification (of this page) unclassified	22. No. of Pages 220	23. Price ----

Transports Canada Transport Canada
Développement Development

FORMULE DOCUMENTAIRE DU RAPPORT

1. Nº du rapport Transports Canada
TP 8136E

2. Nº de l'étude — CDT
4877

3. Nº de catalogue du destinataire

4. Titre et sous-titre
MODEL STUDIES OF ICE INTERACTION WITH SHIP RUDDERS AND STEERING SYSTEMS

5. Date du rapport
novembre 1986

6. Nº du rapport de l'organisme exécutant
1163C

7. Auteur(s)
B. Menon, L.D. Phillips, T. Roots

8. Nº de dossier Transports Canada
D1460-179-2

9. Nom et adresse de l'organisme exécutant
Arctec Canada Limited
311 Legget Drive
Kanata (Ontario)
K2K 1Z8

10. Nº de dossier — ASC
10SD.T8200-3-3519

11. Nº de contrat — ASC ou Transports Canada
1SD85-00077

12. Nom et adresse de l'organisme parrain
Centre de développement des transports (CDT)
Complexe Guy-Favreau
200 ouest, boul. Dorchester, suite 601, tour ouest
Montréal (Québec) H2Z 1X4

13. Genre de rapport et période visée
Final (sept.85-oct.86)

14. Code de l'organisme parrain
CDT 4877

15. Remarques additionnelles
Volume I - Rapport principal
Volume II - Appendices

16. Agent de projet — CDT
C. Nowicki

17. Résumé

Le présent rapport donne les résultats, et explique les méthodes de mise en de deux expérimentations complémentaires visant à approfondir l'action des glaces sur le gouvernail et l'appareil à gouverner d'un navire. Dans un premier temps, des données expérimentales ont été tirées des essais de choc contrôlés qui mettaient en oeuvre un modèle réduit au 1/17 du brise-glace LOUIS-SAINT-LAURENT heurtant une glace synthétique modèle. Dans ces essais dits hors bassin, des variations ont été imposées aux facteurs contrôlés suivants: vitesse à l'impact, taille des fragments de glace, angles de braquage, résistance de la glace, raideur en torsion de la mèche et pression d'ouverture du circuit hydraulique de commande. L'évolution des déformations de torsion et de flexion de la mèche, des efforts sur le gouvernail et d'autres variables a été établie à l'égard des trois modèles réduits représentant le N.M. ARCTIC, le PIERRE-RADISSON et le POLAR 8. Dans un deuxième temps, par des essais de remorquage en bassin rempli de fragments de glace, la fréquence des impacts sur le gouvernail a été chiffrée. Les facteurs contrôlés étudiés ont été les suivants: forme de la coque, vitesse, angle de braquage, tirant d'eau, angle de dérive, sens de rotation des hélices et poussée; l'influence des ces paramètres est commentée, histogrammes à l'appui. Les valeurs de couple mesurées sur le gouvernail lors des essais en bassin servent de point de comparaison aux essais hors bassin. Une fois combinés, les résultats des deux expérimentations permettront de vérifier un modèle mathématique simulant la réponse d'un gouvernail à la charge des glaces et de mettre au point les critères de calcul correspondants.

18. Mots-clés
Gouvernail, mèche, efforts, modèles réduits, modélisation physique, essais sur modèles réduits, appareil à gouverner, couple de référence, choc des glaces.

19. Diffusion
Le Centre de développement des transports dispose d'un nombre limité d'exemplaires.

20. Classification de sécurité (de ce rapport)	21. Classification de sécurité (de cette page)	22. Nombre de pages	23. Prix
non classifié	non classifiée	220	----

CDT/TDC 79-005
Rev 86

Canada

PROJECT TEAM

The project team for Arctec Canada Limited was composed of:

- B. Menon, Program Manager
- L. Phillips, Project Engineer (Dry Impact Tests)
- L. Goossens, Project Engineer (Ice Basin Tests)
- T. Roots, Test Engineer
- R. Brown, In-House Consultant, Numerical Modelling and Data Analysis

with technical assistance from:

- D. Bourne
- A. Karton
- A. Lemieux
- A. Moonah
- R. Nelson
- V. Nisbett.

ACKNOWLEDGEMENTS

The authors would like to acknowledge the support of Mr. Chris Nowicki who, as Scientific Authority at Transportation Development Centre, has patiently directed this project to a satisfactory completion. In addition, we would like to thank Mr. Ian Bayly, also at Transportation Development Centre, who originally supported this important study on rudder/ice loading and who provided valuable guidance at the early stages of development of the experimental programs.

SUMMARY

Two complementary model scale experiments have been carried out to systematically investigate the response characteristics of ship steering systems under the influence of ice loads acting on the rudder.

- In the first phase of the project the rudder-ice interaction problem was addressed by physical modelling. A 1:17 scale model of the rudder assembly of the Canadian Coast Guard icebreaker LOUIS S. ST. LAURENT was designed and parametrically tested over a range of impact conditions. This provided a database of information on rudder loads, torques, bending strains, and other parameters.
- In the second phase of the project, three ship models were tested in the ice basin to measure frequency of ice impacts on the rudder as a function of a range of ship operating conditions.

The work is generally directed towards the development of rudder load design criteria for ship steering systems and the verification of a mathematical model of rudder response to ice impacts. The database and trends determined as a result of these two experiments represents a valuable tool in advancing the design of steering systems for ice-worthy vessels.

Physical Modelling of Dry Impact Test System

The dry mode impact tests were planned to parametrically study the loading and response of a typical rudder assembly and hydraulic steering gear from the perspective of the severe ice impact scenario. The LOUIS S. ST. LAURENT rudder was chosen as the prototype, representative of a typical icebreaker rudder assembly. Physical modelling involved the accurate scaling of pertinent geometric and dynamic properties of the test system; including rudder, stock, tiller, rams, hydraulic actuator system, and ice. A 1:17 scaling was selected on the basis of size and weight considerations. Figure 1 shows a representation of the test system. A scaled model of the rudder and matching rudder stocks were designed and machined from aluminum. The rudder was free to rotate on a pair of pintles and it was supported along the stock by a support bearing and a carrier bearing. Three rudder stocks having different diameters were fabricated to introduce variation of the rudder stock torsional stiffness.

The rudder stock attached to the tiller could be fixed rigidly or could be rotated by the rams of a hydraulic actuator system. The entire rudder assembly was bolted to a steel box which was suspended on a two meter track under the towing carriage. It was possible to add ballast weights to this box, and thereby change the mass involved in the rudder-ice interaction at the impact speed. Since the broken channel ice floes are generally much less massive than the ship, it is valid to consider that this moving box mass represents the mass of the ice pieces.

FIGURE .1

DRY IMPACT EXPERIMENTAL SET-UP

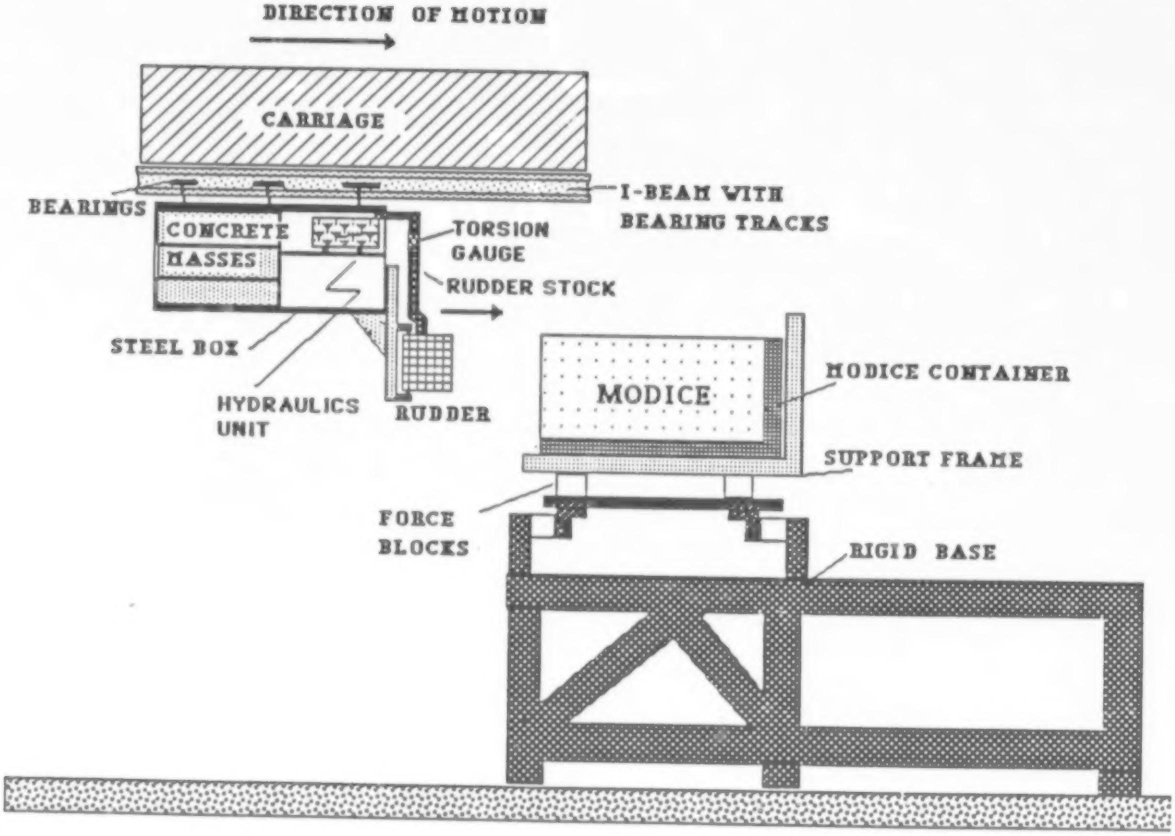
DIRECTION OF MOTION
CARRIAGE
BEARINGS
I-BEAM WITH BEARING TRACKS
CONCRETE MASSES
TORSION GAUGE
RUDDER STOCK
STEEL BOX
HYDRAULICS UNIT
RUDDER
MODICE
MODICE CONTAINER
SUPPORT FRAME
FORCE BLOCKS
RIGID BASE

The synthetic ice, MODICE, used in these tests is a wax-type material, which is formulated as a melt and allowed to set in a mold. Therefore, the testing could be carried out in a 'dry mode', with only a surface spray of water onto the MODICE to improve friction. The strength of the ice was controlled by means of an empirical scaling formula that is considered valid for crushing type application. This relationship was verified through a series of uniaxial crushing tests using Arctec's Closed Loop System. A target strength of 53 kPa was defined. This assumes that multi-year ice fragments represent the most extreme scenario. During testing the entire trailing edge of the rudder was involved in the crushing process. A series of eight ice blocks were prepared which included very strong ice, moderately strong ice, target ice, and relatively weak ice (15-22 kPa, 68 kPa, 86 kPa, 175 kPa). The blocks were mounted on a force balance which measured axial direction and lateral direction forces in the horizontal plane.

Dry Impact Test Results

The test matrix for the dry mode rudder-ice impact tests involved variation in six parameters: velocity of impact, rudder angle, rudder stock torsional stiffness, ice mass, ice strength and hydraulic pressure relief. In excess of 130 tests were carried out. Measured variables included: rudder loads (longitudinal and transverse components), stock torsional strain, bending strain (side and front components), ice indentation and ram hydraulic pressures. The influence of the operational parameters on the measured response has been assessed and represented graphically. Figure 2 provides an example showing the influence of ice strength and velocity on peak torque. The following general trends have been observed, although no definitive functional relationships have been derived in the present analysis:

- The influence of ice strength is strongest for peak rudder loading, longitudinal accelerations and torsional strain response. Indentation length appears to decrease exponentially with increasing ice strength. Torque rise time also decrease over the test range of increasing ice strength.

- Rudder loading and longitudinal acceleration appear to obey power law relationships with respect to increasing velocity, which show a coefficient less than one. Torsional strain and indentation are approximately linear with velocity. Bending strain does not show any significant trend, and torque rise time is constant.

- An increase in rudder angle is observed to cause increased rudder loads, torques and accelerations up to about 60 degrees. The trend appears approximately sinusoidal. Indentation decreases at larger angles of impact.

FIGURE 2

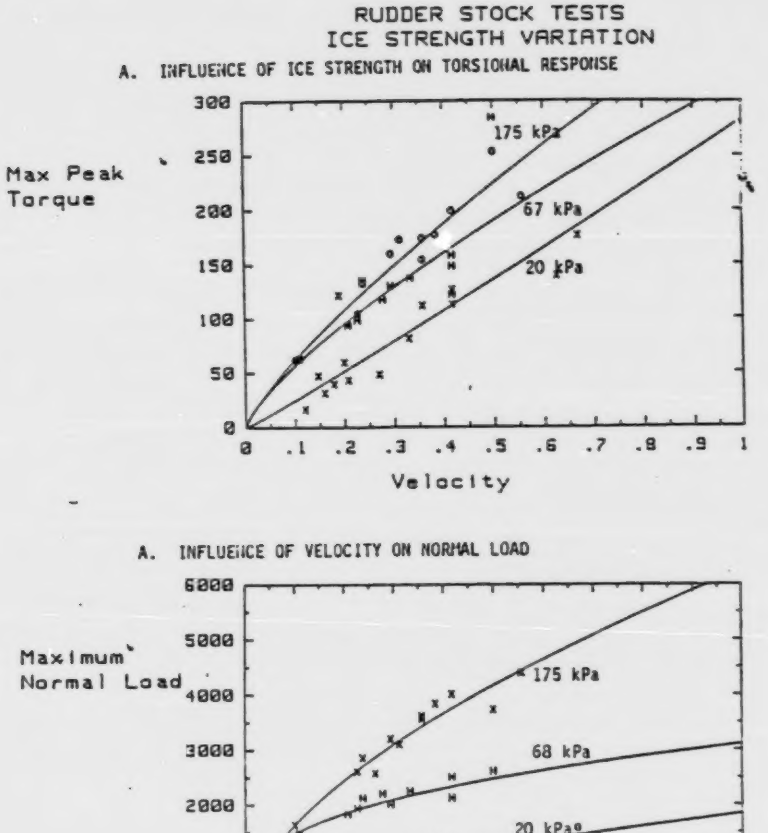
RUDDER STOCK TESTS
ICE STRENGTH VARIATION
A. INFLUENCE OF ICE STRENGTH ON TORSIONAL RESPONSE
Max Peak Torque
300
250
200
150
100
50
0
175 kPa
67 kPa
20 kPa
0
.1
.2
.3
.4
.5
.6
.7
.8
.9
1
Velocity
A. INFLUENCE OF VELOCITY ON NORMAL LOAD
Maximum Normal Load
6000
5000
4000
3000
2000
1000
0
175 kPa
68 kPa
20 kPa
Velocity
B. RELATIONSHIP OF LOAD TO CRUSHED AREA
Maximum Normal Load
175 kPa
68 kPa
20 kPa
0
50
100
150
200
250
300
350
Crushing Area (cm^2)
Ice Block 2= X
Ice Block 5= O
Ice Block 1= H
Stack: 2
Angle: +/- 15 (deg)
Mass: 256.4 (kg)

- The standard ice mass of 256 kg used in the majority of tests corresponds to about 10 percent of ship (mass) displacement. Further increases in mass up to 700 kg caused a linear increase in rudder loads, indentation and torque. Bending strains appear to depend only marginally on ice mass. Axial acceleration decreases inversely with increasing mass. It was not possible to decrease mass below 200 kg with the present set-up.

- Torsional strain and bending strain increase rapidly with reduced stock stiffness. The relationship is approximately inverse squared. The ratio of bending strain to torsional strain is less than 0.1 at target scaling, and therefore bending is only significant for very weak stock stiffnesses. This ratio does not appear sensitive to ice strength variations.

- The majority of parametric testing was carried out with the rudder stock fixed at the tiller. In one set of tests the tiller was instead connected to the hydraulic actuator system via the rams. It was observed that a release pressure of 50 psi caused a significant reduction in the peak torque and loads as compared to the fixed tiller arrangement. At increased release pressures, the maximum pressure difference was found to increase. This effect increased linearly with impact speed.

Ice Basin Towed Tests

The towed test program was developed to investigate a range of operational parameters which influence the frequency of ice impacts with the rudder. Three ship models were identified with the requisite bow forms and stern configurations. The MV ARCTIC is a large ice class bulk carrier/OBO with a single screw and single rudder. The PIERRE RADISSON is an existing Canadian Coast Guard icebreaker with twin screws and a single rudder. The POLAR 8 hull represents a proposed design for a Arctic Class 8 icebreaker. This model has triple screws and a single rudder.

Three similar series of self-propulsion tests were planned and carried out involving the three models. In the case of the MV ARCTIC tests, an additional set of tests was included at a different ice thickness. Four ice sheets were used, the thicknesses of which correspond to the maximum ice thickness for continuous icebreaking for these vessels. Each test series consisted of numerous repetitious of forward and astern trials in pre-cut floes with known dimensions. The initial test involved breaking along a herring bone pattern, which had been formed by 45° cuts outward from the ice basin centerline. The lateral width of the herring bone pattern was 1.1 times the model beam.

The separation of cuts was determined by a characteristic length calculation. The second test run involved backing in the broken channel formed by the first test. The entire ice surface was then cut into pieces corresponding to the model's characteristic cusp length. All subsequent runs in a test series were in the nominally identical piece size distribution. However, the mean size gradually became smaller as a result of interaction between the floes and the ship, as well as by ingestion of ice into the propellers. For this reason it was necessary to stagger the repetitions of a particular test condition, so that the mean ice piece size of each grouping of similar tests would be equivalent. A large range of operating parameters were investigated, including the influence of ship form, forward speed, astern speed, rudder angle, propeller thrust level and direction of rotation, ballast condition (draft), ice thickness and floe size. The principal parameters measured were frequency of impact and rudder torque.

Towed Test Results

Data sets from approximately 150 tests involving four different ice sheets were recorded. In addition, bollard test data and open water self-propulsion trials data for each of the three models was collected. This latter information was obtained at forward and backing velocities corresponding to the ice test conditions for each ship model. Torque time histories from the individual ice transiting tests were examined and the magnitude and number of significant impacts have been extracted. Figure 3 shows a typical torque time history.

The results have been presented in histograms which give the number of impact events (or peaks) at a particular magnitude of torque. For purposes of analysis, the matrix of test parameters has been consolidated into five groups. This was necessary to ensure a statistically meaningful number of impact counts within each histogram.

Table 1 shows the tests which have been included in each of the five categories; designed as: maximum forward speed, yawing forward, mid speed forward, mid speed backing and low speed backing. Histograms are normalized to show the average number of impacts per full scale kilometer of transit (forward or astern). For each ship, this corresponds to a different ice thickness and test velocities. A sample histogram is shown in Figure 4.

It has not been possible to define the influence of some parameters such as thrust level, draft condition and rudder angle because of the limited amount of significant impact data. However, the consolidated histograms have indicated the following general trends:

- There were no ice impacts observed for the MV ARCTIC during forward speed motions. This is likely a result of her length, deep draft and the protection afforded by the propeller nozzle.

FIGURE 3

INFLUENCE OF SHIP FORM IN FULL FORWARD SPEED MANOEUVRES

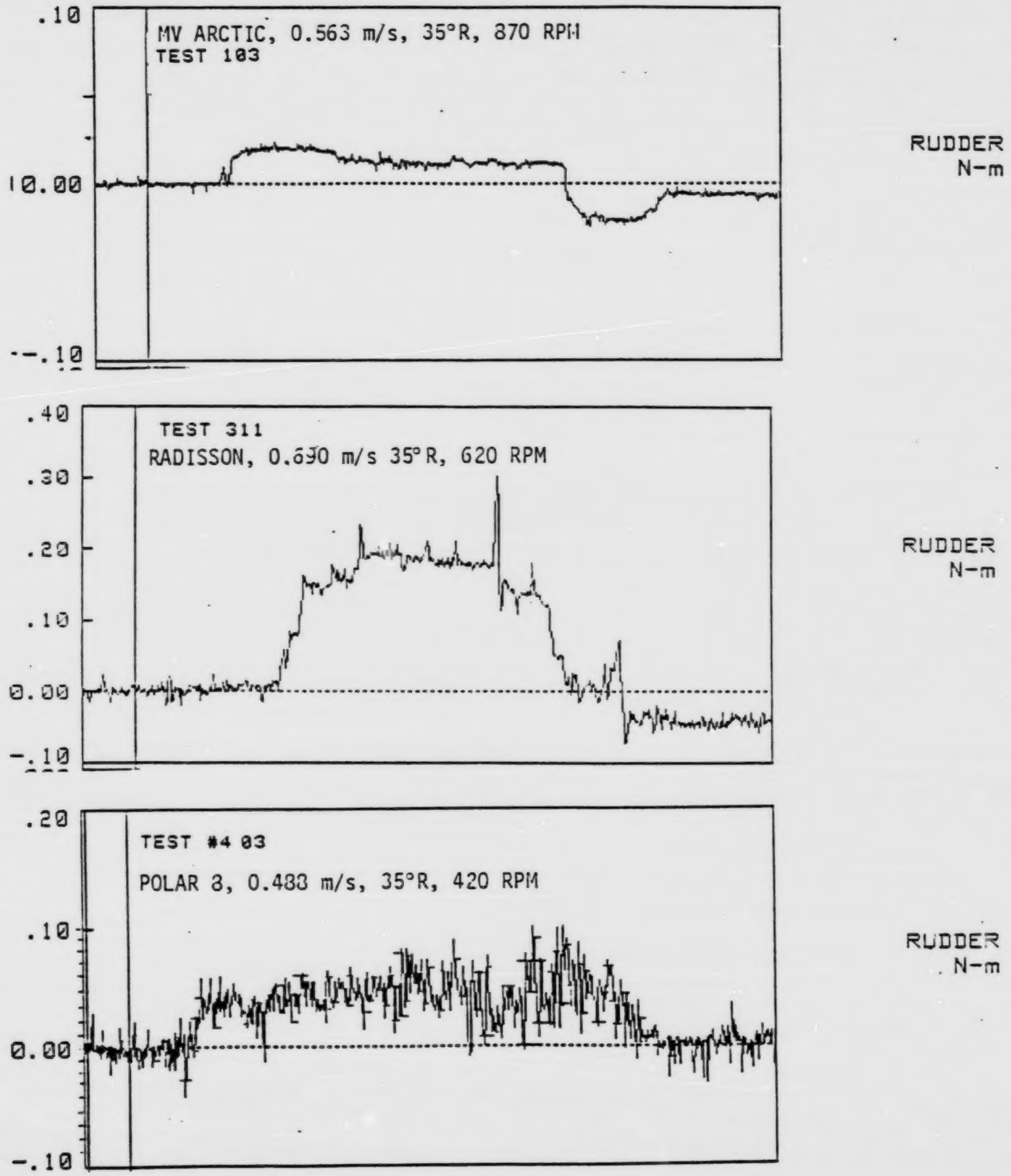

FIGURE 4

FREQUENCY and MAGNITUDE of RUDDER/ICE IMPACTS

M. V. ARCTIC - Mid-speed Backing : .282 m/s

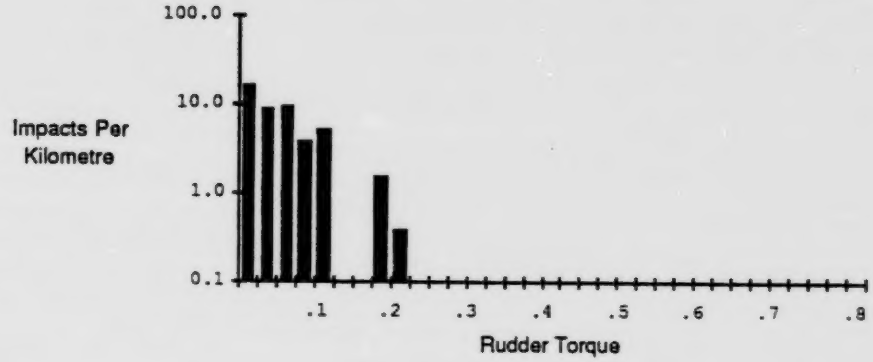

PIERRE RADISSON - Mid-speed Backing : .345 m/s

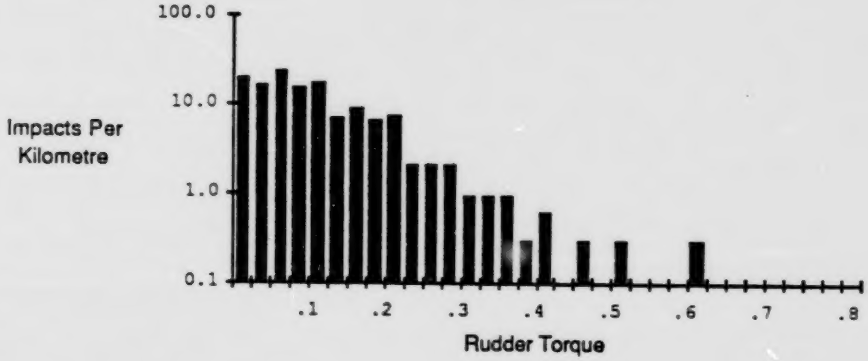

POLAR 8 - Mid-speed Backing : .244 m/s

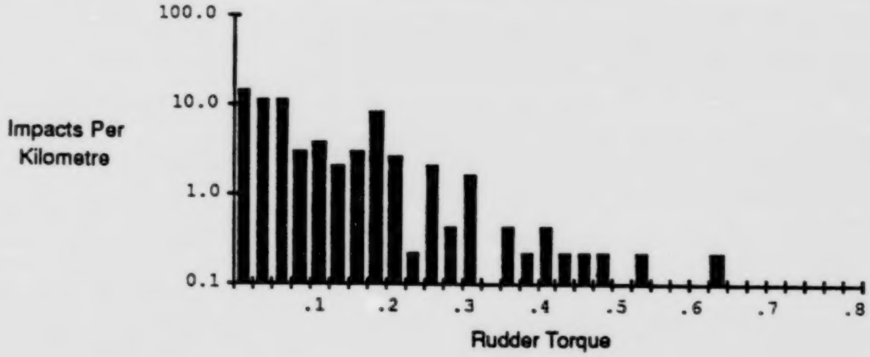

- In astern manoeuvres the MV ARCTIC exhibited a larger number of impacts with moderate torque magnitudes. Additionally, a large number of impacts with low torque values were observed. These may result from continuous ice contact or from enhanced hydrodynamic loads on the rudder. There appears to be no appreciable increase in frequency of impact with increased astern velocity, although a shift towards larger mean torque is seen.

- The PIERRE RADISSON shows the highest frequency of impacts on the rudder during both ahead motions and astern motions of all three test vessels. An increase in frequency with forward speed is observed in both the ice impact torque region and the hydrodynamic loading range. Introduction of a drift angle into the full speed manoeuvres results in an increase in the number of impacts and an upward shift in the mean torque magnitude.

- In astern manoeuvres the RADISSON exhibits a larger number of significant impacts, but about the same hydrodynamic loading as during forward motions. The impact frequency does not appear dependent on velocity; but there is an upward shift in torque magnitude with speed.

- The POLAR 8 icebreaker histograms have a similar pattern to that observed for the RADISSON. In forward motions, the POLAR 8 has a larger number of low magnitude or hydrodynamic events, but fewer ice impacts. This number is speed dependent. In backing the POLAR 8 again shows fewer impacts over a similar torque range.

Some additional comments about individual parameters may be made on the basis of a visual examination of the time histories. It appears that the relative value of steady state rudder torque for each ship in each operating mode is a major factor influencing the histograms. The steady state component in the ice impact environment is similar in magnitude to the corresponding open water value. In general, it is observed that the RADISSON has the larger value; followed by POLAR 8 and MV ARCTIC. This reflects the particular hydrodynamic characteristics of each ship's stern configuration and rudder geometry. Furthermore, it has repercussions on the interpretation of trends in various ship parameters.

The time histories suggest that decreasing draft causes a marginal increase in torque magnitudes; as does increasing RPM or ice thickness. The effect of changing the propeller rotation direction is hidden by the change in steady state torque.

Conclusions

The applicability of dry impact parametric testing by means of a large scale physical model of a ship rudder assembly has been demonstrated. A large range of operational parameters have been assessed, including the influence of: impact velocity, rudder angle, rudder stock torsional stiffness, ice mass, ice strength and hydraulic pressure release. Sets of time histories of rudder loading, stock bending strains and torsional response have been collected and a corresponding data base of peak values established. This has allowed insights into the rudder-ice interaction process and has provided a starting point from which functional relationships between parameters may be derived. Trends between rudder stock torque and other variables and a range of parameters have been presented.

A limited assessment of the influence of steering gear hydraulic pressure relief on rudder loads and motions has been made as a result of the use of the hydraulic rams and control units. The scaled hydraulics system provided a reasonable representation of the release pressure mechanism and illustrated significant trends associated with steering system hydraulic "stiffness". In particular, it showed that the fixed tiller tests represented a conservative loading condition, and that the effect of pressure relief variation was velocity dependent. However, it should be noted that there was no attempt to incorporate feedback control into this hydraulic model. Additional physical modelling using a more complete hydraulics model is needed to study the influence of the pipe orifice diameter, the response and the pumping rate of fluid during pressure release situations.

The data generally represents extreme impact conditions since the test conditions involved large ice masses, full depth ice contact with the rudder edge, large rudder angles, and strong ice. Excepting contact depth, a range of each of these parameters has been tested, which allows extrapolation to less extreme scenarios. However, it is difficult to predict torsional response for ice masses which are less than 5 percent of the RADISSON displacement because of the rapid increase of torque over the lower range of ice mass. The trends defined in this part of the study form the basis for parametric equations which will lead to a realistic validation of the mathematical model of overall rudder torsional response and to more rational design criteria.

The principal outcome of these tests has been the statistics on the frequency of impact during astern manoeuvres in the broken channel. Since it was not possible to accurately scale the crushing strength of the pre-cut urea ice, and maintain it throughout a full day of tests, distortions in the rudder torque values were expected. Nonetheless, the torque values provide an order of magnitude reference in assessing the impact severity.

The comparison between the three vessels has demonstrated the effectiveness of certain hull form characteristics in limiting the number and severity of rudder ice loads. In particular, the nozzle on the MV ARCTIC propeller, in combination with its greater length and draft, resulted in a total protection from impacts during forward manoeuvres. With the limited number of test repetitions, it has not been possible to statistically determine the meaningfulness of the data on opposing propeller rotation directions. Nor has it been possible to differentiate between minor variations of rudder angle or thrust level during astern manoeuvres. These tests have been grouped together to allow comparative statistical assessment between different ships and major operating characteristics.

Recommendations

The present analysis of the 'dry mode' impact data has identified the significant trends of influence between rudder torsional response and a range of operation parameters. A further analysis effort is necessary to reformulate the data into a dimensionless form and then to extract the individual parametric equations. The preliminary evaluation of peak data by means of power regression fits for the figures in the text has shown that this exercise will yield good numerical results. These relationships will form the basis for an validated mathematical model of rudder-ice interaction. For numerical modelling, added mass effects must also be included. In addition, model scale data should be correlated with available full scale LOUIS S. ST. LAURENT trials data.

There were several limitations in the dry impact modelling that resulted in unanswered questions after the present test program. The most serious deficiency was in the range of ice mass. The lower bound on mass in the test range corresponded to approximately seven percent of the LOUIS S. ST. LAURENT displacement. Therefore, only the case of an infinite ship and large ice masses has been treated. Two further cases should be addressed by means of additional testing:

(1) If the stern of a vessel manoeuvring in ice swings into the channel edge, the situation may be considered one of an infinite ice mass and a finite displacement ship. Physical model tests to investigate this case would use an existing ship model backing into a fixed synthetic (MODICE) ice block. Stock torsion would again be modelled. This approach is necessary since it is not possible to support the 1:17 scaled weight of the entire ship in the present experimental apparatus. Other vessels may also be examined in this manner to establish reference comparisons between the dry impact parametric equations and 'wet mode' self propulsion model tests.

(2) If the ice floe mass drops below seven percent of the LOUIS S. ST. LAURENT displacement, the present interpretation of the two body impact problem does not change. The same experimental apparatus may be used to investigate the lower range of ice mass. However, the box frame which constitutes a major part of the mass would have to be redesigned and fabricated out of a lighter material to reduce its minimum, unballasted value.

Other areas in which the dry impact database may be expanded include variation in rudder tip geometry and depth of contact with the ice. Both of these recommendations address the question of the influence of pressure-area effects on rudder loading.

Another aspect of improved physical modelling involves the development of a more complete hydraulic steering gear. This necessitates further work on the modelling of fluid flow rates in the cylinders and orifices of the control unit. In addition, scaled feedback control should be incorporated into the hydraulic control system.

The principal limitation affecting the quality of the towed ice basin test results is in the number of repetitions of each test configuration. It has not been possible to separate the ice related torque peaks from the background hydrodynamic mean values. The towed results should be further reviewed to consider the open water and bollard trials data at each operational condition which was examined in the ice tests. The limited amount of data has necessitated a coarser grouping of different test parameters in the histograms than intended, to ensure more statistically meaningful trends. Additional evaluation of at least one vessel in a significantly larger sample of tests would improve the validity of these statistics and allow a finer differentiation of parametric influences. Furthermore, as a result of the experience with the dry impact physical modelling it is recommended that MODICE should be used in a follow-up towed test program. This ice material has two principal advantages: ice crushing strength can be modelled and maintained during testing; and the density of MODICE is closer to that of full scale ice. The former implies more accurate torque values. The latter implies that ice buoyancy forces will be better simulated and therefore the flow of ice to the rudder will be more representative.

The present 'dry mode' impact tests and 'wet mode' ice basin model tests have established the basic information necessary to confirm or validate a mathematical model of steering response to rudder-ice loads. A valuable continuation involves the combination of the parametric equations of the dry impact tests, with the appropriate statistics from the ice basin tests and comparison to available full scale data. This leads towards the development of a semi-empirical model of the rudder-ice interaction with repercussions for rudder system design and regulation.

SOMMAIRE

Dans le but de caractériser la réponse de l'appareil à gouverner d'un navire à la charge des glaces sur le gouvernail, deux expérimentations complémentaires ont été faites à l'aide de modèles réduits:

- En premier lieu, l'investigation de l'interaction gouvernail-glaces s'est faite à l'aide d'un modèle réduit au 1/17 du gouvernail du brise-glace canadien LOUIS-ST-LAURENT, lequel modèle a été soumis à des essais paramétriques dans toute l'étendue du domaine considéré. Dans cette recherche, divers paramètres ont été pris en compte: efforts sur le gouvernail, couples, déformations dues aux efforts de flexion, etc.

- Ensuite, la recherche a pris la forme d'essais, dans un bassin des glaces, sur les modèles réduits de trois navires, dans le but de chiffrer le nombre d'impacts sur le gouvernail dans des conditions de marche variables.

L'objet de ces travaux était double: (1) mettre au point des critères de calcul de résistance des gouvernails et appareils à gouverner et (2) vérifier un modèle mathématique simulant la réponse d'un gouvernail à la charge des glaces. Tant l'information que les techniques résultant de ces deux expérimentations ont permis de faire progresser les méthodes de conception des appareils à gouverner pour navires appelés à naviguer dans les glaces.

Modèle réduit pour essais de choc hors bassin

Ces essais ont été étudiés en vue de mettre en évidence la charge exercée par les glaces sur un appareil à gouverner type, ainsi que les réactions de celui-ci à des chocs de forte amplitude. Le prototype choisi pour l'expérimentation a été l'appareil à gouverner du LOUIS-ST-LAURENT. Afin de réaliser la maquette, il a fallu procéder à une réduction d'échelle exacte des conditions géométriques et dynamiques des éléments constitutifs: gouvernail, mèche, barre, vérins, actionneur hydraulique et, enfin, glaces. L'échelle de réduction choisie a été de l'ordre du 1/17, pour des considérations à la fois de taille et de poids. La maquette réalisée est illustrée à la figure 1. Le gouvernail a été réalisé en aluminium, ainsi que les trois mèches dont chacune avait un diamètre différent de manière à faire varier la raideur en torsion de cet élément. Le gouvernail tournait sur deux aiguillots et était maintenu en position par l'intermédiaire de la mèche passant dans deux paliers.

FIGURE .1

Montage d'essais hors bassin

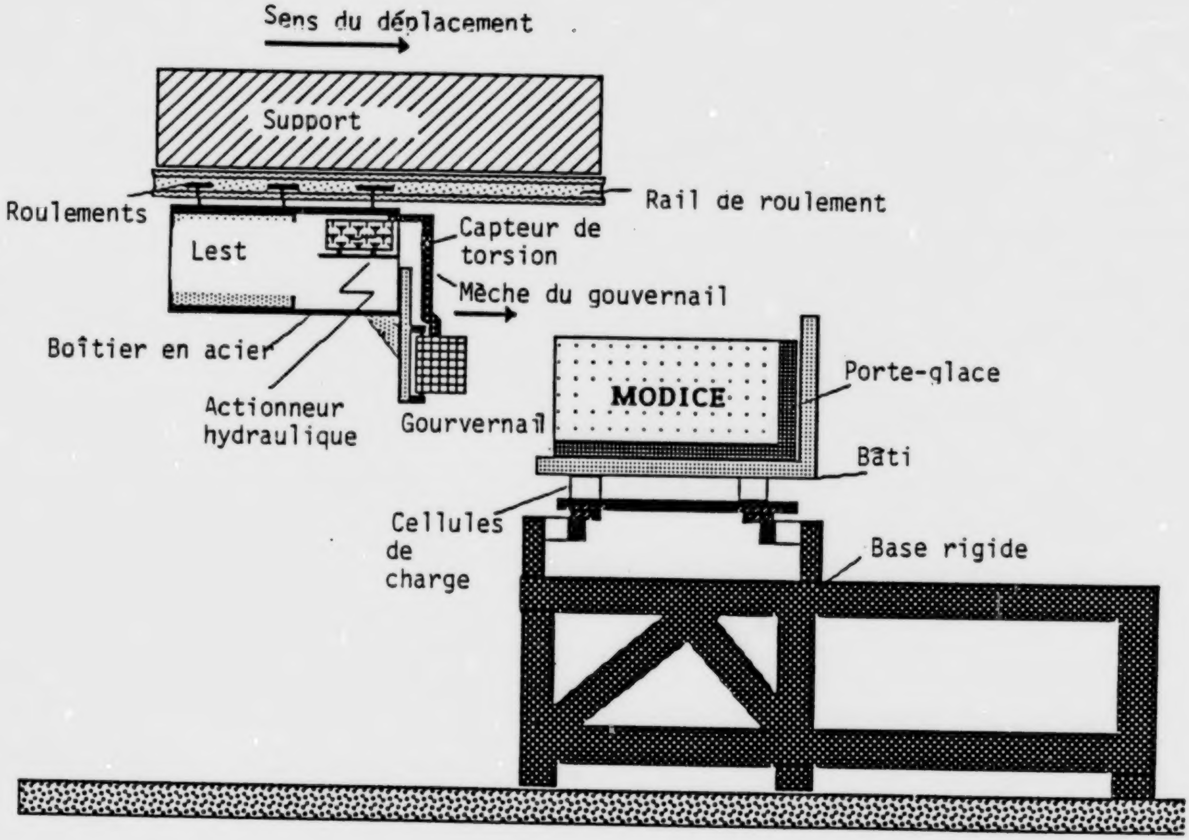
Sens du déplacement
Support
Roulements
Rail de roulement
Lest
Capteur de torsion
Mèche du gouvernail
Boîtier en acier
Actionneur hydraulique
Gourvernail
MODICE
Porte-glace
Bâti
Cellules de charge
Base rigide

La mèche était fixée à la barre, soit rigidement, soit par l'intermédiaire d'un actionneur hydraulique. La maquette était boulonnée à un boîtier en acier qui coulissait sur un rail de deux mètres de long fixé au chariot d'entraînement. Les variations dans la masse mise en oeuvre durant les essais étaient réalisées par des blocs de lest amovibles placés dans le boîtier. Étant donné que les fragments de glace dans le chenal ouvert ont une masse qui représente une petite fraction de la masse du navire, il est raisonnable de considérer la masse du boîtier en mouvement comme représentative de la masse des fragments de glaces.

La glace modèle utilisée dans les expérimentations était à base de cire, élaborée à l'état fondu et placée dans un moule pour figer. Lors des essais hors bassin, la surface des blocs de glace modèle était aspergée d'eau pour réduire le frottement. La résistance de la glace modèle a été déterminée à l'aide d'une équation de similitude obtenue empiriquement et considérée comme valide dans les cas de compression. Cette équation avait été vérifiée par des essais uniaxiaux de résistance à la compression pilotés par un programme informatique propre à Arctec. La résistance de référence de la glace modèle a été fixée à 53 kPa, partant de l'hypothèse que la plus grande probabilité d'endommagement du gouvernail est liée à la présence de fragments de glace de plusieurs années. Un total de huit blocs de glace avaient été préparés; leur résistance était de 175 kPa (très forte), 86 kPa (moyennement forte), 68 kPa (valeur de référence) et 15 à 22 kPa (relativement faible). Ces blocs étaient montés sur une balance comportant des cellules de charge qui mesuraient les forces horizontales, tant axiales que transversales.

Résultats des essais hors bassin

Le plan de l'expérimentation hors bassin prévoyait de faire varier six facteurs contrôlés, à savoir: vitesse à l'impact, angle de braquage, raideur en torsion de la mèche, masse du bloc de glace, résistance de celui-ci et pression limite du circuit hydraulique de commande. Les quelque 130 essais effectués ont permis de chiffrer les variables dépendantes, soit: contraintes dans le gouvernail (composantes axiale et transversale), déformations de la mèche en torsion, moments de flexion (composantes axiale et transversale), pénétration dans la glace et pression dans le circuit hydraulique. L'influence des facteurs contrôlés sur la réponse chiffrée a été évaluée et reproduite graphiquement. La figure 2 donne à titre d'exemple les couples maximums en fonction de la résistance de la glace et de la vitesse. Bien qu'aucune relation fonctionnelle définitive n'ait pu être tirée de la présente analyse, les constatations générales suivantes ont pu être faites:

FIGURE 2

Réponse de la mèche aux
variations de résistance de la glace

A. Influence de la résistance sur le couple de torsion

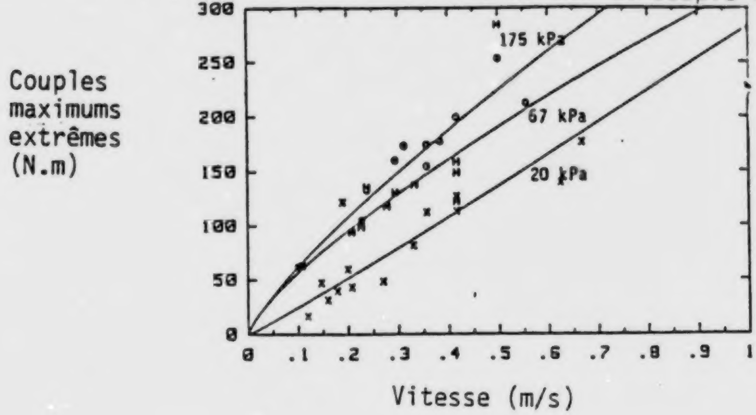

A. Influence de la vitesse sur la charge normale

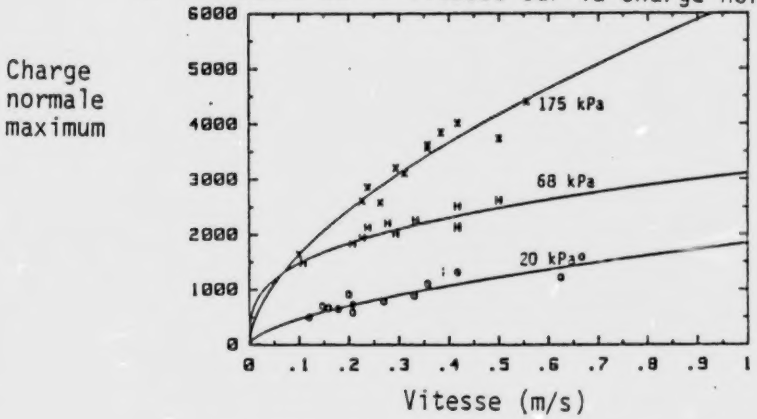

B. Évolution de la charge en fonction de la surface de compression

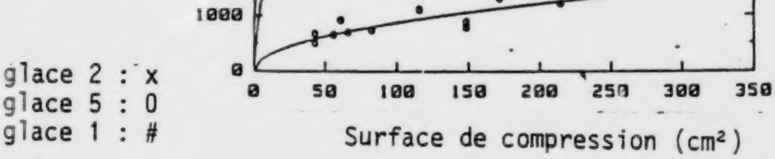

Bloc de glace 2 : x
Bloc de glace 5 : 0
Bloc de glace 1 : #

Mèche : 2
Angle : ± 15°
Masse : 256,4 kg

- Les variables dépendantes qui réagissent le plus fortement à une variation dans la résistance de la glace sont: l'effort maximum sur le gouvernail, l'accélération axiale et la déformation en torsion. La profondeur de pénétration dans la glace décroît exponentiellement à mesure qu'augmente la résistance de la glace. Le temps de réaction en torsion diminue aussi dans toute l'étendue de la plage d'essais.

- Les efforts sur le gouvernail et les accélérations axiales varient avec les vitesses croissantes selon une loi (de) puissance dont l'exposant est inférieur à l'unité. Les déformations en torsion et les profondeurs de pénétration varient à peu près linéairement avec la vitesse. Les déformations en flexion ne montrent pas de variations significatives tandis que les temps de réaction en torsion du gouvernail demeurent inchangés.

- Toute augmentation de l'angle de braquage semble s'accompagner d'un accroissement des efforts sur le gouvernail, des couples et des accélérations, et ce, jusqu'à un angle limite d'environ 60°. Une courbe quasi sïnusoidale a été obtenue dans chaque cas. Aux angles plus élevés, les pénétrations diminuent en profondeur.

- La masse de 256 kg de glace mise en oeuvre dans la plupart des essais correspond à quelque 10 p. 100 du déplacement du navire. Une masse portée graduellement à 700 kg a provoqué un accroissement linéaire des efforts sur le gouvernail, des pénétrations et des couples. Les moments de flexion ne dépendraient de la masse de glace qu'accessoirement. Les accélérations axiales décroissent en raison inverse de l'augmentation de la masse. Sur le montage utilisé, il n'a pas été possible de réduire la masse à moins de 200 kg.

- Les déformations en torsion et en flexion croissent rapidement à mesure que décroît la raideur de la mèche, et ce, dans un rapport non loin d'être inversement proportionnel au carré des valeurs considérées. Le rapport déformations en flexion/déformations en torsion est inférieur à 0,1 à la raideur en flexion de référence. Donc, la flexion ne devient significative qu'à partir de valeurs de raideur très faibles. Ce rapport ne semble pas sensible aux variations dans la résistance de la glace.

- Dans la plupart des essais paramétriques, la mèche était fixée rigidement à la barre. Dans une série d'essais, celle-ci a été reliée à un actionneur hydraulique à vérins. Il a été observé que la pression d'ouverture du circuit hydraulique, réglée à 50 lb/po^2, a provoqué une réduction notable des couples et contraintes maximums, comparativement au système rigide. À mesure qu' augmentent les pressions de réglage, la pression différentielle maximum dans les vérins croît, elle aussi, selon une relation linéaire avec la vitesse à l'impact.

Résultats des essais de remorquage en bassin

Les essais de remorquage en bassin étaient destinés à élucider les paramètres déterminant la fréquence des impacts gouvernail-glaces ainsi que leur domaine d'action. Les essais en bassin ont été conduits sur les modèles réduits de trois navires ayant les formes de proue et de poupe requises: le N.M. ARCTIC, un gros minéralier-vraquier-pétrolier de cote arctique, à une seule hélice et un seul gouvernail; le PIERRE-RADISSON, brise-glace canadien à deux hélices et un gouvernail; et la représentation de la coque du POLAR 8, brise-glace proposé doté de trois hélices et d'un gouvernail.

Trois séries d'essais en autopropulsion ont été effectuées sur chacun des trois modèles, et une série supplémentaire a été faite dans une glace d'une épaisseur différente dans le cas de l'ARCTIC. Quatre couches de glace ont été mises en oeuvre, dont l'épaisseur a été choisie pour correspondre à l'épaisseur maximum dans laquelle les navires représentés peuvent avancer en marche continue. Chaque série d'essais a comporté des marches avant et arrière répétées dans une glace préalablement entaillée pour former des fragments de dimensions précises. Le premier essai consistait à casser la glace selon un motif en chevrons formant un angle de 45° avec l'axe du bassin. La largeur de la glace ainsi découpée correspondait à 1,1 fois la largeur du modèle. Quant à la distance séparant les chevrons, elle correspondait à une longueur caractéristique obtenue par calcul. L'essai suivant consistait à lancer le modèle en marche arrière dans le chenal ouvert lors de l'essai précédent. Ensuite, la surface de la couche glacée a été coupée en fragments de longueur correspondant à la longueur caractéristique pour le modèle considéré. Pour les essais subséquents de chaque série, la taille des fragments a été maintenue afin de respecter une distribution nominalement identique. Mais comme la taille moyenne des fragments diminuait après chaque essai, en raison des chocs répétés avec les modèles et aussi du broyage par les hélices, il a fallu disperser les répétitions d' essais particuliers, de manière à assurer une distribution équivalente particuliers, de la taille moyenne des fragments, d'un groupe d'essais homologues à l'autre. Parmi les nombreux facteurs contrôlés qui ont été étudiés figurent: la forme de la coque, la vitesse avant et arrière, l'angle de braquage, la poussée, le sens de rotation de l'hélice, le tirant d'eau (ballast), l'épaisseur de la glace et la taille des fragments. Les principales variables dépendantes mesurées ont été la fréquence des impacts et l'amplitude du couple agissant sur le gouvernail.

Analyse des résultats

Les résultats de quelque 150 essais dans quatre couches de glace différentes ont été enregistrés, de même que ceux d'essais de traction au point fixe et d'autopropulsion en eau libre. Ces derniers ont été faits à des vitesses de marche avant et arrière correspondant à celles pratiquées lors des essais dans les glaces. Des courbes d'évolution des couples obtenues de chacun des essais individuels dans la glace a été extraite l'information correspondante sur l'amplitude et la fréquence des impacts. Une courbe d'évolution type des couples est illustrée à la figure 3.

Le résultat a été présenté sous la forme d'histogrammes donnant le nombre d'impacts (ou de crêtes) au regard d'une amplitude donnée. Aux fins d'analyse statistique, l'information obtenue a été organisée en cinq catégories générales, de manière à donner des histogrammes où le nombre d'impacts mis en évidence est significatif du point de vue statistique.

Le tableau 1 dénombre les essais faisant partie de ces cinq catégories: vitesse avant maximum, vitesse avant modifiée par la dérive, vitesse avant intermédiaire, vitesse arrière intermédiaire et vitesse arrière basse. Les histogrammes ont été normalisés de manière à donner le nombre moyen d'impacts par kilomètre réel de marche (avant ou arrière), paramètre qui, lors des essais, a varié en fonction de l'épaisseur de la glace et de la vitesse. Un histogramme type est illustré à la figure 4.

Il n'a pas été possible de chiffrer l'influence de certains paramètres tels que la poussée, le tirant d'eau et l'angle de braquage, vu la quantité restreinte de données utiles disponibles. Néanmoins, les constatations suivantes ont pu être faites à partir des histogrammes normalisés obtenus:

- Aucun impact avec la glace n'a été observé avec l'ARCTIC durant les essais en marche avant. Cela peut s'expliquer par la longueur du navire, son grand tirant d'eau et la protection assurée par la tuyère.

- En marche arrière, avec l'ARCTIC, un nombre élevé d'impacts ont été observés ainsi que des valeurs de couple modérées. De nombreux impacts à des valeurs de couple faibles ont également été observés. Cela peut être attribué à un contact continu avec la glace ou à une charge hydrodynamique accrue sur le gouvernail. Il ne semble pas y avoir un accroissement notable dans la fréquence des impacts lorsque la vitesse en marche arrière est augmentée, bien qu'une tendance vers des valeurs moyennes de couple plus élevées ait été observée.

FIGURE 3

Influence de la forme de coque à vitesse avant maximum

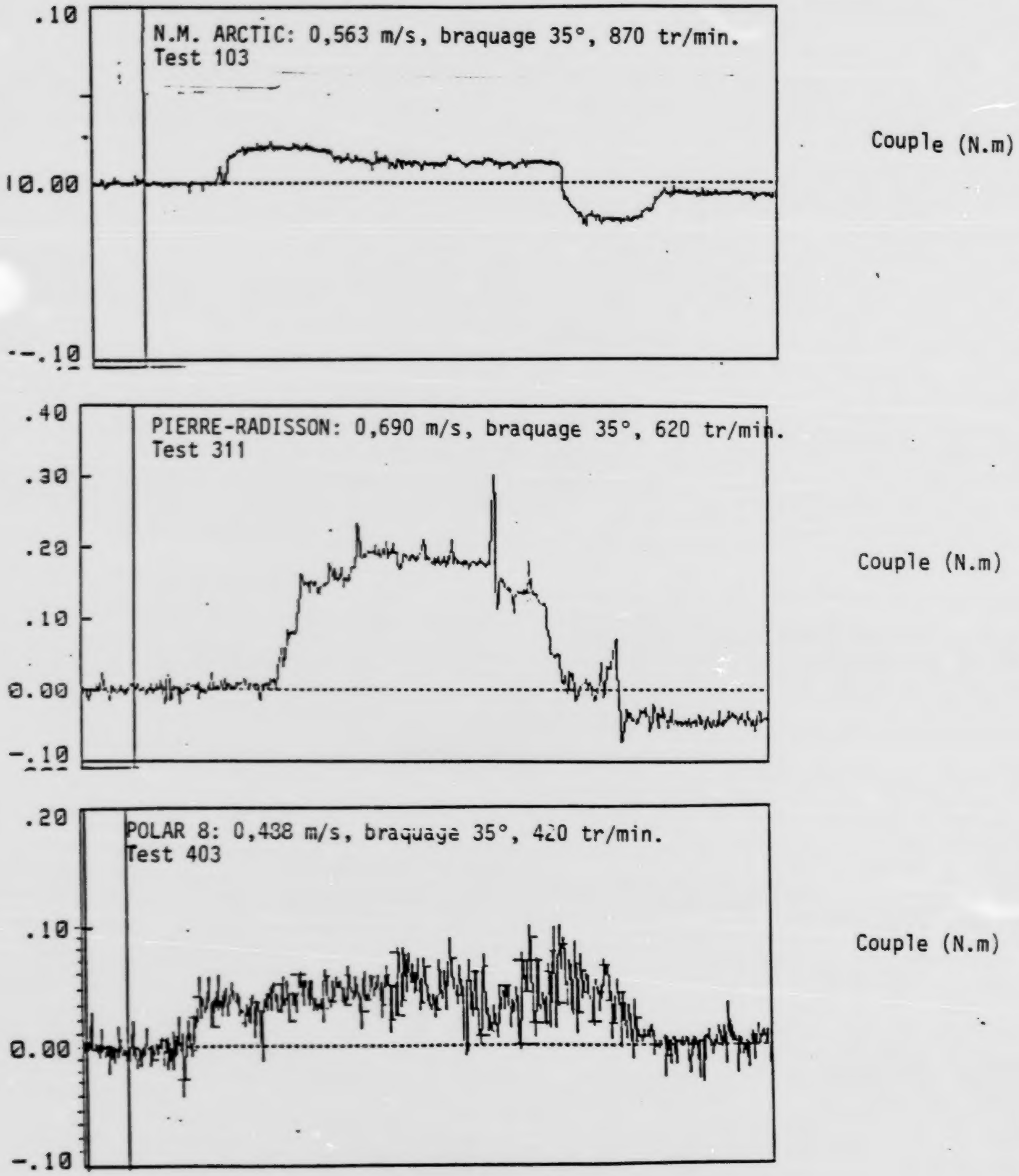

FIGURE 4

Fréquence et amplitude des impacts de glace

N.M. Arctic - Marche arrière à vitesse intermédiare : 0.282 m/s

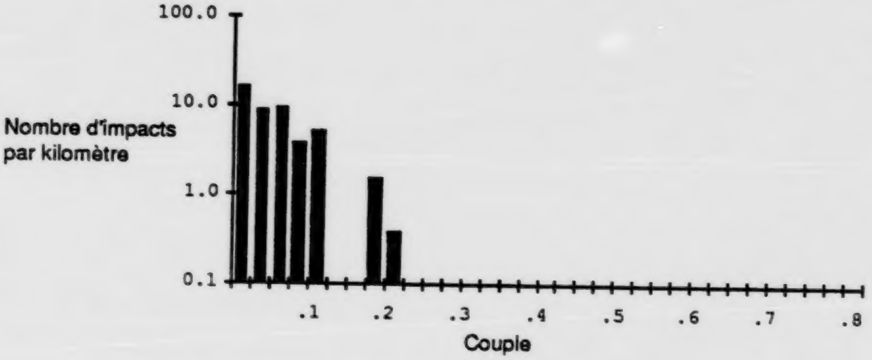

Pierre-Radisson - Marche arrière à vitesse intermédiare : 0.345 m/s

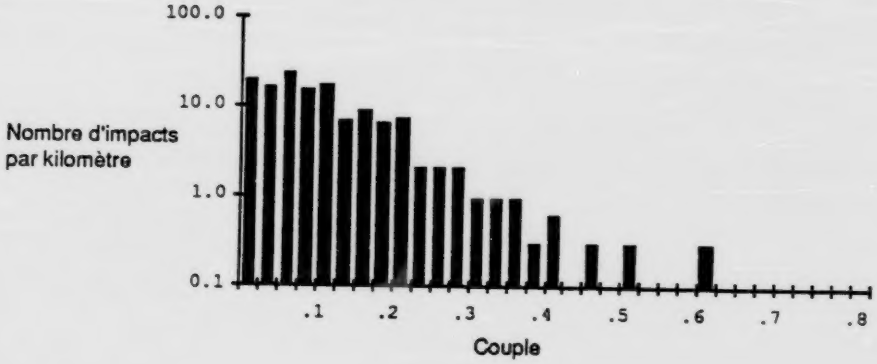

Polar 8 - Marche arrière à vitesse intermédiare : 0.244 m/s

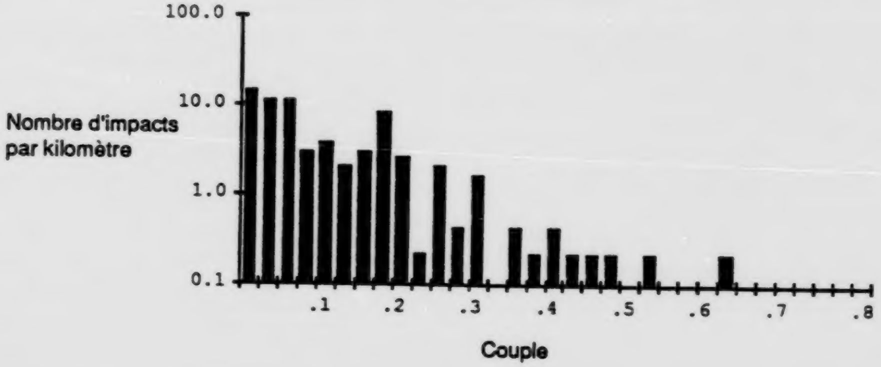

- De tous les modèles, c'est celui du PIERRE-RADISSON qui a montré la fréquence d'impact la plus élevée sur le gouvernail, tant en marche avant qu'en marche arrière. Un accroissement de cette fréquence avec la vitesse avant a également été observé, tant dans le domaine des couples correspondant au choc des glaces que dans celui des surcharges hydrodynamiques. La prise en compte d'un angle de dérive durant les essais à vitesse maximale s'est traduite par un accroissement dans le nombre d'impacts et par un relèvement des valeurs moyennes de couple.

- En marche arrière, le modèle du PIERRE-RADISSON a montré un nombre d'impacts significatifs plus élevé qu'en marche avant, le régime de surcharge hydrodynamique restant à peu près le même. Il ne semble pas que la fréquence des impacts soit fonction de la vitesse, mais un relèvement des valeurs de couple avec la vitesse a été observé.

- Les histogrammes relatifs au POLAR 8 ressemblent à ceux du PIERRE-RADISSON. En marche avant, il y a eu un nombre plus élevé d'événements à faible valeur de couple assimilables à des surcharges hydrodynamiques, mais moins d'impacts avec les glaces. Le nombre de ces événements varie avec la vitesse. En marche arrière, le POLAR 8 a eu encore une fois moins d'impacts avec les glaces, pour des valeurs de couple identiques.

D'autres constatations concernant certains paramètres peuvent être tirées d'un examen des courbes d'évolution dans le temps. Il semble que le couple en régime permanent qui agit sur le gouvernail des trois navires représentés, et à toutes les allures essayées, serait un des principaux paramètres influençant les résultats; il semble également que la composante en régime permanent durant la marche dans les glaces se compare en amplitude à la valeur correspondante en eau libre. De façon générale, il a été observé que, à ce point de vue, le PIERRE-RADISSON vient en tête, suivi du POLAR 8 et de l'ARCTIC, reflétant les caractéristiques hydrodynamiques particulières propres tant à la forme de la poupe qu'à la géométrie du gouvernail des navires représentés. L'interprétation des résultats relatifs à divers paramètres a pu également s'en ressentir.

Les courbes d'évolution dans le temps montrent que l'amplitude des couples augmente très légèrement lorsqu'on réduit le tirant d'eau ou bien lorsque le nombre de tr/min ou l'épaisseur de la glace est augmenté. Quant à l'effet apporté par un changement dans le sens de rotation de l'hélice, il a été masqué par les fluctuations dans le couple en régime permanent.

Conclusions

L'utilité des essais hors bassin, sur un gros modèle réduit du gouvernail, en vue de mettre en évidence l'influence des divers paramètres a été amplement démontrée. D'importantes variations ont été données aux facteurs contrôlés, à savoir: vitesse à l'impact, angle de braquage, raideur en torsion de la mèche, masse du bloc de glace, résistance de celui-ci et, enfin, pression d'ouverture du circuit hydraulique de commande. Des courbes d'évolution dans le temps ont été obtenues en ce qui concerne les efforts sur le gouvernail, les déformations en flexion et en torsion de la mèche et, à partir de ces courbes, une base de données sur les valeurs extrêmes a été élaborée. La recherche a débouché sur des connaissances approfondies concernant le phénomène d'interaction gouvernail-glace et a été le point de départ d'une étude sur les relations fonctionnelles pouvant exister entre les divers paramètres en jeu. Des courbes d'évolution sont présentées et montrent les variations du couple de torsion qui agit sur la mèche du gouvernail et sur d'autres variables, en fonction des paramètres pris en compte.

La mise en oeuvre d'un actionneur hydraulique en modèle réduit a permis d'évaluer dans une certaine mesure l'influence de la pression hydraulique d'ouverture sur le gouvernail: déplacements et efforts exercés. Cet actionneur, qui peut être considéré comme représentant assez fidèlement le mécanisme de déblocage hydraulique, a mis en évidence l'influence de la variation de "raaideur" de l'appareil à gouverner; il a particulièrement démontré que les essais faits à mèche rigidement fixée à la barre représentaient un mode de charge classique et que l'influence des variations de réglage de la pression hydraulique était liée à la vitesse. À noter cependant l'absence d'asservissement par rétroaction dans le modèle réduit. Des études complémentaires visant la mise au point d'un modèle réduit plus complet d'un appareil à gouverner hydraulique seront nécessaires afin d'approfondir l'influence du diamètre de la vanne de commande, la réponse du gouvernail et les débits, lorsque la pression d'ouverture du circuit hydraulique est atteinte.

Les données tirées des expérimentations se rapportent généralement à des conditions extrêmes, étant donné la mise en oeuvre de blocs de glace massifs, les contacts pleine hauteur entre le gouvernail et la glace, les angles de braquage importants et la forte résistance de la glace modèle. Excepté la hauteur du contact, chacun des facteurs contrôlés a été soumis à d'importantes variations. À partir de là, il est donc possible de procéder à des extrapolations reflétant des conditions moins rigoureuses. Mais il est difficile de calculer les déformations en torsion lorsque la masse de la glace est inférieure à 5 p. 100 du déplacement du PIERRE-RADISSON, vu l'accroissement rapide des valeurs de couple dans ces conditions. Les résultats de ces expérimentations serviront à établir les relations pouvant exister entre les facteurs contrôlés et, de la sorte, permettront de valider le modèle mathématique élaboré pour simuler la réponse d'un gouvernail à la charge des glaces et de déboucher sur des critères de calcul plus logiques.

Le principal résultat de cette recherche aura été la mise en évidence des statistiques concernant la fréquence des impacts lorsque le navire recule dans le chenal qu'il vient d'ouvrir. Étant donné qu'il est impossible d'obtenir une similitude parfaite en résistance à la compression dans le cas de la couche de glace dopée à l'urée et pré-entaillée et, au surplus, de maintenir une même résistance en compression durant toute une journée, il fallait s'attendre à une distorsion dans les valeurs de couples de torsion du gouvernail. Néanmoins, un ordre de grandeur des impacts enregistrés a pu être dégagé de ces valeurs.

La comparaison des trois modèles de navire a mis en évidence l'apport de certaines caractéristiques géométriques de leur coque à la réduction du nombre et de l'amplitude des impacts gouvernail-glaces. Dans le cas de l'ARCTIC en particulier, la conjonction d'une tuyère protégeant l'hélice, d'une grande longueur de coque et d'un grand tirant d'eau, s'est traduite par une absence totale de chocs en marche avant. À cause du nombre restreint de répétitions des essais, il n'a pas été possible de déterminer statistiquement l'utilité des données tirées des essais durant lesquels le sens de rotation des hélices a été inversé. Il n'a pas non plus été possible de distinguer l'effet des faibles variations dans l'angle de braquage ou la poussée durant les manoeuvres en marche arrière. Ces essais ont été groupés pour autoriser une analyse statistique comparée des navires en fonction de leurs principales caractéristiques.

Recommandations

L'analyse des résultats des essais hors bassin a permis d'approfondir l'influence des principaux facteurs contrôlés sur le comportement en torsion du gouvernail. Cependant, une analyse plus poussée est nécessaire pour réécrire les résultats sous forme adimensionnelle de manière à déboucher sur des équations paramétriques spécifiques. Le traitement préliminaire des valeurs extrêmes par une analyse de régression de la variable puissance promet de déboucher sur d'intéressants résultats numériques. Les relations ainsi mises en évidence seront le fondement sur lequel asseoir un modèle de simulation des forces d'interaction dûment validé qui devra également tenir compte du phénomène de la masse entraînée. En outre, une corrélation devra être faite entre, d'une part, le résultat des essais sur modèle réduit du LOUIS-ST-LAURENT et, d'autre part, les données d'essais en vraie grandeur du même brise-glace.

Diverses limitations des essais sur modèles réduits hors bassin ont fait que certaines questions sont restées sans réponse à l'issue du présent programme d'essais. La plus importante lacune a été la limitation de la masse de glace modèle pouvant être mise en oeuvre. Les valeurs minimales de masse prises en compte durant les essais correspondent à quelque 7 p. 100 du déplacement du LOUIS-ST-LAURENT. Donc, le seul scénario envisagé dans les essais a été de considérer le déplacement du brise-glace comme étant infini et la masse de glace comme quelconque, mais finie. Il faudrait faire d'autres essais pour approfondir les deux scénarios suivants:

(1) Celui de la poupe heurtant le bord du chenal ouvert par le brise-glace, où la situation est inversée: masse de glace infinie et déplacement fini. Les essais sur modèle réduit s'effectueraient au moyen du modèle existant que l'on ferait reculer dans un bloc de glace synthétique fixe. Là encore il faudrait utiliser des mèches dont la résistance en torsion aurait été calculée par voie de similitude. Cette méthode s'impose étant donné que le montage servant aux expérimentations ne peut supporter le poids du modèle réduit au 1/17. Des essais sur d'autres modèles pourraient être faits dans cette optique afin d'établir une corrélation entre les équations paramétriques résultant des essais hors bassin et les résultats des essais d'autopropulsion en bassin.

(2) Masse de glace inférieure à 7 p. 100 du déplacement du LOUIS-ST-LAURENT. Dans ce cas, l'interprétation retenue quant au choc de deux corps reste inchangée. Le montage actuel pourrait servir à la recherche dans la plage inférieure des masses de glace. Mais il faudrait alléger le boîtier métallique qui représente la plus grande part de la masse mise en oeuvre.

Parmi les autres secteurs, auxquels la base de données résultant des essais hors bassin mériterait d'être étendue, citons celui des variations dans les deux paramètres suivants: géométrie du bord de gouvernail et hauteur de contact avec la glace. Cette recherche permettrait d'approfondir l'influence de la surface de contact sur les efforts s'exerçant sur le gouvernail.

Il y a aussi le perfectionnement du modèle réduit par l'adjonction d'un appareil à gouverner hydraulique plus complet; mais cela suppose des recherches sur la modélisation des débits dans les vérins et à travers la vanne de commande. En outre, il y aurait lieu de définir et de réaliser un dispositif d'asservissement par rétroaction, également en modèle réduit.

La grande faiblesse des essais de remorquage en bassin, responsable de la qualité réduite des résultats, a été le petit nombre de répétitions faites de chaque essai. À partir des résultats obtenus, il n'a pas été possible d'extraire les deux composantes que sont les impacts dus aux glaces et aux charges hydrodynamiques normales. Les résultats de ces essais devraient être examinés à la lumière des données résultant des essais en eau libre et des essais de traction au point fixe faits dans les mêmes conditions "opérationnelles" que les essais dans les glaces. Le nombre restreint de données a nécessité un groupage moins fin que prévu des paramètres d'essais, afin de pouvoir dégager des tendances statistiquement plus significatives. La solution réside dans une recherche ultérieure, sur au moins un des trois modèles, par des essais plus nombreux visant à confirmer les résultats statistiques déjà obtenus et à permettre une distinction plus fine entre le degré d'influence des différents facteurs contrôlés. De plus, suite aux expérimentations hors bassin, il est recommandé d'utiliser la glace modèle "MODICE" dans un programme ultérieur d'essais en bassin, étant donné les deux avantages offerts par ce type de glace: (1) bonne aptitude à la modélisation en résistance de compression de la glace réelle et stabilité de cette résistance dans le temps, et (2) densité plus proche de celle de la vraie glace. Le premier facteur apporte une plus grande précision dans les valeurs de couple, le deuxième une simulation plus réaliste de la flottabilité de la glace et, par conséquent, une modélisation plus fidèle de l'écoulement des fragments de glace par rapport au gouvernail.

Les essais réalisés dans le cadre de la présente recherche, tant en bassin que hors bassin, ont fourni l'information de base nécessaire pour confirmer ou vérifier un modèle mathématique permettant de simuler la réponse du gouvernail d'un navire à la charge des glaces. Il serait intéressant de poursuivre ces travaux par l'intégration des équations paramétriques découlant des essais hors bassin aux statistiques tirées des essais en bassin et d'en comparer le résultat final aux données disponibles tirées des essais en vraie grandeur. Cela autoriserait la mise au point d'un modèle semi-empirique simulant l'interaction gouvernail-glaces qui aurait certainement des répercussions sur la conception des gouvernails et appareils à gouverner ainsi que sur la réglementation en la matière.

TABLE OF CONTENTS

VOLUME I

1. INTRODUCTION....1
2. BACKGROUND AND STATE-OF-THE ART....3
3. DRY IMPACT TESTING OF RUDDER MODEL....5
    3.1 Physical Modelling of Rudder/Ice Interaction....5
        3.1.1 Physical Model System....5
        3.1.2 Scaling Criteria and Similitude Principle....6
        3.1.3 Ice Model....14
    3.2 Parametric Test Program....19
        3.2.1 Matrix of Test Parameters....19
        3.2.2 Experimental Set-up....21
        3.2.3 Instrumentation and Data Collection....25
        3.2.4 Test Data....27
    3.3 Discussion of Dry Impact Test Results....41
        3.3.1 Influence of Test Parameters....41
    3.4 Dry Impact Tests Astern Results, Remarks and Recommendations....65
        3.4.1 Dry Impact Astern Tests Results....65
        3.4.2 Remarks on Dry Impact Astern Tests....67
        3.4.3 Recommendations Regarding Dry Impact Astern Tests...68
4. ICE BASIN TOWED MODEL TESTS....72
    4.1 Background....72
    4.2 Test Objectives....72
    4.3 Scope of Test Program....73
    4.4 Models and Modelling Criteria....76
        4.4.1 Ship Models....76
        4.4.2 Modelling Criteria....76
    4.5 Ice Basin Test set-up....78
        4.5.1 Rudder Torque....78
        4.5.2 Propeller Shaft RPM....80
        4.5.3 Model Speed and Drag....80
        4.5.4 Drift Angle....80
        4.5.5 Data Acquisition....80
    4.6 Test Procedure....82
        4.6.1 Bollard Testing....82
        4.6.2 Open Water Testing....82
        4.6.3 Level Ice Testing....82
        4.6.4 Broken Channel Testing....84
        4.6.5 Photographic Documentation of the Towed Tests....87
    4.7 Data Reduction and Results....91
        4.7.1 Histograms of Peak Torque Magnitude and Frequency of Impact....95
        4.7.2 Influence of Parameters....105

4.8 Remarks and Recommendations on Towed Tests................113
4.8.1 Remarks..................................113
4.8.2 Recommendations..........................114

5. GENERAL REMARKS...115

REFERENCES...116

APPENDIX A - MATHEMATICAL MODELS OF RUDDER LOAD AND STEERING GEAR RESPONSE.............117

APPENDIX B - BIBLIOGRAPHY......................................129

APPENDIX C - DETAILED STATEMENT OF WORK.........................137

VOLUME II - **TYPICAL DRY IMPACT RUDDER TORQUE AND ICE BASIN TOWED TEST DATA**

APPENDIX D - TYPICAL DRY IMPACT TESTS

APPENDIX E - ICE BASIN TOWED TEST DATA

LIST OF FIGURES

1.1 ARCTIC SHIP RUDDER RESEARCH AND DEVELOPMENT PROGRAM..........2
3.1 DRY IMPACT EXPERIMENTAL SET-UP....................................7
3.2 PHYSICAL MODEL OF RUDDER ASSEMBLY..............................9
3.3 STRAIN RATE DEPENDENCE OF MODICE..............................15
3.4 TEMPERATURE DEPENDENCE OF MODICE..............................16
3.5 GRAECO-LATIN SQUARE ARRANGEMENT OF TEST VARIABLES...........20
3.6 TEST ASSEMBLY...22
3.7 HYDRAULIC SYSTEM..23
3.8 TYPICAL SET OF TIME HISTORIES..................................28
3.9 TYPICAL TORSIONAL RESPONSE.....................................29
3.10 TORSIONAL RESPONSE ILLUSTRATING PEAK REVERSALS..............30
3.11 TYPICAL TORQUES AND BENDING MOMENTS IN TARGET STRENGTH ICE..31
3.12 RUDDER STOCK TESTS ICE STRENGTH VARIATION...................42
3.13 MAXIMUM RUDDER LOAD INFLUENCE OF VELOCITY & CRUSHING AREA...43
3.14 RUDDER STOCK TESTS ICE STRENGTH VARIATION...................45
3.15 RUDDER STOCK TESTS ICE STRENGTH VARIATION...................46
3.16 RUDDER STOCK TESTS ICE STRENGTH VARIATION...................47
3.17 RUDDER STOCK TESTS ANGLE VARIATION..........................48
3.18 RUDDER STOCK TESTS ANGLE VARIATION..........................49
3.19 RUDDER STOCK TESTS ANGLE VARIATION..........................50
3.20 RUDDER STOCK TESTS RATIO OF BENDING STRAIN TO TORQUE STRAIN.51
3.21 TORQUE RISE TIME INFLUENCE OF VELOCITY & MAX. TORQUE........53
3.22 RUDDER STOCK TESTS MASS VARIATION...........................54
3.23 RUDDER STOCK TESTS MASS VARIATION...........................56
3.24 RUDDER STOCK TESTS MASS VARIATION...........................57
3.25 RUDDER STOCK TESTS MASS VARIATION...........................58
3.26 RUDDER STOCK TESTS RELIEF VARIATION.........................59
3.27 RUDDER STOCK TESTS RELIEF VARIATION.........................60
3.28 RUDDER STOCK TESTS RELIEF VARIATION.........................61
3.29 RUDDER STOCK TESTS VELOCITY VARIATION.......................63
3.30 RUDDER STOCK TESTS VELOCITY VARIATION.......................64
4.1 TOWED TESTS EXPERIMENTAL SET-UP...............................79
4.2 SCHEMATIC OF TOWING ARRANGEMENT...............................81
4.3 PRE-SAWN PLAN...83
4.4 ICEBREAKING TEST IN PRE-CUT ICE...............................86
4.5 PRE-CUT BROKEN CHANNEL DISTRIBUTION..........................88
4.6 TYPICAL TEST RUNS...90
4.7 RADISSON MODEL ICEBREAKING TEST...............................92
4.8 INFLUENCE OF AHEAD VELOCITY ON OPEN WATER TORQUE............93
4.9 INFLUENCE OF ASTERN VELOCITY ON OPEN WATER TORQUE...........94
4.10 FREQUENCY AND MAGNITUDE OF RUDDER ICE IMPACTS...............99
4.11 FREQUENCY AND MAGNITUDE OF RUDDER ICE IMPACTS..............100
4.12 FREQUENCY AND MAGNITUDE OF RUDDER ICE IMPACTS..............101
4.13 FREQUENCY AND MAGNITUDE OF RUDDER ICE IMPACTS..............102
4.14 FREQUENCY AND MAGNITUDE OF RUDDER ICE IMPACTS..............103
4.15 INFLUENCE OF SHIP FORM IN HULL FORWARD SPEED MANOEUVRES....106
4.16 INFLUENCE OF SHIP FORM IN MID SPEED BACKING MANOEUVRES.....107

LIST OF FIGURES (CONTINUED)

4.17 INFLUENCE OF DRAFT CONDITION DURING BACKING MANOEUVRES.....109
4.18 INFLUENCE OF PROPELLER SPEED DURING BACKING MANOEUVRES.....110
4.19 INFLUENCE OF PROPELLER ROTATIONAL DIRECTION DURING FORWARD MANOEUVRES.....111
4.20 INFLUENCE OF ICE THICKNESS DURING BACKING.....112
A.1 SCHEMATIC OF A TYPICAL HYDRAULIC STEERING GEAR.....125
A.2 PRINCIPLE OF OPERATION OF A HYDRAULIC STEERING GEAR.....126
A.3 TYPES OF TILLER ARRANGEMENTS.....126

LIST OF TABLES

3.1 PERTINENT VARIABLES IN DIMENSIONAL ANALYSIS.....10
3.2 PRINCIPAL DIMENSIONLESS PARAMETERS.....11
3.3 DESIGN EQUATIONS BASED ON DYNAMIC (FROUDE) SCALING.....12
3.4 PRINCIPAL PROTOTYPE AND MODEL SCALE DIMENSIONS.....13
3.5 DENSITY, FRICTION, UNIAXIAL CRUSHING STRENGTH PROPERTIES.....18
3.6 TEST MATRIX AND PEAK DATA SUMMARY.....33
4.1 INDEPENDENT TEST VARIABLES.....74
4.2 TYPICAL TEST MATRIX.....75
4.3 TOWED TEST MODEL PARTICULARS.....77
4.4 ICE SHEET CHARACTERISTICS.....85
4.5 ICE BASIN TOWED TESTS.....96
4.6 ICE BASIN TOWED MODEL DATA.....97
A.1 DESIGN EQUATIONS BASED ON DYNAMIC (FROUDE) SCALING.....122

NOMENCLATURE

A	Area of contact
b	Width of contact area
d	Diameter
g	Acceleration due to gravity
G	Load, Force, Shear Modulus
i	Moment of Inertia
K	Torsional Stiffness
l	Characteristic length
L	Any length variable
M_I, M_R, M_S	Mass (Ice, Rudder, Ship)
P	Hydraulic pressure
Q	Torque
S	Ratio of Full Scale to Model Scale
t	Time
T	Temperature
v	Velocity
x,y,z	Displacement Coordinate
δ	Rudder Angle
μ	Friction Coefficient
σ_c	Crushing Strength
ρ	Mass Density
λ	Geometric Scale Factor
θ	Crushed depth
ε	Strain

APPENDIX D

TYPICAL DRY IMPACT TORQUES

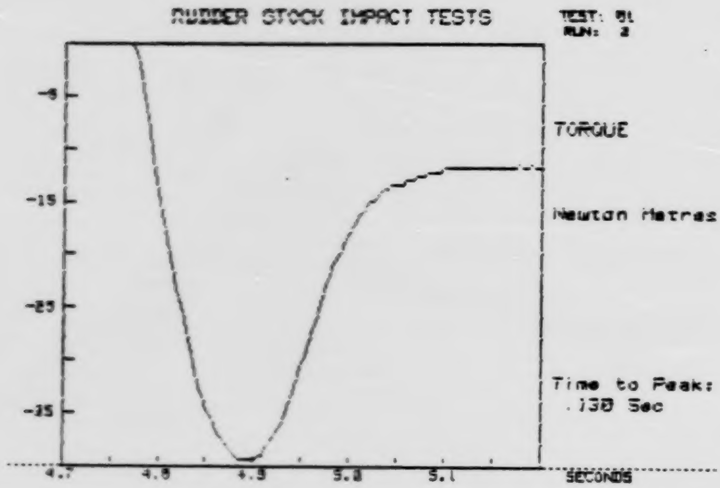
RUDDER STOCK IMPACT TESTS
TEST: 01
RUN: 2
-5
-15
-25
-35
TORQUE
Newton Metres
Time to Peak:
.130 Sec
4.7
4.8
4.9
5.0
5.1
SECONDS

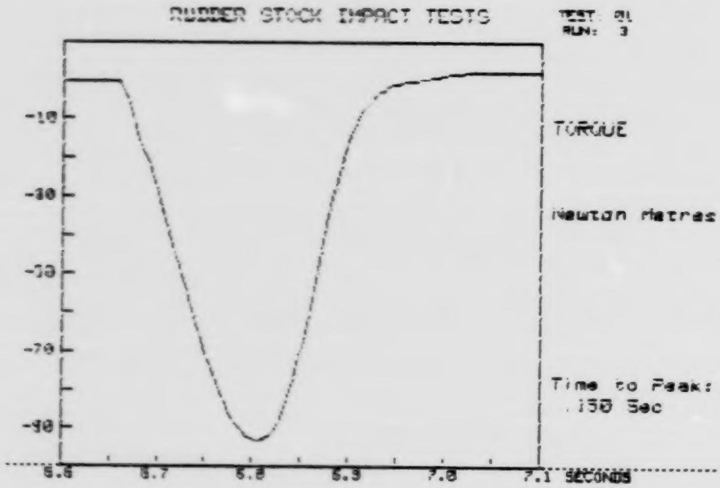
RUDDER STOCK IMPACT TESTS
TEST: 01
RUN: 3
-10
-30
-50
-70
-90
TORQUE
Newton Metres
Time to Peak:
.150 Sec
6.6
6.7
6.8
6.9
7.0
7.1
SECONDS

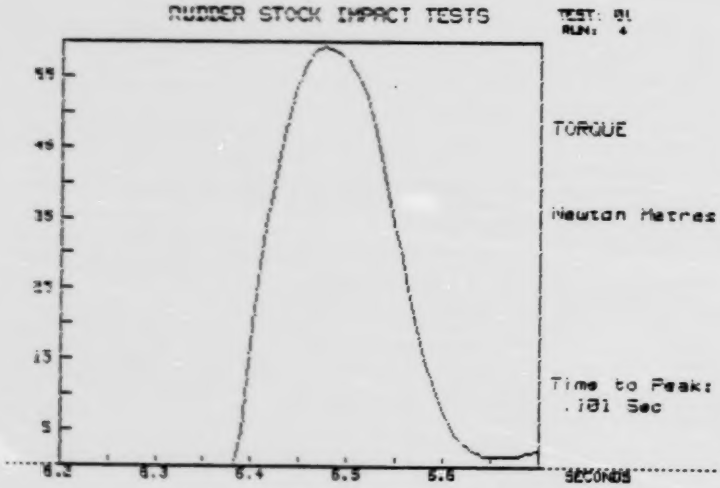
RUDDER STOCK IMPACT TESTS
TEST: 01
RUN: 4
55
45
35
25
15
5
TORQUE
Newton Metres
Time to Peak:
.101 Sec
6.2
6.3
6.4
6.5
6.6
SECONDS

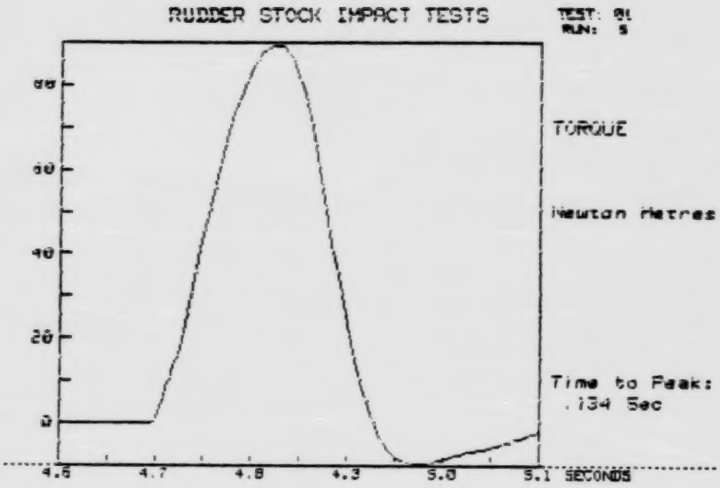
RUDDER STOCK IMPACT TESTS
TEST: 01
RUN: 5
80
60
40
20
0
TORQUE
Newton Metres
Time to Peak:
.134 Sec
4.6
4.7
4.8
4.9
5.0
5.1
SECONDS

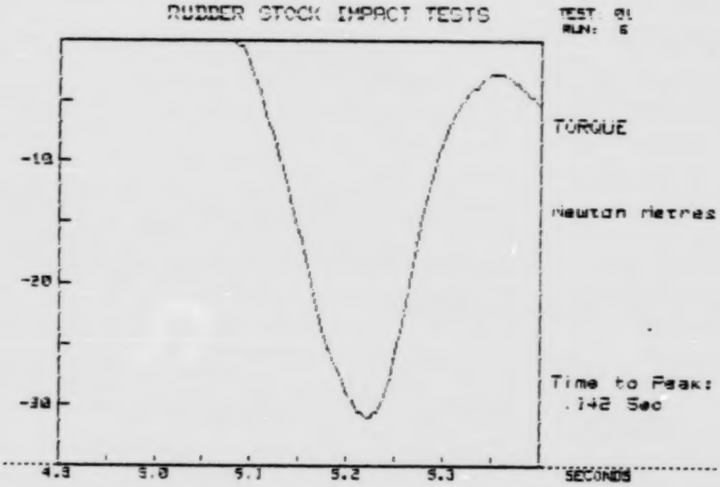
RUDDER STOCK IMPACT TESTS
TEST: 01
RUN: 6
-10
-20
-30
TORQUE
Newton Metres
Time to Peak:
.142 Sec
4.9
5.0
5.1
5.2
5.3
SECONDS

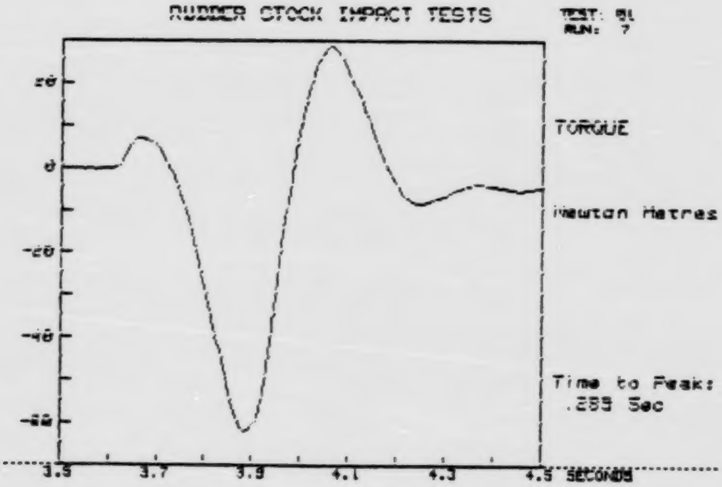
RUDDER STOCK IMPACT TESTS
TEST: 01
RUN: 7
20
0
-20
-40
-60
TORQUE
Newton Metres
Time to Peak:
.283 Sec
3.5
3.7
3.9
4.1
4.3
4.5
SECONDS

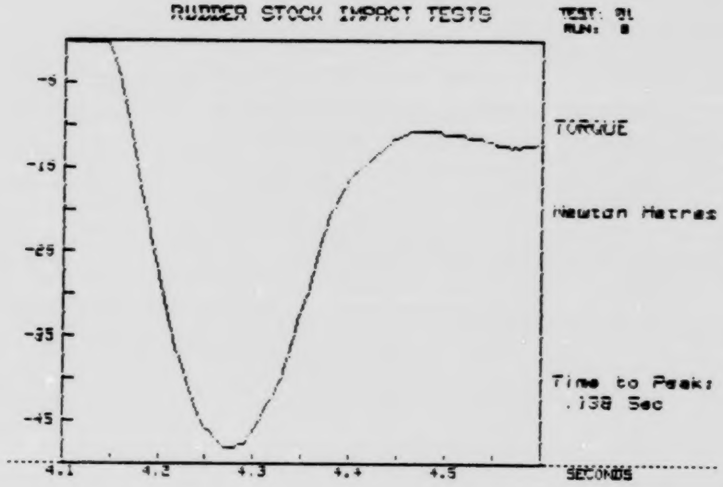
RUDDER STOCK IMPACT TESTS
TEST: 01
RUN: 8
-5
-15
-25
-35
-45
TORQUE
Newton Metres
Time to Peak:
.138 Sec
4.1
4.2
4.3
4.4
4.5
SECONDS

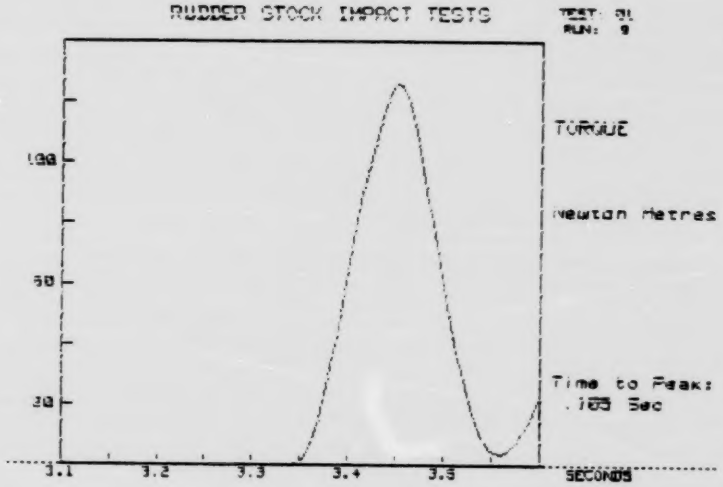
RUDDER STOCK IMPACT TESTS
TEST: 01
RUN: 9
100
60
20
TORQUE
Newton Metres
Time to Peak:
.105 Sec
3.1
3.2
3.3
3.4
3.5
SECONDS

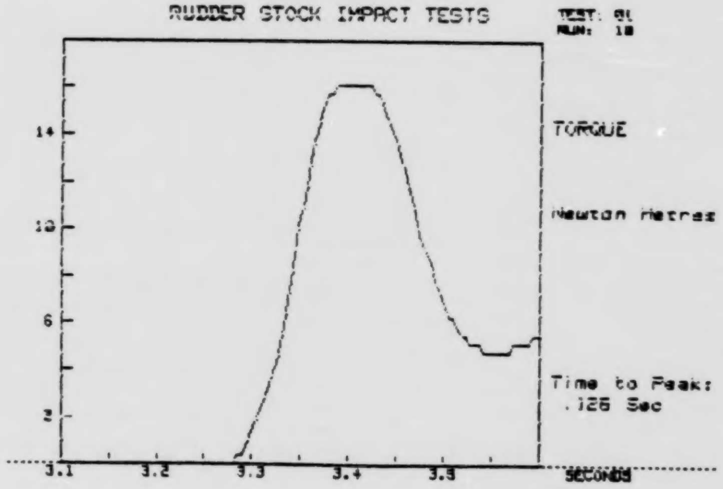
RUDDER STOCK IMPACT TESTS
TEST: 01
RUN: 10
14
10
6
2
TORQUE
Newton Metres
Time to Peak:
.126 Sec
3.1
3.2
3.3
3.4
3.5
SECONDS

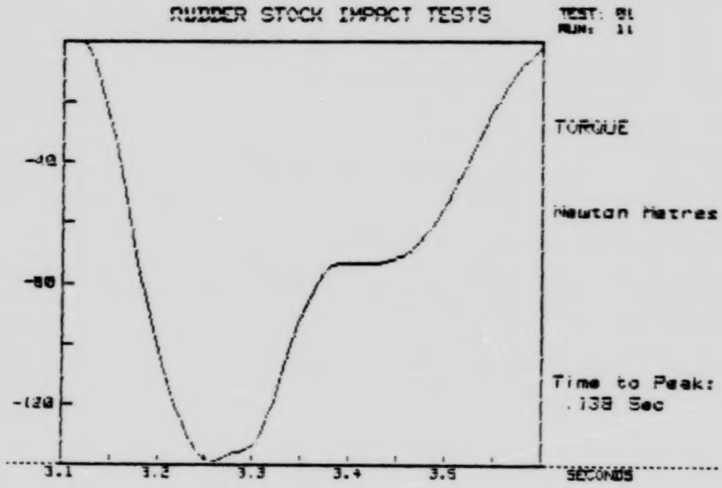
RUDDER STOCK IMPACT TESTS
TEST: 01
RUN: 11
TORQUE
Newton Metres
Time to Peak:
.138 Sec
-40
-80
-120
3.1
3.2
3.3
3.4
3.5
SECONDS

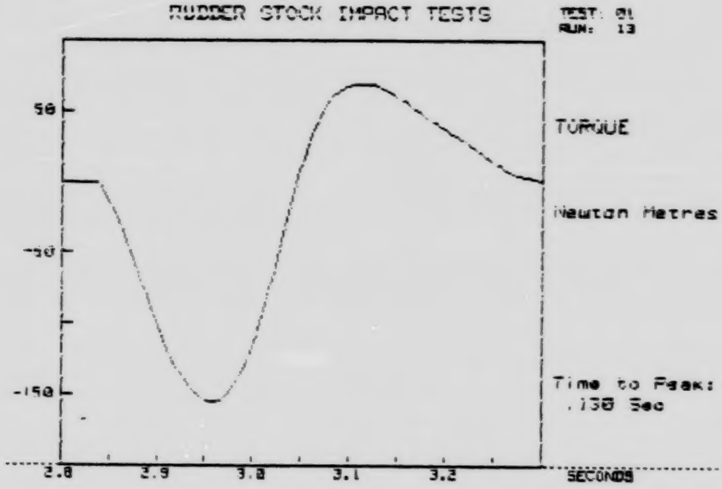
RUDDER STOCK IMPACT TESTS
TEST: 01
RUN: 13
TORQUE
Newton Metres
Time to Peak:
.138 Sec
50
-50
-150
2.8
2.9
3.0
3.1
3.2
SECONDS

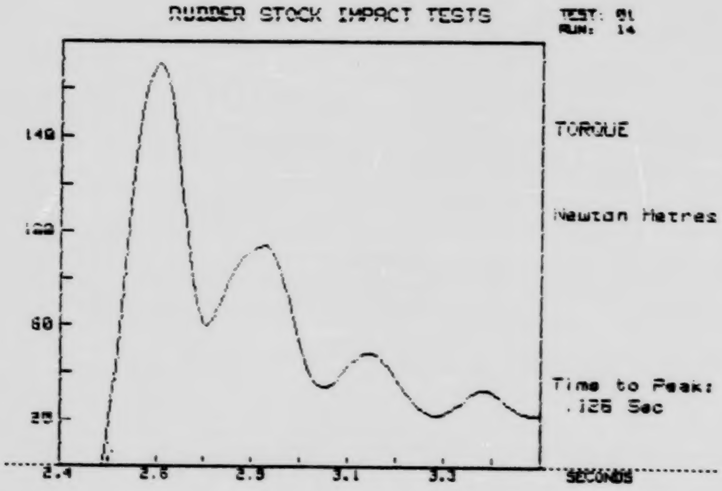
RUDDER STOCK IMPACT TESTS
TEST: 01
RUN: 14
TORQUE
Newton Metres
Time to Peak:
.126 Sec
140
100
60
20
2.5
2.7
2.9
3.1
3.3
SECONDS

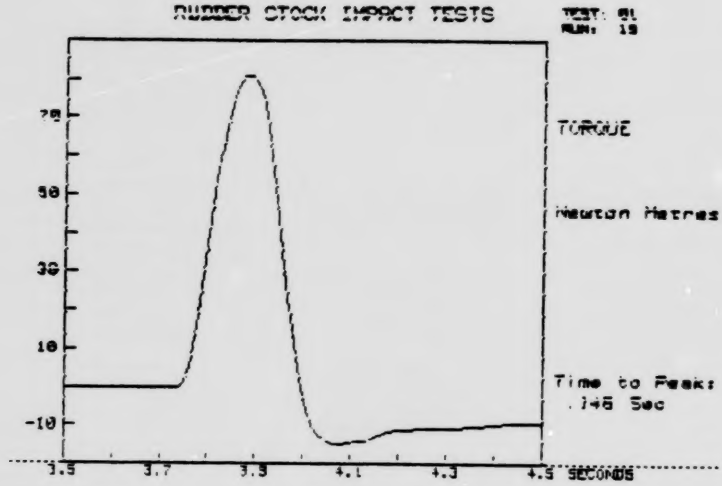
RUDDER STOCK IMPACT TESTS
TEST: 01
RUN: 19
70
50
30
10
-10
TORQUE
Newton Metres
Time to Peak:
.146 Sec
3.5
3.7
3.9
4.1
4.3
4.5
SECONDS

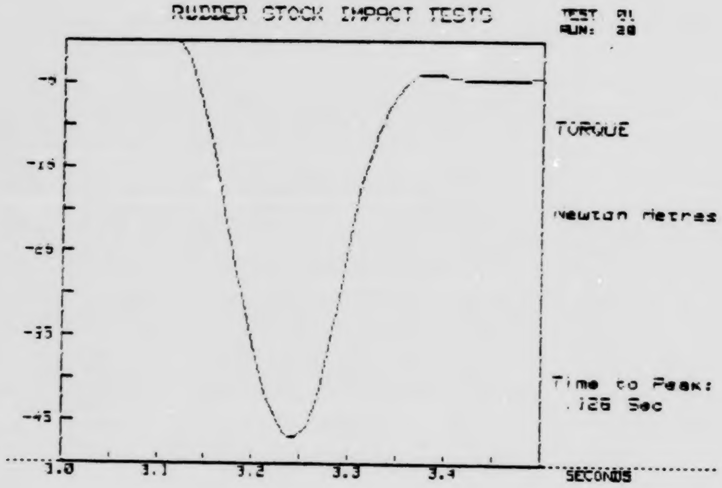
RUDDER STOCK IMPACT TESTS
TEST 01
RUN: 20
-5
-15
-25
-35
-45
TORQUE
Newton Metres
Time to Peak:
.126 Sec
3.0
3.1
3.2
3.3
3.4
SECONDS

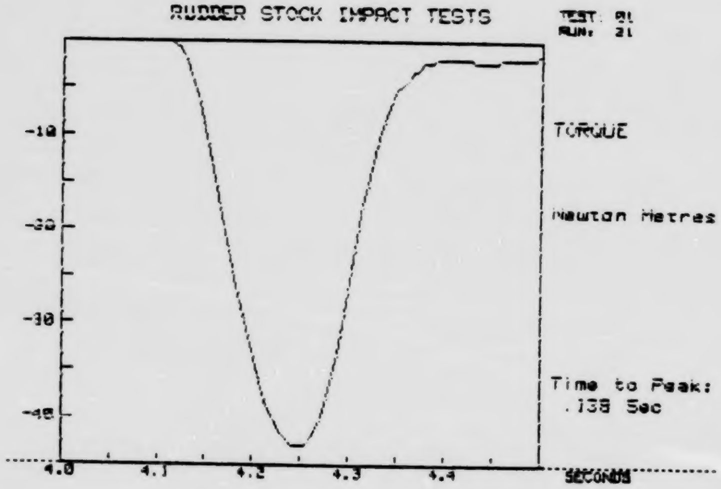
RUDDER STOCK IMPACT TESTS
TEST: 01
RUN: 21
-10
-20
-30
-40
TORQUE
Newton Metres
Time to Peak:
.138 Sec
4.0
4.1
4.2
4.3
4.4
SECONDS

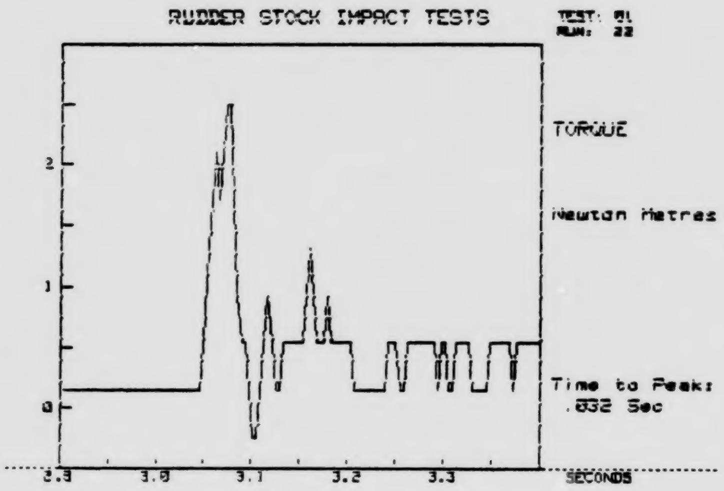
RUDDER STOCK IMPACT TESTS
TEST: 01
RUN: 22
TORQUE
Newton Metres
Time to Peak:
.032 Sec
2
1
0
2.9
3.0
3.1
3.2
3.3
SECONDS

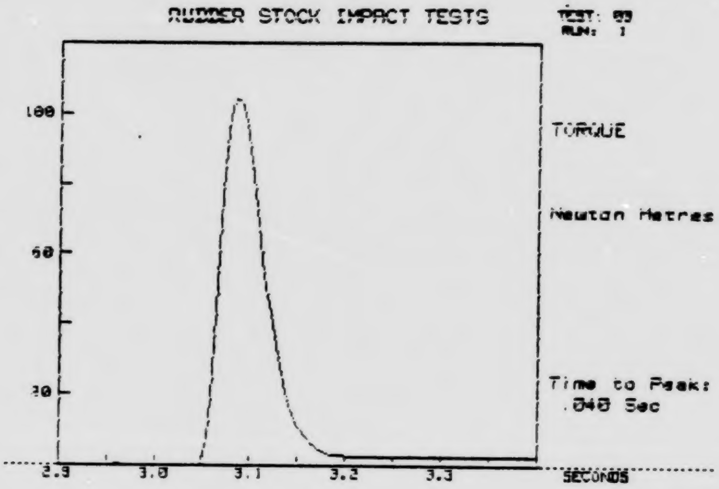
RUDDER STOCK IMPACT TESTS
TEST: 03
RUN: 1
100
60
20
TORQUE
Newton Metres
Time to Peak:
.040 Sec
2.9
3.0
3.1
3.2
3.3
SECONDS

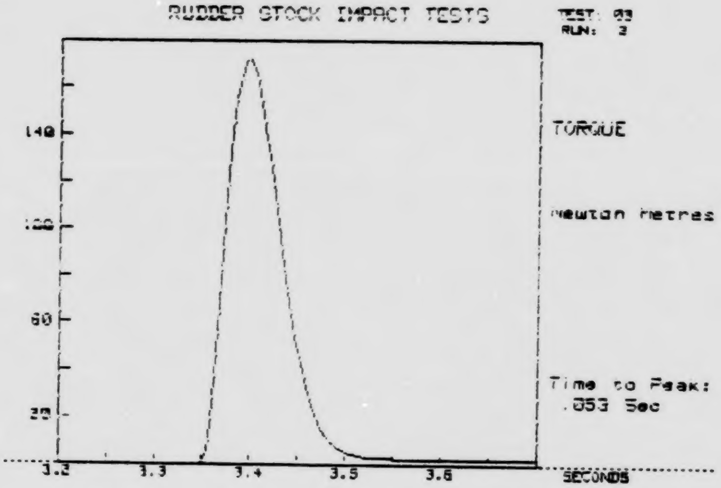
RUDDER STOCK IMPACT TESTS
TEST: 03
RUN: 2
140
100
60
20
TORQUE
Newton Metres
Time to Peak:
.053 Sec
3.2
3.3
3.4
3.5
3.6
SECONDS

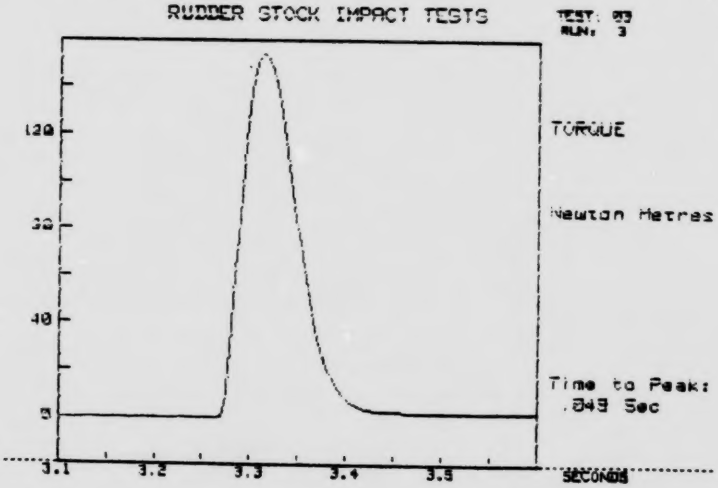
RUDDER STOCK IMPACT TESTS
TEST: 03
RUN: 3
120
80
40
0
TORQUE
Newton Metres
Time to Peak:
.049 Sec
3.1
3.2
3.3
3.4
3.5
SECONDS

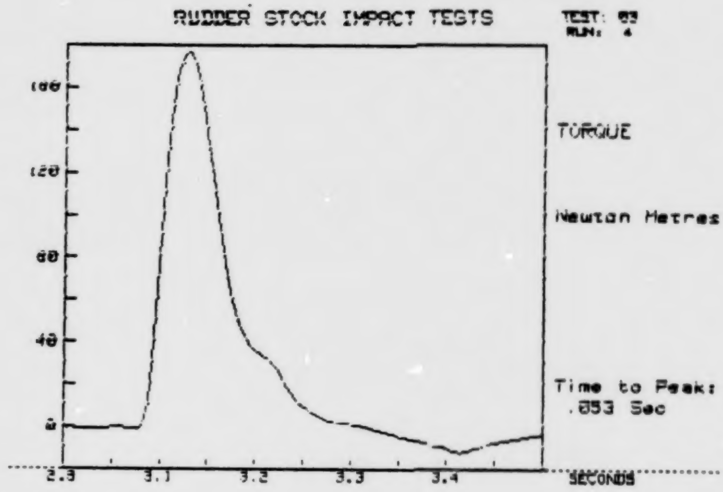

RUDDER STOCK IMPACT TESTS

TEST: 03
RUN: 4

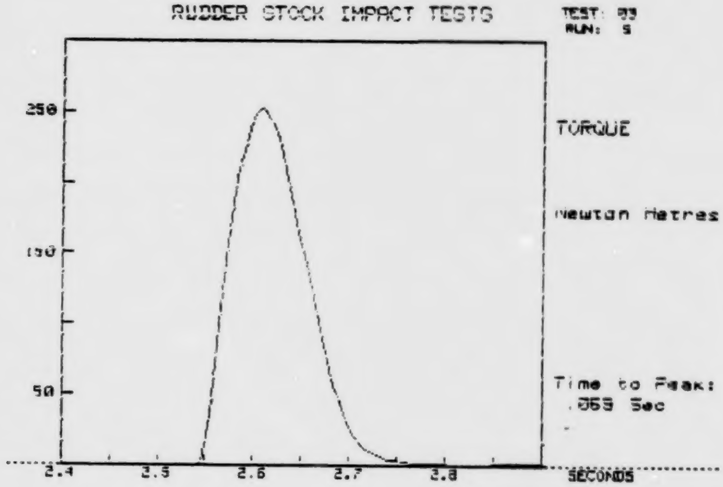

RUDDER STOCK IMPACT TESTS

TEST: 03
RUN: 5

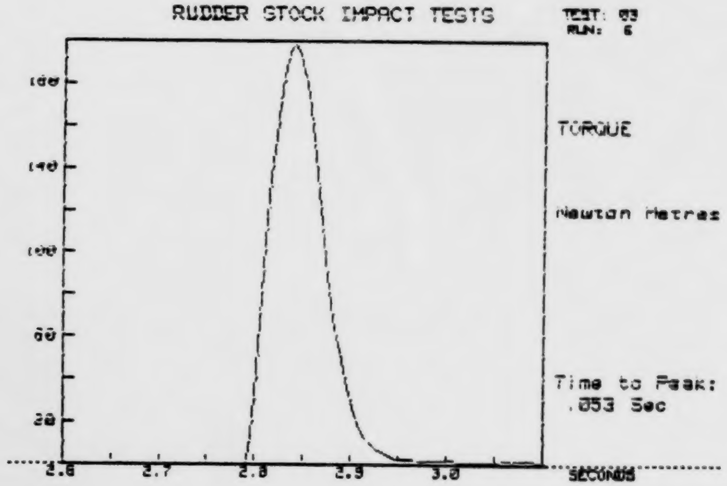

RUDDER STOCK IMPACT TESTS

TEST: 03
RUN: 6

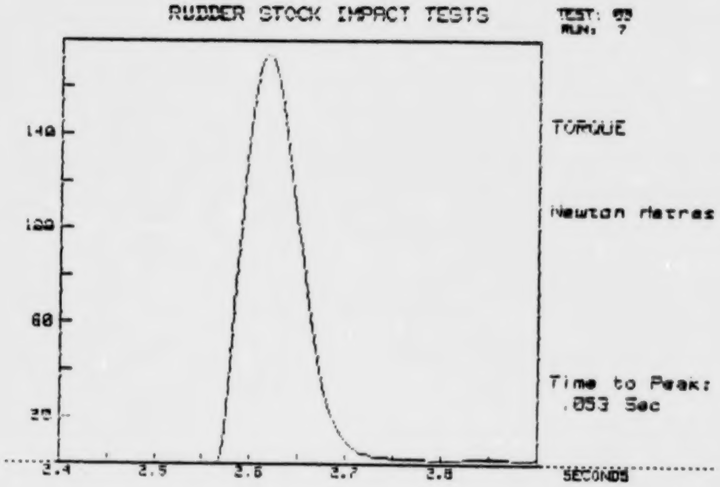
RUDDER STOCK IMPACT TESTS
TEST: 03
RUN: 7
140
100
60
20
2.4
2.5
2.6
2.7
2.8
SECONDS
TORQUE
Newton Metres
Time to Peak:
.053 Sec

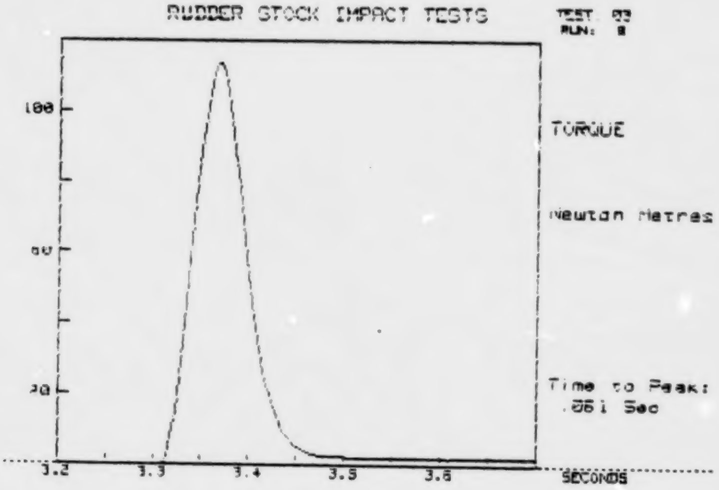
RUDDER STOCK IMPACT TESTS
TEST: 03
RUN: 8
100
60
20
3.2
3.3
3.4
3.5
3.6
SECONDS
TORQUE
Newton Metres
Time to Peak:
.061 Sec

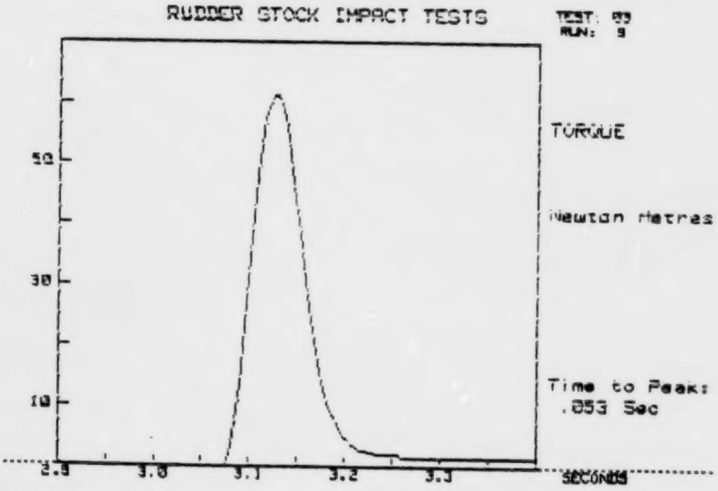
RUDDER STOCK IMPACT TESTS
TEST: 03
RUN: 9
50
30
10
2.9
3.0
3.1
3.2
3.3
SECONDS
TORQUE
Newton Metres
Time to Peak:
.053 Sec

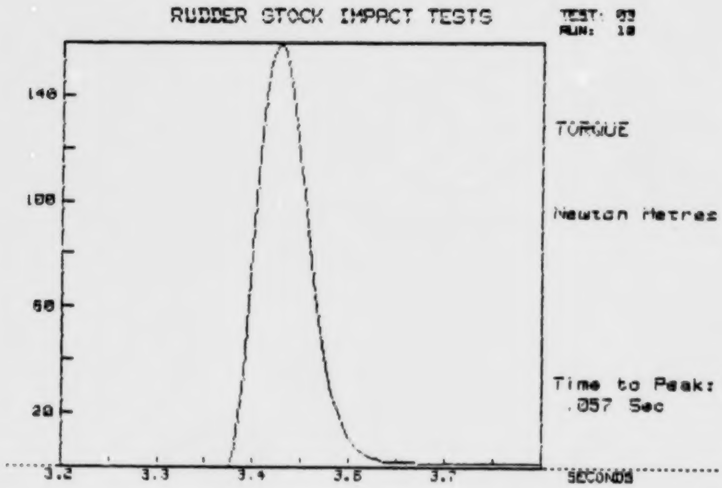
RUDDER STOCK IMPACT TESTS
TEST: 03
RUN: 10
140
100
60
20
TORQUE
Newton Metres
Time to Peak:
.057 Sec
3.2
3.3
3.4
3.5
3.6
SECONDS

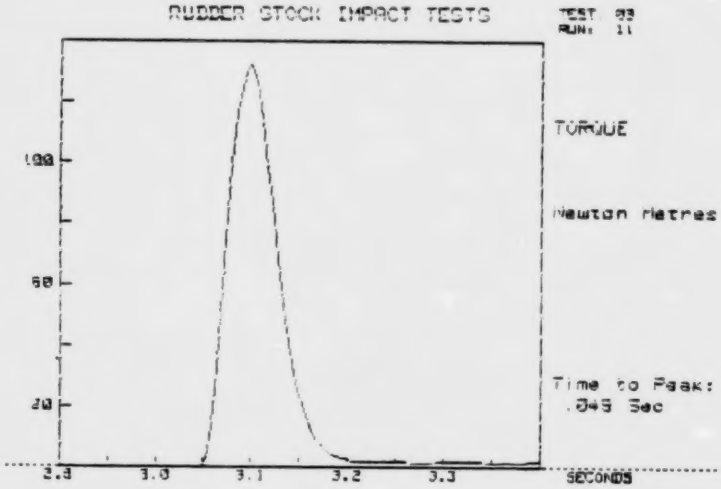
RUDDER STOCK IMPACT TESTS
TEST: 03
RUN: 11
100
60
20
TORQUE
Newton Metres
Time to Peak:
.045 Sec
2.9
3.0
3.1
3.2
3.3
SECONDS

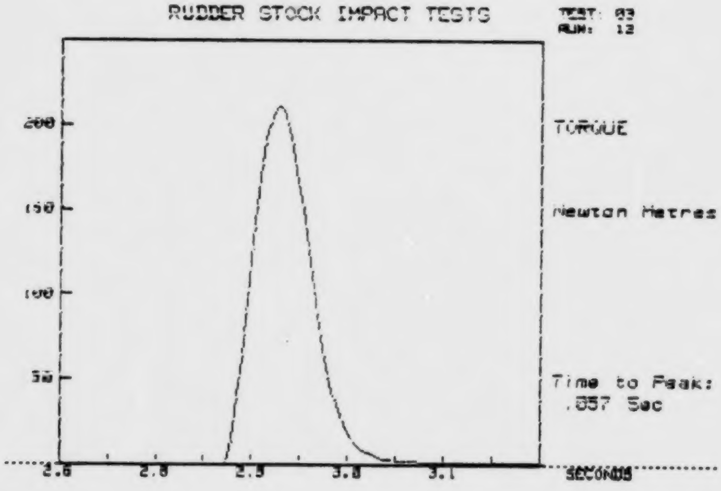
RUDDER STOCK IMPACT TESTS
TEST: 03
RUN: 12
200
150
100
50
TORQUE
Newton Metres
Time to Peak:
.057 Sec
2.7
2.8
2.9
3.0
3.1
SECONDS

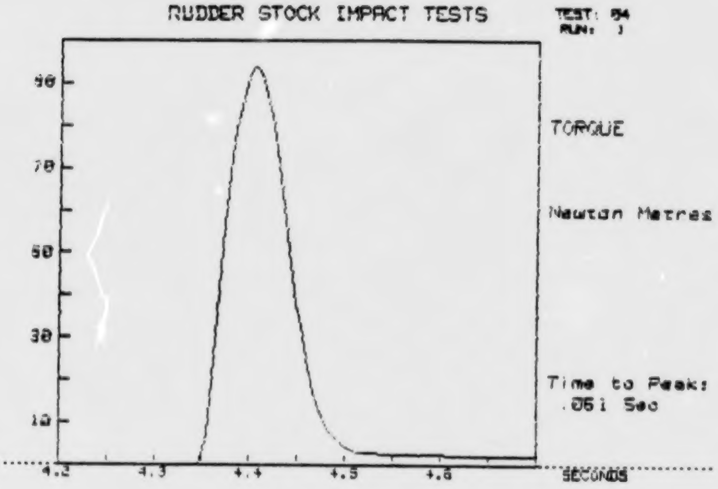
RUDDER STOCK IMPACT TESTS
TEST: 04
RUN: 1
TORQUE
Newton Metres
Time to Peak:
.061 Sec
90
70
50
30
10
4.2
4.3
4.4
4.5
4.6
SECONDS

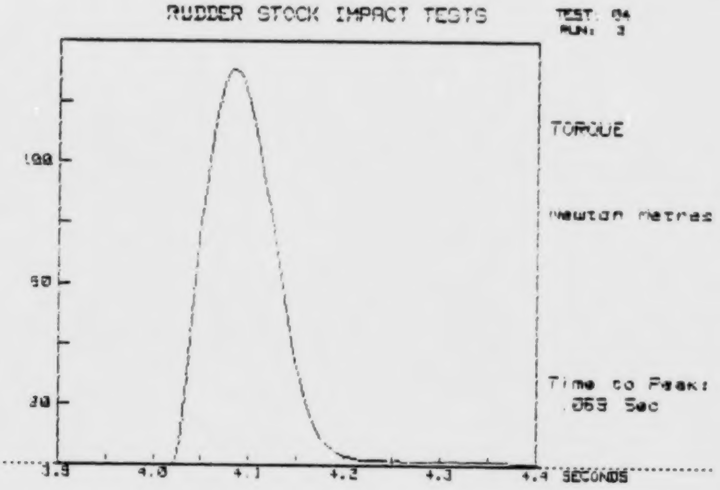
RUDDER STOCK IMPACT TESTS
TEST: 04
RUN: 2
TORQUE
Newton Metres
Time to Peak:
.063 Sec
100
60
20
3.9
4.0
4.1
4.2
4.3
4.4
SECONDS

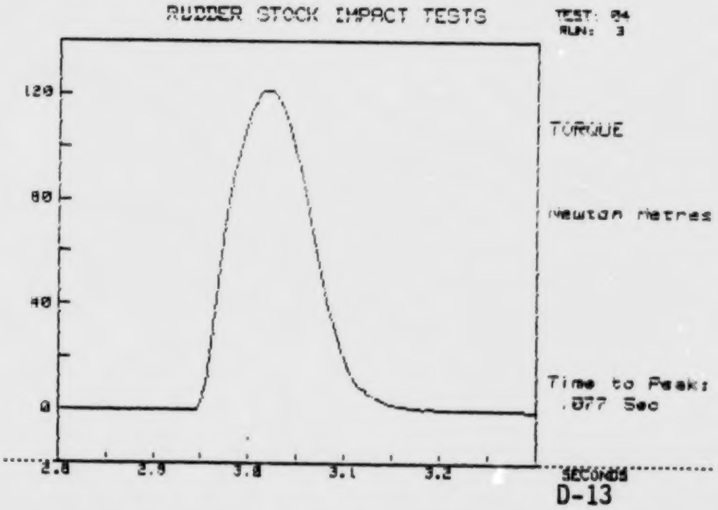
RUDDER STOCK IMPACT TESTS
TEST: 04
RUN: 3
TORQUE
Newton Metres
Time to Peak:
.077 Sec
120
80
40
0
2.8
2.9
3.0
3.1
3.2
SECONDS

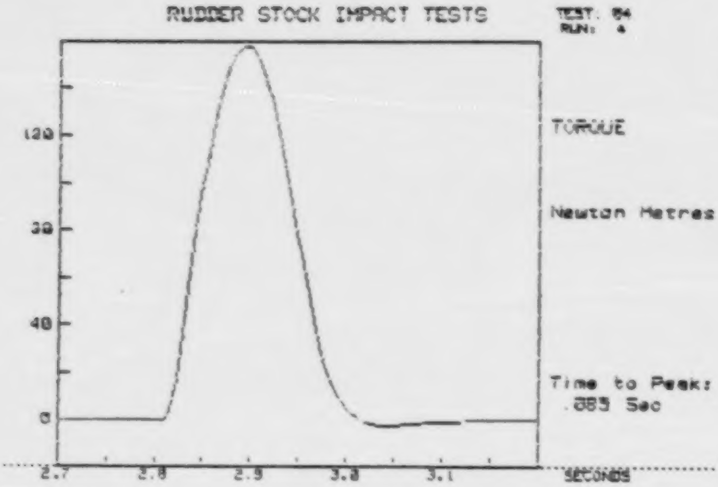
RUDDER STOCK IMPACT TESTS
TEST: 04
RUN: 4
120
80
40
0
TORQUE
Newton Metres
Time to Peak:
.085 Sec
2.7
2.8
2.9
3.0
3.1
SECONDS

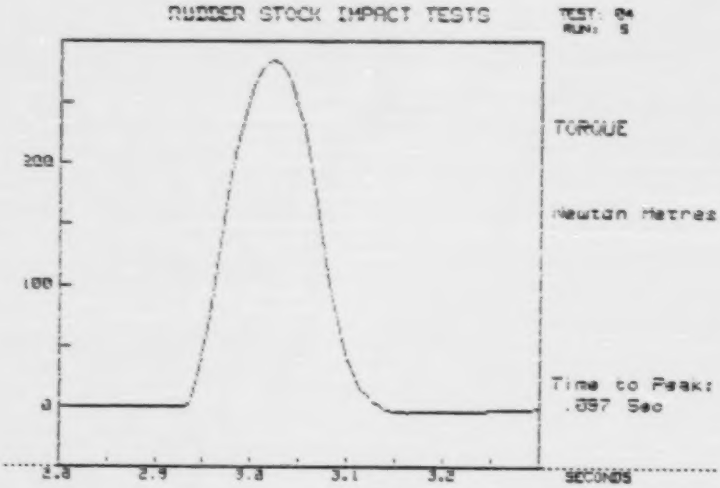
RUDDER STOCK IMPACT TESTS
TEST: 04
RUN: 5
200
100
0
TORQUE
Newton Metres
Time to Peak:
.097 Sec
2.8
2.9
3.0
3.1
3.2
SECONDS

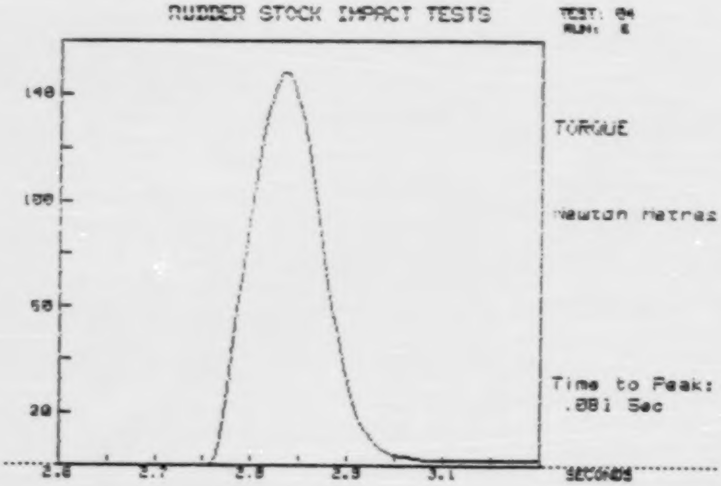
RUDDER STOCK IMPACT TESTS
TEST: 04
RUN: 6
140
100
50
20
TORQUE
Newton Metres
Time to Peak:
.081 Sec
2.6
2.7
2.8
2.9
3.1
SECONDS

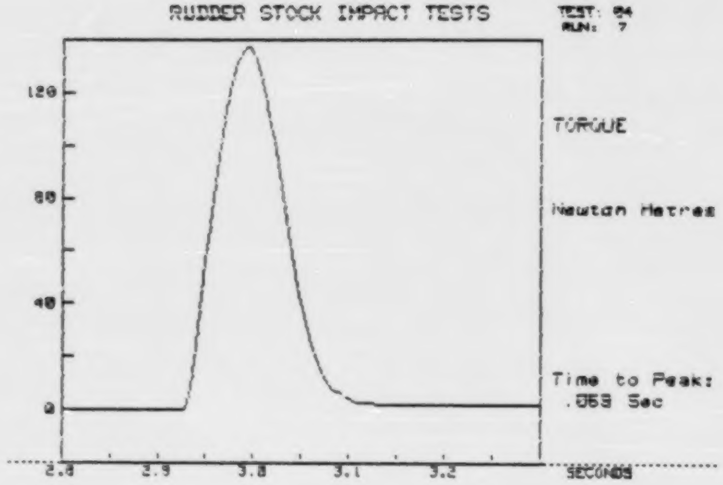
RUDDER STOCK IMPACT TESTS
TEST: 04
RUN: 7
120
80
40
0
TORQUE
Newton Metres
Time to Peak:
.063 Sec
2.8
2.9
3.0
3.1
3.2
SECONDS

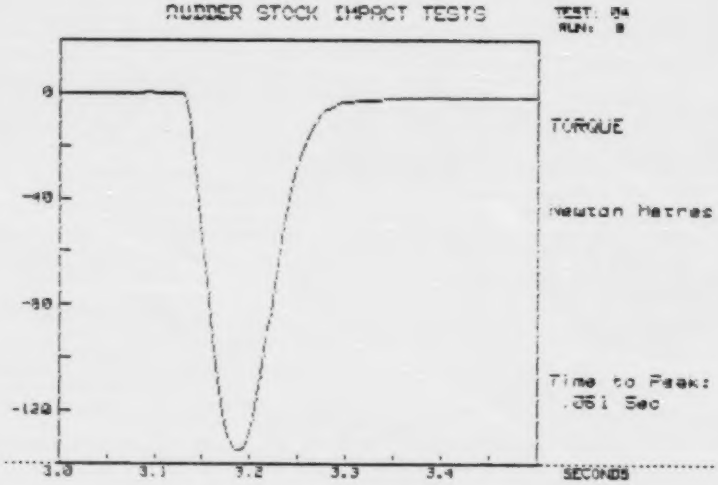
RUDDER STOCK IMPACT TESTS
TEST: 04
RUN: 8
0
-40
-80
-120
TORQUE
Newton Metres
Time to Peak:
.061 Sec
3.0
3.1
3.2
3.3
3.4
SECONDS

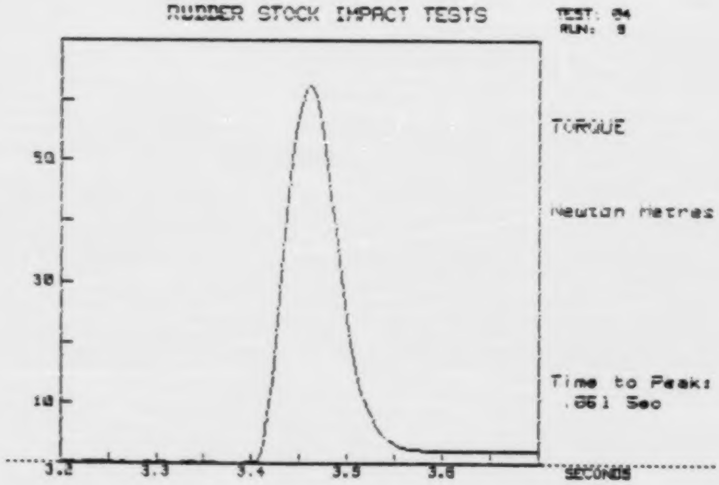
RUDDER STOCK IMPACT TESTS
TEST: 04
RUN: 9
50
30
10
TORQUE
Newton Metres
Time to Peak:
.061 Sec
3.2
3.3
3.4
3.5
3.6
SECONDS

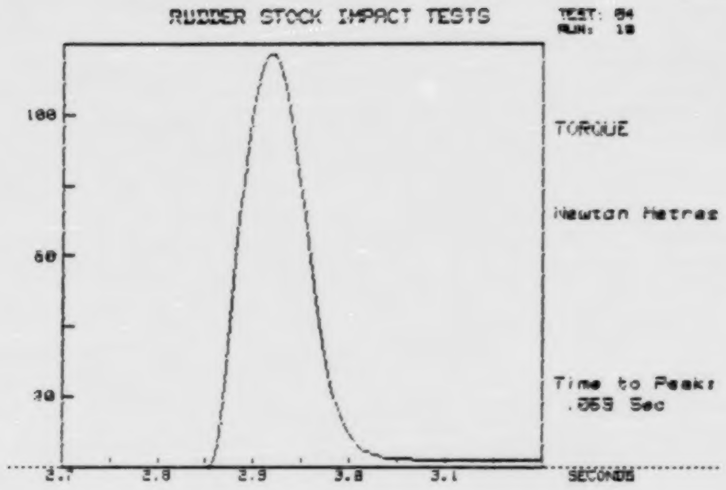
RUDDER STOCK IMPACT TESTS
TEST: 04
RUN: 10
100
60
20
TORQUE
Newton Metres
Time to Peak:
.063 Sec
2.7
2.8
2.9
3.0
3.1
SECONDS

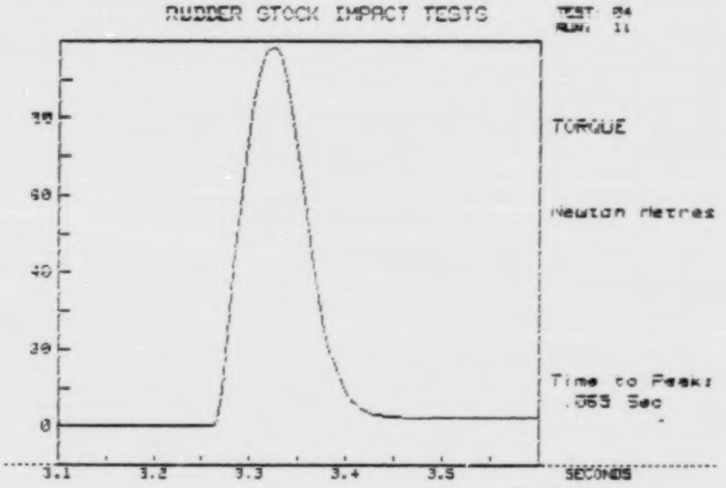
RUDDER STOCK IMPACT TESTS
TEST: 04
RUN: 11
80
60
40
20
0
TORQUE
Newton Metres
Time to Peak:
.063 Sec
3.1
3.2
3.3
3.4
3.5
SECONDS

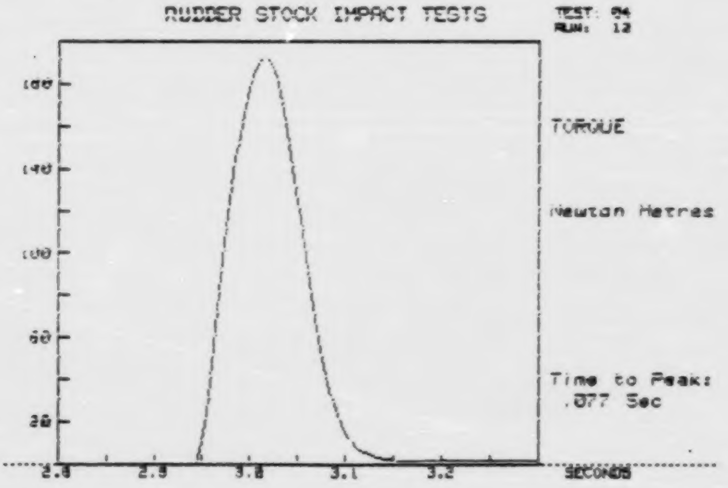
RUDDER STOCK IMPACT TESTS
TEST: 04
RUN: 12
180
140
100
60
20
TORQUE
Newton Metres
Time to Peak:
.077 Sec
2.8
2.9
3.0
3.1
3.2
SECONDS

APPENDIX E

ICE BASIN TOWED TEST DATA

ICE BASIN TOWED TESTS

HISTOGRAMS: CATEGORIES SELECTED AND TEST RUNS INCLUDED

CONDITIONS THRUST (FWD/BACK) VELOCITY RUDDER ANGLE DRIFT ANGLE		SHIPS MVA / R / P8 TEST 01, 03, 04 RUNS AT DESIGN DRAFT	SHIPS MV / R TEST 01, 03 RUNS AT LIGHT DRAFT	SHIPS P8 TEST 04 OTHER RUNS, DESIGN DRAFT
1 FULL SPEED FRWD	FF,V_1,35°R, 0°D	3, 11, 19	27	3a
	TF	5, 13, 21	23	5a
2 YAWED FRWD	FF,V_1,35°R,5°D	7, 15, 23	31	7a
3 MID SPEED FRWD	FF,V_2,35°R,0°D	9, 17, 25	33	
4 MID SPEED BACK	FB,V_2, 0°R,0°D	4, 12, 20	28	49
	TB,V_2, 0°R,0°D	6, 14, 22	30	69
	FB,V_2,10°R,0°D	8, 16, 24	32	89
5 SPEED BACK	FB V_3 0°R 0°D	10 18 26	34	

NOMINAL SPEEDS	MVA(01)	MVA(02)	R(03)	P8(04)
V_1 m/s	.563		.690	.488
V_2 m/s	.282		.345	.244
V_3 m/s	.141		.173	.122
SCALE	30	30	20	40
NOMINAL ICE (mm) THICKNESS	70	40	50	50

NOTE: Open water test runs are not shown.

TEST 101

TEST #1 RUN 01

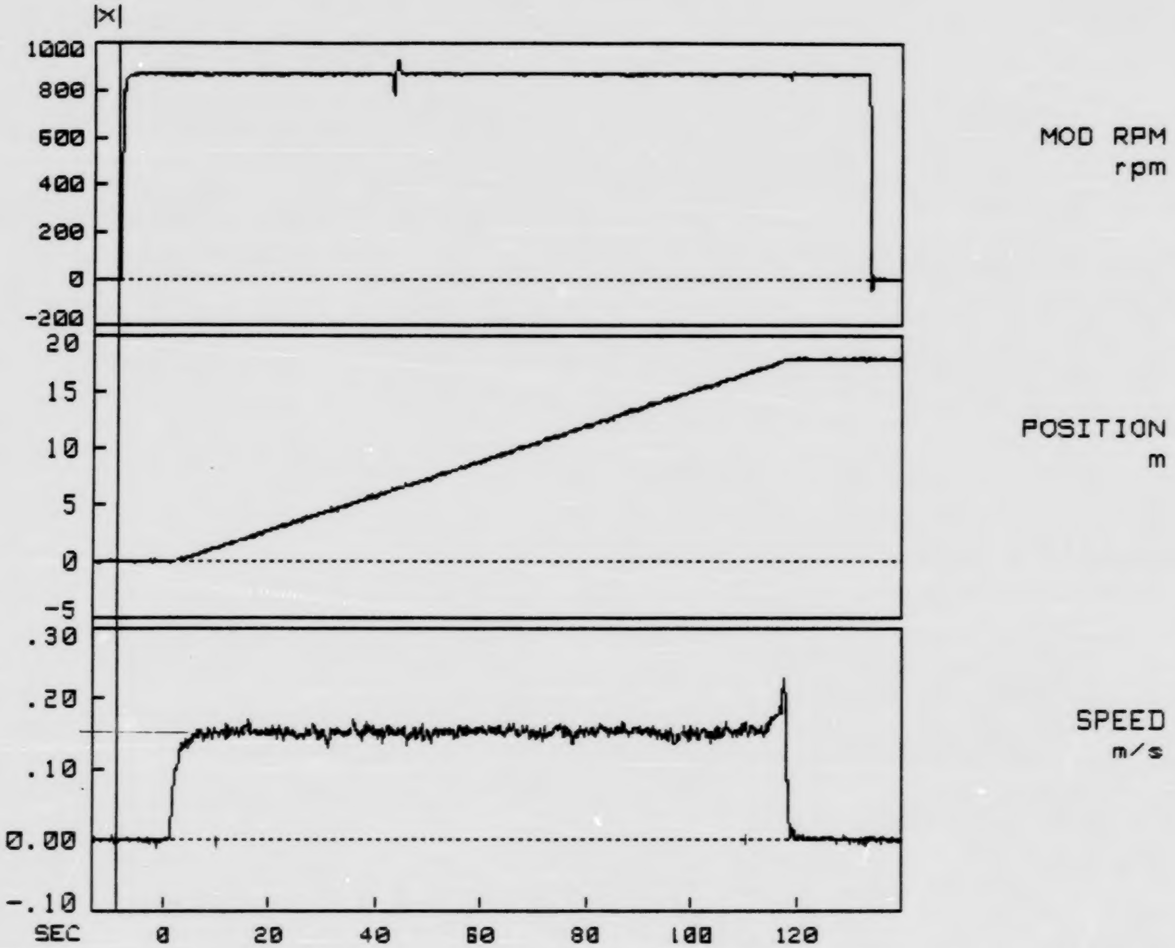

TEST #1 RUN 01 TEST 101

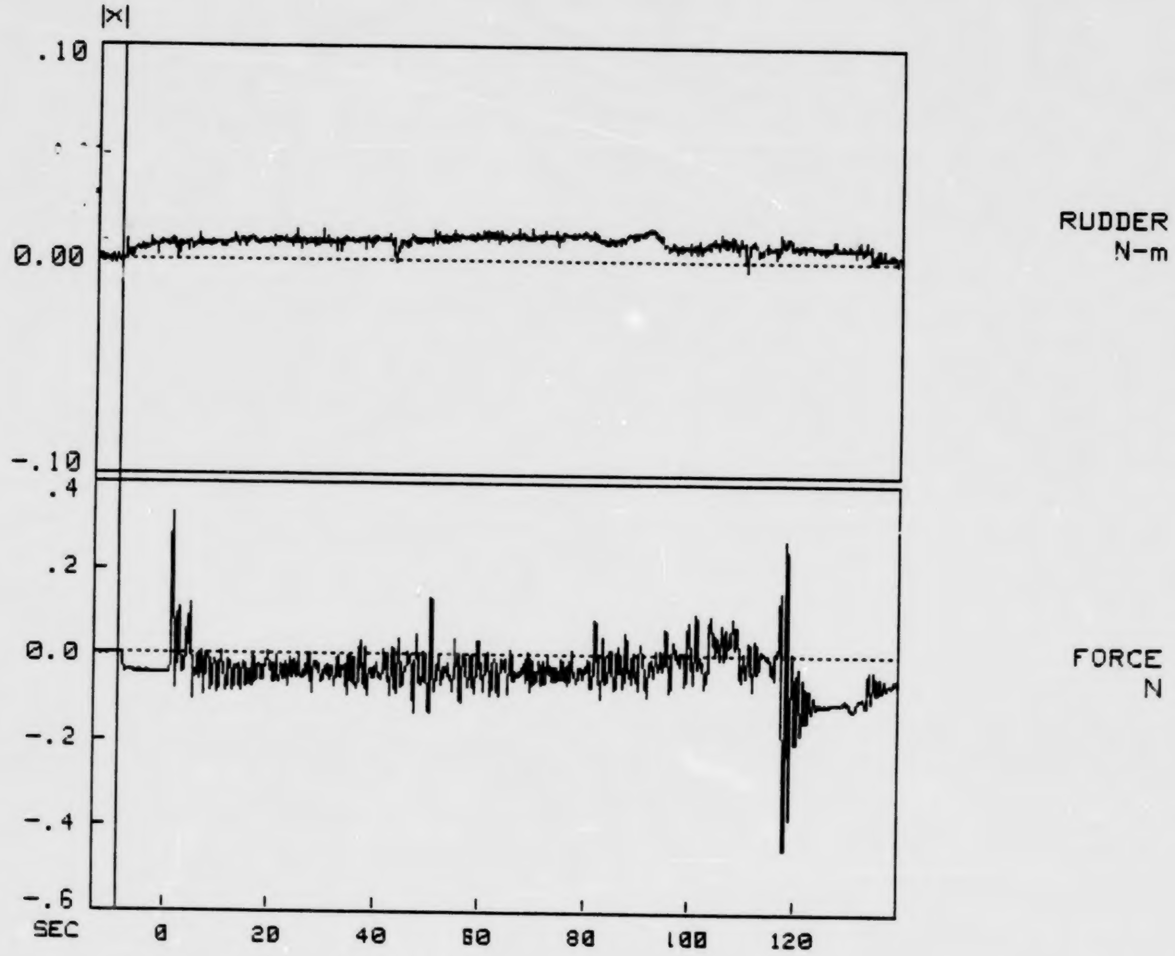

TEST 102

TEST #1 RUN 02

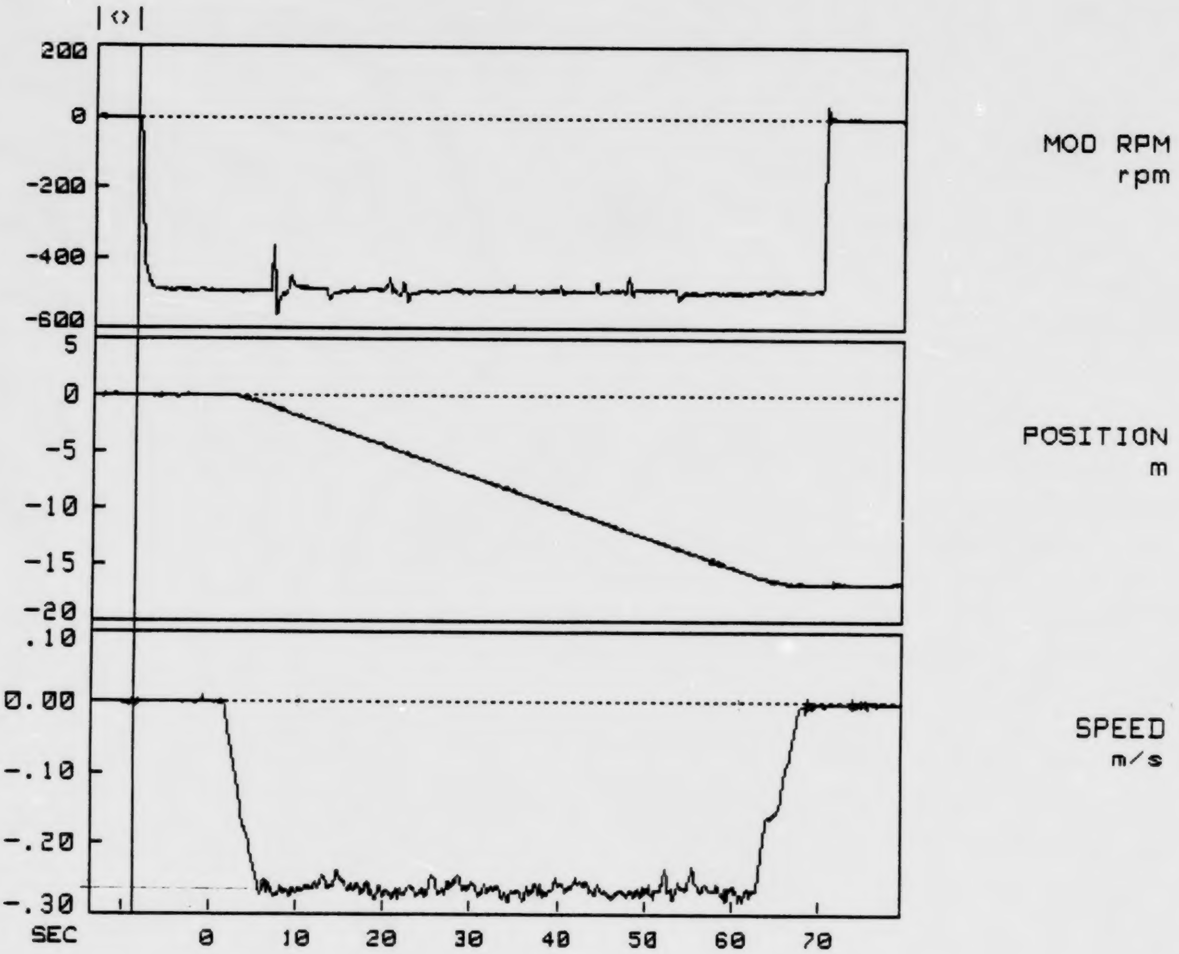

TEST #1 RUN 02 TEST 102

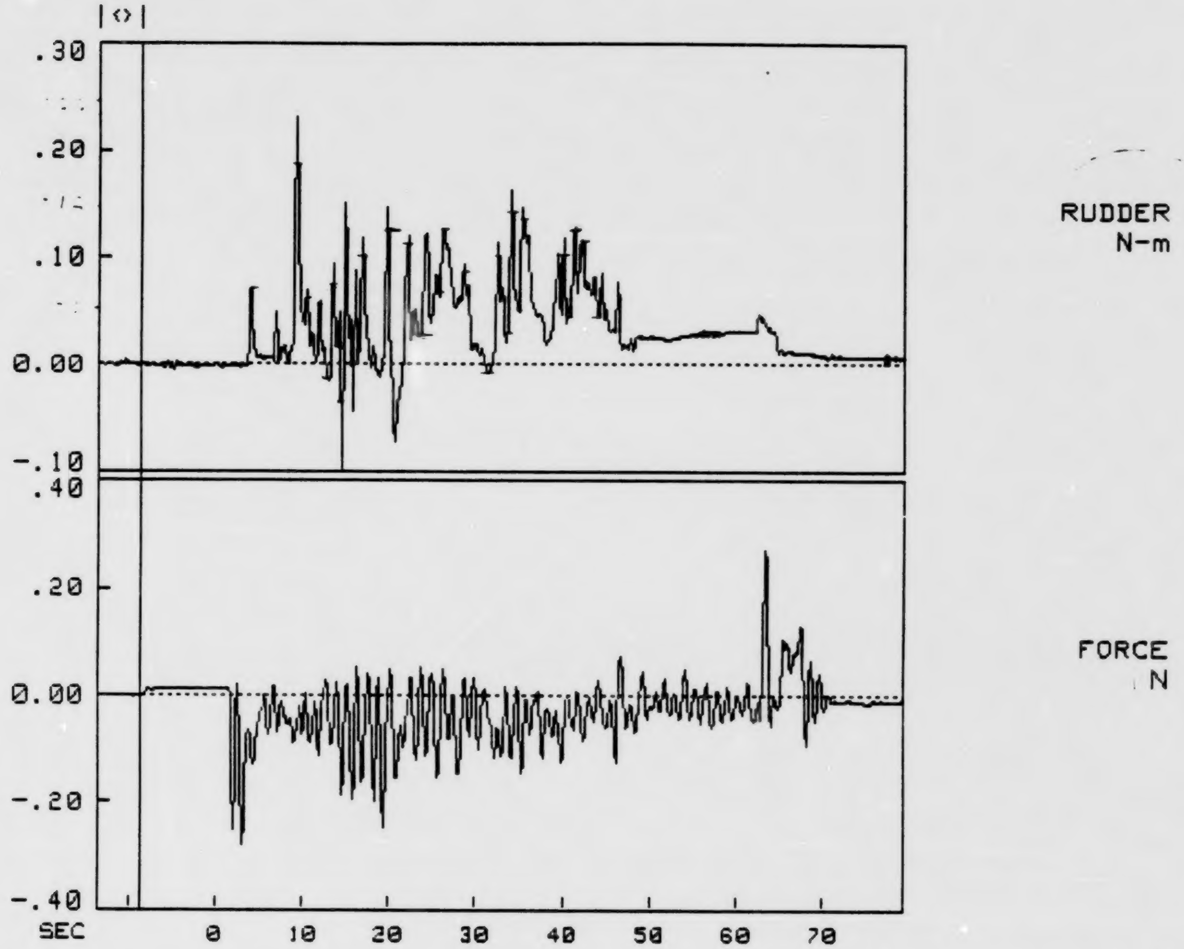

TEST #1 RUN 03 TEST 103

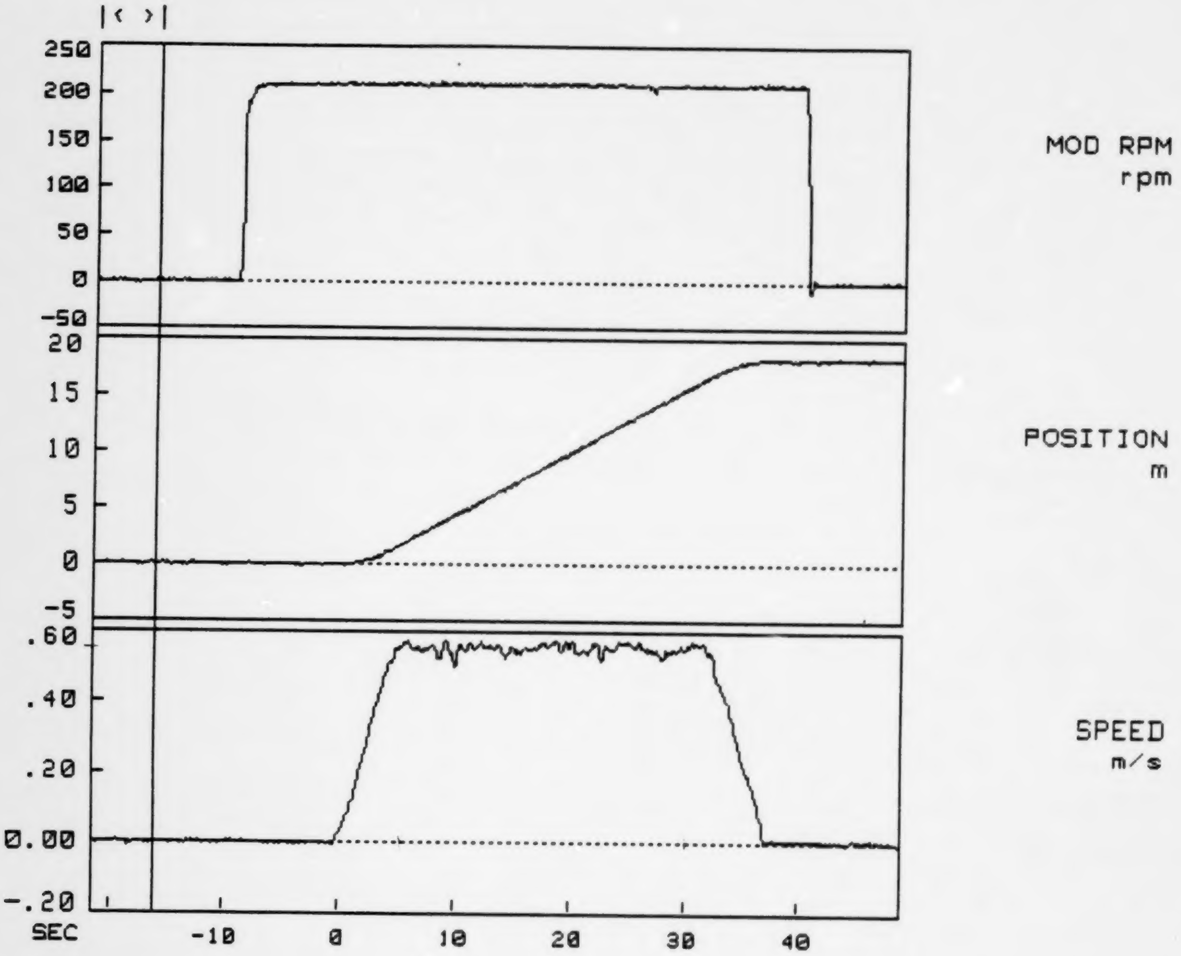

TEST 103

TEST #1 RUN 03

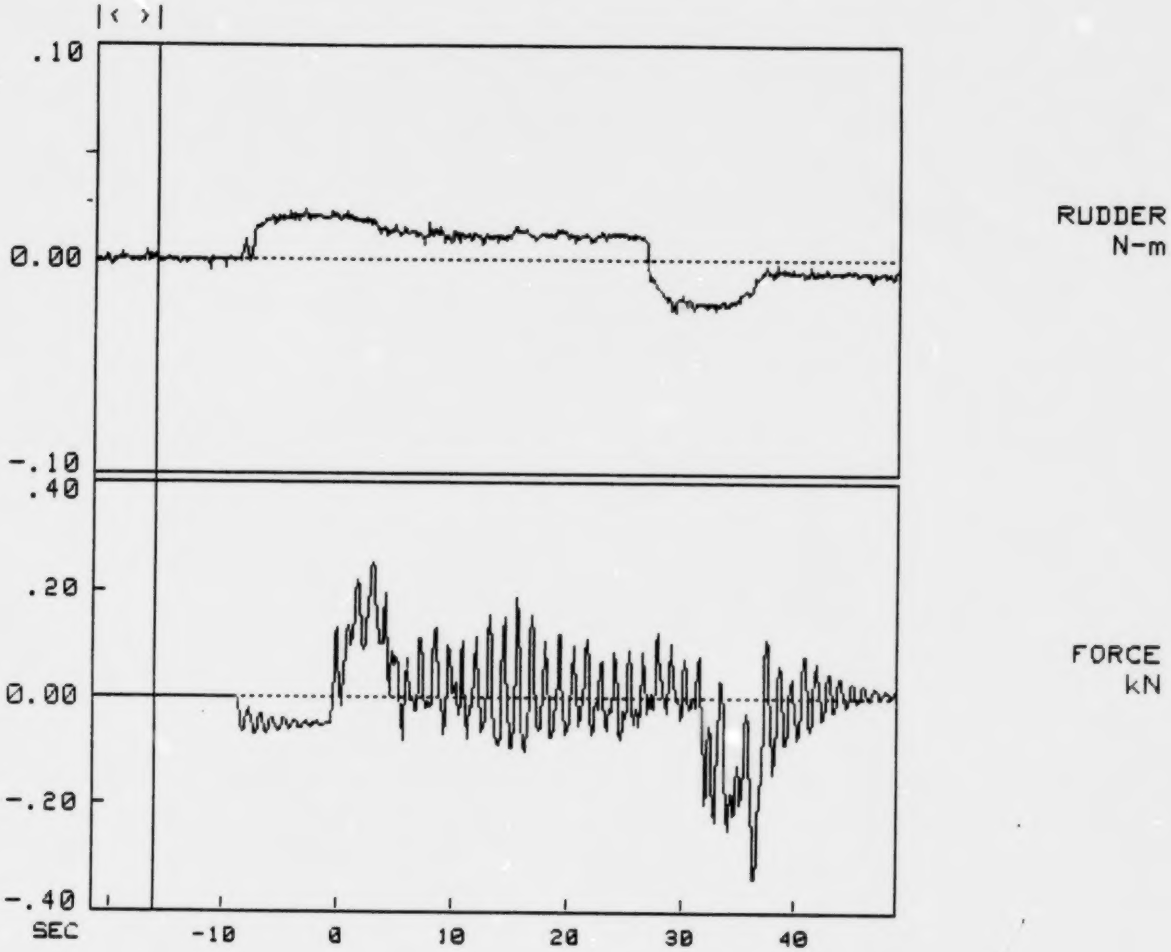

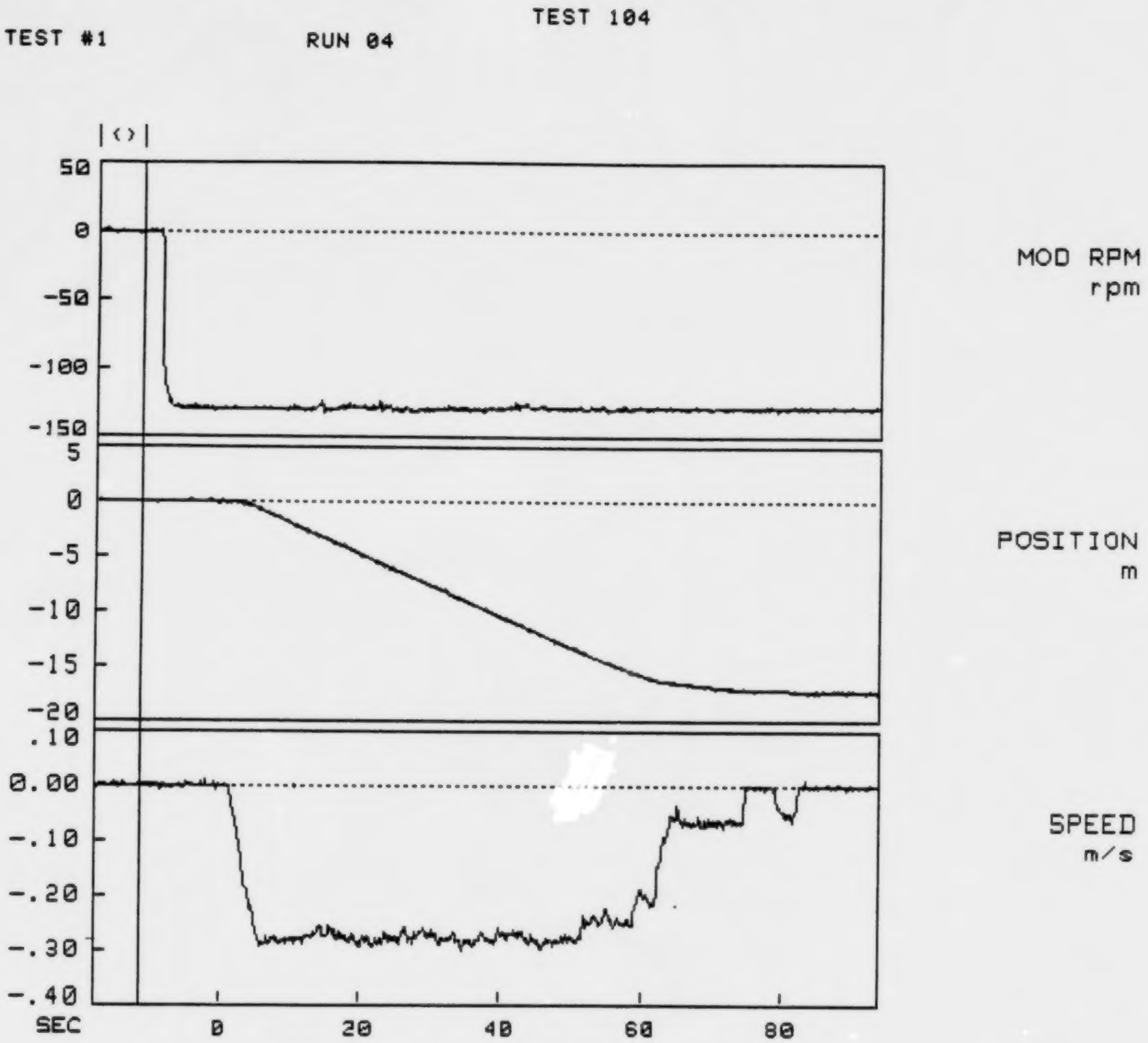
TEST #1
RUN 04
TEST 104
|<>|
50
0
-50
-100
-150
MOD RPM
rpm
5
0
-5
-10
-15
-20
POSITION
m
.10
0.00
-.10
-.20
-.30
-.40
SPEED
m/s
SEC
0
20
40
60
80

TEST #1 RUN 04 TEST 104

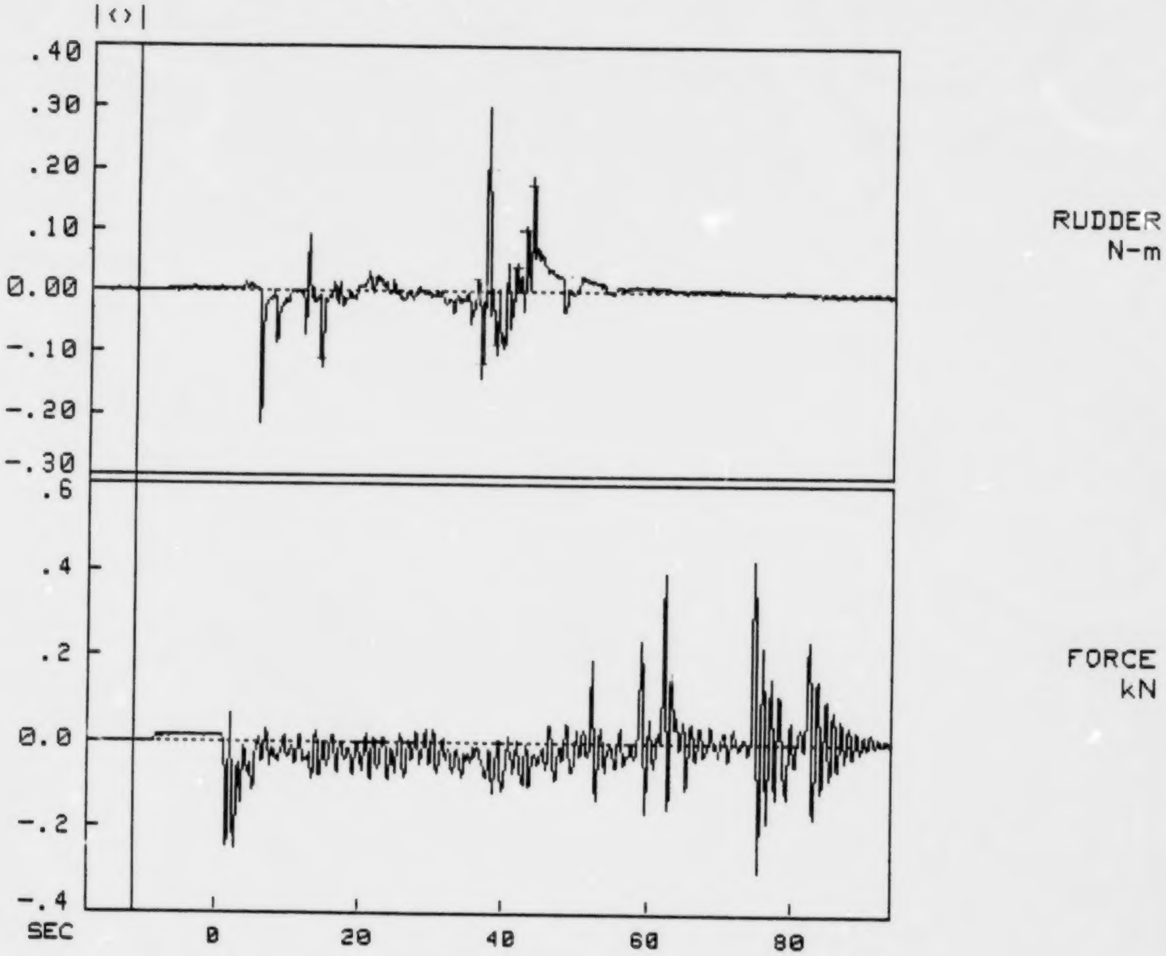

TEST #1 RUN 05 TEST 105

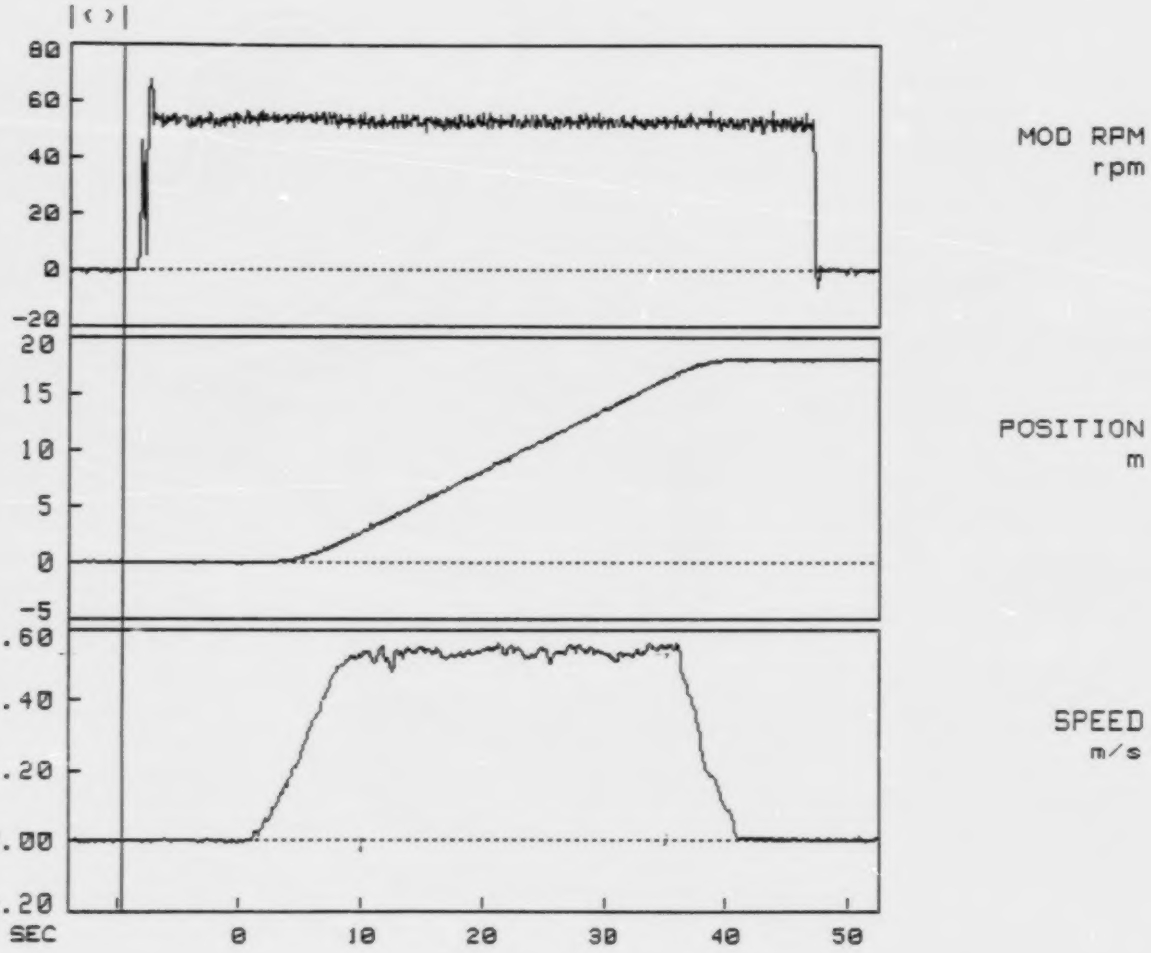

TEST #1 RUN 05 TEST 105

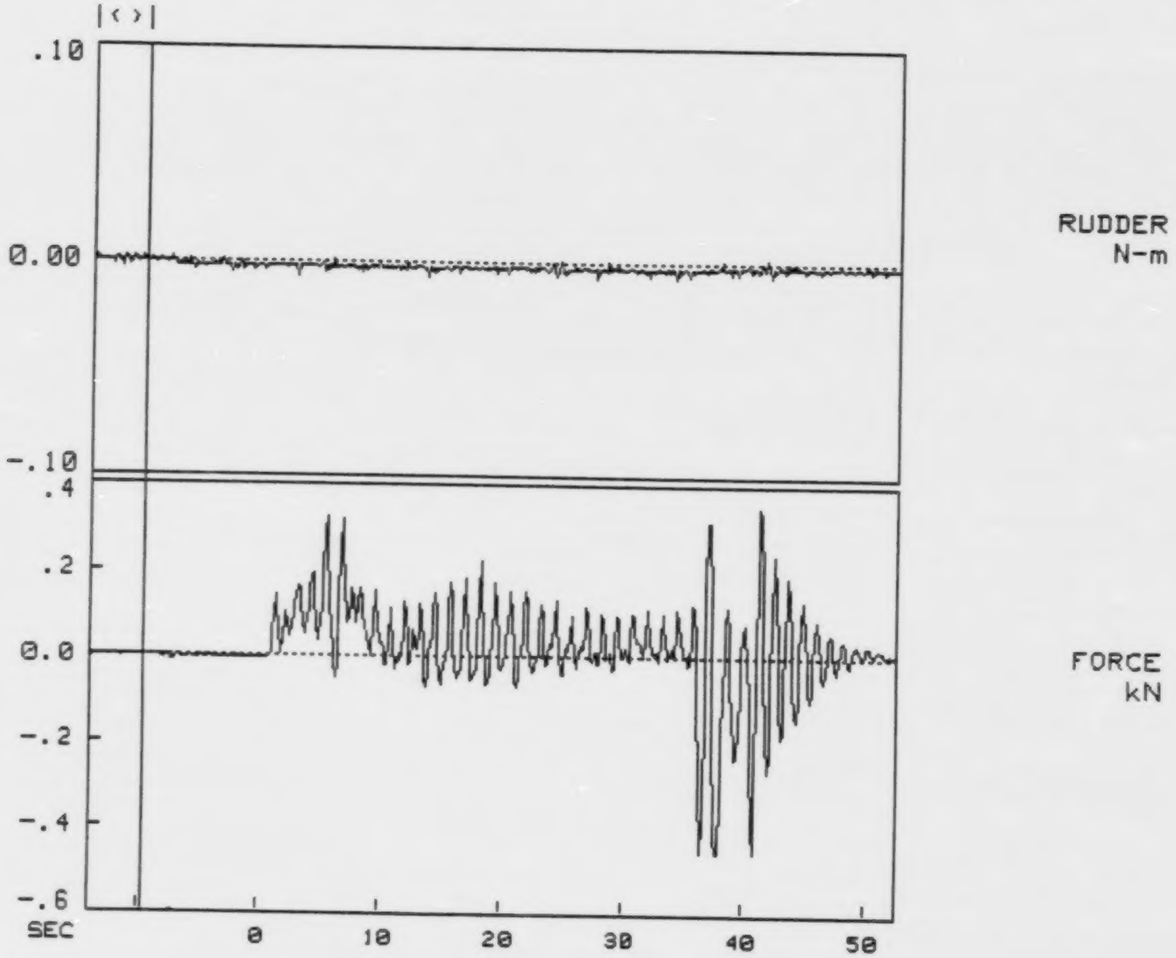

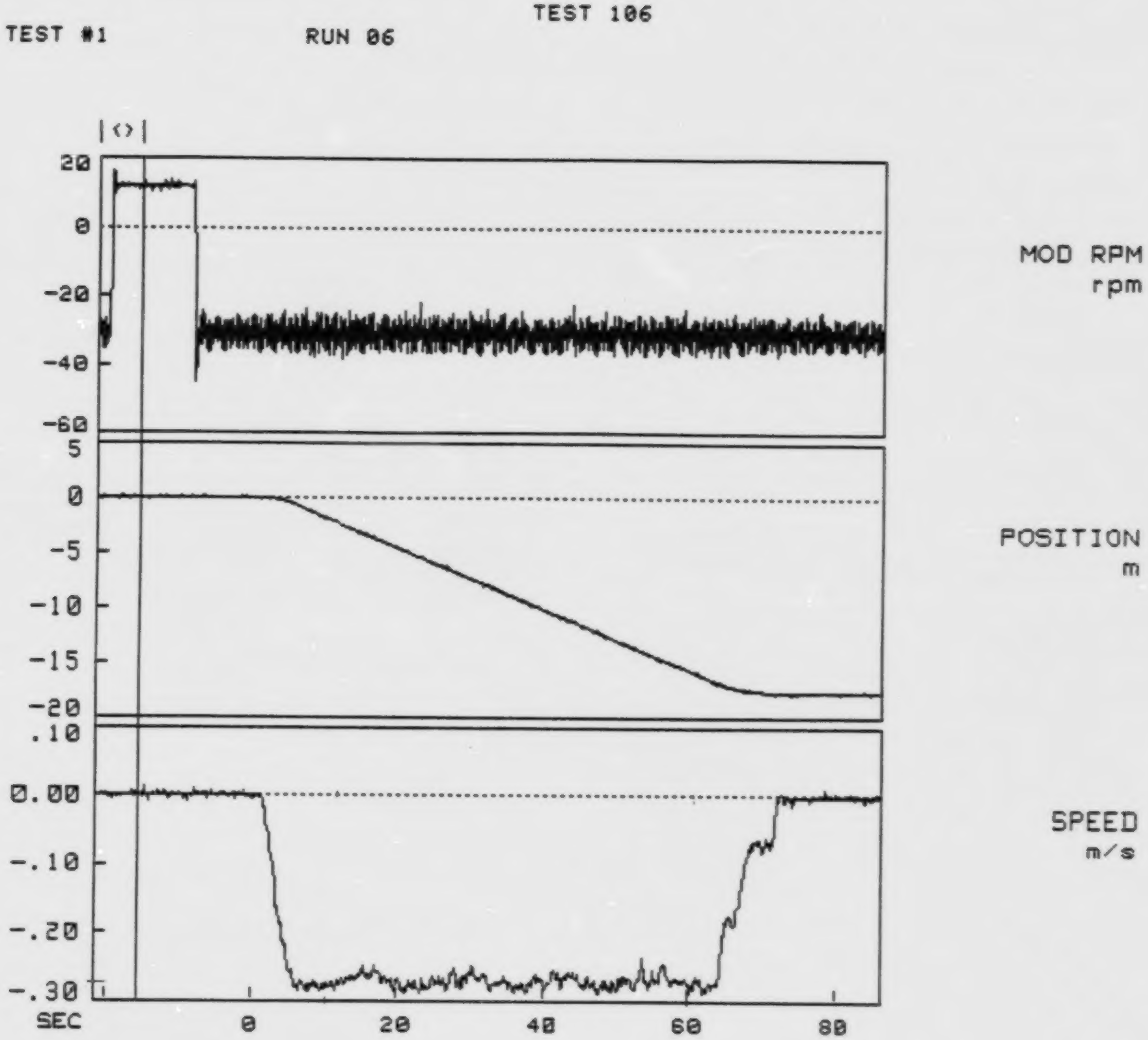

TEST 106
TEST #1
RUN 06
|<>|
20
0
-20
-40
-60
MOD RPM
rpm
5
0
-5
-10
-15
-20
POSITION
m
.10
0.00
-.10
-.20
-.30
SPEED
m/s
SEC
0
20
40
60
80

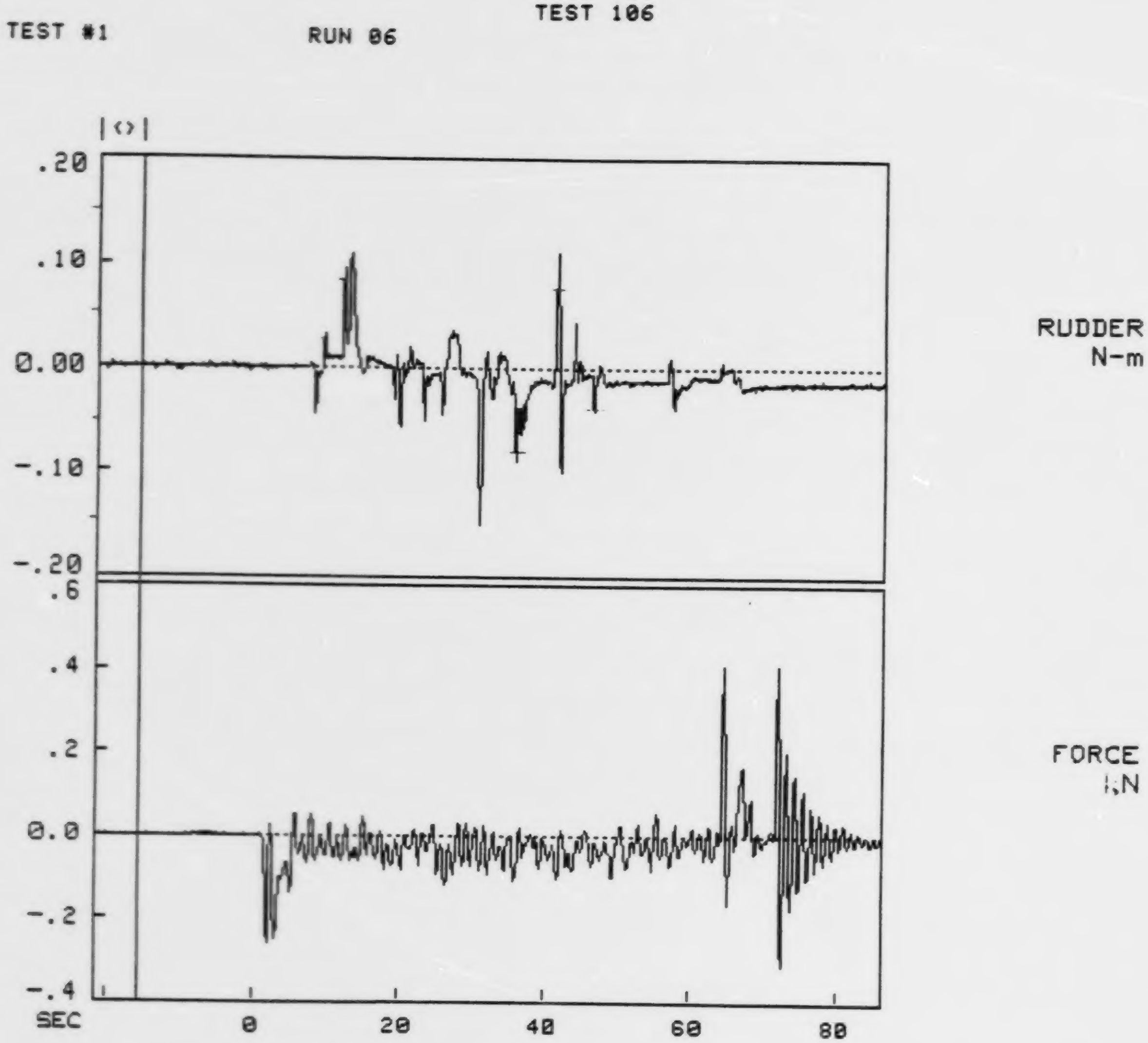
TEST #1
RUN 06
TEST 106
|<>|
.20
.10
0.00
-.10
-.20
RUDDER
N-m
.6
.4
.2
0.0
-.2
-.4
FORCE
kN
SEC
0
20
40
60
80

TEST 107

TEST #1 RUN 07

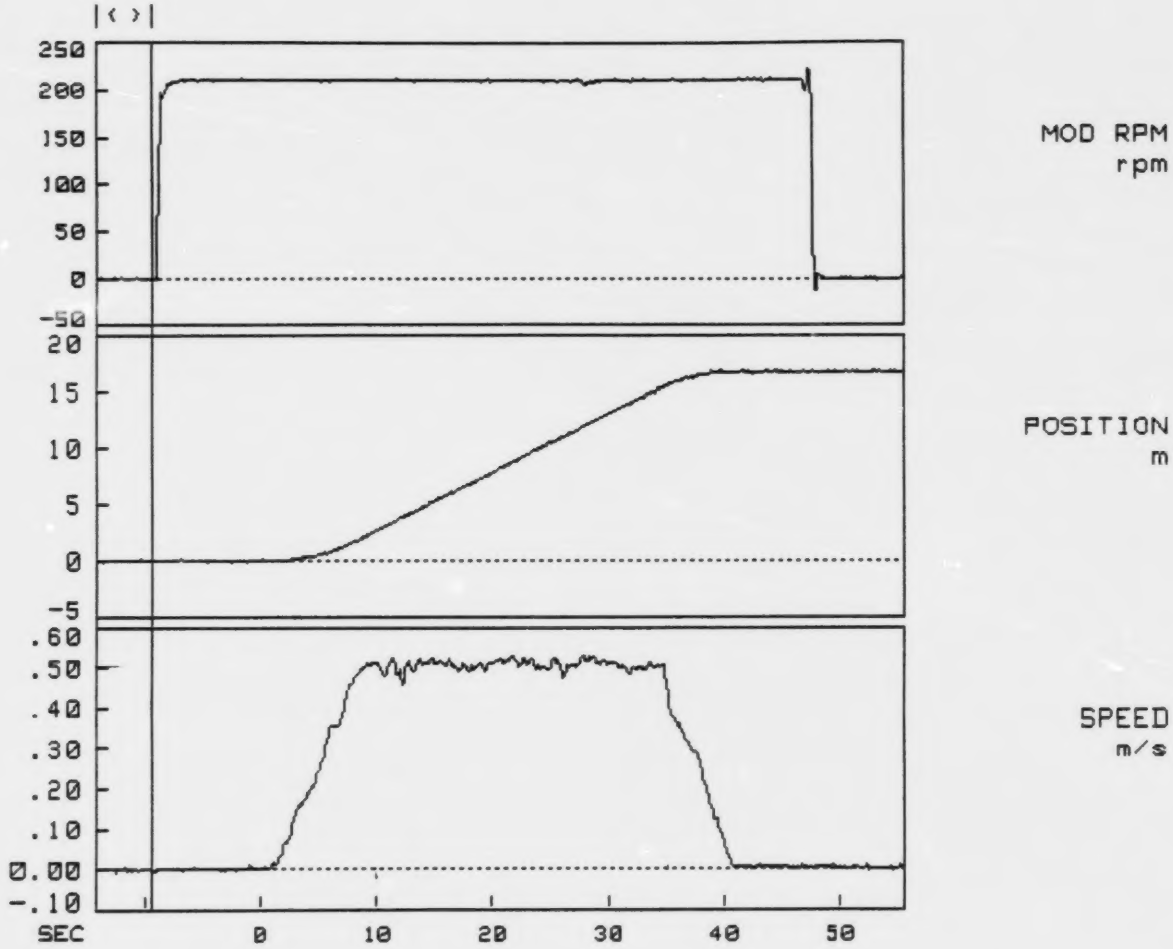

TEST #1 RUN 07 TEST 107

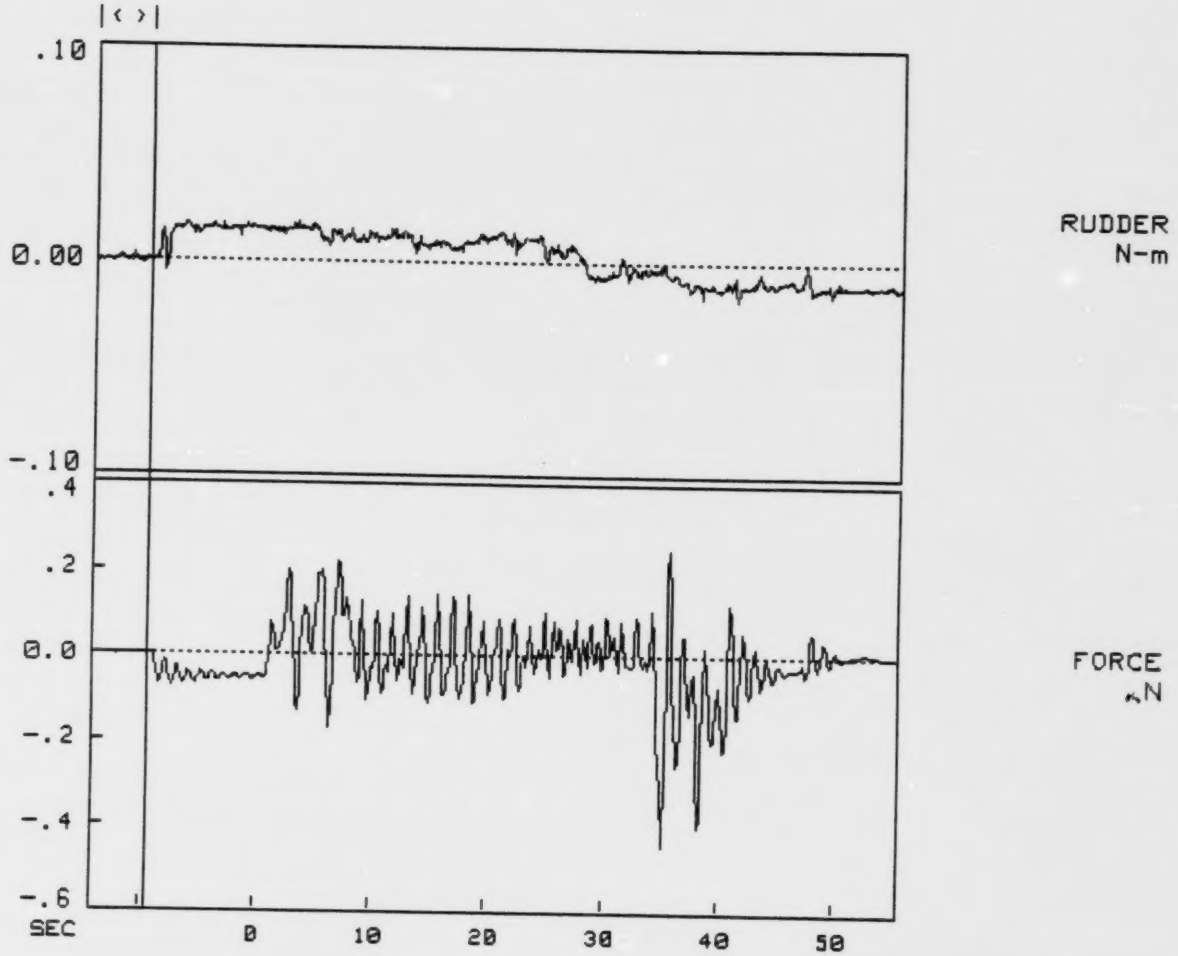

TEST 108

TEST #1 RUN 08

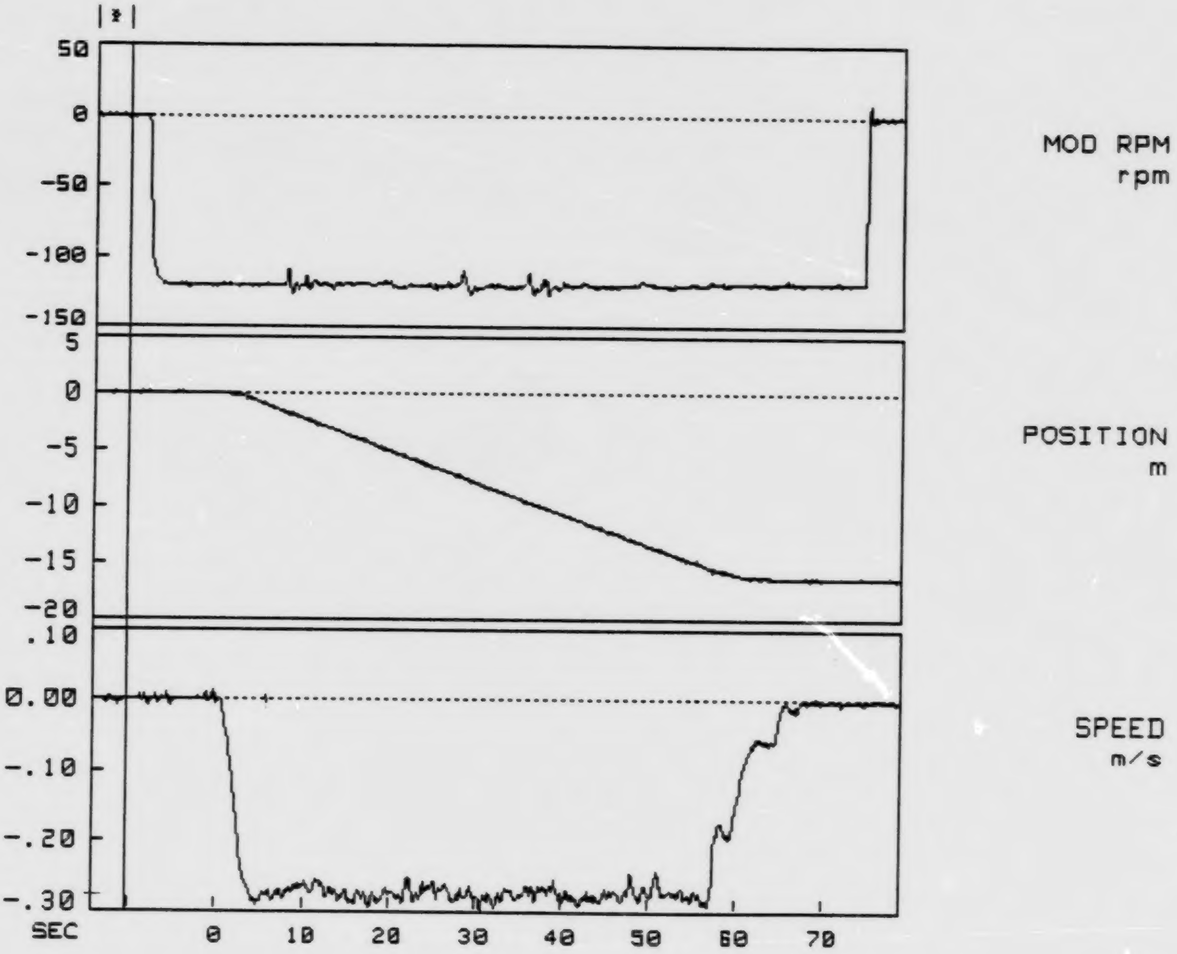

TEST #1 RUN 08 TEST 108

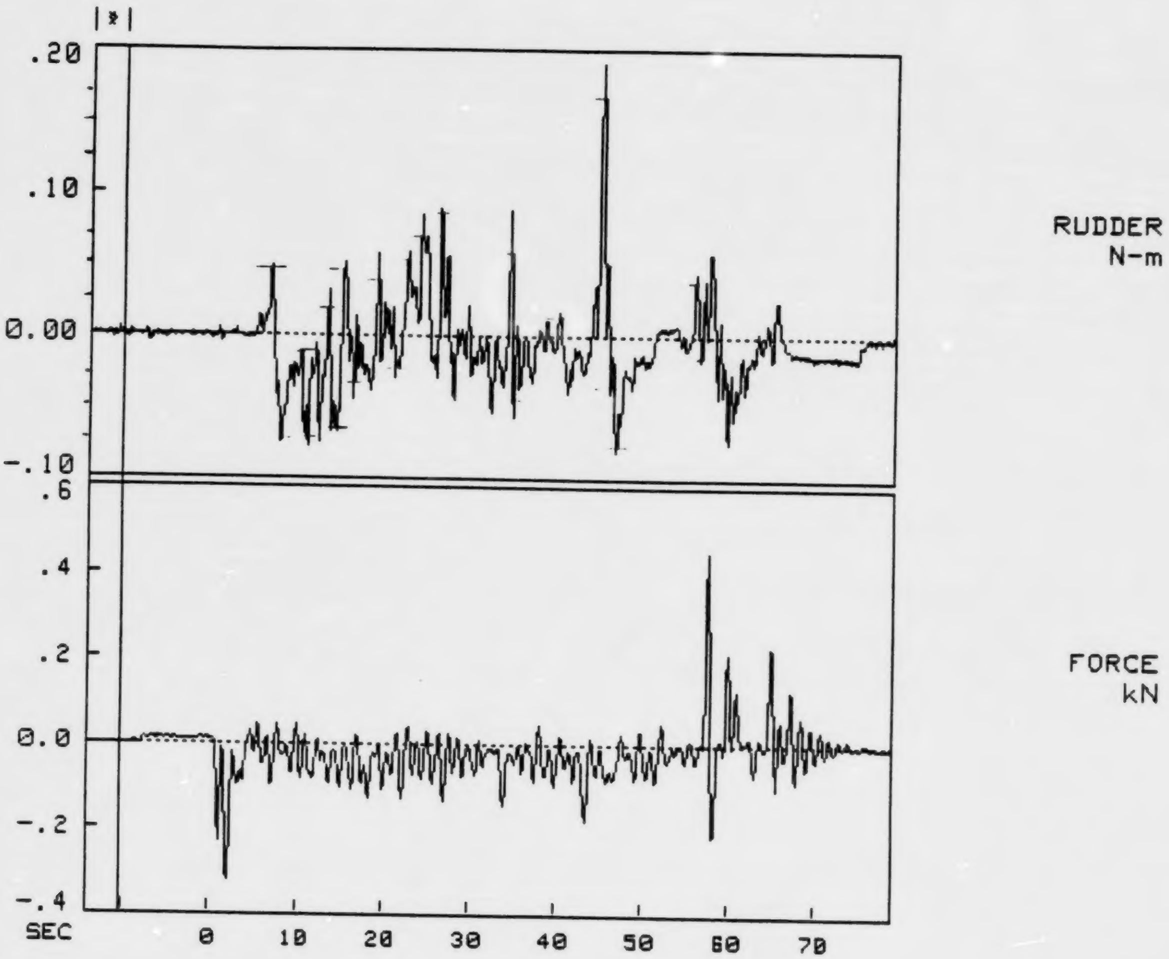

TEST 109

TEST #1 RUN 09

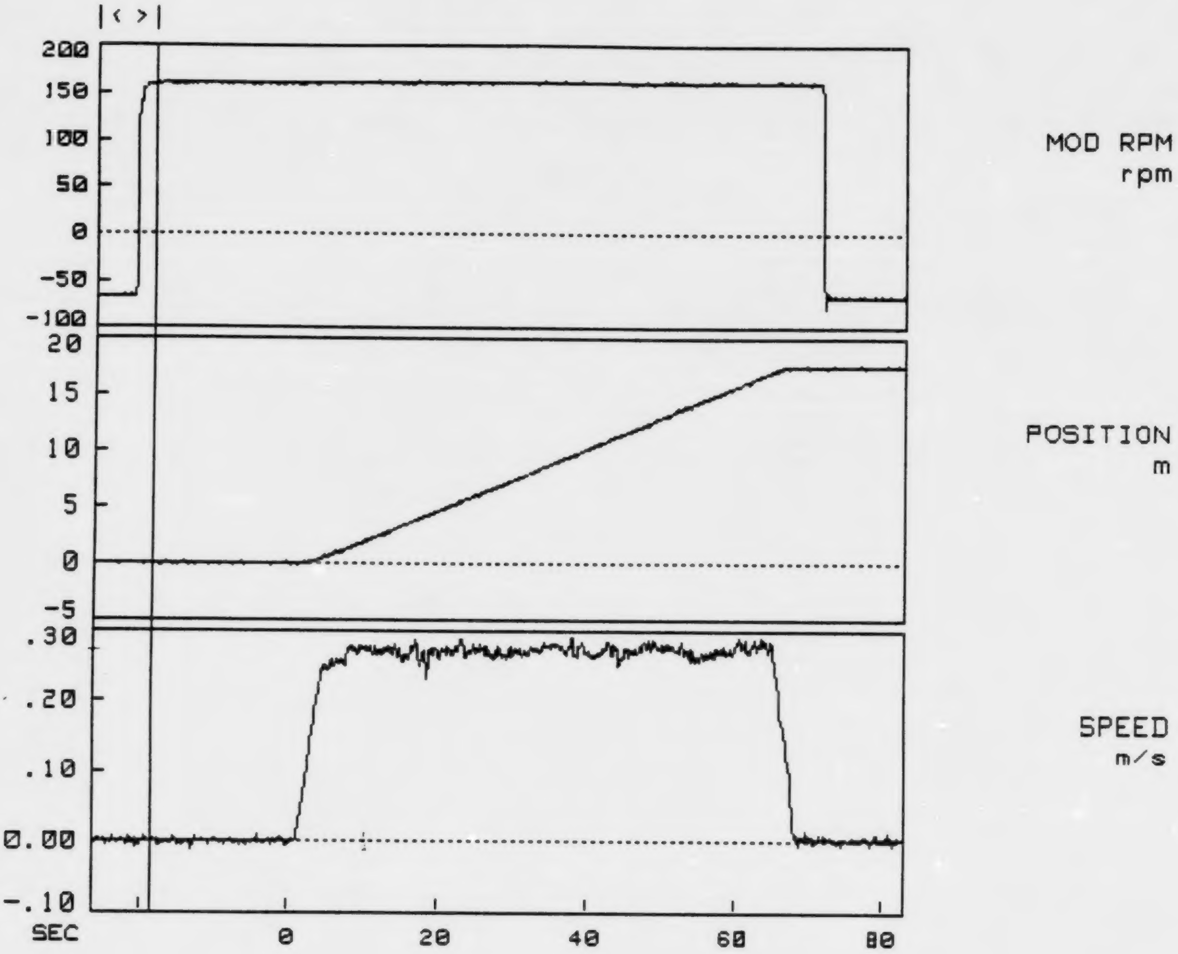

TEST #1 RUN 09 TEST 109

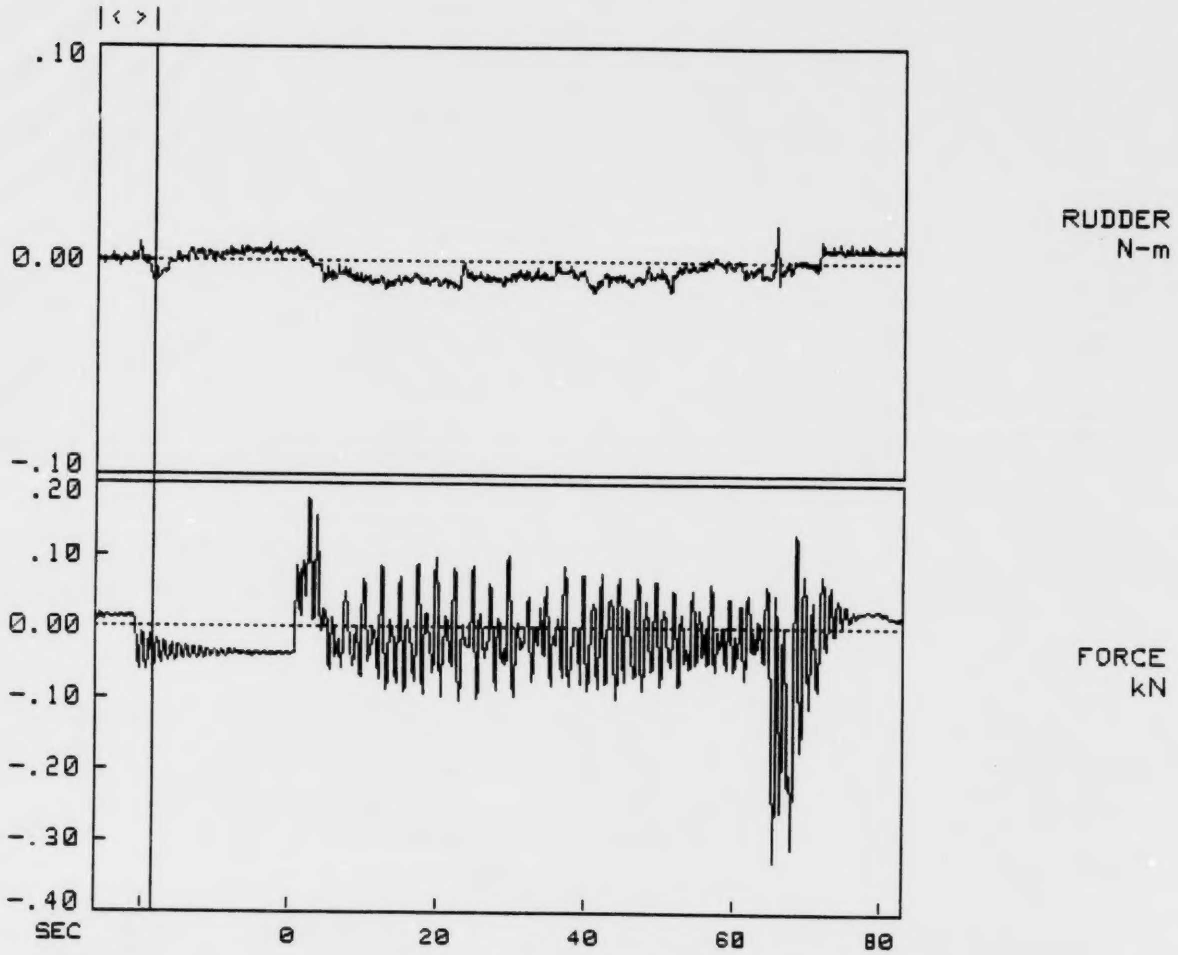

TEST 110

TEST #1 RUN 10

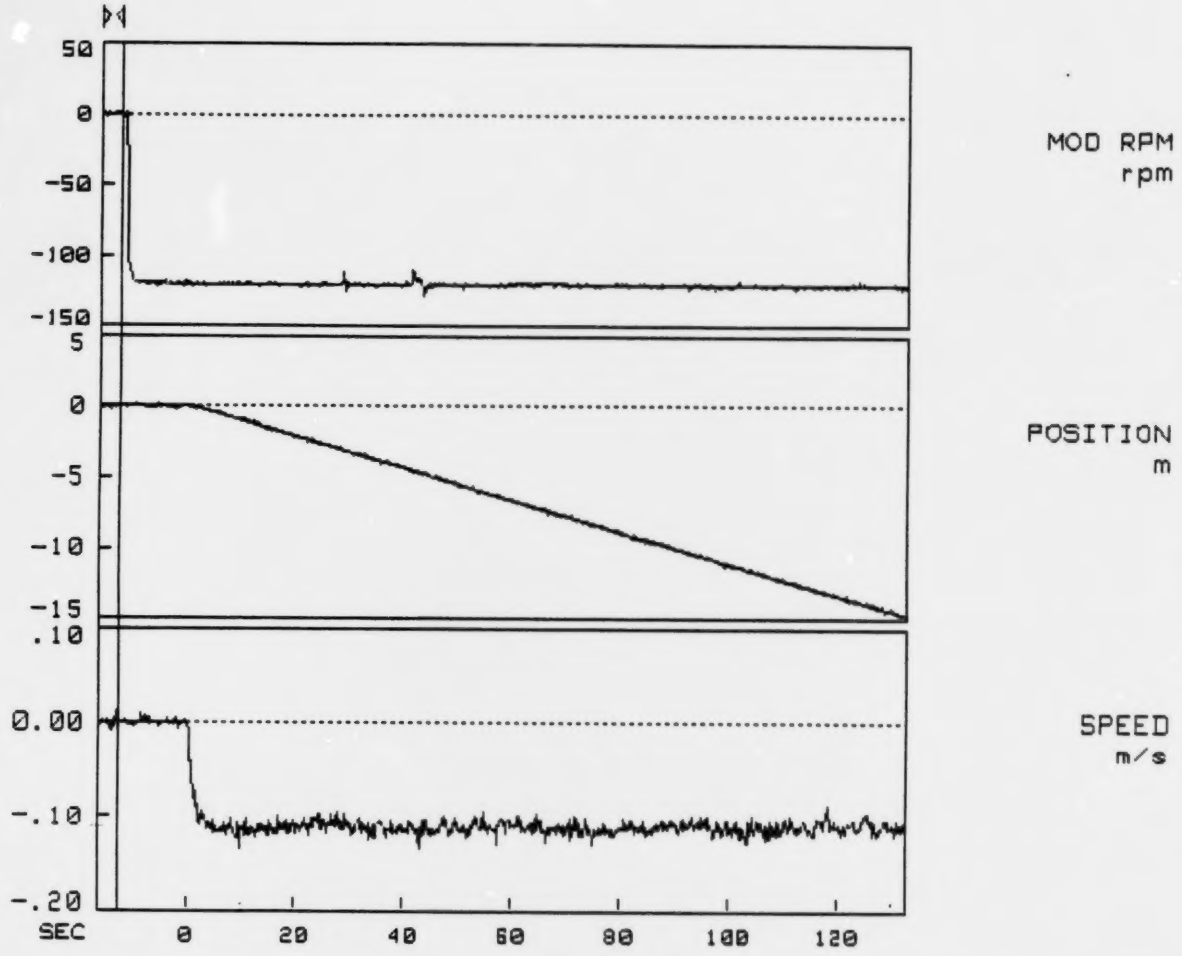

TEST #1 RUN 10 TEST 110

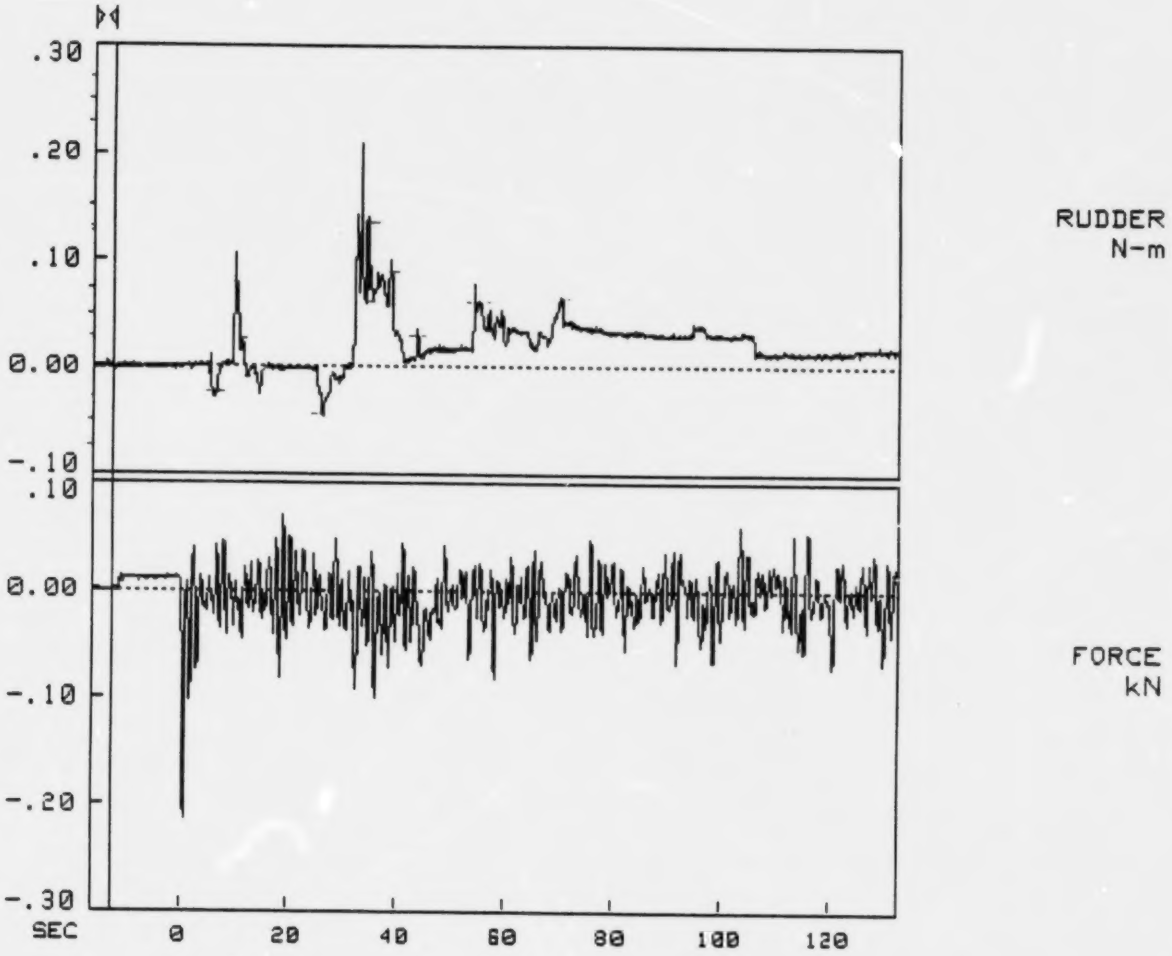

TEST #1 RUN 11 TEST 111

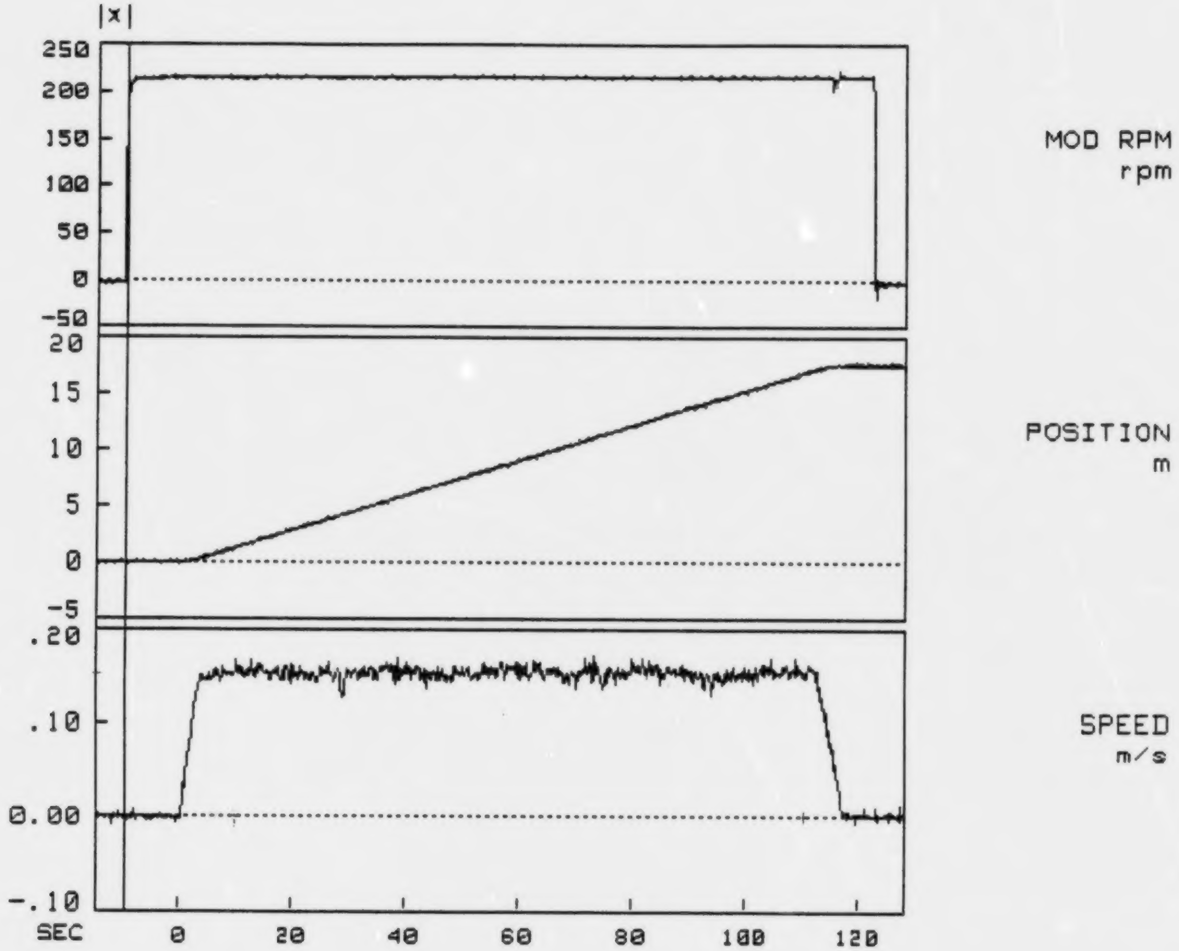

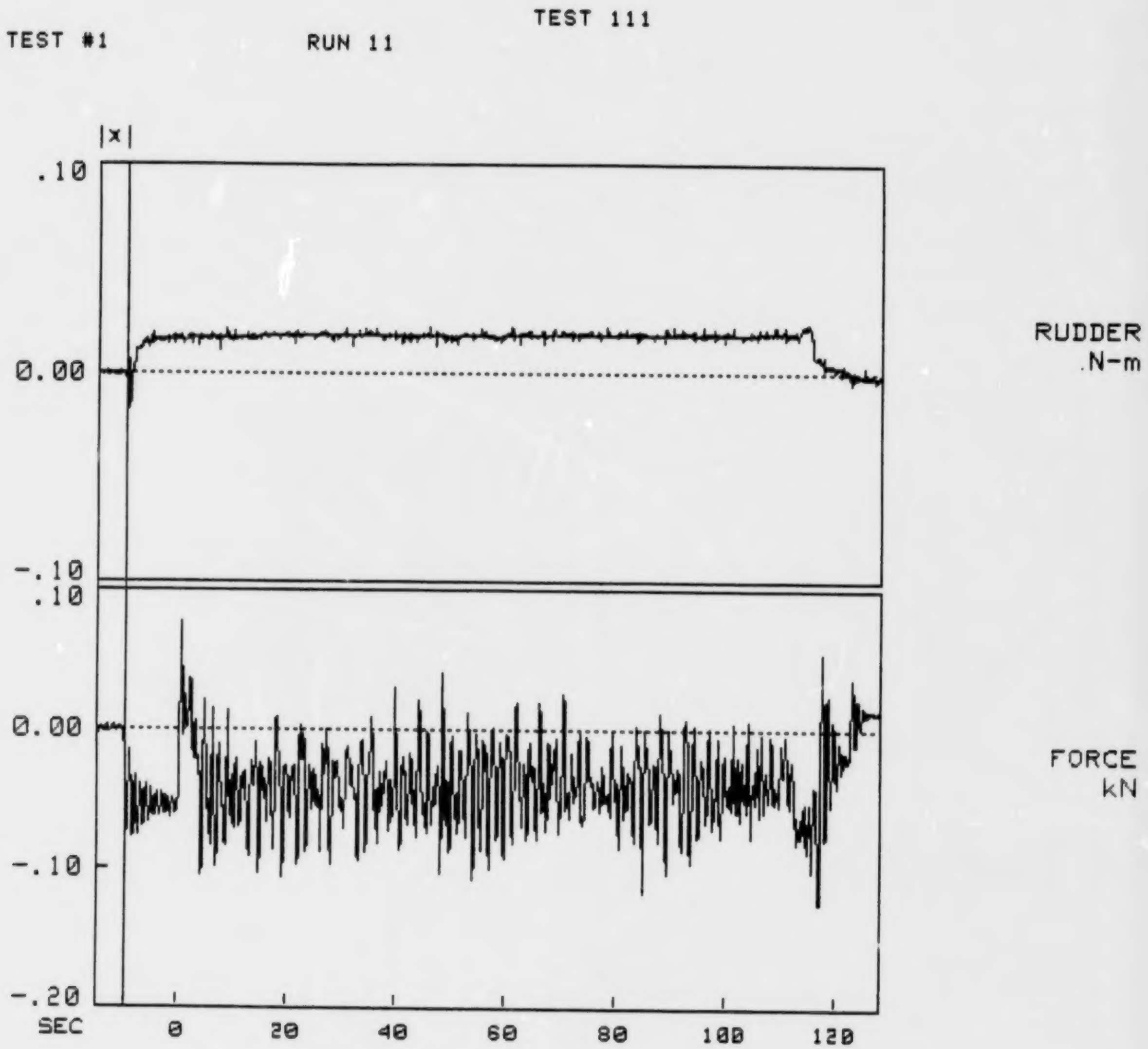
TEST 111
TEST #1
RUN 11
|x|
.10
0.00
-.10
.10
0.00
-.10
-.20
SEC
0
20
40
60
80
100
120
RUDDER
N-m
FORCE
kN

TEST 112

TEST #1 RUN 12

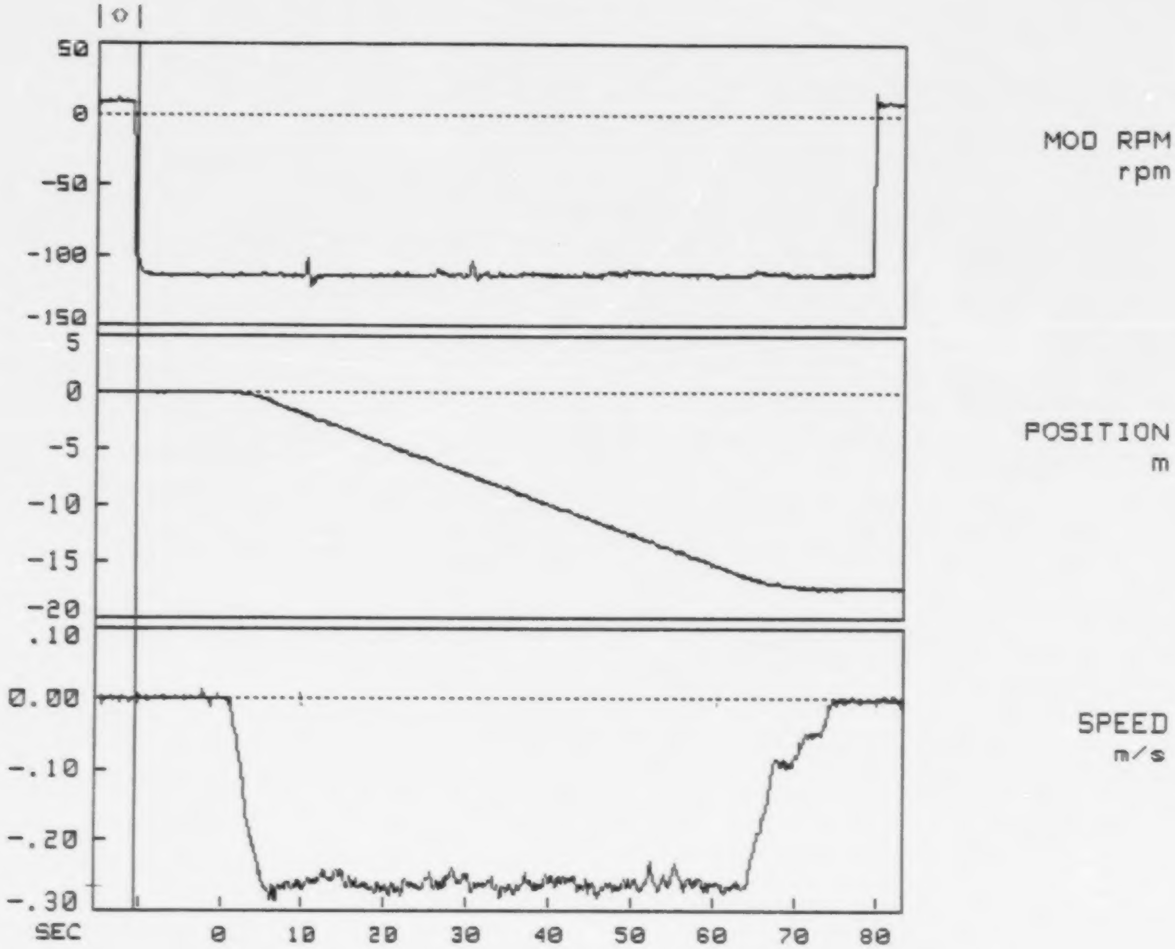

TEST #1 RUN 12 TEST 112

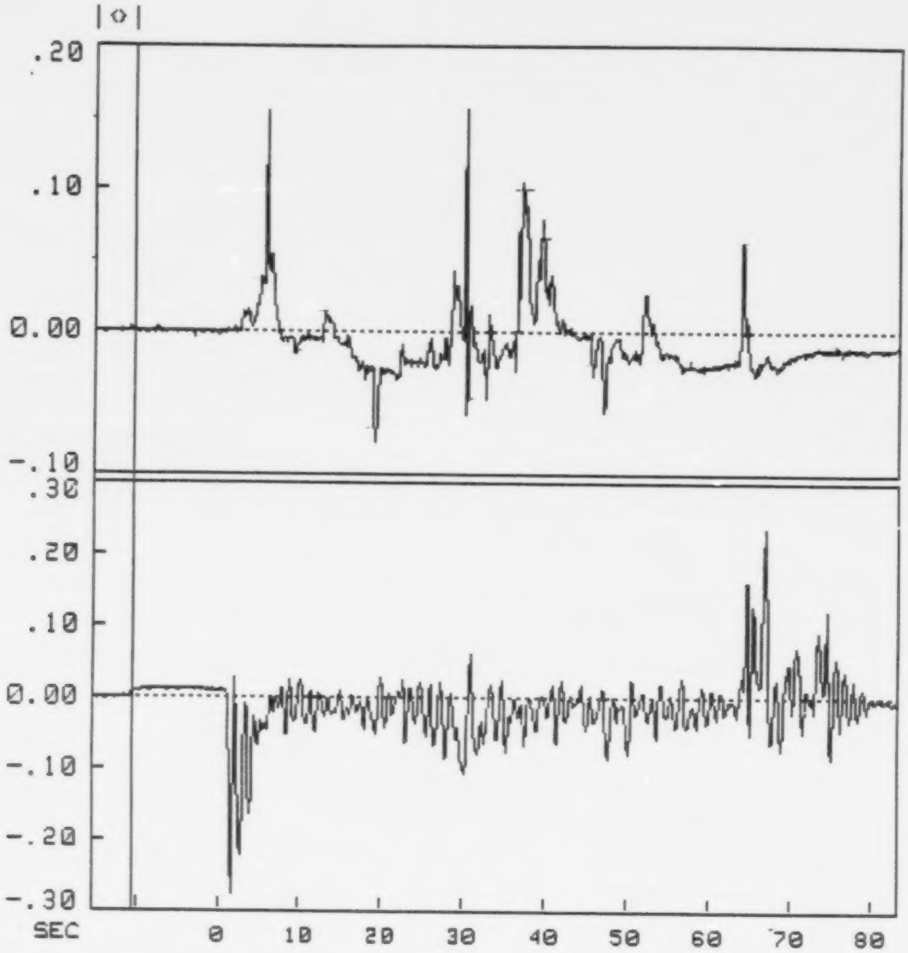

RUDDER
N-m

FORCE
kN

TEST #1 RUN 13 TEST 113

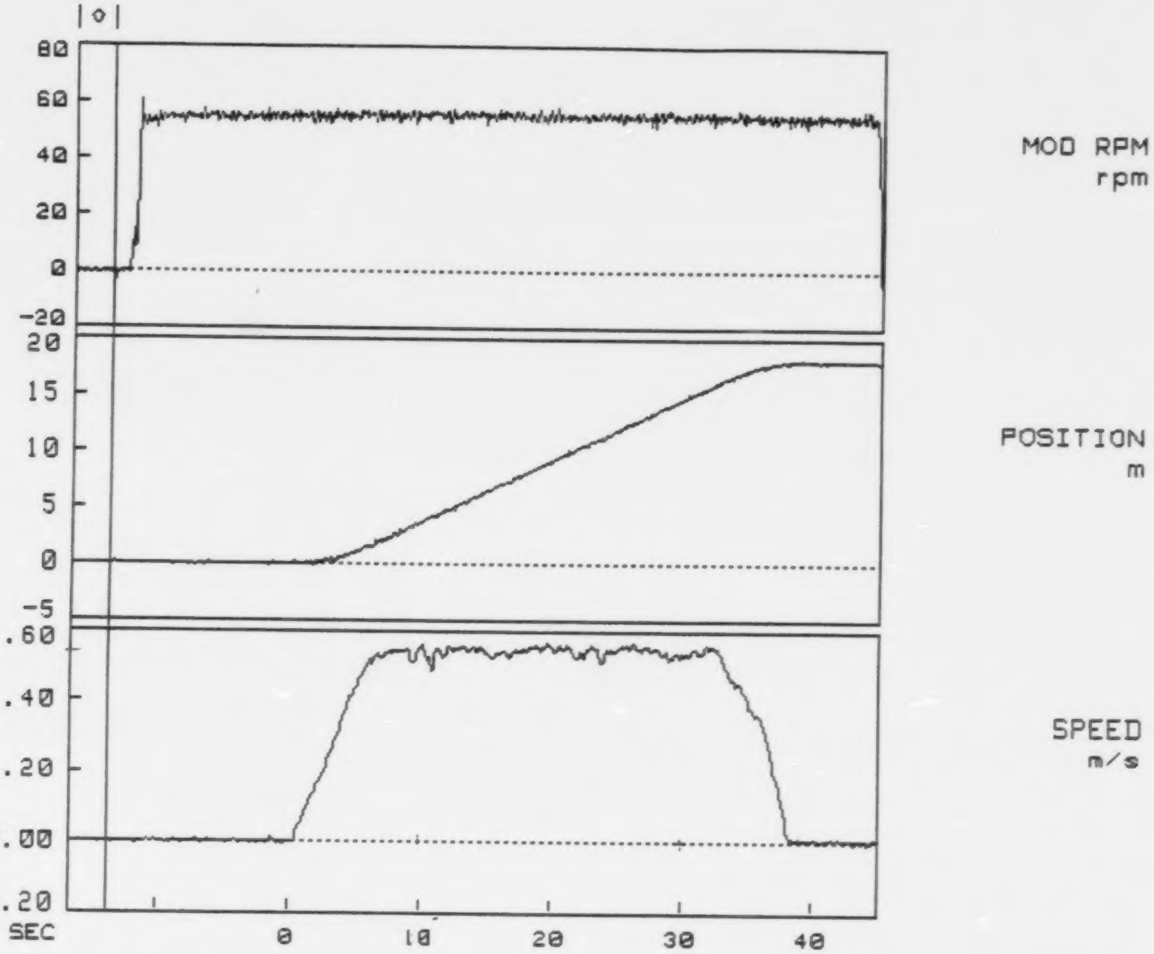

TEST #1 RUN 13 TEST 113

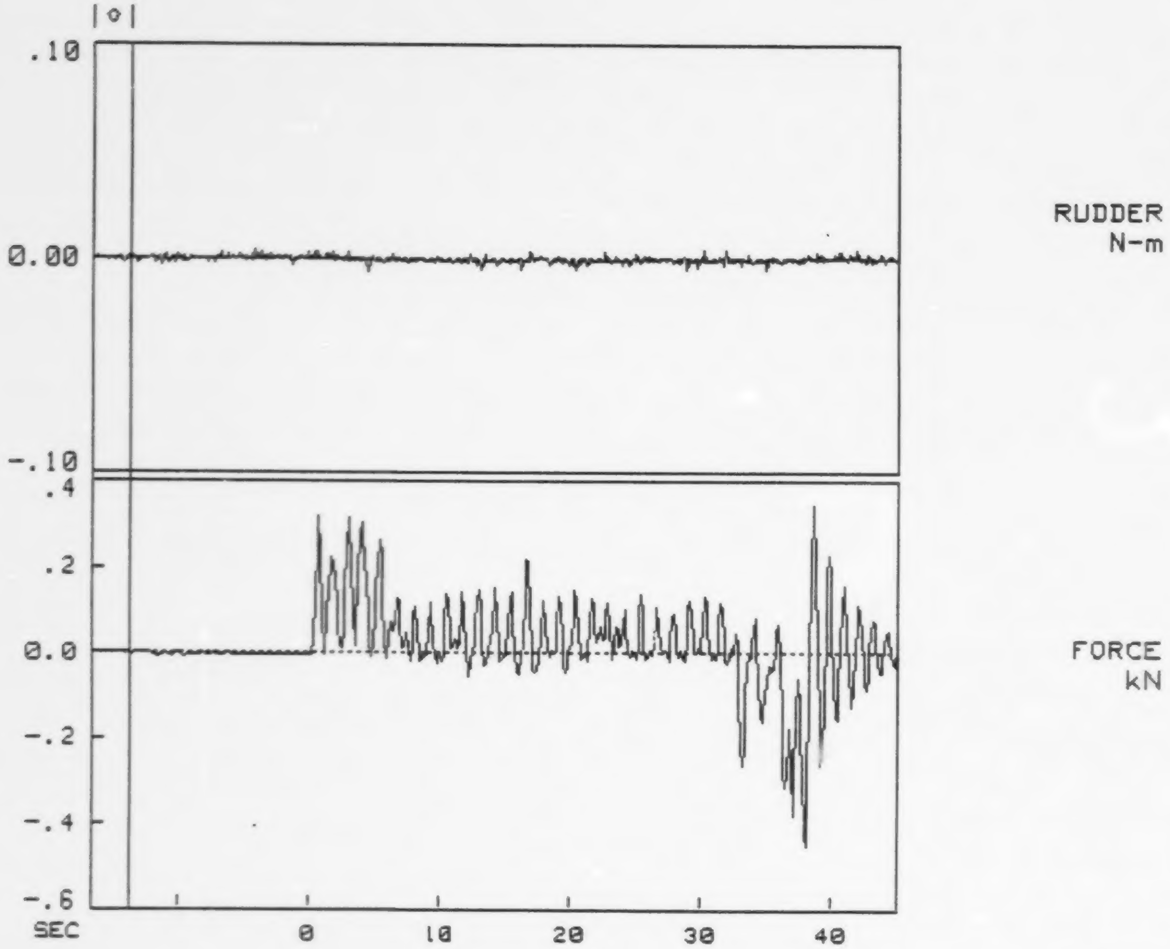

TEST #1 RUN 14 TEST 114

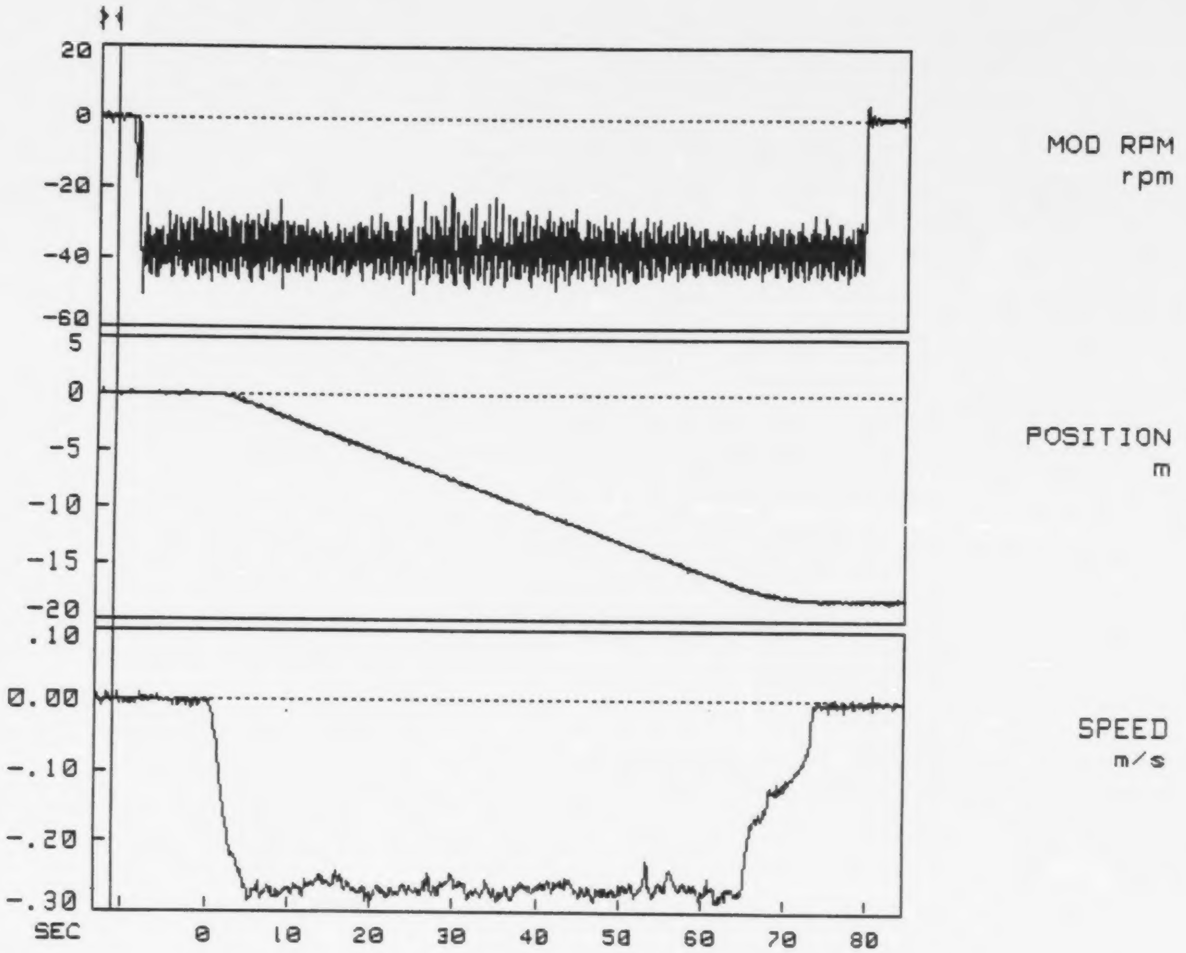

TEST #1 RUN 14 TEST 114

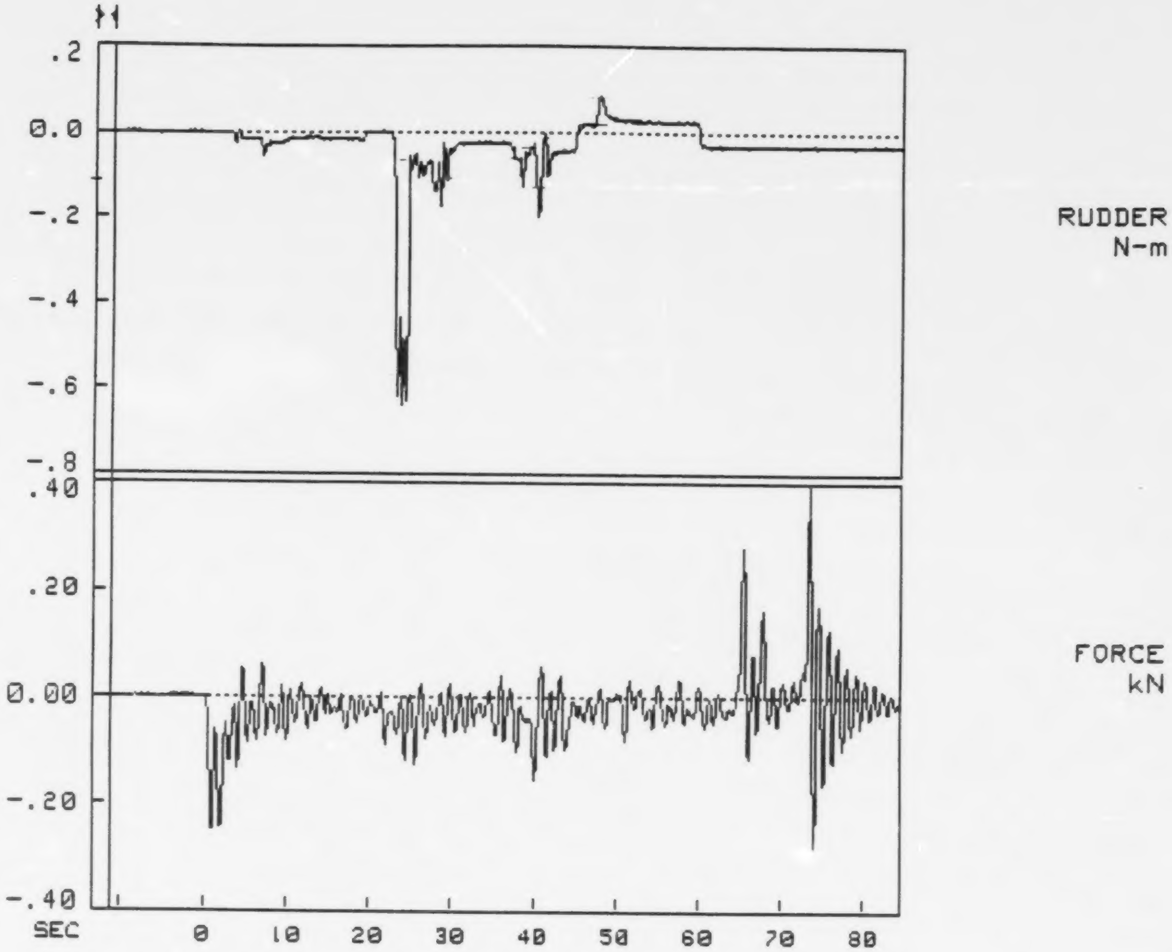

TEST #1 RUN 15 TEST 115

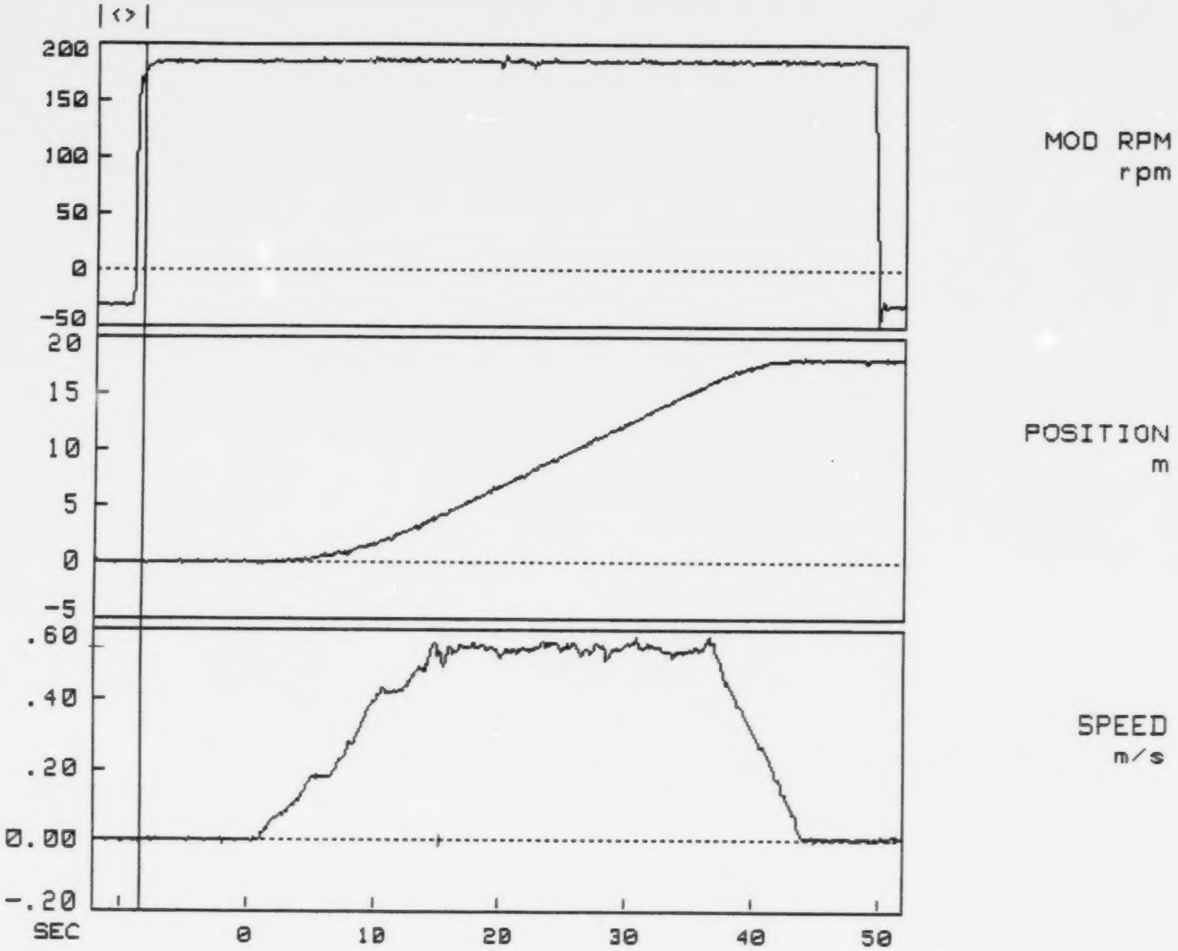

TEST #1 RUN 15 TEST 115

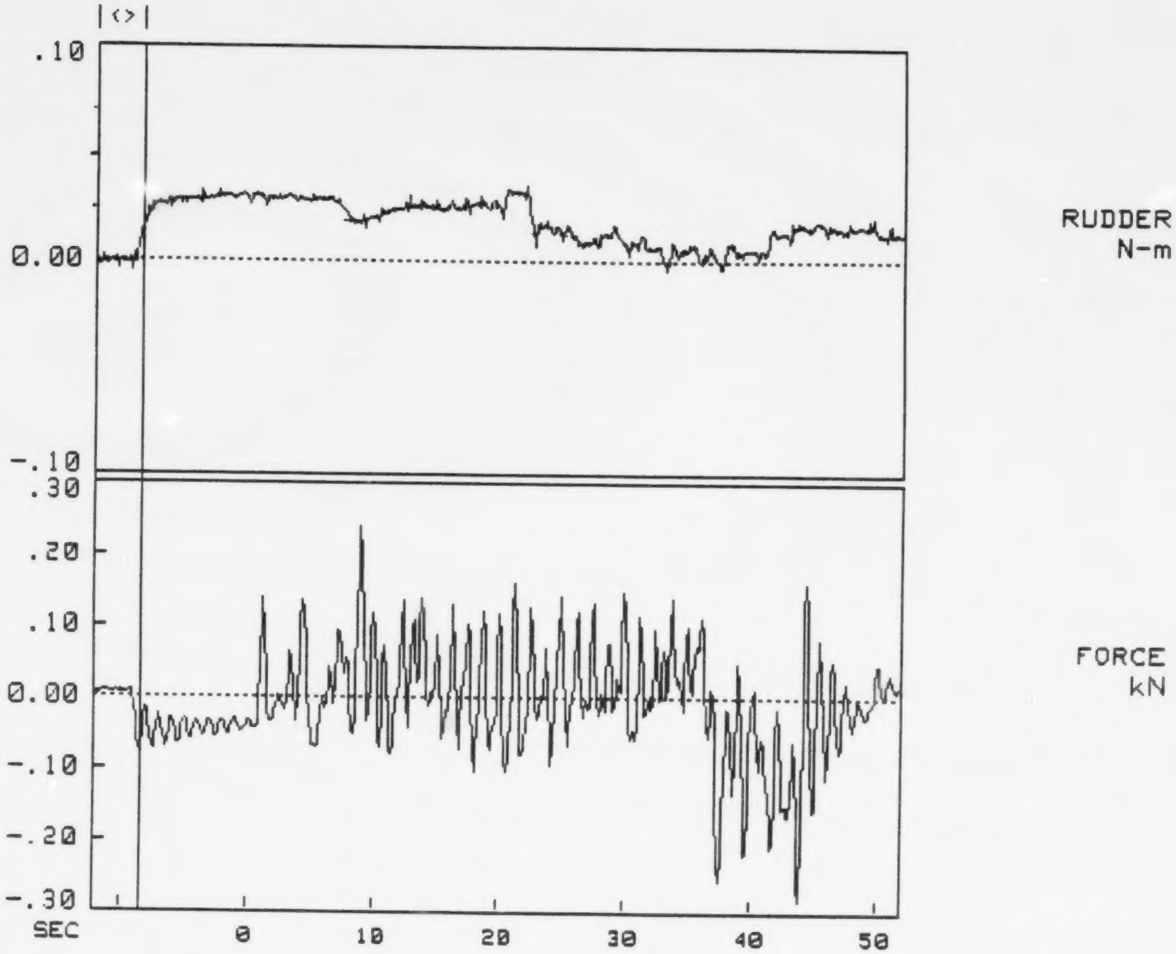

TEST #1 RUN 16 TEST 116

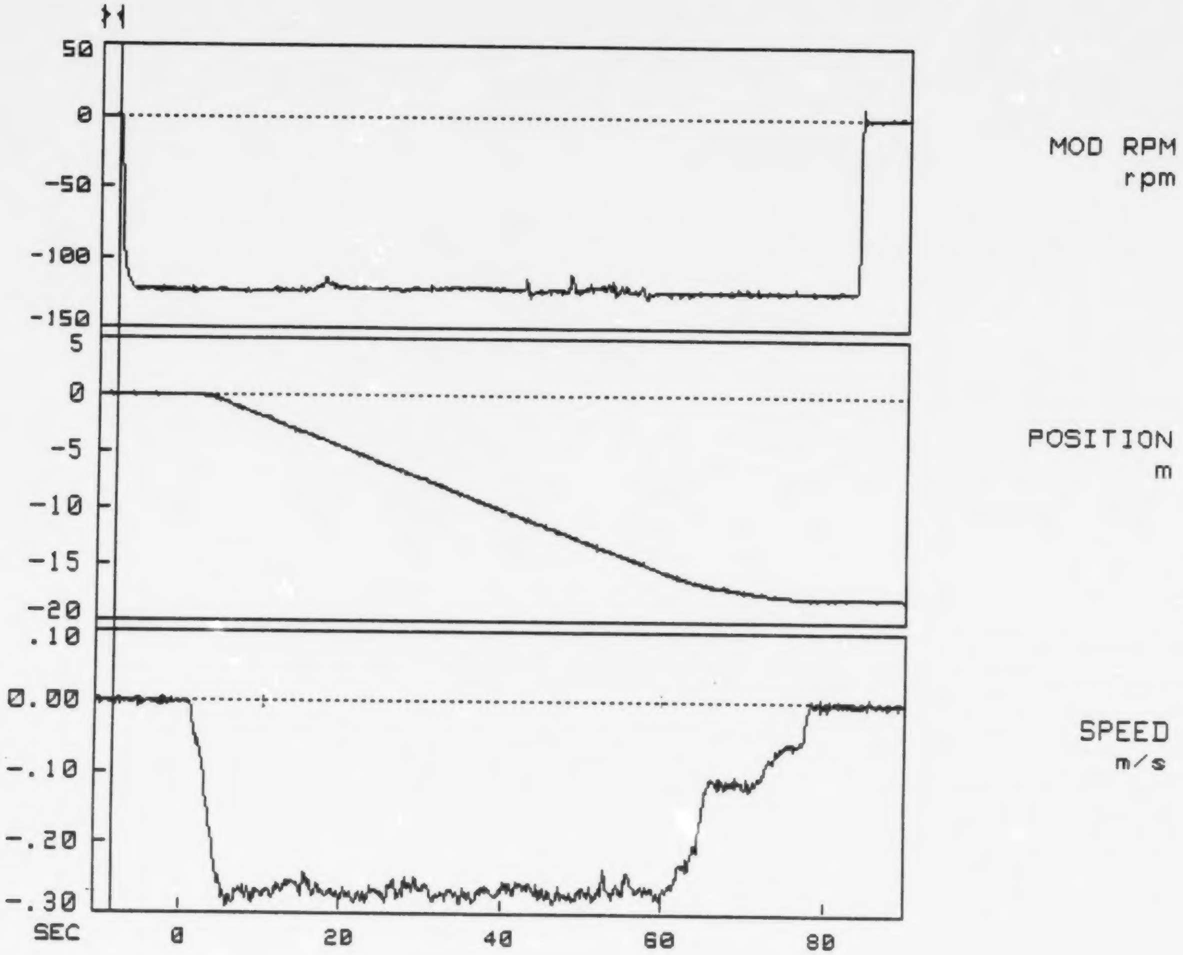

TEST 116

TEST #1 RUN 16

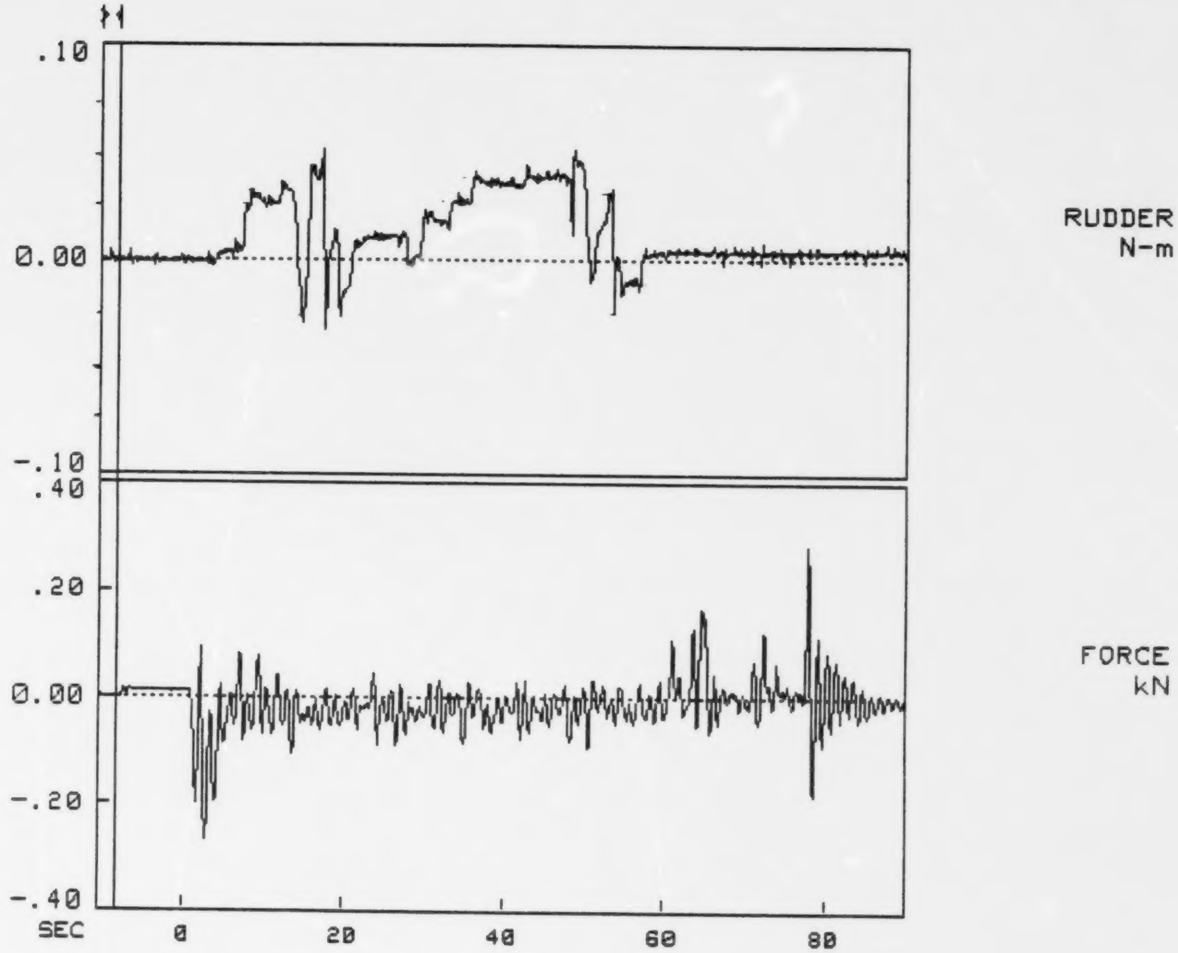

TEST #1 RUN 17 TEST 117

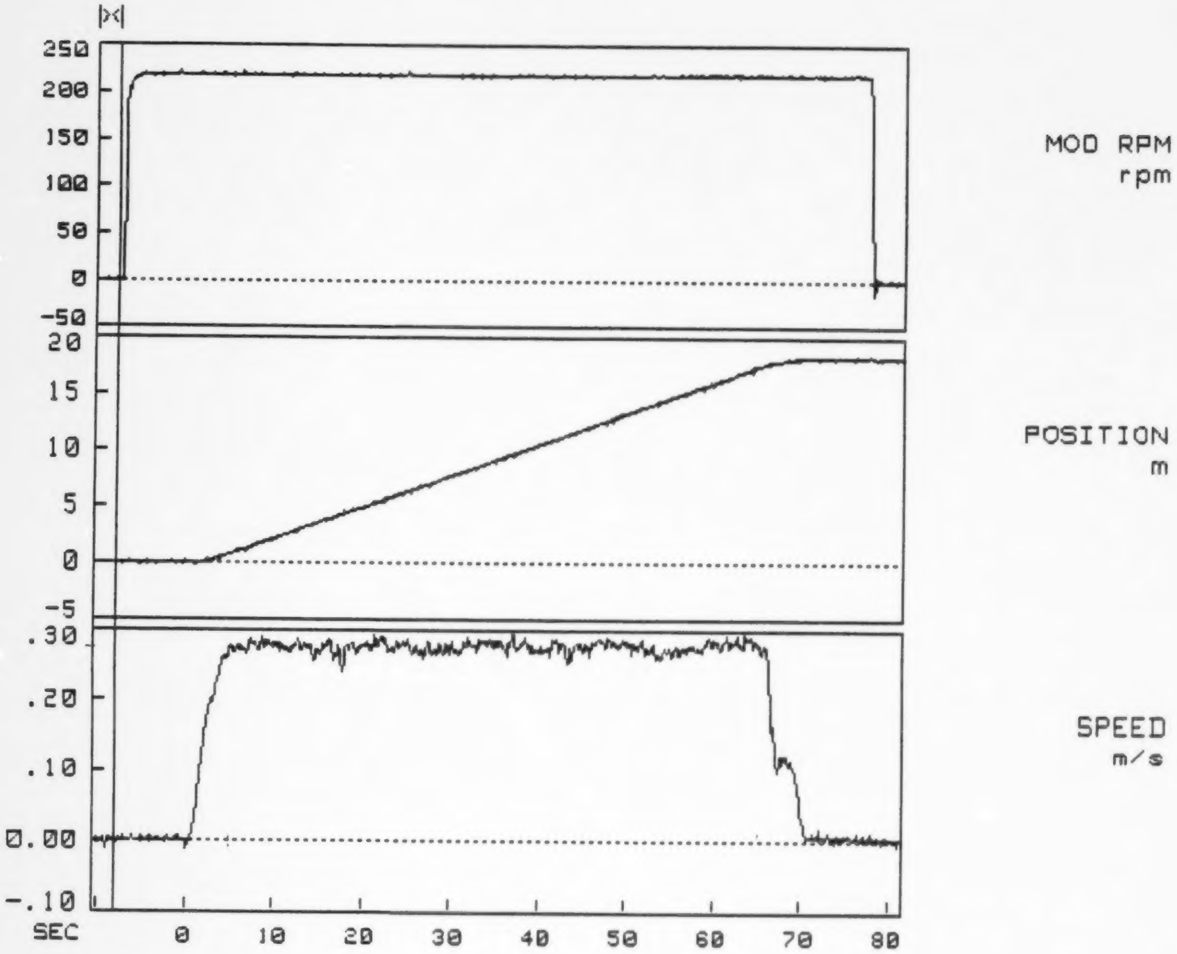

TEST 117

TEST #1 RUN 17

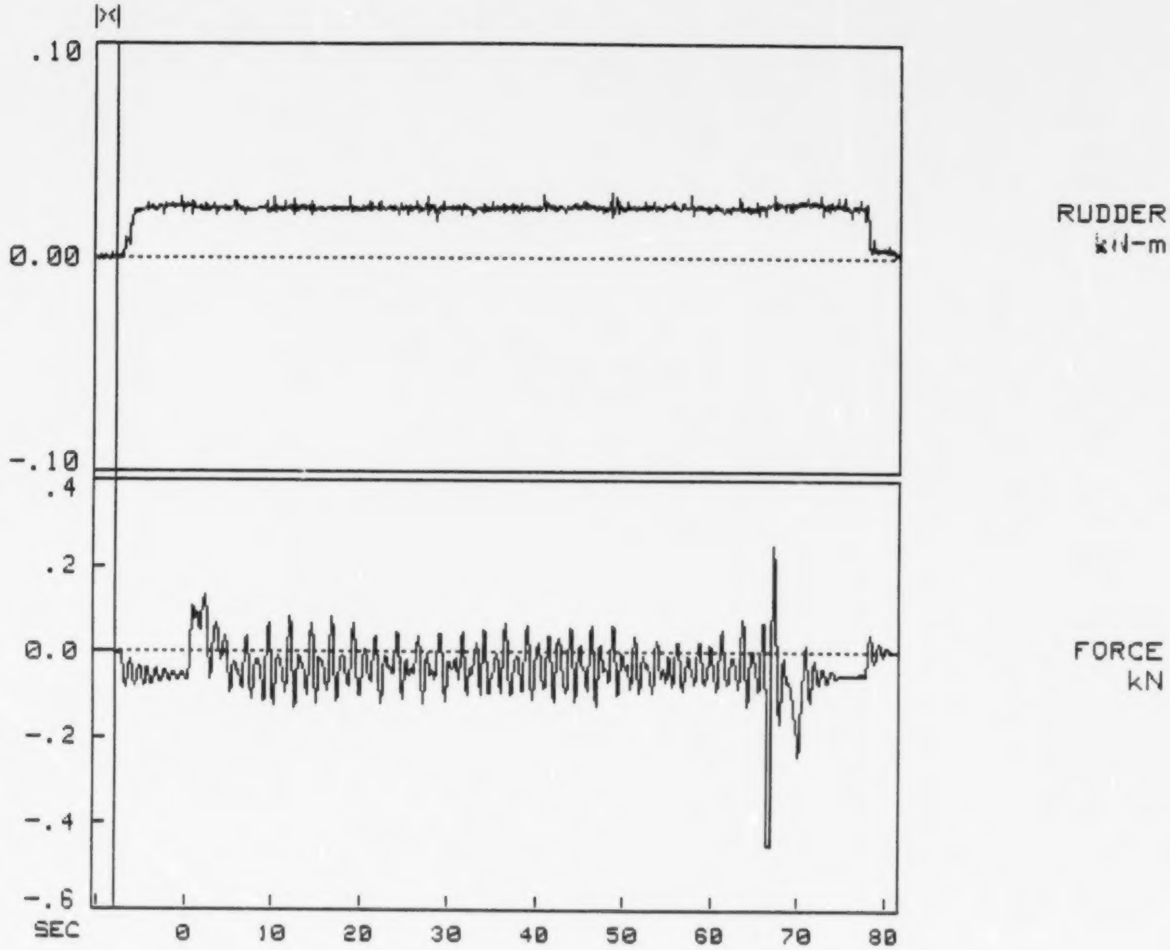

TEST #1 RUN 18 TEST 118

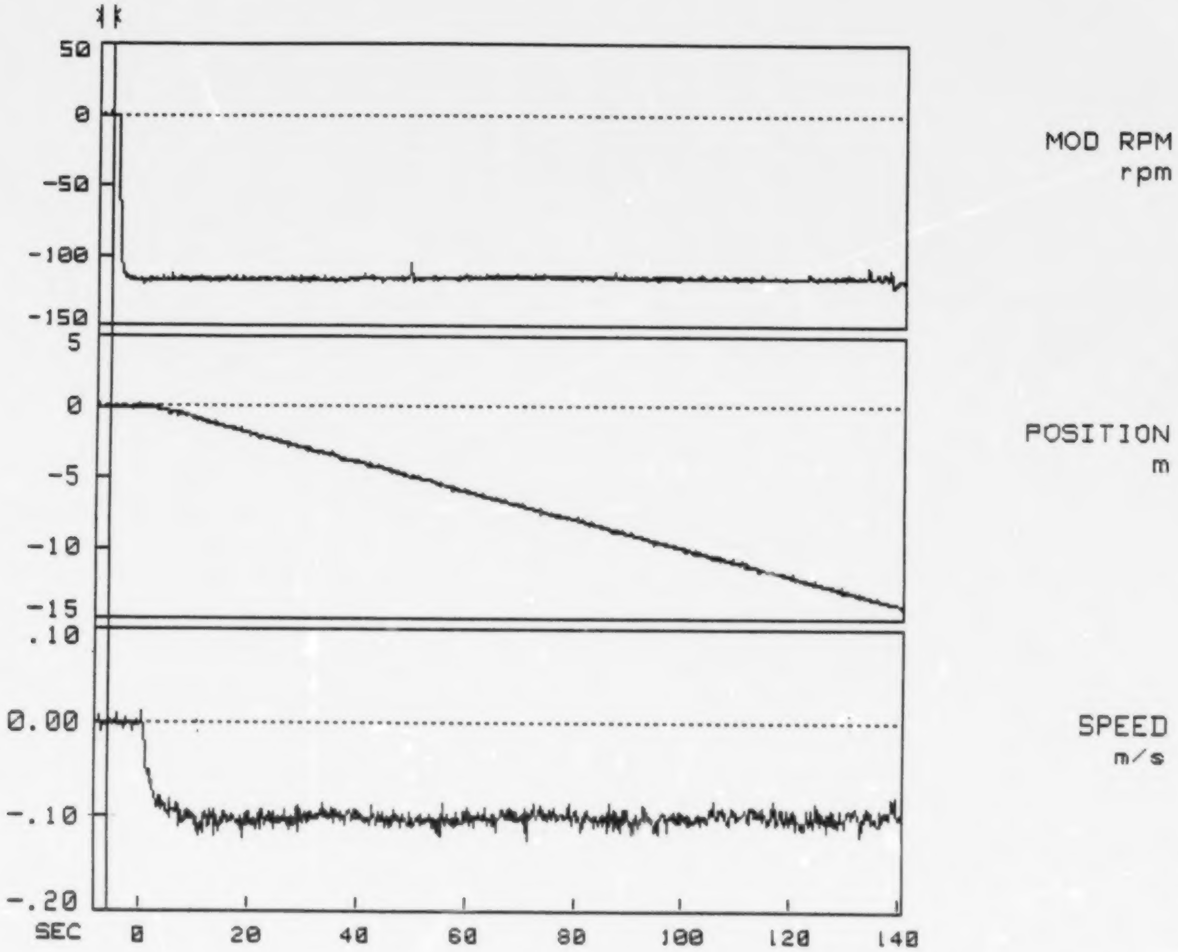

TEST 118

TEST #1 RUN 18

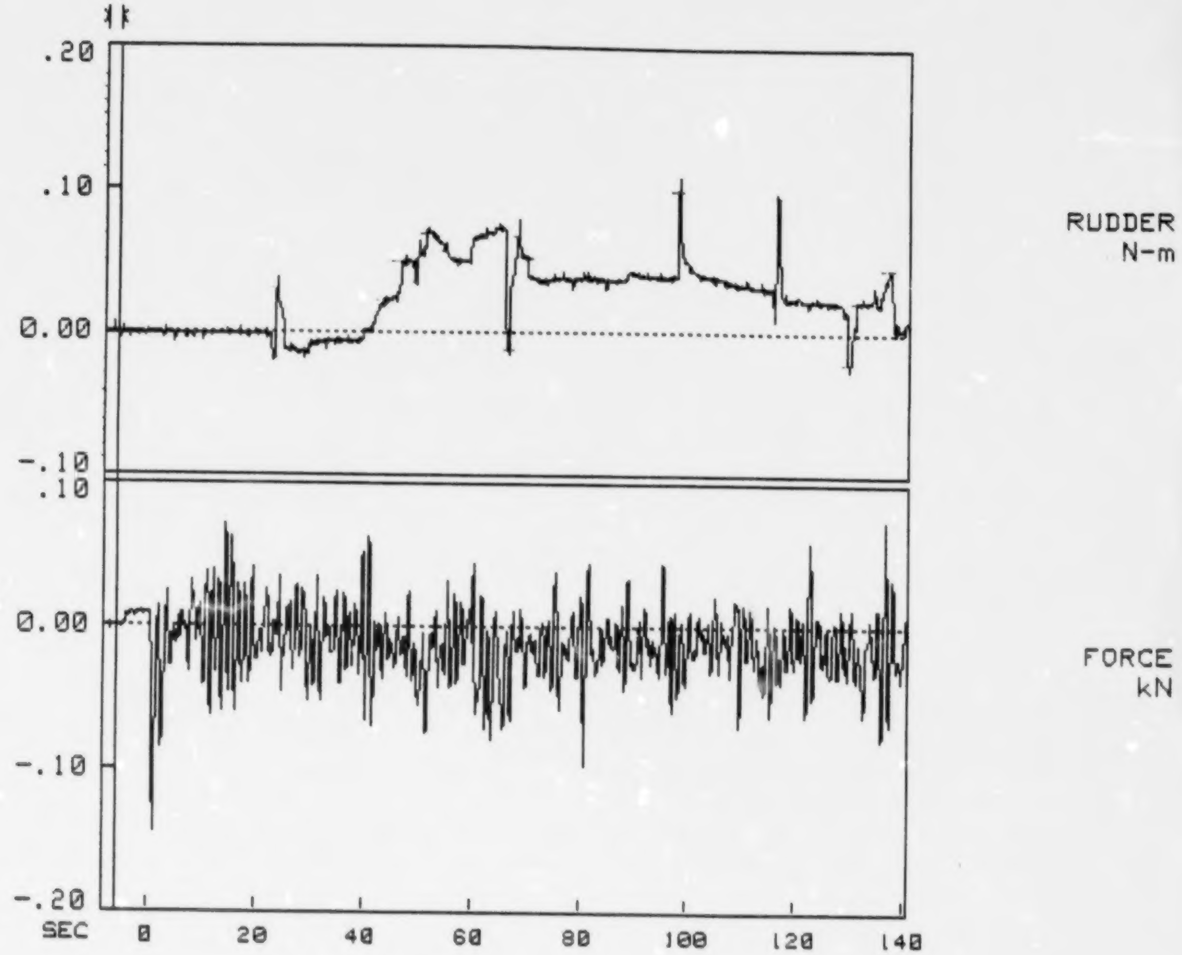

TEST 301

TEST #3 RUN 01

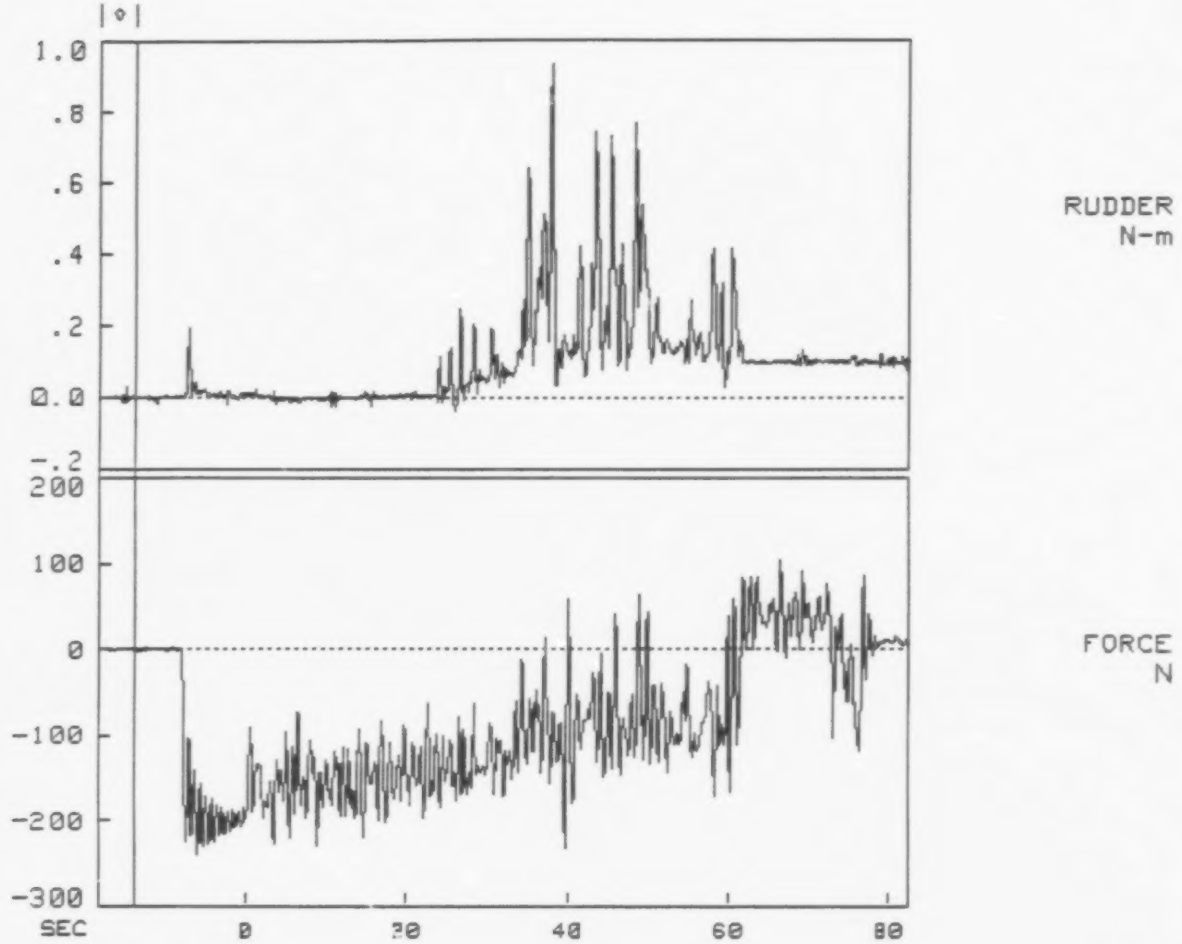

TEST #3 RUN 01 TEST 301

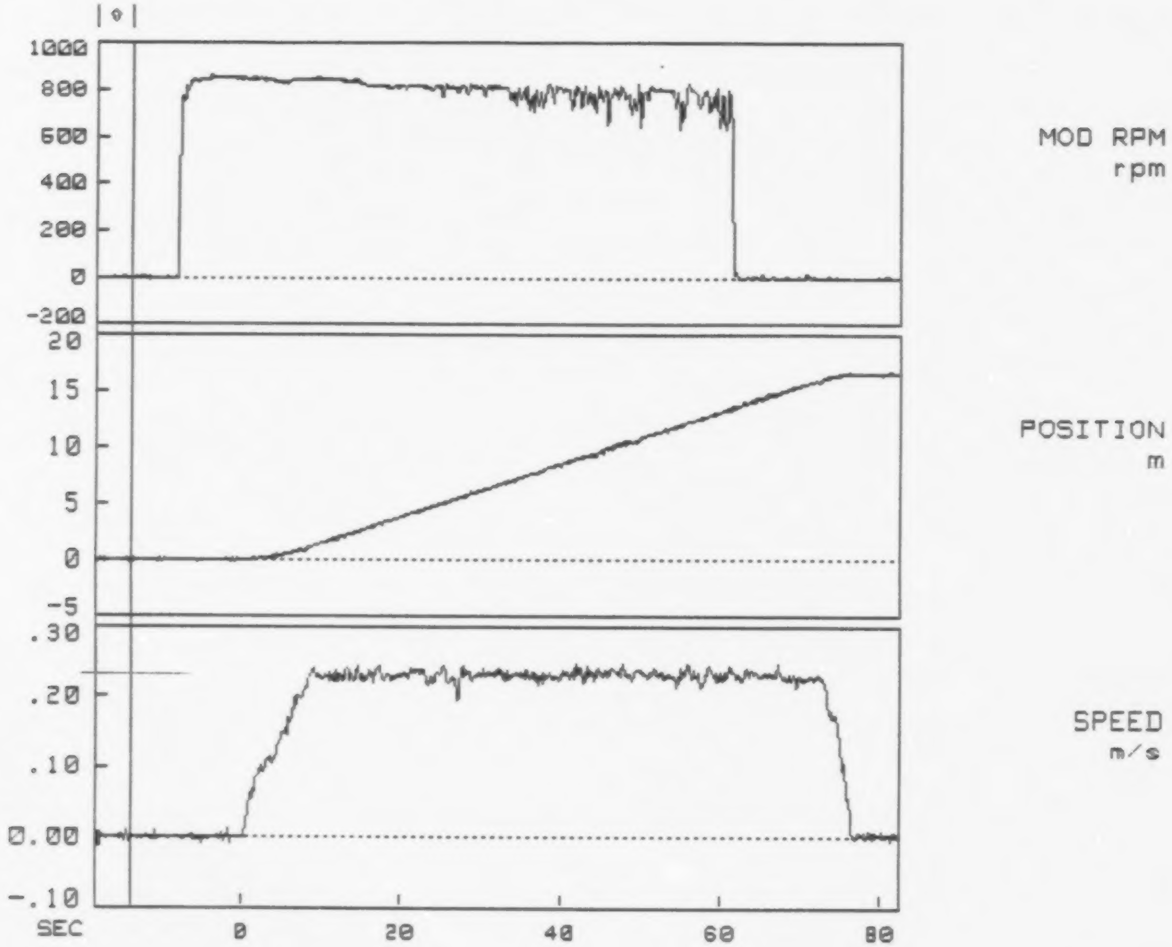

TEST 302

TEST #3 RUN 02

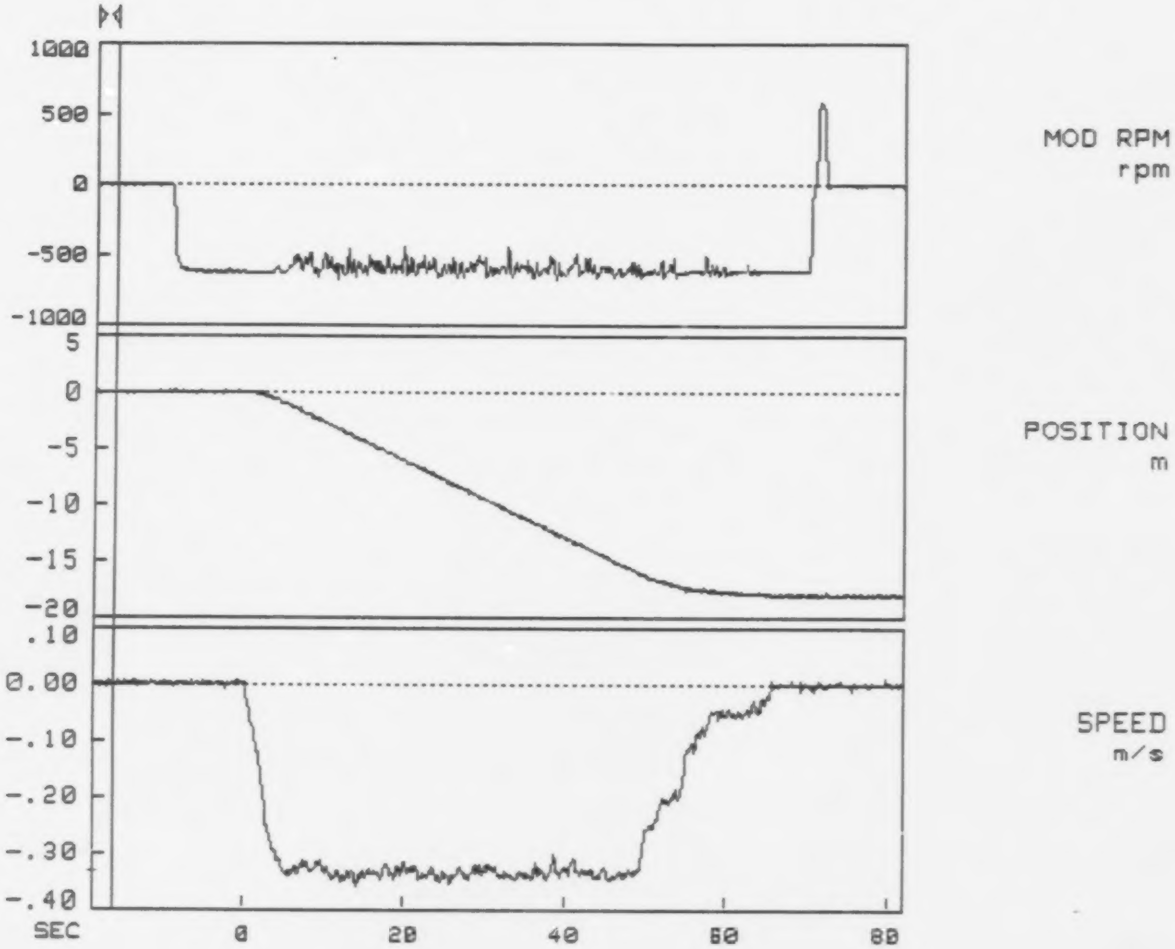

TEST #3 RUN 02 TEST 302

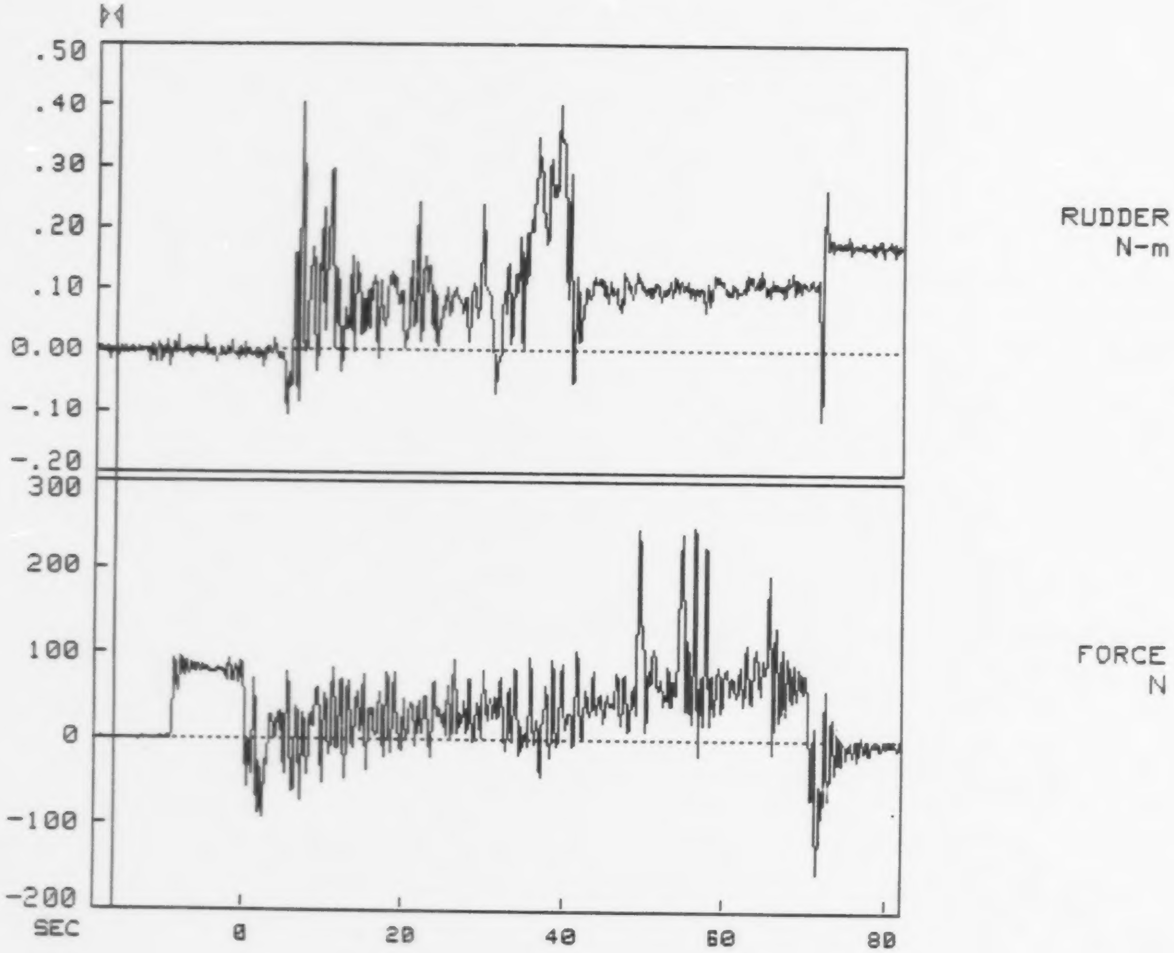

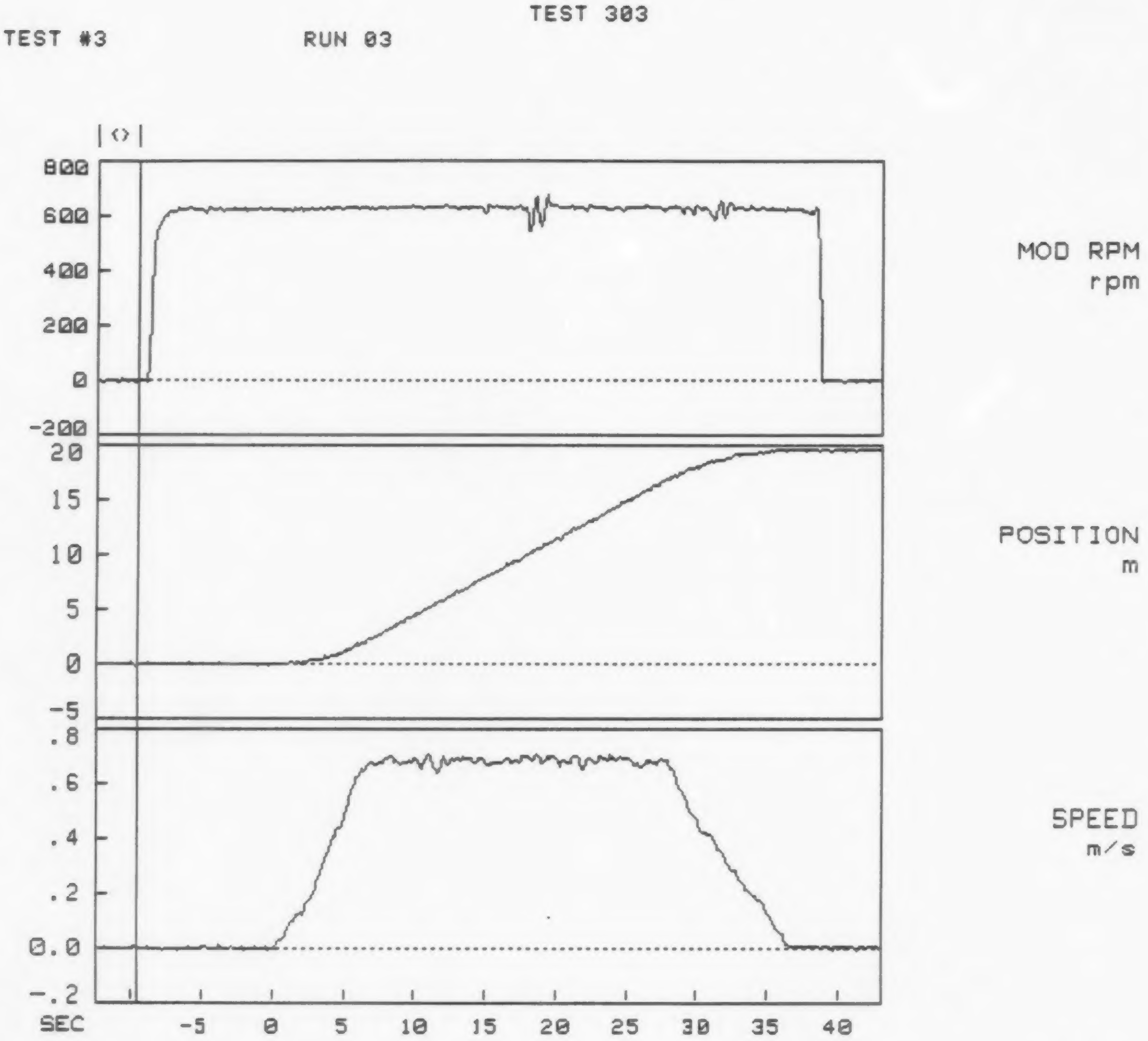

TEST 303
TEST #3
RUN 03
|<>|
800
600
400
200
0
-200
MOD RPM
rpm
20
15
10
5
0
-5
POSITION
m
.8
.6
.4
.2
0.0
-.2
SPEED
m/s
SEC
-5
0
5
10
15
20
25
30
35
40

TEST #3 RUN 03 TEST 303

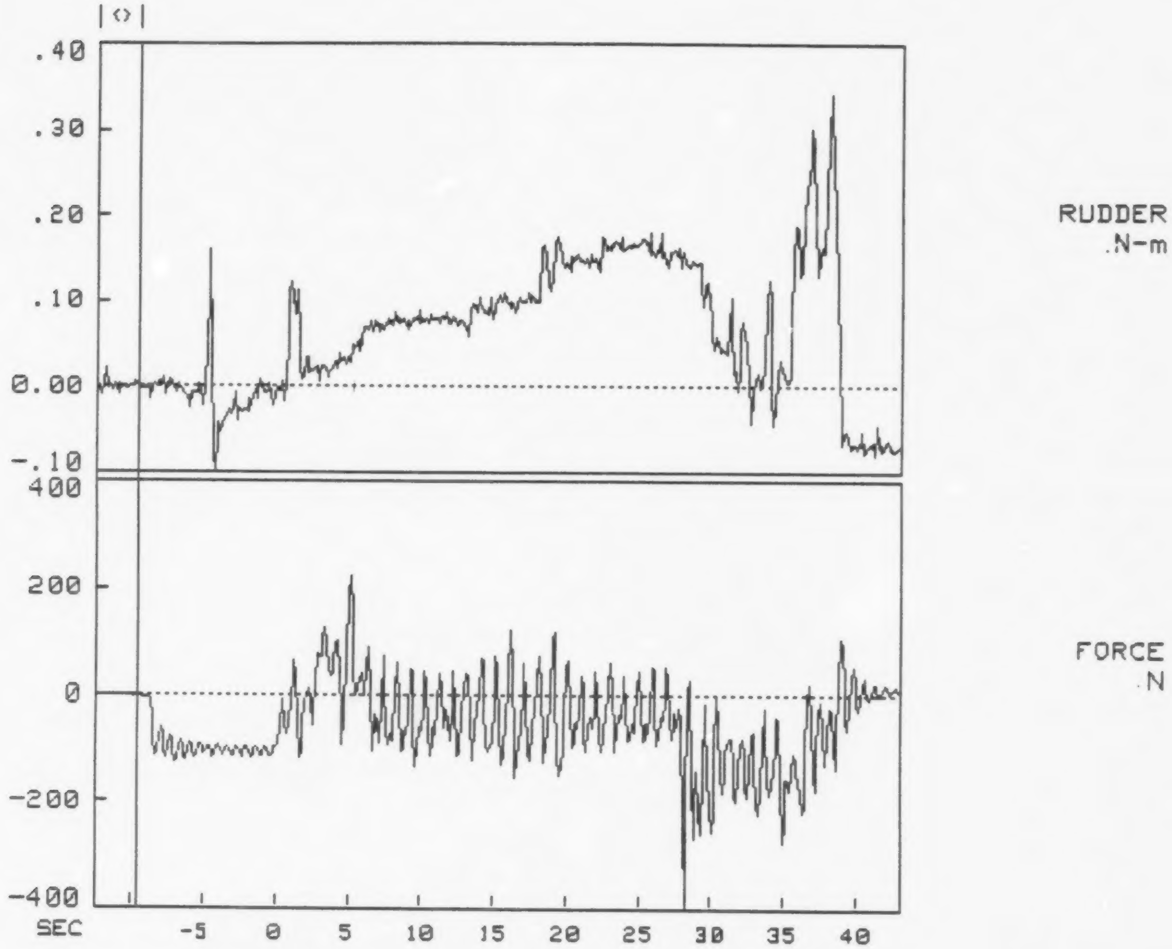

TEST 304

TEST #3 RUN 04

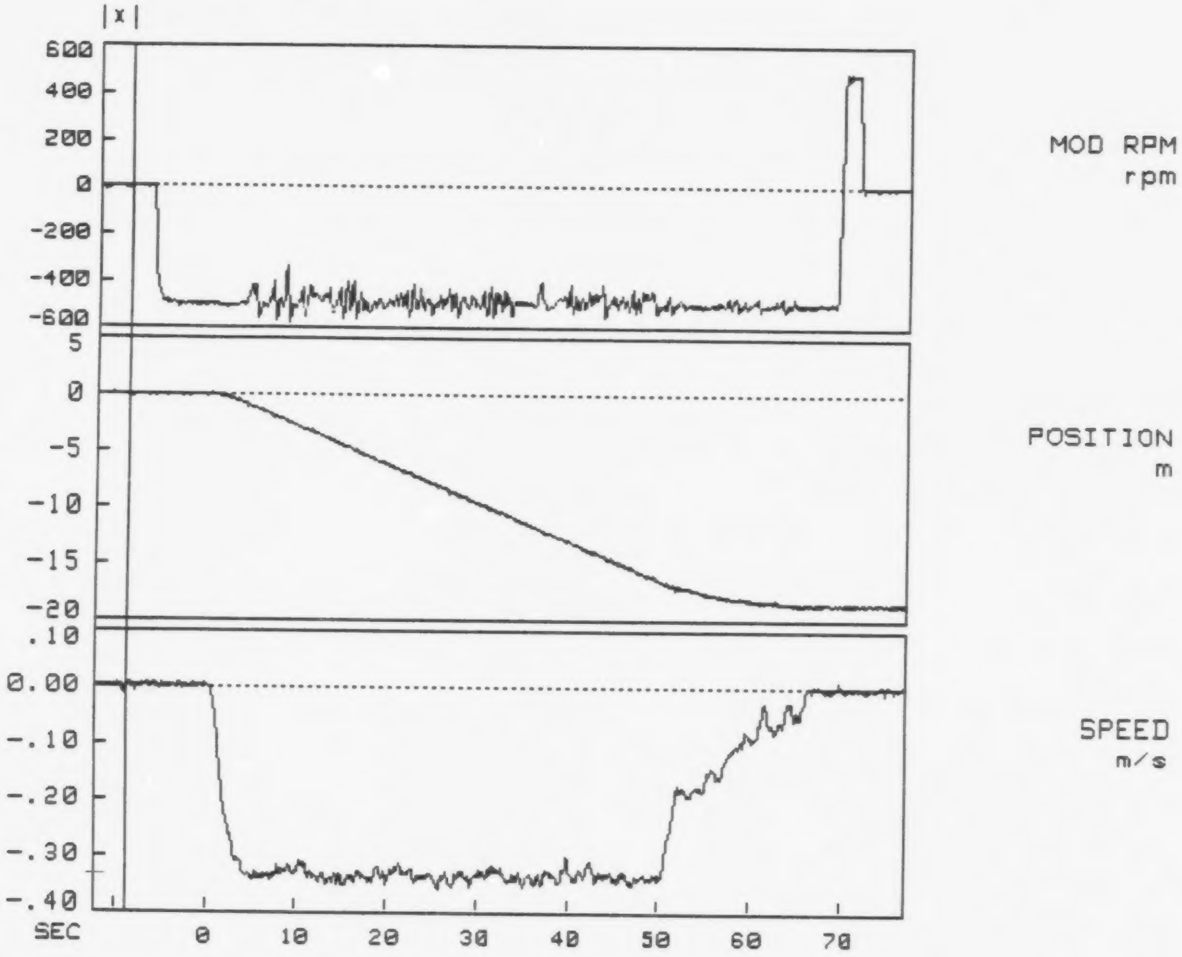

TEST 304

TEST #3 RUN 04

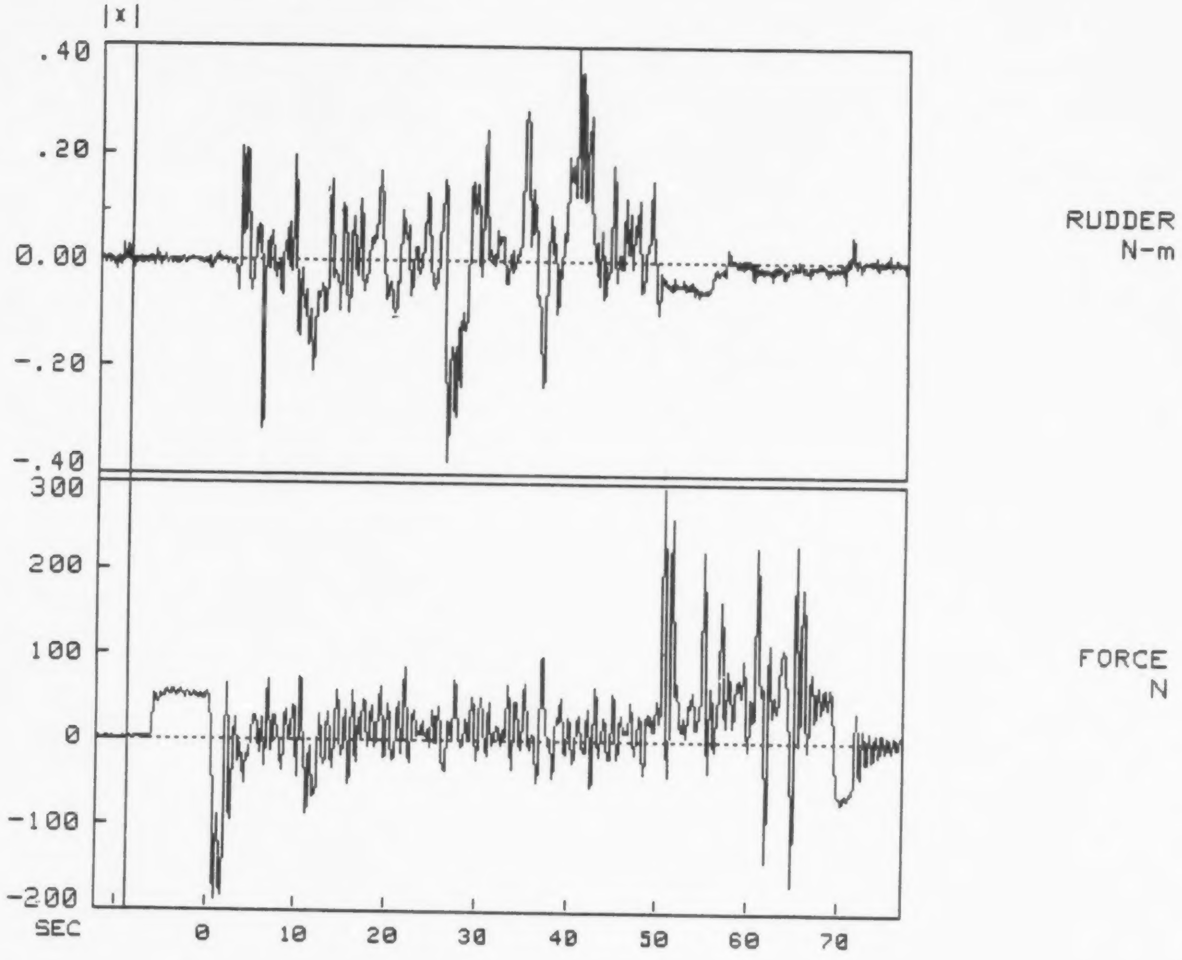

TEST #3 RUN 05 TEST 305

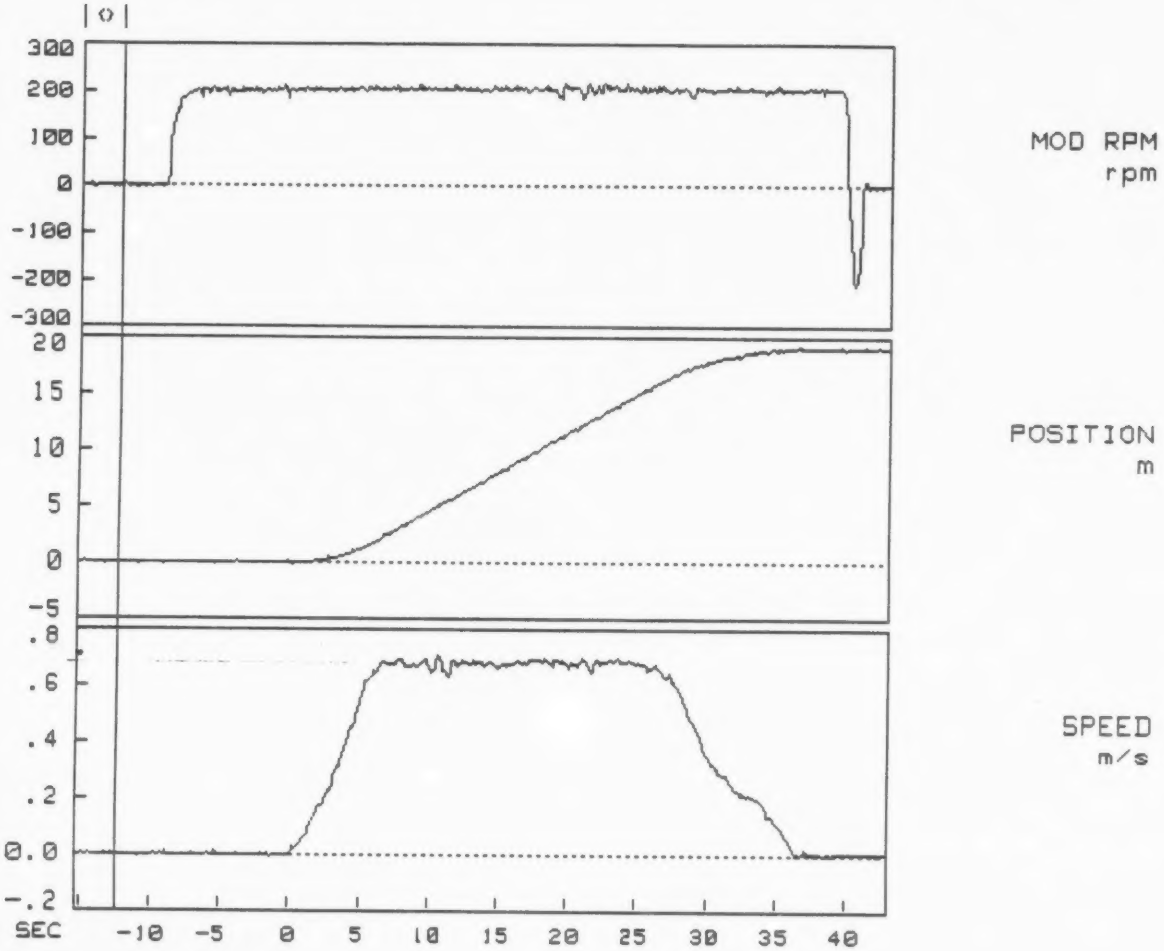

TEST #3 RUN 05 TEST 305

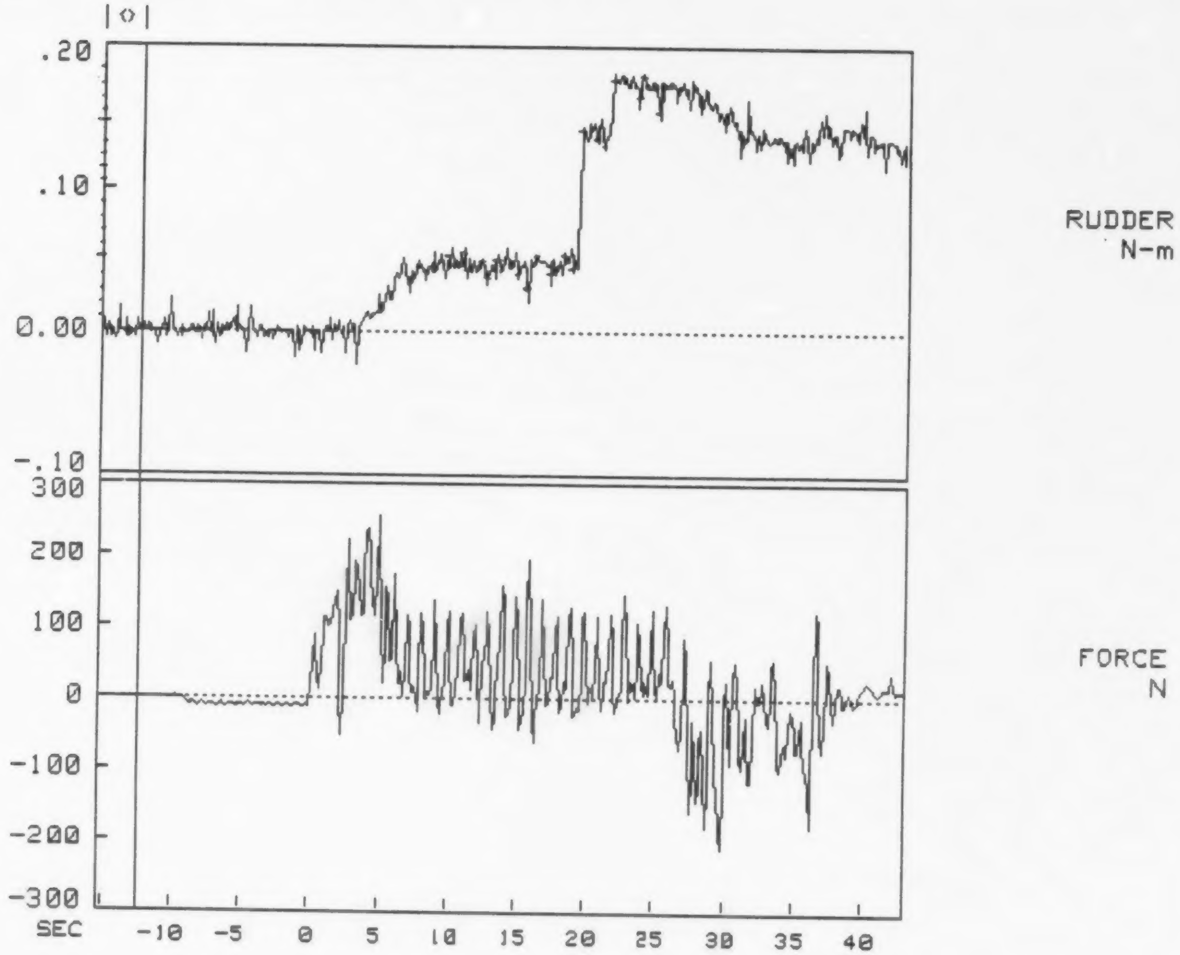

TEST 306

TEST #3 RUN 06

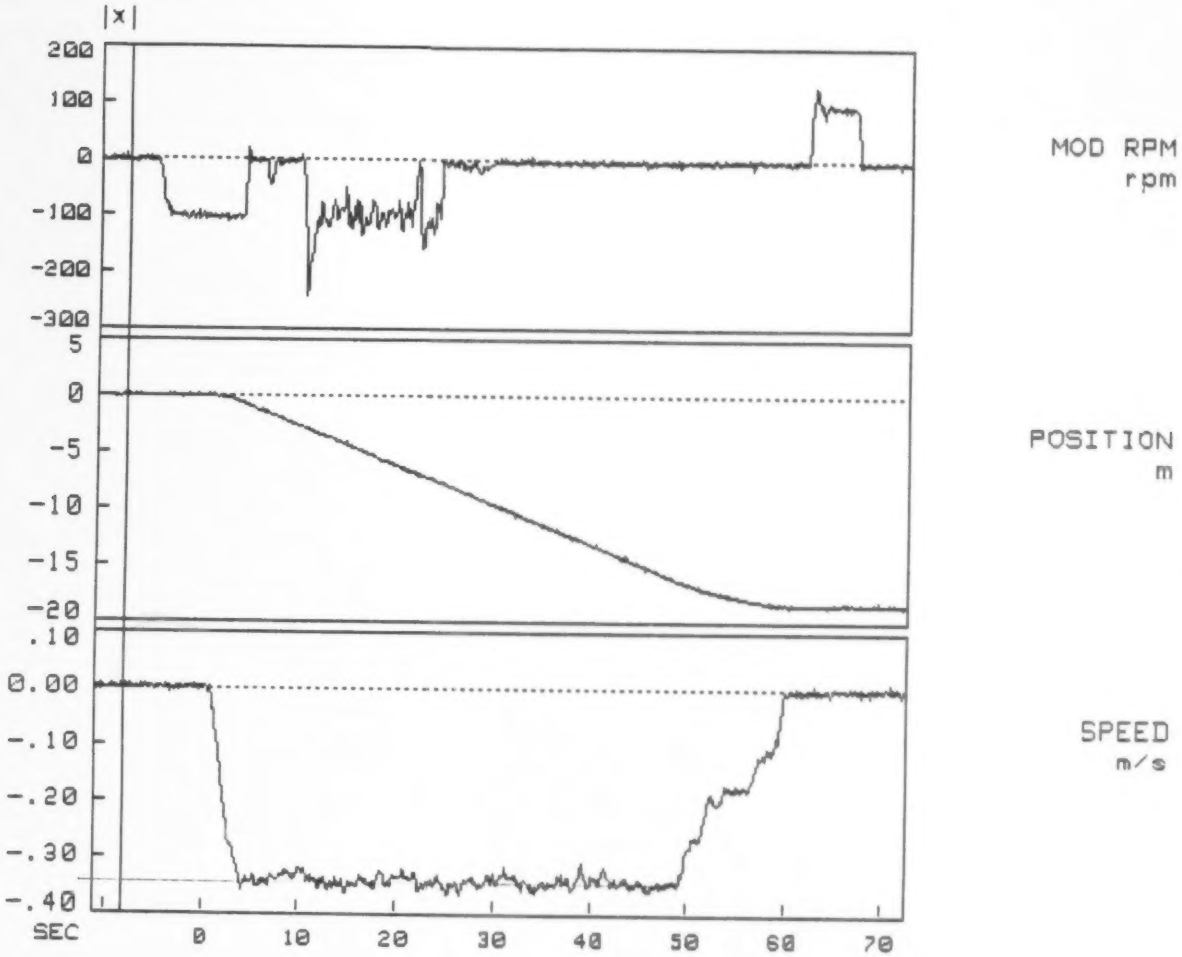

TEST #3 RUN 06 TEST 306

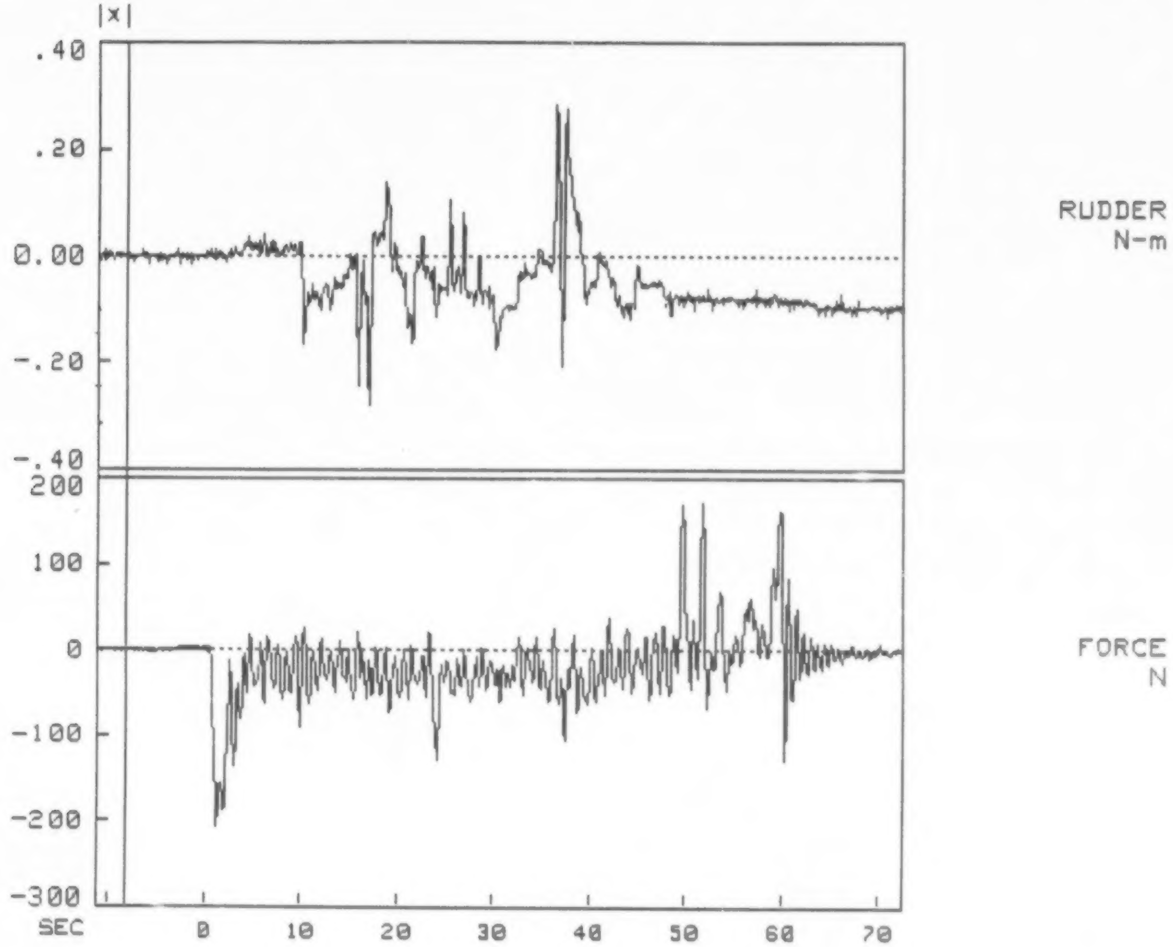

TEST #~~6~~ 3

RUN 07

TEST 607
3

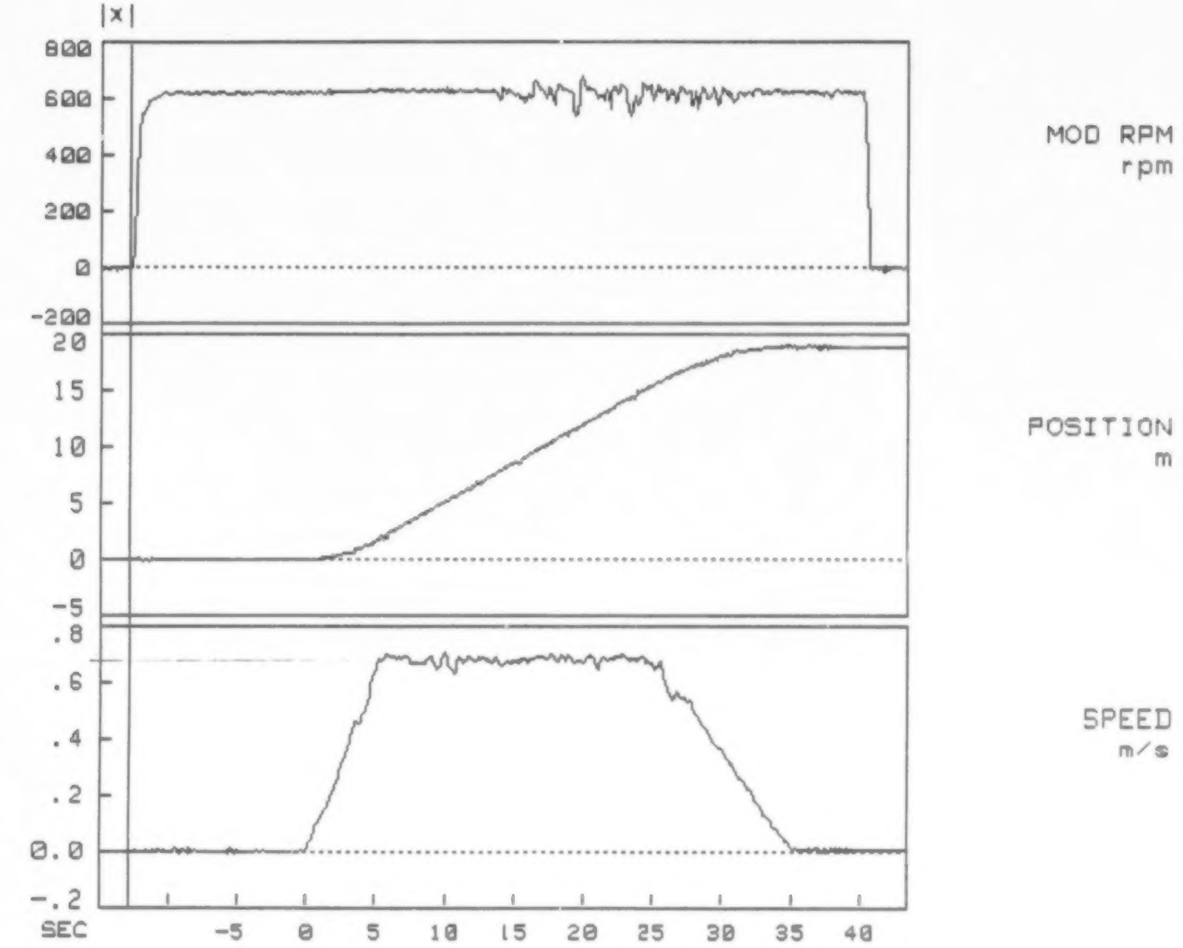

TEST #6
3

RUN 07

TEST 607
3

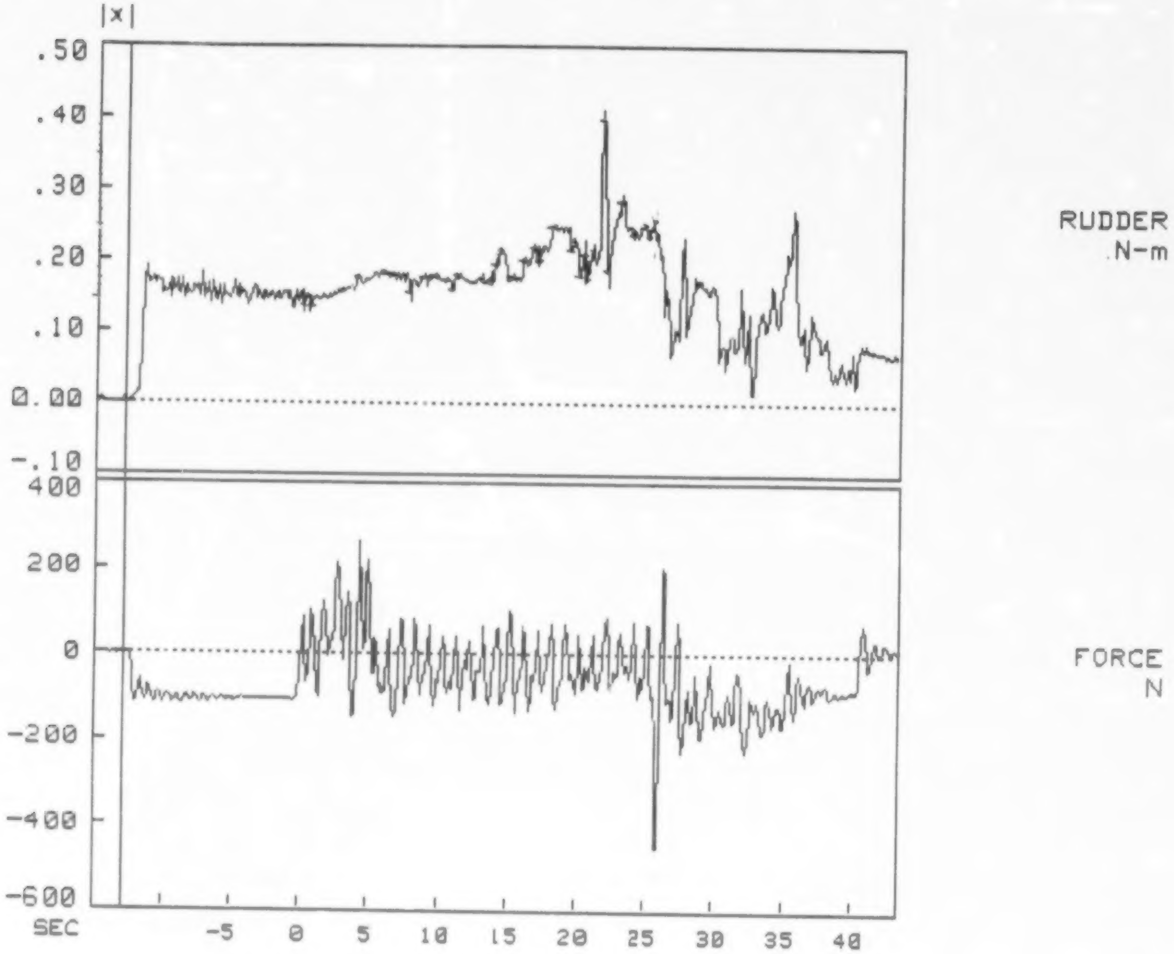

TEST #6 3 RUN 08 .ES. 608 3

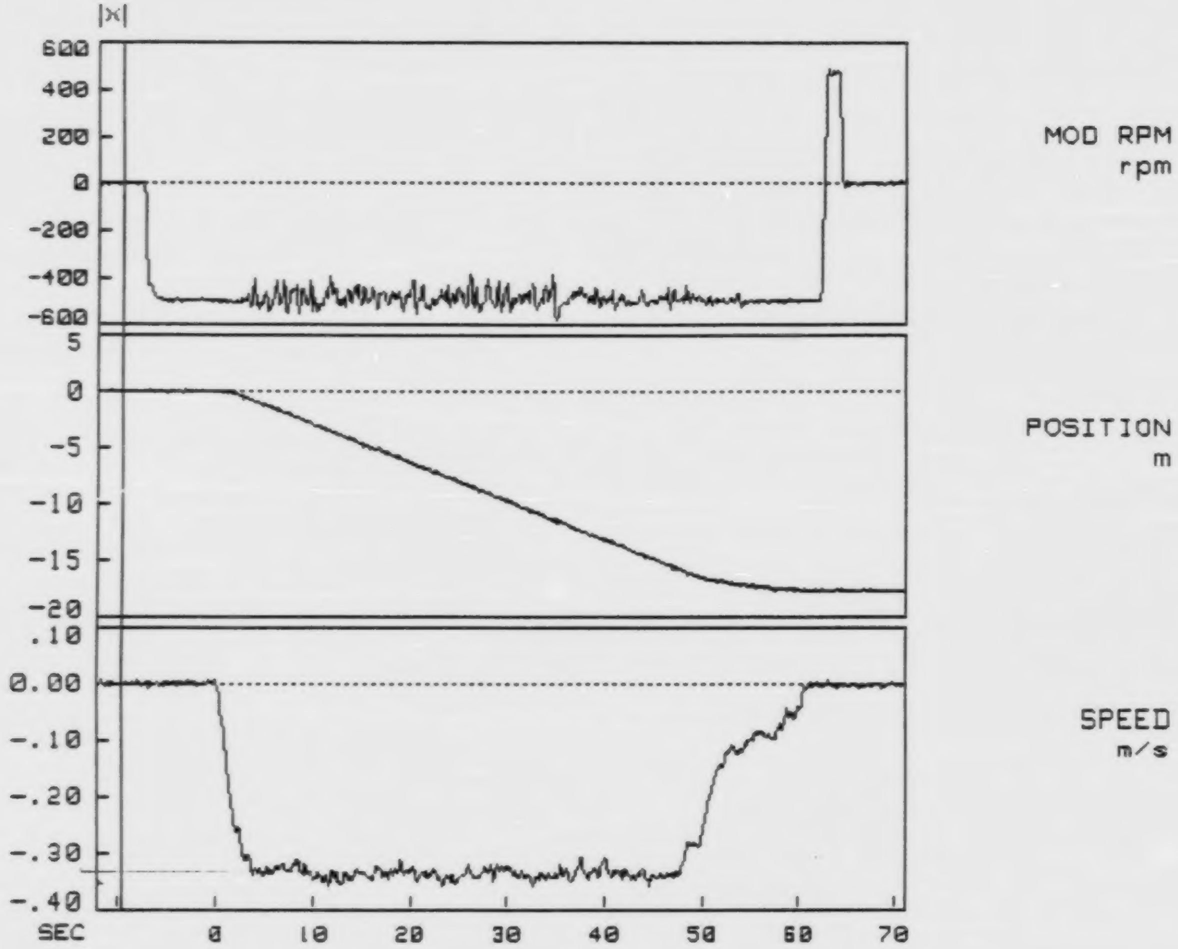

TEST #6
3

RUN 08

TEST 608
3

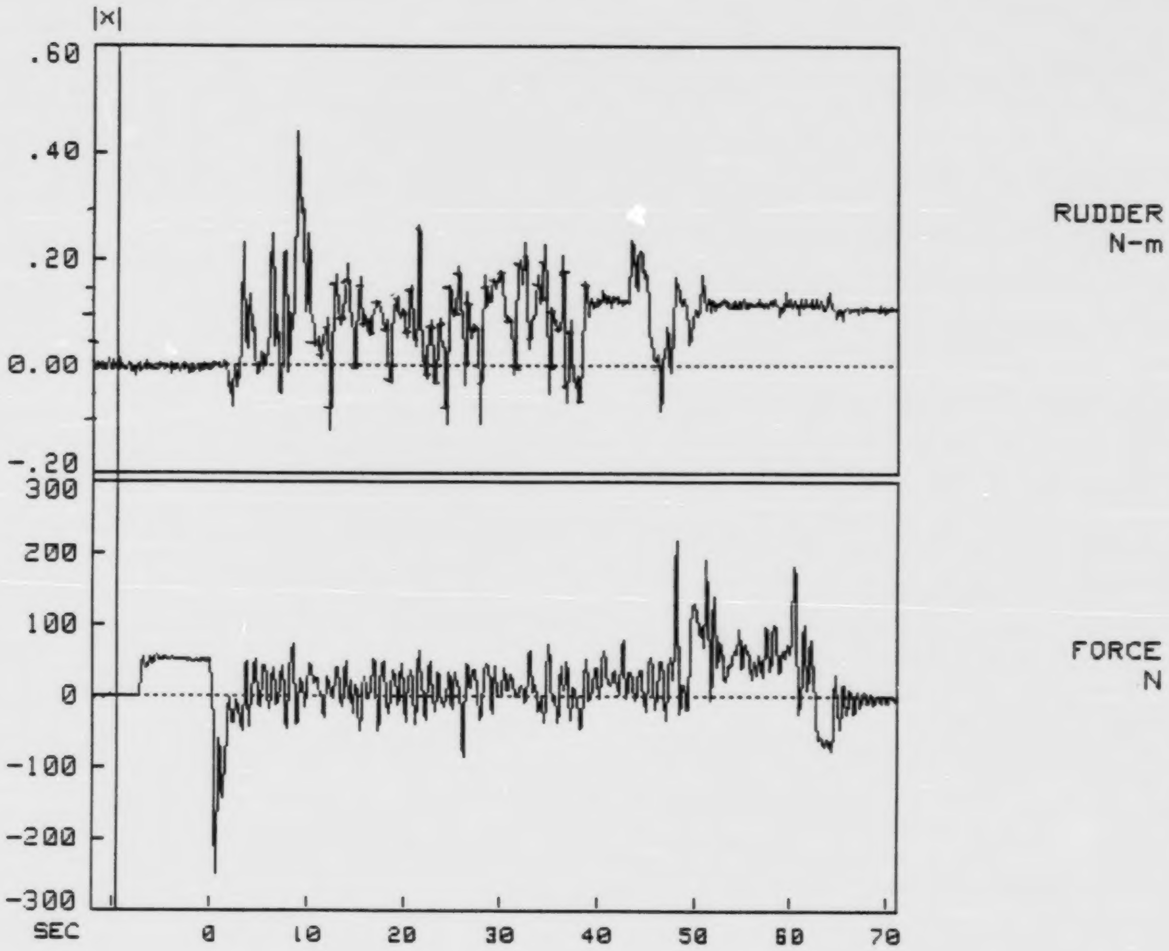

TEST #3 RUN 09 TEST 309

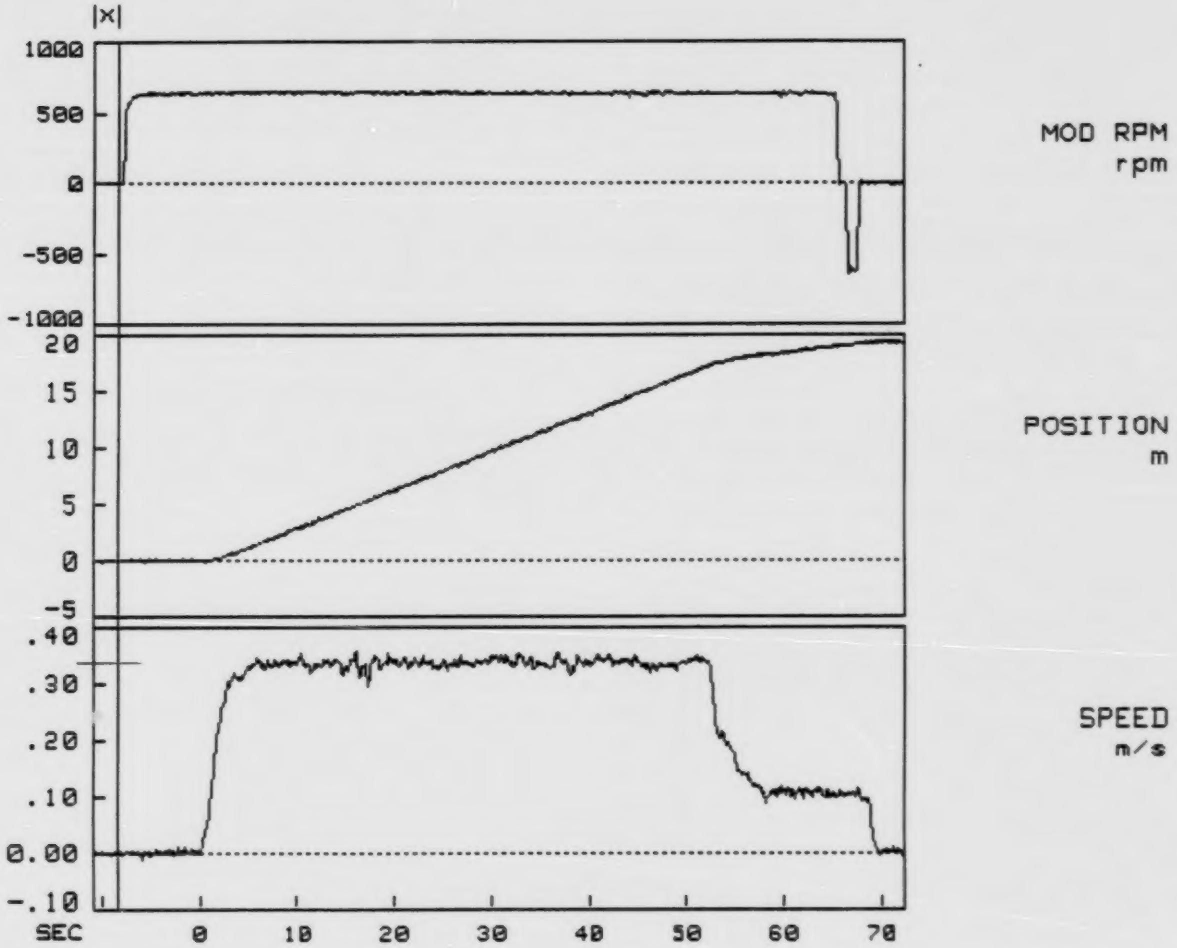

TEST 309

TEST #3 RUN 09

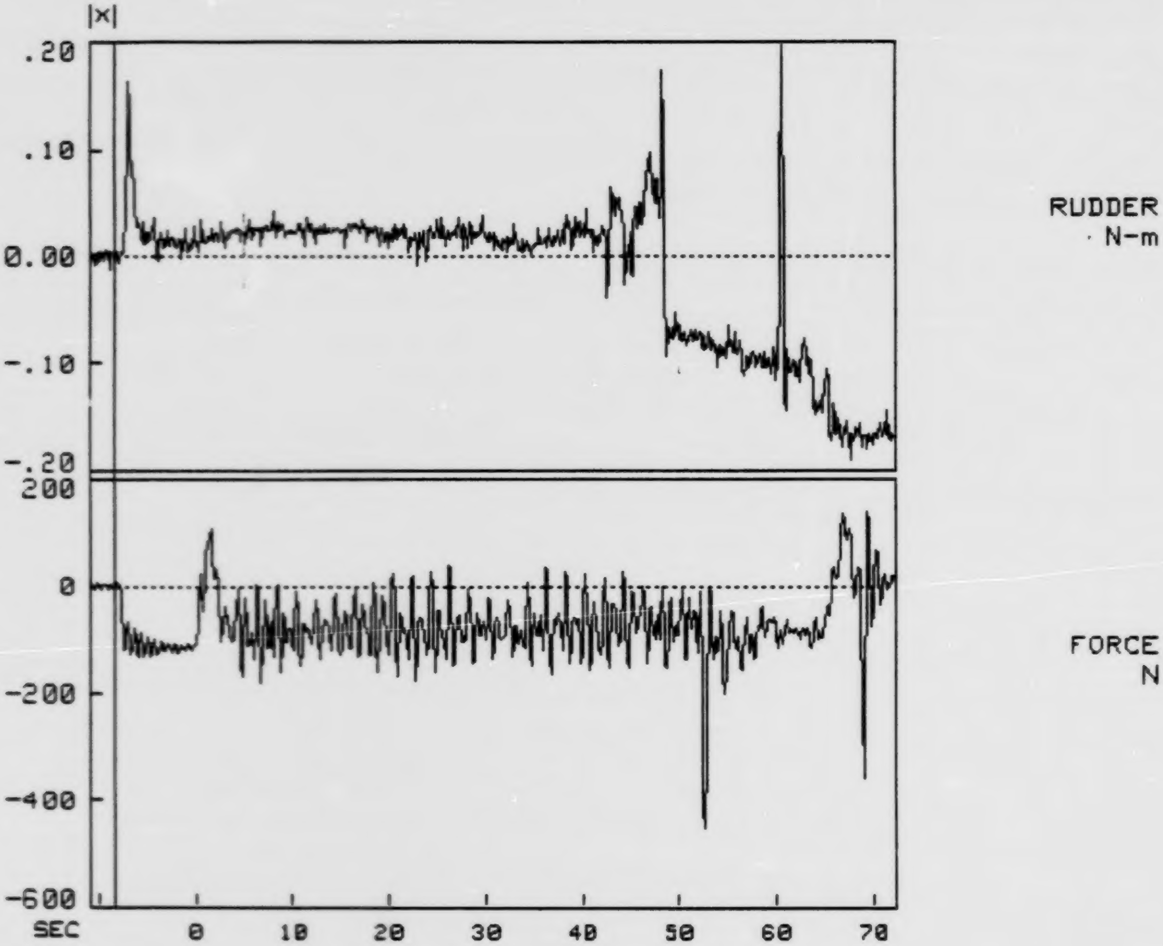

TEST 310

TEST #3 RUN 10

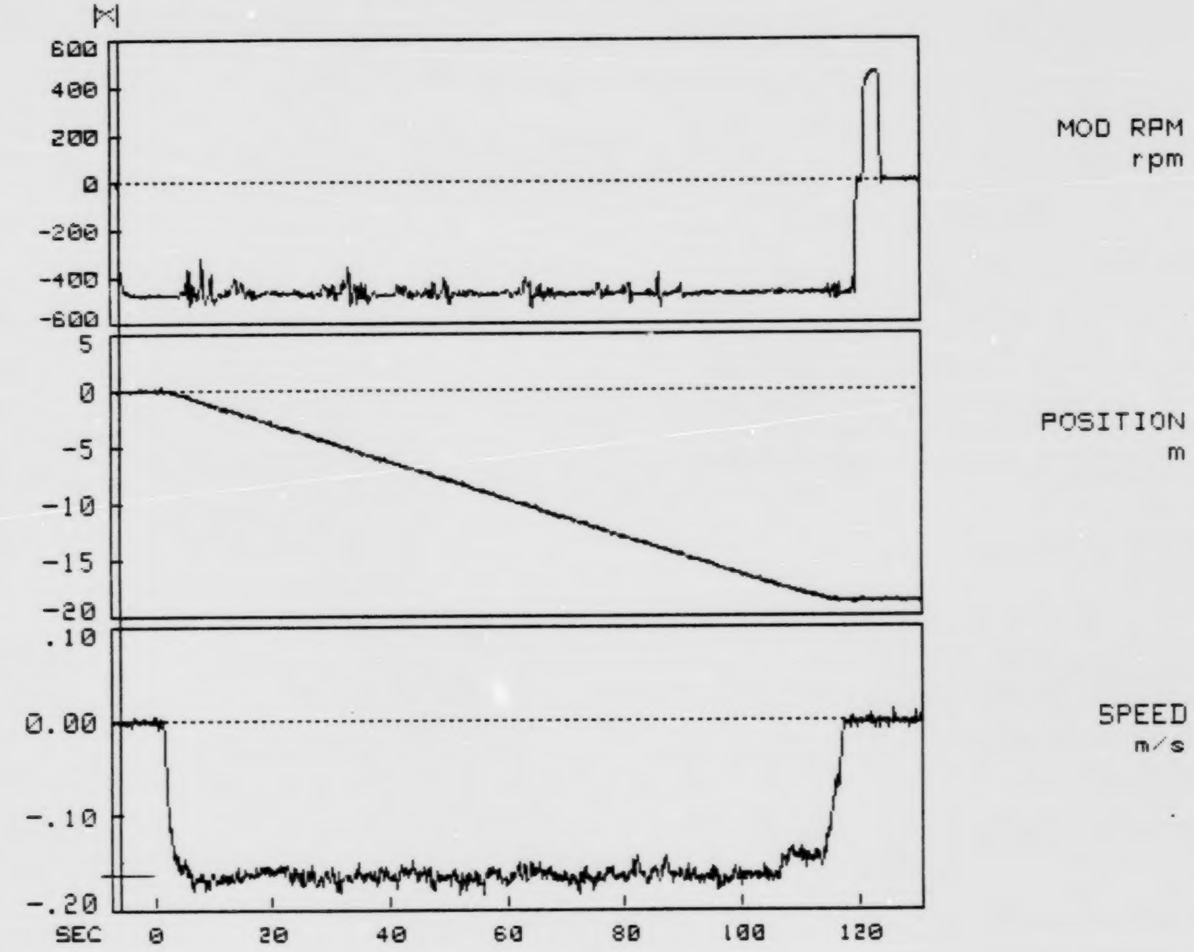

TEST 310

TEST #3 RUN 10

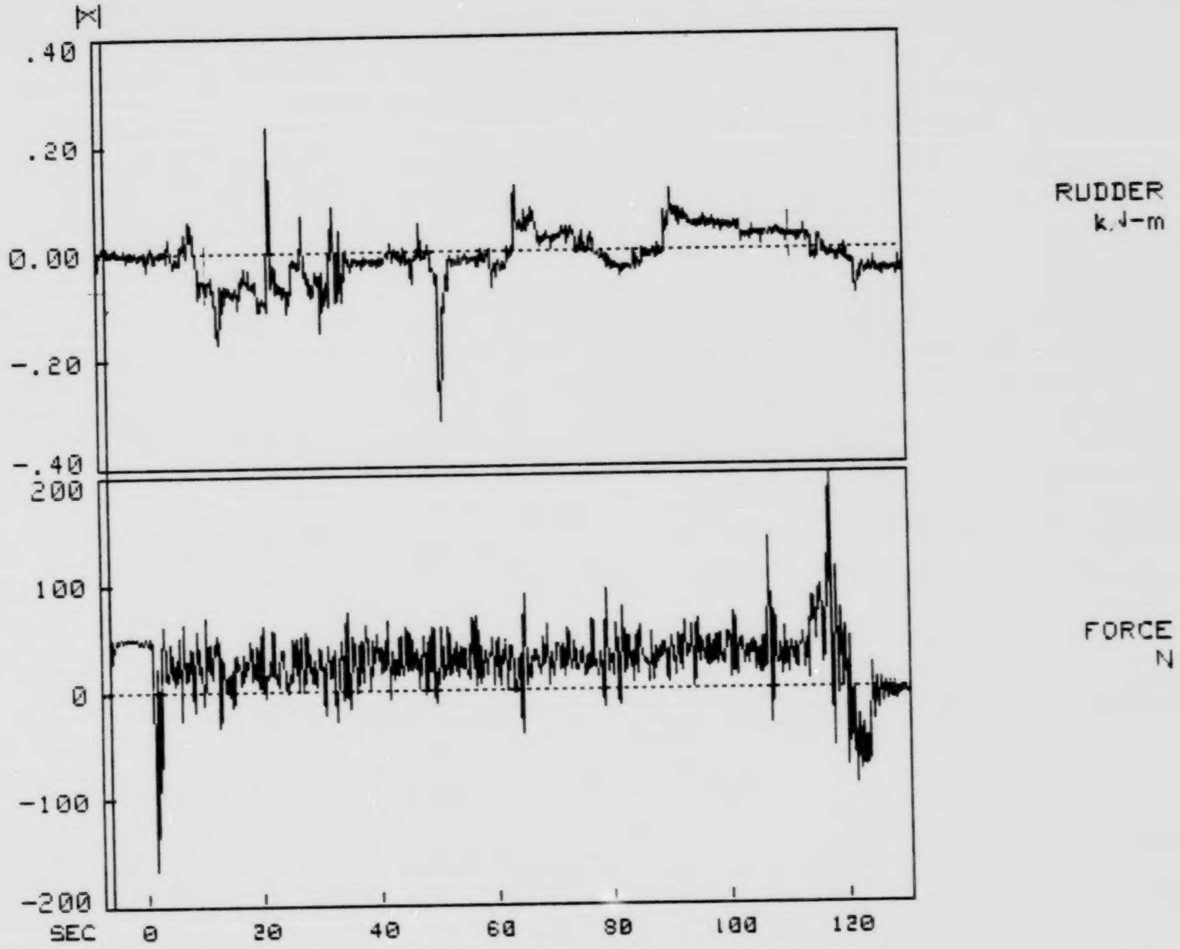

TEST 311

TEST #3 RUN 11

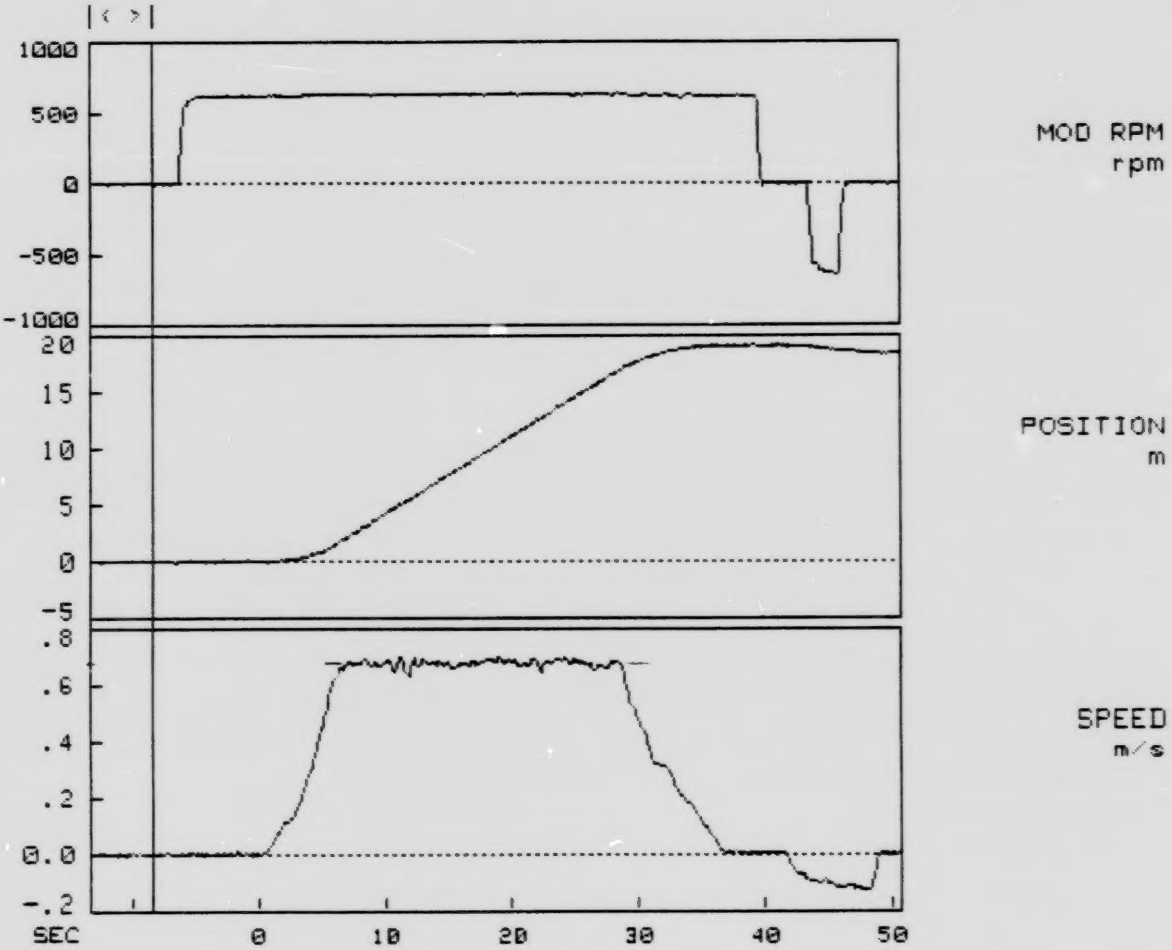

TEST 311

TEST #3 RUN 11

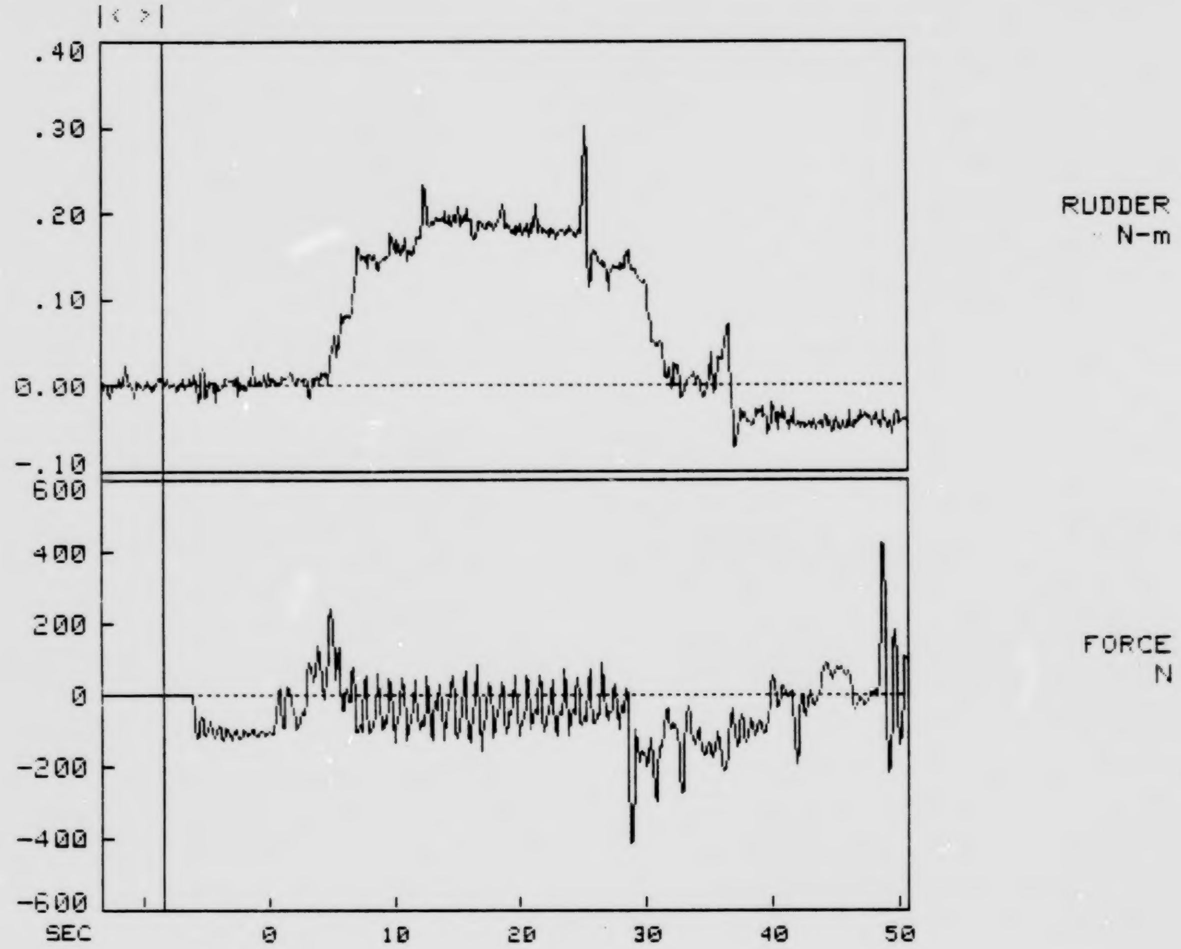

TEST 312

TEST #3 RUN 12

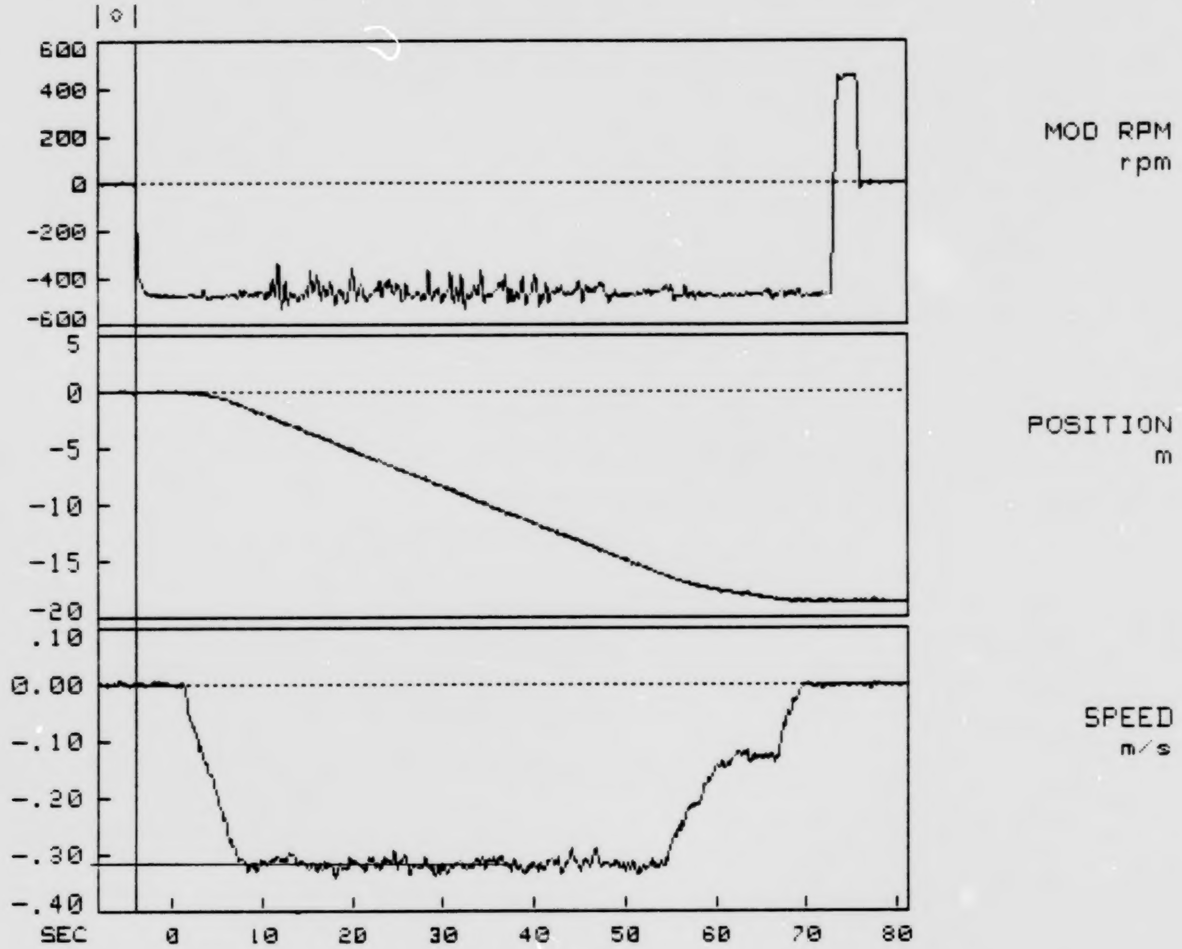

TEST 312

TEST #3 RUN 12

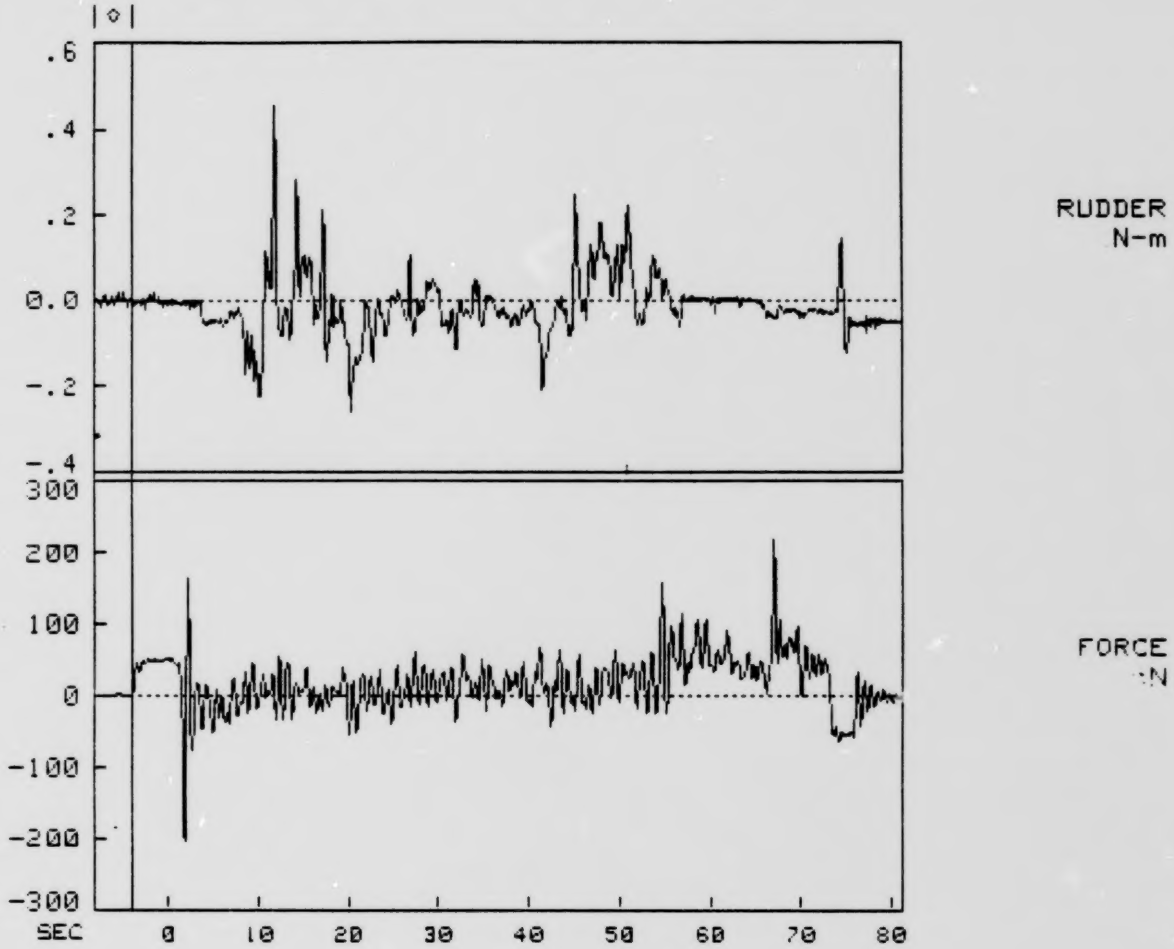

TEST 313

TEST #3 RUN 13

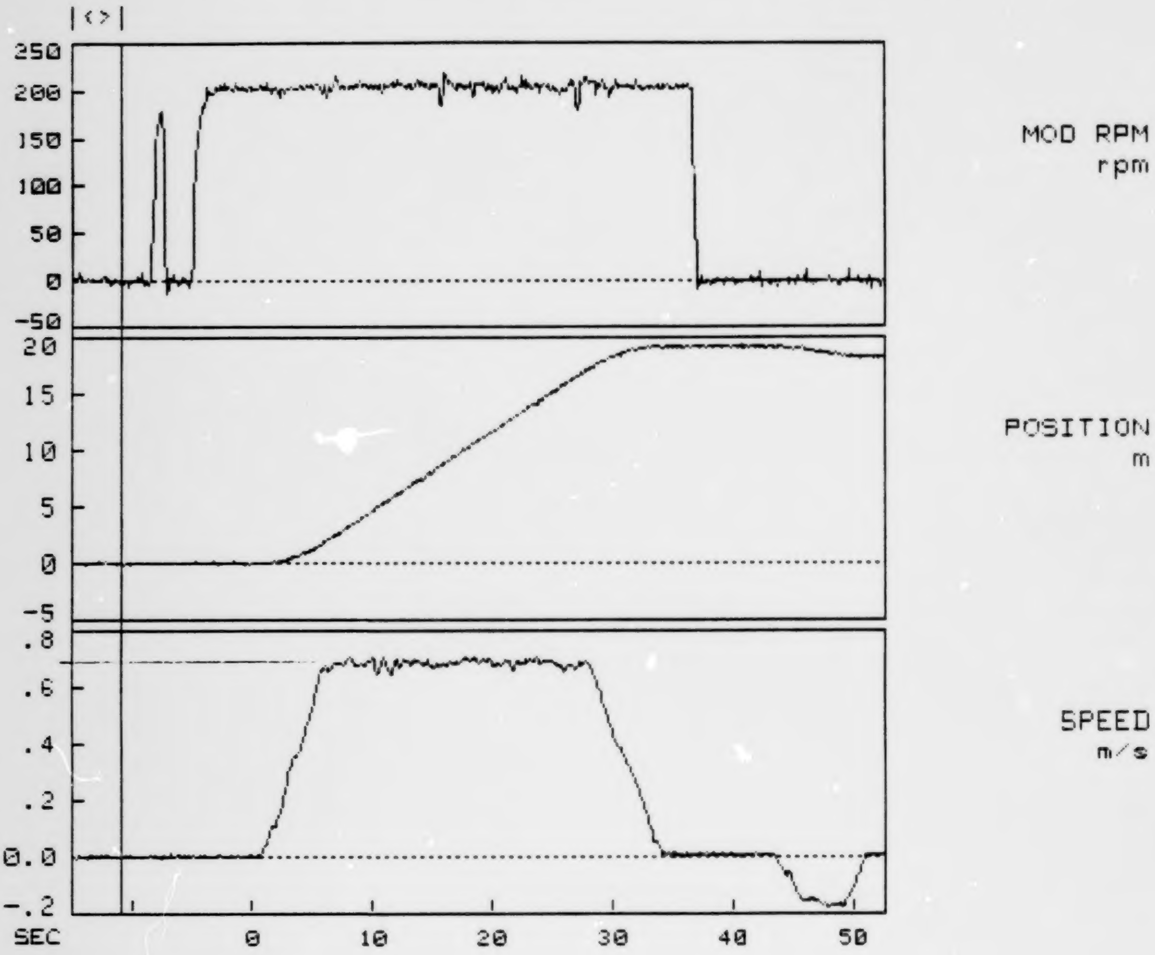

TEST #3 RUN 13 TEST 313

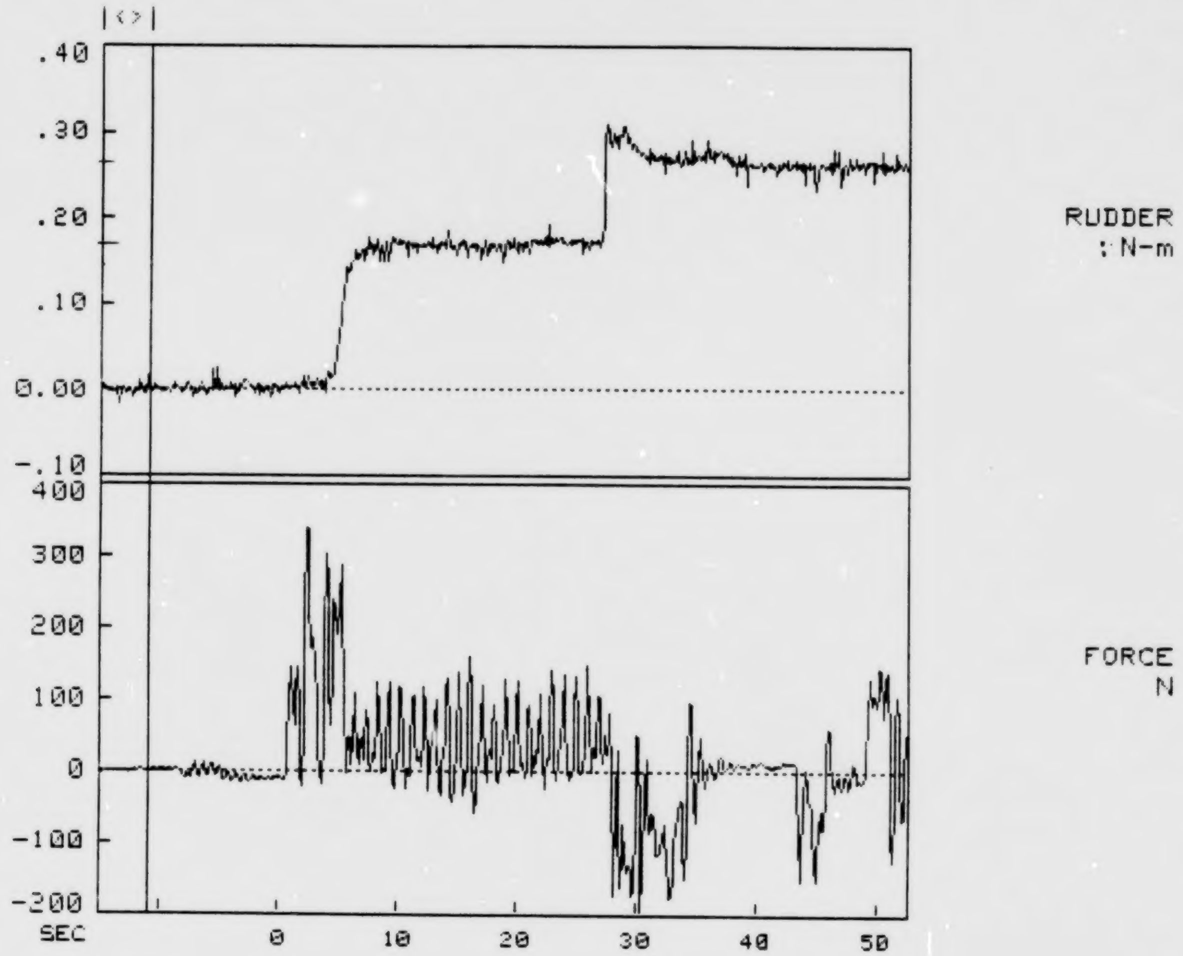

TEST 314

TEST #3 RUN 14

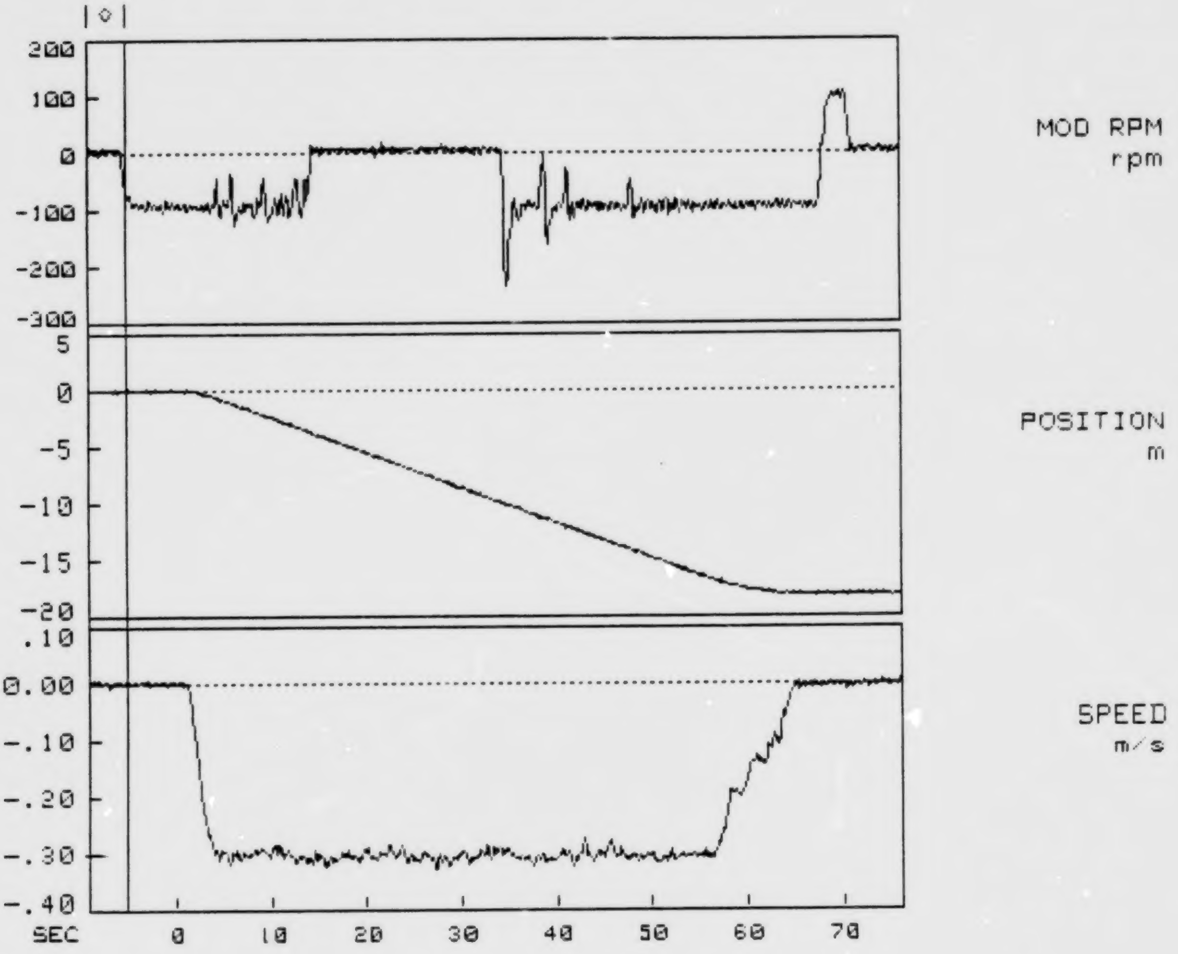

TEST 314

TEST #3 RUN 14

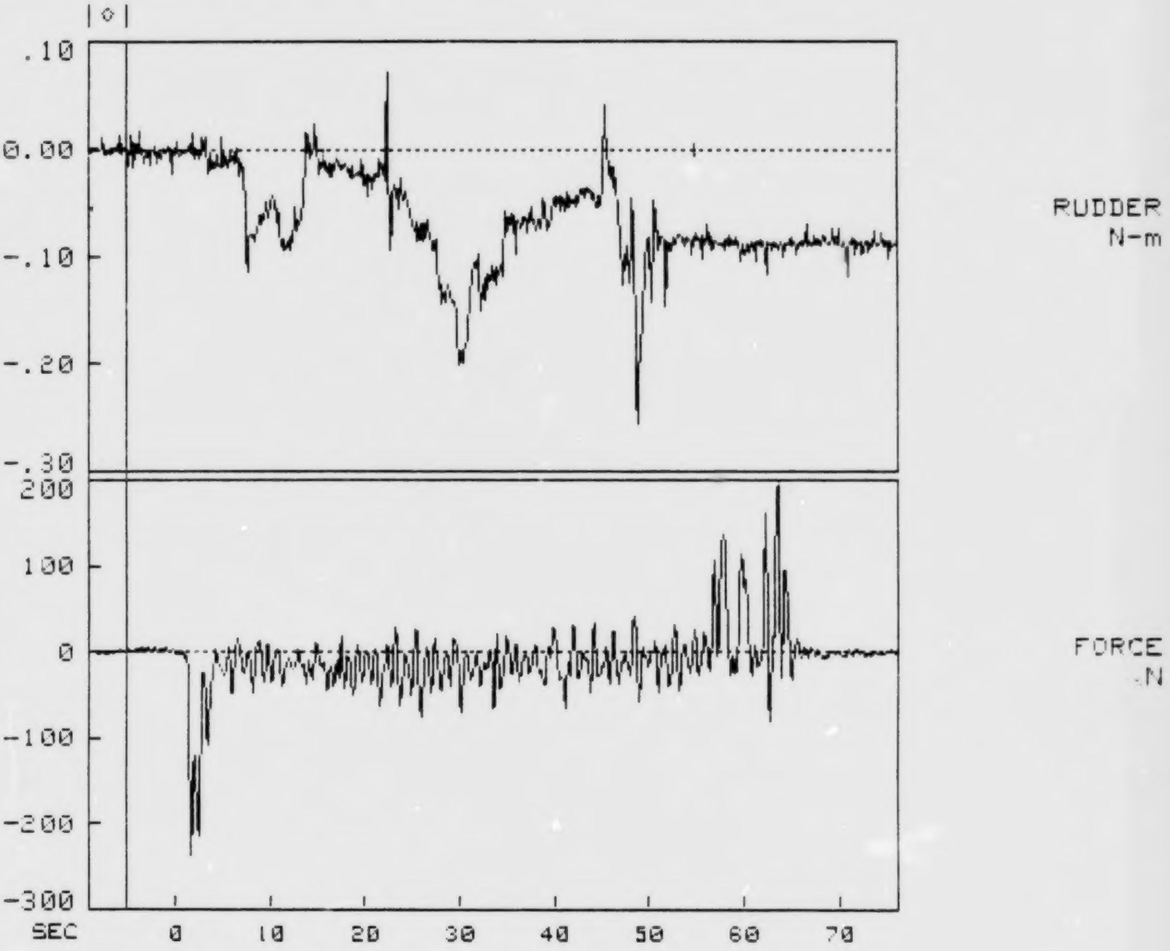

TEST 315

TEST #3 RUN 15

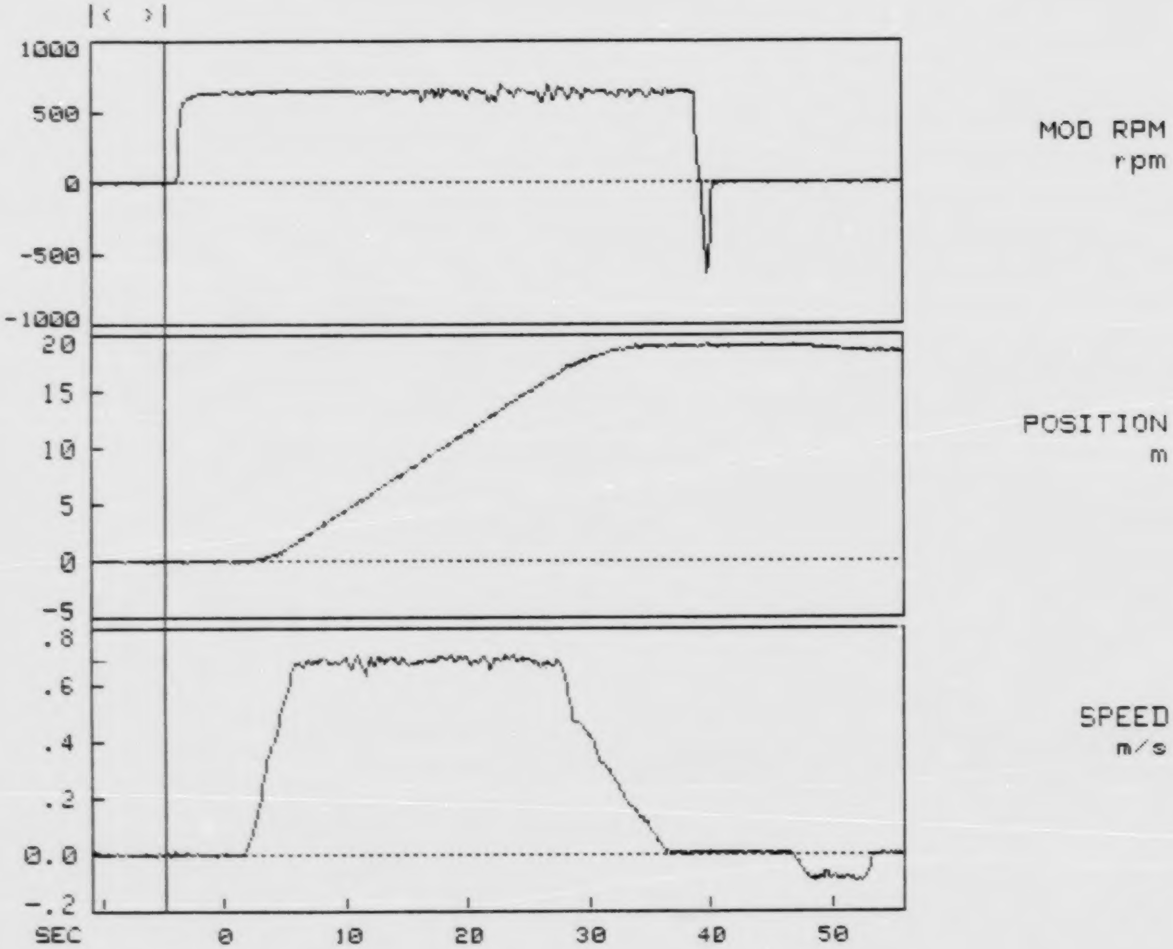

TEST 315

TEST #3 RUN 15

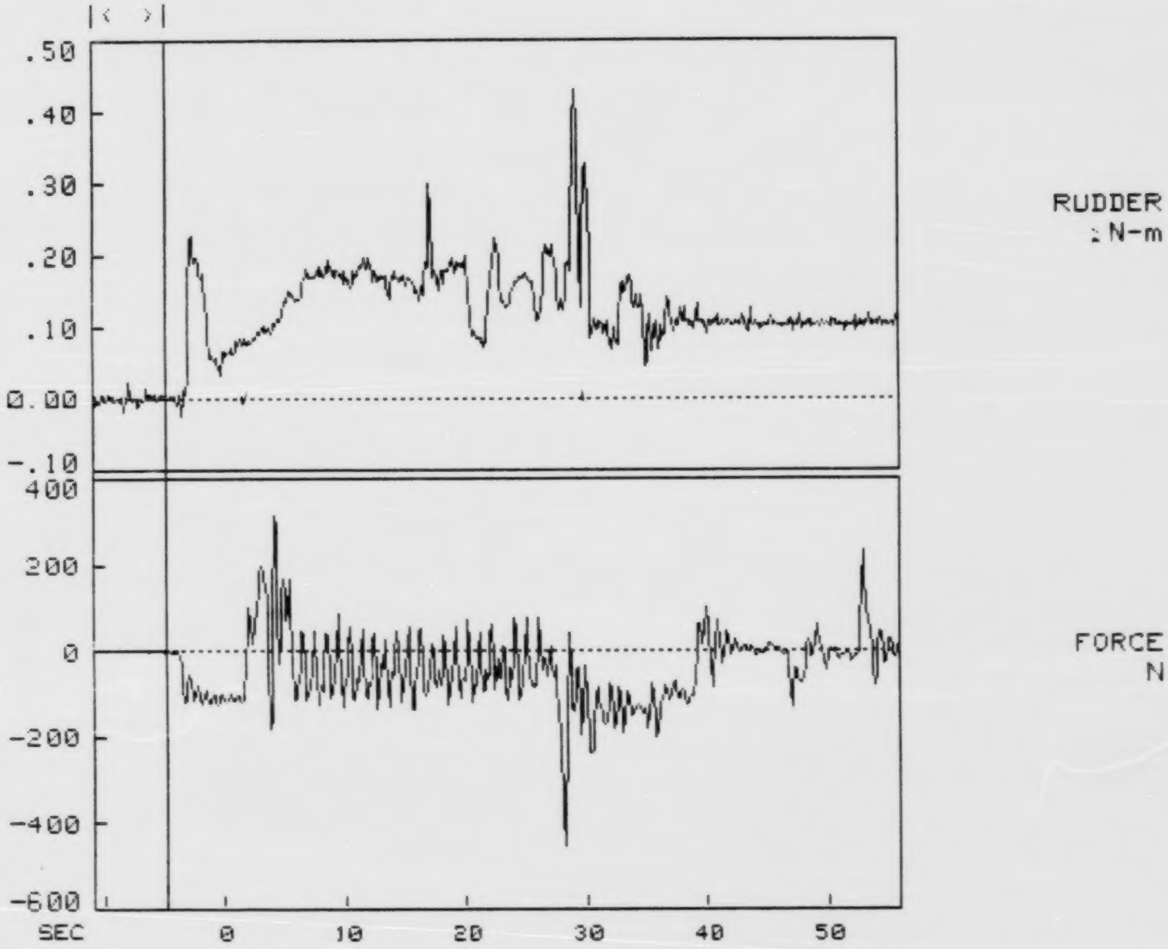

TEST 316

TEST #3 RUN 16

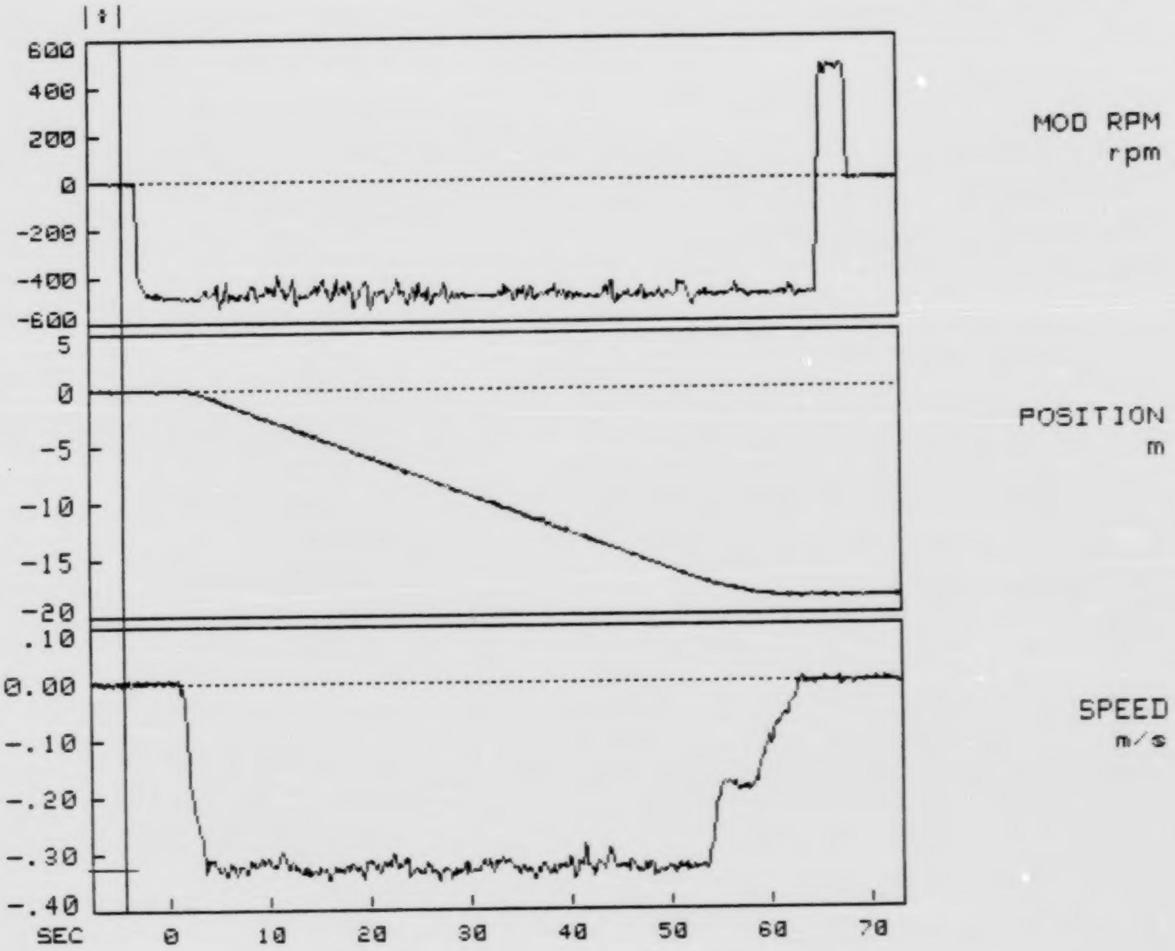

TEST 316

TEST #3 RUN 16

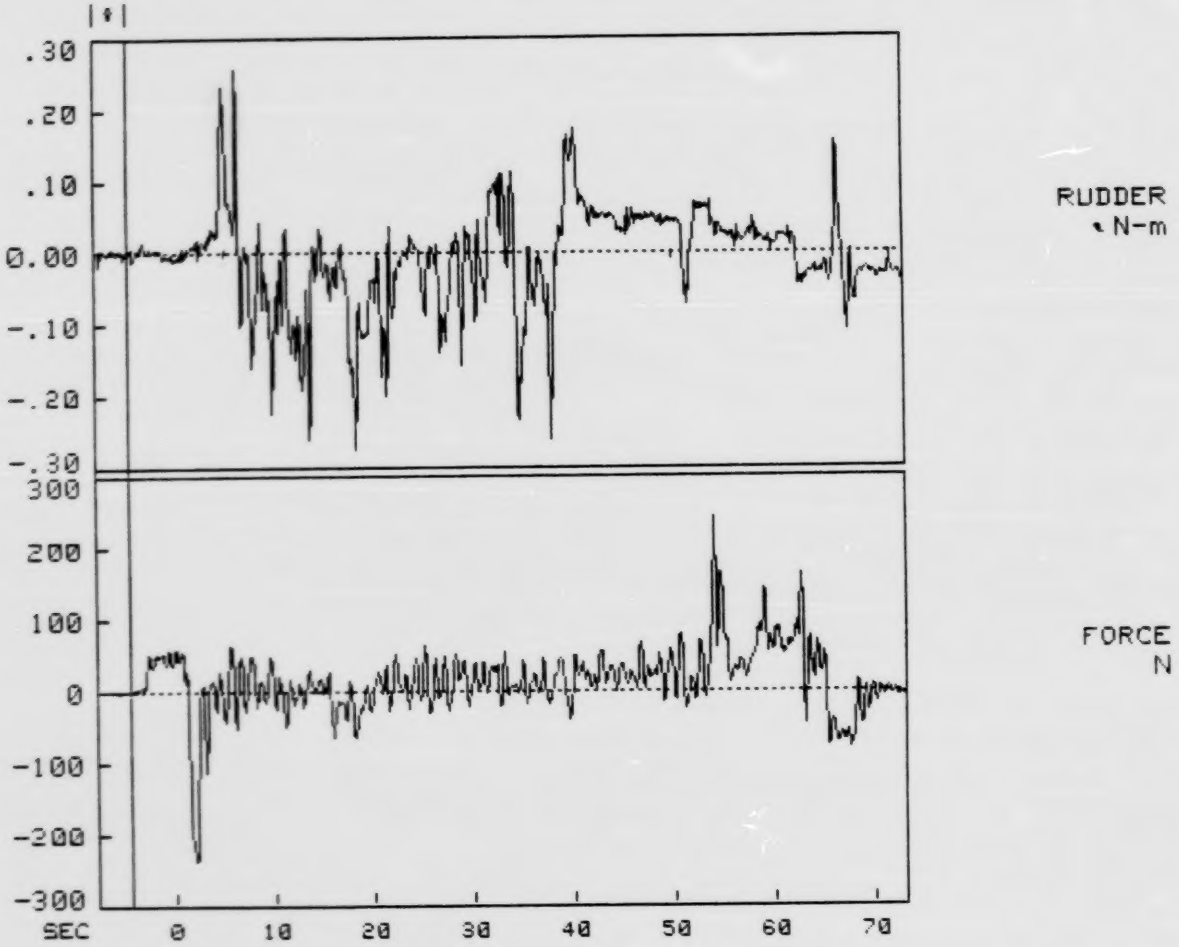

TEST 317

TEST #3 RUN 17

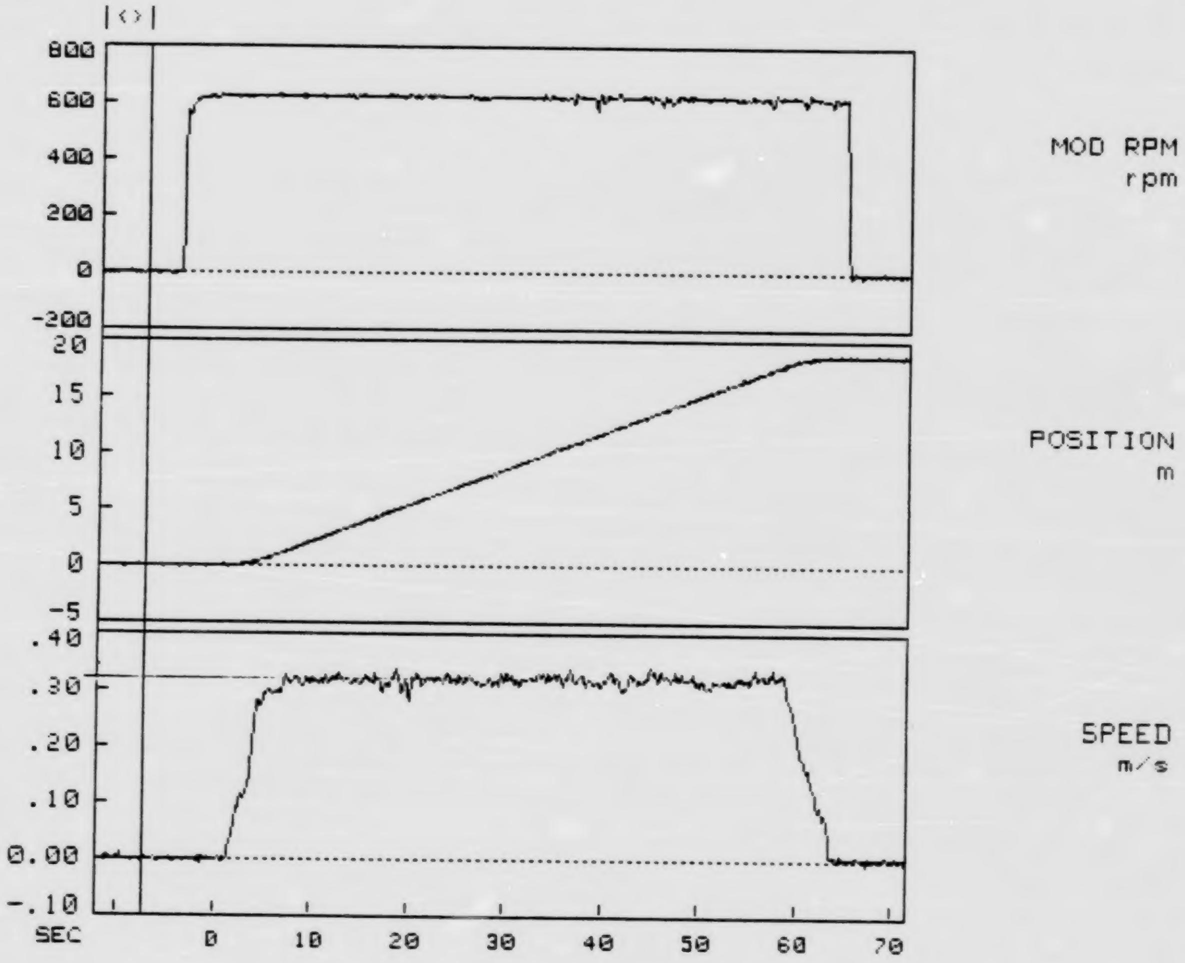

TEST 317

TEST #3 RUN 17

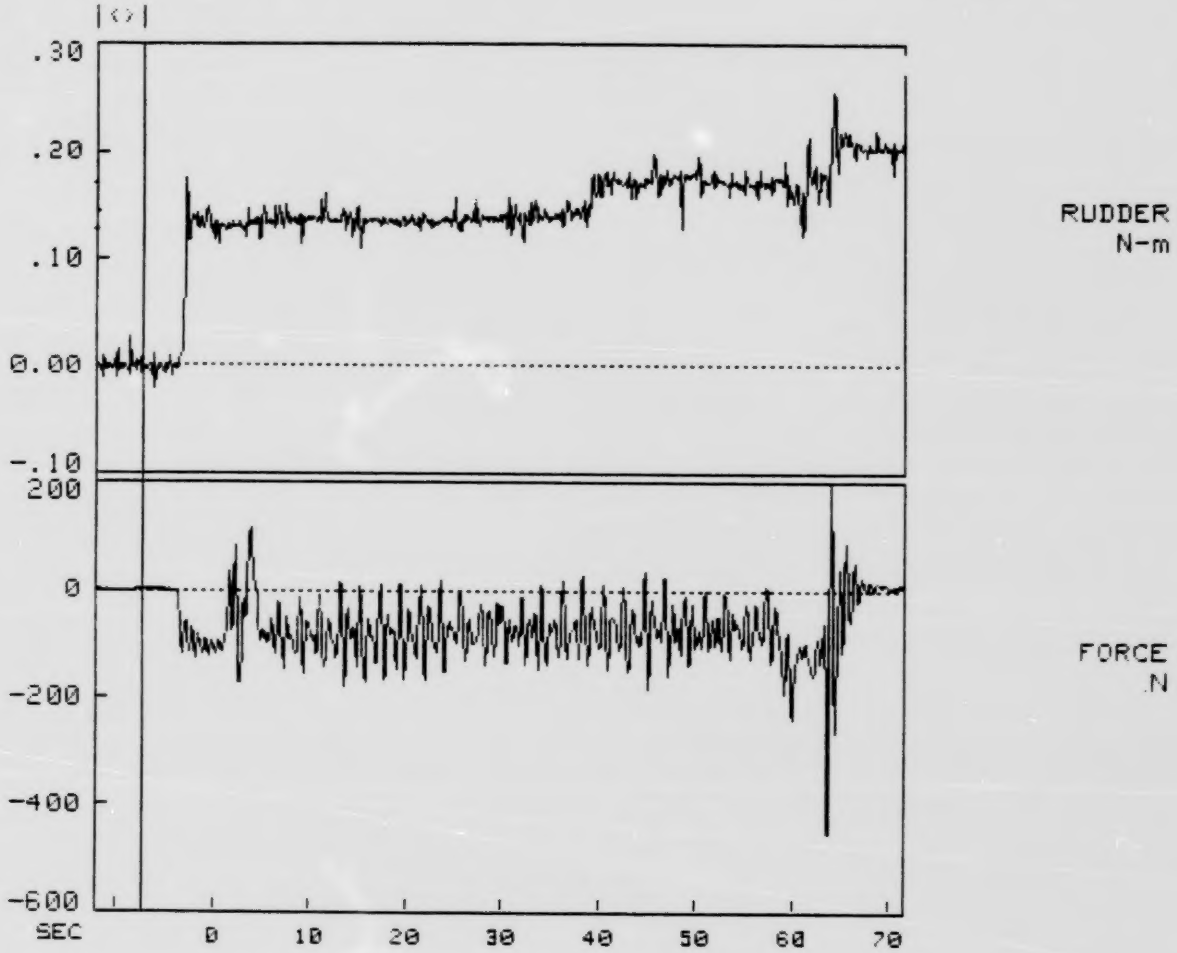

TEST 318

TEST #3 RUN 18

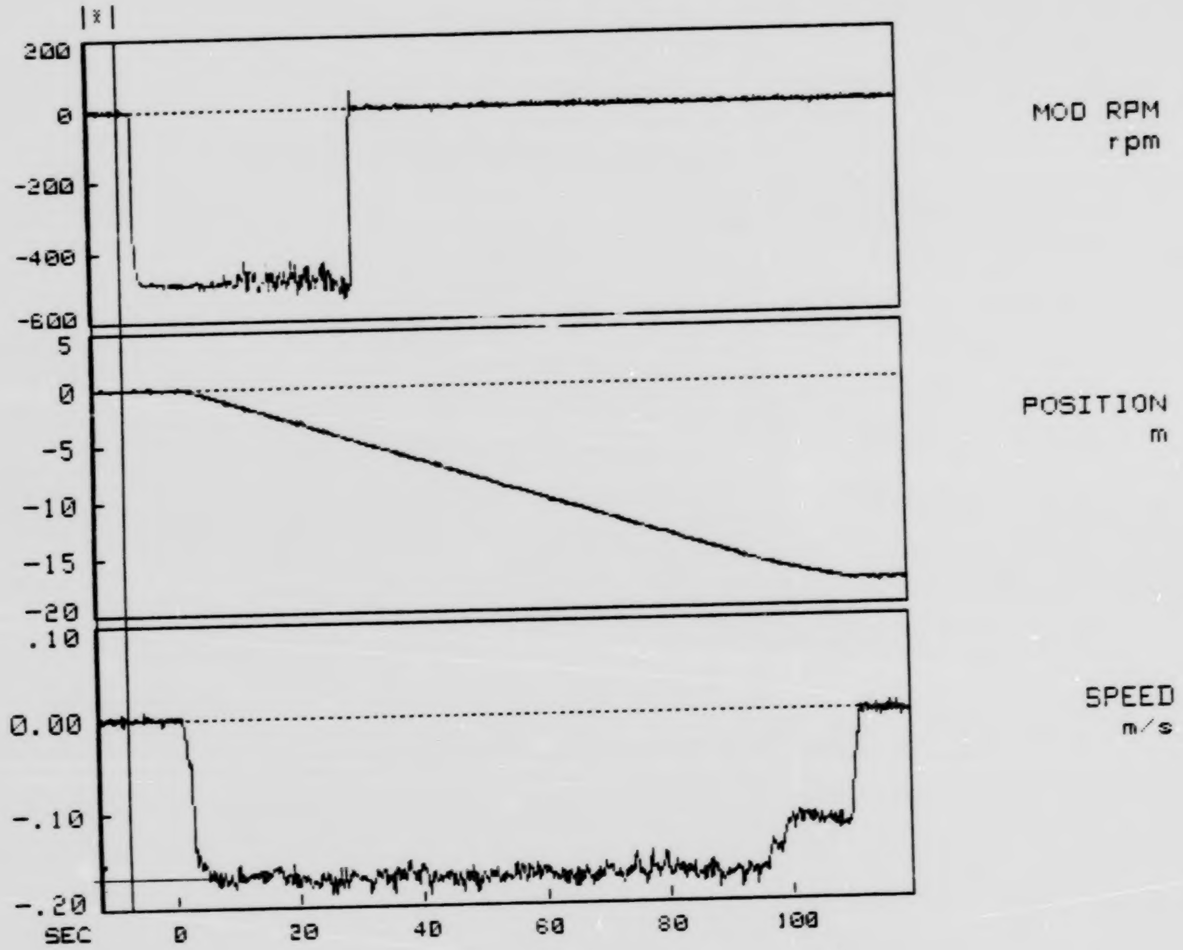

TEST #3 RUN 18 TEST 318

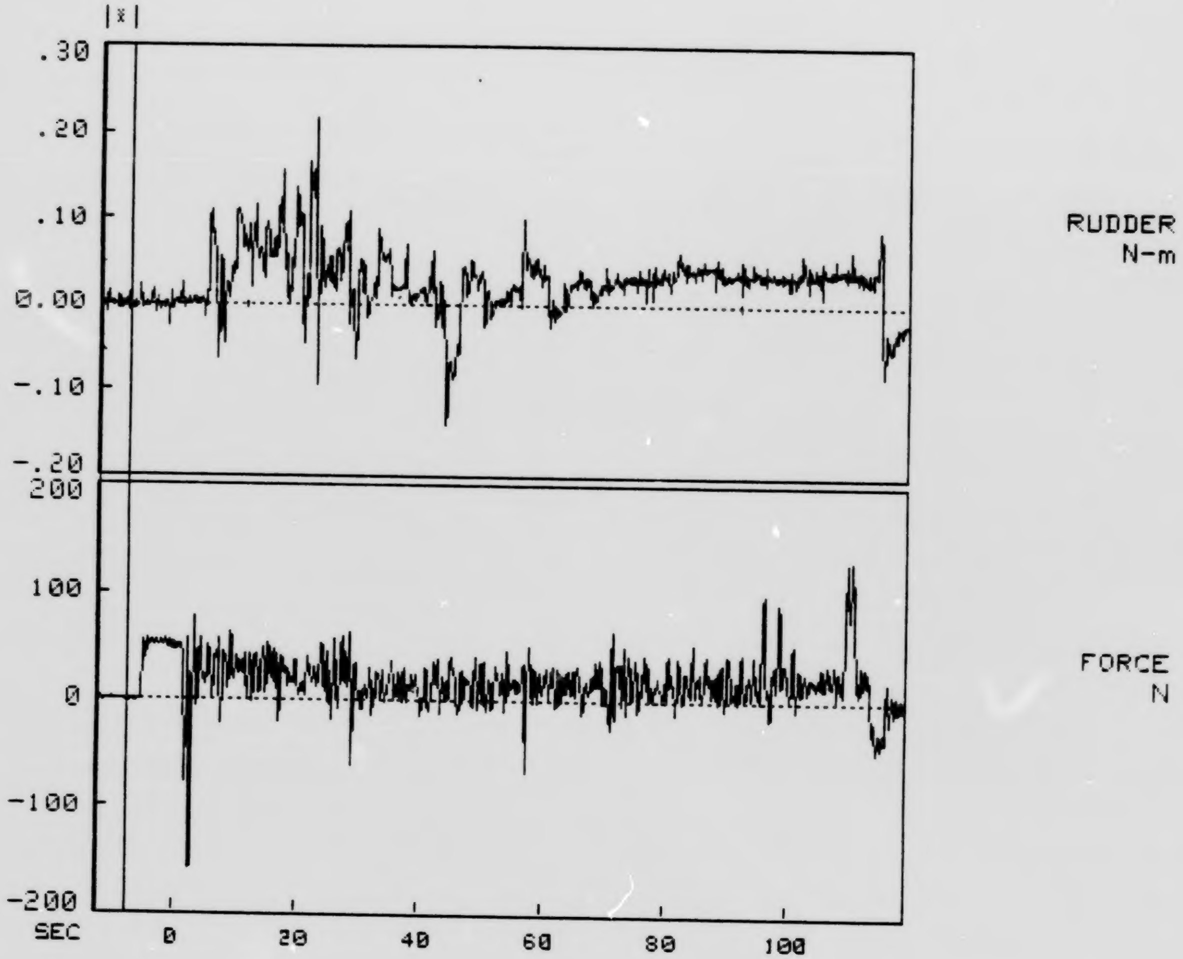

TEST 319

TEST #3 RUN 19

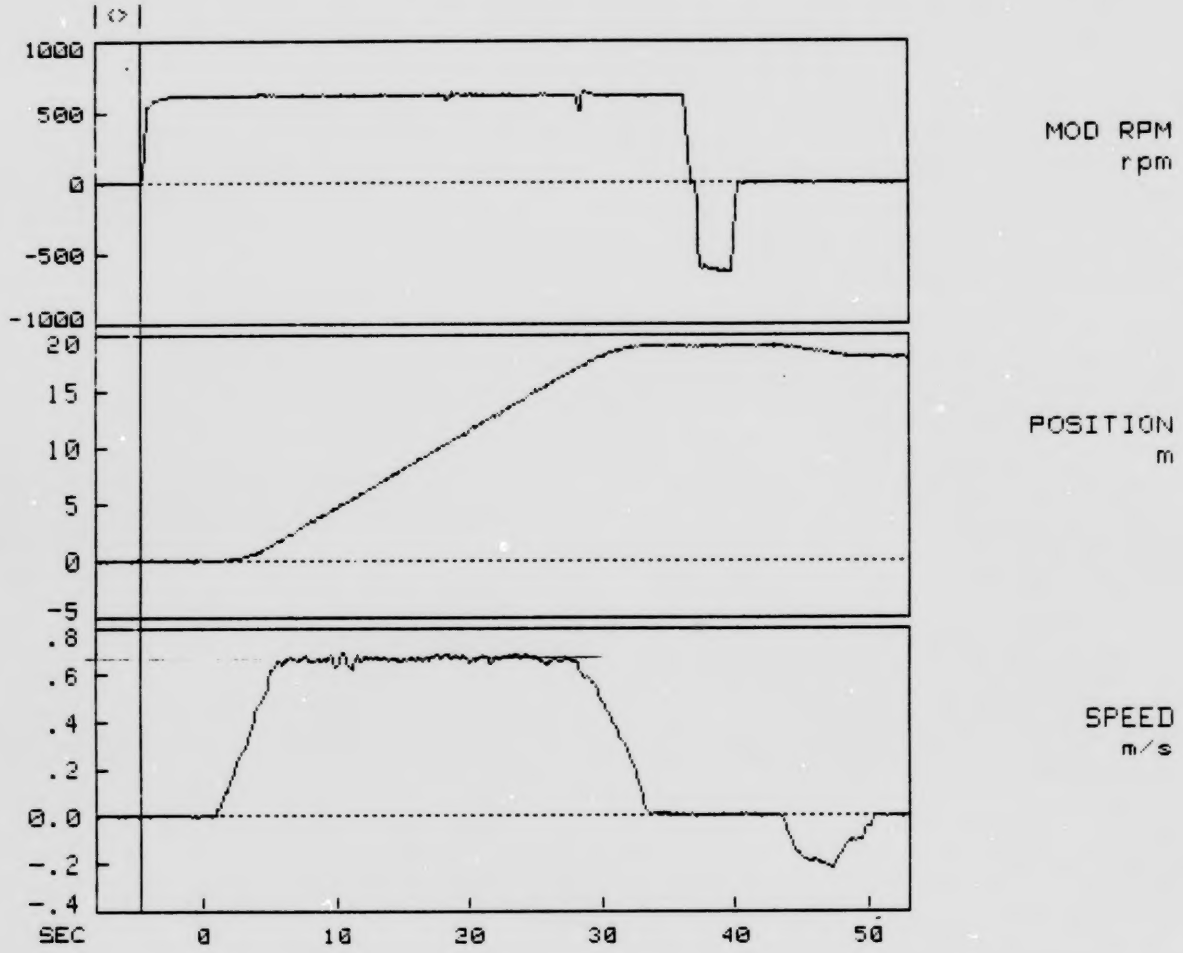

TEST 319

TEST #3 RUN 19

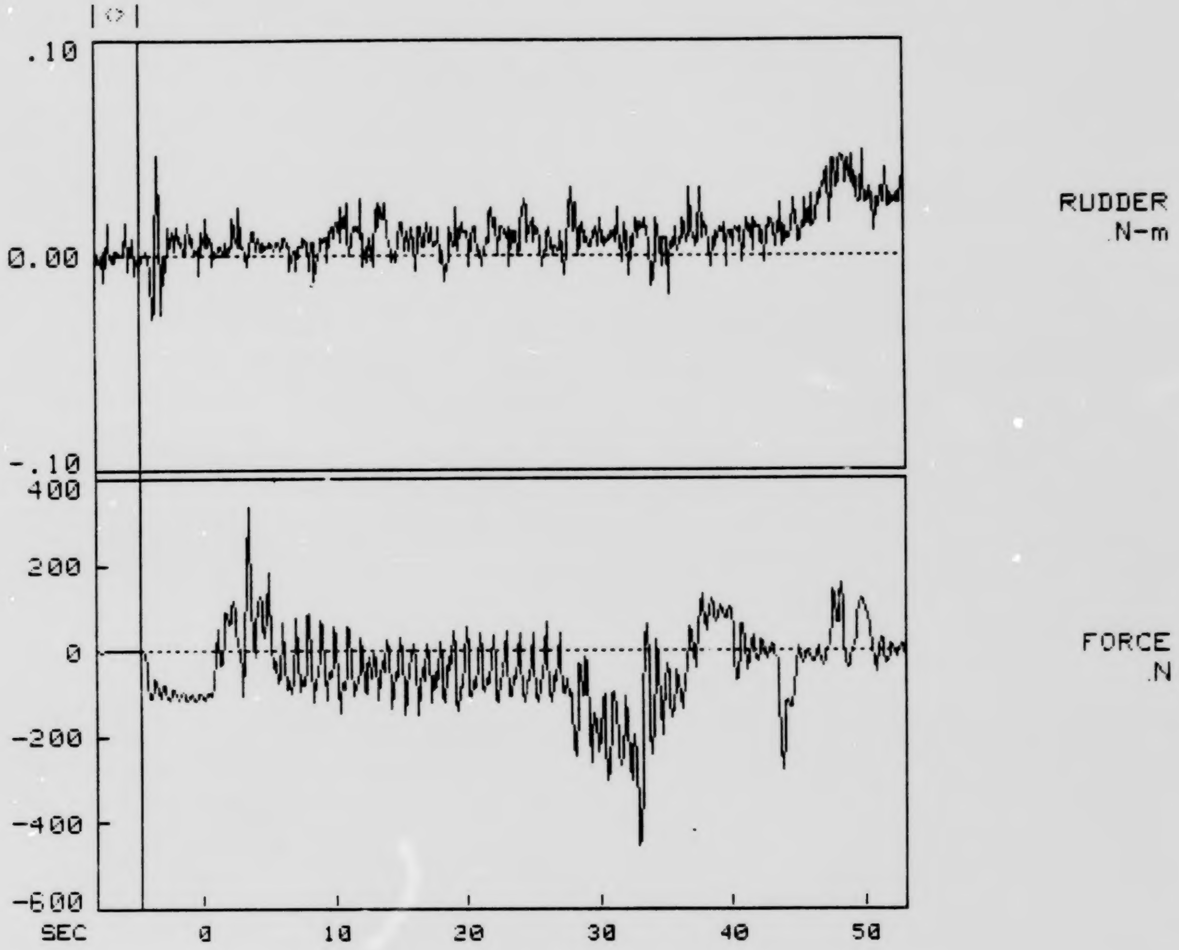

TEST 320

TEST #3 RUN 20

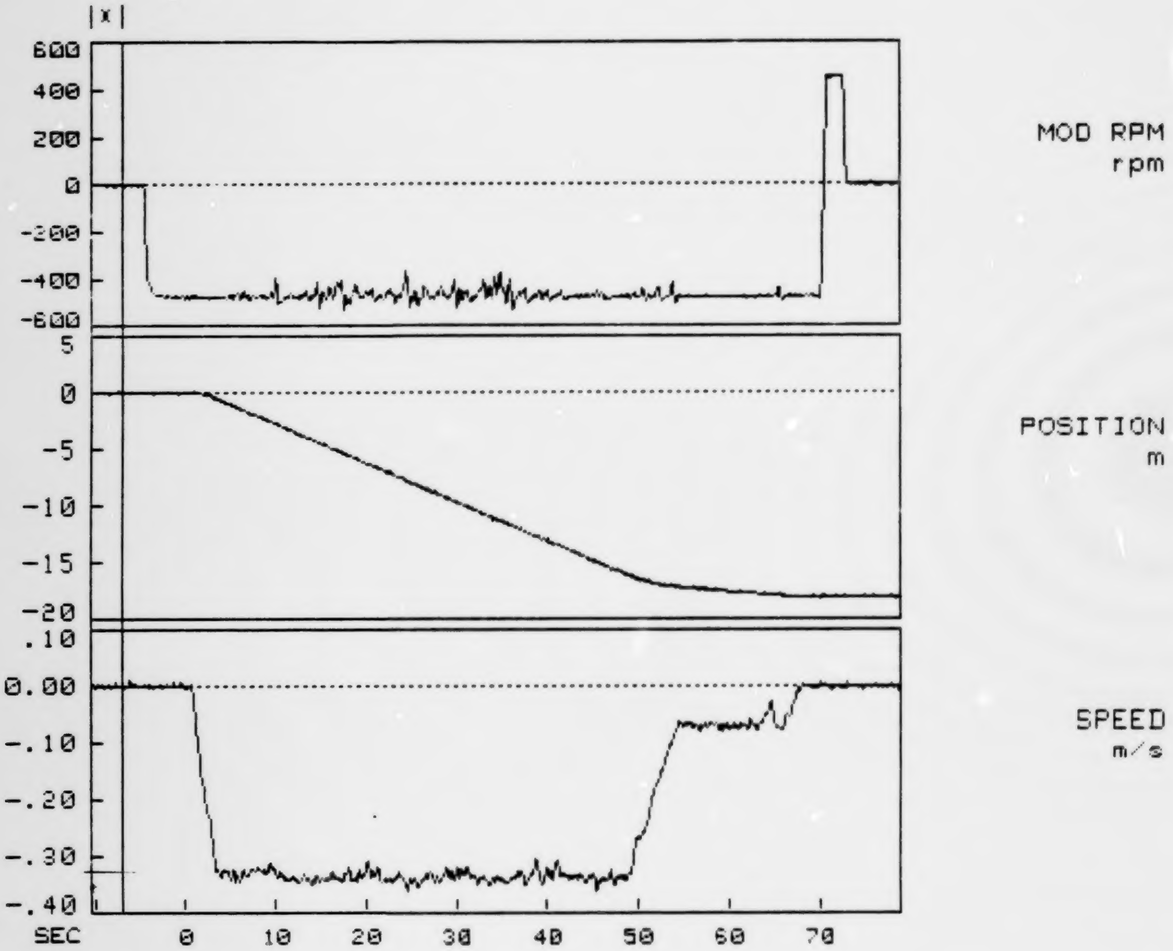

TEST 320

TEST #3 RUN 20

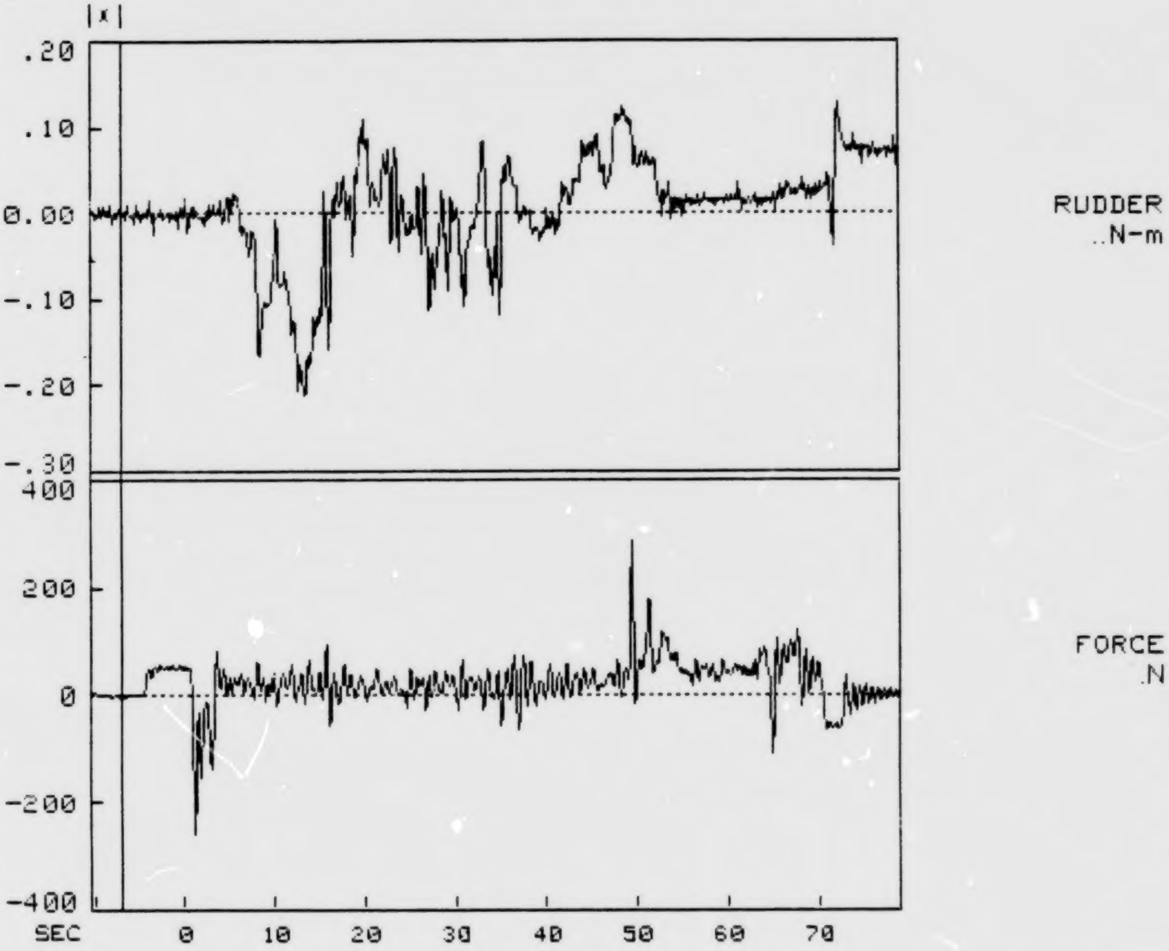

TEST 321

TEST #3 RUN 21

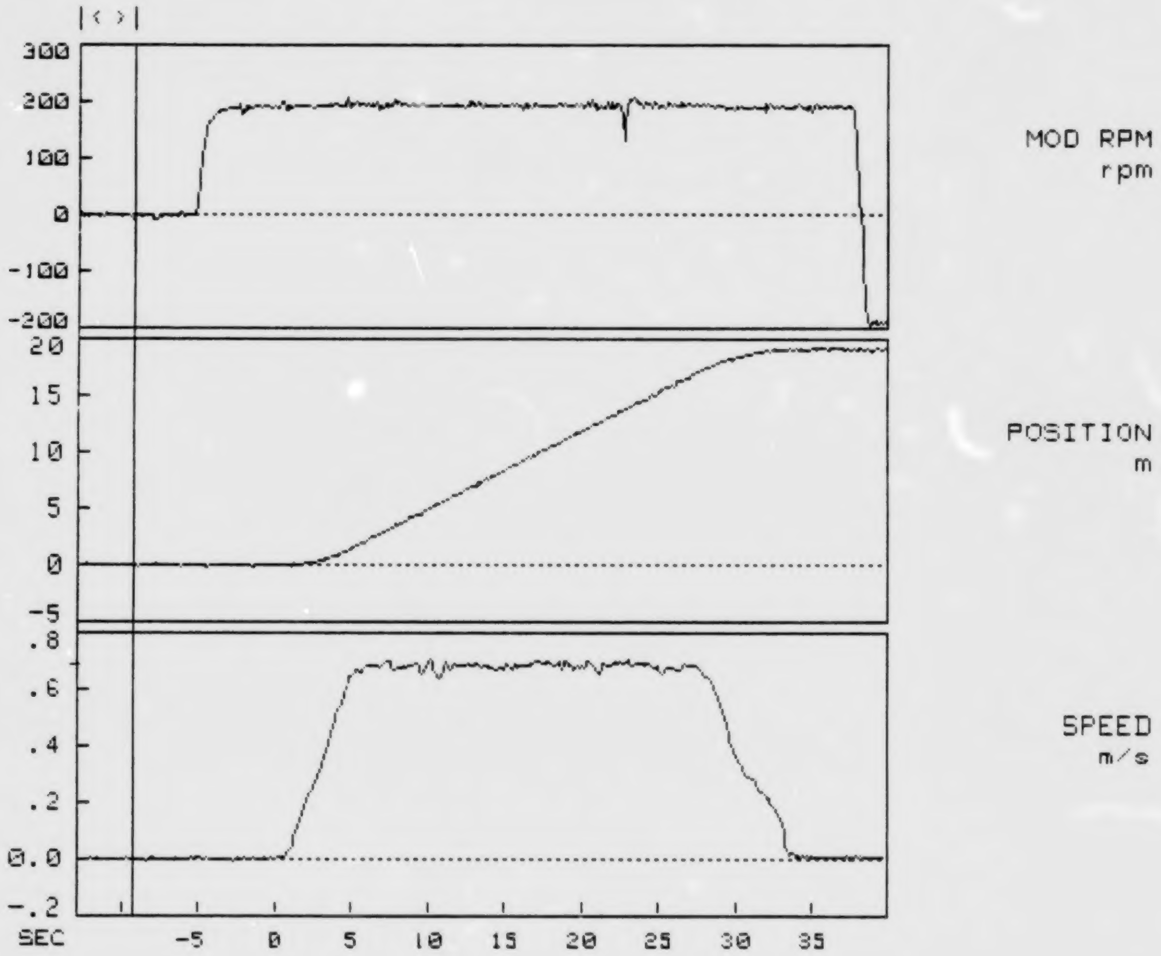

TEST #3 RUN 21 TEST 321

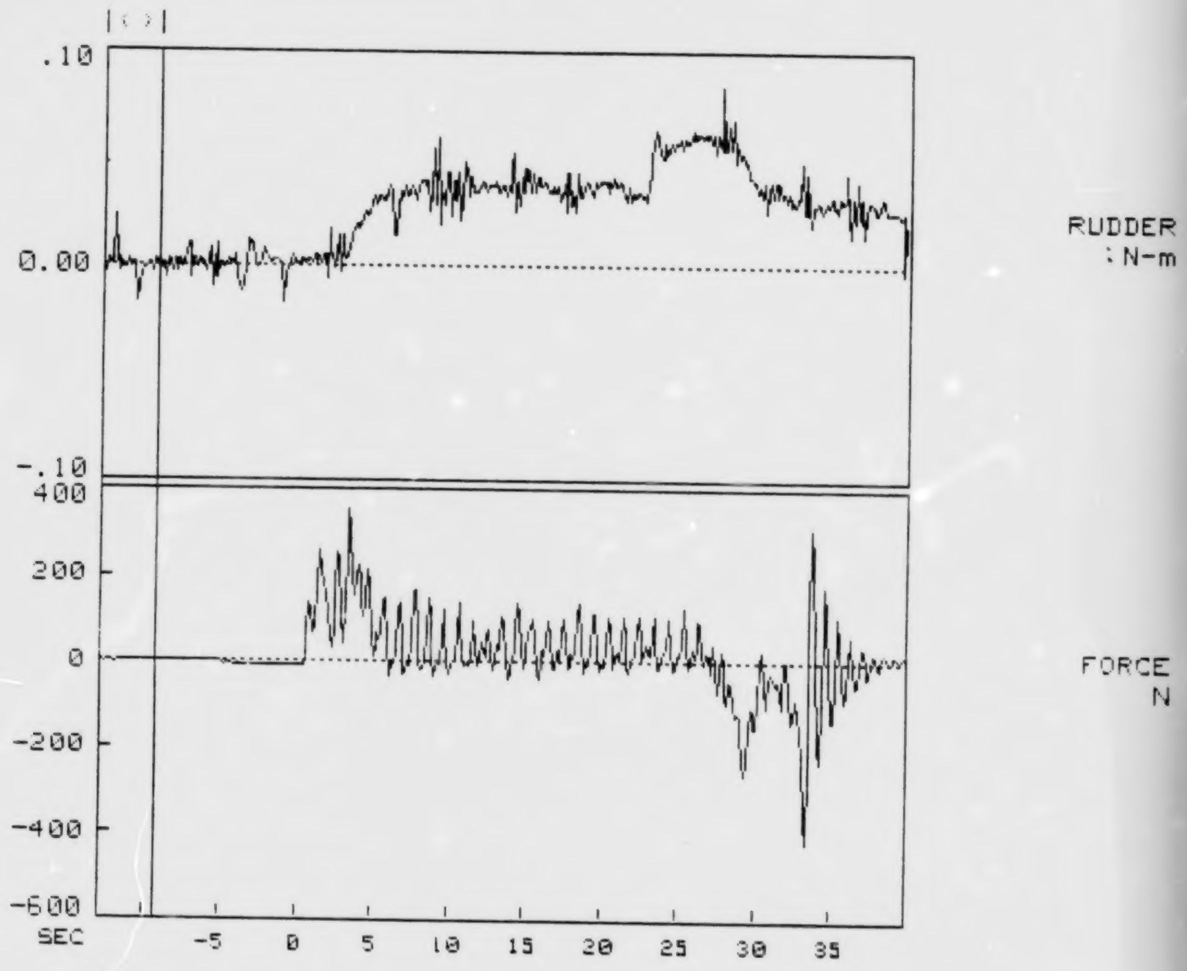

TEST #3 RUN 22 TEST 322

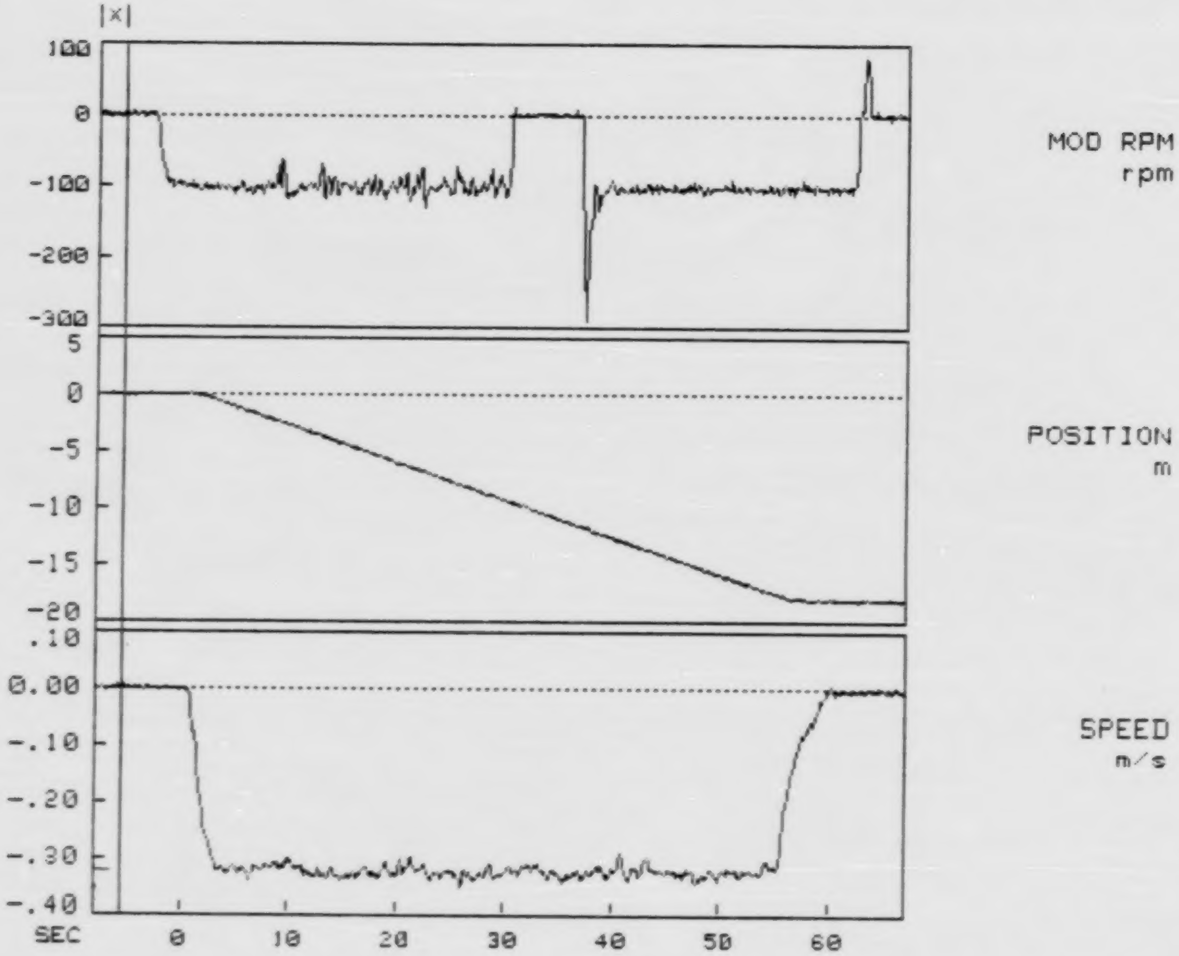

TEST #3 RUN 22 TEST 322

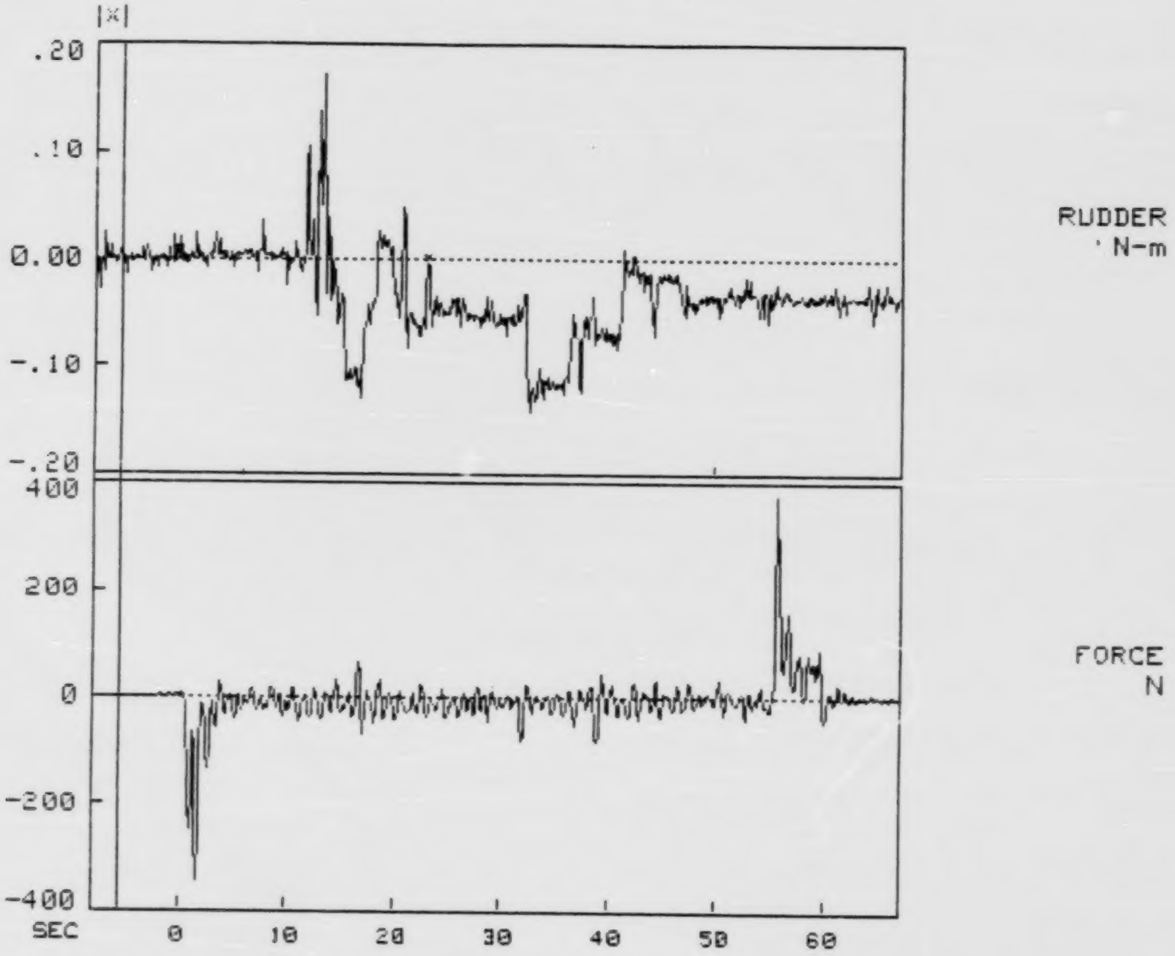

TEST #3 RUN 23 TEST 323

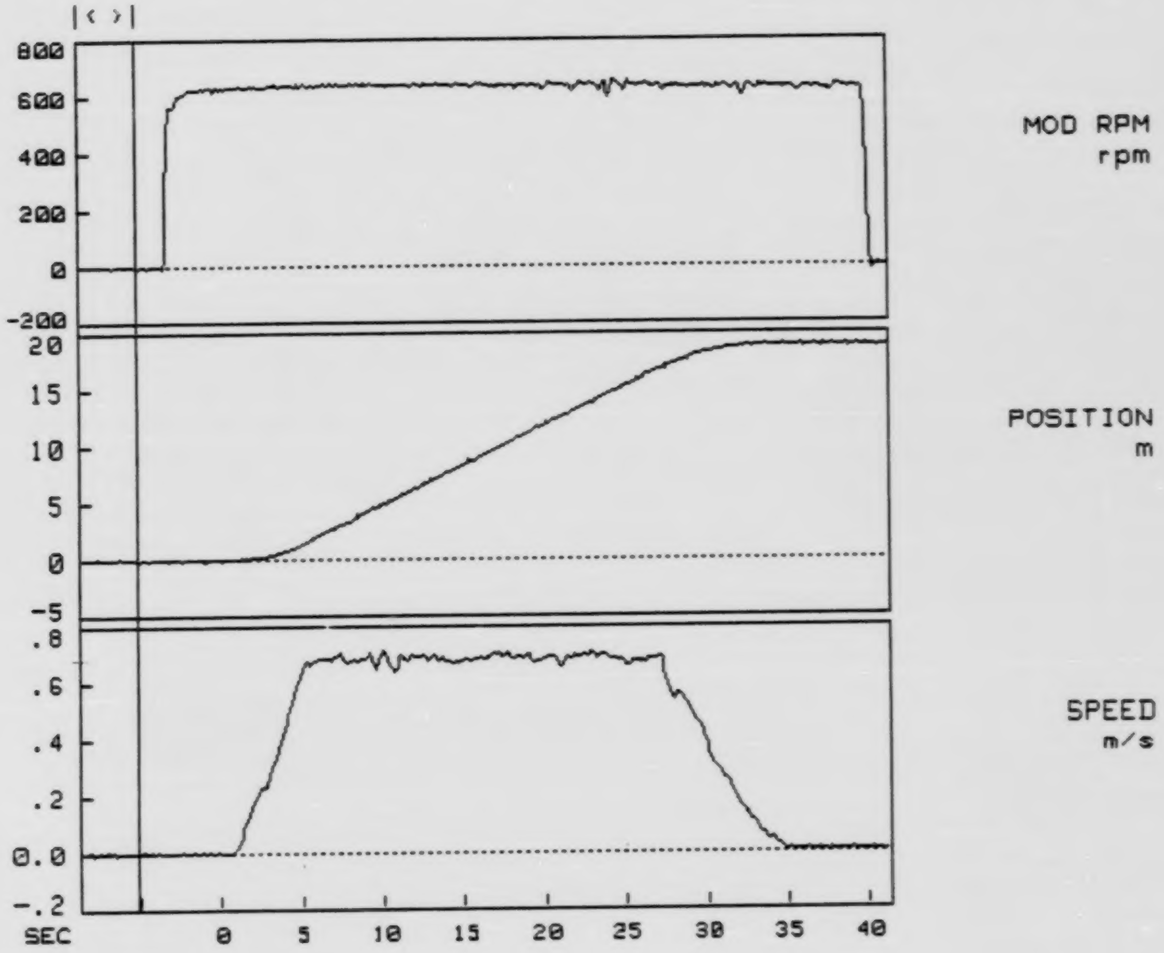

TEST 323

TEST #3 RUN 23

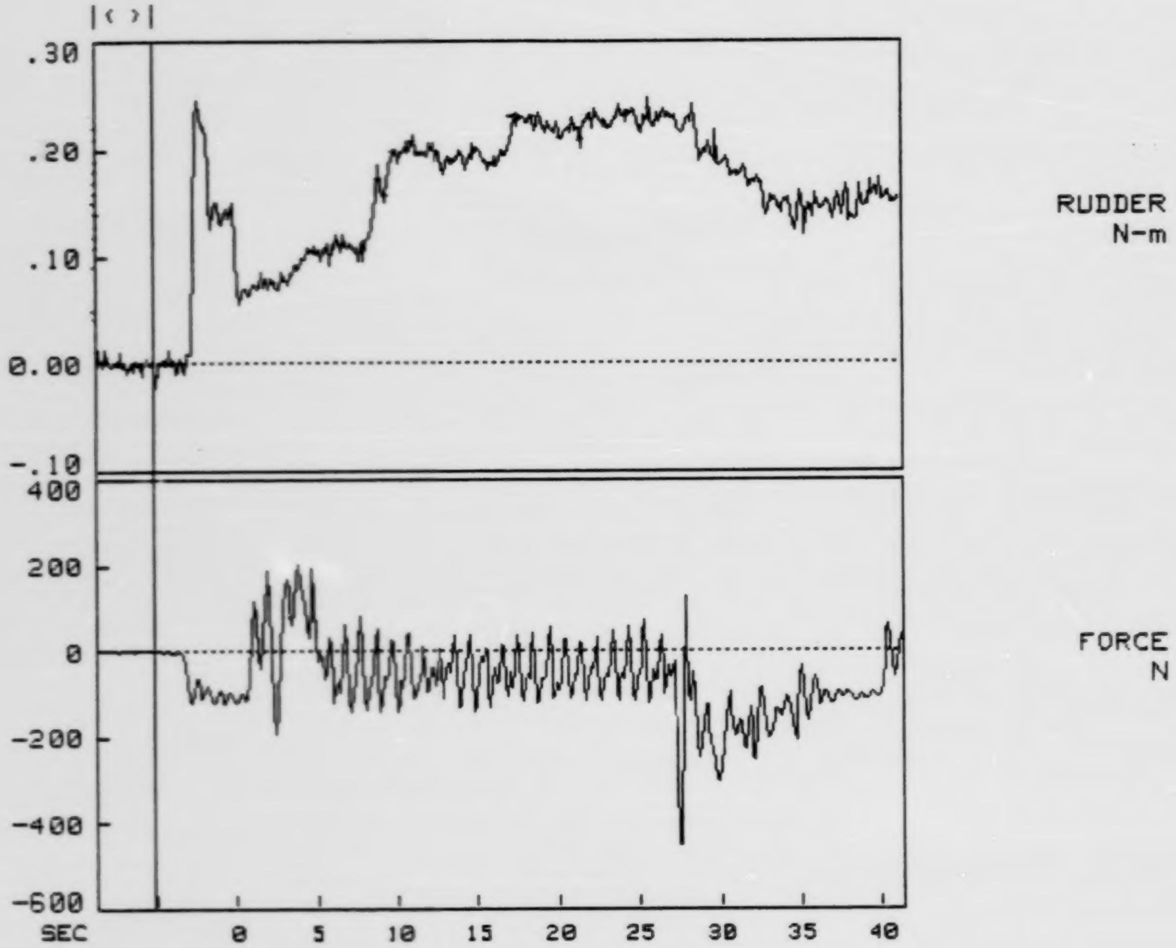

TEST 324

TEST #3 RUN 24

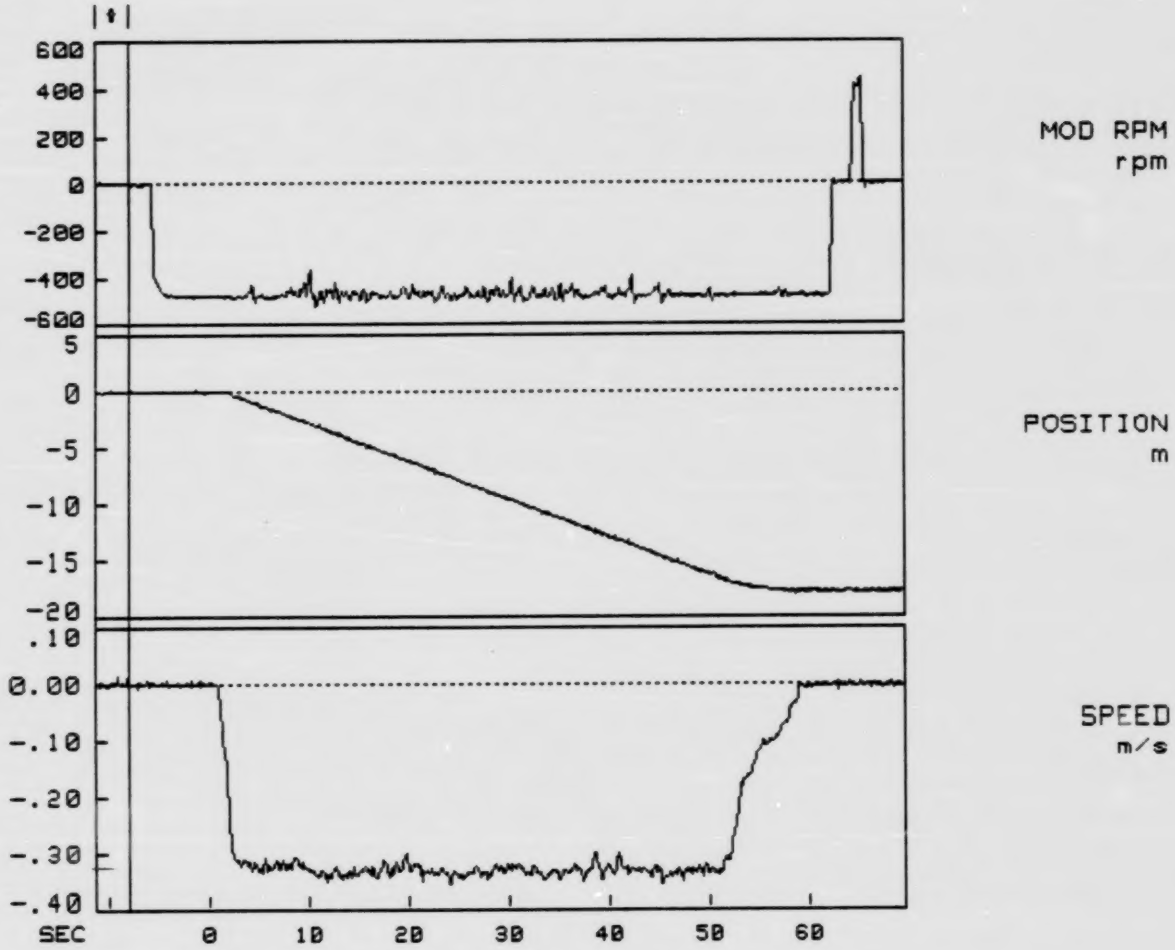

TEST 324

TEST #3 RUN 24

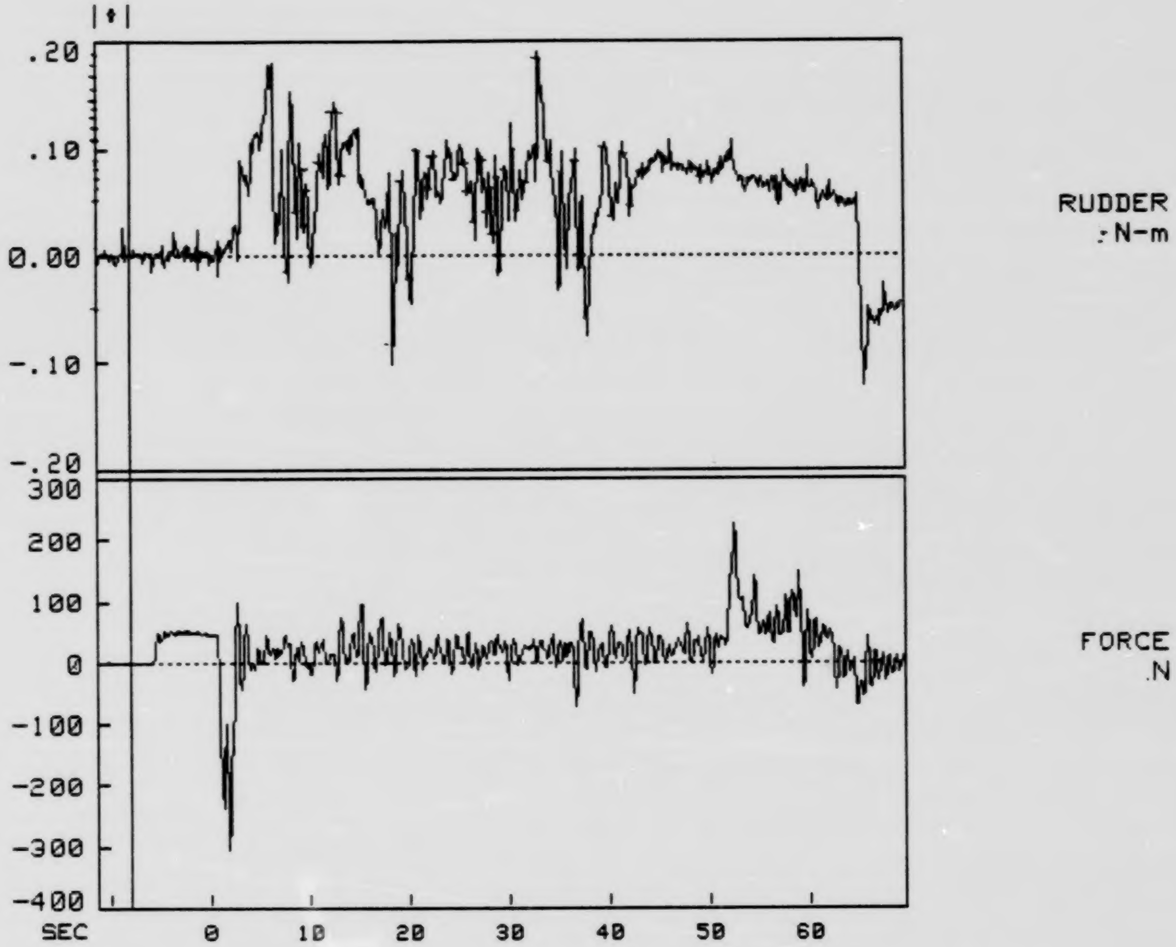

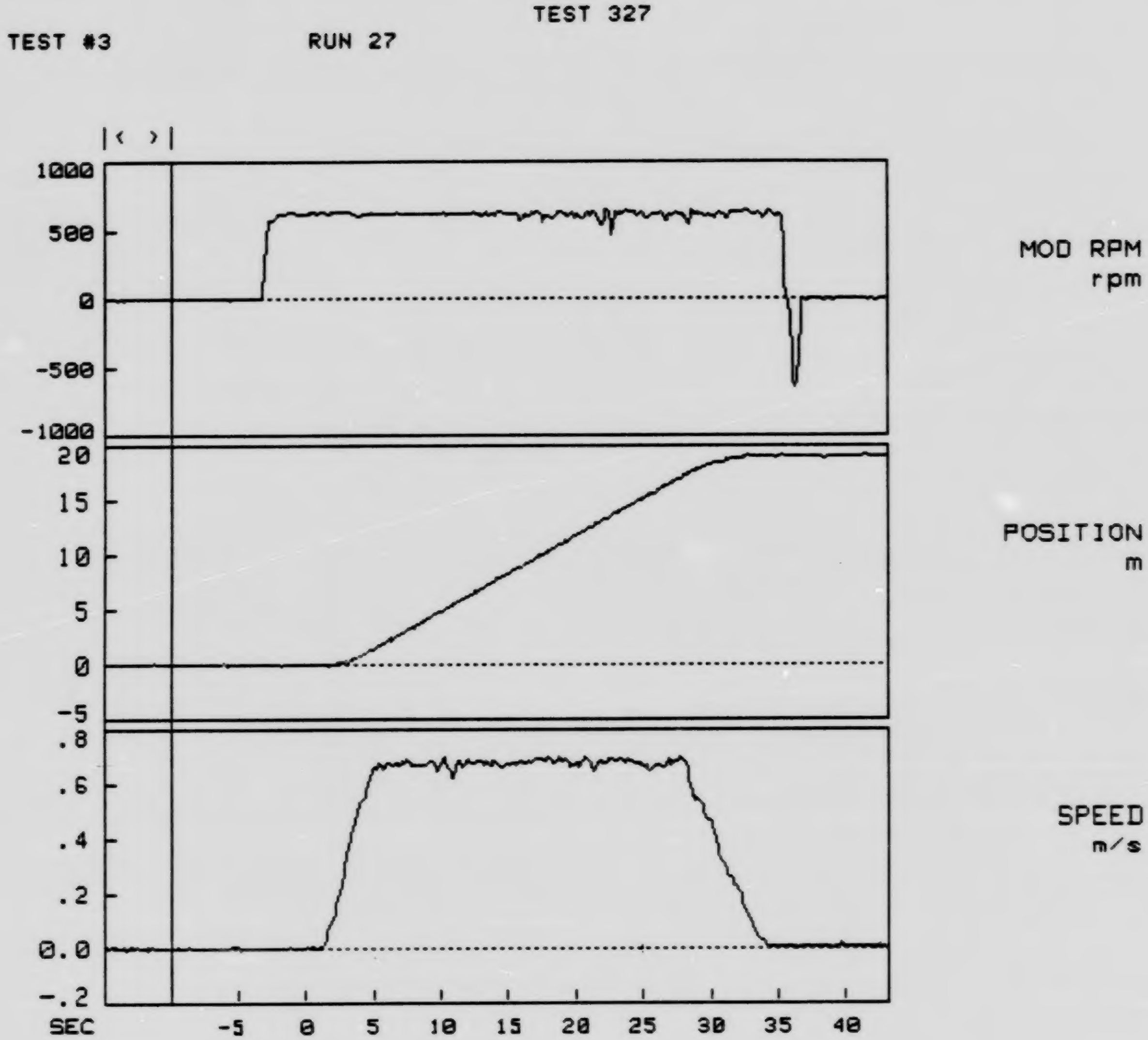
TEST 327
TEST #3
RUN 27
|< >|
1000
500
0
-500
-1000
MOD RPM
rpm
20
15
10
5
0
-5
POSITION
m
.8
.6
.4
.2
0.0
-.2
SPEED
m/s
SEC
-5
0
5
10
15
20
25
30
35
40

TEST 327

TEST #3 RUN 27

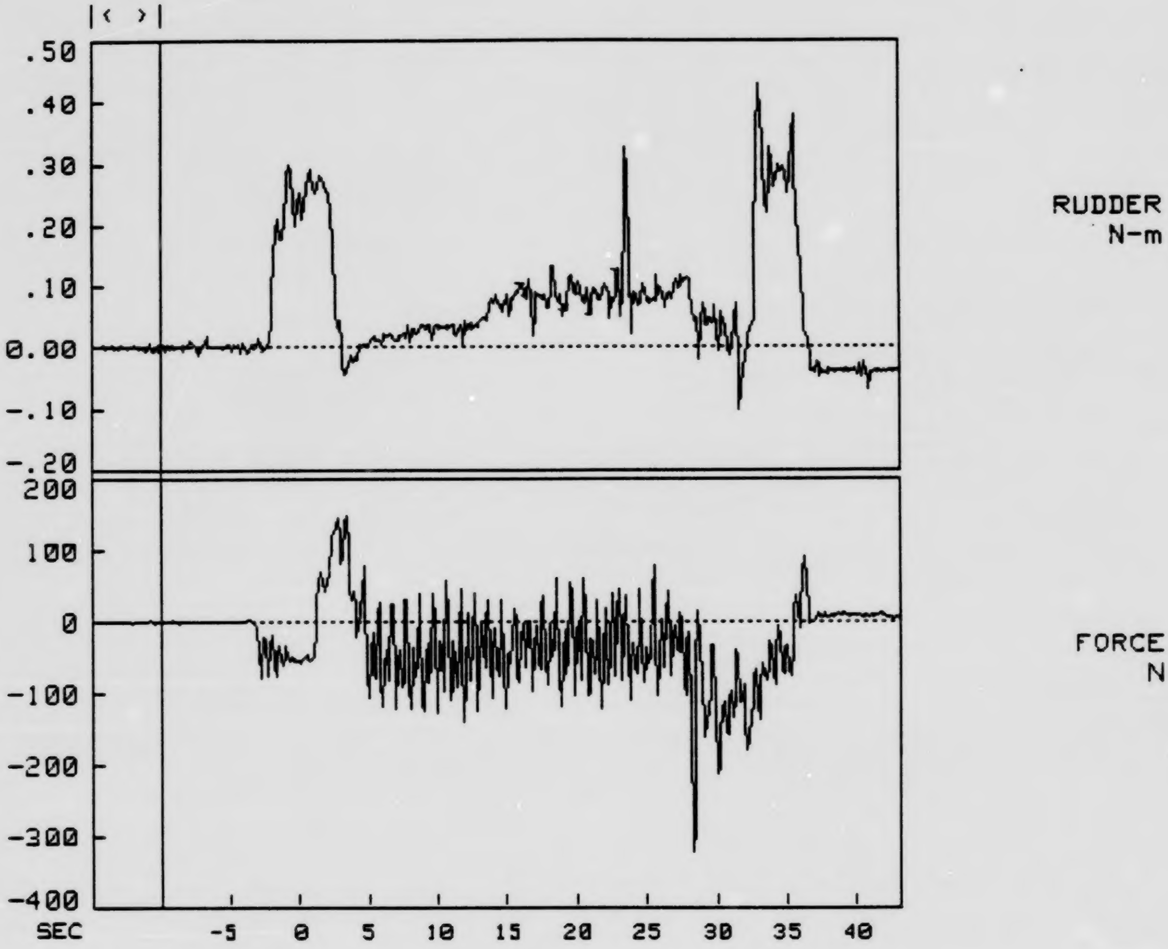

TEST 328

TEST #3 RUN 28

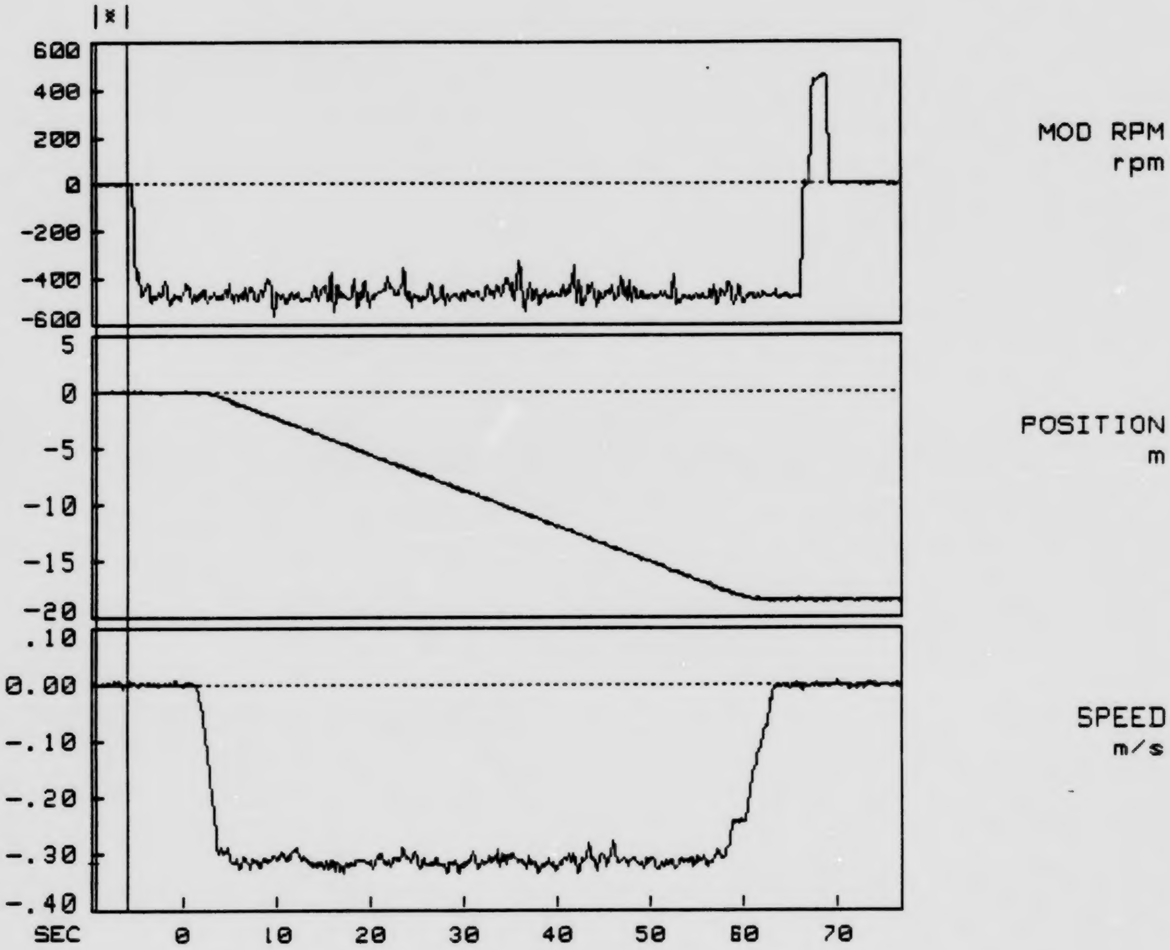

TEST 328

TEST #3 RUN 28

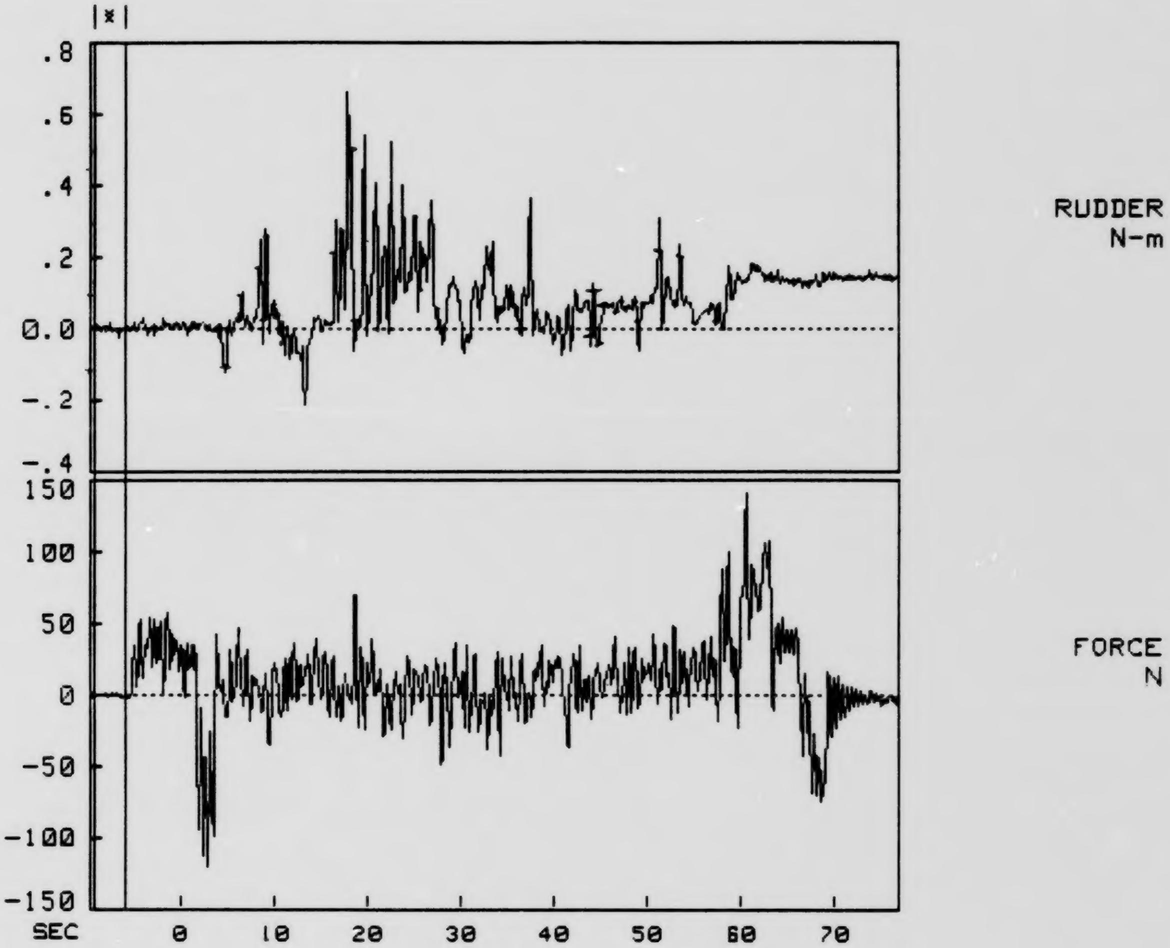

TEST 329

TEST #3 RUN 29

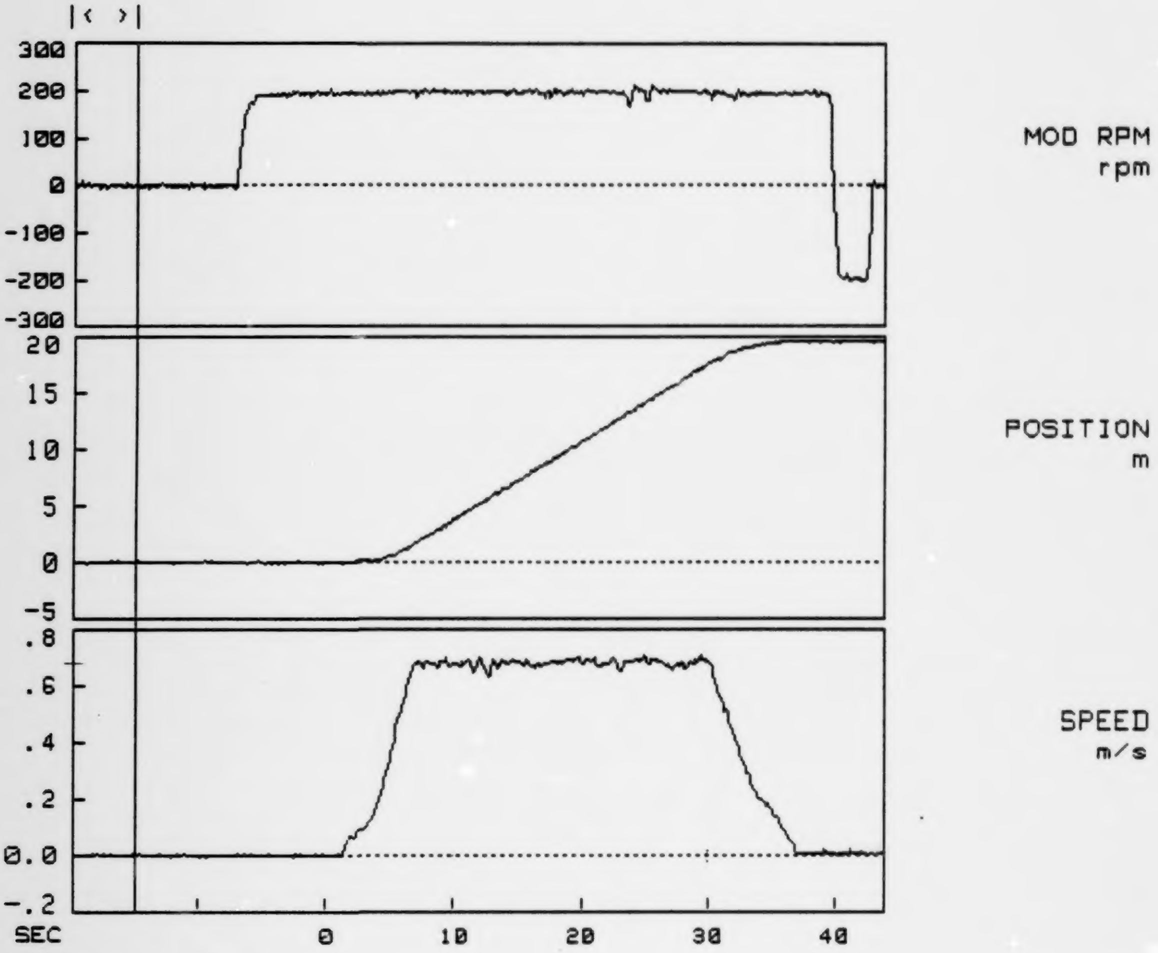

TEST 329

TEST #3 RUN 29

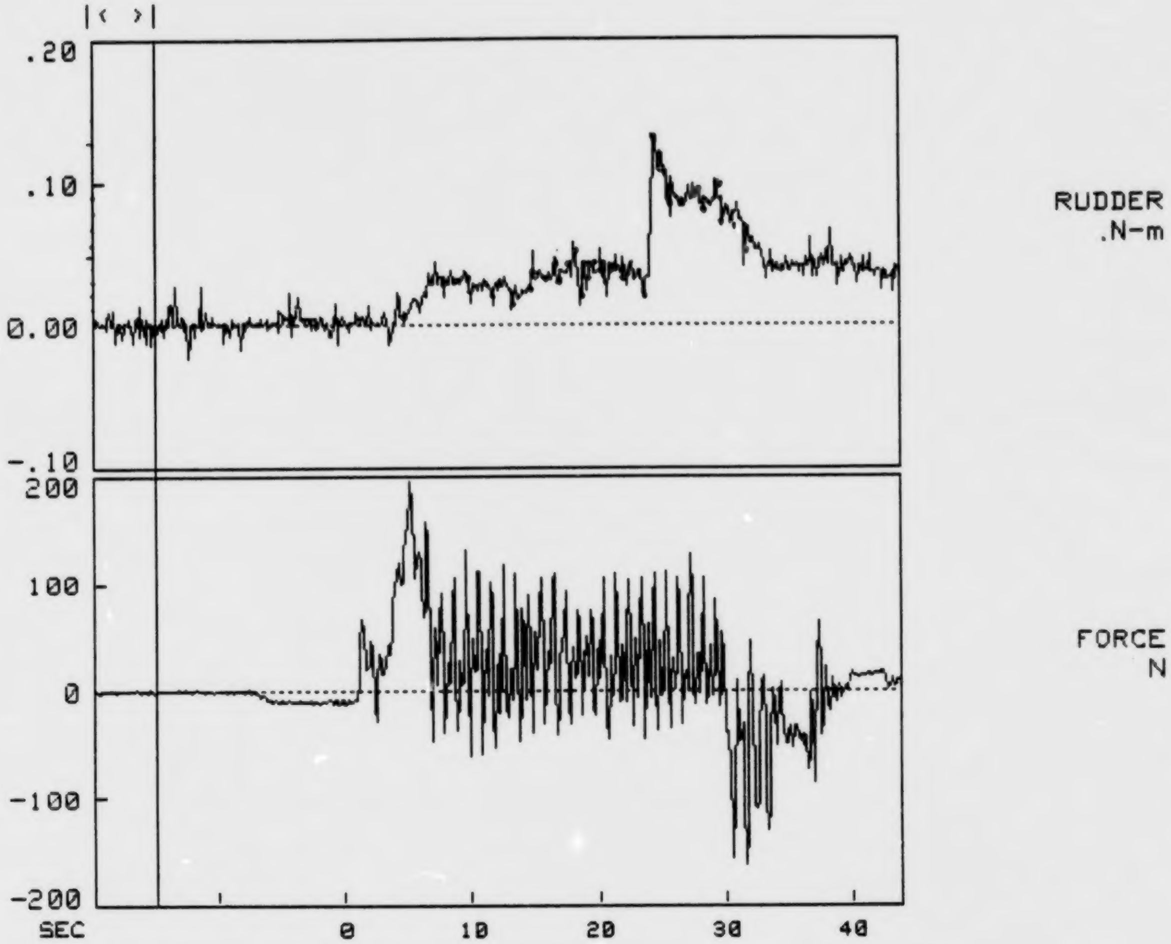

TEST 330

TEST #3 RUN 30

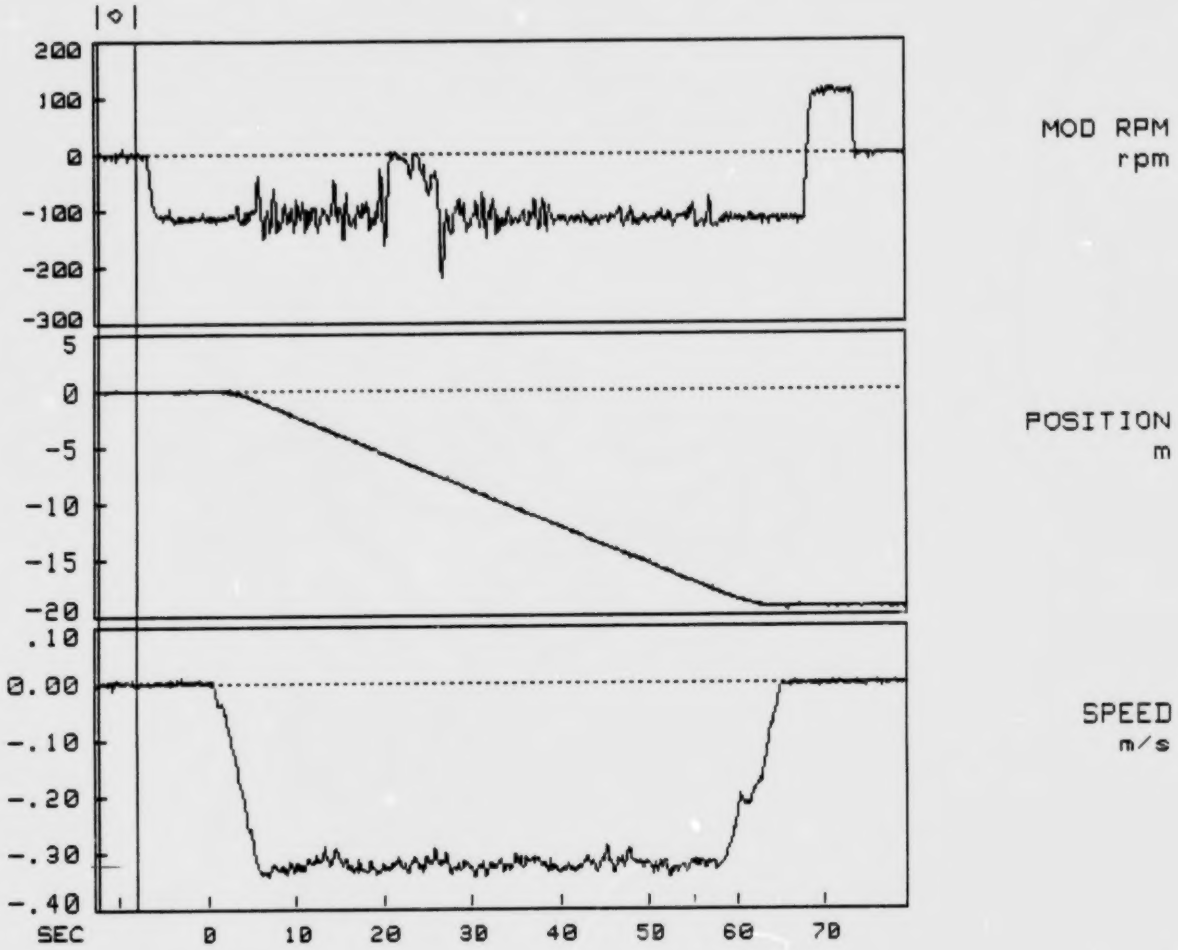

TEST 330

TEST #3 RUN 30

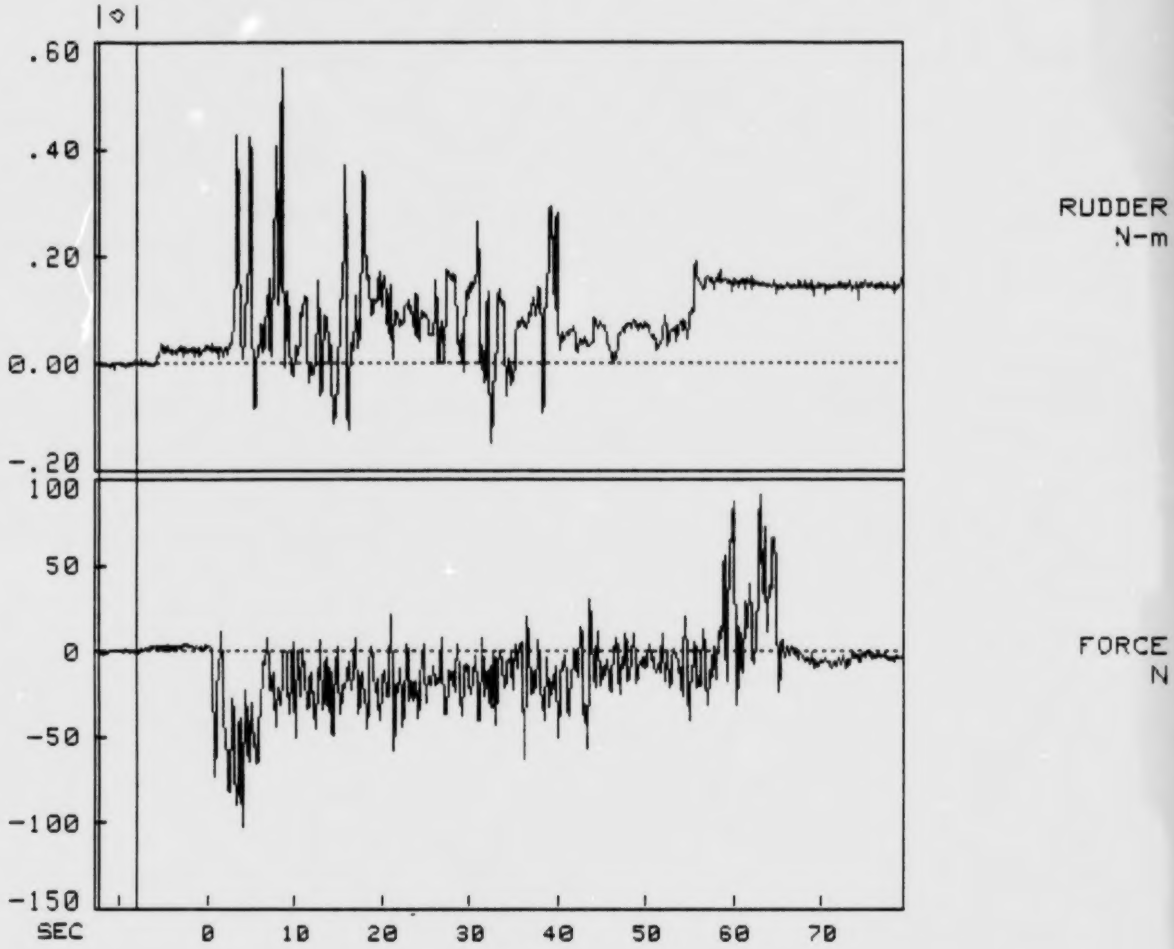

TEST #3 RUN 31 TEST 331

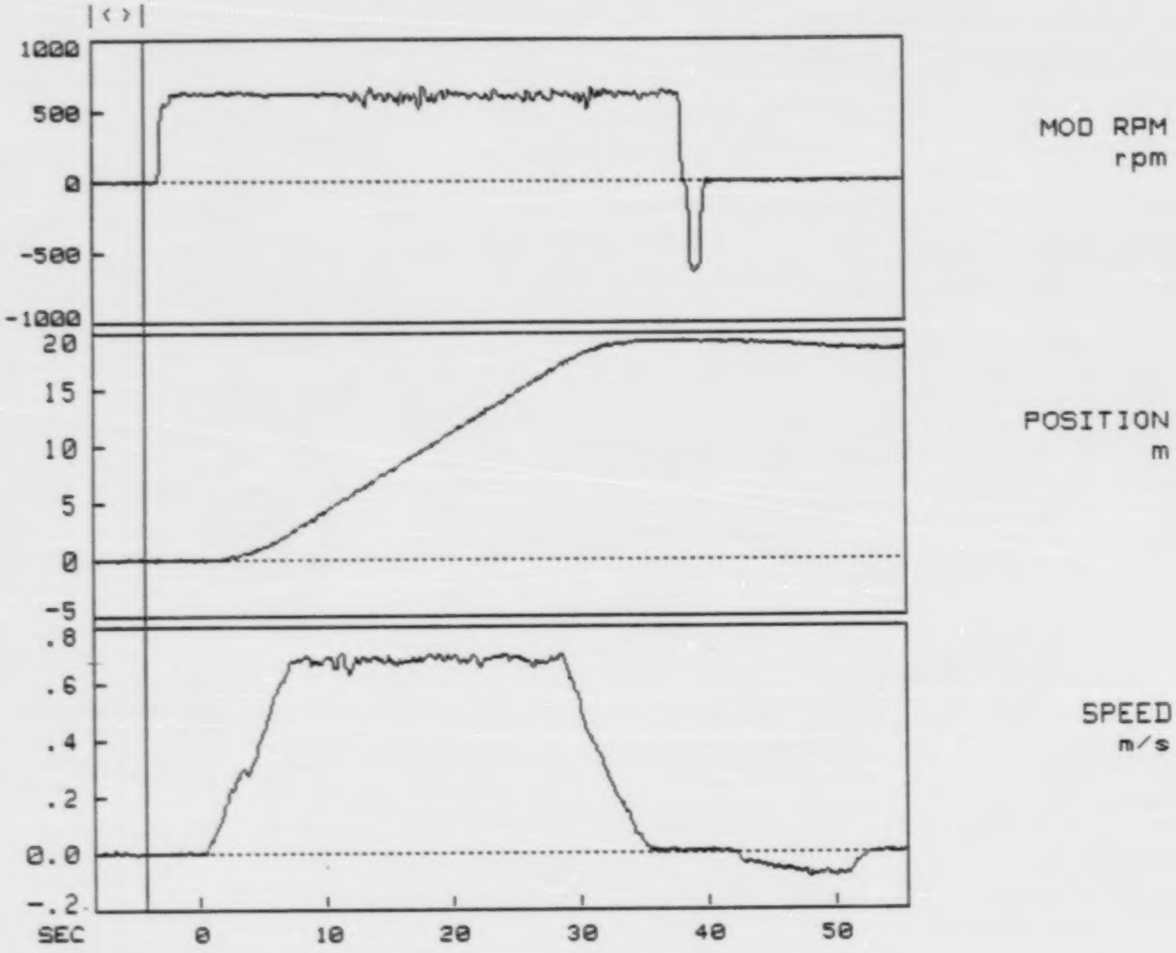

TEST #3 RUN 31 TEST 331

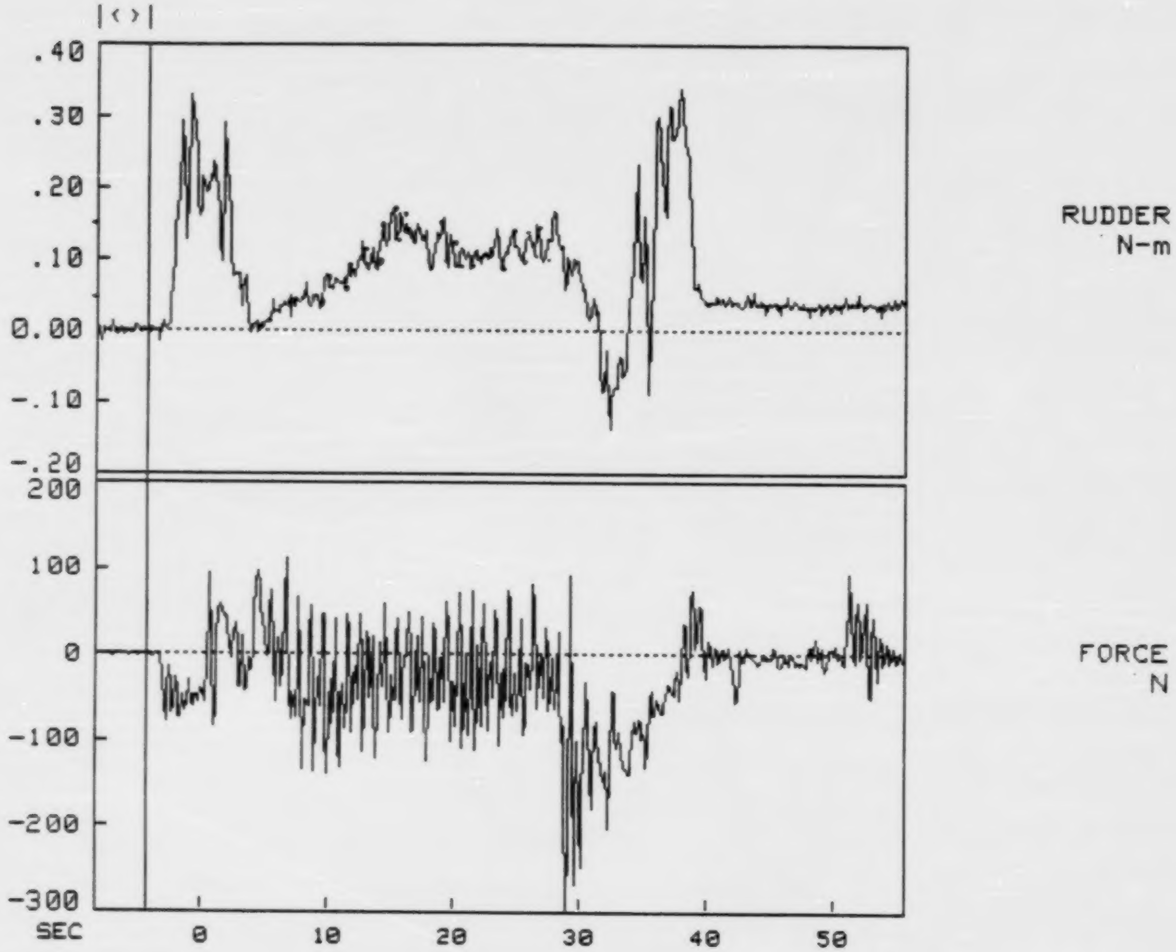

TEST #3 RUN 32 TEST 332

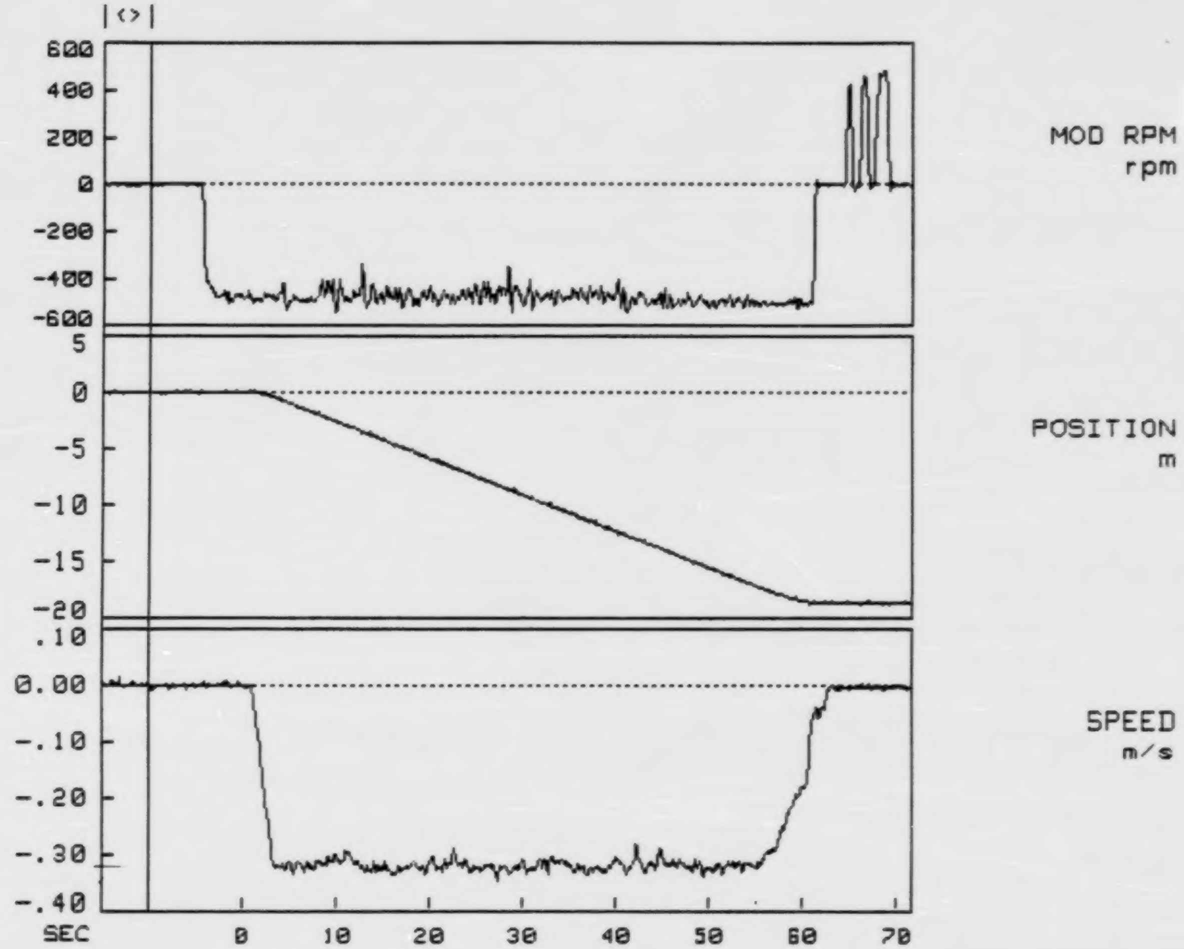

TEST 332

TEST #3 RUN 32

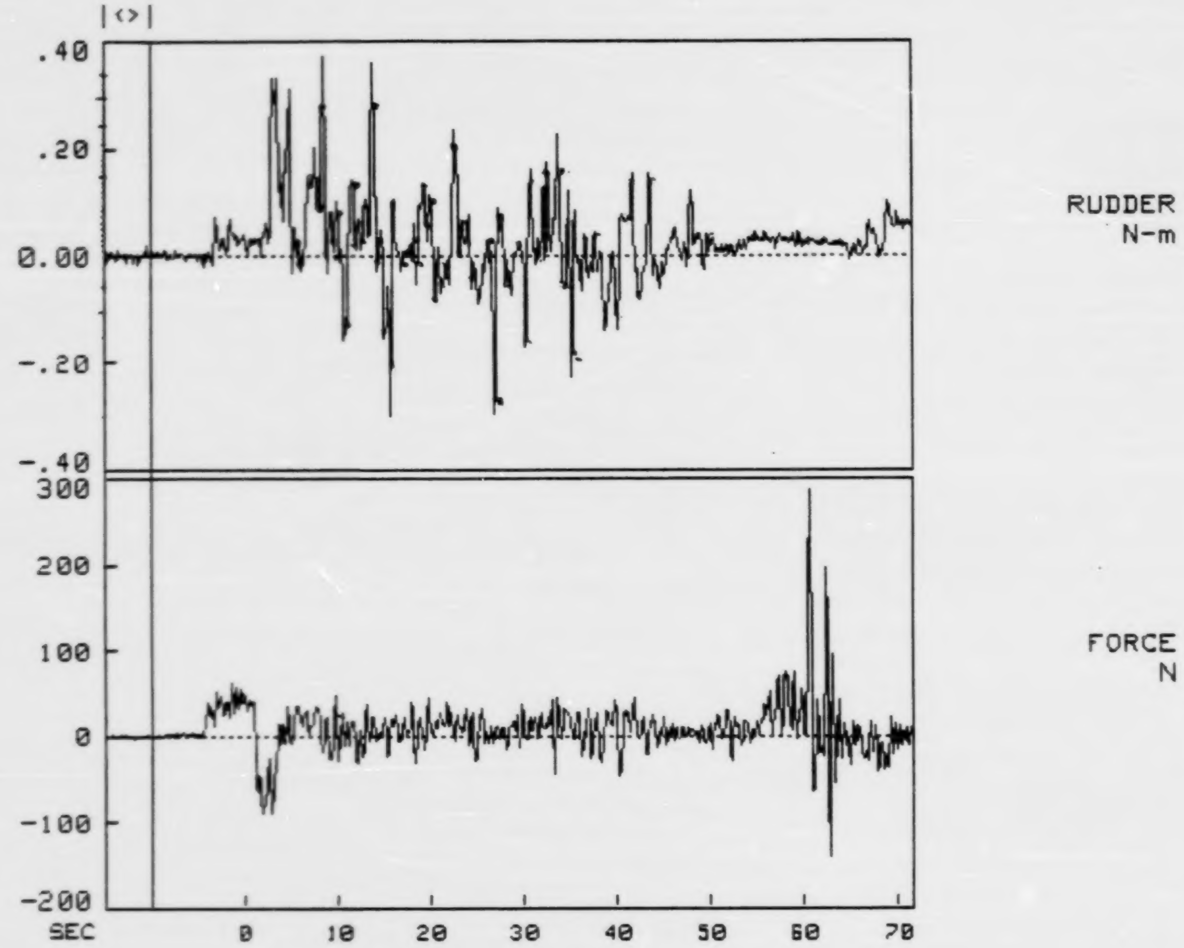

TEST 333

TEST #3 RUN 33

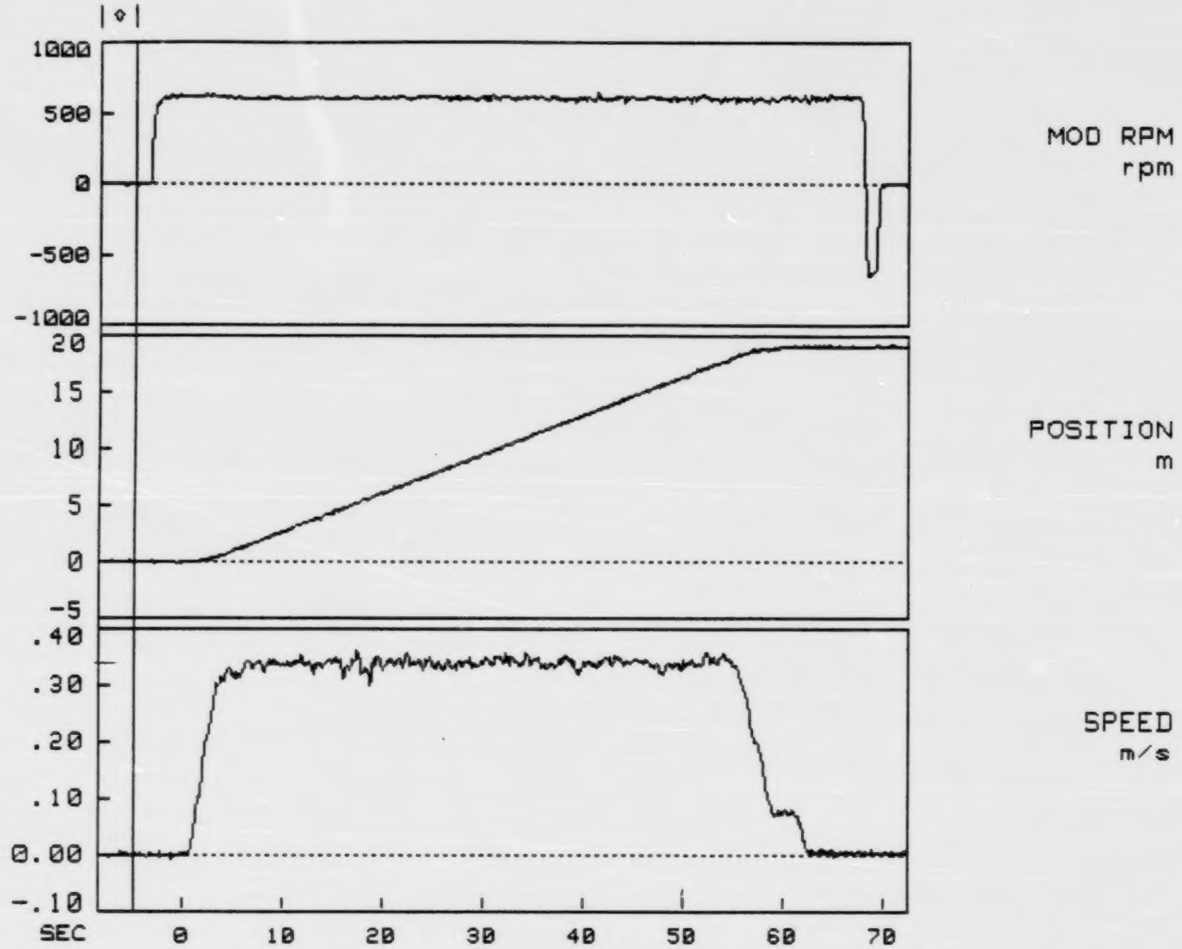

TEST 333

TEST #3 RUN 33

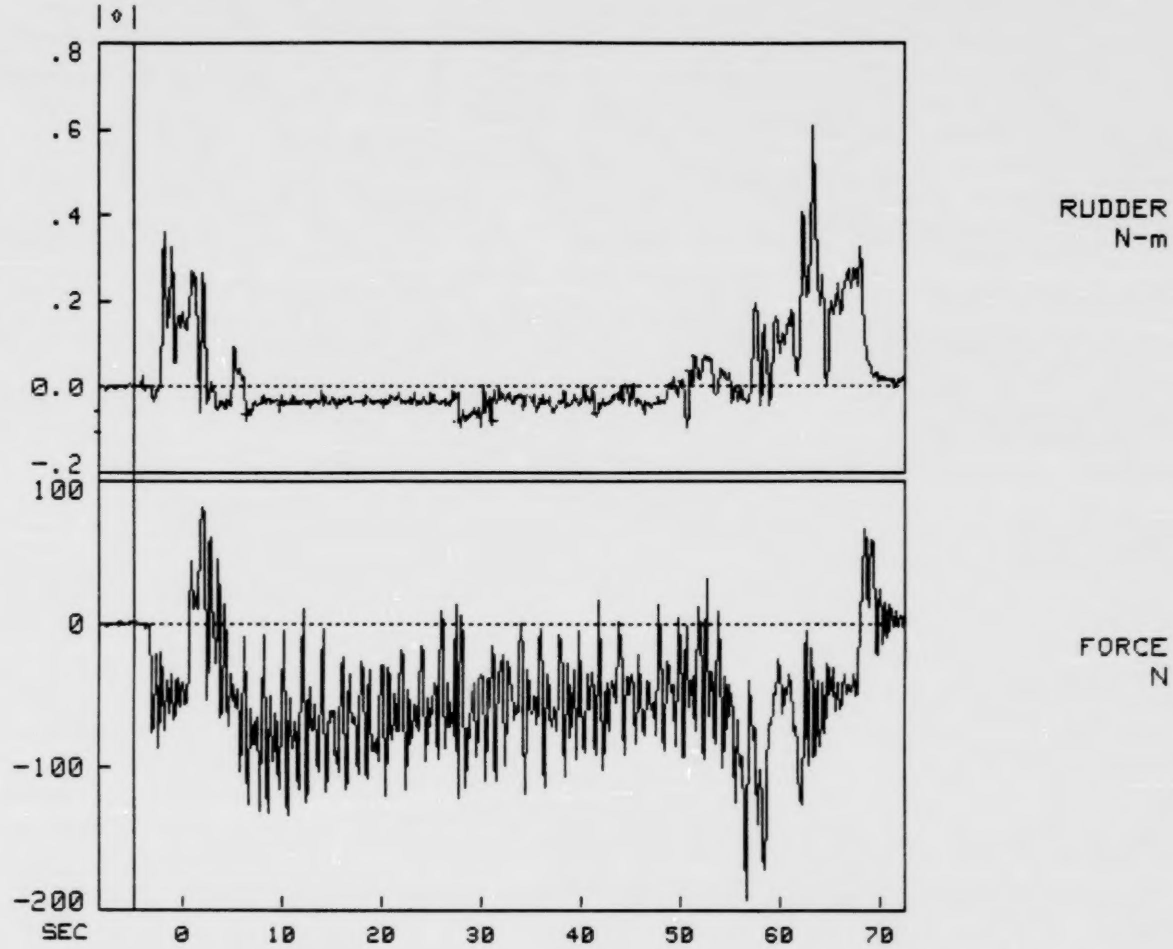

TEST 334

TEST #3 RUN 34

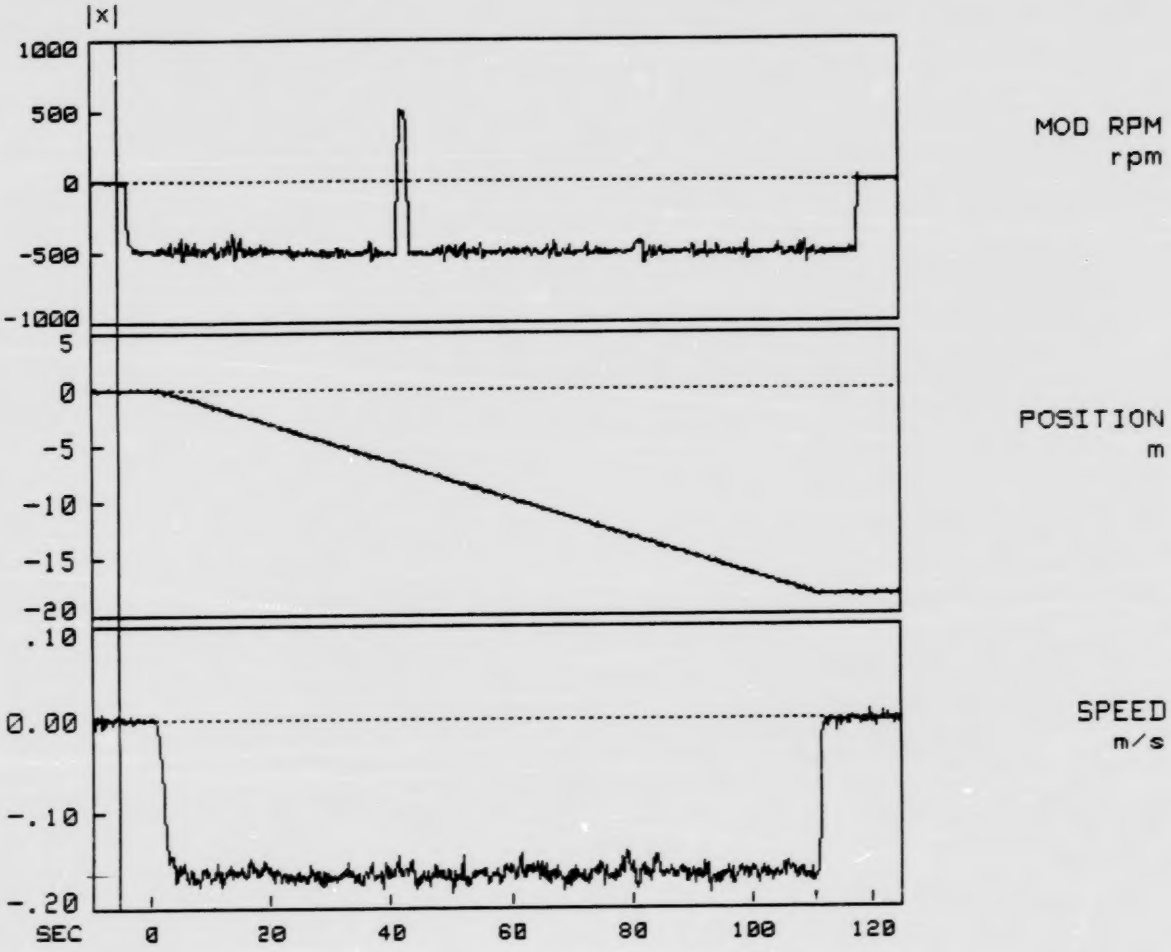

TEST 334

TEST #3 RUN 34

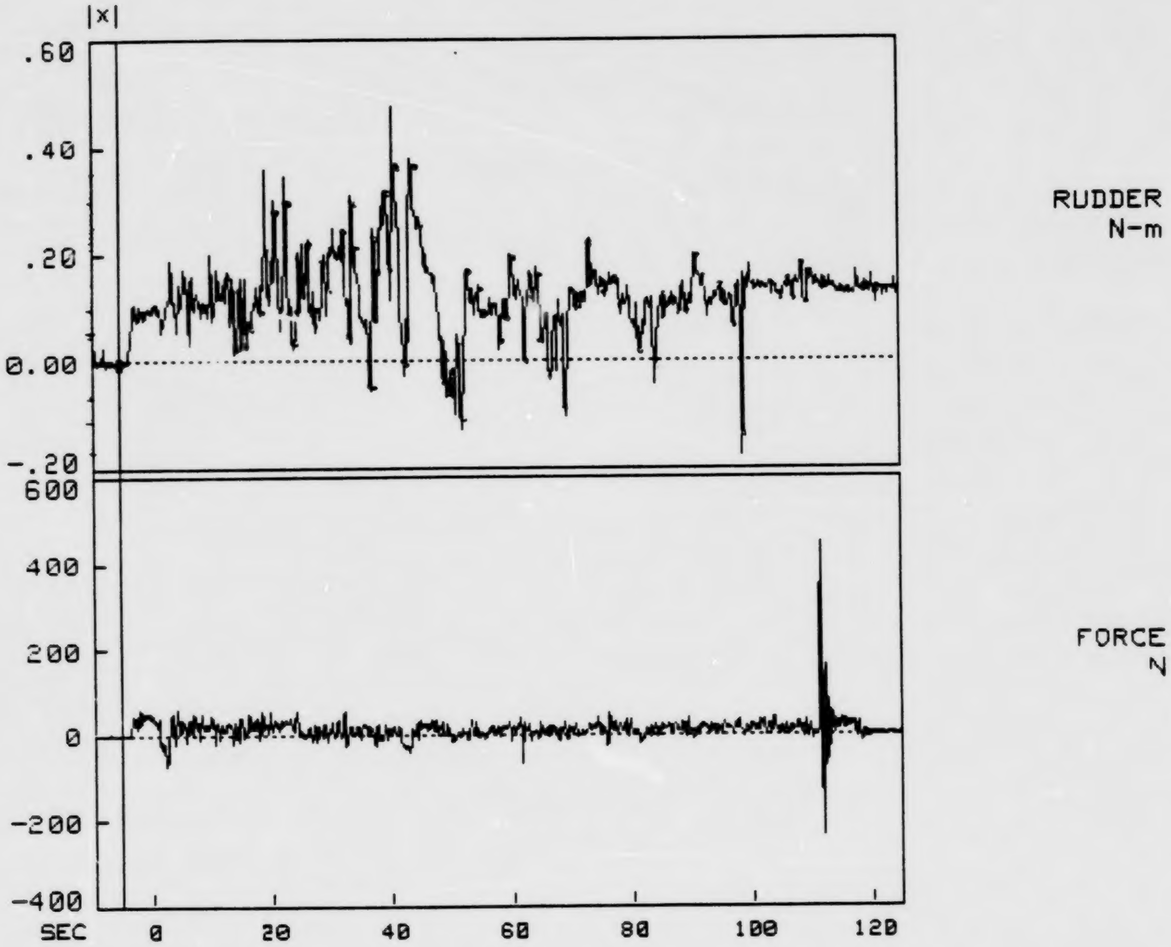

TEST 401

TEST #4 RUN 01

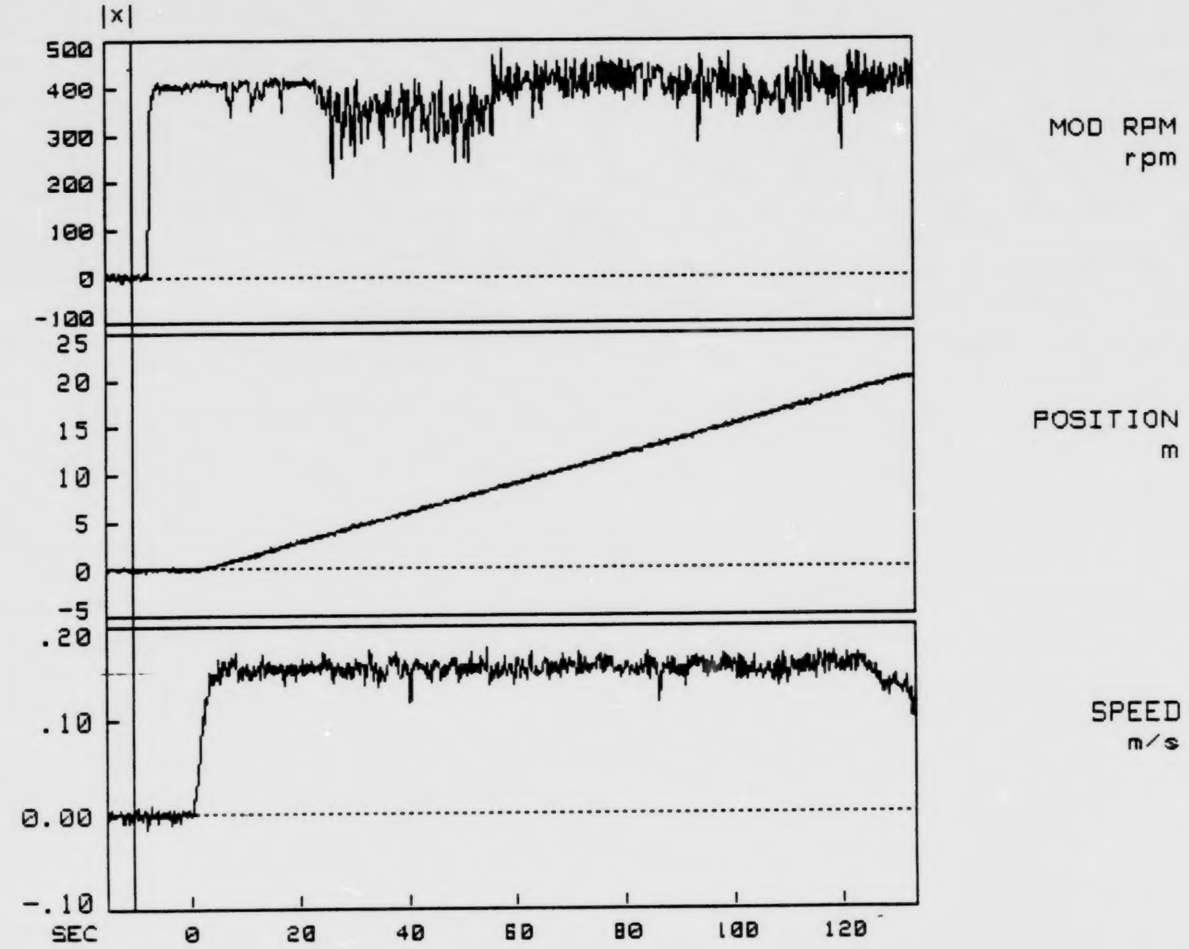

TEST 401

TEST #4 RUN 01

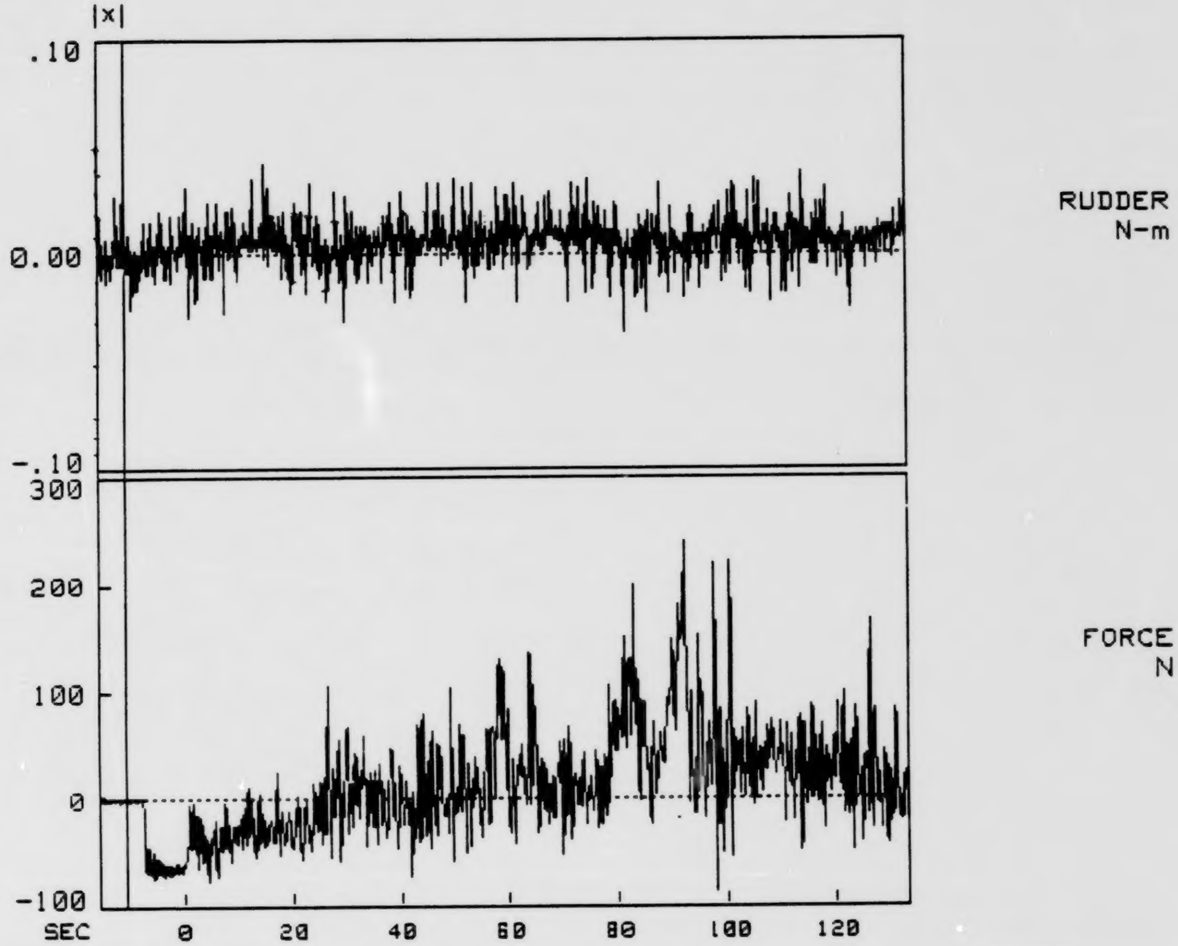

TEST #4 RUN 03 TEST 40 3

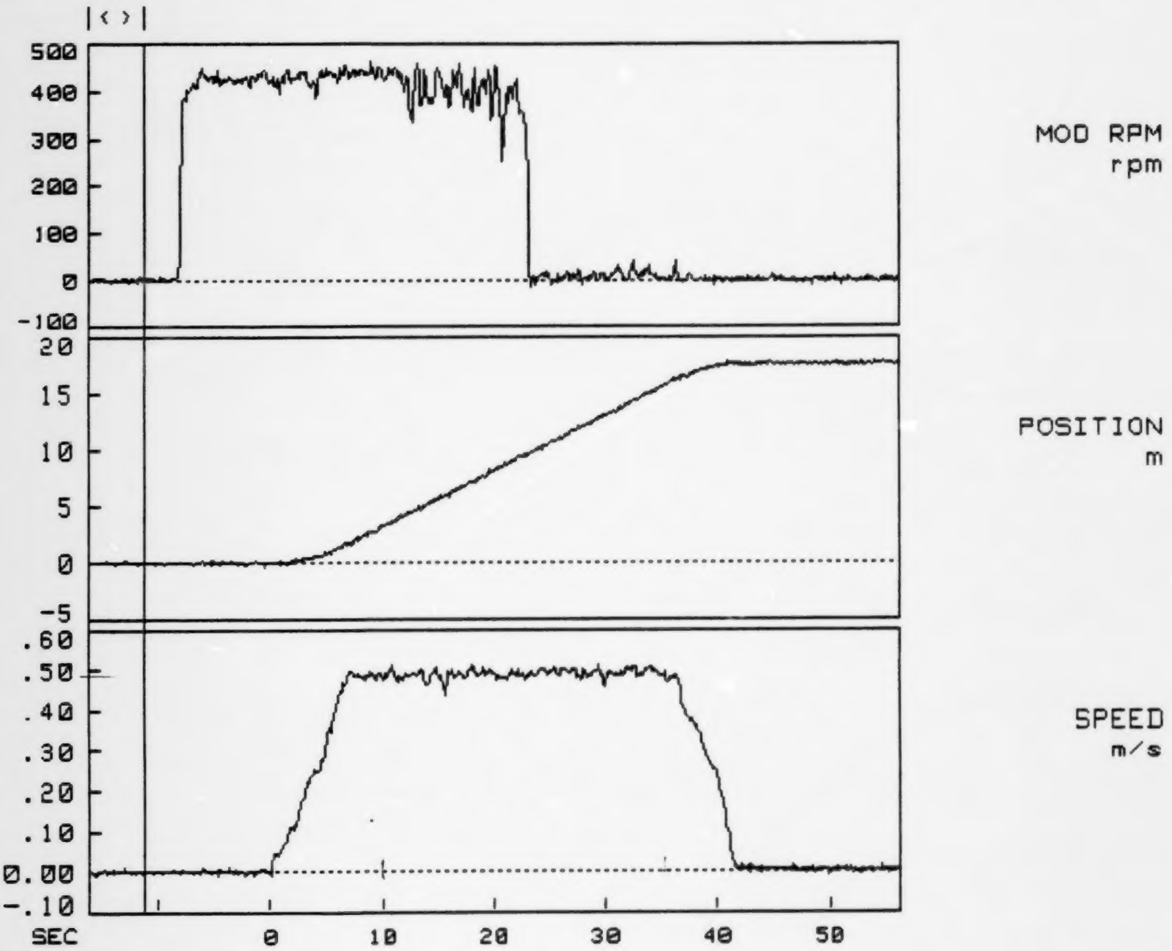

TEST #4 RUN 03 TEST 40^{3}

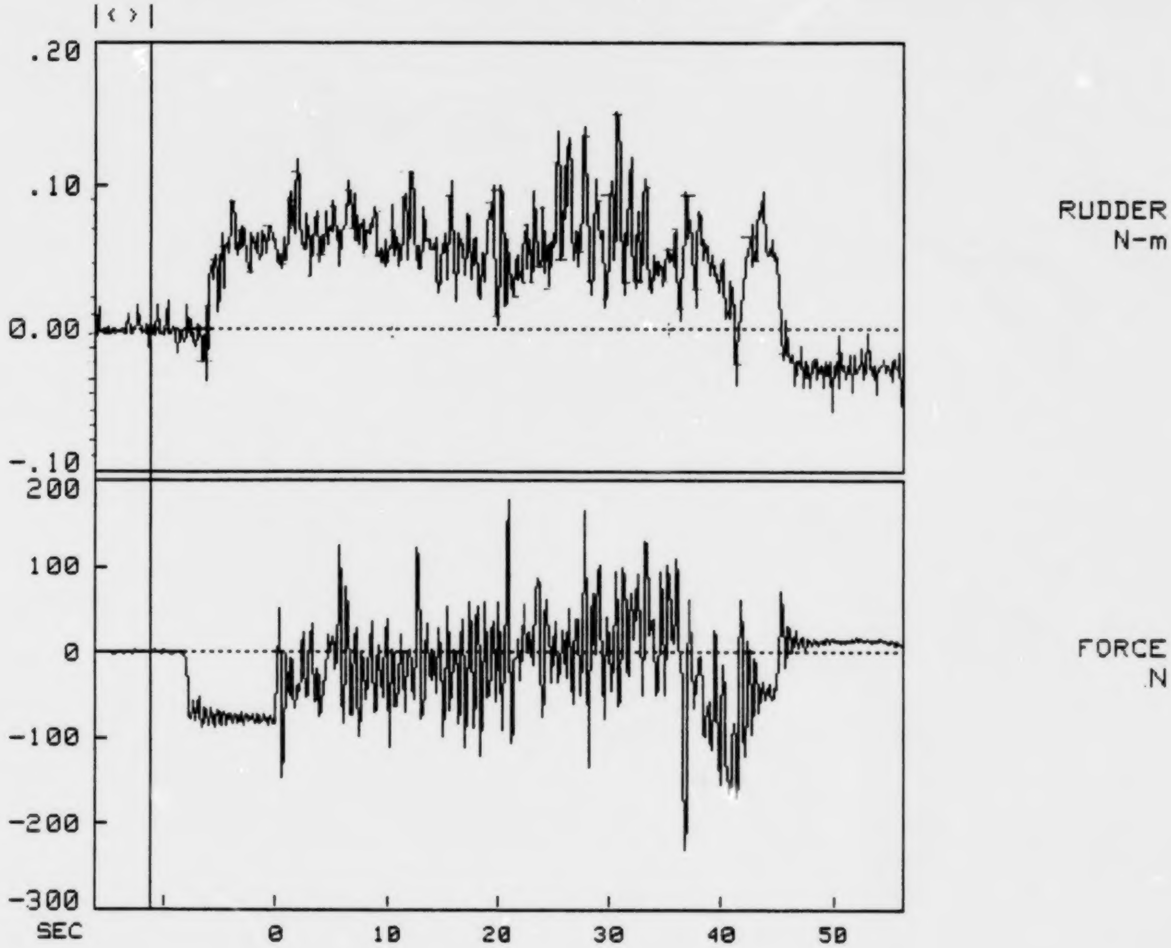

TEST 403-A

TEST #4 RUN 03

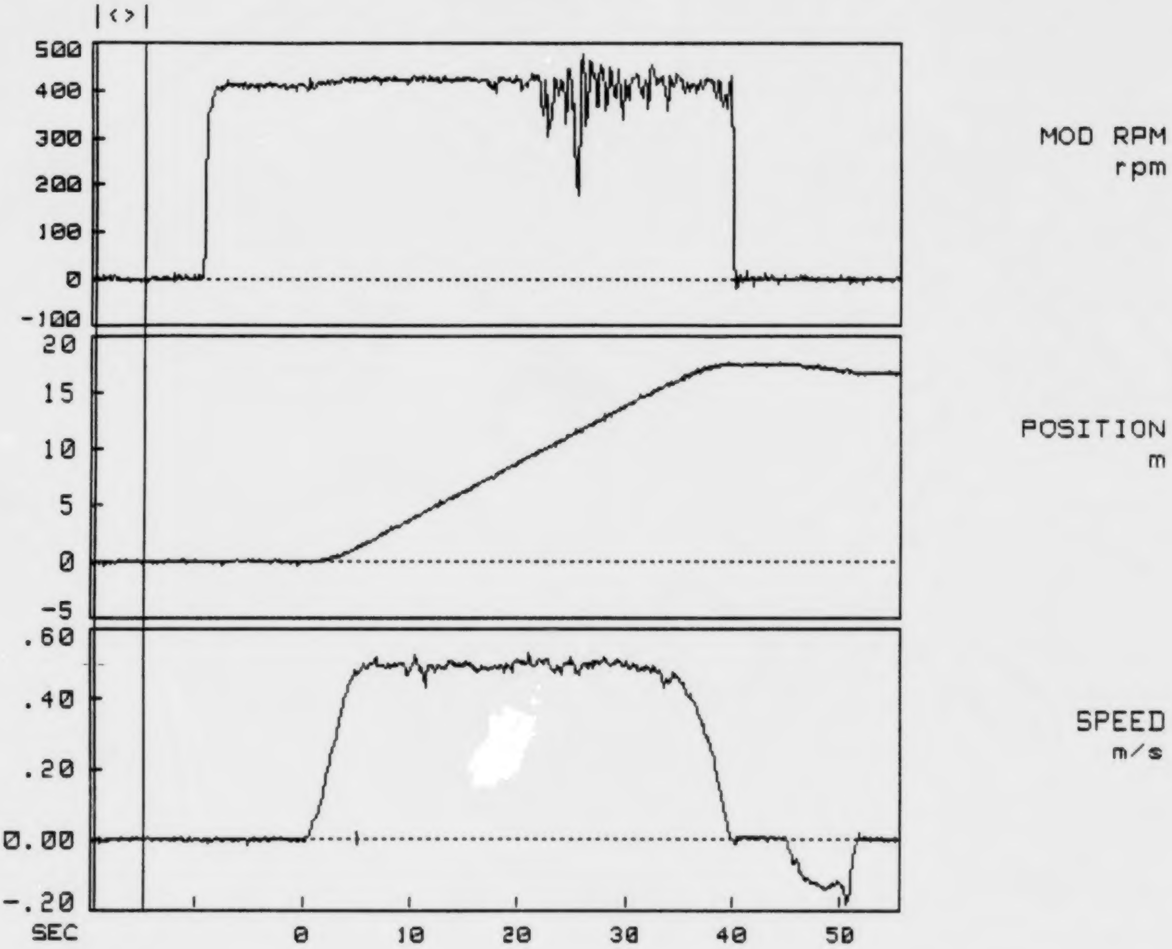

TEST #4 RUN 03 TEST 403-A

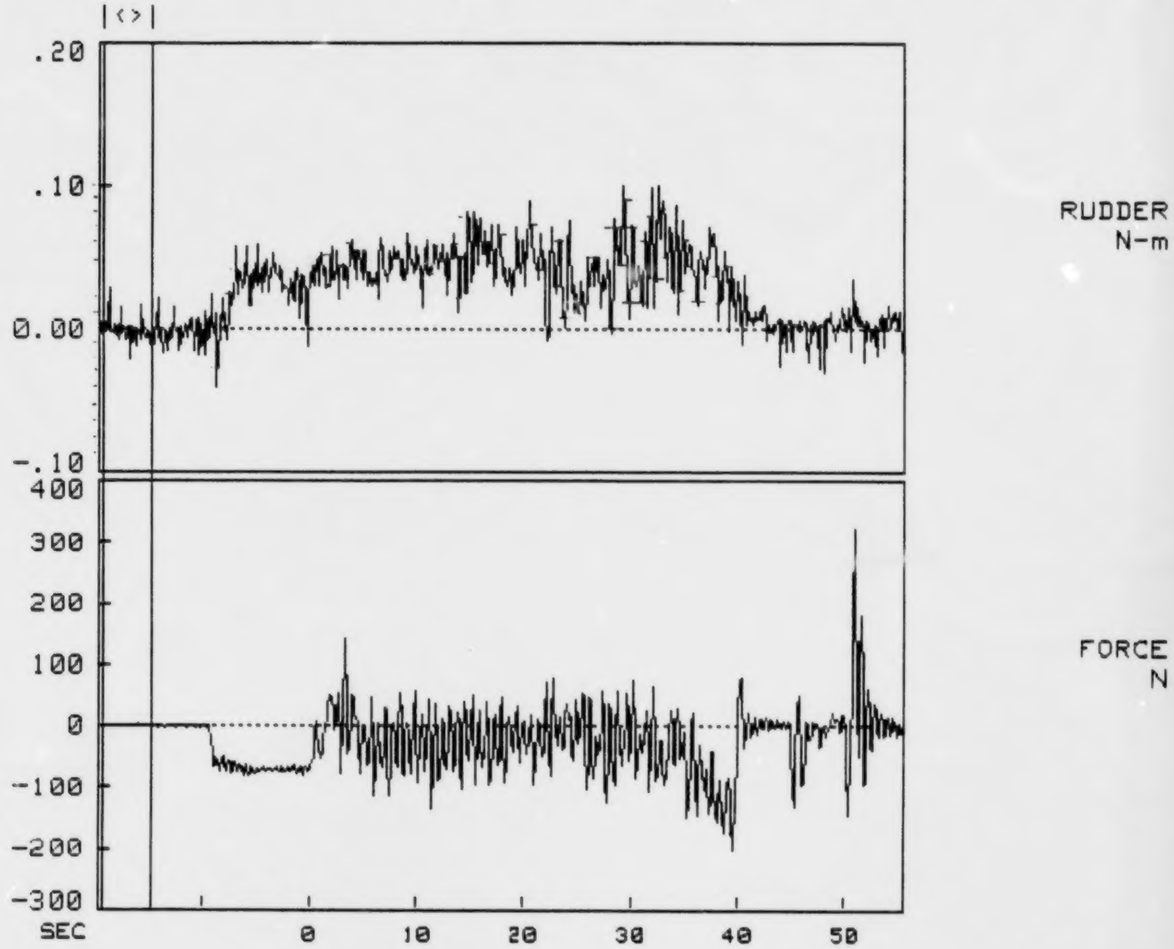

TEST 404

TEST #4 RUN 04

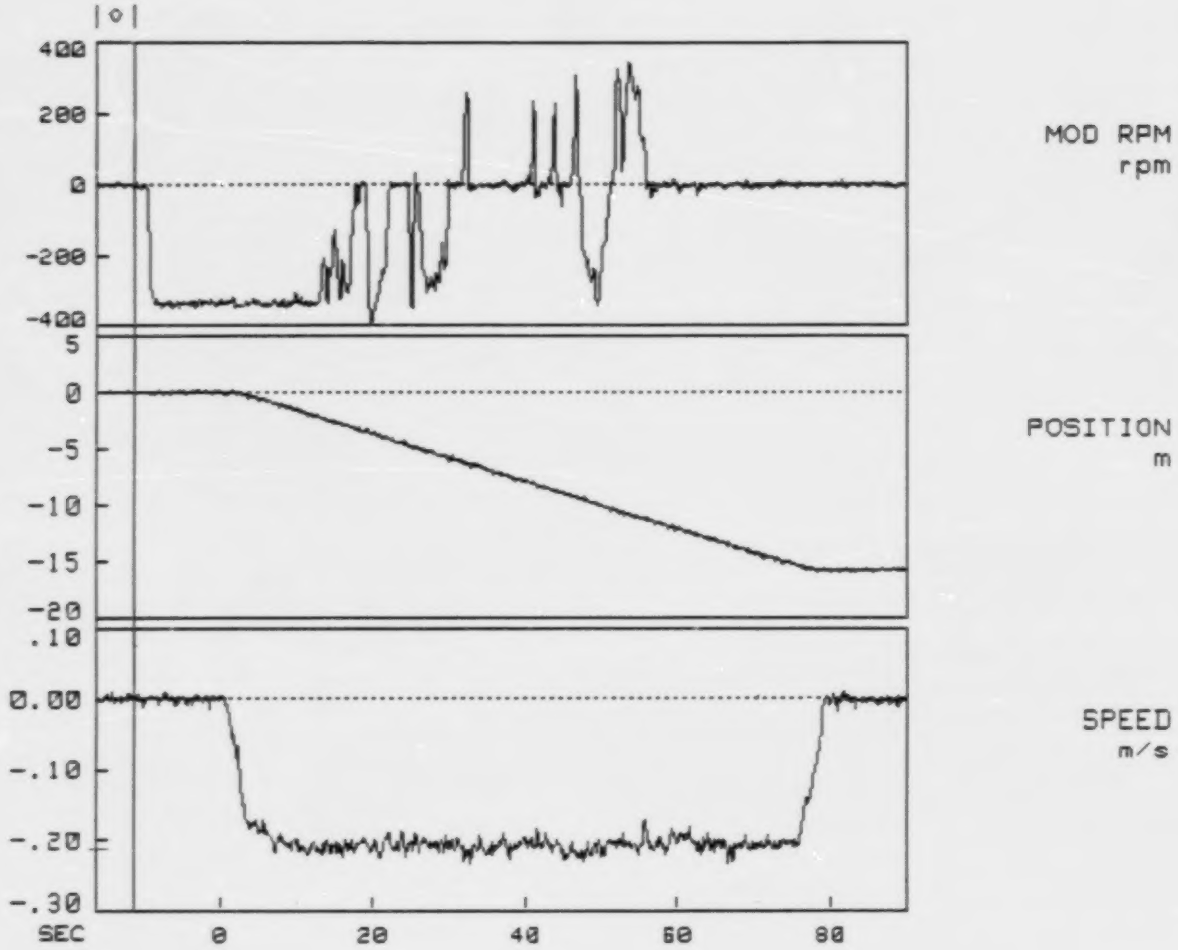

TEST 404

TEST #4 RUN 04

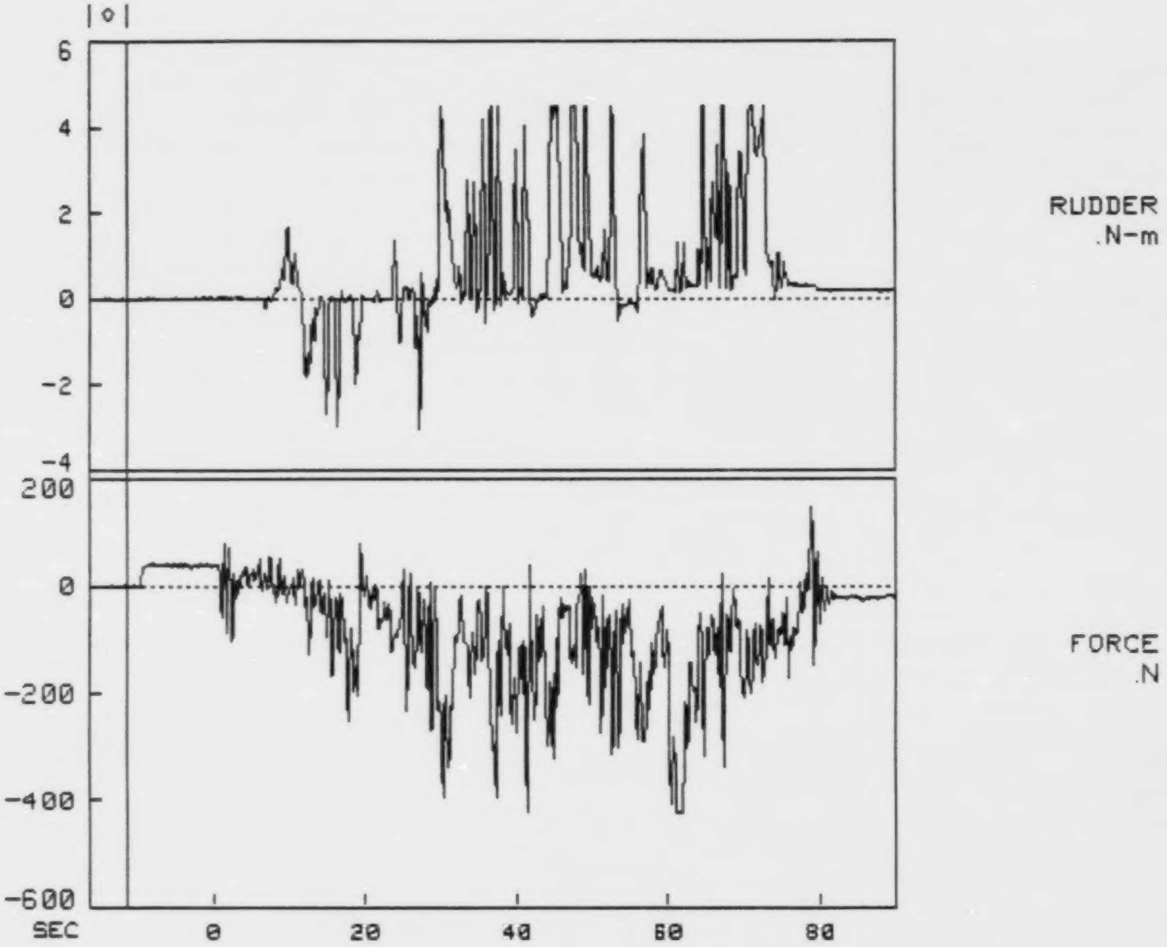

TEST 404-A

TEST #4 RUN 04

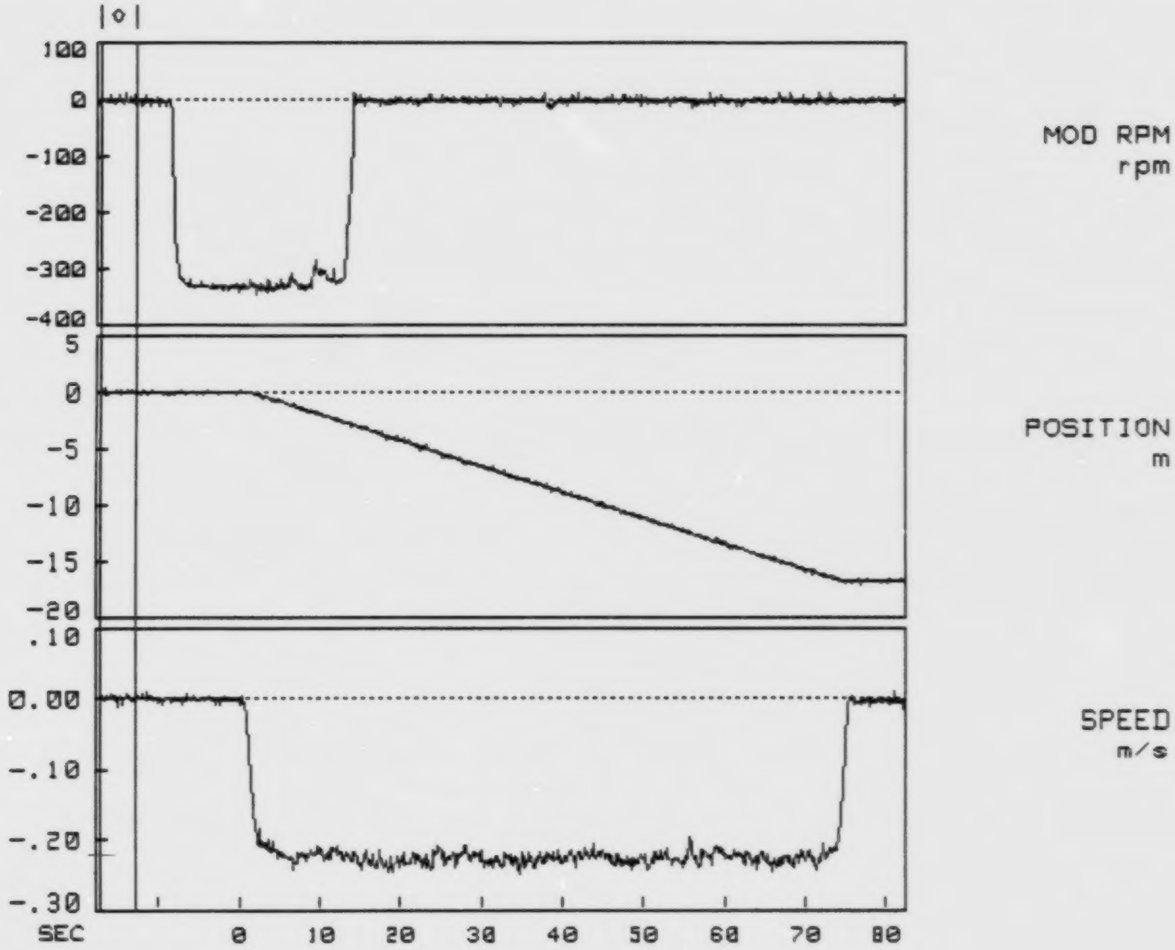

TEST 404-A

TEST #4 RUN 04

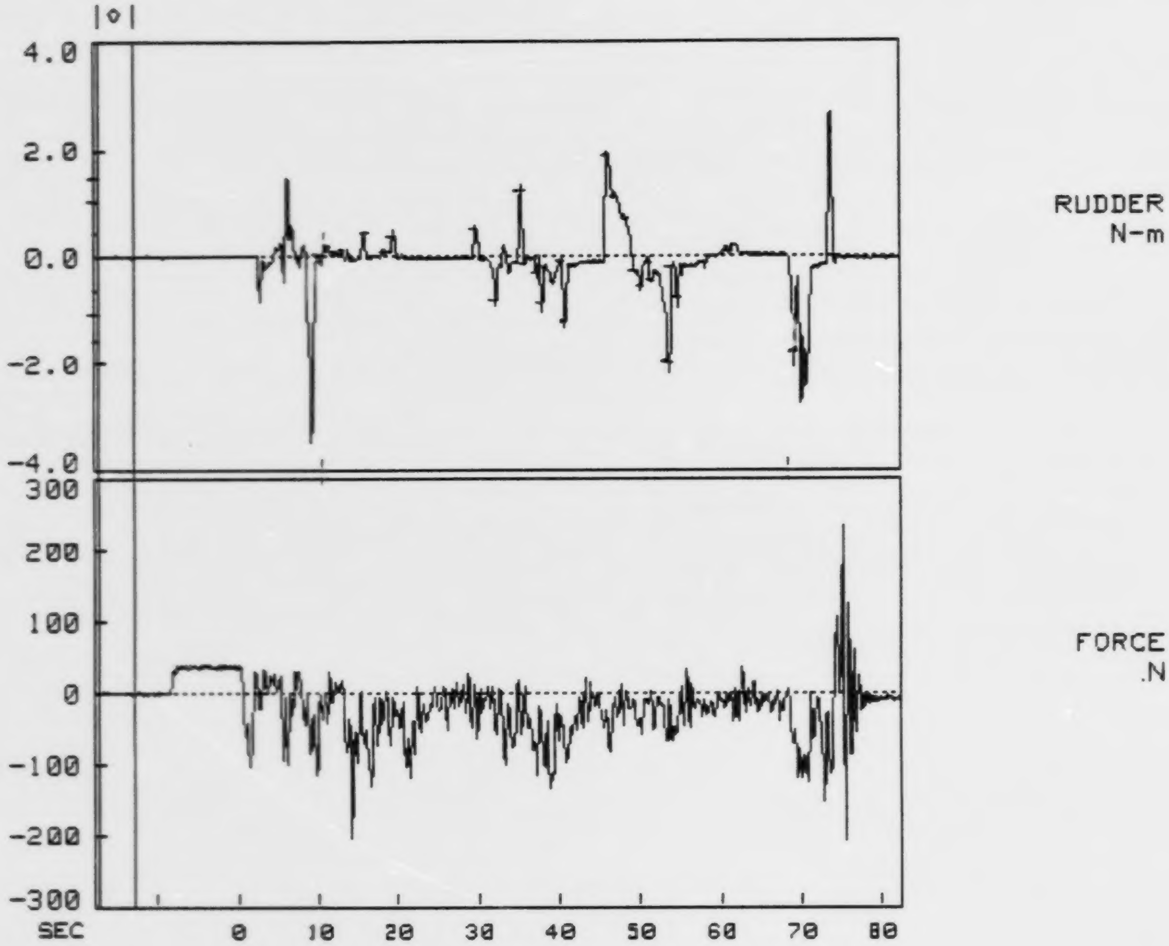

TEST ~~3~~405

TEST ~~#3~~ 4 RUN 05

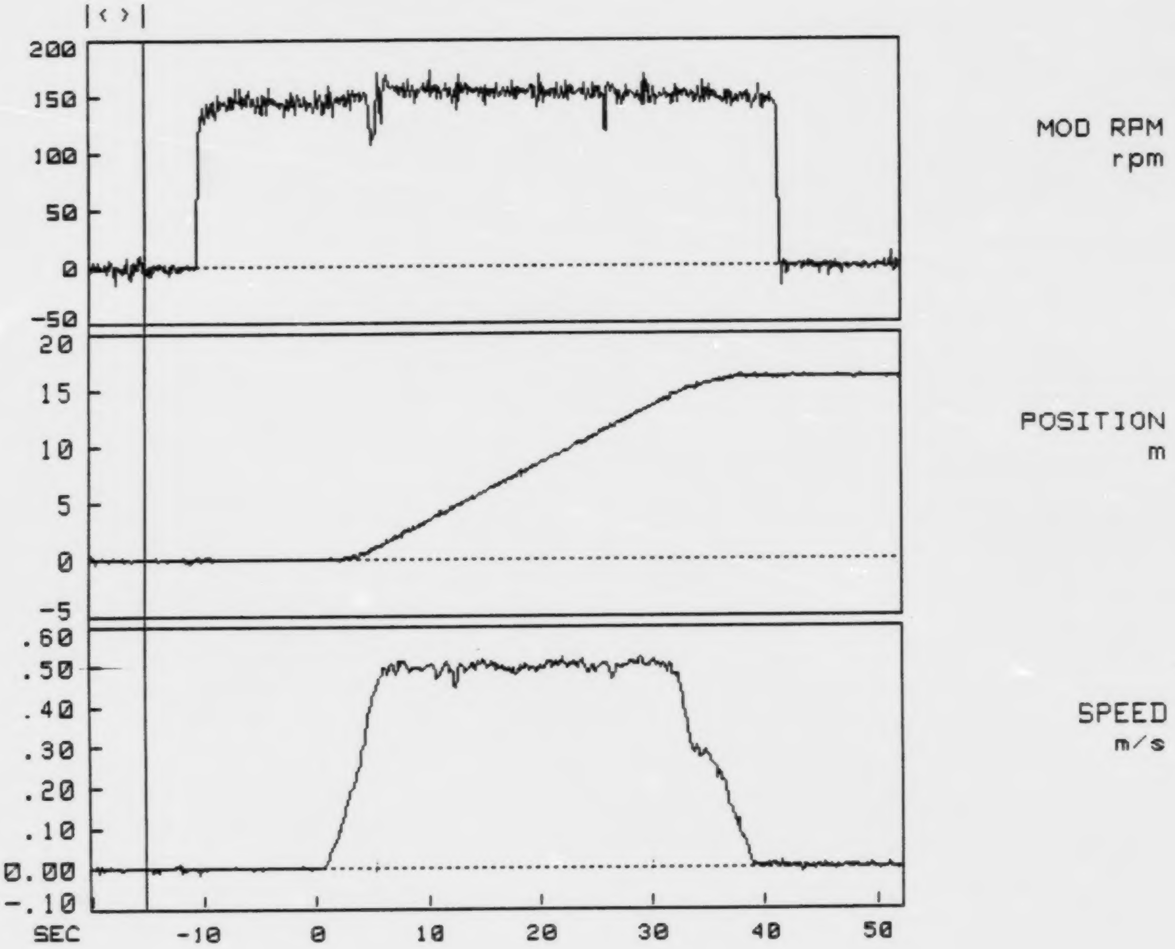

TEST # 4 RUN 05 TEST 4 05

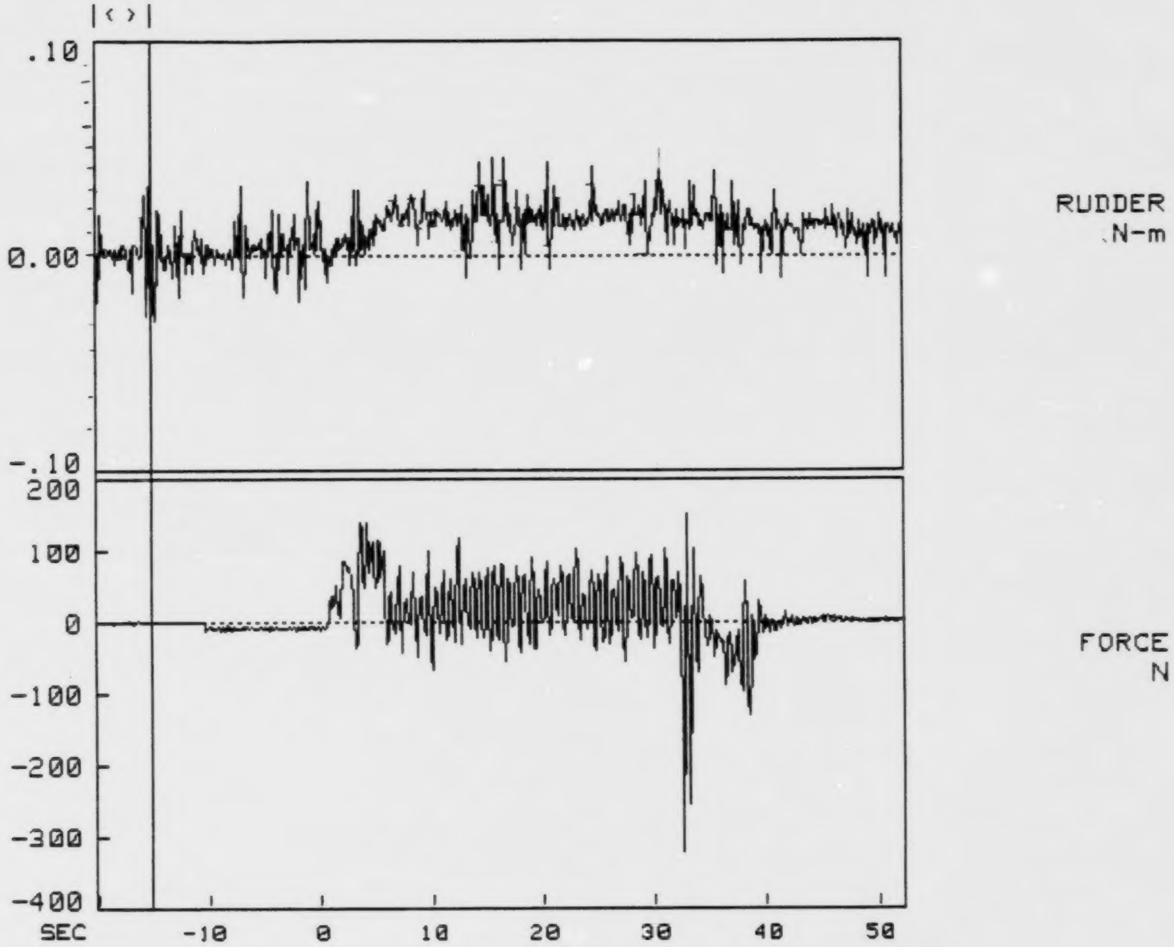

TEST 405-A

TEST #4 RUN 05

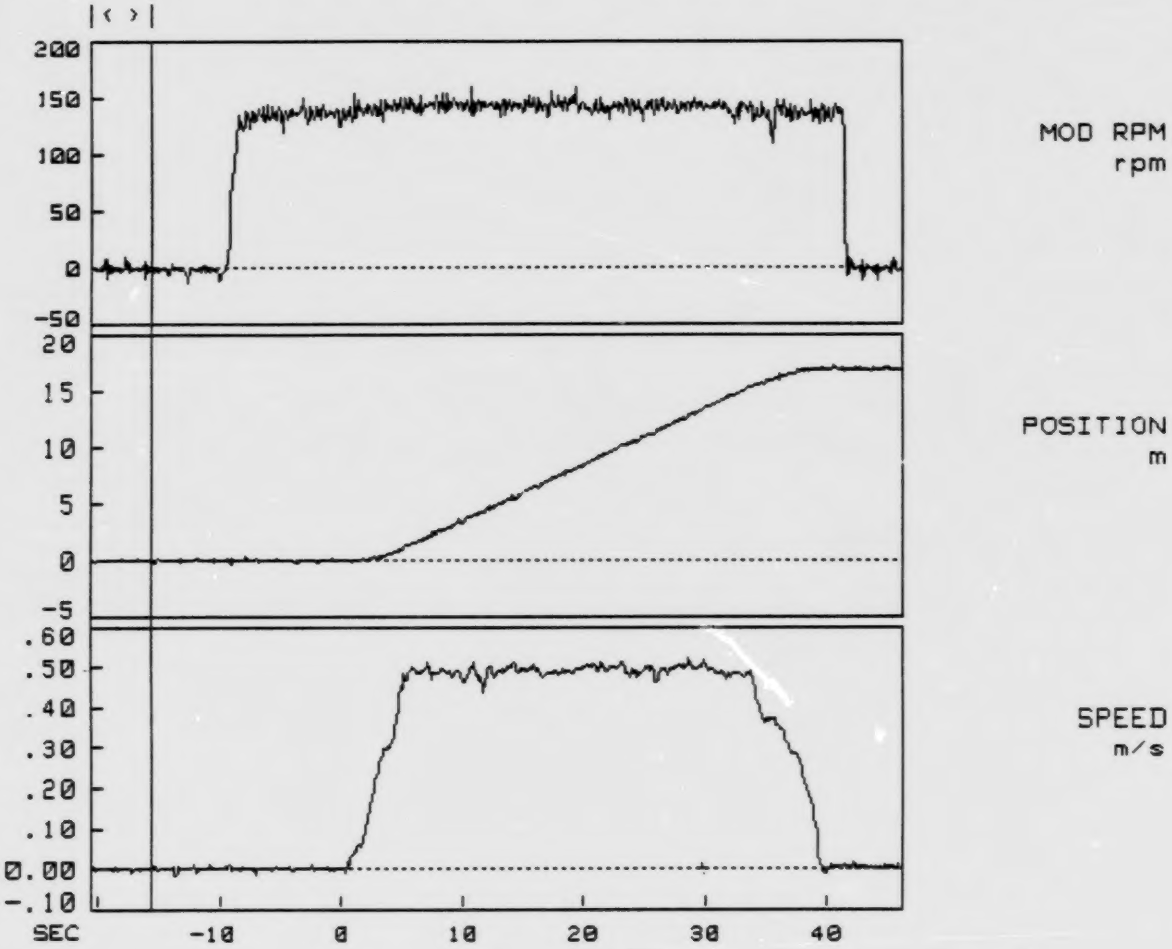

TEST 405-A

TEST #4 RUN 05

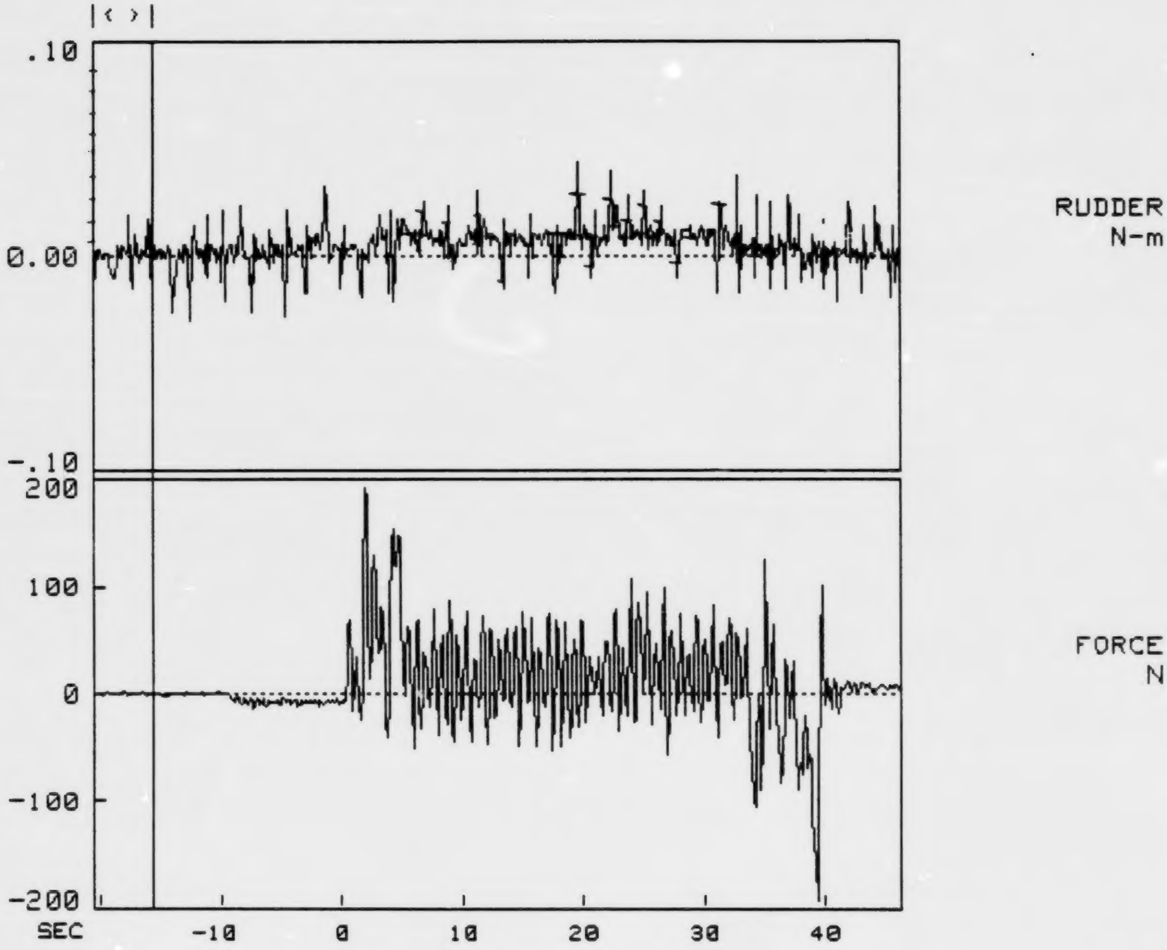

TEST 406

TEST #4 RUN 06

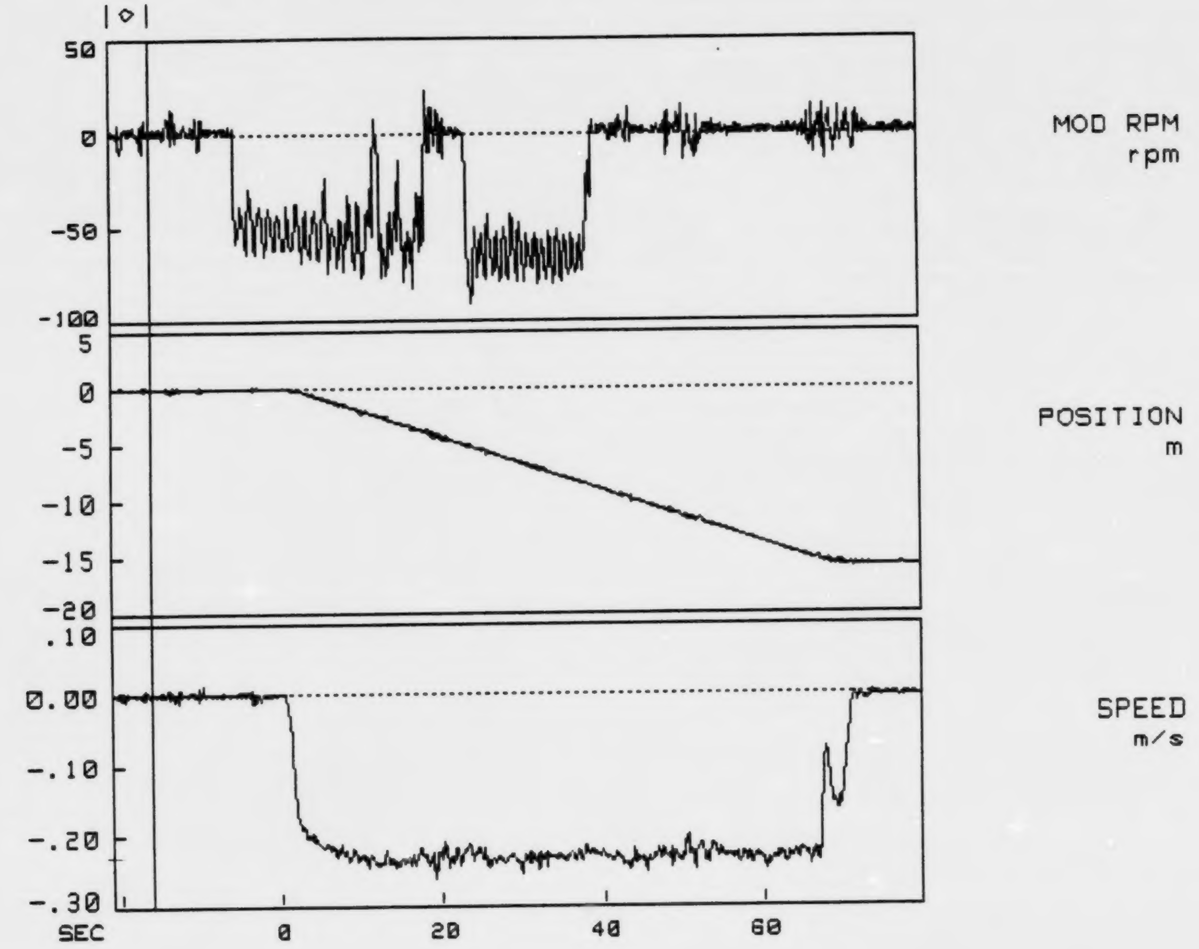

TEST 406

TEST #4 RUN 06

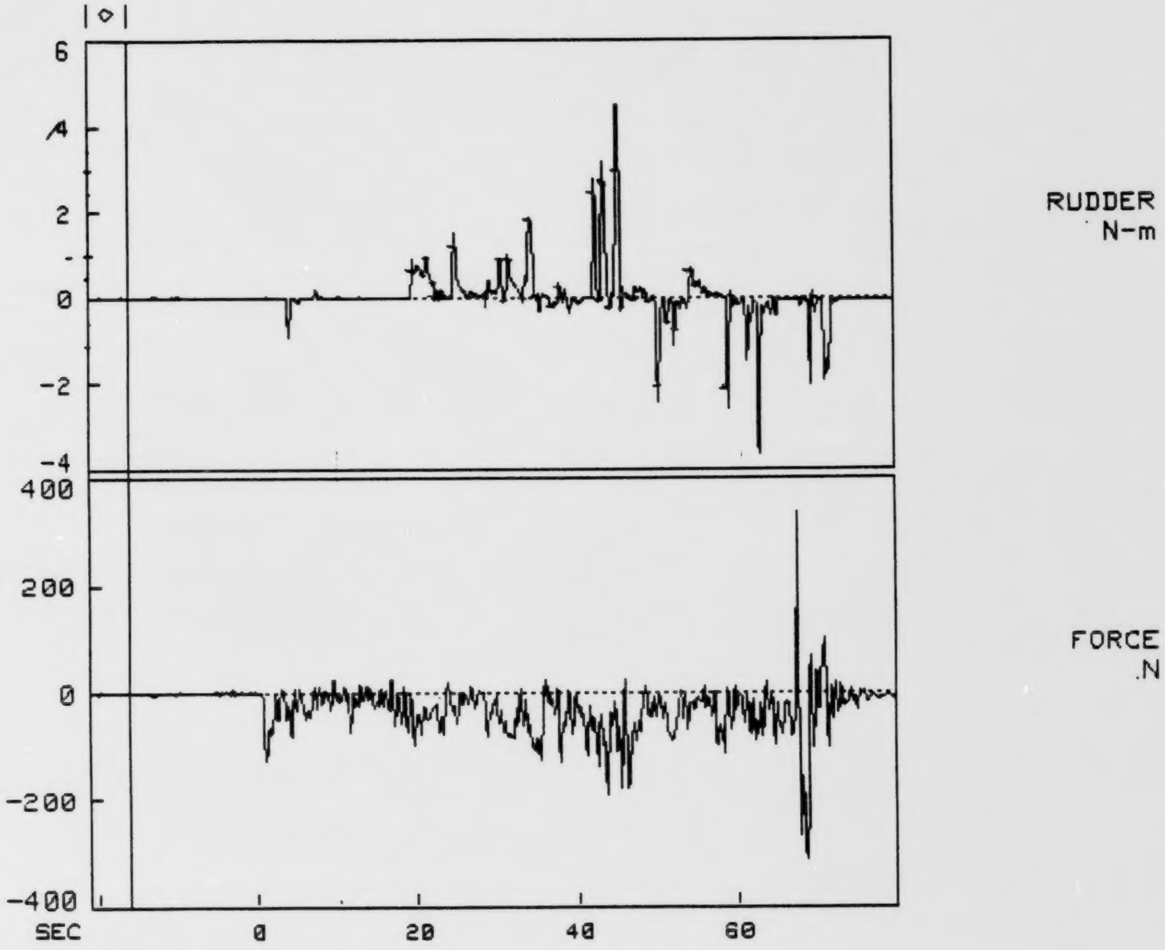

TEST 406-A

TEST #4 RUN 06

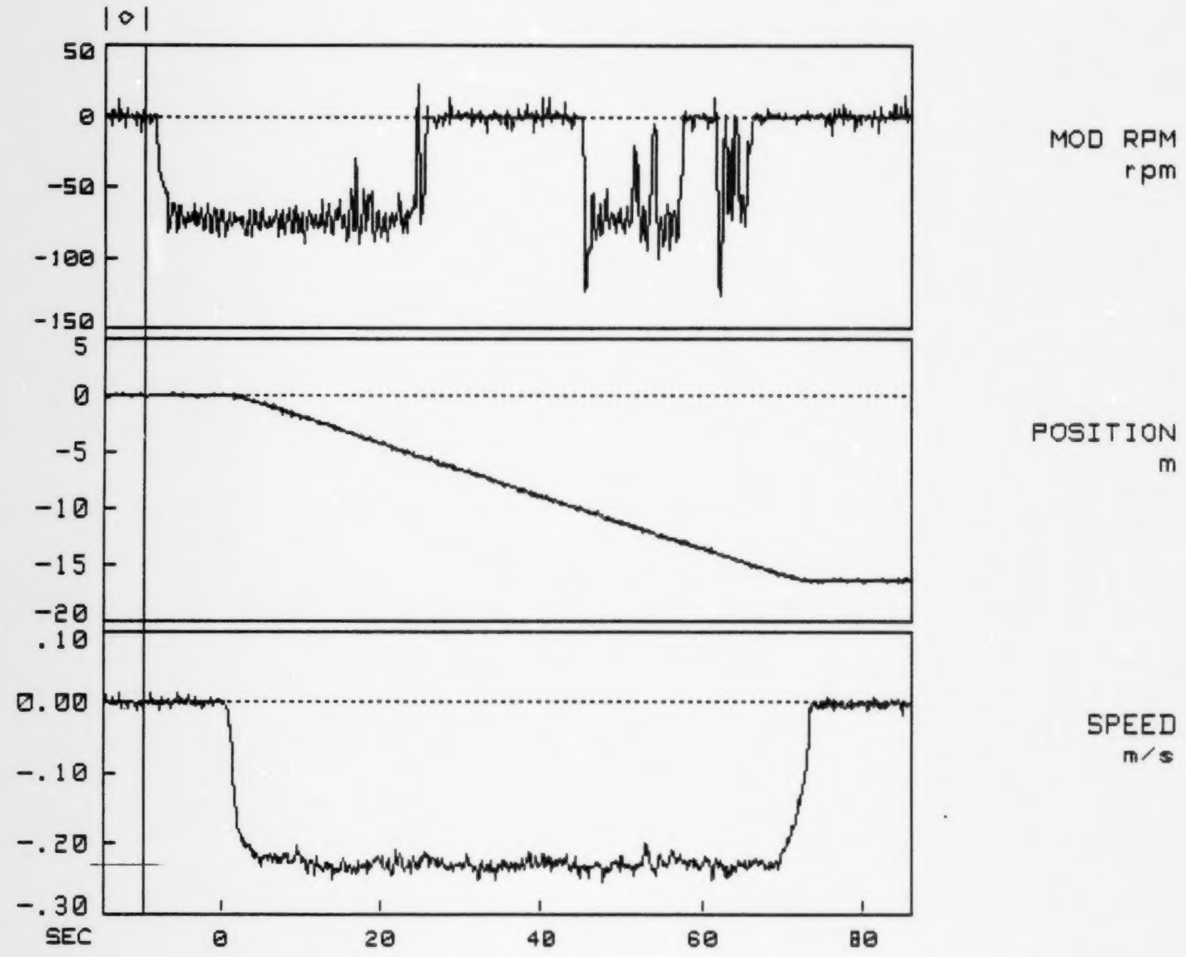

TEST #4 RUN 06 TEST 406-A

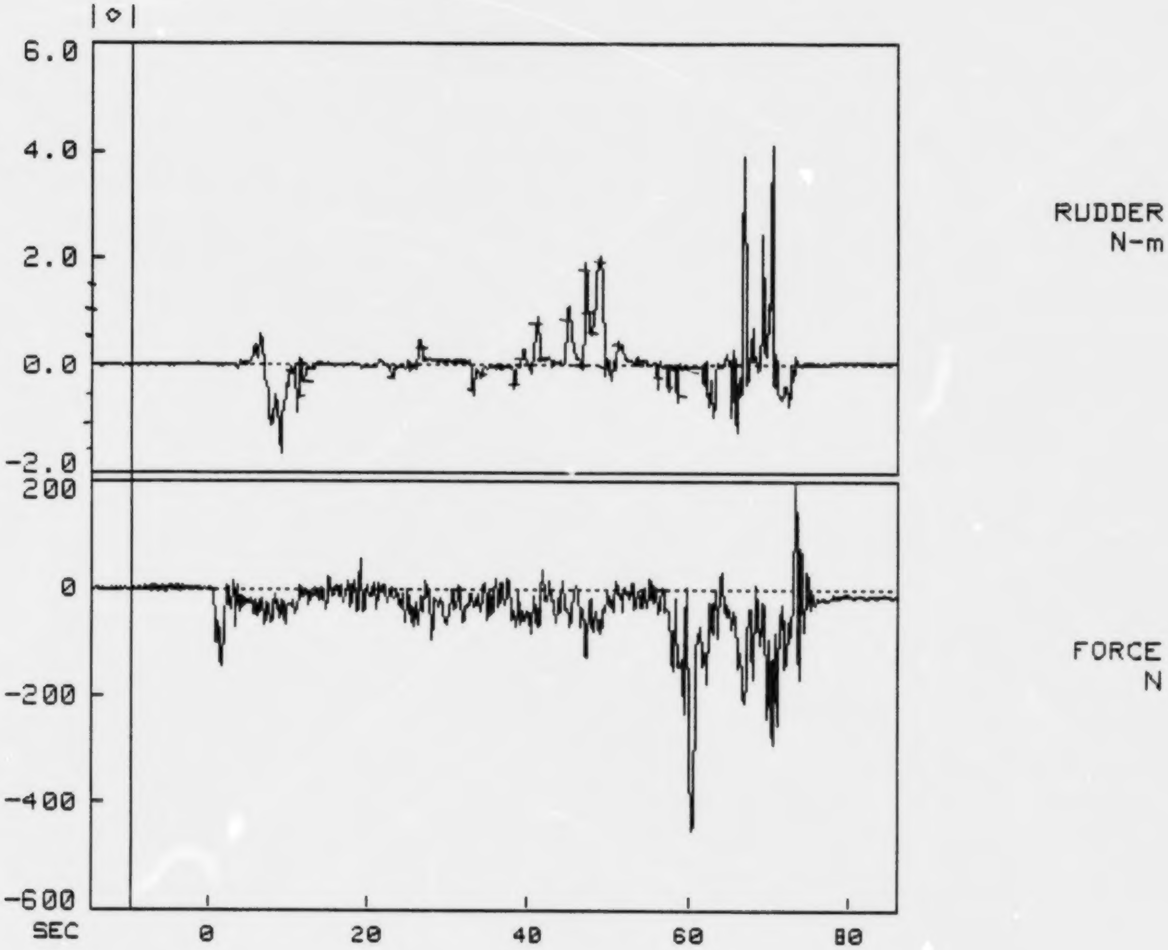

TEST 407-A

TEST #4 RUN 07

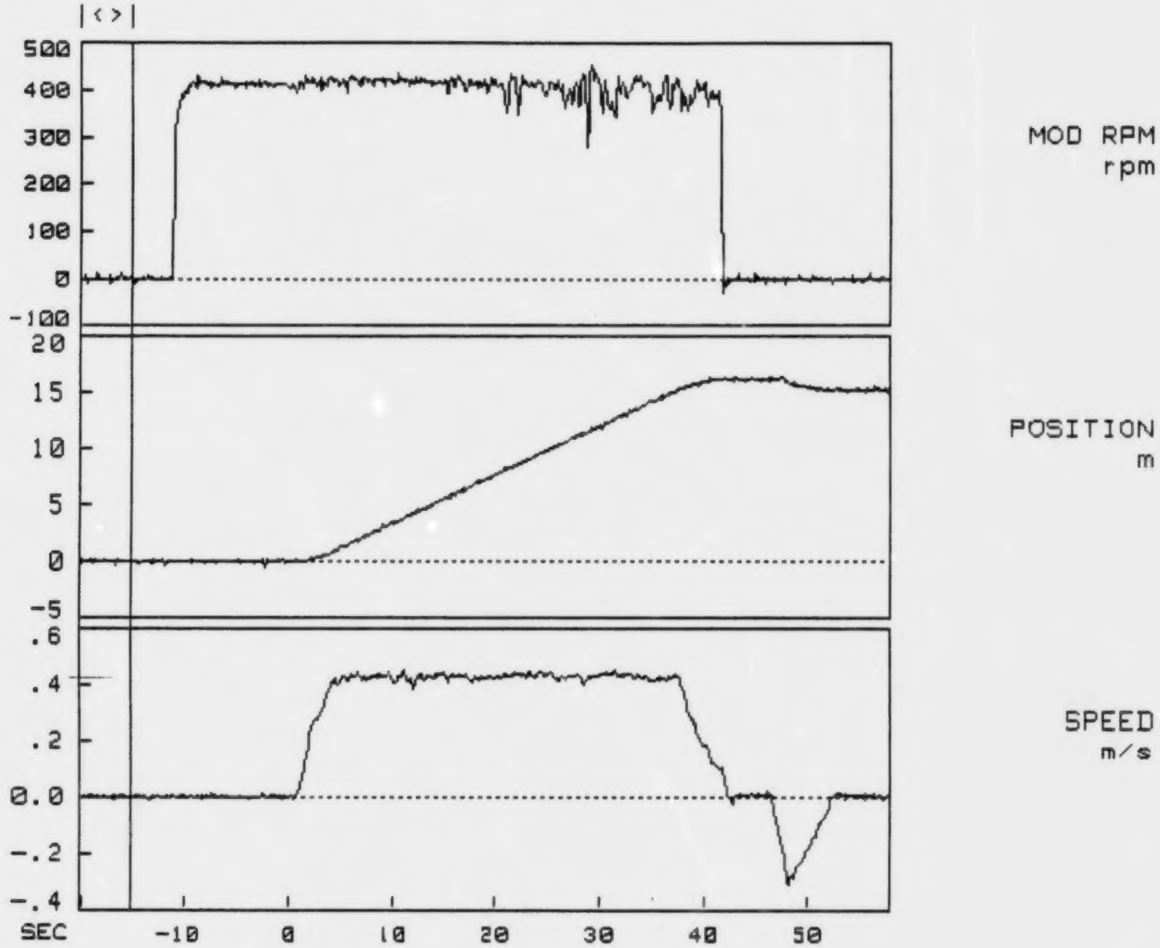

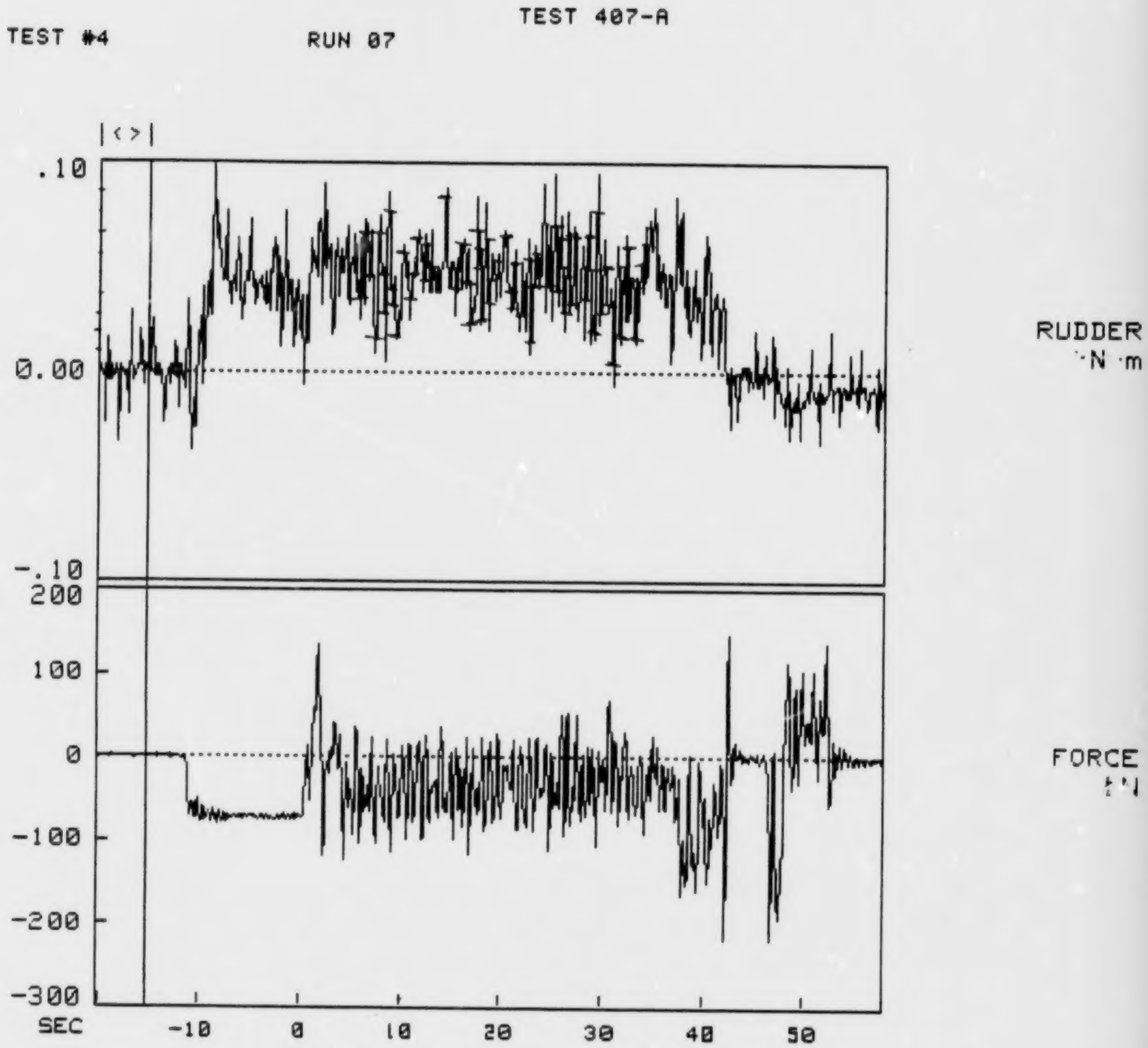
TEST #4
RUN 07
TEST 407-A
|<>|
.10
0.00
-.10
RUDDER
N·m
200
100
0
-100
-200
-300
FORCE
kN
SEC
-10
0
10
20
30
40
50

TEST 408

TEST #4 RUN 08

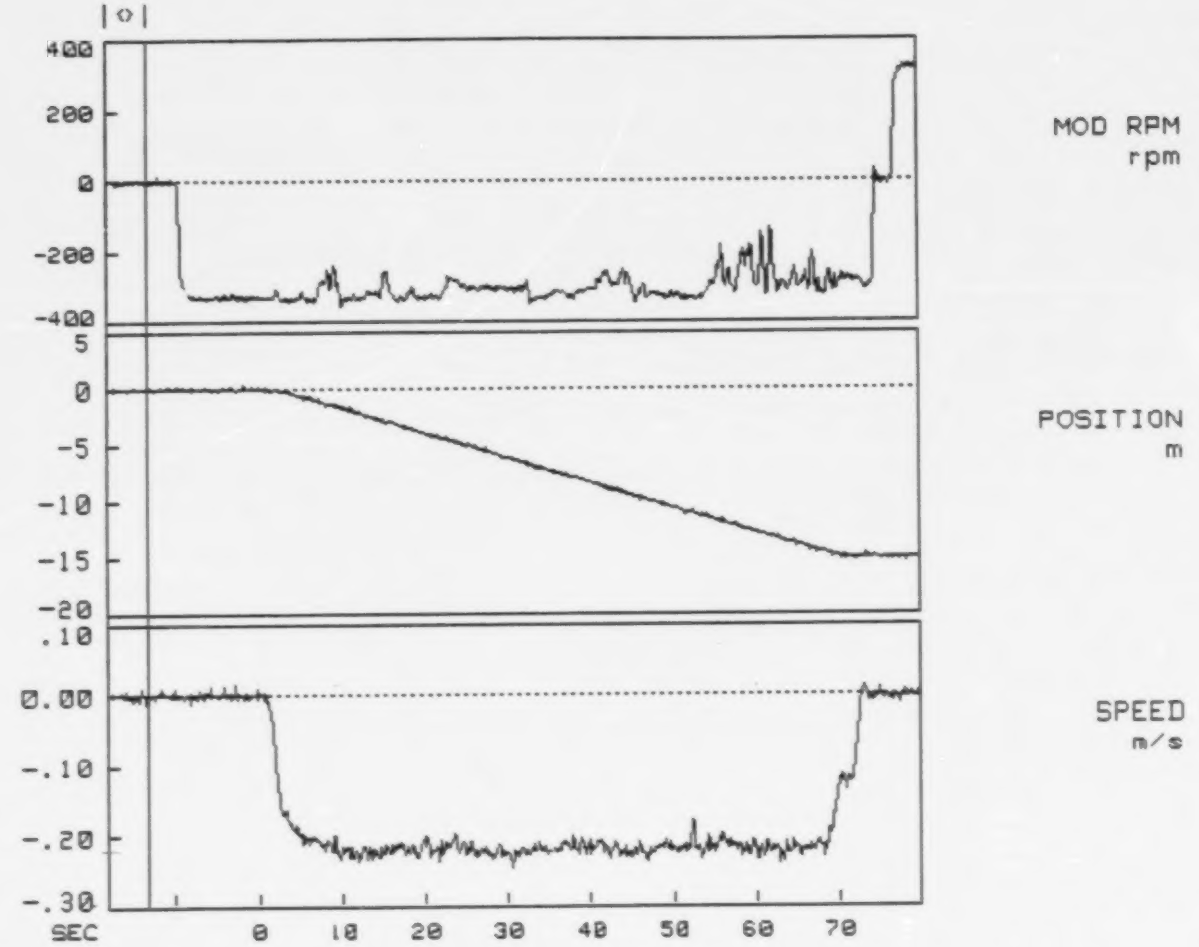

TEST 408

TEST #4 RUN 08

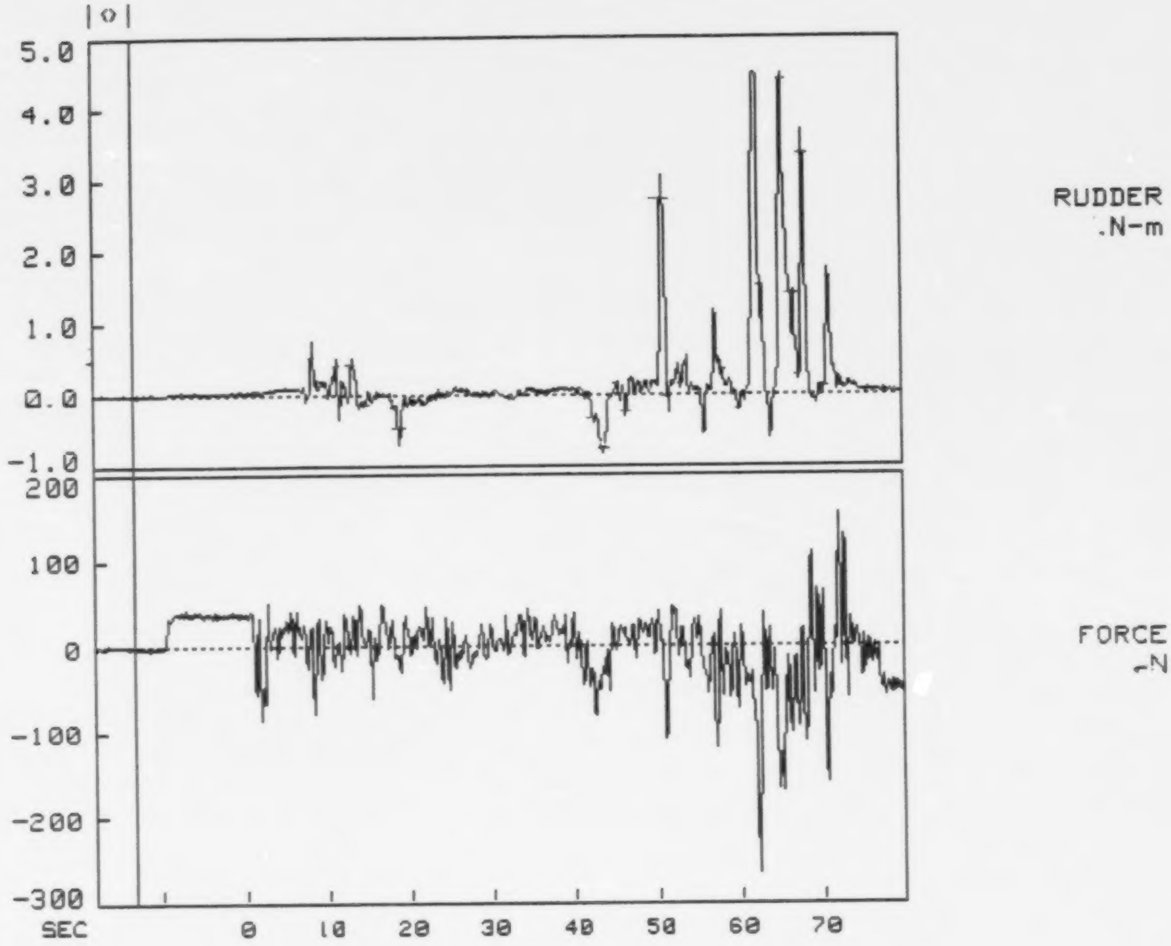

TEST #4 RUN 09 TEST 409

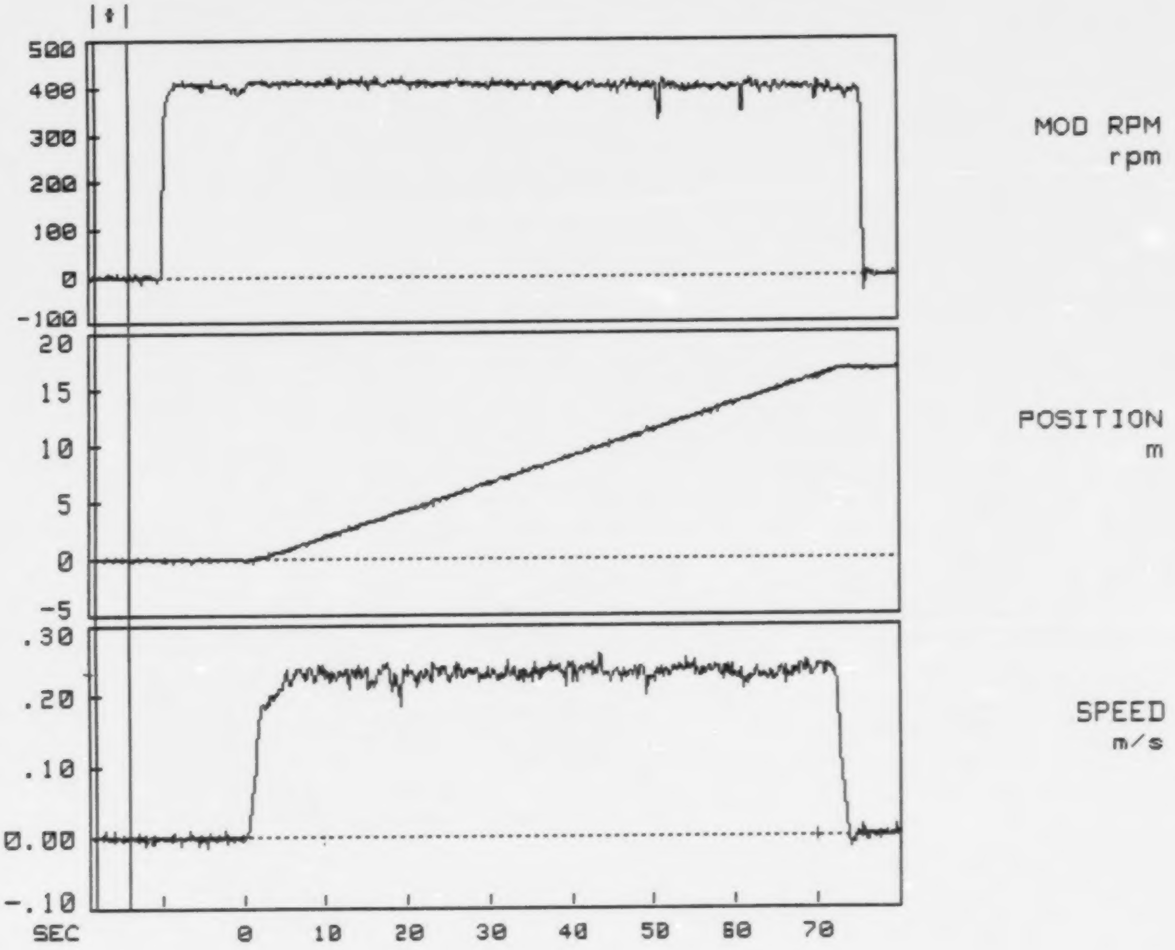

TEST #4 RUN 09 TEST 409

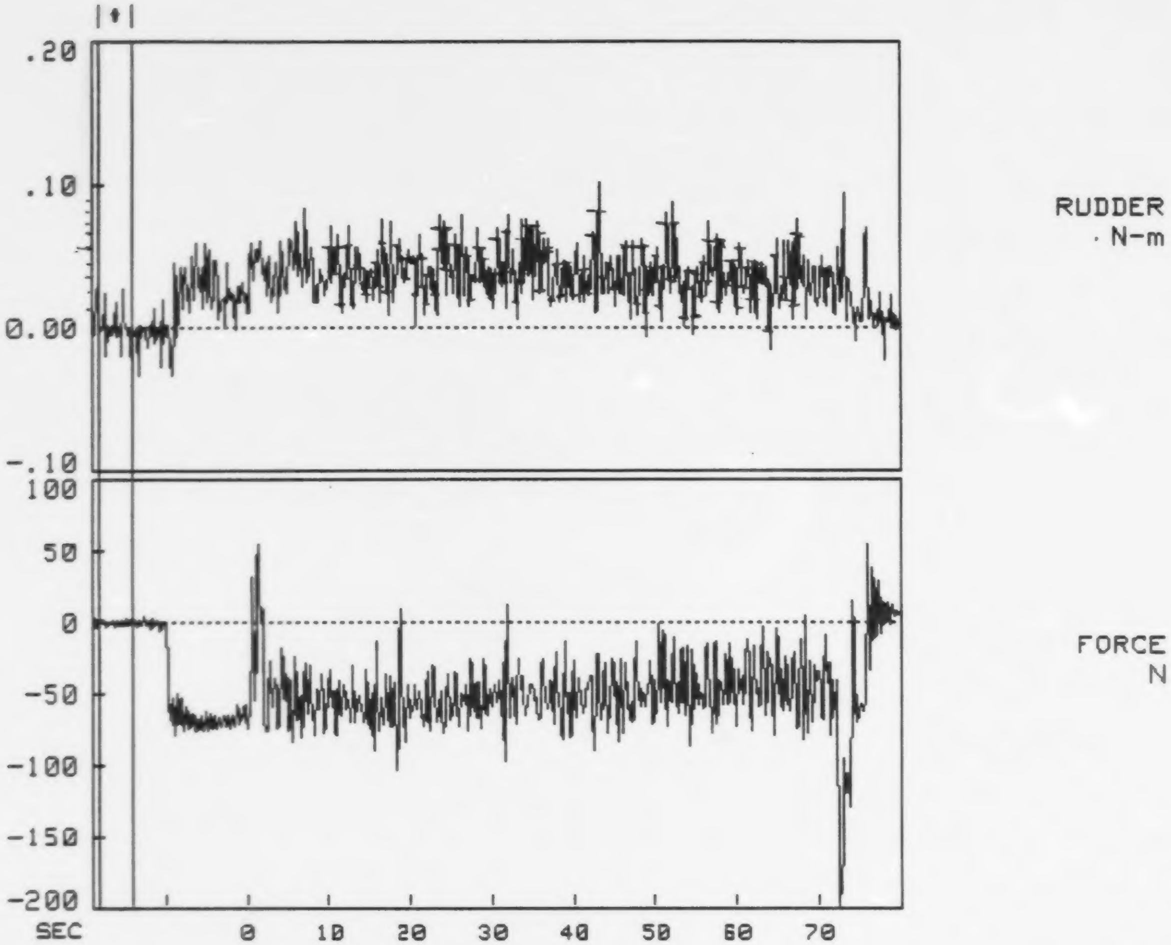

TEST 410

TEST #4 RUN 10

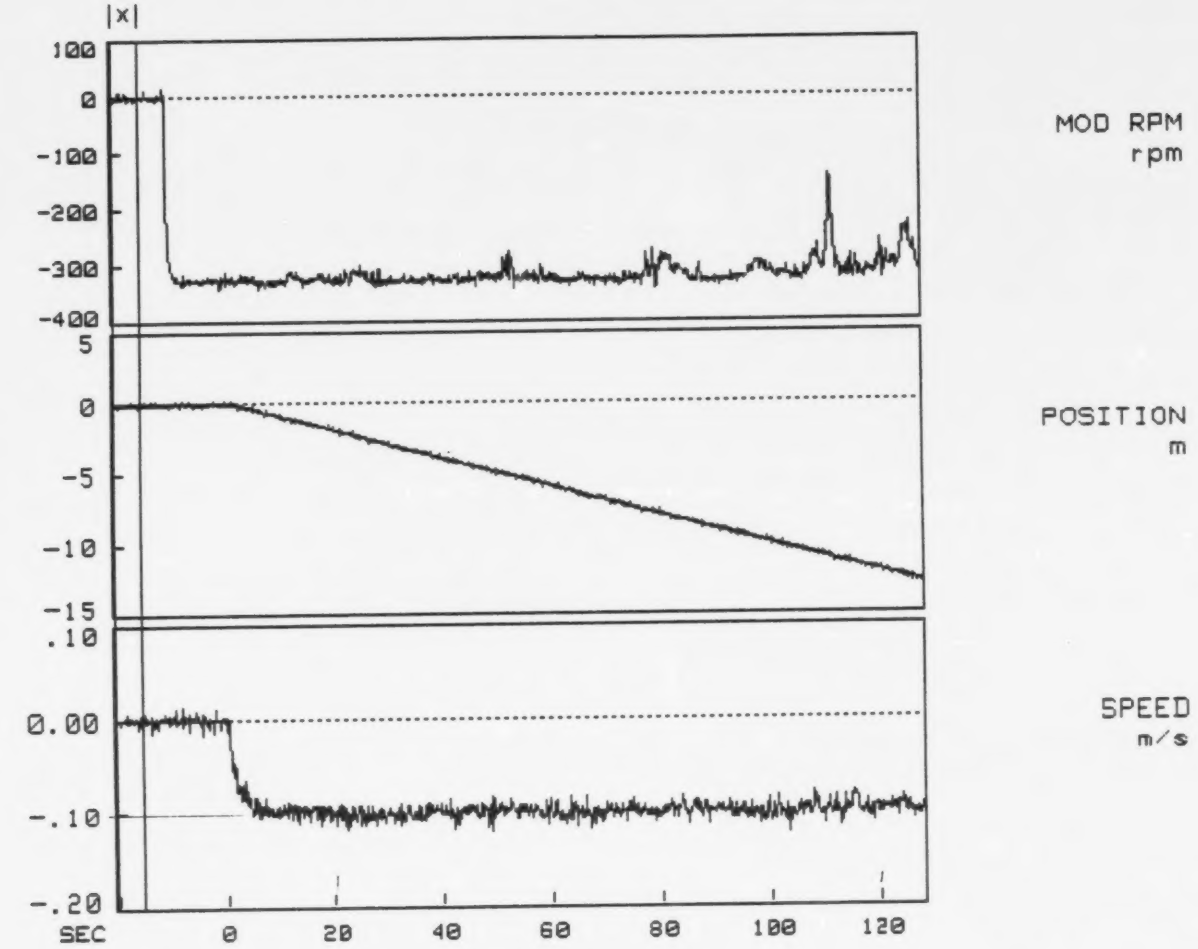

TEST 410

TEST #4 RUN 10

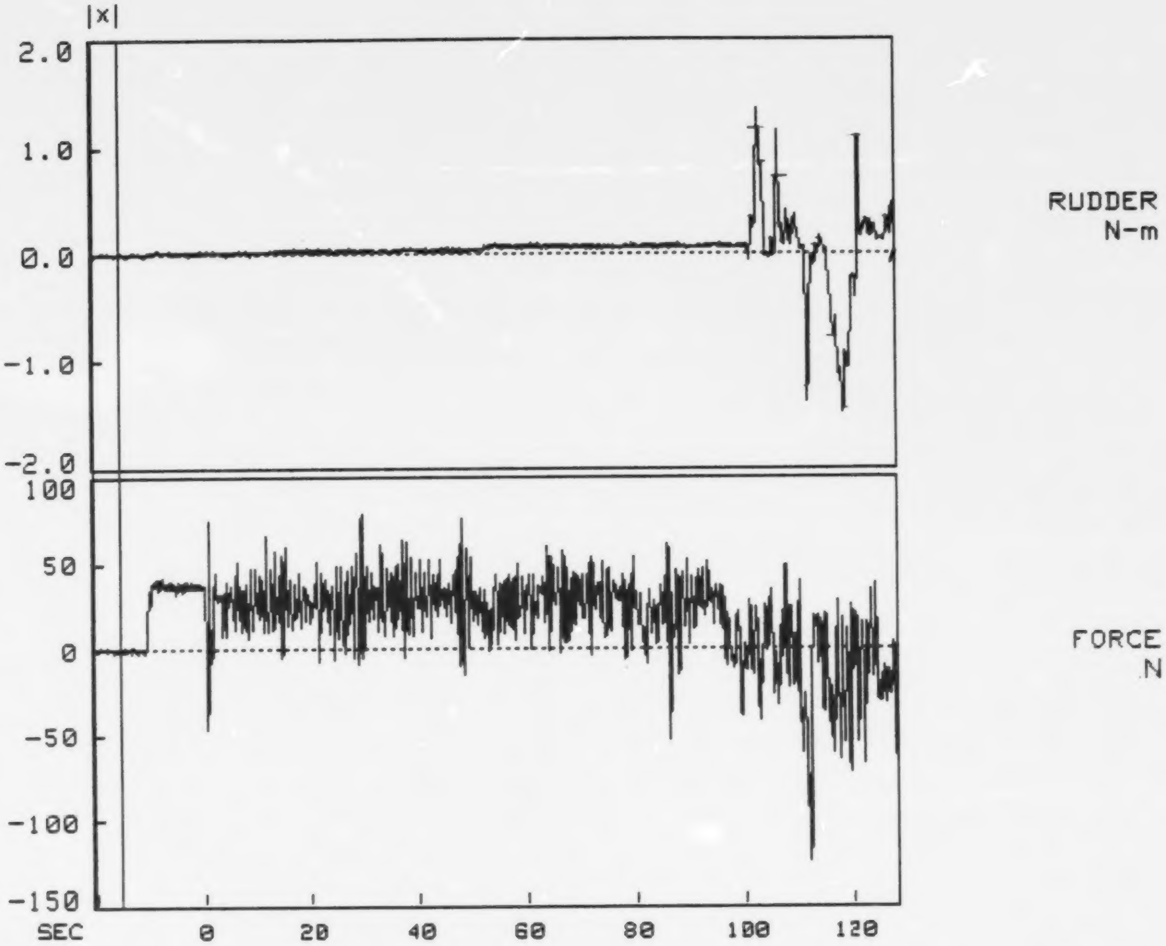

TEST 411

TEST #4 RUN 11

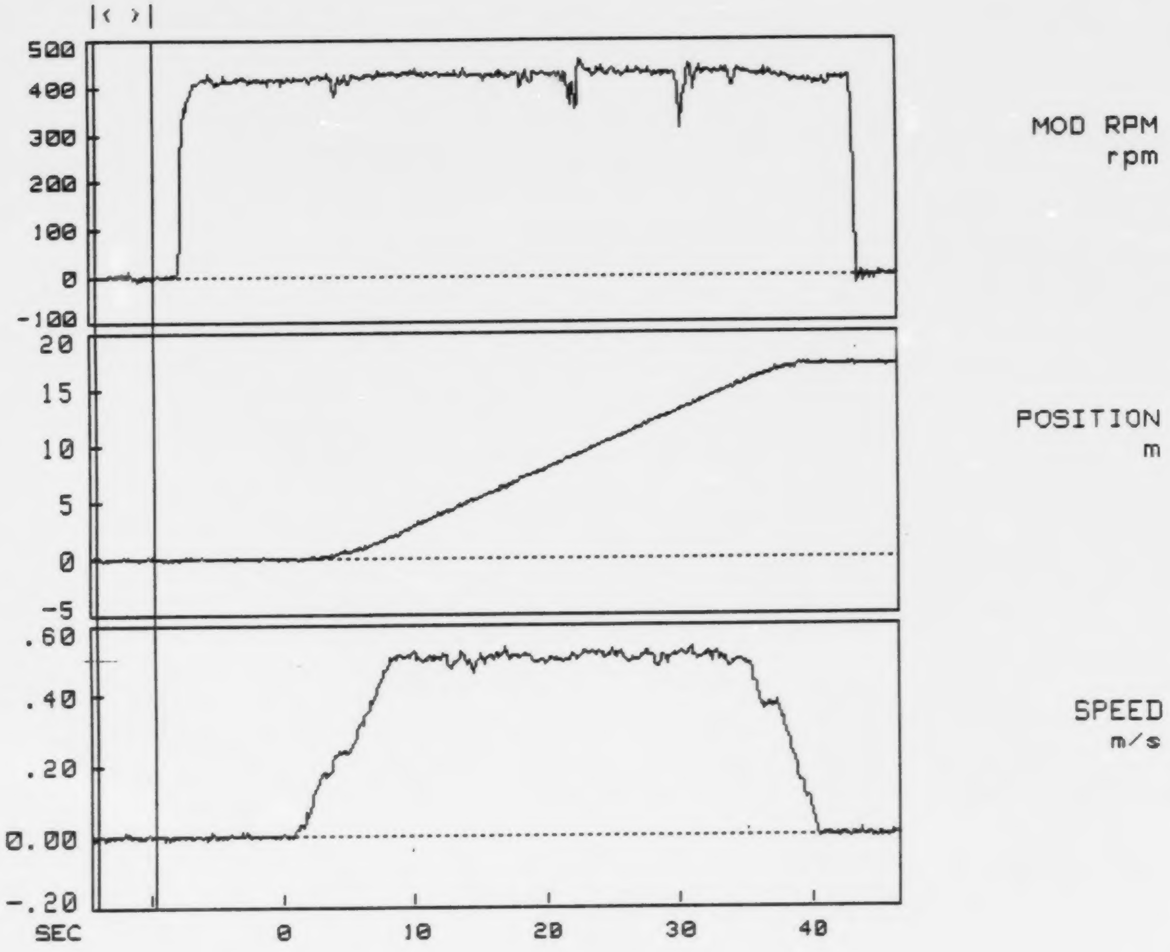

TEST 411

TEST #4 RUN 11

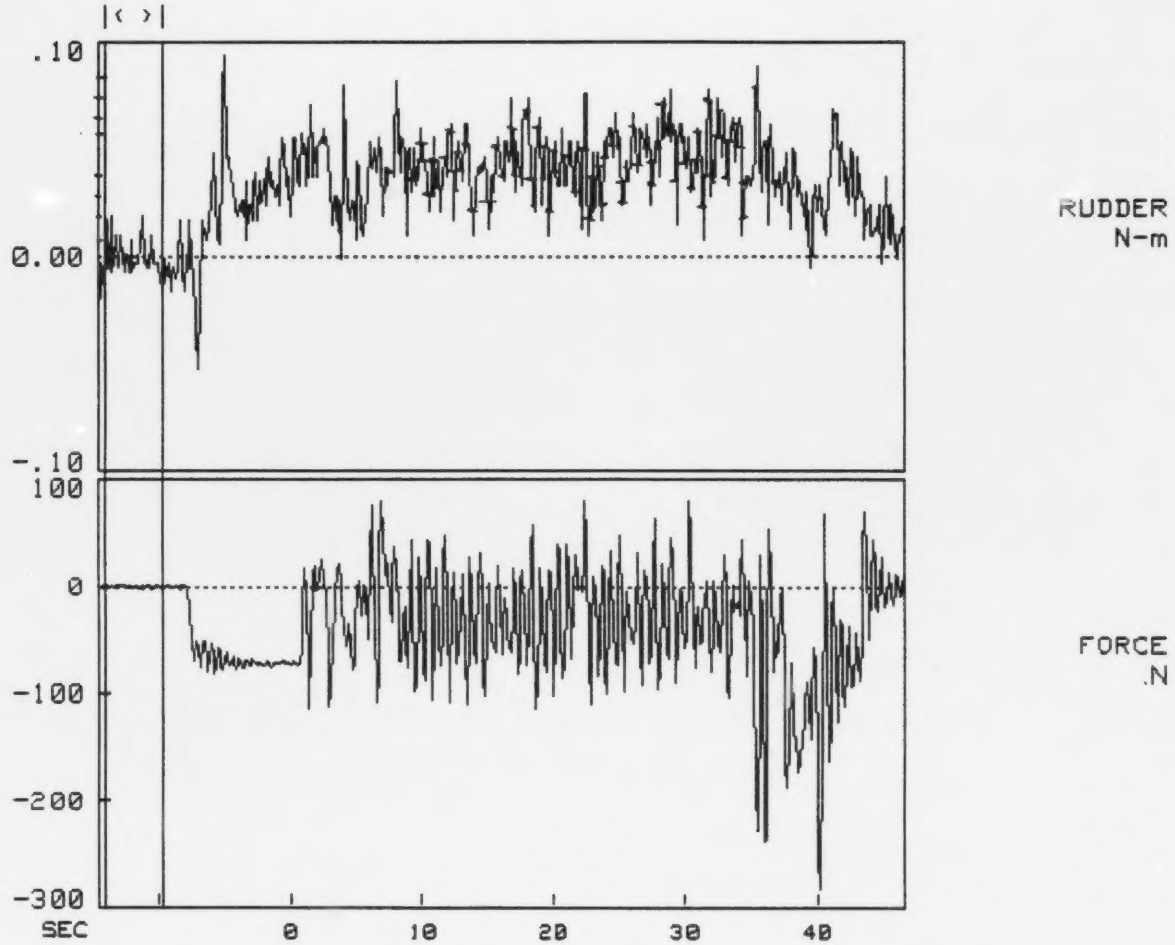

TEST 412

TEST #4 RUN 12

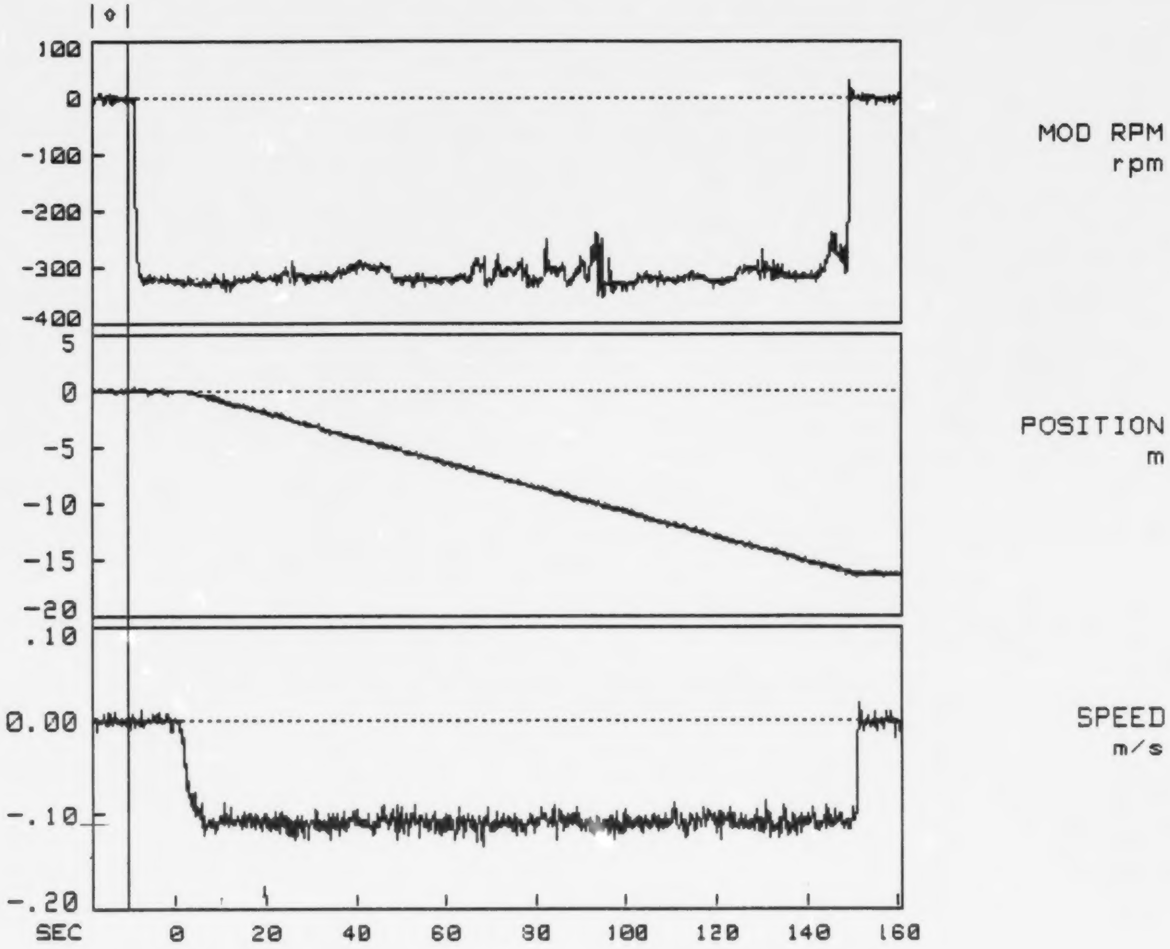

TEST 412

TEST #4 RUN 12

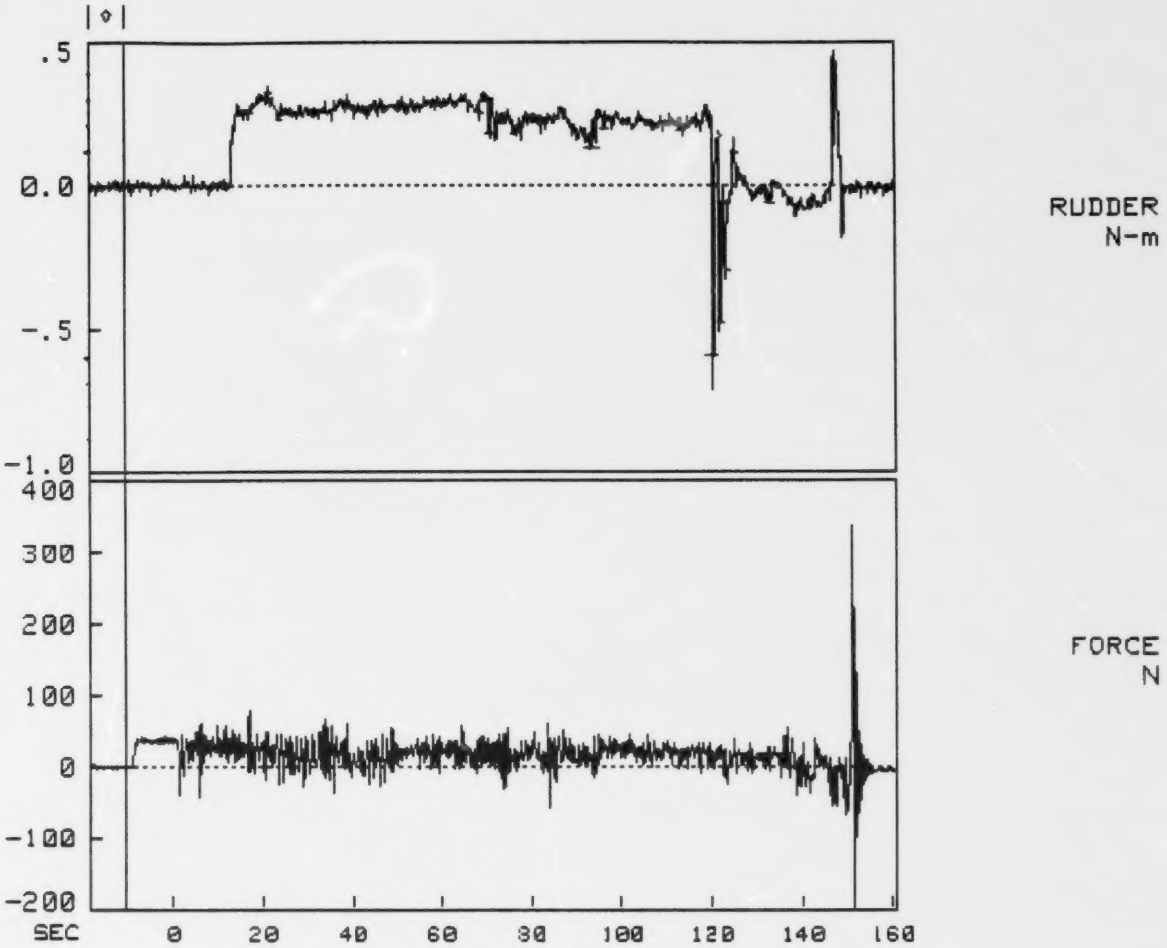

TEST 413

TEST #4 RUN 13

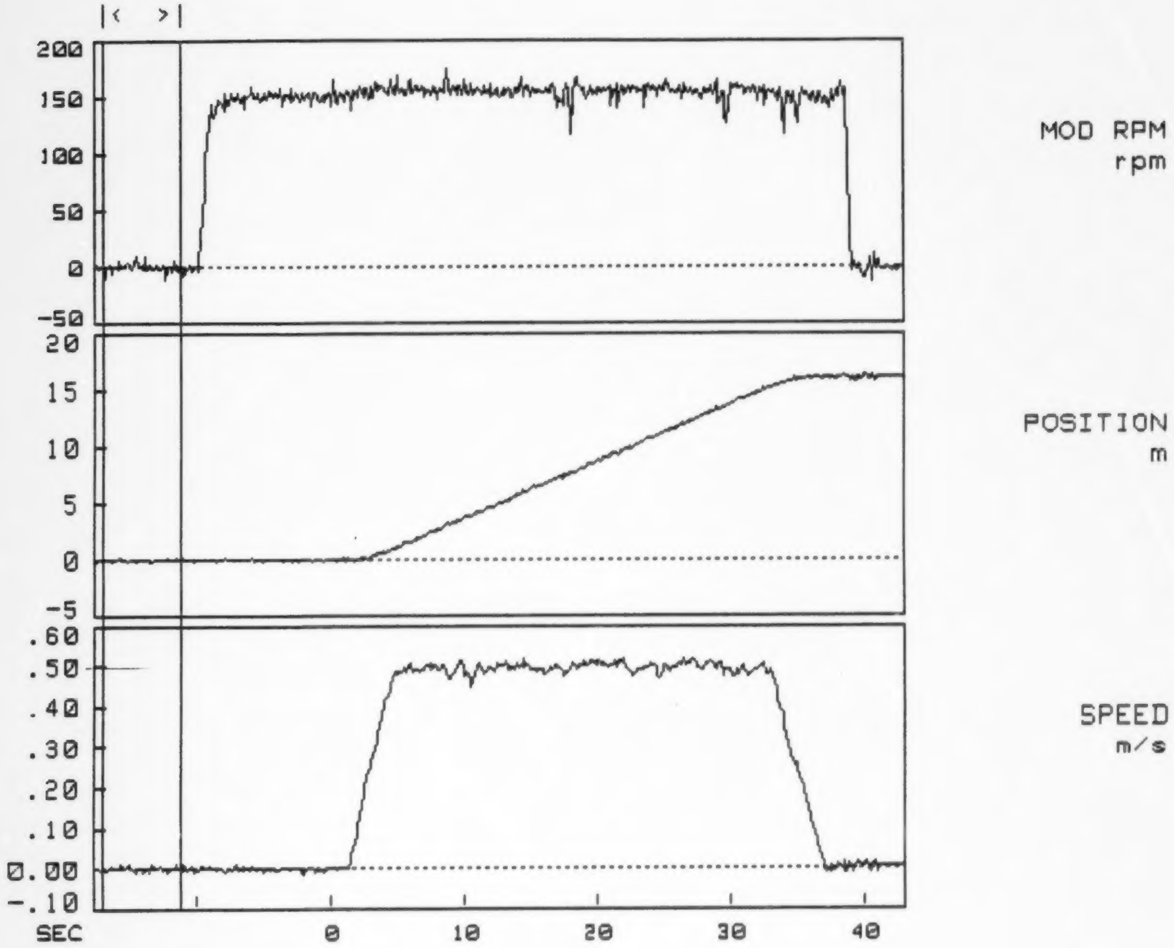

TEST 413

TEST #4 RUN 13

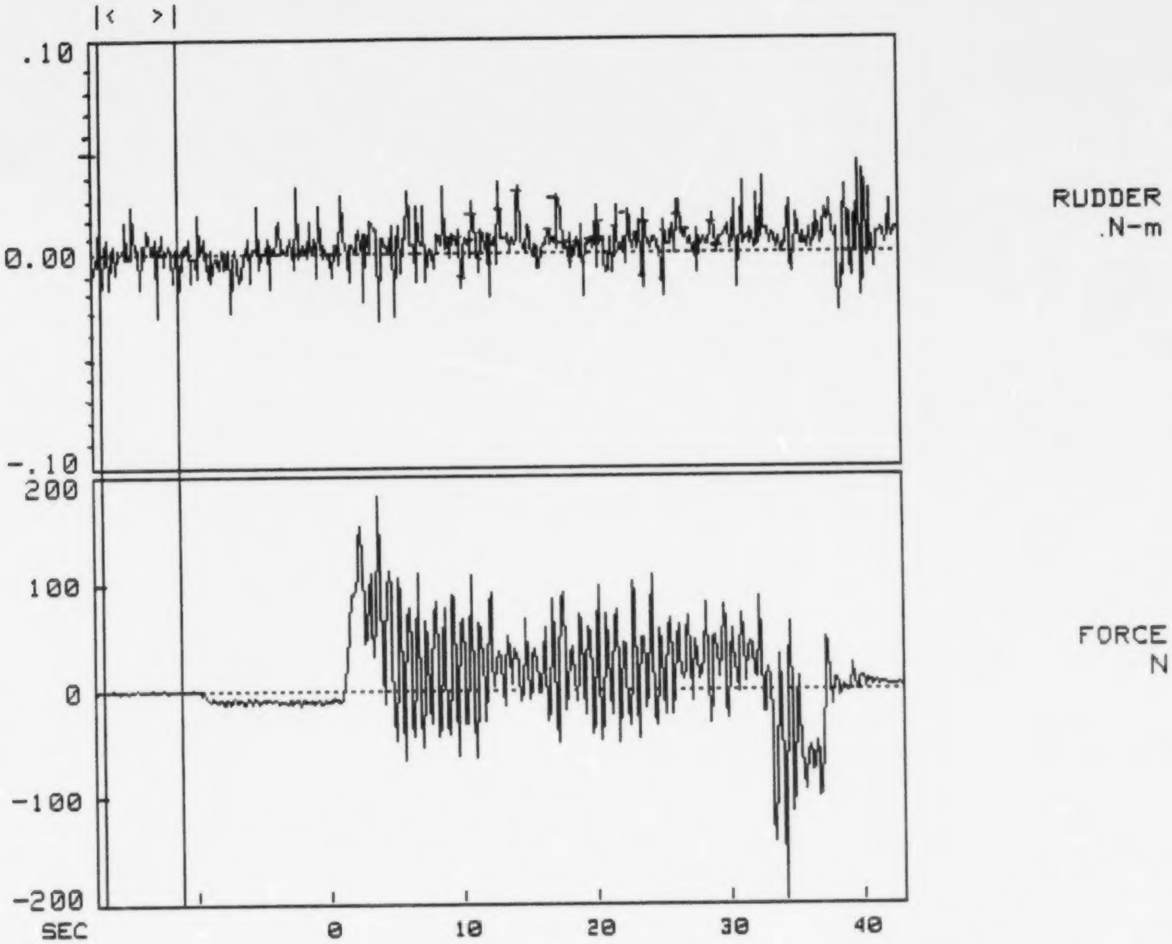

TEST 414

TEST #4 RUN 14

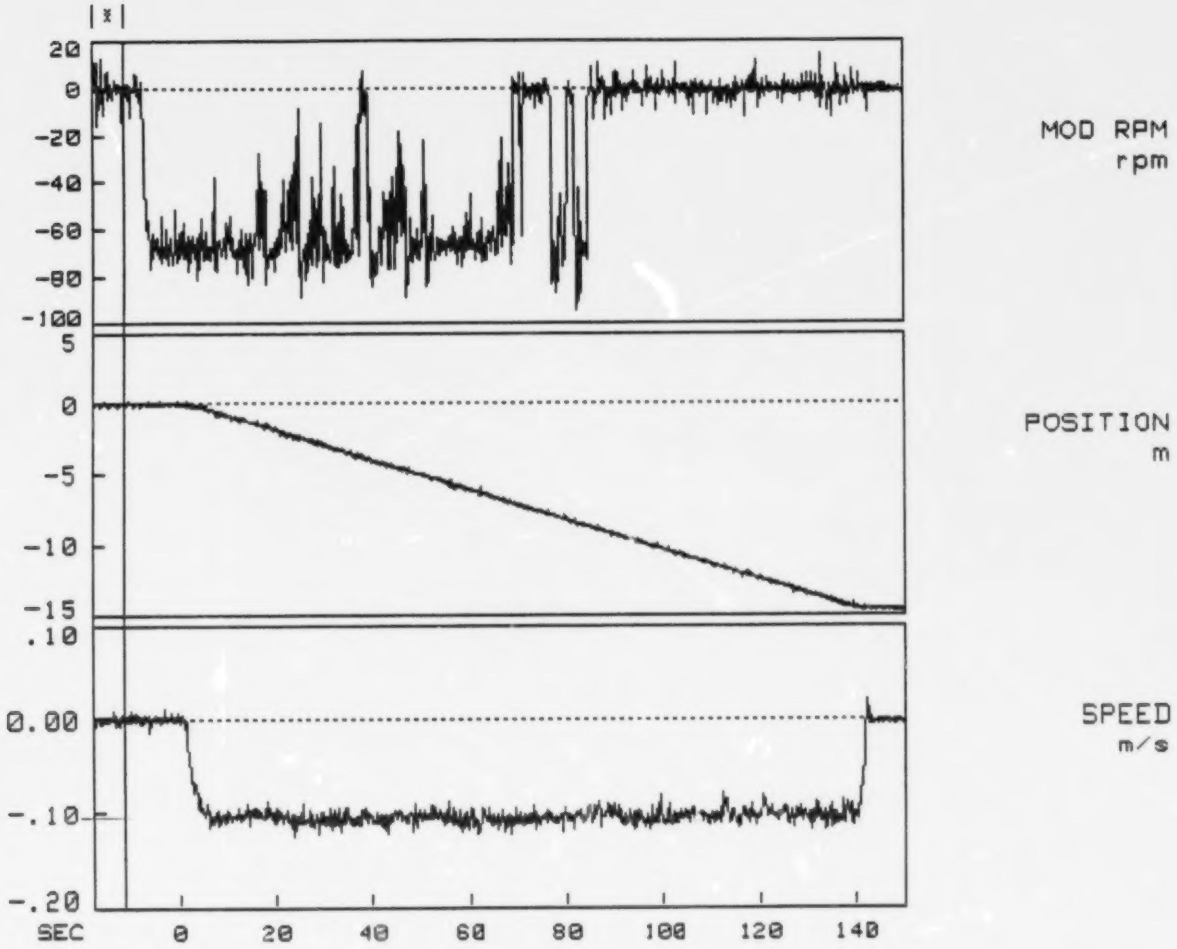

TEST 414

TEST #4 RUN 14

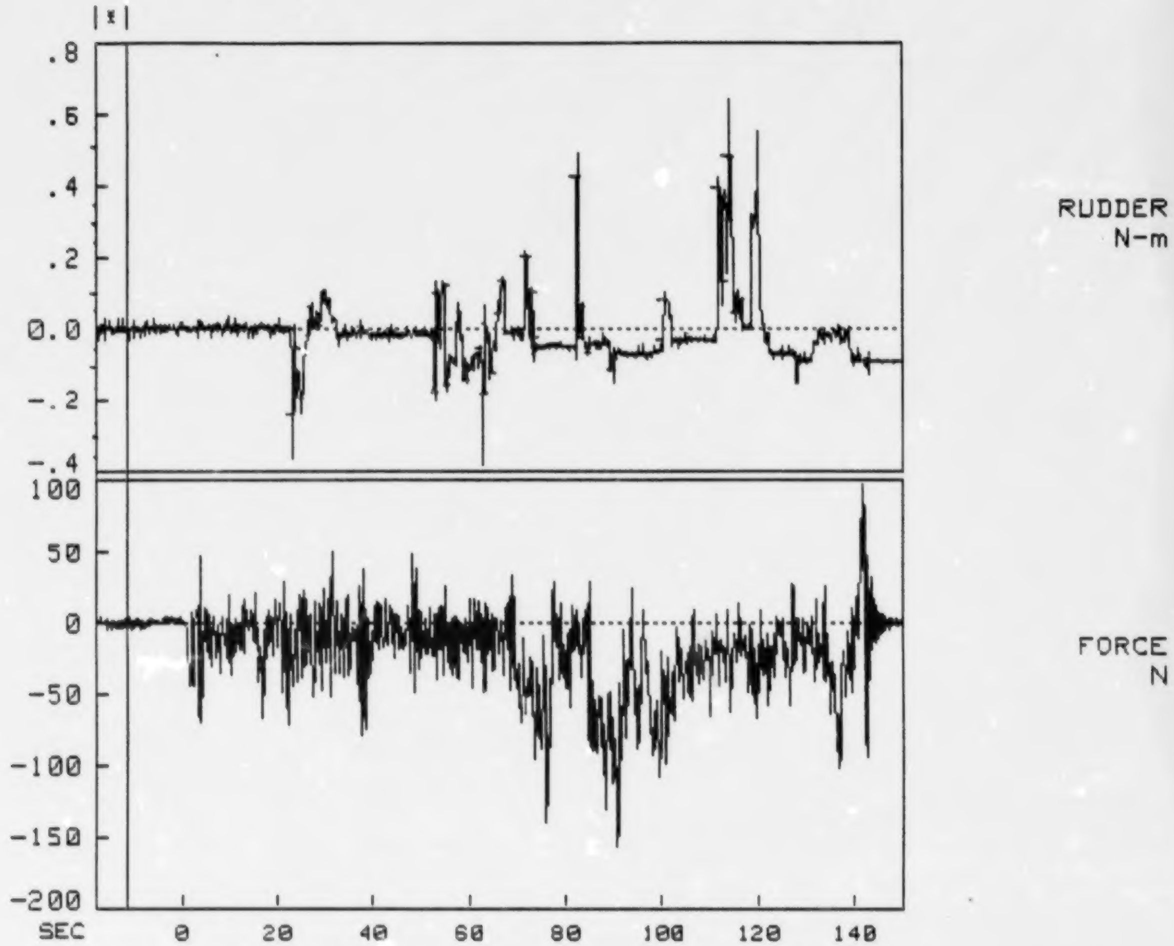

TEST #4 RUN 15 TEST 415

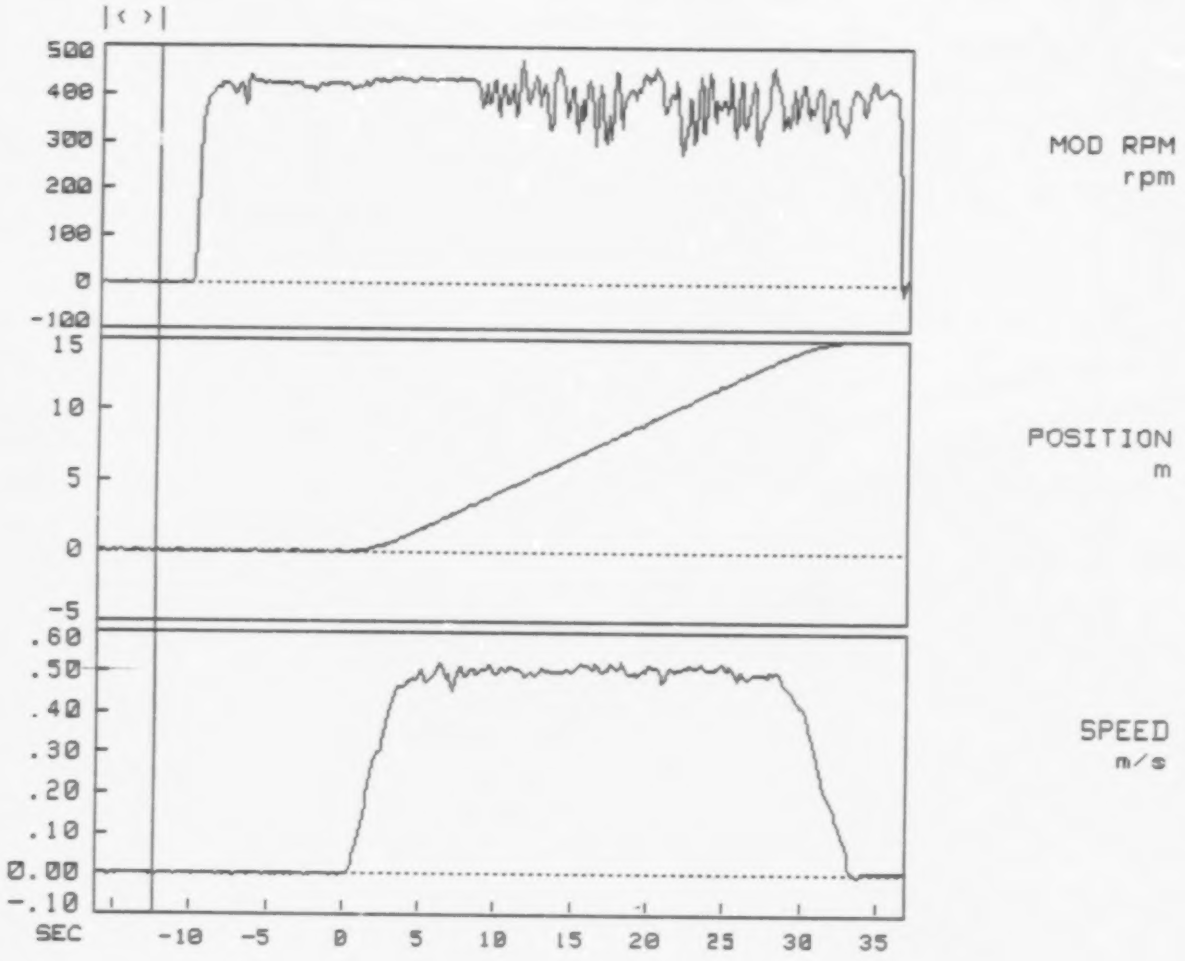

TEST #4 RUN 15 TEST 415

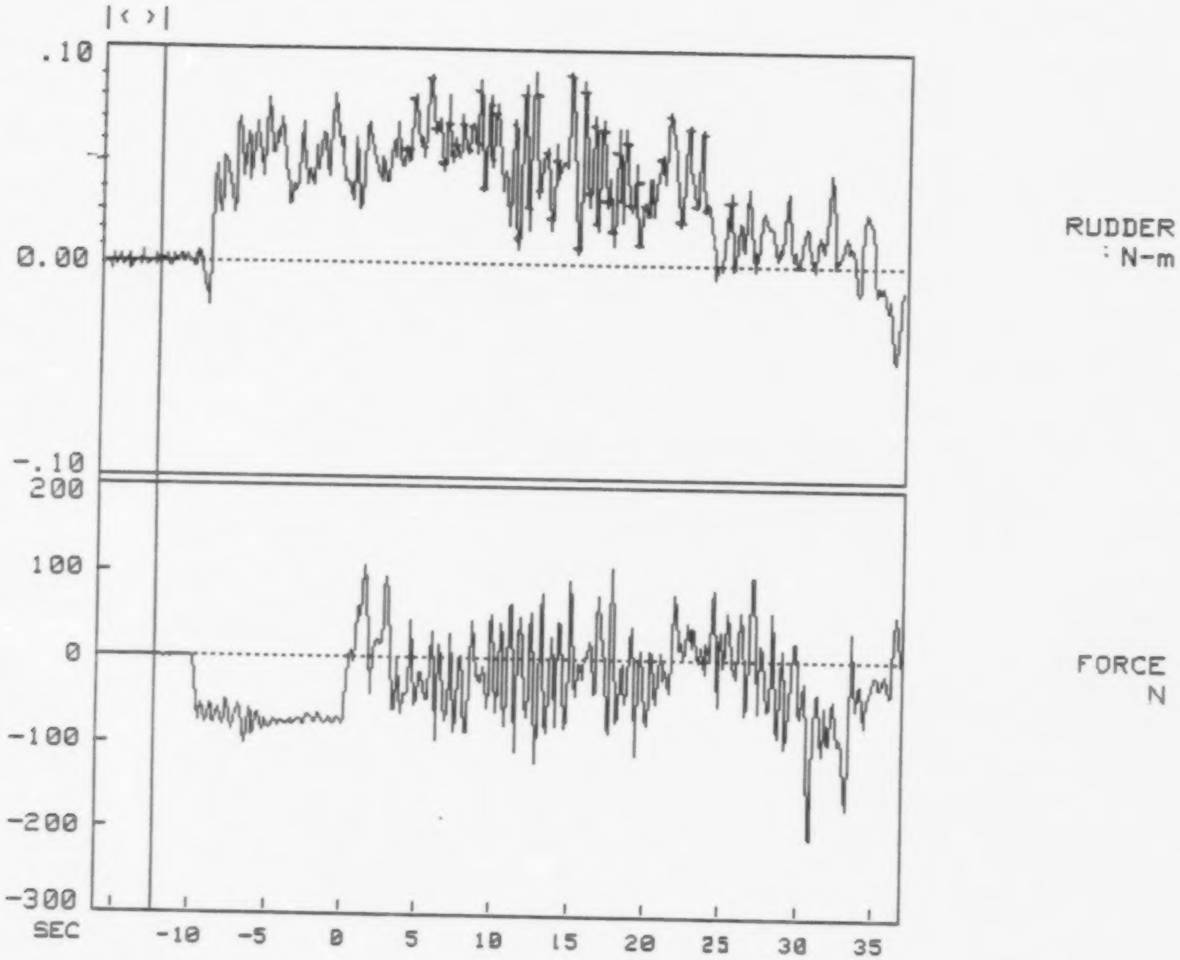

TEST 416

TEST #4 RUN 16

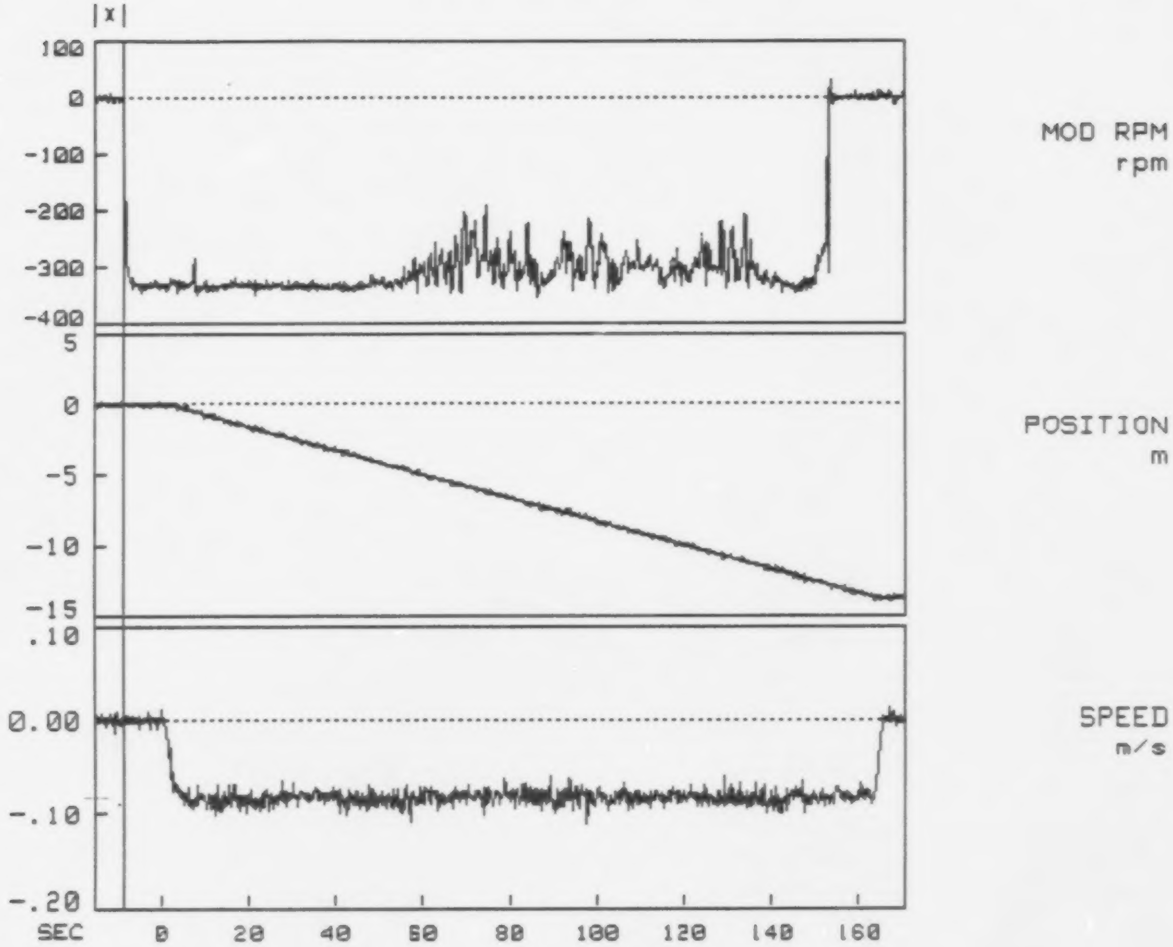

TEST 416

TEST #4 RUN 16

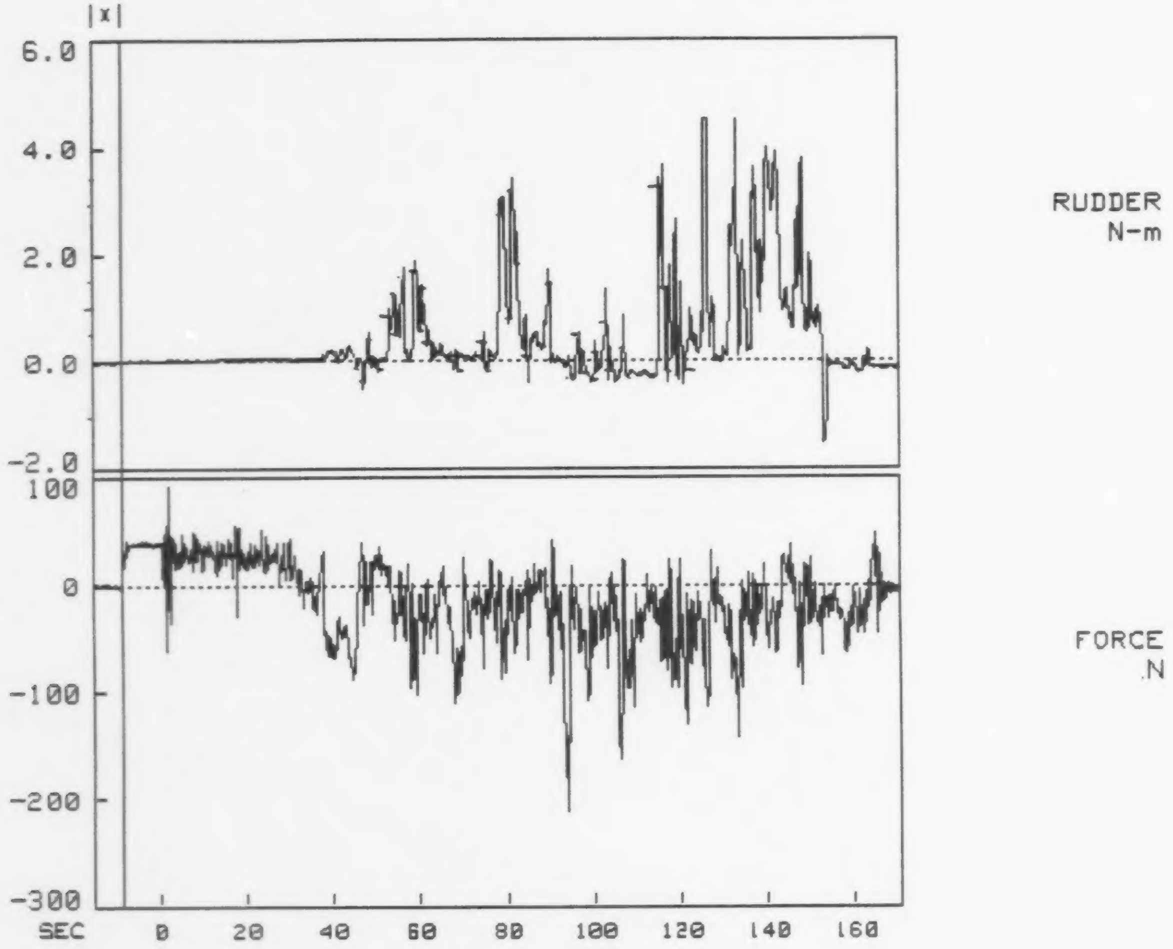

TEST #4 RUN 17 TEST 417

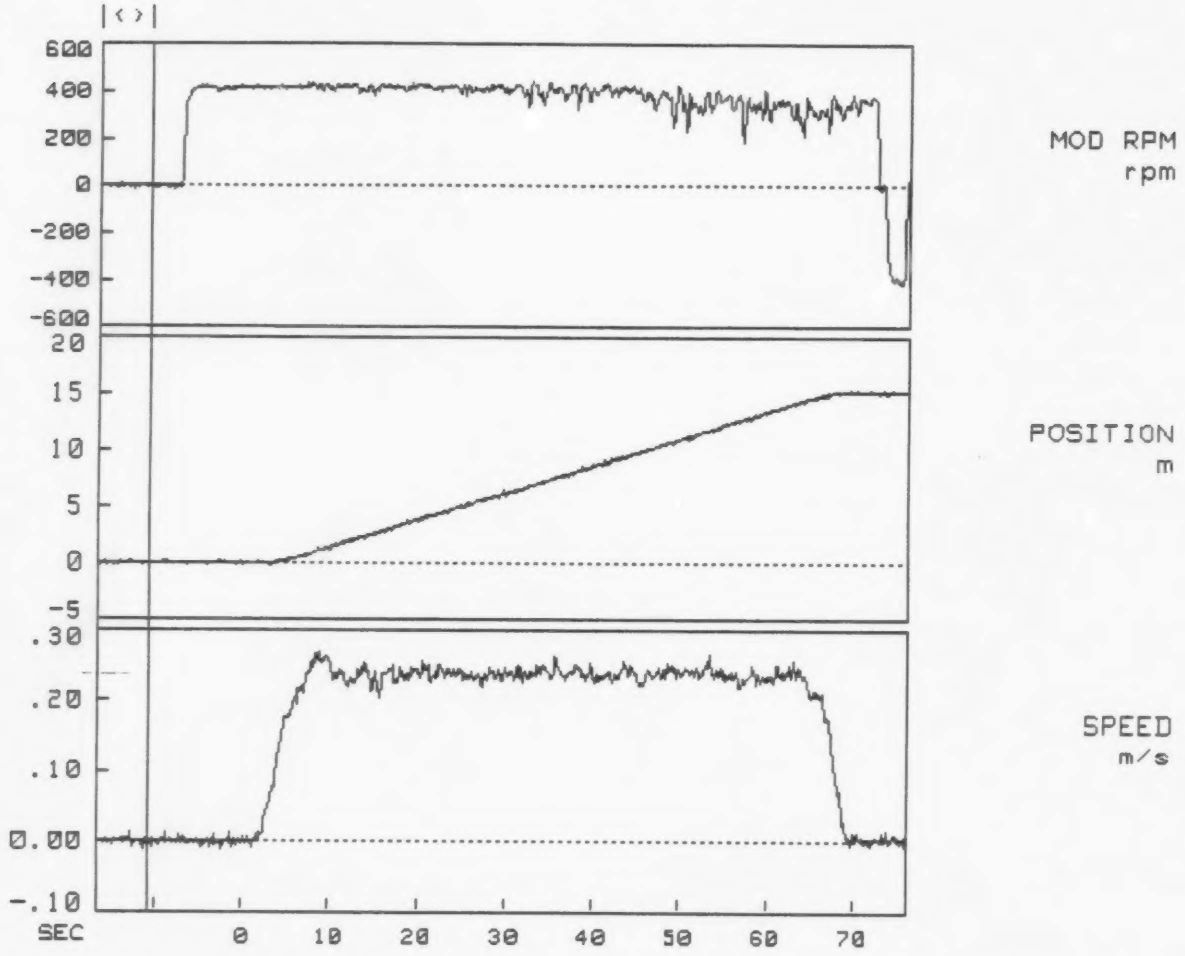

TEST #4 RUN 17 TEST 417

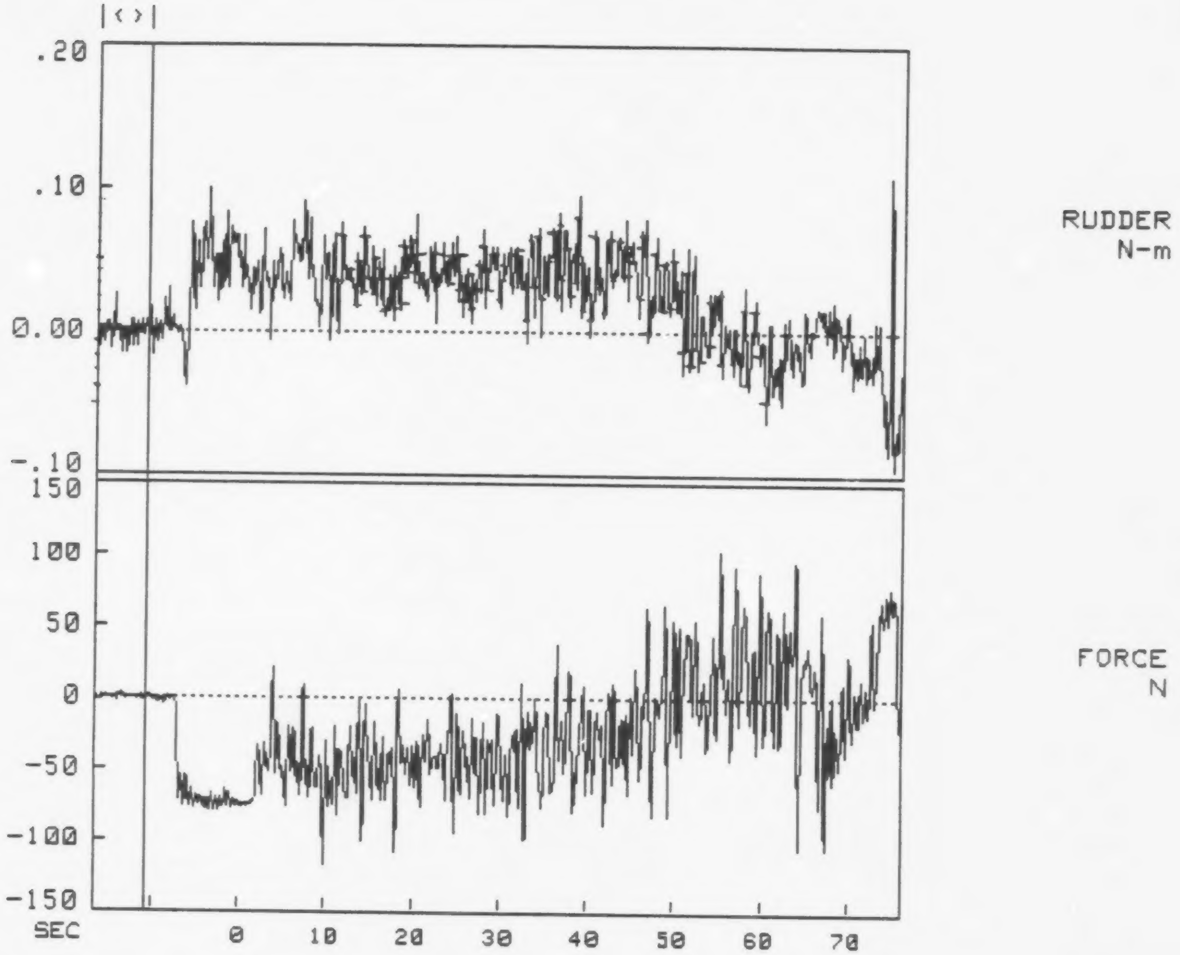

TEST #4 RUN 18 TEST 418

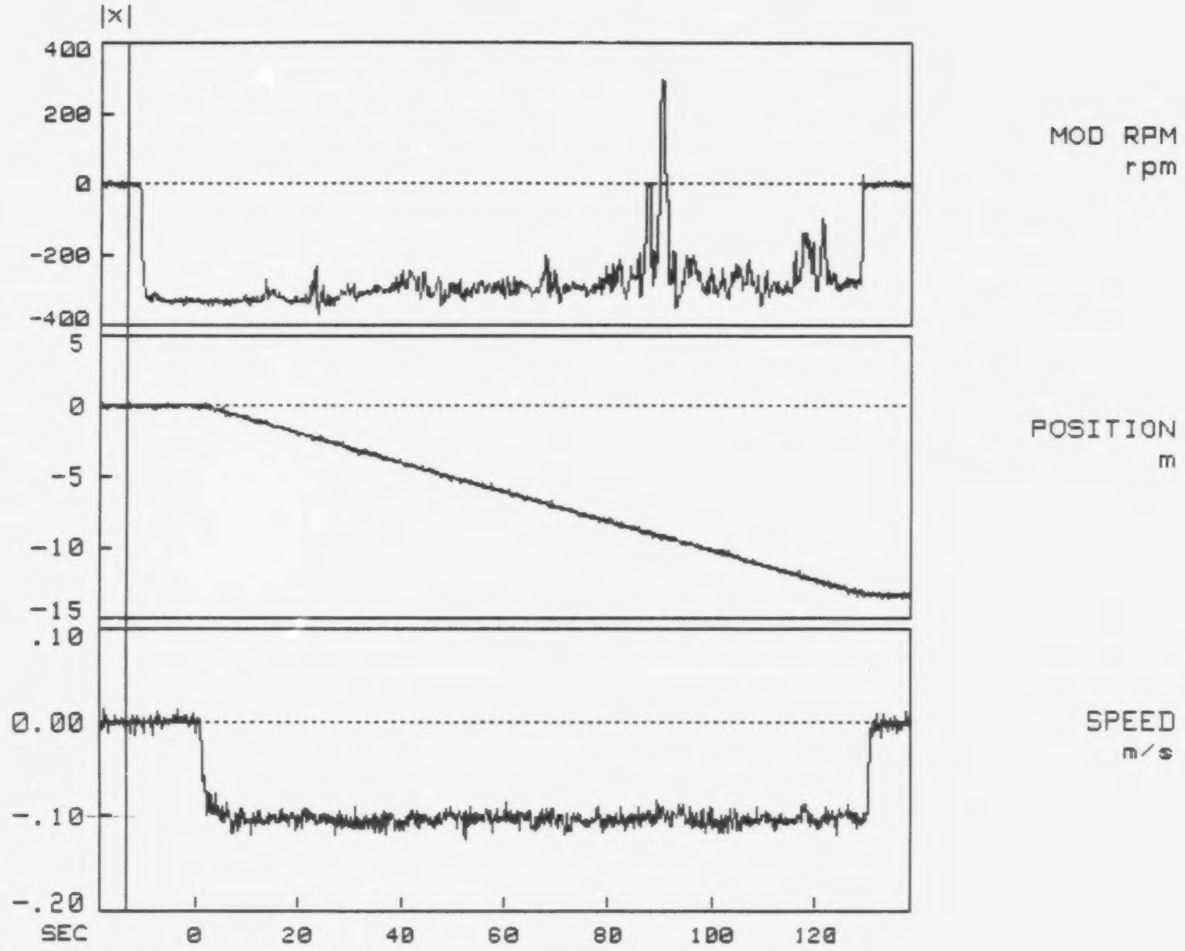

TEST #4 RUN 18 TEST 418

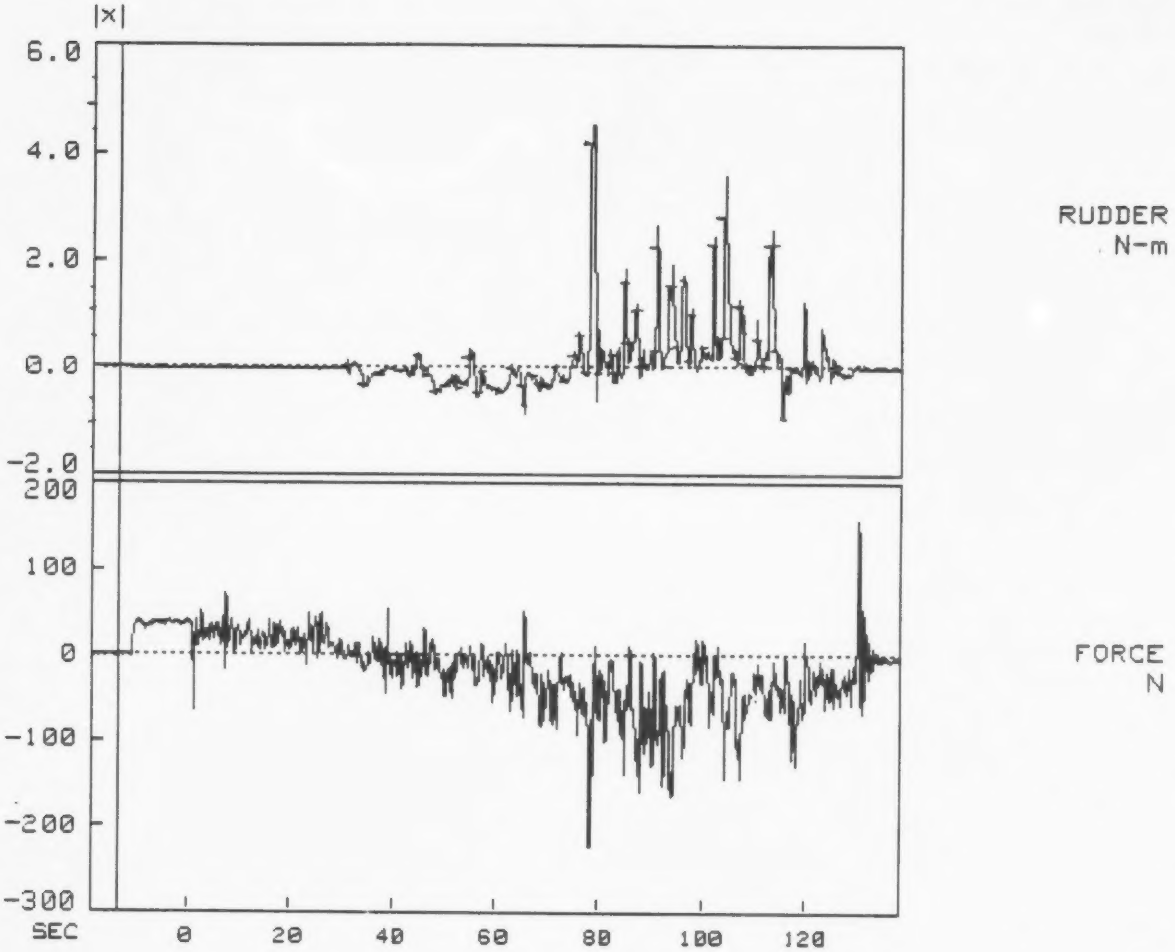

TEST 421

TEST #4 RUN 21

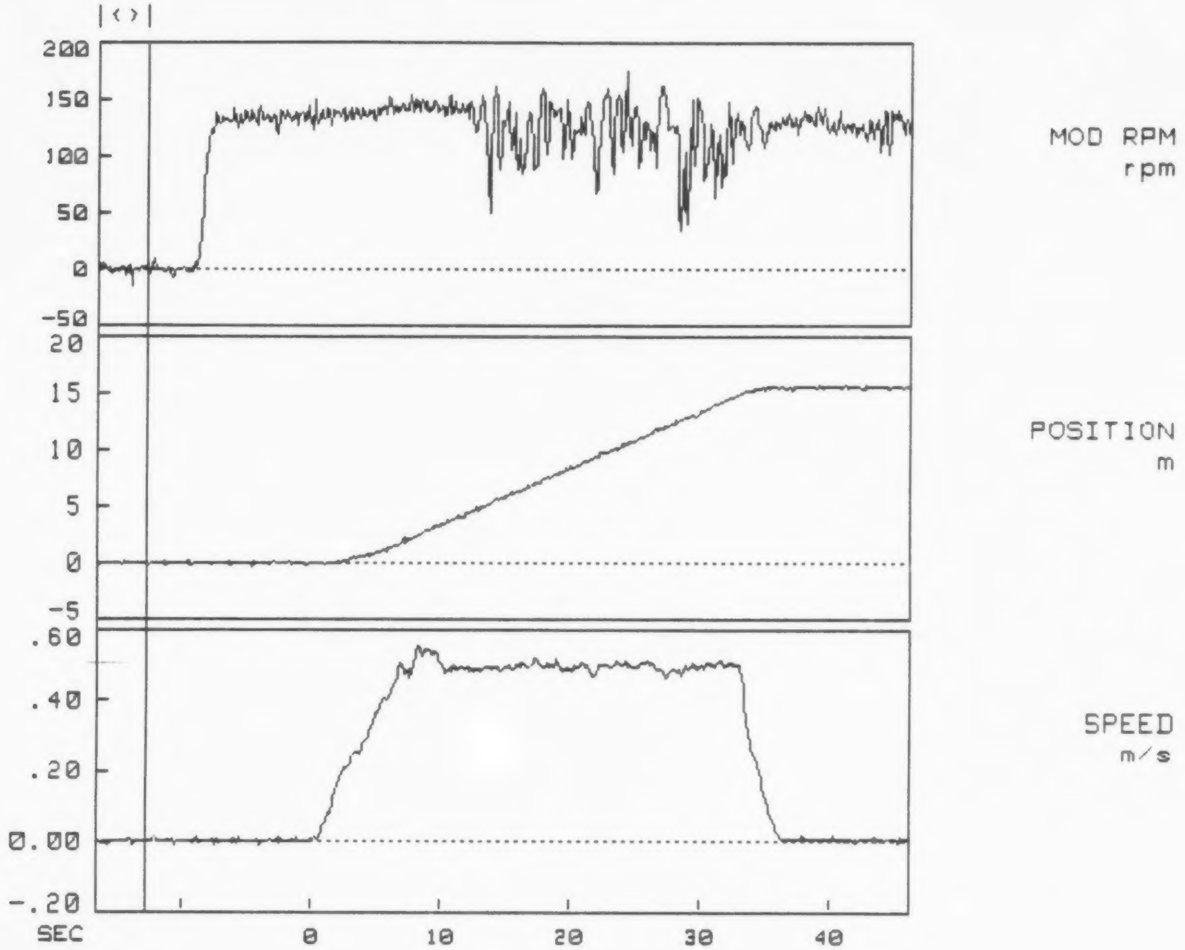

TEST #4 RUN 21 TEST 421

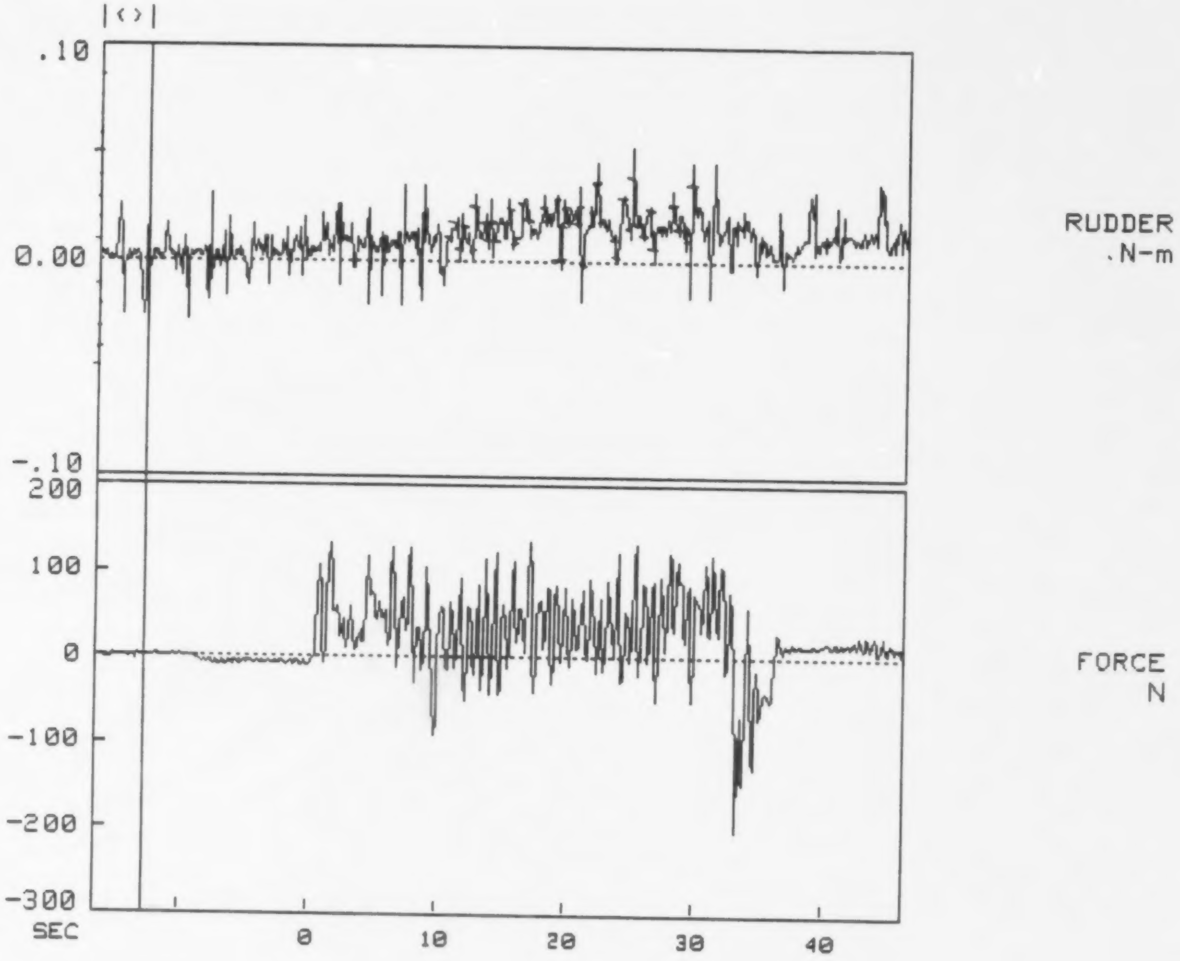

TEST #4 RUN 22 TEST 422

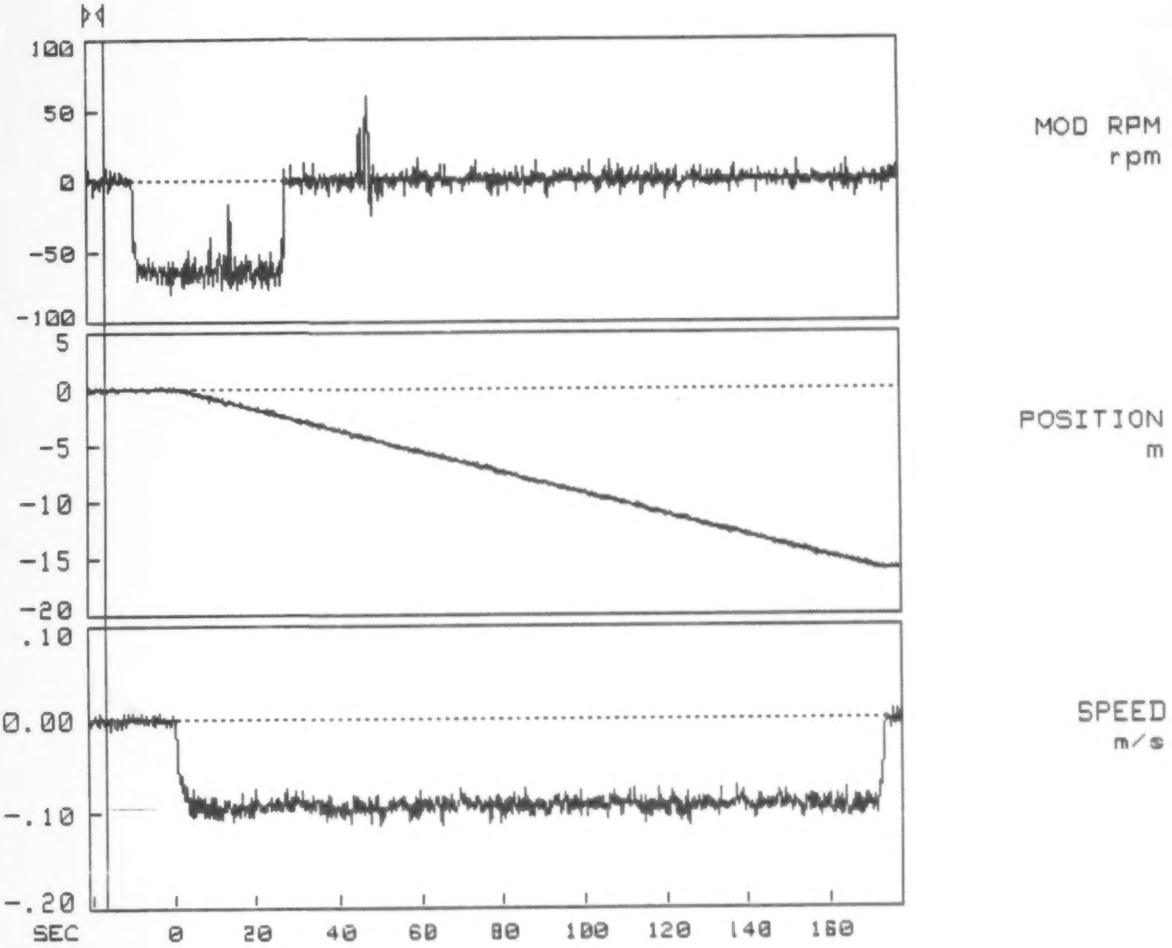

TEST 422

TEST #4 RUN 22

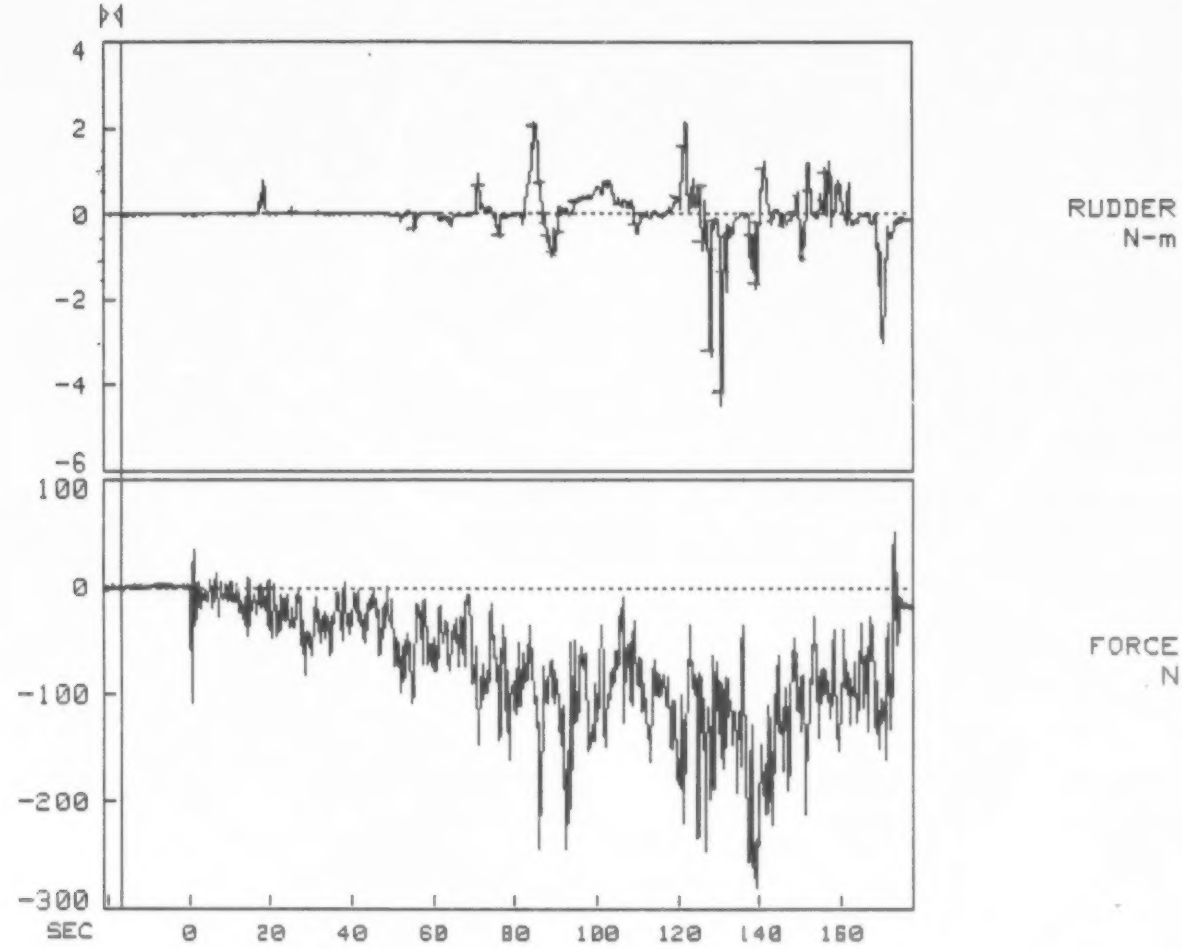

TEST 423

TEST #4 RUN 23

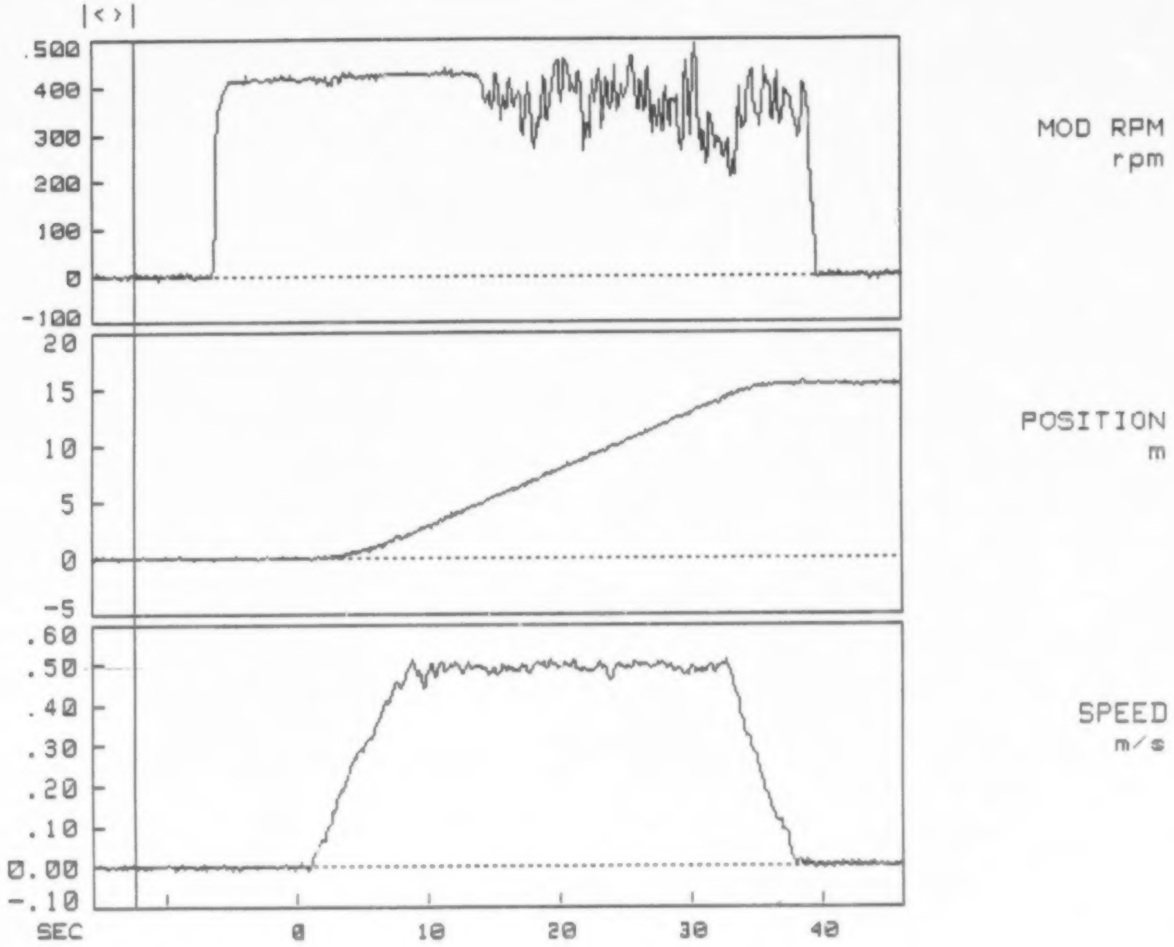

TEST 423

TEST #4 RUN 23

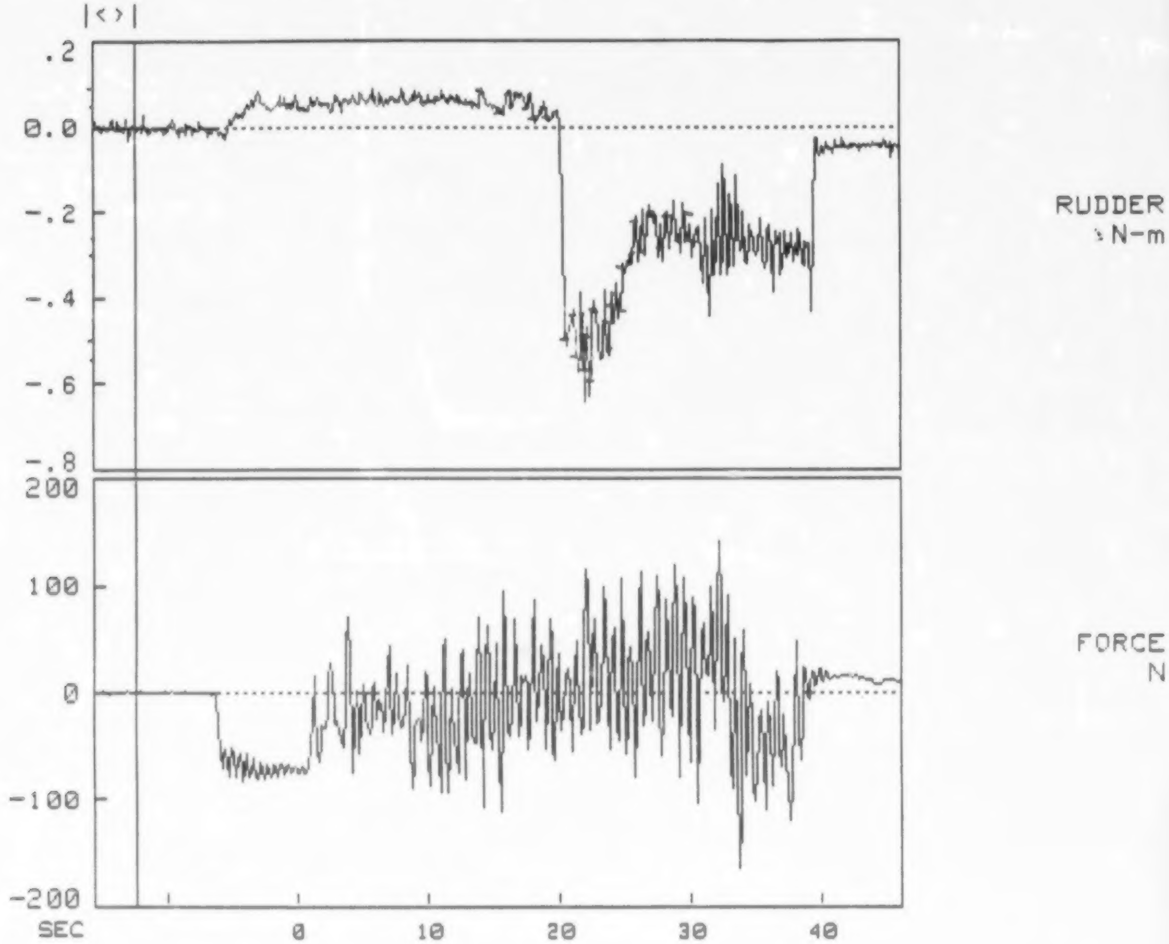

TEST 424

TEST #4 RUN 24

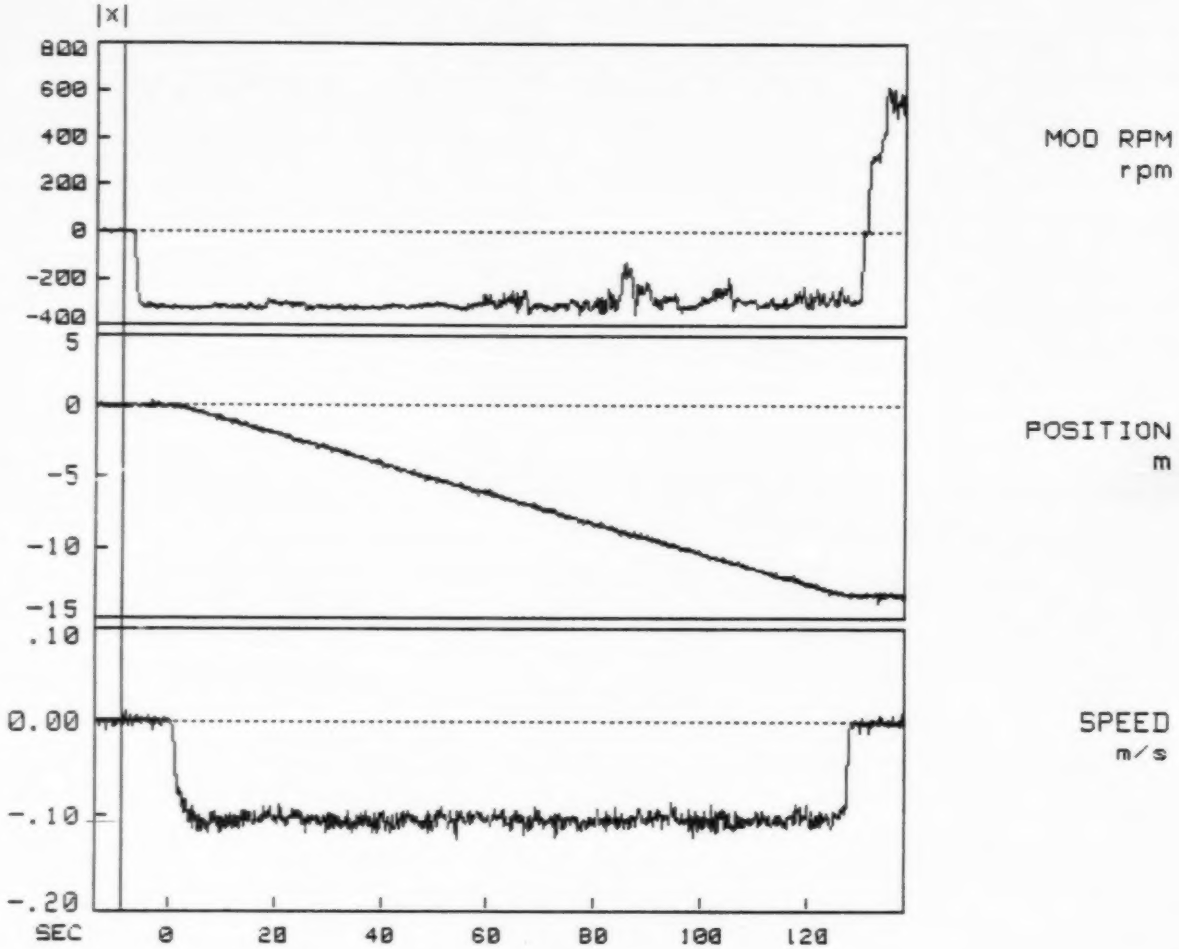

TEST 424

TEST #4 RUN 24

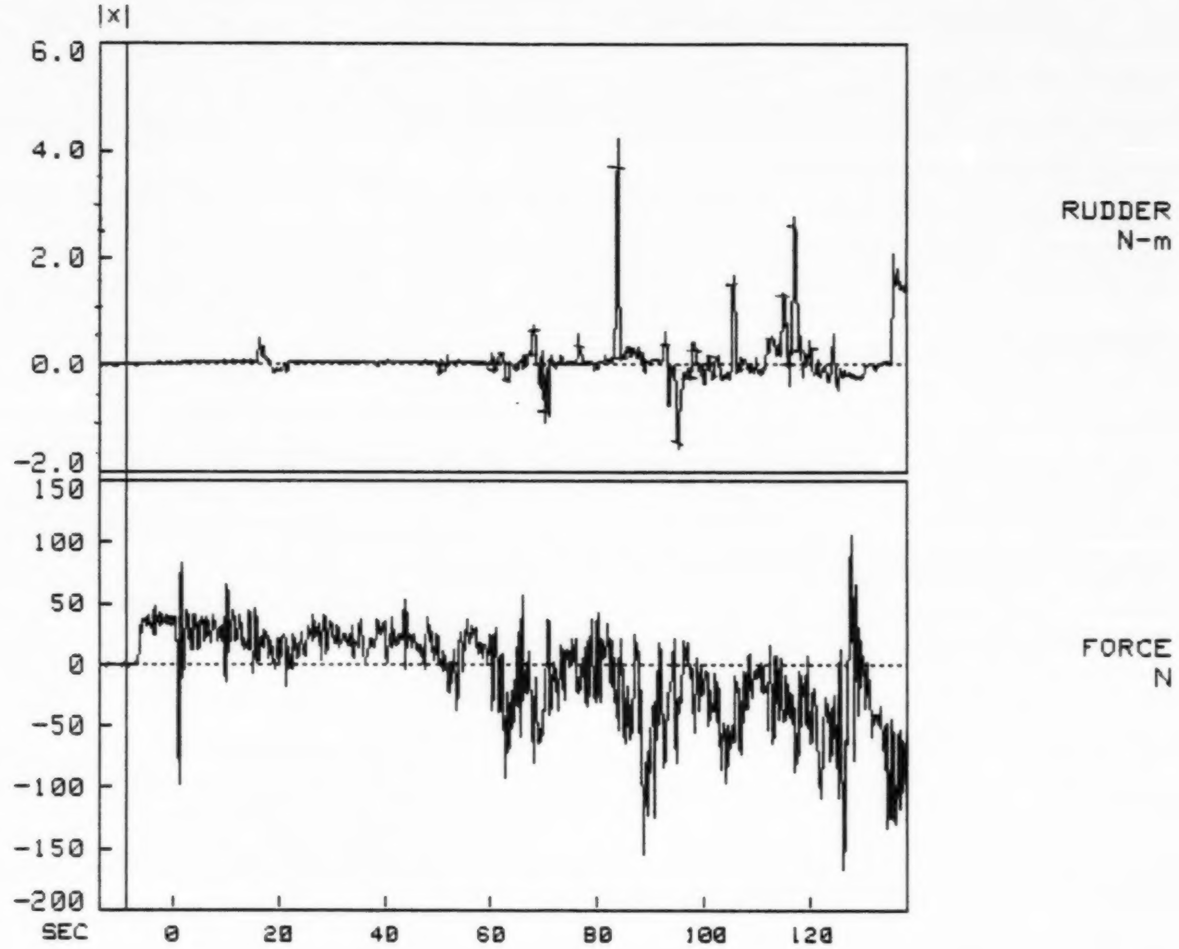

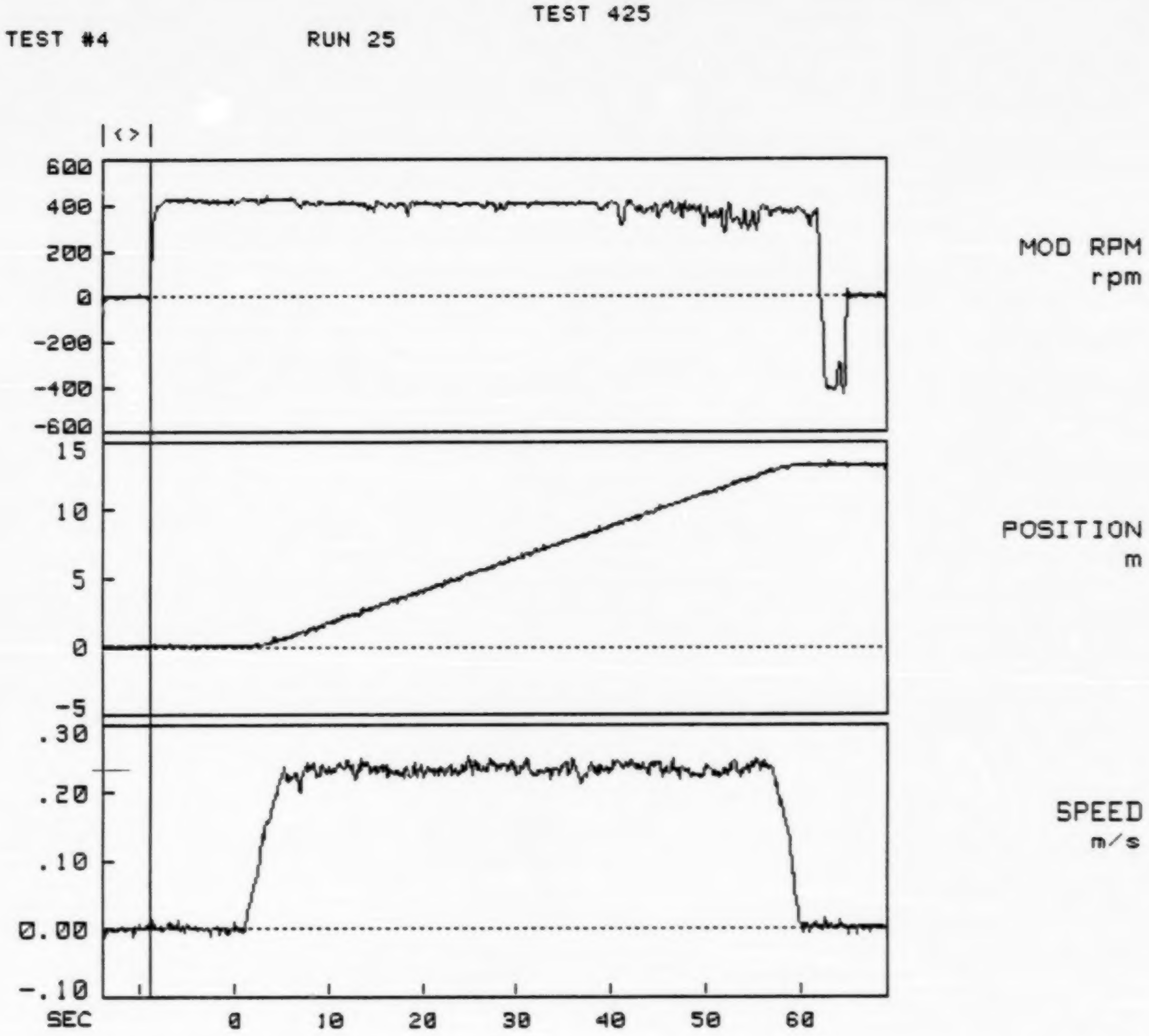
TEST 425
TEST #4
RUN 25
|<>|
600
400
200
0
-200
-400
-600
MOD RPM
rpm
15
10
5
0
-5
POSITION
m
.30
.20
.10
0.00
-.10
SPEED
m/s
SEC
0
10
20
30
40
50
60

TEST #4 RUN 25 TEST 425

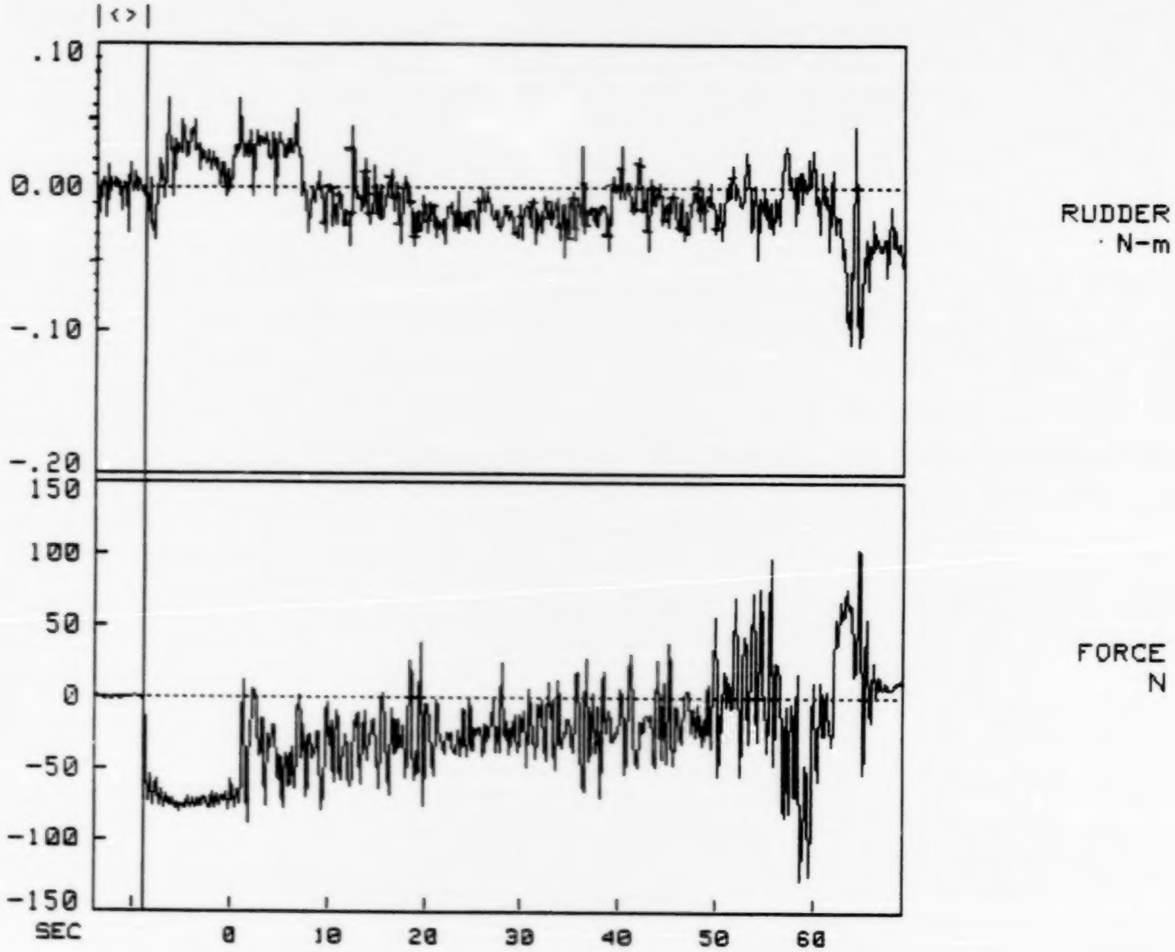

TEST #4 RUN 35 TEST 435

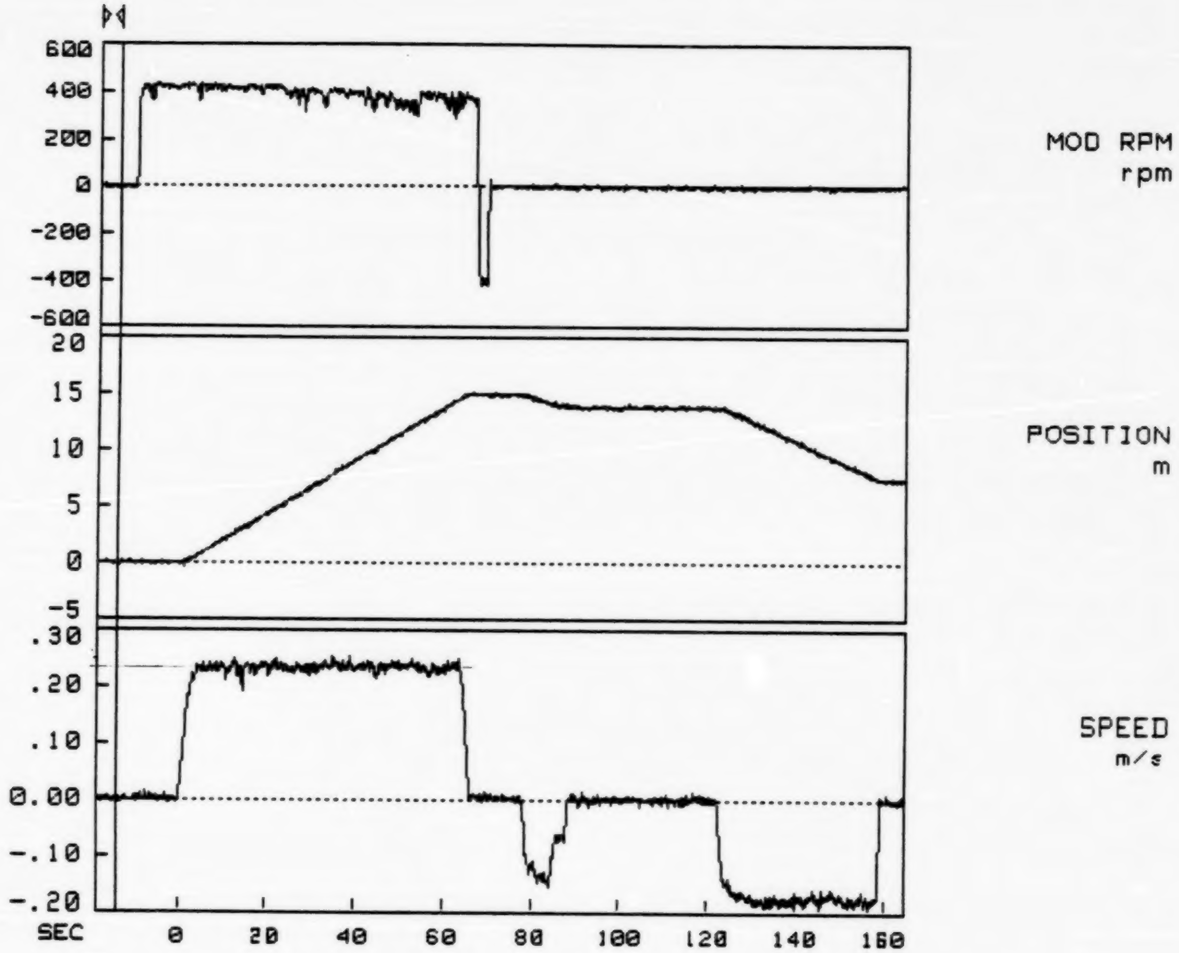

TEST #4 RUN 35 TEST 435

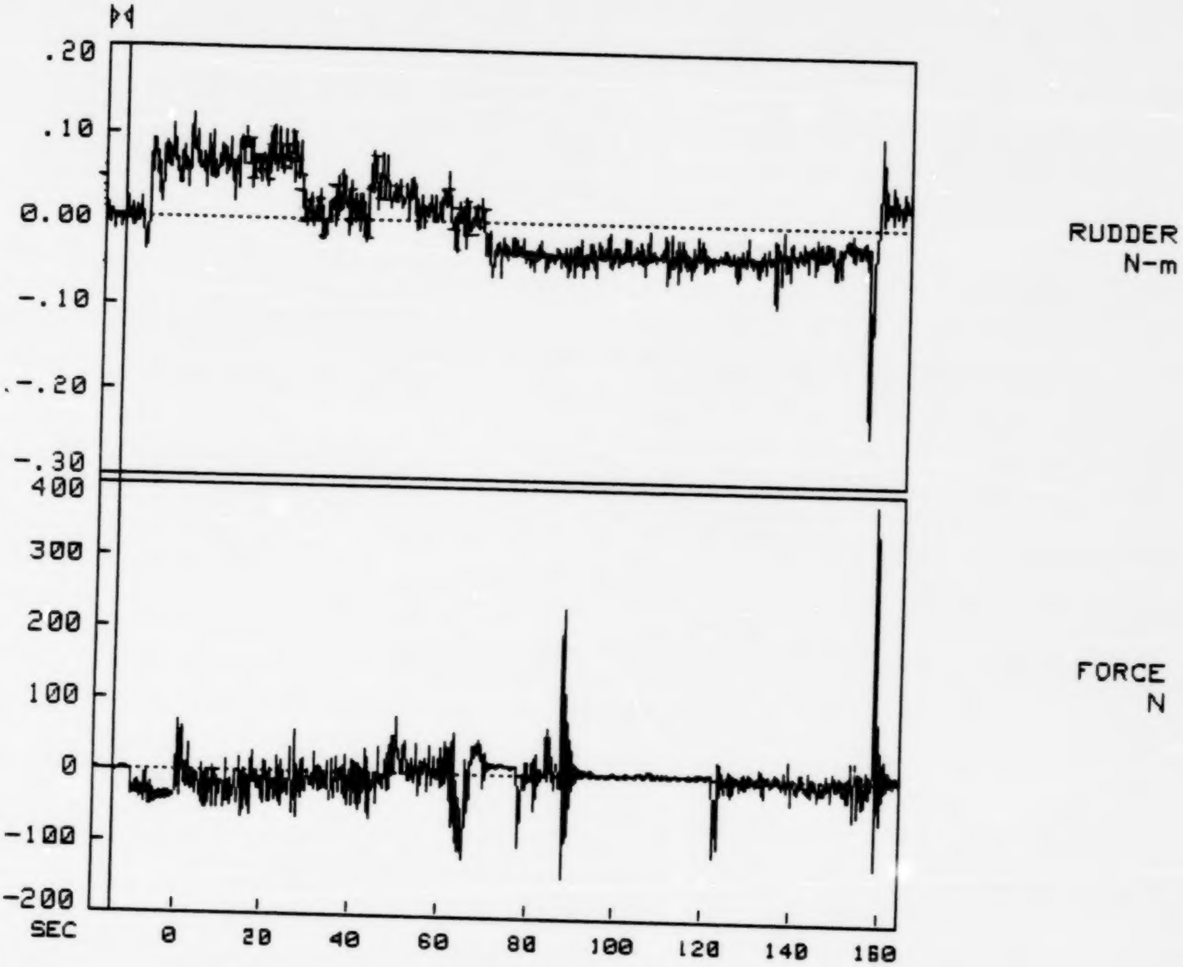

TEST 436

TEST #4 RUN 36

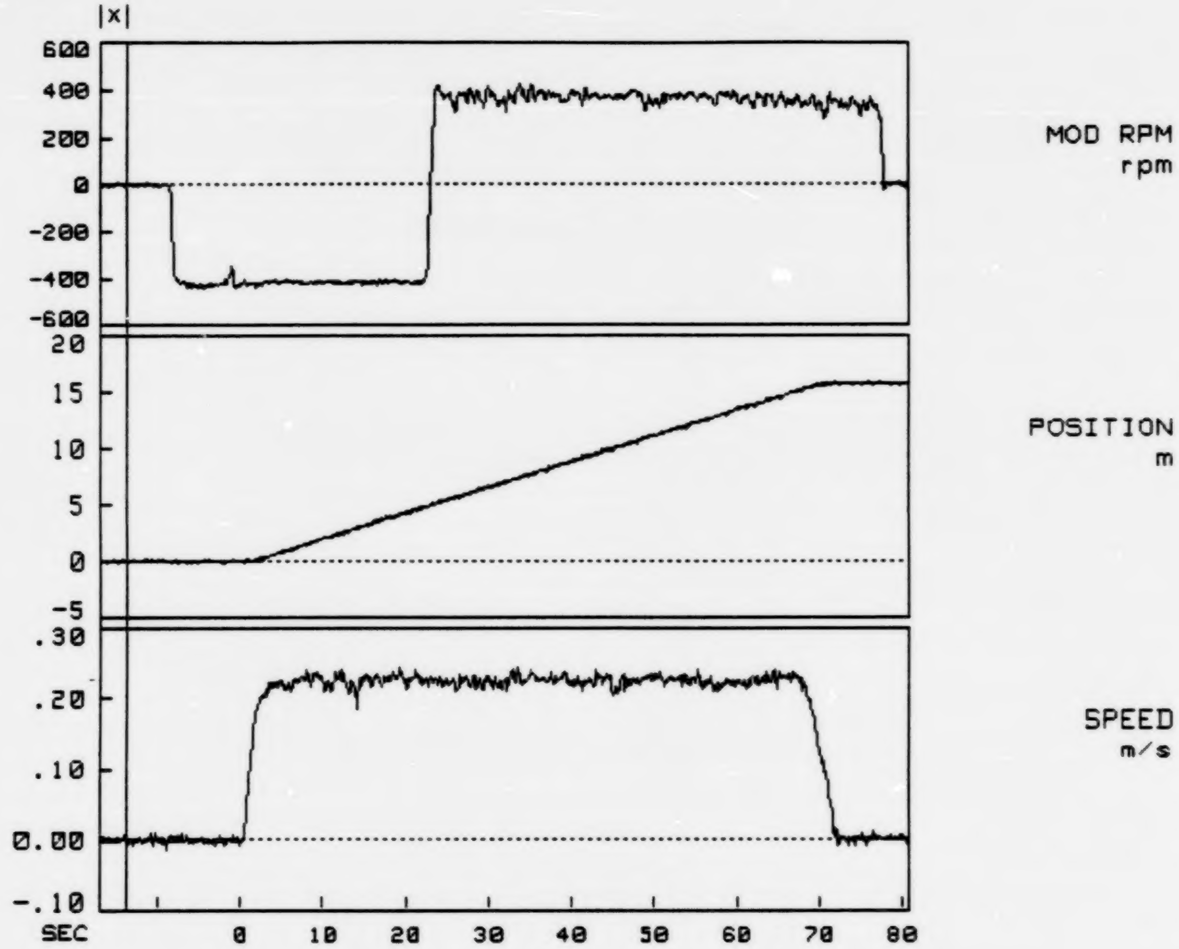

TEST 436

TEST #4 RUN 36

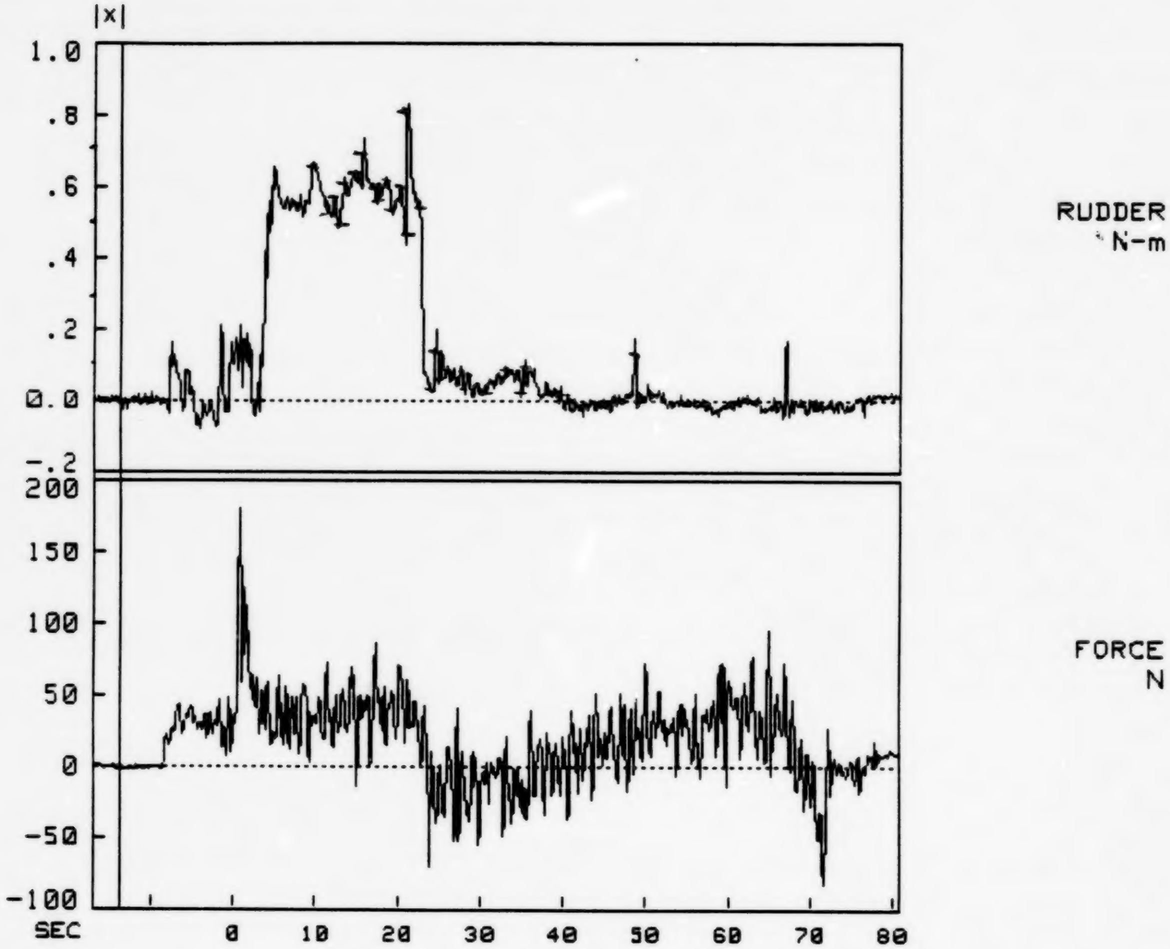

TEST 437

TEST #4 RUN 37

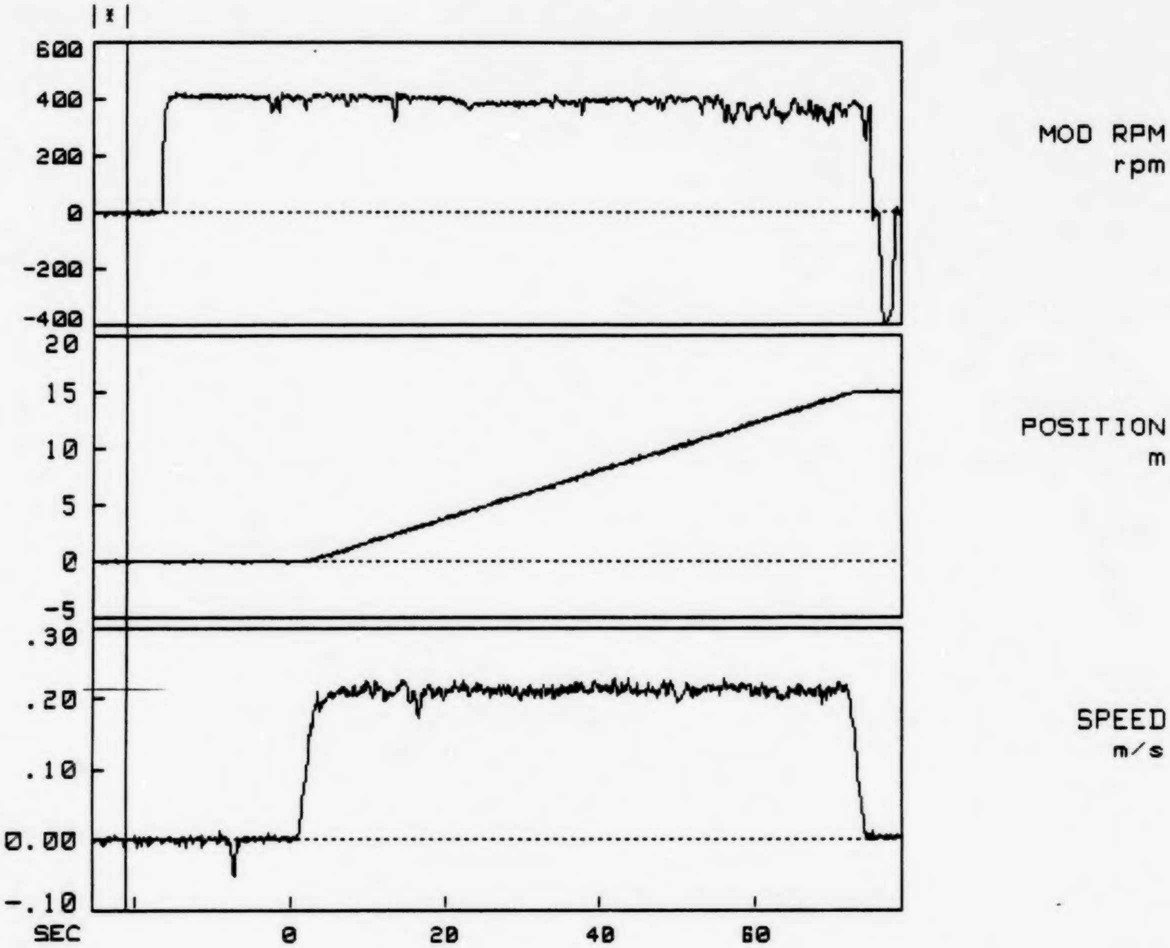

TEST 437

TEST #4 RUN 37

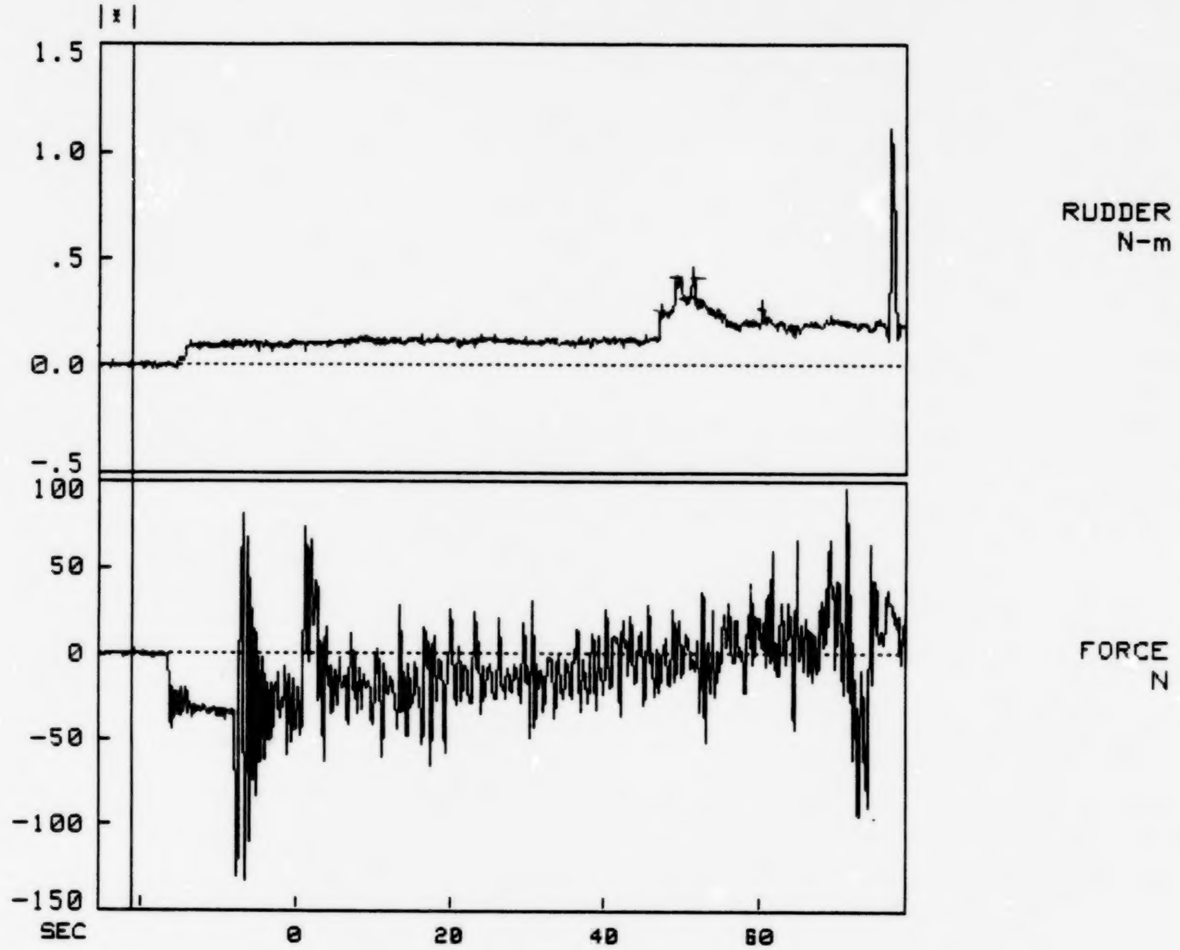

TEST 438

TEST #4 RUN 38

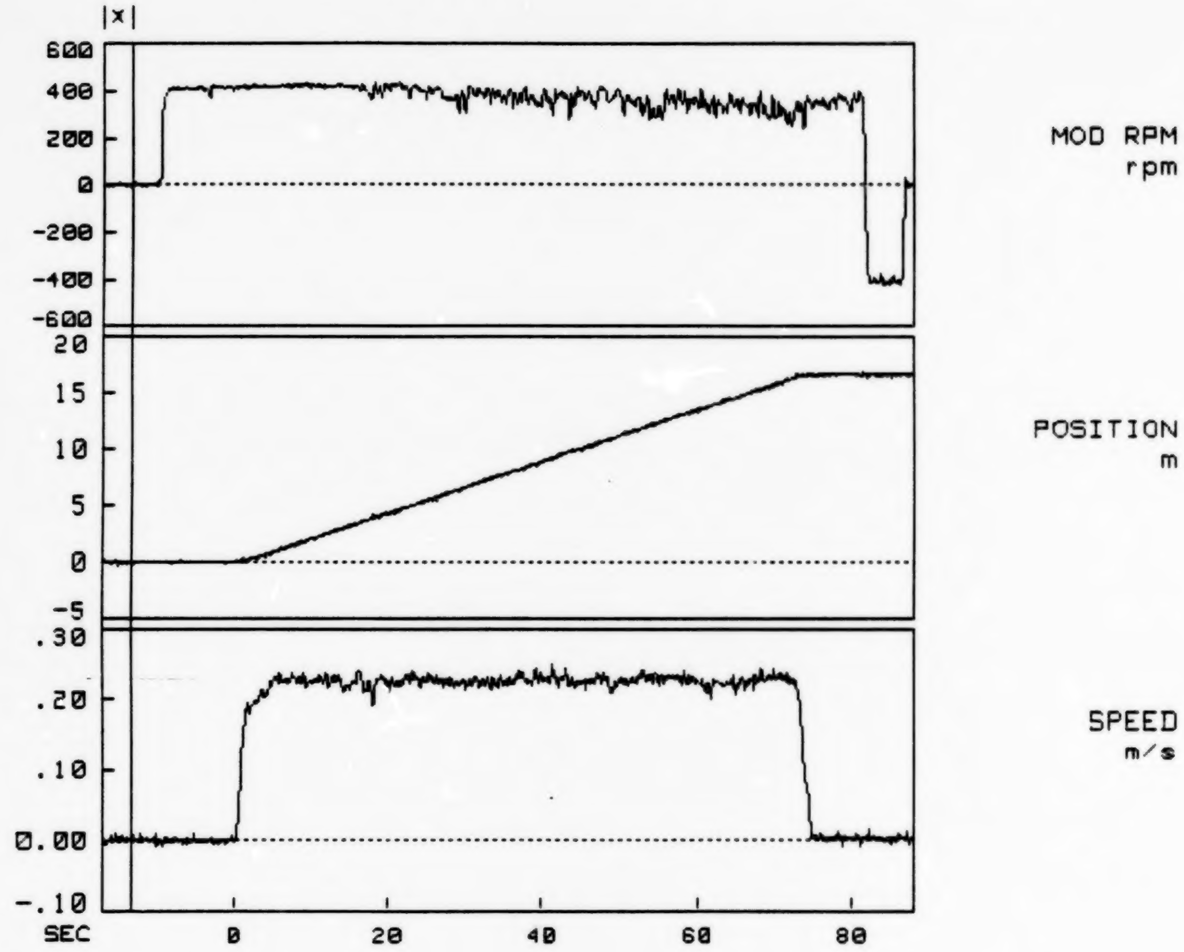

TEST 438

TEST #4 RUN 38

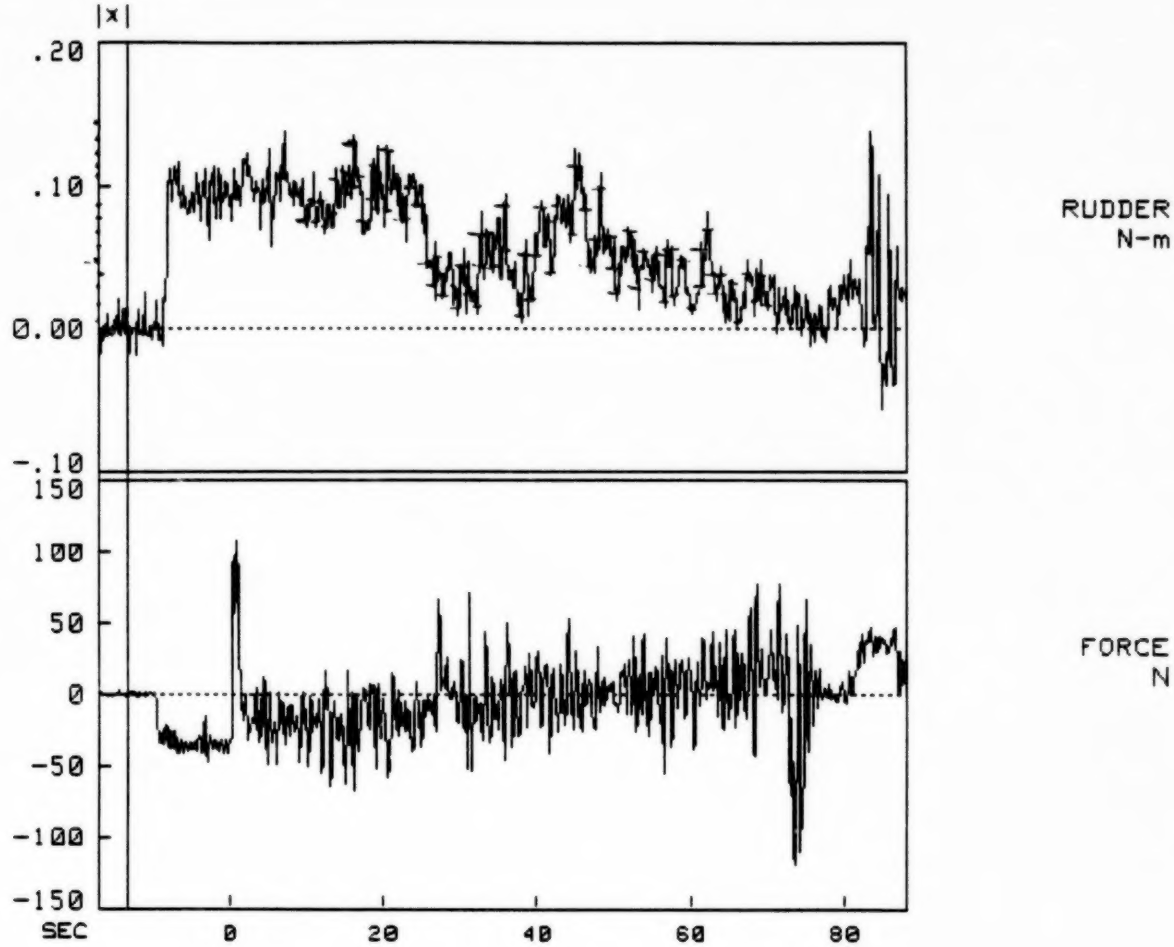

TEST 439

TEST #4 RUN 39

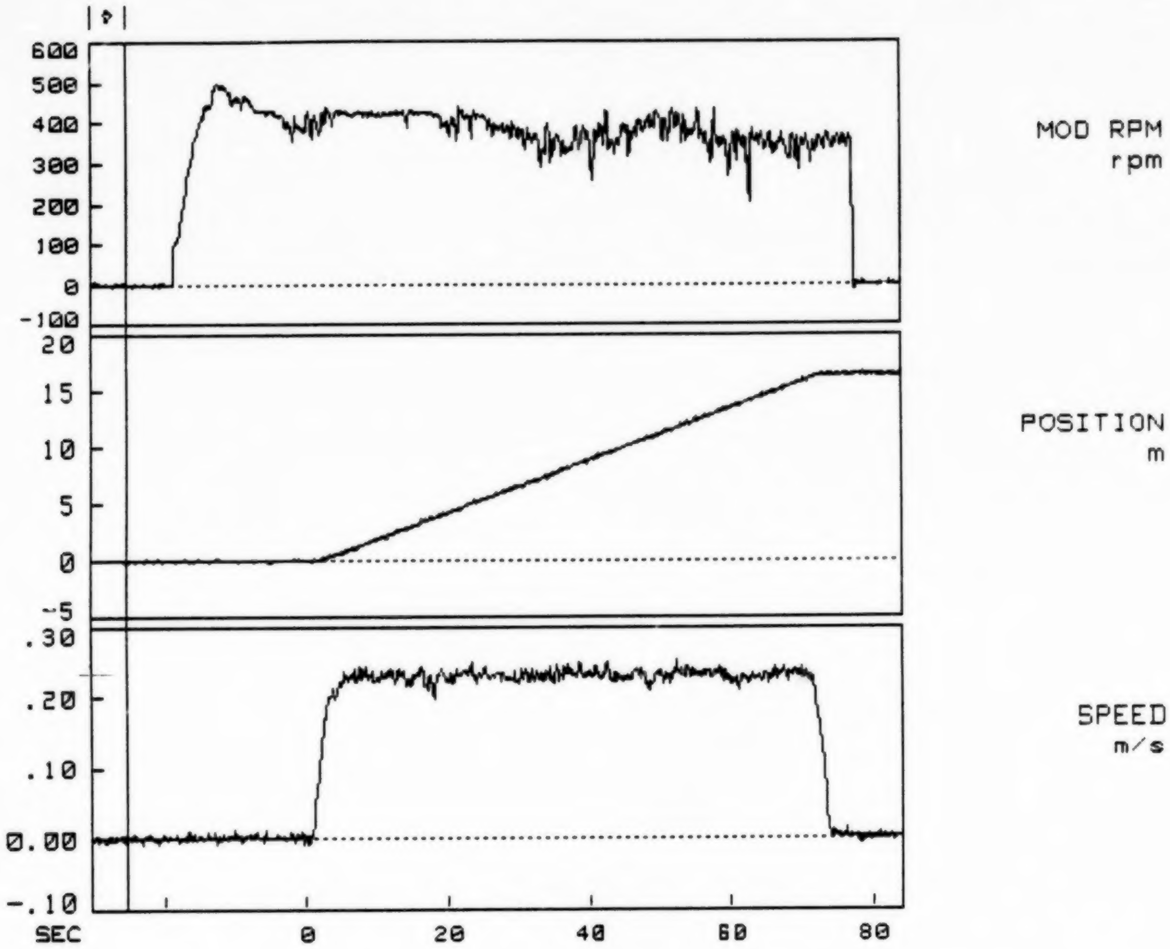

TEST 439

TEST #4 RUN 39

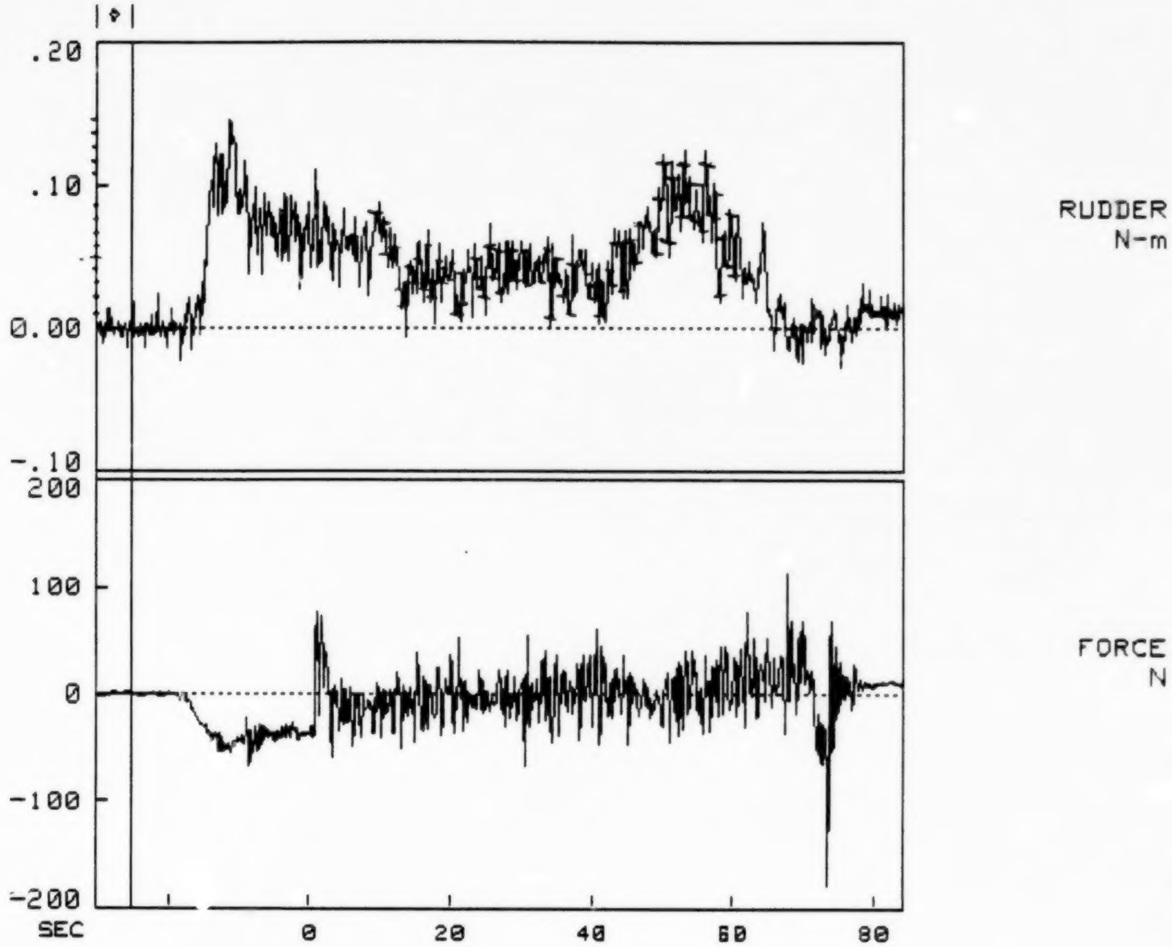

TEST 440

TEST #4 RUN 40

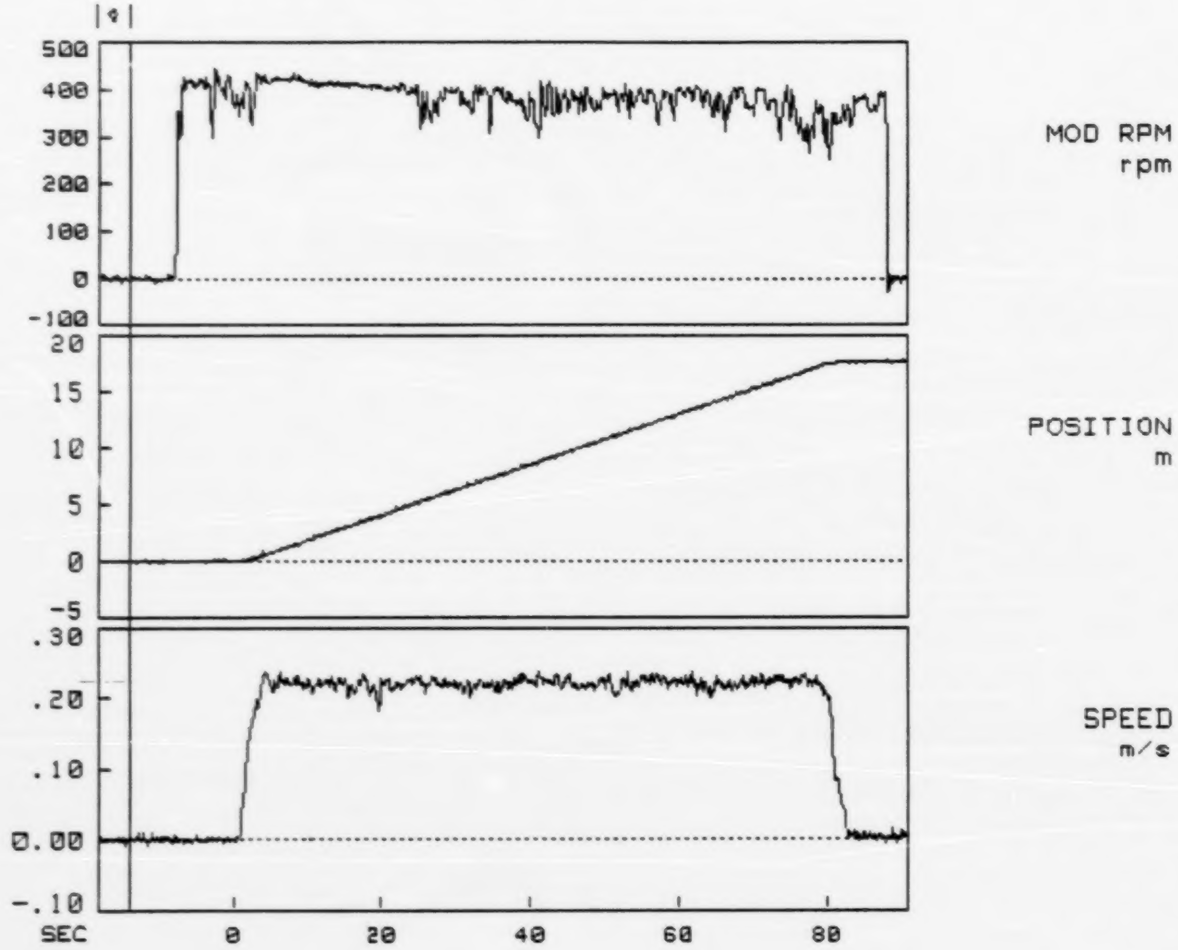

TEST 440

TEST #4 RUN 40